FACULTY OF SCIENCE·MASARYK UNIVERSITY
Institute of Experimental Biology

Hormonal Regulations of Plant Development

Jan Hejátko

Habilitation Thesis
Brno 2010

Acknowledgements

I would like to thank all my mentors and teachers who contributed to my scientific education, the formation of my critical thinking, and my love of science. In particular, these include Jiřina Kalabisová, who cultivated my early relationship to nature, Prof. Jan Šmarda, M.D., my first teacher of science, and his colleague, Assoc. Prof. David Šmajs, M.D., my dear friend. I would like to thank Prof. Břetislav Brzobohatý and Prof. Klaus Palme for introducing me into the world of top science. I would like to express my deep appreciation to Prof. Jiří Fajkus and Assoc. Prof. Eva Zažímalová for their trust and generosity. I would not have been able to do all my work without great support from my dear friends Prof. Jiří Friml and Assoc. Prof. Eva Benková. Finally, this thesis would not exist were it not for my team at the Laboratory of Molecular Plant Biology. My thanks go also to all my collaborators for their great and kind approach. Last but not least, I am deeply indebted to my family and particularly to Romana for her passionate and gratuitous support.

Contents

1. Introduction

This work is a compilation of publications to which I have contributed either as the first author, the last and/or corresponding author, respectively (see the list of enclosed publications, page 39). The introductory part presents an overview of the contribution by my colleagues and me to the field of molecular and developmental plant biology, and particularly with regard to elucidating hormonal regulations of plant development. This overview serves to facilitate the reader's understanding of our results in the contexts of time and the findings of the broader research community. To obtain a detailed understanding, however, careful reading of the original publications would be necessary. In these publications, all figures and explanatory schemes can also be found.

The enclosed publications include three reviews which may serve to acquaint the reader with the recent status of our knowledge on two important topics of my work: ***i)*** the role and underlying molecular mechanisms of signalling and its specificity via multistep phosphorelay in *Arabidopsis* (Horák et al., 2011), and ***ii)*** the role and molecular mechanisms of interactions of two principal regulators of plant development, the phytohormones auxin and cytokinins (Pernisová et al., 2011) and/or interactions of other phytohormones (Benkova and Hejatko, 2009). The enclosed six papers and one submitted manuscript describe original results that I have obtained together with my colleagues in our efforts to understand the aforementioned topics in the field of hormonal regulations of plant development.

2. Postembryonic *De Novo* Organogenesis in Plants

2.1. Postembryonic *De Novo* Organogenesis as a Plant Adaptation Strategy

The general problem of developmental biology is to decipher the molecular mechanisms that allow formation of a multicellular, fully differentiated organism from a single-celled zygote. In most animals, the majority of these processes take place during embryogenesis, wherein all tissues and organs are formed. By contrast, the embryogenesis of seed plants (to which the term embryogenesis will refer throughout the text) results in the formation of a simply organized embryo, wherein primordia of only a few organs (i.e. root, hypocotyl and cotyledons) are briefly specified. Hence, in plants, most of the tissues, cell types and organs differentiate during postembryonic development.

An important prerequisite for the aforementioned developmental strategy is a developmental plasticity of plant cells that allows substantial changes of their developmental status. Thus, virtually any cell of the fully differentiated plant body could become the progenitor of an entire new organism. Connection of regulatory mechanisms of this developmental plasticity with environmental inputs provides a sessile plant an ability for developmental adaptation to changing environmental conditions that include both biotic and abiotic stresses. While the involvement of plant hormones, namely cytokinins and auxin, in these processes has been known for decades (Skoog and Miller, 1957), the molecular nature of this developmental strategy has begun to be elucidated only recently. The identification of molecular mechanisms regulating cell division and differentiation in plants is of general biological importance, and comparison of such mechanisms with those being identified in animals can provide us with understanding of the basic developmental principles employed by self-organizing living systems on planet Earth.

2.2. The Concept of Meristems

Postembryonic plant development is accomplished via the action of specific structures known as meristems. There are two apical meristems in plants, the shoot and root apical meristem (SAM and RAM, respectively), secondary meristems (i.e. inflorescence meristems, floral meristems, axillary meristems in shoots, and lateral root meristems in roots), and lateral meristems formed by the (pro)cambium in vascular tissues. Apical meristems ensure the apical growth of the root and shoot, while secondary and lateral meristems allow radial plant expansion.

SAM undergoes several developmental switches, first forming what is called inflorescence apical meristem that later allows formation of individual floral meristems. After the onset of flowering, axillary meristems, the secondary inflorescence meristems, are formed and give rise to lateral inflorescences (coflorescences) in the axils of 2–5 cauline leaves in *Arabidopsis* (Dubova et al., 2005).

The two apical meristems share structural similarities. SAM and RAM contain what are called organization centres that are formed by the expression domains of the homeobox genes *WUSCHEL* (*WUS*) and *WUSCHEL-RELATED HOMEOBOX 5 (WOX5*) in the SAM and RAM, respectively. The activity of complex regulatory circuits involving WUS and WOX5 controls

the equilibrium between cell division and cell differentiation in the pool of stem cells that are under direct control of the organization centres in a cell-nonautonomous way (for review, see e.g. (Carles and Fletcher, 2003; Petricka and Benfey, 2008)). Thus, meristems act as sources of pluripotent stem cells that differentiate into newly formed plant tissues and organs. The tight control between cell division and cell differentiation as well as the providing of positional information in meristems determine postembryonic plant growth and development. Both of these processes are under direct control of the cytokinins and auxin phytohormones (for more details, see enclosed publication #1 (Pernisová et al., 2011)]).

2.3. The Origin of Meristems

The meristems in plants can be of two principal origins: embryonic and postembryonic. During embryogenesis, formation of the two apical meristems is an important part and a consequence of apical-basal symmetry acquisition. The first asymmetric zygote division leads to formation of a smaller apical cell and a larger suspensor. The smaller apical cell undergoes an additional three rounds of division, which result in formation of the octant embryo stage. The upper four cells (the upper tier) will further develop into the shoot part, while the lower four cells (the lower tier) together with the uppermost cell (hypophysis) of the twice-divided suspensor will result in formation of the root (Capron et al., 2009). One of the important molecular determinants as to the further developmental fate of individual embryo cell lineages is the expression of genes from the *WUS* gene family, which were found to be differentially expressed immediately after the first asymmetric zygote division (Haecker et al., 2004; Nawy et al., 2008; Capron et al., 2009). Auxin signalling is necessary for proper acquisition of shoot and root identity (Hamann et al., 2002; Szemenyei et al., 2008), and formation of local auxin maxima was found to be critical for determination of the apical-basal axis (Friml et al., 2003). Differential formation of auxin maxima seems to be instructive for determination of the apical-basal axis, and *WUS* genes were shown to be among the potential molecular targets of auxin-dependent regulations (Ding and Friml, 2010). Auxin and its interaction with cytokinins was also found to be important for positioning of the root pole and particularly the RAM organization centre (Muller and Sheen, 2008). The role of auxin in positioning of the SAM organization centre remains unclear, but the recently identified auxin/cytokinins interaction in the regulation of SAM activity (Gordon et al., 2009;

Zhao et al., 2010) suggests that similar mechanisms might play a role in the specification of *WUS* expression during embryogenesis.

Lateral root formation is an example of postembryonic meristem formation. Lateral roots in *Arabidopsis* develop from the pericycle founder cells (for review, see (Peret et al., 2009) that are located at the pericycle xylem pole (pericycle cells located opposite the xylem). The pericycle founder cells divide and allow formation of lateral root primordia, which might eventually emerge and form lateral root. Recently, it was found that specification of the pericycle founder cells could be induced by auxin in the region located proximally to the RAM (De Smet et al., 2007) that is referred to as basal meristem or transition zone (Dello Ioio et al., 2007; Peret et al., 2009). This process, also called priming, occurs in a regularly cyclic way, approximately every 15 hours. Later, the pre-specified pericycle founder cells accumulate auxin that triggers lateral root formation (Dubrovsky et al., 2008). Under normal conditions, only primed cells of the xylem pole pericycle become pericycle founder cells. However, exogenous auxin application might also activate other xylem pole pericycle cells (Boerjan et al., 1995; Dubrovsky et al., 2008). In addition to the auxin-mediated priming, there is also auxin-independent, mechanically induced priming that allows induction of lateral root primordia in a response to environmental inputs, e.g. gravistimulation (Ditengou et al., 2008; Lucas et al., 2008b; Peret et al., 2009).

The pericycle xylem pole cells that eventually become pericycle founder cells might be considered as 'extended meristem' (Casimiro et al., 2003). In contrast to pericycle cells located at the phloem pole, which remain in the G1 phase of the cell cycle, the xylem pole pericycle cells leave the apical meristem in the G2 stage (Beeckman et al., 2001), thus maintaining their ability to divide. It remains a question, therefore, whether auxin-mediated induction leads to complete, *de novo* re-specification of the developmental fate of completely differentiated cells or whether the auxin-mediated induction of postembryonic organogenesis allows activation of meristem pre-programmed cells with higher mitotic potential. In that regard, it is worthy of note that in addition to doing so in the roots, the exogenously applied auxin might induce postembryonic *de novo* organogenesis also in other organs, e.g. hypocotyls, petals or cotyledons (Pernisova et al., 2009; Sugimoto et al., 2010). Even in the shoot-derived tissues, however, auxin-induced organogenesis is accompanied by the expression of pericycle marker, suggesting that the auxin-induced organogenesis occurs

by default through the root developmental pathway (Sugimoto et al., 2010). Despite that neither the cell cycle status nor the lineage origin of the auxin-responsive cells in the shoot has been determined, the expression of pericycle-specific marker (Sugimoto et al., 2010) implies the possible existence of specific, meristem-derived cell lineages with higher mitotic and auxin-response potential throughout the plant body.

3. Auxin and Cytokinins as Principal Regulators of Plant Development

The plant hormones auxin and cytokinins are key regulators of plant development during both embryogenesis and the postembryonic stage. Auxin has been described as a principle regulator of plant cell polarity and cell patterning during embryogenesis and postembryonic development (Sachs, 1991; Sabatini et al., 1999; Friml et al., 2002c; Blilou et al., 2005; Pagnussat et al., 2009), plant tropic responses (Friml et al., 2002b; Lucas et al., 2008a), phyllotaxis (Reinhardt et al., 2003), and vascular tissue formation (Sachs, 2000; Scarpella et al., 2006; Donner et al., 2009). Cytokinins were originally identified as factors promoting cell division (Miller et al., 1955). Similar to auxin, cytokinins are involved in regulating many important developmental processes, e.g. regulation of both shoot and root meristem activity (Medford et al., 1989; Smigocki, 1991; Higuchi et al., 2004; Nishimura et al., 2004; Kurakawa et al., 2007; Kuroha et al., 2009), activity of axillary meristems (Sachs and Thimann, 1967; Tanaka et al., 2006), senescence (Hewelt et al., 1994; Kim et al., 2006), stress response (Tran et al., 2007), and vascular tissue formation (Matsumoto-Kitano et al., 2008; Nieminen et al., 2008; Hejatko et al., 2009b). Both cytokinins and auxin are important regulators of postembryonic *de novo* organogenesis, including regulation of the root architecture via modulation of the lateral root formation (Medford et al., 1989; Smigocki, 1991; Himanen et al., 2002; Benkova et al., 2003; Li et al., 2006; De Smet et al., 2007; Laplaze et al., 2007; Dubrovsky et al., 2008; Kuderova et al., 2008) or *in vitro* induced *de novo* organogenesis (Skoog and Miller, 1957; Cary et al., 2002; Gordon et al., 2007; Che et al., 2007; Pernisova et al., 2009). For more detailed description of the aforementioned regulatory roles of both phytohormones and their interactions, see enclosed publication #1 (Pernisová et al., 2011).

In the following sections, I will describe in more detail regulatory roles of cytokinins and auxin in selected developmental processes, emphasizing those for which my colleagues and I have contributed to the identification of underlying molecular mechanisms.

4. Multistep Phosphorelay Signalling and its Role in Developmental Regulations

4.1. Multistep Phosphorelay Signalling and Overview of its Role in the Regulation of Plant Development

In bacteria, sensor histidine kinases (HKs) comprise a part of what are called two-component signalling (TCS) systems, which were found to be important regulators of a wide spectrum of adaptive responses in bacteria, including e.g. nitrogen and carbon usage, phosphate assimilation, chemotaxis, sporulation or virulence (for review, see (Stock et al., 1989; Gao et al., 2007). TCS systems are composed of an HK that is recognized by its signalling partner, the cognate response regulator (RR). Upon interaction of the usually low molecular weight signalling molecule with the extracellular portion of the HK, the intracellular (kinase) domain is activated and the conserved histidine residue is phosphorylated. The phosphate group is then transferred from the phosphorylated histidine to the aspartate of the N-terminal regulatory or receiver domain of the RR, which leads to the activation of its output domain. In bacteria, the RRs are mostly transcription factors and activation of their output domains leads to the regulation of target gene expression. However, bacterial response regulators might also be involved in other processes, e.g. regulation of target effectors via protein-protein interactions, interactions with RNA, or enzymatic regulations (Gao et al., 2007).

In some eukaryotic systems, too, TCS systems were adopted. In eukaryotic systems (and in some bacteria), however, modifications of the TCS were introduced, resulting in a modified signalling pathway known as multistep phosphorelay (MSP). In comparison to the aforementioned TCS, signal transduction via MSP contains two more signalling modules. The sensor histidine kinases (called hybrid histidine kinases) in MSP contain an additional, response regulator-like receiver domain and the first phosphotransfer reaction is intramolecular. Further, an additional histidine-containing phosphotransfer protein (HPt) serves as a shuttle between (mostly) membrane-localized sensor histidine kinase and the nucleus, where it allows phosphorylation of the terminal phosphate acceptor, the response regulator. Thus, in comparison to simple His-to-Asp phosphotransfer taking place in prototypical bacterial TCS systems, the aforementioned modifications lead to sequential His-to-Asp-to-His-to-Asp phosphorelay being employed by some bacteria and eukaryotes (Chang

and Stewart, 1998). For more details on the molecular mechanisms of the signal transduction via MSP and related figures, see enclosed publication #2 (Horák et al., 2011).

In *Arabidopsis*, 11 HKs, 6 HPts and 23 RRs were identified (for review, see e.g. (To and Kieber, 2008)). Upon interaction with usually low molecular weight signalling molecules, HKs trigger the MSP signalling cascade and regulate a spectrum of developmental responses. Hybrid histidine kinases AHK2, AHK3 and AHK4 act as cytokinin receptors and trigger the cytokinin-regulated MSP-mediated responses during both root and shoot development (Higuchi et al., 2004; Nishimura et al., 2004; Riefler et al., 2006; Dello Ioio et al., 2007; Gordon et al., 2009), vascular tissue formation (Matsumoto-Kitano et al., 2008; Nieminen et al., 2008; Hejatko et al., 2009b), senescence (Kim et al., 2006), abiotic stress response (Tran et al., 2007), and postembryonic *de novo* organogenesis (Kakimoto, 1996; Inoue et al., 2001; Higuchi et al., 2004; Nishimura et al., 2004; Pernisova et al., 2009). In addition to cytokinins, receptors of another phytohormone, ethylene, reveal similarity with the histidine kinases, and ETR1 was proven also to affect developmental responses in *Arabidopsis* via MSP (Hass et al., 2004; Scharein et al., 2008; Voet-van-Vormizeele and Groth, 2008; Pernisova et al., 2009). In addition to hormonal regulation, the MSP in *Arabidopsis* mediates osmoregulation (AHK1) (Urao et al., 1999; Urao et al., 2000; Tran et al., 2007), stomatal signalling (AHK5) (Desikan et al., 2008), root growth (AHK5) (Iwama et al., 2007), and megagametogenesis (CKI1) (Pischke et al., 2002; Hejatko et al., 2003; Deng et al., 2010). Six HPt proteins mediate the signal transduction via MSP in *Arabidopsis*. Five of these, ARABIDOPSIS HISTIDINE PHOSPHOTRANSFER PROTEIN 1-5 (AHP1-5), are positive regulators (Hutchison et al., 2006; Deng et al., 2010) and act to shuttle between the membrane-located HKs and the nuclear-located RRs. AHP6 has lost the conserved His and was found to be a negative regulator of MSP-mediated cytokinin signalling in the vascular tissue development in the root (Mahonen et al., 2006b). There are two types of final phosphate acceptors, the RRs in *Arabidopsis,* encoded by *ARABIDOPSIS RESPONSE REGULATOR* (*ARR*) genes. Type-B RRs act as transcription factors and are activated by phosphate transferred from AHP1-5. Type-A RRs are among the targets of type-B RRs, and, based on the very rapid up-regulation of their transcription by cytokinins (D'Agostino et al., 2000), they are considered as cytokinin primary response genes. Type-A RRs are negative regulators of cytokinin signalling and mediate the negative feedback loop in MSP signalling (To et al., 2004).

4.2. Isolation of the *CKI1* Gene

In spite of cytokinins' general importance for plant development, about 10 years ago the signalling machinery involved in transduction of the cytokinin signal from the plasma membrane to the nucleus was still completely unknown. The first evidence of a possible molecular mechanism for the cytokinin signalling came from work of the exceptional Japanese scientist Tatsuo Kakimoto. Tatsuo used an activation mutagenesis approach to find genes potentially involved in the cytokinin signalling. He transformed *Arabidopsis* with tetramer of the cauliflower mosaic virus 35S rRNA gene promoter (CaMV35S) and performed a genetic screen for the *Arabidopsis* hypocotyls that would show the cytokinin-like response (i.e. formation of shoots from the hypocotyl explants *in vitro*, a process also called 'shooting') but in the absence of exogenously added hormones. Cloning of DNA in close proximity to the integration site of the T-DNA with 35S tetramer led to the isolation of a gene encoding a putative amino acid sequence with similarity to bacterial sensor histidine kinases. It was proven that ectopic overexpression of its cDNA leads to cytokinin independent shooting and hence the gene was designated *CYTOKININ-INDEPENDENT 1* (*CKI1*) (Kakimoto, 1996).

4.3. The Role of CKI1 in Female Gametophyte Development

At the time of *CKI1's* cloning, the role of bacterial TCS-like sensor histidine kinases was also known in yeast and some other eukaryotes (for review, see (Chang and Stewart, 1998)) and even in hormonal regulations by ethylene in *Arabidopsis* (Chang et al., 1993). On that basis, Tatsuo concluded that CKI1 might be a cytokinin receptor, the overexpression of which leads to higher sensitivity to endogenous cytokinins and thus the cytokinin independent phenotype (Kakimoto, 1996).

We used the reverse genetics approach to identify the potential regulatory role of CKI1 in the development of *Arabidopsis* (see enclosed publication #3 (Hejatko et al., 2003)). We identified insertion of maize transposable element En-1 in the coding sequence of CKI1 via screening of a mutant library constructed by Ellen Wisman (Wisman et al., 1998) and found out that plants homozygous for the insertion allele *cki1-i* cannot be identified in the segregating population, thus leading to a distortion of expected Mendelian segregation ratios. Based on the results of reciprocal crosses, we found that *cki1-i* cannot be transferred

through the female germ line. In good agreement with that, the plants heterozygous for the insertion allele were semi-sterile, having the seed set reduced to approximately one-half of that found in the sibling wild type (WT) lines. That led us to conclude that the female gametogenesis (megagametogenesis) might potentially be compromised in female gametophytes (embryo sacs) carrying the *cki1-i* allele. That hypothesis was confirmed by detailed microscopy analysis which proved that half of the embryo sacs in *CKI1/cki1-i* plants aborted their development at a specific stage of megagametogenesis (FG5). Based on the mutant phenotypes, we found that the most probable primary effect of the absence of *CKI1* is a collapse of the central vacuole that might lead to subsequent and probably only secondary effects (e.g. abnormal mitosis, cellularization defects, and final degradation of the entire embryo sac). Thus, based on these data, we concluded that "the integrity of the central vacuole is important for the timing and spatial distribution of specific cellular events (e.g. mitosis) during female gametophyte development" (Hejatko et al., 2003). However, what is the exact role of CKI1 in maintenance of the central vacuole remains to be clarified.

Interestingly, the expression of *CKI1* as revealed by analysis of transgenic lines carrying transcriptional fusion of *CKI1* promoter with the bacterial β-GLUCURONIDASE (GUS) encoding gene (*ProCKI1:GUS*) suggested the transcriptional activity of *CKI1* from the very beginning of female gametophyte development (FG0 or FG1). That was confirmed by *in situ* localization of *CKI1* mRNA according to the protocol that we have adopted (Hartmann et al., 2000) and further optimized (see enclosed publication #4, (Hejatko et al., 2006) and (Brewer et al., 2006)). Thus, CKI1 might be involved in processes that take place throughout megagametogenesis but become manifest only later during female gametophyte development. Alternatively, the signalling molecule recognized by CKI1 might appear later, in stage FG4 or FG5 (Hejatko et al., 2003).

We have further inspected the expression of *CKI1* in the newly developing sporophyte, immediately after fertilization. To avoid possible contamination of the developing embryo and seed sporophyte by GUS originating from gametophytic expression, we inspected the GUS activity in WT developing seeds after pollination with pollen from *ProCKI1:GUS* lines. In that experimental setup, we detected the GUS activity as soon as 12 hours after pollination (HAP). The expression was most prominent at 24 HAP and further decreased, with only residual GUS staining being detectable at 48 HAP. At 72 HAP, no more GUS staining was

detectable, suggesting transient transcriptional activation of *CKI1* during early seed development. At that time, there was published the hypothesis about genome-wide male imprinting, based upon which the male genome is completely silenced in the early stages of seed development (Grossniklaus and Schneitz, 1998; Luo et al., 2000). However, our data together with that of others (Weijers et al., 2001) have strongly suggested that the hypothesis should be revised.

Taken together, we have shown that *CKI1* expression starts very early in female gametophyte formation and that CKI1 is critical for proper female gametophyte development (Hejatko et al., 2003). Similar results were obtained by the competing group of Professor Sussman for *cki1-5* and *cki1-6* alleles (Pischke et al., 2002). As CKI1 is supposed to act through the MSP in *Arabidopsis*, these data might also suggest involvement of HPTs, the predicted downstream signalling partners of CKI1, in the female gametogenesis. That was recently confirmed by the Chinese group of Professor Zuo. In their publication by Deng et al. (2010) they have shown that pentaple *ahp1,2,3,4,5* mutant ovules reveal a phenotype similar to that of *cki1-i*. Interestingly*, ahk2,3,4* ovules carrying multiple mutations in cytokinin receptors similar to *wol* ovules (see next section) showed no substantial phenotypic alterations, thus suggesting specificity of CKI1-mediated MSP signalling in the female gametophyte development (see also section 4.7).

4.4. MSP and Vascular Tissue Formation

During our work on identifying the role of CKI1 in female gametogenesis, additional sensor histidine kinases were isolated in *Arabidopsis*. ARABIDOPSIS HISTIDINE KINASES 2, 3, and 4 (AHK2, AHK3 and AHK4, respectively) were proven to activate MSP in a cytokinin-dependent way and to act as cytokinin receptors *in planta* (Inoue et al., 2001; Suzuki et al., 2001; Ueguchi et al., 2001b; Ueguchi et al., 2001a; Yamada et al., 2001; Higuchi et al., 2004; Nishimura et al., 2004; Riefler et al., 2006). The first of these, AHK4, was identified as a *wooden leg* (*wol*) allele. The *wol* mutant was identified in a screen for lines deficient in radial organization of the root (Scheres et al., 1995). Out of the vascular tissue cell types normally present in the WT (i.e. phloem [PH], protoxylem [PX] and metaxylem [MX]), only PX was identifiable in the vascular tissue of the *wol* mutant (therefore the designation '*wooden leg*'). The *WOL* gene was cloned (Mahonen et al., 2000) and later it was found to be allelic to

CYTOKININ RESPONSE 1 (*CRE1*), the gene for the sensor histidine kinase responsible for the cytokinin response in *Arabidopsis* hypocotyls (the 'shooting' described in section 3.1 (Inoue et al., 2001)) and to *AHK4* (Suzuki et al., 2001). Importantly, AHK4/CRE1/WOL was proven to mediate the MSP activation in yeast and in *E. coli* in a cytokinin-dependent way (Inoue et al., 2001; Suzuki et al., 2001; Yamada et al., 2001) and the extracellular domain of AHK4 and AHK3, containing what is called the CHASE domain (Anantharaman and Aravind, 2001; Mougel and Zhulin, 2001), was found to directly bind cytokinins (Yamada et al., 2001; Spichal et al., 2004).

Later, the role of cytokinin signalling in the vascular tissue was corroborated by the group of Yka Helariutta. Ari Pekka Mahonen et al. (2006b) have shown that cytokinin signalling via AHK4 is necessary for PH and MX formation in the vascular tissue of the root. According to this scenario, in the absence of cytokinin signal, the 'default' developmental pathway leads to formation of PX cells. However, AHK4-mediated cytokinin signalling results in inhibition or perhaps rather modification of this 'default' developmental pathway, thus allowing formation of PH and MX cell types (Mahonen et al., 2006b). As previously mentioned in section 3.1, the spatiotemporal specificity of the cytokinin pathway is modulated via multiple negative regulators and feedback loops. Specific expression of negative regulator *AHP6* was proven to delimit the activity of MSP to the pericycle cells outside the xylem poles, where PX cells differentiate (Mahonen et al., 2006b).

4.5. The Role of CKI1 in Shoot Vascular Tissue Development

As mentioned in section 4.3, we have found the expression of *CKI1* throughout megagametogenesis and transient *CKI1* expression was detectable in the sporophytic tissue during early seed development (Hejatko et al., 2003). We have seen the transcriptional activity of *CKI1* also during the generative growth phase, however, and dominantly in the shoot vascular tissues. Based on the analysis of GUS activity in *ProCKI1:GUS* and *in situ* localization of *CKI1* mRNA, the expression was detectable in vascular tissue of the inflorescence stem and of all floral organs, while weak but distinct GUS activity was also detectable in the tapetum (see enclosed publication #5 (Hejatko et al., 2009b)). In the vascular tissue of the inflorescence stem, the expression of *CKI1* (both *CKI1* promoter activity and *CKI1* mRNA localization) was detectable in cells adjacent to the vascular bundles

forming what is called the vascular bundle sheath and in the xylem. To prove the presence of CKI1 protein in those tissues, we prepared an antibody recognizing the extracellular part of CKI1. Surprisingly, using these antibodies, we have detected the presence of CKI1 not only in the aforementioned cells revealing *CKI1* transcription, but also in adjacent procambial cells. That implied potential presence of localization signal in the CKI1 protein, which was confirmed in lines with ectopic overexpression of *CKI1* (*Pro35S:CKI1* lines), where the signal was localized dominantly also in the procambial cells.

Thus, these data on expression of *CKI1* in specific cell types of vascular tissue suggested a potential role of CKI1 in vascular tissue formation. That was confirmed by the phenotype analysis of *Pro35S:CKI1* lines, where we have detected increased number of procambial cells forming the stem cell pool of the lateral meristem. The opposite phenotype (i.e. reduction in the number of procambial cells) we found in lines with down-regulated *CKI1* activity via RNA interference (RNAi) as well as in lines heterozygous for the *cki1-6* allele. We observed reduction in the number of procambial cells also in the single mutants *ahk2* and *ahk3*, with more pronounced phenotype in the *ahk2 ahk3* double mutant line. Similar phenotype was found also in transgenic lines with depleted endogenous cytokinins via overexpression of the gene encoding cytokinin degradation enzymes, CYTOKININ OXIDASE/DEHYDROGENASE 2 and 3 [*Pro35S:AtCKX2(3*)]. Complementary results regarding the cytokinin action in the cambium activity were obtained in parallel by two other groups (Matsumoto-Kitano et al., 2008; Nieminen et al., 2008).

Taken together, our results provided experimental evidence that CKI1 acts together with cytokinins as a positive regulator of procambial cells division and/or the maintenance of their identity, thus directly affecting radial plant growth. These results are important not only as a part of our knowledge of molecular principles involved in regulating fundamental developmental processes in plants, but they might be used also to improve the quality of our life. Knowledge of molecular mechanisms regulating plant growth might be employed in the development of novel technologies that would decrease our dependence on petroleum products and increase the use of biomass production as a sustainable alternative energy resource (Hejatko et al., 2009a).

4.6. The Mechanism of CKI1 Action and Its Role in Cytokinin Signalling

CKI1 was originally supposed to be a cytokinin receptor. Our findings as to the role of CKI1 in the vascular tissue development have suggested that CKI1 acts together with cytokinins in the regulation of vascular tissue formation and radial plant growth (Hejatko et al., 2009b). Nonetheless, neither cytokinin binding (Yamada et al., 2001) nor cytokinin-dependent activation of MSP by CKI1 has been shown. CKI1 was found to be able to activate MSP in *E. coli* and yeast, however, in a cytokinin-independent way [T. Kakimoto, personal communication], thus impugning a role for CKI1 in cytokinin perception.

To find the molecular mechanism of CKI1's action, we analysed its ability to mediate MSP signalling in plant protoplast assay. In this assay, established in the laboratory of Professor Jen Sheen, plant protoplasts are transformed by the DNA construct carrying the gene encoding firefly LUCIFERASE (LUC) under control of the cytokinin primary response gene *ARR6* (*ProARR6:LUC*) and the activity of MSP signalling is quantified in proportion to the LUC activity (Hwang and Sheen, 2001). Using that assay, it was shown that CKI1 is able to induce MSP signalling in a cytokinin-independent way (Hwang and Sheen, 2001). In our work, we have shown that CKI1 lacking the conserved His residue (CKI1H^{405Q} mutant) has a dominant negative role in MSP signalling and interferes with cytokinin-dependent signalling mediated by the cytokinin receptor AHK4. Further, we have shown that CKI1 phosphorylates ARR2, a type-B response regulator that is involved in cytokinin-mediated two-component responses, (again, however, in a cytokinin-independent way). Finally, we have shown that the expression of type-A RRs, the expression of which is considered to be a measure of the MSP signalling, is affected in the *CKI1/cki1-5(6)* mutants and in transgenic lines overexpressing both WT CKI1 and CKI1H^{405Q} (Hejatko et al., 2009b). Thus, our data have provided clear experimental evidence that CKI1 acts through MSP signalling in *Arabidopsis* and shares common regulatory proteins with the cytokinin signalling pathway. That was later proven by an independent group using analysis of pentaple *ahp* mutants (Deng et al., 2010), as mentioned previously in section 4.3. However, CKI1 seems to act independent of the presence or absence of cytokinins. Thus, the potential regulatory role of CKI1 in cytokinin signalling remains to be clarified. One of the possibilities could be a direct interaction of CKI1 with some of the cytokinin receptors and formation of heterodimers, as was shown in the case of ethylene receptors (Grefen et al., 2008). That might eventually lead to changed

binding specificity and/or kinase activity of such heterodimers. We have shown formation of CKI1 homodimers both *in vitro* and *in vivo*, but no interaction of CKI1 has been proven with either AHK3 or AHK4 (Hejatko et al., 2009b). Thus, most probably, CKI1 interferes with the cytokinin signalling at the level of interaction with its closest downstream signalling partners, the HPt proteins.

A similar model was predicted in the work of Mahonen et al. (2006a). In their work, they have shown that AHK4 might act as a kinase or phosphatase dependent on the presence or absence of cytokinins, respectively. This ability to switch between kinase and phosphatase activities might be unique to AHK4 among all cytokinin receptors, as AHK2 and AHK3 seem able only to act in the kinase mode (Mahonen et al., 2006a). According to this model, the final output of the MSP comprises a combined contribution of both types of sensor HKs (kinases/phosphatases and kinases), both cytokinin-regulated and cytokinin-independent (Mahonen et al., 2006a). Although phosphatase activity of the CKI1 receiver domain was proven *in vitro* (Nakamura et al., 1999), the potential regulatory role of CKI1 phosphatase activity in the MSP remains to be clarified. Finally, differential regulation of *CKI1* expression might be another regulatory mechanism of the CKI1-dependent modulation of both cytokinin signalling and MSP in general, which is a subject of our recent work.

4.7. Specificity of Multistep Phosphorelay Signalling

As mentioned in section 4.1, MSP signalling in plants seems to integrate different signalling pathways into a common output. Accordingly, the individual members of the MSP (i.e. HK, HPt proteins and RRs) appear, at least in part, to act redundantly (Higuchi et al., 2004; Nishimura et al., 2004; To et al., 2004; Mason et al., 2005; Hutchison et al., 2006; Riefler et al., 2006). For review, see (Horák et al., 2011). In addition to signal integration, however, the independence and specificity of individual signalling pathways must be preserved. Accordingly, signalling through the MSP in *Arabidopsis* reveals a certain level of specificity, as manifested e.g. by the ligand specificity of individual cytokinin receptors (Spichal et al., 2004) and/or their involvement in different, spatiotemporal-specific developmental regulations (Dello Ioio et al., 2007). For more details, see enclosed publication #2 (Horák et al., 2011). However, the developmental specificity and underlying molecular mechanisms in plant MSP signalling remain mostly elusive.

4.8. Structure and Binding Specificity of the Receiver Domain of CKI1

In our work on identifying potential specificity in the MSP signalling in *Arabidopsis* and of its molecular determinants (see enclosed publications #6 and #7 (Klumpler et al., 2009; Pekárová et al., 2011)), we have been inspired by the mechanisms of specificity that have evolved in ancestors of MSP, the TCS in bacteria. The prototypical TCS systems in bacteria are formed by rather rigid couples of cognate signalling partners, consisting of histidine kinase and corresponding response regulator. In spite of their high sequential and structural similarity, physiologically relevant cross-reactivity among non-cognate signalling proteins in bacterial TCS is usually not detected (Laub and Goulian, 2007). The molecular recognition of the individual pairs is mediated by protein-protein interaction between the dimerization histidine-containing phosphotransfer domain (DHpD) of the histidine kinases and the receiver domain of response regulators. This molecular recognition is a prerequisite for the effective support of TCS specificity by such other molecular mechanisms as phosphatase activity of bifunctional histidine kinases or substrate competition (for review, see (Laub and Goulian, 2007; Horák et al., 2011). Taking into account the evolutionary relationship between TCS and MSP, one could predict that similar mechanisms could be at least partially preserved in the plant MSP signalling.

To prove that hypothesis, we performed screening of the protein-protein interactions of CKI1 with all six *Arabidopsis* HPt proteins. Using two independent *in vivo* assays – the yeast two-hybrid (Y2H) and bimolecular fluorescence complementation (BiFC) assays – we found that CKI1 interacts with only a subset of *Arabidopsis* HPt proteins: AHP1, AHP2 and AHP5. The same results were obtained using full-length CKI1 and only the receiver domain of CKI1 ($CKI1_{RD}$), suggesting that $CKI1_{RD}$ is sufficient and responsible for molecular recognition of the specific signalling partner of CKI1. These results were confirmed by ELISA measurements of apparent dissociation constants. While K_ds of the interaction between $CKI1_{RD}$ and AHP2 and AHP3 were comparable (9.17 ± 0.49 and 10.5 ± 0.73, respectively), the K_d of the $CKI1_{RD}$ complex with AHP5 was an order of magnitude higher (108 ± 18) (Pekárová et al., 2011).

To elucidate determinants of these specific interactions at the atomic level, we determined the structure of $CKI1_{RD}$ using X-ray diffraction (Klumpler et al., 2009). Similarly to receiver domains from the CheY-like superfamily (Wilson et al., 2009), $CKI1_{RD}$ was found to be folded in an $(\alpha/\beta)_5$ manner with the central β-sheet formed from five parallel β-strands

(β2-β1-β3-β4-β5), and surrounded on both sides by two (α1, α5) and three (α2, α3, α4), α-helices. Secondary structure elements are connected with five loops, L1–L5, on the face side of the domain and by four loops ℓ1–ℓ4 on the opposite side (Pekárová et al., 2011).

Magnesium ions (Mg^{2+}) are necessary cofactors for both the kinase autophosphorylation and transphosphorylation reactions (Lukat et al., 1990). Binding of the Mg^{2+} to the receiver domain of bacterial response regulators and subsequent phosphorylation was shown to be associated with structural rearrangements (Bourret et al., 1993; Stock et al., 1993; Lee et al., 2001; Rogov et al., 2008). To investigate the potential Mg^{2+}-mediated structural changes of $CKI1_{RD}$, we analysed the structure of a co-crystal of $CKI1_{RD}$ with Mg^{2+}. We found that the secondary structure of the $CKI1_{RD}$ complex with Mg^{2+} in comparison to the structure of the free $CKI1_{RD}$ protein was only slightly affected. The most dramatic changes occurred in the position of the side chain of the conserved Asp that is directly involved in the transphosphorylation reaction (change of the chi angle of the D1050 side chain [C-terminal part of strand β3]). Upon magnesium binding, the side chain of D1050 rotates by 90° towards the divalent cation. As the D1050 is connected via a salt bridge with K1105, the rotation of D1050 induces rotation of K1105 (see also supplemental video, enclosed with the electronic version of this work). This change induces a 3.4 Å shift of N^{ζ} (K1105) and 2 Å shift of O^{δ} (D1050), thus resulting in an appropriate geometry in the acidic pocket required for acceptance of the phosphate group (Pekárová et al., 2011).

To determine the potential structural changes of $CKI1_{RD}$ induced by Mg^{2+} or phosphorylation in solution, a ^{13}C, ^{15}N-labelled $CKI1_{RD}$ sample was prepared. Backbone amide as well as $^{13}C^{\alpha}$ and $^{13}C^{\beta}$ resonances were assigned using standard triple resonance NMR experiments in the presence and absence of Mg^{2+} and phosphorylation mimicking BeF_3^-. The major effect observed after addition of Mg^{2+} was loss of the conformational heterogeneity observed in the loop 3. In general, the chemical shift changes observed suggest that the Mg^{2+} might be responsible for major structural rearrangements, while phosphorylation (as mimicked by the binding of BeF_3^-) results in rather minor structural modifications. This is in contrast to what could be seen in bacterial MSP, where phosphorylation in e.g. RcsC-PR/RcsD-mediated MSP was identified as inducing major structural rearrangements and subsequent changes in the protein affinity (Rogov et al., 2006).

Finally, we have inspected potential influence of Mg^{2+}- and BeF_3^--induced structural changes on the binding specificity of $CKI1_{RD}$. In comparison to free $CKI1_{RD}$, the presence of Mg^{2+} ions slightly favoured interactions with AHP2 at the expense of interactions with AHP3, thus resulting in a two-fold preference for AHP2 when compared to AHP3. In contrast, the addition of phosphorylation mimicking BeF_3^- in the presence of Mg^{2+} reversed the binding affinities, leading to 1.5-fold higher preference for AHP3 as compared to AHP2. Thus, while either the presence of Mg^{2+} or beryllofluoridation has only limited influence on the interactions between $CKI1_{RD}$ and AHP proteins, these can further modulate the relative specificity of $CKI1_{RD}$ to individual AHPs (Pekárová et al., 2011).

Taken together, our work proves for the first time a certain level of specificity in the MSP signalling in plants and allows first insights into the structure of the CKI1 receiver domain as a molecular determinant of this specificity. Our work thus provides an initial platform for identifying molecular factors determining signalling specificity in various plant MSP signalling pathways.

5. Molecular Mechanisms of Auxin-Dependent Regulations of Plant Development

Detailed description of all developmental processes controlled by auxin and their molecular mechanisms is beyond the scope of this work and can be found in several recent reviews (e.g. (Teale et al., 2006; De Smet and Jurgens, 2007; Vieten et al., 2007; Benkova et al., 2009; Peret et al., 2009; Vanneste and Friml, 2009; Bennett and Scheres, 2010)). Here, I will only briefly describe the essential features of auxin-mediated developmental regulations for the better understanding of our work and its background.

Auxin is synthesized in cotyledons, leaves and roots. It is actively transported from the place of its biosynthesis by influx and efflux carriers. Of these, AUX1 and PIN proteins, respectively, are among the best characterized (Bennett et al., 1996; Galweiler et al., 1998; Muller et al., 1998; Marchant et al., 1999; Friml et al., 2002c; Friml et al., 2002a; Friml et al., 2003; Mravec et al., 2009). Dynamic polar localization of auxin carriers is determinative for intercellular auxin distribution and spatiotemporal-specific formation of auxin concentration maxima (Geldner et al., 2001; Benkova et al., 2003; Dhonukshe et al., 2007; Feraru and Friml, 2008). Localization of auxin maxima may be visualized in transgenic lines carrying reporter genes under control of auxin-responsive promoter, e.g. *DR5rev:GFP* or *DR5:GUS* (Ulmasov et

al., 1997; Benkova et al., 2003). Interference with formation of the auxin concentration maxima compromises several critical aspects of plant development, e.g. formation of apical-basal axis during embryogenesis (Friml et al., 2003; Geldner et al., 2003; Weijers et al., 2005), tropic responses (Friml et al., 2002a), lateral root formation (Benkova et al., 2003; De Smet et al., 2007; Dubrovsky et al., 2008; Kuderova et al., 2008), positioning of root meristem stem cell niche (Sabatini et al., 1999; Blilou et al., 2005), phyllotaxis (Reinhardt et al., 2003; Bainbridge et al., 2008), or vascular tissue formation and patterning (Scarpella et al., 2006; Bayer et al., 2009; Donner et al., 2009).

The intracellular auxin signal is recognized by the TRANSPORT INHIBITOR RESPONSE 1 (TIR1) protein, which upon auxin binding mediates targeted degradation of AUXIN/INDOLE-3-ACETIC ACID (AUX/IAA) proteins. That releases their inhibitory effect on AUXIN-RESPONSIVE FACTORS (ARFs) that are thus allowed to initiate transcription of auxin-regulated genes (Dharmasiri et al., 2005; Okushima et al., 2005; Overvoorde et al., 2005).

6. Auxin and Cytokinins Interactions

6.1. Developmental Importance of Auxin and Cytokinins Interactions

Auxin and cytokinins interactions are important for several aspects of plant development. In spite of the fact that the developmental impact of these interactions has been known for decades (Skoog and Miller, 1957), the molecular nature and cellular and tissue aspects of respective developmental regulations are just emerging. These include positioning and maintenance of apical meristem organization centres (Muller and Sheen, 2008; Gordon et al., 2009; Zhao et al., 2010), regulation of root meristem size via control over the equilibrium between cell division and cell differentiation (Beemster and Baskin, 2000; Dello Ioio et al., 2007; Dello Ioio et al., 2008), and postembryonic *de novo* organogenesis (Cary et al., 2002; Gordon et al., 2007; Che et al., 2007; Laplaze et al., 2007; Kuderova et al., 2008; Pernisova et al., 2009). For more details on respective developmental regulations and underlying molecular mechanisms, see enclosed publication #1 (Pernisová et al., 2011).

6.2. Auxin and Cytokinins Interactions During *De Novo* Organogenesis

In contrast to most animals, plants evolved postembryonic *de novo* organogenesis as an important developmental adaptation (see section 2.1). The regulatory role of cytokinins and auxin in these processes was identified in the early 1950s, when Folke Skoog and Carlos O. Miller showed that the concentration ratio of these two phytohormones determines the developmental fate of plant tissues *in vitro*. Under high auxin-to-cytokinin concentration ratios, roots were initiated from cultivated plant explants. Under cytokinin abundance, meanwhile, shooting (i.e. formation of the aerial portion of the plant) was observed (Skoog and Miller, 1957). Since then, the interaction of these two hormones has been found to be important also for the regulation of other aspects of development *in planta*, e.g. regulation of the root meristem size (Beemster and Baskin, 2000). However, the underlying molecular mechanism of this important phenomenon remained unknown.

In our work (see enclosed publication #8, (Pernisova et al., 2009)), we have employed a well-established technique involving *Arabidopsis* hypocotyl explants (Kubo and Kakimoto, 2000). Briefly, the hypocotyls of etiolated seedlings are collected and further cultivated on media with varying ratios of cytokinins and auxin. Using this assay, we have found that, after reaching a certain minimal concentration, auxin is able to induce formation of root-like organs, even in the absence of exogenously added cytokinins. We designated this minimal auxin concentration leading to organogenic response as the auxin threshold (30 ng/mL [135 nM] for 2,4-dichlorophenoxyacetic acid [2,4-D] and 100 ng/mL [537 nM] for naphthalene-1-acetic acid [NAA], (Pernisova et al., 2009)). By contrast, in the absence of auxin or at concentrations below the auxin threshold, cytokinins were unable to induce any organogenesis, even at the highest concentration used. At the auxin threshold, however, increasing concentration of cytokinins led to gradual loss of the organization of auxin-induced organs. After reaching a certain cytokinin concentration (300 ng/mL of kinetin, [1.4 uM]), we observed formation of only disorganized calli and we referred to this cytokinin concentration as the cytokinin threshold. Based on these findings, we have concluded that auxin, but not cytokinins, is able to induce organogenic response and that cytokinins modulate the auxin-induced organogenesis. We have further shown that the cytokinin-dependent modulation of organogenesis is mediated via MSP signalling with a dominant effect of AHK4, followed by AHK3 and AHK2 (AHK4≥AHK3>AHK2). Position-specific activation

of MSP signalling was detected in the newly formed organs by GUS staining of hypocotyls from transgenic lines carrying the GUS encoding gene under control of the promoter of *ARR5*, one of the cytokinin primary response genes (*ProARR5:GUS,* (D'Agostino et al., 2000)*)*.

To analyse the potential role of endogenous cytokinins, we inspected the organogenic response in transgenic lines with depleted endogenous cytokinins (*Pro35S:AtCKX2(3*)). When cultivated at the cytokinin threshold, *Pro35S:AtCKX2(3)* hypocotyl explants still revealed formation of root-like organs in contrast to WT, where only disorganized calli were detectable. Measurements of endogenous cytokinins confirmed the production of endogenous cytokinins in hypocotyl explants showing organogenic response and its decrease to approximately half of WT levels in *Pro35S:AtCKX2(3)* lines.

Further, we were interested in the possible mechanism for cytokinin-dependent modulation of *de novo* organogenesis. Interestingly, use of NAA or 2,4-D as auxins in cultivation media led to different organogenic responses. The use of 2,4-D in the absence of cytokinins resulted in the formation of poorly specified organs that only partially resembled roots. With increasing concentration of exogenously applied cytokinins, these organs were gradually disorganized. By contrast, NAA induced production of root-like structures and the increasing cytokinin concentration led to only partial loss of their organization. In hypocotyl explants cultivated in the presence of either 2,4-D or NAA at the cytokinin threshold, however, we observed complete loss of organ formation and disorganized calli production.

NAA and 2,4-D differ in their mechanisms of cellular transport. While 2,4-D is transported inside the cell via the active transport, NAA enters the cell passively. Conversely, while 2,4-D is only a very poor substrate of auxin efflux carriers that transport auxin outside the cell, NAA can leave the cell exclusively via the action of auxin efflux carriers. Thus, the observed differences in the sensitivity of induced organs to cytokinins suggested that auxin transport might be a potential target of cytokinins during its modulation of *de novo* organogenesis. That conclusion was further supported by our analysis of auxin concentration maxima formation as estimated in hypocotyl explants from *DR5rev:GFP* and *DR5:GUS* transgenic lines. In the 2,4-D-induced organs, multiple auxin maxima were detectable that became less focused and their spreading and disorganization were observed with the increasing cytokinin concentration. In contrast, NAA-induced organs formed single auxin maxima that, similarly to roots, were located in their tips, and the presence of cytokinins below the cytokinin

threshold had only weak effect on their intensity. Under no circumstances did we observe any changes in their localization. In organs induced by either 2,4-D or NAA, however, reaching the cytokinin threshold led to complete loss of the ability to form auxin concentration maxima (Pernisova et al., 2009).

Taken together, all these data strongly suggested the involvement of auxin transport in the observed cytokinin-mediated regulations of organogenic response. To prove that hypothesis, we used the auxin-transport assay system employing tobacco BY-2 tissue cultures that was established in the lab of Professor Eva Zažímalová. In that system, the accumulation of [^{3}H]NAA in cultured tobacco BY-2 cells was proven to be dependent exclusively on the auxin efflux (Petrasek et al., 2003). When [^{3}H]NAA was added to the BY-2 cells together with cytokinin, no effect on the [^{3}H]NAA accumulation was detected even in the presence of high cytokinin concentrations. When the BY-2 cells were pre-treated with cytokinin for approximately 16 hours, however, we observed dramatic increase in the [^{3}H]NAA accumulation, thus suggesting cytokinin interference with auxin efflux.

PIN auxin efflux carriers have been shown to be rate-limiting factors of auxin efflux in plant cells (Petrasek et al., 2006) and changes in their expression have been suggested to occur in plants treated with cytokinins (Laplaze et al., 2007), potentially leading to changes in auxin concentration maxima during lateral root formation in transgenic lines with elevated levels of endogenous cytokinins (see enclosed publication #9 (Kuderova et al., 2008)). Therefore, we inspected the expression of *PIN* genes (*PIN1-8*) in our system. In good accordance with our results from the auxin transport assay in BY-2 cells, we observed differential regulation of individual *PIN* genes in hypocotyl explants cultivated at the auxin threshold and in the presence of increasing cytokinin concentrations. Interestingly, in the case of PIN1, we detected no apparent changes in the *PIN1* mRNA levels. With the increasing cytokinin concentration, however, the PIN1 protein was internalized (changing its plasma membrane localization to internal cell compartments) and gradually disappeared, as detected in transgenic lines carrying translational fusion of PIN1 with GFP (*ProPIN1:PIN1-GFP*). Thus, we have shown that cytokinins regulate the expression of auxin efflux carriers from the PIN family at both the transcriptional and post-transcriptional levels.

Finally, to prove the validity of the observed effects for *in planta* developmental regulations, we inspected the auxin maxima formation in transgenic lines with depleted

endogenous cytokinins. In comparison to WT, we observed lateral expansion of auxin maxima in both *Pro35S:AtCKX2* and *Pro35S:AtCKX3* lines associated with decrease of *PIN2* and *PIN4* expression. This suggests that certain levels of endogenous cytokinins are necessary for expression of the genes for PIN auxin efflux carriers and thus proper intercellular auxin distribution, as suggested in our previous publication (see enclosed publication #9 (Kuderova et al., 2008)).

Taken together, in this work we have identified a completely new mechanism for the regulation of intercellular auxin distribution. Two other groups obtained similar results in parallel (Dello Ioio et al., 2008; Ruzicka et al., 2009), thus confirming an important and novel role of auxin and cytokinins interaction in the regulation of plant development (see also enclosed publication #10 (Benkova and Hejatko, 2009). Based on our aforementioned findings, we suggested a developmental model in which auxin maxima trigger organogenesis that is associated with endogenous cytokinin production. The cytokinins produced in turn regulate expression of *PIN* genes, thus modulating auxin-induced organogenic response (see enclosed publication #1 (Pernisová et al., 2011)).

7. Future Prospects

Great progress has been made during the last decade in the field of hormonal regulations of plant development. Important questions remain to be answered, however, and, as a consequence of obtaining new data, novel questions are emerging. In terms of the general regulatory mechanisms, one of the crucial questions is whether auxin is able to induce *de novo* organogenesis in all the cells throughout the plant body or whether the developmental plasticity is limited to a specific subset of cells pre-programmed in meristems, as suggested by recent findings (De Smet et al., 2007; Sugimoto et al., 2010). Further, if auxin is really the general trigger of organogenesis (Benkova et al., 2009; Pernisova et al., 2009), what determines the identity of newly formed organs? Most probably, the interactions of auxin with other regulatory pathways, including MSP, will play important roles in those processes (Muller and Sheen, 2008; Gordon et al., 2009; Moubayidin et al., 2010; Zhao et al., 2010). Also, the molecular targets of the auxin gradients and molecular mechanisms allowing translation of these gradients into spatiotemporal-specific regulation of gene expression remain to be identified, although the first mechanisms

seem recently to have appeared (Galinha et al., 2007; Parry et al., 2009; Calderon-Villalobos et al., 2010). In terms of MSP specificity, the story has just begun. To what extent is the signal integrated and, on the contrary, to what extent is signalling specificity maintained in the MSP-mediated signalling? What are the molecular determinants at the atomic level? What is the role of potential structural dynamics of individual proteins that mediate MSP signalling? Are there any other, yet unknown regulators that would connect MSP with other signalling pathways in plants?

More intense use and/or implementation of several novel approaches in the plant sciences will be necessary to allow solving these problems. In particular, the connection of structural biology with recent genetic and molecular biology approaches will be critical in improving our understanding of several aspects of hormonal regulations of plant development, including the aforementioned specificity of both cytokinin and auxin signalling (Calderon-Villalobos et al., 2010; Horák et al., 2011). Recent technological improvements and reductions in their costs will allow novel approaches to be employed for data acquisition, including genome-wide studies using next-generation sequencing on the one hand (Weber et al., 2007; Eveland et al., 2008; Lister et al., 2008) and high-resolution approaches on the other, thus allowing transcriptome and/or proteome analysis at single-cell or even sub-cellular resolution (Schrader et al., 2004; Holmes-Davis et al., 2005; Zhao et al., 2008; Yadav et al., 2009). Last but not least, the growing complexity of our understanding will require novel procedures for data processing and data mining, and particularly for implementing systemic biology and modelling approaches (de Reuille et al., 2006; Teale et al., 2008; Gordon et al., 2009).

Recently, my colleagues and I from the Department of Functional Genomics and Proteomics have prepared a novel study programme, “Genomics and Proteomics”, to be taught at Masaryk University. That programme will encompass some of the aforementioned aspects of recent molecular biology and biochemistry, and it will allow for preparing the new generation of students that will be tasked with meeting the future challenges of modern life sciences.

8. References

Anantharaman, V., and Aravind, L. (2001). The CHASE domain: a predicted ligand-binding module in plant cytokinin receptors and other eukaryotic and bacterial receptors. Trends Biochem Sci **26,** 579-582.

Bainbridge, K., Guyomarc'h, S., Bayer, E., Swarup, R., Bennett, M., Mandel, T., and Kuhlemeier, C. (2008). Auxin influx carriers stabilize phyllotactic patterning. Genes Dev **22,** 810-823.

Bayer, E.M., Smith, R.S., Mandel, T., Nakayama, N., Sauer, M., Prusinkiewicz, P., and Kuhlemeier, C. (2009). Integration of transport-based models for phyllotaxis and midvein formation. Genes Dev **23,** 373-384.

Beeckman, T., Burssens, S., and Inze, D. (2001). The peri-cell-cycle in Arabidopsis. J Exp Bot **52,** 403-411.

Beemster, G.T., and Baskin, T.I. (2000). Stunted plant 1 mediates effects of cytokinin, but not of auxin, on cell division and expansion in the root of Arabidopsis. Plant Physiol **124,** 1718-1727.

Benkova, E., and Hejatko, J. (2009). Hormone interactions at the root apical meristem. Plant Mol Biol **69,** 383-396.

Benkova, E., Ivanchenko, M.G., Friml, J., Shishkova, S., and Dubrovsky, J.G. (2009). A morphogenetic trigger: is there an emerging concept in plant developmental biology? Trends Plant Sci **14,** 189-193.

Benkova, E., Michniewicz, M., Sauer, M., Teichmann, T., Seifertova, D., Jurgens, G., and Friml, J. (2003). Local, efflux-dependent auxin gradients as a common module for plant organ formation. Cell **115,** 591-602.

Bennett, M.J., Marchant, A., Green, H.G., May, S.T., Ward, S.P., Millner, P.A., Walker, A.R., Schulz, B., and Feldmann, K.A. (1996). Arabidopsis AUX1 gene: a permease-like regulator of root gravitropism. Science **273,** 948-950.

Bennett, T., and Scheres, B. (2010). Root development-two meristems for the price of one? Curr Top Dev Biol **91,** 67-102.

Blilou, I., Xu, J., Wildwater, M., Willemsen, V., Paponov, I., Friml, J., Heidstra, R., Aida, M., Palme, K., and Scheres, B. (2005). The PIN auxin efflux facilitator network controls growth and patterning in Arabidopsis roots. Nature **433,** 39-44.

Boerjan, W., Cervera, M.T., Delarue, M., Beeckman, T., Dewitte, W., Bellini, C., Caboche, M., Van Onckelen, H., Van Montagu, M., and Inze, D. (1995). Superroot, a recessive mutation in Arabidopsis, confers auxin overproduction. Plant Cell **7,** 1405-1419.

Bourret, R.B., Drake, S.K., Chervitz, S.A., Simon, M.I., and Falke, J.J. (1993). Activation of the phosphosignaling protein CheY. II. Analysis of activated mutants by 19F NMR and protein engineering. J Biol Chem **268,** 13089-13096.

Brewer, P.B., Heisler, M.G., Hejatko, J., Friml, J., and Benkova, E. (2006). In situ hybridization for mRNA detection in Arabidopsis tissue sections. Nat Protoc **1,** 1462-1467.

Calderon-Villalobos, L.I., Tan, X., Zheng, N., and Estelle, M. (2010). Auxin perception--structural insights. Cold Spring Harb Perspect Biol **2,** a005546.

Capron, A., Chatfield, S., Provart, N., and Berleth, T. (2009). Embryogenesis: Pattern Formation from a Single Cell. In The Arabidopsis Book (Rockville, MD: American Society of Plant Biologists, doi: 10.1199/tab.0126, http://www.aspb.org/publications/arabidopsis/.

Carles, C.C., and Fletcher, J.C. (2003). Shoot apical meristem maintenance: the art of a dynamic balance. Trends Plant Sci **8,** 394-401.

Cary, A.J., Che, P., and Howell, S.H. (2002). Developmental events and shoot apical meristem gene expression patterns during shoot development in Arabidopsis thaliana. Plant J **32,** 867-877.

Casimiro, I., Beeckman, T., Graham, N., Bhalerao, R., Zhang, H., Casero, P., Sandberg, G., and Bennett, M.J. (2003). Dissecting Arabidopsis lateral root development. Trends Plant Sci **8,** 165-171.

D'Agostino, I.B., Deruere, J., and Kieber, J.J. (2000). Characterization of the response of the Arabidopsis response regulator gene family to cytokinin. Plant Physiol **124,** 1706-1717.

de Reuille, P.B., Bohn-Courseau, I., Ljung, K., Morin, H., Carraro, N., Godin, C., and Traas, J. (2006). Computer simulations reveal properties of the cell-cell signaling network at the shoot apex in Arabidopsis. Proc Natl Acad Sci U S A **103,** 1627-1632.

De Smet, I., and Jurgens, G. (2007). Patterning the axis in plants--auxin in control. Curr Opin Genet Dev **17,** 337-343.

De Smet, I., Tetsumura, T., De Rybel, B., Frey, N.F.D., Laplaze, L., Casimiro, I., Swarup, R., Naudts, M., Vanneste, S., Audenaert, D., Inze, D., Bennett, M.J., and Beeckman, T. (2007). Auxin-dependent regulation of lateral root positioning in the basal meristem of Arabidopsis. Development **134,** 681-690.

Dello Ioio, R., Linhares, F.S., Scacchi, E., Casamitjana-Martinez, E., Heidstra, R., Costantino, P., and Sabatini, S. (2007). Cytokinins determine Arabidopsis root-meristem size by controlling cell differentiation. Curr Biol **17,** 678-682.

Dello Ioio, R., Nakamura, K., Moubayidin, L., Perilli, S., Taniguchi, M., Morita, M.T., Aoyama, T., Costantino, P., and Sabatini, S. (2008). A genetic framework for the control of cell division and differentiation in the root meristem. Science **322,** 1380-1384.

Deng, Y., Dong, H., Mu, J., Ren, B., Zheng, B., Ji, Z., Yang, W.C., Liang, Y., and Zuo, J. (2010). Arabidopsis Histidine Kinase CKI1 Acts Upstream of HISTIDINE PHOSPHOTRANSFER PROTEINS to Regulate Female Gametophyte Development and Vegetative Growth. Plant Cell.

Desikan, R., Horak, J., Chaban, C., Mira-Rodado, V., Witthoft, J., Elgass, K., Grefen, C., Cheung, M.K., Meixner, A.J., Hooley, R., Neill, S.J., Hancock, J.T., and Harter, K. (2008). The histidine kinase AHK5 integrates endogenous and environmental signals in Arabidopsis guard cells. PLoS One **3,** e2491.

Dharmasiri, N., Dharmasiri, S., and Estelle, M. (2005). The F-box protein TIR1 is an auxin receptor. Nature **435,** 441-445.

Dhonukshe, P., Aniento, F., Hwang, I., Robinson, D.G., Mravec, J., Stierhof, Y.D., and Friml, J. (2007). Clathrin-mediated constitutive endocytosis of PIN auxin efflux carriers in Arabidopsis. Curr Biol **17,** 520-527.

Ding, Z., and Friml, J. (2010). Auxin regulates distal stem cell differentiation in Arabidopsis roots. Proc Natl Acad Sci U S A.

Ditengou, F.A., Teale, W.D., Kochersperger, P., Flittner, K.A., Kneuper, I., van der Graaff, E., Nziengui, H., Pinosa, F., Li, X., Nitschke, R., Laux, T., and Palme, K. (2008). Mechanical induction of lateral root initiation in Arabidopsis thaliana. Proc Natl Acad Sci U S A **105,** 18818-18823.

Donner, T.J., Sherr, I., and Scarpella, E. (2009). Regulation of preprocambial cell state acquisition by auxin signaling in Arabidopsis leaves. Development **136,** 3235-3246.

Dubova, J., Hejatko, J., and Friml, J. (2005). Reproduction of Plants. (Weinheim: Wiley-VCH Verlag).

Dubrovsky, J.G., Sauer, M., Napsucialy-Mendivil, S., Ivanchenko, M.G., Friml, J., Shishkova, S., Celenza, J., and Benkova, E. (2008). Auxin acts as a local morphogenetic trigger to specify lateral root founder cells. Proc Natl Acad Sci U S A **105,** 8790-8794.

Eveland, A.L., McCarty, D.R., and Koch, K.E. (2008). Transcript profiling by 3'-untranslated region sequencing resolves expression of gene families. Plant Physiol **146,** 32-44.

Feraru, E., and Friml, J. (2008). PIN polar targeting. Plant Physiol **147,** 1553-1559.

Friml, J., Wisniewska, J., Benkova, E., Mendgen, K., and Palme, K. (2002a). Lateral relocation of auxin efflux regulator PIN3 mediates tropism in Arabidopsis. Nature **415,** 806-809.

Friml, J., Wisniewska, J., Benkova, E., Mendgen, K., and Palme, K. (2002b). Lateral relocation of auxin efflux regulator PIN3 mediates tropism in Arabidopsis. Nature **415,** 806-809.

Friml, J., Vieten, A., Sauer, M., Weijers, D., Schwarz, H., Hamann, T., Offringa, R., and Jurgens, G. (2003). Efflux-dependent auxin gradients establish the apical-basal axis of Arabidopsis. Nature **426,** 147-153.

Friml, J., Benkova, E., Blilou, I., Wisniewska, J., Hamann, T., Ljung, K., Woody, S., Sandberg, G., Scheres, B., Jurgens, G., and Palme, K. (2002c). AtPIN4 mediates sink-driven auxin gradients and root patterning in Arabidopsis. Cell **108,** 661-673.

Galinha, C., Hofhuis, H., Luijten, M., Willemsen, V., Blilou, I., Heidstra, R., and Scheres, B. (2007). PLETHORA proteins as dose-dependent master regulators of Arabidopsis root development. Nature **449,** 1053-1057.

Galweiler, L., Guan, C., Muller, A., Wisman, E., Mendgen, K., Yephremov, A., and Palme, K. (1998). Regulation of polar auxin transport by AtPIN1 in Arabidopsis vascular tissue. Science **282,** 2226-2230.

Gao, R., Mack, T.R., and Stock, A.M. (2007). Bacterial response regulators: versatile regulatory strategies from common domains. Trends Biochem Sci **32,** 225-234.

Geldner, N., Friml, J., Stierhof, Y.D., Jurgens, G., and Palme, K. (2001). Auxin transport inhibitors block PIN1 cycling and vesicle trafficking. Nature **413,** 425-428.

Geldner, N., Anders, N., Wolters, H., Keicher, J., Kornberger, W., Muller, P., Delbarre, A., Ueda, T., Nakano, A., and Jurgens, G. (2003). The Arabidopsis GNOM ARF-GEF mediates endosomal recycling, auxin transport, and auxin-dependent plant growth. Cell **112,** 219-230.

Gordon, S.P., Chickarmane, V.S., Ohno, C., and Meyerowitz, E.M. (2009). Multiple feedback loops through cytokinin signaling control stem cell number within the Arabidopsis shoot meristem. Proc Natl Acad Sci U S A **106,** 16529-16534.

Gordon, S.P., Heisler, M.G., Reddy, G.V., Ohno, C., Das, P., and Meyerowitz, E.M. (2007). Pattern formation during de novo assembly of the Arabidopsis shoot meristem. Development **134,** 3539-3548.

Grefen, C., Stadele, K., Ruzicka, K., Obrdlik, P., Harter, K., and Horak, J. (2008). Subcellular localization and in vivo interactions of the Arabidopsis thaliana ethylene receptor family members. Molecular Plant **1,** 308-320.

Grossniklaus, U., and Schneitz, K. (1998). The molecular and genetic basis of ovule and megagametophyte development. Semin Cell Dev Biol **9,** 227-238.

Haecker, A., Gross-Hardt, R., Geiges, B., Sarkar, A., Breuninger, H., Herrmann, M., and Laux, T. (2004). Expression dynamics of WOX genes mark cell fate decisions during early embryonic patterning in Arabidopsis thaliana. Development **131,** 657-668.

Hamann, T., Benkova, E., Baurle, I., Kientz, M., and Jurgens, G. (2002). The Arabidopsis BODENLOS gene encodes an auxin response protein inhibiting MONOPTEROS-mediated embryo patterning. Genes Dev **16,** 1610-1615.

Hartmann, U., Hohmann, S., Nettesheim, K., Wisman, E., Saedler, H., and Huijser, P. (2000). Molecular cloning of SVP: a negative regulator of the floral transition in Arabidopsis. Plant J **21,** 351-360.

Hass, C., Lohrmann, J., Albrecht, V., Sweere, U., Hummel, F., Yoo, S.D., Hwang, I., Zhu, T., Schafer, E., Kudla, J., and Harter, K. (2004). The response regulator 2 mediates ethylene signalling and hormone signal integration in Arabidopsis. EMBO J **23,** 3290-3302.

Hejatko, J., Pernisova, M., Eneva, T., Palme, K., and Brzobohaty, B. (2003). The putative sensor histidine kinase CKI1 is involved in female gametophyte development in Arabidopsis. Mol Genet Genomics **269,** 443-453.

Hejatko, J., Dobesova, R., Dubova, J., Hwang, I., and Ryu, H. (2009a). Method of regulation of biomass production in plants, DNA sequences and method of preparation thereof. Patent # 300145, M.U.a.P.A.I. Foundation, ed (Czech Republic).

Hejatko, J., Blilou, I., Brewer, P.B., Friml, J., Scheres, B., and Benkova, E. (2006). In situ hybridization technique for mRNA detection in whole mount Arabidopsis samples. Nat Protoc **1,** 1939-1946.

Hejatko, J., Ryu, H., Kim, G.T., Dobesova, R., Choi, S., Choi, S.M., Soucek, P., Horak, J., Pekarova, B., Palme, K., Brzobohaty, B., and Hwang, I. (2009b). The Histidine Kinases CYTOKININ-INDEPENDENT1 and ARABIDOPSIS HISTIDINE KINASE2 and 3 Regulate Vascular Tissue Development in Arabidopsis Shoots. Plant Cell **21,** 2008-2021.

Hewelt, A., Prinsen, E., Schell, J., Van Onckelen, H., and Schmulling, T. (1994). Promoter tagging with a promoterless ipt gene leads to cytokinin-induced phenotypic variability in transgenic tobacco plants:implications of gene dosage effects. Plant J **6,** 879-891.

Higuchi, M., Pischke, M.S., Mahonen, A.P., Miyawaki, K., Hashimoto, Y., Seki, M., Kobayashi, M., Shinozaki, K., Kato, T., Tabata, S., Helariutta, Y., Sussman, M.R., and Kakimoto, T. (2004). In planta functions of the Arabidopsis cytokinin receptor family. Proc Natl Acad Sci U S A **101,** 8821-8826.

Himanen, K., Boucheron, E., Vanneste, S., de Almeida Engler, J., Inze, D., and Beeckman, T. (2002). Auxin-mediated cell cycle activation during early lateral root initiation. Plant Cell **14,** 2339-2351.

Holmes-Davis, R., Tanaka, C.K., Vensel, W.H., Hurkman, W.J., and McCormick, S. (2005). Proteome mapping of mature pollen of Arabidopsis thaliana. Proteomics **5,** 4864-4884.

Horák, J., Janda, L., Pekárová, B., and Hejátko, J. (2011). Molecular determinants of the signalling specificity via phosphorelay pathways in Arabidopsis. Curr Protein Pept Sci in press.

Hutchison, C.E., Li, J., Argueso, C., Gonzalez, M., Lee, E., Lewis, M.W., Maxwell, B.B., Perdue, T.D., Schaller, G.E., Alonso, J.M., Ecker, J.R., and Kieber, J.J. (2006). The Arabidopsis histidine phosphotransfer proteins are redundant positive regulators of cytokinin signaling. Plant Cell **18,** 3073-3087.

Hwang, I., and Sheen, J. (2001). Two-component circuitry in Arabidopsis cytokinin signal transduction. Nature **413,** 383-389.

Chang, C., and Stewart, R.C. (1998). The two-component system. Regulation of diverse signaling pathways in prokaryotes and eukaryotes. Plant Physiol **117,** 723-731.

Chang, C., Kwok, S.F., Bleecker, A.B., and Meyerowitz, E.M. (1993). Arabidopsis ethylene-response gene ETR1: similarity of product to two-component regulators. Science **262,** 539-544.

Che, P., Lall, S., and Howell, S.H. (2007). Developmental steps in acquiring competence for shoot development in Arabidopsis tissue culture. Planta **226,** 1183-1194.

Inoue, T., Higuchi, M., Hashimoto, Y., Seki, M., Kobayashi, M., Kato, T., Tabata, S., Shinozaki, K., and Kakimoto, T. (2001). Identification of CRE1 as a cytokinin receptor from Arabidopsis. Nature **409,** 1060-1063.

Iwama, A., Yamashino, T., Tanaka, Y., Sakakibara, H., Kakimoto, T., Sato, S., Kato, T., Tabata, S., Nagatani, A., and Mizuno, T. (2007). AHK5 histidine kinase regulates root elongation through an ETR1-dependent abscisic acid and ethylene signaling pathway in Arabidopsis thaliana. Plant Cell Physiol **48,** 375-380.

Kakimoto, T. (1996). CKI1, a histidine kinase homolog implicated in cytokinin signal transduction. Science **274,** 982-985.

Kim, H.J., Ryu, H., Hong, S.H., Woo, H.R., Lim, P.O., Lee, I.C., Sheen, J., Nam, H.G., and Hwang, I. (2006). Cytokinin-mediated control of leaf longevity by AHK3 through phosphorylation of ARR2 in Arabidopsis. Proc Natl Acad Sci U S A **103,** 814-819.

Klumpler, T., Pekarova, B., Marek, J., Borkovcova, P., Janda, L., and Hejatko, J. (2009). Cloning, purification, crystallization and preliminary X-ray analysis of the receiver domain of the histidine kinase CKI1 from Arabidopsis thaliana. Acta Crystallogr Sect F Struct Biol Cryst Commun **65,** 478-481.

Kubo, M., and Kakimoto, T. (2000). The Cytokinin-hypersensitive genes of Arabidopsis negatively regulate the cytokinin-signaling pathway for cell division and chloroplast development. Plant J **23,** 385-394.

Kuderova, A., Urbankova, I., Valkova, M., Malbeck, J., Nemethova, D., and Hejatko, J. (2008). Effects of conditional IPT-dependent cytokinin overproduction on root architecture of Arabidopsis seedlings. Plant Cell Physiol **49,** 570-582.

Kurakawa, T., Ueda, N., Maekawa, M., Kobayashi, K., Kojima, M., Nagato, Y., Sakakibara, H., and Kyozuka, J. (2007). Direct control of shoot meristem activity by a cytokinin-activating enzyme. Nature **445,** 652-655.

Kuroha, T., Tokunaga, H., Kojima, M., Ueda, N., Ishida, T., Nagawa, S., Fukuda, H., Sugimoto, K., and Sakakibara, H. (2009). Functional analyses of LONELY GUY cytokinin-activating enzymes reveal the importance of the direct activation pathway in Arabidopsis. Plant Cell **21,** 3152-3169.

Laplaze, L., Benkova, E., Casimiro, I., Maes, L., Vanneste, S., Swarup, R., Weijers, D., Calvo, V., Parizot, B., Herrera-Rodriguez, M.B., Offringa, R., Graham, N., Doumas, P., Friml, J., Bogusz, D., Beeckman, T., and Bennett, M. (2007). Cytokinins act directly on lateral root founder cells to inhibit root initiation. Plant Cell **19,** 3889-3900.

Laub, M.T., and Goulian, M. (2007). Specificity in two-component signal transduction pathways. Annu Rev Genet **41,** 121-145.

Lee, S.Y., Cho, H.S., Pelton, J.G., Yan, D., Berry, E.A., and Wemmer, D.E. (2001). Crystal structure of activated CheY. Comparison with other activated receiver domains. J Biol Chem **276,** 16425-16431.

Li, X., Mo, X., Shou, H., and Wu, P. (2006). Cytokinin-mediated cell cycling arrest of pericycle founder cells in lateral root initiation of Arabidopsis. Plant Cell Physiol **47,** 1112-1123.

Lister, R., O'Malley, R.C., Tonti-Filippini, J., Gregory, B.D., Berry, C.C., Millar, A.H., and Ecker, J.R. (2008). Highly integrated single-base resolution maps of the epigenome in Arabidopsis. Cell **133,** 523-536.

Lucas, M., Godin, C., Jay-Allemand, C., and Laplaze, L. (2008a). Auxin fluxes in the root apex co-regulate gravitropism and lateral root initiation. J Exp Bot **59,** 55-66.

Lucas, M., Guedon, Y., Jay-Allemand, C., Godin, C., and Laplaze, L. (2008b). An auxin transport-based model of root branching in Arabidopsis thaliana. PLoS One **3,** e3673.

Lukat, G.S., Stock, A.M., and Stock, J.B. (1990). Divalent metal ion binding to the CheY protein and its significance to phosphotransfer in bacterial chemotaxis. Biochemistry **29,** 5436-5442.

Luo, M., Bilodeau, P., Dennis, E.S., Peacock, W.J., and Chaudhury, A. (2000). Expression and parent-of-origin effects for FIS2, MEA, and FIE in the endosperm and embryo of developing Arabidopsis seeds. Proc Natl Acad Sci U S A **97,** 10637-10642.

Mahonen, A.P., Bonke, M., Kauppinen, L., Riikonen, M., Benfey, P.N., and Helariutta, Y. (2000). A novel two-component hybrid molecule regulates vascular morphogenesis of the Arabidopsis root. Genes Dev **14,** 2938-2943.

Mahonen, A.P., Higuchi, M., Tormakangas, K., Miyawaki, K., Pischke, M.S., Sussman, M.R., Helariutta, Y., and Kakimoto, T. (2006a). Cytokinins regulate a bidirectional phosphorelay network in Arabidopsis. Curr Biol **16,** 1116-1122.

Mahonen, A.P., Bishopp, A., Higuchi, M., Nieminen, K.M., Kinoshita, K., Tormakangas, K., Ikeda, Y., Oka, A., Kakimoto, T., and Helariutta, Y. (2006b). Cytokinin signaling and its inhibitor AHP6 regulate cell fate during vascular development. Science **311,** 94-98.

Marchant, A., Kargul, J., May, S.T., Muller, P., Delbarre, A., Perrot-Rechenmann, C., and Bennett, M.J. (1999). AUX1 regulates root gravitropism in Arabidopsis by facilitating auxin uptake within root apical tissues. EMBO J **18,** 2066-2073.

Mason, M.G., Mathews, D.E., Argyros, D.A., Maxwell, B.B., Kieber, J.J., Alonso, J.M., Ecker, J.R., and Schaller, G.E. (2005). Multiple type-B response regulators mediate cytokinin signal transduction in Arabidopsis. Plant Cell **17,** 3007-3018.

Matsumoto-Kitano, M., Kusumoto, T., Tarkowski, P., Kinoshita-Tsujimura, K., Vaclavikova, K., Miyawaki, K., and Kakimoto, T. (2008). Cytokinins are central regulators of cambial activity. Proc Natl Acad Sci U S A **105,** 20027-20031.

Medford, J.I., Horgan, R., El-Sawi, Z., and Klee, H.J. (1989). Alterations of Endogenous Cytokinins in Transgenic Plants Using a Chimeric Isopentenyl Transferase Gene. Plant Cell **1,** 403-413.

Miller, C.O., Skoog, F., Vonsaltza, M.H., and Strong, F.M. (1955). Kinetin, a Cell Division Factor from Deoxyribonucleic Acid. Journal of the American Chemical Society **77,** 1392-1392.

Moubayidin, L., Perilli, S., Dello Ioio, R., Di Mambro, R., Costantino, P., and Sabatini, S. (2010). The rate of cell differentiation controls the Arabidopsis root meristem growth phase. Curr Biol **20,** 1138-1143.

Mougel, C., and Zhulin, I.B. (2001). CHASE: an extracellular sensing domain common to transmembrane receptors from prokaryotes, lower eukaryotes and plants. Trends Biochem Sci **26,** 582-584.

Mravec, J., Skupa, P., Bailly, A., Hoyerova, K., Krecek, P., Bielach, A., Petrasek, J., Zhang, J., Gaykova, V., Stierhof, Y.D., Dobrev, P.I., Schwarzerova, K., Rolcik, J., Seifertova, D., Luschnig, C., Benkova, E., Zazimalova, E., Geisler, M., and Friml, J. (2009). Subcellular homeostasis of phytohormone auxin is mediated by the ER-localized PIN5 transporter. Nature **459,** 1136-1140.

Muller, A., Guan, C., Galweiler, L., Tanzler, P., Huijser, P., Marchant, A., Parry, G., Bennett, M., Wisman, E., and Palme, K. (1998). AtPIN2 defines a locus of Arabidopsis for root gravitropism control. EMBO J **17,** 6903-6911.

Muller, B., and Sheen, J. (2008). Cytokinin and auxin interaction in root stem-cell specification during early embryogenesis. Nature **453,** 1094-1097.

Nakamura, A., Kakimoto, T., Imamura, A., Suzuki, T., Ueguchi, C., and Mizuno, T. (1999). Biochemical characterization of a putative cytokinin-responsive His-kinase, CKI1, from Arabidopsis thaliana. Biosci Biotechnol Biochem **63,** 1627-1630.

Nawy, T., Lukowitz, W., and Bayer, M. (2008). Talk global, act local-patterning the Arabidopsis embryo. Curr Opin Plant Biol **11,** 28-33.

Nieminen, K., Immanen, J., Laxell, M., Kauppinen, L., Tarkowski, P., Dolezal, K., Tahtiharju, S., Elo, A., Decourteix, M., Ljung, K., Bhalerao, R., Keinonen, K., Albert, V.A., and Helariutta, Y. (2008). Cytokinin signaling regulates cambial development in poplar. Proc Natl Acad Sci U S A **105,** 20032-20037.

Nishimura, C., Ohashi, Y., Sato, S., Kato, T., Tabata, S., and Ueguchi, C. (2004). Histidine kinase homologs that act as cytokinin receptors possess overlapping functions in the regulation of shoot and root growth in Arabidopsis. Plant Cell **16,** 1365-1377.

Okushima, Y., Overvoorde, P.J., Arima, K., Alonso, J.M., Chan, A., Chang, C., Ecker, J.R., Hughes, B., Lui, A., Nguyen, D., Onodera, C., Quach, H., Smith, A., Yu, G., and Theologis, A. (2005). Functional genomic analysis of the AUXIN RESPONSE FACTOR gene family members in Arabidopsis thaliana: unique and overlapping functions of ARF7 and ARF19. Plant Cell **17,** 444-463.

Overvoorde, P.J., Okushima, Y., Alonso, J.M., Chan, A., Chang, C., Ecker, J.R., Hughes, B., Liu, A., Onodera, C., Quach, H., Smith, A., Yu, G., and Theologis, A. (2005). Functional genomic analysis of the AUXIN/INDOLE-3-ACETIC ACID gene family members in Arabidopsis thaliana. Plant Cell **17,** 3282-3300.

Pagnussat, G.C., Alandete-Saez, M., Bowman, J.L., and Sundaresan, V. (2009). Auxin-dependent patterning and gamete specification in the Arabidopsis female gametophyte. Science **324,** 1684-1689.

Parry, G., Calderon-Villalobos, L.I., Prigge, M., Peret, B., Dharmasiri, S., Itoh, H., Lechner, E., Gray, W.M., Bennett, M., and Estelle, M. (2009). Complex regulation of the TIR1/AFB family of auxin receptors. Proc Natl Acad Sci U S A **106,** 22540-22545.

Pekárová, B., Klumpler, T., Třísková, O., Horák, J., Jansen, S., Dopitová, R., Papoušková, V., Nejedlá, E., Žídek, L., Sklenář, V., Marek, J., Hejátko, J., and Janda, L. (2011).

Structure and binding specificity of the receiver domain of sensor histidine kinase CKI1 from Arabidopsis thaliana. Submitted.

Peret, B., De Rybel, B., Casimiro, I., Benkova, E., Swarup, R., Laplaze, L., Beeckman, T., and Bennett, M.J. (2009). Arabidopsis lateral root development: an emerging story. Trends Plant Sci **14,** 399-408.

Pernisova, M., Klima, P., Horak, J., Valkova, M., Malbeck, J., Soucek, P., Reichman, P., Hoyerova, K., Dubova, J., Friml, J., Zazimalova, E., and Hejatko, J. (2009). Cytokinins modulate auxin-induced organogenesis in plants via regulation of the auxin efflux. Proc Natl Acad Sci U S A **106,** 3609-3614.

Pernisová, M., Kuderová, A., and Hejátko, J. (2011). Cytokinin and auxin interactions in plant development: Metabolism, signalling, transport and gene expression. Curr Protein Pept Sci**,** in press.

Petrasek, J., Cerna, A., Schwarzerova, K., Elckner, M., Morris, D.A., and Zazimalova, E. (2003). Do phytotropins inhibit auxin efflux by impairing vesicle traffic? Plant Physiol **131,** 254-263.

Petrasek, J., Mravec, J., Bouchard, R., Blakeslee, J.J., Abas, M., Seifertova, D., Wisniewska, J., Tadele, Z., Kubes, M., Covanova, M., Dhonukshe, P., Skupa, P., Benkova, E., Perry, L., Krecek, P., Lee, O.R., Fink, G.R., Geisler, M., Murphy, A.S., Luschnig, C., Zazimalova, E., and Friml, J. (2006). PIN proteins perform a rate-limiting function in cellular auxin efflux. Science **312,** 914-918.

Petricka, J.J., and Benfey, P.N. (2008). Root layers: complex regulation of developmental patterning. Curr Opin Genet Dev **18,** 354-361.

Pischke, M.S., Jones, L.G., Otsuga, D., Fernandez, D.E., Drews, G.N., and Sussman, M.R. (2002). An Arabidopsis histidine kinase is essential for megagametogenesis. Proc Natl Acad Sci U S A **99,** 15800-15805.

Reinhardt, D., Pesce, E.R., Stieger, P., Mandel, T., Baltensperger, K., Bennett, M., Traas, J., Friml, J., and Kuhlemeier, C. (2003). Regulation of phyllotaxis by polar auxin transport. Nature **426,** 255-260.

Riefler, M., Novak, O., Strnad, M., and Schmulling, T. (2006). Arabidopsis cytokinin receptor mutants reveal functions in shoot growth, leaf senescence, seed size, germination, root development, and cytokinin metabolism. Plant Cell **18,** 40-54.

Rogov, V.V., Rogova, N.Y., Bernhard, F., Koglin, A., Lohr, F., and Dotsch, V. (2006). A new structural domain in the Escherichia coli RcsC hybrid sensor kinase connects histidine kinase and phosphoreceiver domains. J Mol Biol **364,** 68-79.

Rogov, V.V., Schmoe, K., Lohr, F., Rogova, N.Y., Bernhard, F., and Dotsch, V. (2008). Modulation of the Rcs-mediated signal transfer by conformational flexibility. Biochem Soc Trans **36,** 1427-1432.

Ruzicka, K., Simaskova, M., Duclercq, J., Petrasek, J., Zazimalova, E., Simon, S., Friml, J., Van Montagu, M.C., and Benkova, E. (2009). Cytokinin regulates root meristem activity via modulation of the polar auxin transport. Proc Natl Acad Sci U S A **106,** 4284-4289.

Sabatini, S., Beis, D., Wolkenfelt, H., Murfett, J., Guilfoyle, T., Malamy, J., Benfey, P., Leyser, O., Bechtold, N., Weisbeek, P., and Scheres, B. (1999). An auxin-dependent distal organizer of pattern and polarity in the Arabidopsis root. Cell **99,** 463-472.

Sachs, T. (1991). Pattern formation in plant tissues. (Cambridge University Press).

Sachs, T. (2000). Integrating cellular and organismic aspects of vascular differentiation. Plant Cell Physiol **41,** 649-656.

Sachs, T., and Thimann, V. (1967). Role of Auxins and Cytokinins in Release of Buds from Dominance. American Journal of Botany **54,** 136-&.

Scarpella, E., Marcos, D., Friml, J., and Berleth, T. (2006). Control of leaf vascular patterning by polar auxin transport. Genes Dev **20,** 1015-1027.

Scharein, B., Voet-van-Vormizeele, J., Harter, K., and Groth, G. (2008). Ethylene signaling: identification of a putative ETR1-AHP1 phosphorelay complex by fluorescence spectroscopy. Anal Biochem **377,** 72-76.

Scheres, B., Dilaurenzio, L., Willemsen, V., Hauser, M.T., Janmaat, K., Weisbeek, P., and Benfey, P.N. (1995). Mutations Affecting the Radial Organization of the Arabidopsis Root Display Specific Defects Throughout the Embryonic Axis. Development **121,** 53-62.

Schrader, J., Nilsson, J., Mellerowicz, E., Berglund, A., Nilsson, P., Hertzberg, M., and Sandberg, G. (2004). A high-resolution transcript profile across the wood-forming meristem of poplar identifies potential regulators of cambial stem cell identity. Plant Cell **16,** 2278-2292.

Skoog, F., and Miller, C.O. (1957). Chemical regulation of growth and organ formation in plant tissues cultured in vitro. Symp Soc Exp Biol **54,** 118-130.

Smigocki, A.C. (1991). Cytokinin content and tissue distribution in plants transformed by a reconstructed isopentenyl transferase gene. Plant Mol Biol **16,** 105-115.

Spichal, L., Rakova, N.Y., Riefler, M., Mizuno, T., Romanov, G.A., Strnad, M., and Schmulling, T. (2004). Two cytokinin receptors of Arabidopsis thaliana, CRE1/AHK4 and AHK3, differ in their ligand specificity in a bacterial assay. Plant Cell Physiol **45,** 1299-1305.

Stock, A.M., Martinez-Hackert, E., Rasmussen, B.F., West, A.H., Stock, J.B., Ringe, D., and Petsko, G.A. (1993). Structure of the Mg(2+)-bound form of CheY and mechanism of phosphoryl transfer in bacterial chemotaxis. Biochemistry **32,** 13375-13380.

Stock, J.B., Ninfa, A.J., and Stock, A.M. (1989). Protein phosphorylation and regulation of adaptive responses in bacteria. Microbiol Rev **53,** 450-490.

Sugimoto, K., Jiao, Y., and Meyerowitz, E.M. (2010). Arabidopsis regeneration from multiple tissues occurs via a root development pathway. Dev Cell **18,** 463-471.

Suzuki, T., Miwa, K., Ishikawa, K., Yamada, H., Aiba, H., and Mizuno, T. (2001). The Arabidopsis sensor His-kinase, AHK4, can respond to cytokinins. Plant and Cell Physiology **42,** 107-113.

Szemenyei, H., Hannon, M., and Long, J.A. (2008). TOPLESS mediates auxin-dependent transcriptional repression during Arabidopsis embryogenesis. Science **319,** 1384-1386.

Tanaka, H., Dhonukshe, P., Brewer, P.B., and Friml, J. (2006). Spatiotemporal asymmetric auxin distribution: a means to coordinate plant development. Cell Mol Life Sci **63,** 2738-2754.

Teale, W.D., Paponov, I.A., and Palme, K. (2006). Auxin in action: signalling, transport and the control of plant growth and development. Nat Rev Mol Cell Biol **7,** 847-859.

Teale, W.D., Ditengou, F.A., Dovzhenko, A.D., Li, X., Molendijk, A.M., Ruperti, B., Paponov, I., and Palme, K. (2008). Auxin as a model for the integration of hormonal signal processing and transduction. Mol Plant **1,** 229-237.

To, J.P., and Kieber, J.J. (2008). Cytokinin signaling: two-components and more. Trends Plant Sci **13,** 85-92.

To, J.P., Haberer, G., Ferreira, F.J., Deruere, J., Mason, M.G., Schaller, G.E., Alonso, J.M., Ecker, J.R., and Kieber, J.J. (2004). Type-A Arabidopsis response regulators are partially redundant negative regulators of cytokinin signaling. Plant Cell **16,** 658-671.

Tran, L.S., Urao, T., Qin, F., Maruyama, K., Kakimoto, T., Shinozaki, K., and Yamaguchi-Shinozaki, K. (2007). Functional analysis of AHK1/ATHK1 and cytokinin receptor histidine kinases in response to abscisic acid, drought, and salt stress in Arabidopsis. Proc Natl Acad Sci U S A **104,** 20623-20628.

Ueguchi, C., Sato, S., Kato, T., and Tabata, S. (2001a). The AHK4 gene involved in the cytokinin-signaling pathway as a direct receptor molecule in Arabidopsis thaliana. Plant Cell Physiol **42,** 751-755.

Ueguchi, C., Koizumi, H., Suzuki, T., and Mizuno, T. (2001b). Novel family of sensor histidine kinase genes in Arabidopsis thaliana. Plant Cell Physiol **42,** 231-235.

Ulmasov, T., Murfett, J., Hagen, G., and Guilfoyle, T.J. (1997). Aux/IAA proteins repress expression of reporter genes containing natural and highly active synthetic auxin response elements. Plant Cell **9,** 1963-1971.

Urao, T., Miyata, S., Yamaguchi-Shinozaki, K., and Shinozaki, K. (2000). Possible His to Asp phosphorelay signaling in an Arabidopsis two-component system. FEBS Lett **478,** 227-232.

Urao, T., Yakubov, B., Satoh, R., Yamaguchi-Shinozaki, K., Seki, M., Hirayama, T., and Shinozaki, K. (1999). A transmembrane hybrid-type histidine kinase in Arabidopsis functions as an osmosensor. Plant Cell **11,** 1743-1754.

Vanneste, S., and Friml, J. (2009). Auxin: a trigger for change in plant development. Cell **136,** 1005-1016.

Vieten, A., Sauer, M., Brewer, P.B., and Friml, J. (2007). Molecular and cellular aspects of auxin-transport-mediated development. Trends Plant Sci **12,** 160-168.

Voet-van-Vormizeele, J., and Groth, G. (2008). Ethylene controls autophosphorylation of the histidine kinase domain in ethylene receptor ETR1. Mol Plant **1,** 380-387.

Weber, A.P., Weber, K.L., Carr, K., Wilkerson, C., and Ohlrogge, J.B. (2007). Sampling the Arabidopsis transcriptome with massively parallel pyrosequencing. Plant Physiol **144,** 32-42.

Weijers, D., Geldner, N., Offringa, R., and Jurgens, G. (2001). Seed development: Early paternal gene activity in Arabidopsis. Nature **414,** 709-710.

Weijers, D., Sauer, M., Meurette, O., Friml, J., Ljung, K., Sandberg, G., Hooykaas, P., and Offringa, R. (2005). Maintenance of embryonic auxin distribution for apical-basal patterning by PIN-FORMED-dependent auxin transport in Arabidopsis. Plant Cell **17,** 2517-2526.

Wilson, D., Pethica, R., Zhou, Y., Talbot, C., Vogel, C., Madera, M., Chothia, C., and Gough, J. (2009). SUPERFAMILY--sophisticated comparative genomics, data mining, visualization and phylogeny. Nucleic Acids Res **37,** D380-386.

Wisman, E., Hartmann, U., Sagasser, M., Baumann, E., Palme, K., Hahlbrock, K., Saedler, H., and Weisshaar, B. (1998). Knock-out mutants from an En-1 mutagenized Arabidopsis thaliana population generate phenylpropanoid biosynthesis phenotypes. Proc Natl Acad Sci U S A **95,** 12432-12437.

Yadav, R.K., Girke, T., Pasala, S., Xie, M., and Reddy, G.V. (2009). Gene expression map of the Arabidopsis shoot apical meristem stem cell niche. Proc Natl Acad Sci U S A **106,** 4941-4946.

Yamada, H., Suzuki, T., Terada, K., Takei, K., Ishikawa, K., Miwa, K., Yamashino, T., and Mizuno, T. (2001). The Arabidopsis AHK4 histidine kinase is a cytokinin-binding receptor that transduces cytokinin signals across the membrane. Plant and Cell Physiology **42,** 1017-1023.

Zhao, Z., Zhang, W., Stanley, B.A., and Assmann, S.M. (2008). Functional proteomics of Arabidopsis thaliana guard cells uncovers new stomatal signaling pathways. Plant Cell **20,** 3210-3226.

Zhao, Z., Andersen, S.U., Ljung, K., Dolezal, K., Miotk, A., Schultheiss, S.J., and Lohmann, J.U. (2010). Hormonal control of the shoot stem-cell niche. Nature **465,** 1089-1092.

9. Applicant's Contribution

My scientific contributions to the field of plant molecular and developmental biology are documented particularly by the enclosed publications (publications #1 to 10), where I have contributed either as the first author, the last and/or corresponding author, respectively. The principal achievements are summarized as follows:

- Identification of the importance of the MSP signalling in general and sensory histidine kinase CKI1 in particular in the regulation of specific developmental processes during development of both gametophytic and sporophytic tissues in *Arabidopsis*
    - Identification of the role of CKI1 in the maintenance of the central vacuole integrity during megagametogenesis
    - Identification of paternally inherited *CKI1* expression as a proof of transcriptional activity of male genome early after fertilization
    - Deciphering the role of CKI1 and cytokinin-mediated MSP signalling in the regulation of procambial cells division and/or the maintenance of their identity
    - Identification of specificity in the CKI1-mediated MSP signalling and determination of the structure of the CKI1 receiver domain as a potential determinant of this specificity

- Elucidation the novel mechanism of the auxin and cytokinins interaction in the plant development at the level of modulation of auxin efflux via regulation of expression of auxin efflux carriers from the PIN family

10. List of the Enclosed Publications of the Applicant

1. Pernisová, M., Kuderová, A. and **Hejátko, J.** (2011) Cytokinin and auxin interactions in plant development: Metabolism, signalling, transport and gene expression. *Current Protein & Peptide Science*, in press. IF_{2009} = 3,854

2. Horák, J., Janda, L., Pekárová, B. and **Hejátko, J.** (2011) Molecular mechanisms of the signalling specificity via phosphorelay pathways in *Arabidopsis*. *Current Protein & Peptide Science*, in press. IF_{2009} = 3,854

3. **Hejátko, J**., Pernisová, M., Eneva, T., Palme, K. and Brzobohatý, B. (2003) The putative sensor histidine kinase CKI1 is involved in female gametophyte development in *Arabidopsis*. *Molecular Genetics and Genomics*, **269**, 443-453. IF_{2008}=2.838

4. **Hejátko, J.,** Blilou, I., Brewer, P.B., Friml, J., Scheres, B. and Benková, E. (2006) *In situ* hybridisation technique for mRNA detection in whole mount *Arabidopsis* samples. *Nature Protocols*, **1**, 1939 – 1946. IF_{2008}= 4.170

5. **Hejátko, J.,** Ryu, H., Kim, G.T., Dobešová, R., Choi, S., Choi, S.M., Souček, P., Horák, J., Pekárová, B., Palme, K., Brzobohatý, B. and Hwang, I. (2009) The Histidine kinases CYTOKININ-INDEPENDENT1 and ARABIDOPSIS HISTIDINE KINASE2 and 3 regulate vascular tissue development in *Arabidopsis* shoots. *Plant Cell*, **21**, 2008-2021. IF_{2008}= 9.296

6. Klumpler, T., Pekárová, B., Marek, J., Borkovcová, P., Janda, L. and **Hejátko, J.** (2009) Cloning, purification, crystallization and preliminary X-ray analysis of the receiver domain of the histidine kinase CKI1 from *Arabidopsis thaliana*. *Acta Crystallographica Section F*, **F65**, 478-481. IF_{2008}= 0.606

7. Pekárová, B., Klumpler, T., Třísková, O., Horák, J., Jansen, S., Dopitová, R., Papoušková, V., Nejedlá, E., Žídek, L., Sklenář, V., Marek, J., **Hejátko, J.**, Janda, L. Dynamic structure and binding specificity of the receiver domain of sensor histidine kinase CKI1 from *Arabidopsis thaliana*. Submitted.

8. Pernisová, M., Klíma, P., Horák, J., Válková, M., Malbeck, J., Souček, P., Reichman, P., Hoyerová, K., Dubová, J., Friml, J., Zažímalová, E. and **Hejátko, J.** (2009) Cytokinins modulate auxin-induced organogenesis in plants via regulation of the auxin efflux. *Proceedings of the National Academy of Sciences of the U.S.A.*, **106**, 3609-3614. IF_{2008}= 9.380

9. Kuderová, A., Urbánková, I., Válková, M., Malbeck, J., Brzobohatý, B., Némethová, D. and **Hejátko, J.** (2008) Effects of conditional IPT-dependent cytokinin overproduction

on root architecture of *Arabidopsis* seedlings. *Plant and Cell Physiology*, **49**, 570-582. IF_{2008}= 3.542

10. Benková, E. and **Hejátko, J.** (2009) Hormone interactions at the root apical meristem. *Plant Molecular Biology*, **69**, 383-396. IF_{2008}= 3.541

11. Summary

In contrast to animals, plant have evolved postembryonic *de novo* organogenesis as a developmental adaptation to the changing environmental conditions. The necessary prerequisite of this adaptation is a developmental plasticity of plant cells, i.e. their ability to respecify developmental status of differentiated cells. Plant hormones (phytohormones) are principal regulators of both embryonic and postembryonic plant development. In this work I provide an analysis of molecular factors that regulate particularly perception of the cytokinin signal and its interaction with auxin in the regulation of plant development.

Cytokinin signalling in plants is mediated via signalling pathway that employs what is known as a multistep phosphorelay (MSP) system. This signalling pathway consists of sensory histidine kinases that bind signalling molecule and transmit the signal into the nucleus via histidine phosphotrasfer proteins. In the nucleus, the final phosphate acceptors are response regulators that regulate the gene expression. One of the first signalling proteins form the family of sensor histidine kinases that was identified in plants (*Arabidopsis thaliana*) is CKI1 (Kakimoto, 1996). Originally, CKI1 was implicated to be a cytokinin receptor. We have shown that CKI1 is necessary for proper female gametogenesis (Hejatko et al., 2003). Further, we have shown that CKI1 together with cytokinins is a positive regulator of stem cell formation in the lateral meristem, the procambium. We have found that CKI1 shares its signalling partners with cytokinin signalling pathway and mediates the signalling in the aforementioned processes via MSP, however, in a cytokinin-independent way (Hejatko et al., 2009b). Further we found that receiver domain of CKI1 mediates specificity in the CKI1-mediated signalling and using X-ray diffraction we have determined the structure of this domain at the atomic level (Klumpler et al., 2009; Pekárová et al., 2011). We learned that Mg^{2+}, the necessary cofactors of signalling via MSP, modify the structure of the CKI1 active centre. These structural changes are most probably essential for the proper function

of CKI1 and together with structural rearrangements induced by the binding of phosphorylation-mimicking BeF_3^- result into changes of CKI1 signalling specificity.

Auxin regulates the whole spectrum of important developmental processes in plants. For that, formation of what is known as auxin concentration maxima is necessary. We found that auxin, but not cytokinins, is able to induce *de novo* organogenesis and that cytokinins modulate the auxin-induced organogenic response. We have also found that the auxin-induced organogenesis is associated with production of endogenous cytokinins that contribute to the modulation of the organogenic response. Using assay employing accumulation of radioactively labeled auxin in tobacco BY-2 cells and expression assays in hypocotyl explants we have found that cytokinins modulate auxin transport via regulation of transcription of auxin carriers from the PIN family at both, transcriptional and posttranscriptional levels. Finally, we have found that a certain levels of endogenous cytokinins is necessary for proper expression of genes for PIN proteins and contributes thus to the regulation of intercellular auxin distribution in the roots. Based on these results, we have suggested model, where the auxin-induced organogenesis is associated with endogenous cytokinins production that in turn regulates the organogenic response via regulation of auxin carriers' expression.

12. Abstrakt

Rostliny, na rozdíl od živočichů, vyvinuly během evoluce postembryonální organogenezi *de novo* jako vývojovou adaptaci na změny vnějšího prostředí. Nutným předpokladem této adaptace je značná vývojová plasticita rostlinných buněk, tedy jejich schopnost zásadně měnit vývojové programy již diferencovaných buněk a pletiv. Rostlinné hormony (fytohoromony) cytokininy a auxin jsou důležitými regulátory embryonálního i postembryonálního vývoje rostlin. V této práci se zabývám analýzou molekulárních faktorů, které řídí zejména vnímání cytokininového signálu a jeho interakci s auxiny v regulaci vývoje rostlin.

Cytokininové signály jsou v rostlinách přenášeny signální drahou, která využívá systém tzv. vícekrokového přenosu fosfátu (VPF). Tato signální dráha sestává z receptorových histidin kináz, které po navázání signální molekuly přenášejí signál do jádra prostřednictvím histidinových proteinů přenášejících fosfát, kde finální akceptory fosfátu, regulátory odezvy,

řídí genovou expresi. Jedním z prvních signálních proteinů, patřících do skupiny receptorových histidin kináz a který byl identifikován v rostlinách (*Arabidopsis thaliana*), byl protein CKI1 (Kakimoto, 1996). Původně předpovězenou funkcí tohoto proteinu bylo vnímání cytokininového signálu. My jsme ukázali, že CKI1 je zásadní pro úspěšný průběh megagametogeneze (Hejatko et al., 2003). Dále jsme zjistili, že CKI1 je společně právě s cytokininy pozitivním regulátorem tvorby kmenových buněk tzv. laterálního meristému, prokambia. Zjistili jsme také, že molekulárním mechanismem, kterým CKI1 přenáší signál během těchto procesů, je na cytokininech nezávislý systém VPF a že CKI1 sdílí v této signální dráze proteiny s cytokininovou signální drahou (Hejatko et al., 2009b). Dále jsme zjistili, že tzv. přijímačová doména CKI1 umožňuje specifický přenos signálu v systému VPF a pomocí rentgenové difrakce se nám podařilo určit strukturu této domény na atomární úrovni (Klumpler et al., 2009; Pekárová et al., 2011). Zjistili jsme, že hořečnaté ionty, které jsou nezbytnými kofaktory v systému VPF, způsobují strukturní změny v aktivním centru CKI1, které jsou pravděpodobně zásadní pro správnou funkci CKI1 a které společně se změnami vyvolanými ionty BeF_3^-, které napodobují fosforylaci CKI1, vedou ke změně signální specificity CKI1 (Pekárová et al., 2011).

Auxin reguluje celou řadu důležitých vývojových procesů u rostlin a pro tuto regulaci je zásadní tvorba tzv. auxinových koncentračních maxim. Zjistili jsme, že auxin, nikoliv však cytokininy, je schopen vyvolávat organogenezi *de novo* a že cytokininy modulují tuto auxiny vyvolanou organogenní odpověď. Zjistili jsme také, že auxinem indukovaná organogeneze je doprovázena tvorbou endogenních cytokininů, které přispívají k regulaci organogenní odpovědi. Pomocí systému měření akumulace radioaktivně značeného auxinu v tkáňových kulturách tabáku a pomocí expresních analýz v hypokotylových explantátech jsme zjistili, že cytokininy regulují transport auxinu prostřednictvím regulace exprese auxinových přenašečů z rodiny PIN a to jak na úrovni transkripce, tak na úrovni posttranskripční. V transegnních rostlinách se sníženými hladinami endogenních cytokininů jsme ukázali, že určitá úroveň endogenních cytokininů je nebytná pro normální míru exprese těchto přenašečů a přispívá tak k regulaci mezibuněčné distribuce auxinů (Pernisova et al., 2009). Na základě těchto výsledků jsme navrhli model, ve kterém je auxiny indukovaná organogeneze doprovázena produkcí cytokininů, které pak zpětně modifikují organogenní odpověď modulací tvorby

auxinových maxim prostřednictvím regulace exprese auxinových přenašečů (Pernisová et al., 2011).

Enclosed Publication # 1

Pernisová, M., Kuderová, A. and **Hejátko, J.** (2011) Cytokinin and auxin interactions in plant development: Metabolism, signalling, transport and gene expression. *Current Protein & Peptide Science*, in press. IF_{2009} = 3,854

Cytokinin and Auxin Interactions in Plant Development: Metabolism, Signalling, Transport and Gene Expression

Markéta Pernisová, Alena Kuderová and Jan Hejátko*

Laboratory of Molecular Plant Physiology, Division of Functional Genomics and Proteomics, Department of Experimental Biology, Faculty of Science, Masaryk University, Kotlářská 2, CZ-61137 Brno, Czech Republic

* *Corresponding Author:*

Jan Hejátko
Laboratory of Molecular Plant Physiology
Division of Functional Genomics and Proteomics, Department of Experimental Biology, Faculty of Science, Masaryk University
Kotlářská 2
CZ-61137 Brno
Czech Republic
E-mail: hejatko@sci.muni.cz
Tel: +420-549494165 Fax: +420-549492640

Abstract: Auxin and cytokinins have been identified as key regulators of plant development. Recently, these phytohormones have been shown to interact during important developmental processes, including positioning, identity acquisition and maintenance of meristem organizing centres, regulation of balance between cell division and differentiation, and postembryonic *de novo* organogenesis. Here, we discuss recent advances in our understanding of the underlying molecular mechanisms at the levels of regulating metabolism, signalling, gene expression and protein stability.

Key words: *Arabidopsis thaliana,* auxin/cytokinin interaction, *de novo* organogenesis, lateral roots, RAM, SAM

Cytokinins and auxin, the key regulators of plant development

Two major principles evolved in the formation of multicellular organisms: The "animal" type relies on the formation of all tissues and organs during embryogenesis. The "plant" type, on the other hand, is based on the strategy that only a basic body plan is established during embryonic development and most of the tissues and organs are formed during post-embryonic *de novo* organogenesis. Consequently, the latter model allows much greater regenerative ability, which is a major adaptation of sessile plants to changing environmental conditions.

The plant hormones known as auxin and cytokinins are key regulators of plant development during both embryogenesis and the postembryonic stage. Auxin has been described as the principle regulator of plant cell polarity and cell patterning during embryogenesis and postembryonic development [1-5], plant tropic responses [6, 7], phyllotaxis [8], vascular tissue formation [9], as well as postembryonic *de novo* organogenesis including lateral root formation [10-13] and *in vitro* induced *de novo* organogenesis [14, 15]. Cytokinins were originally identified as factors promoting cell division [16]. Similarly to auxin, cytokinins are involved in regulating many important developmental processes, e.g. regulation of both shoot and root meristem activity [17-22], activity of axillary meristems [23, 24], senescence [25, 26], stress response [27], vascular tissue formation [28-30], as well as regulation of post-embryonic *de novo* organogenesis including regulation of root architecture via modulation of lateral root formation [21, 22, 31-33] or *in vitro* induced *de novo* organogenesis [14, 15, 34-36].

Recently, important crosstalk between the actions of auxin and cytokinins has been revealed in several important developmental processes in plants. During embryogenesis, shoot and root apical meristems (SAM and RAM, respectively) are established. Both apical meristems contain organizing centres (OCs) that are surrounded by a supply of pluripotent stem cells. The OCs control spatial organization of cell division and differentiation, thus allowing proper growth and novel organ and tissue formation. Formation, localization and maintenance of OCs all represent crucial developmental processes in which both auxin and cytokinins were recently shown to interfere [37-39]. Maintenance of the equilibrium between cell division and cell differentiation is also under control of these two important phytohormones: while auxin induces cell division, cytokinins induce cell differentiation in the root meristem [40-42]. Another important developmental process in which cytokinins and auxin have been shown to interact with one another is regulation of postembryonic *de novo* organogenesis. Interaction of cytokinins and auxin was demonstrated in the case of *de novo* organogenesis induced *in vitro* from stem explants, a phenomenon known for decades [34]. The molecular nature of these interactions has been recently revealed [14, 15, 35, 36], and it implies common developmental regulations of both root and shoot [14, 31, 42-44].

Auxin/cytokinin crosstalk is evident at several levels (i.e. metabolism, signalling, transport, gene expression and protein stability) and it depends on their concentrations. Here we summarize recent advances in our understanding as to the molecular nature of the crosstalk between auxin and cytokinins and its consequences for the developmental processes mentioned above.

Interactions between auxin's and cytokinins' metabolism

Metabolism represents one of the possible regulatory areas in which cytokinins and auxin have been shown to interact. Metabolism of cytokinins includes their biosynthesis, degradation and modification. The current model for cytokinin biosynthesis suggests two possible pathways: one using free adenine nucleotides and another derived from tRNA degradation. The initial step of isoprenoid cytokinin biosynthesis is catalysed by

ATP/ADP-ISOPENTENYLTRANSFERASE (IPT) and involves the transfer of an isopentenyl residue from dimethylallyl diphosphate (DMAPP) onto an ATP or ADP to form N6-isopentenyl-adenine (iP) nucleotide or iP riboside [45-47]. However, a DMAPP-independent pathway might also exist [48]. In *Arabidopsis thaliana,* nine IPTs have been identified (AtIPT1 – AtIPT9), with distinct functions and spatial localizations in the plant [46, 47, 49]. Hydroxylation of the prenyl side chain of the iP nucleotide in a trans position by cytokinin hydroxylase then leads to formation of *trans*-zeatin (*tZ*) [50] that is, together with iP, the major form of active cytokinins in *Arabidopsis* [20]. A second possible biosynthetic pathway gives rise to cytokinins of a *cis*-zeatin (*cZ*) type through tRNA degradation. DMAPP serves as a substrate and tRNA-IPT catalyses the reaction via prenyl-tRNA to final active *cZ* [51]. The mechanisms and enzymes for these conversions, however, have not yet been characterized. Similarly, enzymes leading to biosynthesis of the aromatic cytokinins (6-benzyl adenine [BA] and its hydroxyl derivatives known as topolins) have not yet been identified and the origin of aromatic cytokinins in plants is still unknown. The final step in formation of the most active forms of cytokinins, the free nucleobases, is mediated via the action of the cytokinin riboside 5'-monophosphate phosphoribohydrolase, encoded by the *LONELY GUY (LOG)* gene family in rice and *Arabidopsis* [18, 20]. Irreversible cytokinin degradation is catalysed by CYTOKININ OXIDASE/DEHYDROGENASE (CKX), which cleaves the unsaturated N^6 isoprenoid side chain from Z, iP, and their ribosides [52]. CKX activity was first observed about 30 years ago in tobacco [53], and since then it has been characterized in many plant species. The *Arabidopsis* genome contains seven *CKX* genes (*AtCKX1 – AtCKX7*), which differ in the specificity of their expression and cellular localization [54], substrate specificity [55], or pH optimum [56] of AtCKX proteins. These spatial, and probably also temporal, differences in *AtCKX* gene expression and protein localization [54, 57] point to an importance as to the specificity of cytokinin degradation during plant development.

Auxin biosynthesis occurs in young leaves – that place with the highest synthetic activity – as well as in cotyledons and roots [58]. Indole-3-acetic acid (IAA) is proposed to be synthesised by several biosynthetic routes, designated according to their intermediates. There is one Trp-independent pathway and four Trp-dependent pathways: the indole-3-pyruvic acid (IPA) pathway, the indole-3-acetamide (IAM) pathway, the tryptamine (TAM) pathway, and the indole-3-acetaldoxime (IAOx) pathway [59, 60]. TAM and IPA pathways were described to function in plants, and it is still not clear whether they represent independent or overlapping routes for auxin biosynthesis. In addition to free auxin, its conjugates to sugars, amino acids and small peptides were identified [61], including indole-3-butyric acid (IBA), which can be a source of free IAA by hydrolysis or by β-oxidation in peroxisomes. These conjugates might have roles in storage, transport, compartmentalization, IAA detoxification, and protection against degradation [61]. Several IAA conjugates are physiologically active, representing thus probably not just intermediates in IAA degradation. Another possibility for inactivating IAA besides conjugation is oxidative catabolism. This process is based on chemical modification of the indole nucleus or side chain and results in loss of auxin activity. To date, this is the only known irreversible step regulating IAA levels in plants [62]. Degradation, biosynthesis, conjugation and deconjugation, together with intercellular transport, provide a multistep control over auxin levels.

It is well known that cytokinins and auxin mutually regulate their endogenous levels, but little is thus far known about the molecular mechanisms of these interactions. Exogenous auxin in tobacco cell lines can inhibit cytokinin accumulation and its levels [63], and the overproduction of IAA in transgenic tobacco plants results in reduction of the cytokinins pool size [64] (Fig. 1). More than 20 years ago, auxin was shown to affect

the stability of zeatin riboside [65]. Freshly excised tobacco pith explants grown on incubation medium supplemented with higher auxin (1-naphthaleneacetic acid (NAA)) concentration contained higher levels of degraded zeatin riboside metabolites [65]. Similarly, conversion of Z-type cytokinins to adenine derivates by NAA treatment has been observed [66]. *In vitro* experiments using partially purified CKX supported an idea that auxin can regulate cytokinin levels via stimulation of CKX activity [65]. Recently, genes for AtCKX enzymes were shown to be differentially regulated by auxin. NAA slightly down-regulates mRNA levels of *AtCKX1, 2, 4, 5* and *7*, but it up-regulates levels of *AtCKX3* and *6*, as determined by semiquantitative RT-PCR [57]. *AtCKX4* was also identified among IAA-repressed genes in *Arabidopsis* transcriptome studies [67, 68]. On the contrary, the *Arabidopsis* microarray gene expression database [69] reports *AtCKX1* and *AtCKX6* expression as being up-regulated by IAA. Interestingly, auxin transport inhibitor 1-naphthylphthalamic acid (NPA) strongly decreases transcripts of both these genes [57], thus pointing to possible regulation connected with auxin transport. Furthermore, auxin up-regulates *AtCKX6* expression [70] induced by a low ratio of red to far-red light in the vasculature of developing leaf primordia [71] (Fig. 1). Besides its effect on cytokinin degradation, auxin also influences endogenous cytokinin levels by regulation of cytokinin biosynthesis. NAA treatment of *Arabidopsis* seedlings resulted in a relatively quick repression of cytokinin biosynthesis via an isopentenyladenosine-5-monophosphate-independent pathway in a dose-dependent manner. The pool of Z-type cytokinins was strongly decreased after 24 h of NAA treatment, while the pool of iP-type cytokinins was nearly unaffected [72]. In contrast, gene expression of cytokinin biosynthetic enzymes *AtIPT5* and *AtIPT7* is up-regulated by auxin [49]. Induction of *AtIPT5* expression has been shown to occur through SHY2-mediated signalling [42] (see also below). However, not just cytokinin biosynthesis or degradation is influenced by auxin. Beta-glucosidase, releasing free cytokinins from cytokinin-O-glucosides, can also be inhibited by IAA-glucose esters [73, 74].

On the other hand, little is known about the effect of cytokinins on auxin metabolism. Exogenous cytokinin application or transgenic lines overproducing cytokinins via a bacterial *IPT* gene demonstrate increase in auxin content [75-77]. On the other hand, another study shows decreased auxin levels in bacterial *IPT*-expressing transgenic plants [64]. There is also evidence of indirect cytokinin regulation of auxin biosynthesis. Cytokinins have been shown to enhance ethylene biosynthesis [78, 79] and ethylene to stimulate auxin biosynthesis [80-83].

These results point to complex mutual interactions in the regulation of endogenous auxin and cytokinin levels. Auxin seems to regulate endogenous cytokinin levels via inhibition or stimulation of cytokinin metabolic pathways both at the levels of biosynthesis and degradation. This regulation is very probably tissue- or even cell-specific and may depend on hormone concentration or developmental stage. Spatiotemporal specificity should be considered in future studies to avoid often even contradictory results in describing the effects of auxin on the cytokinin pool (see Fig. 1). On the other hand, cytokinin effect on auxin levels is rather slow and probably occurs through changes in plant development.

Interactions through signalling pathways

The cytokinin signal is transduced by a modified two-component signalling system, originally described in bacteria. In plants and some other eukaryotes, a complex multistep phosphorelay (MSP) signalling system has evolved (for review see [84]). In the MSP, dimers of hybrid histidine kinases (hHKs) – cytokinin receptors – perceive the signal and autophosphorylate. The phosphoryl group is further transferred via histidine-containing

phosphotransfer proteins (HPts) to the nucleus, where it activates the final phosphate acceptors, the response regulators (RRs). There are two major types of response regulators in plant MSP: The type-B RRs act as transcription factors, while type-A RRs lack the DNA-binding domain and act as negative regulators of cytokinin signalling or interact with target effector proteins, e.g. light receptors (reviewed in [85] and Horák *et al.*, this issue). The genome of *Arabidopsis* encodes three cytokinin receptors (*ARABIDOPSIS HISTIDINE KINASES*; *AHK2*, *AHK3* and *AHK4*), six *HPts* (*ARABIDOPSIS HISTIDINE-CONTAINING PHOSPHOTRANSFER PROTEINS*; *AHP1-6*), and 23 *RRs* (*ARABIDOPSIS RESPONSE REGULATORS*; *ARRs*).

In contrast to cytokinin signalling that employs phosphorylation cascades, auxin signalling acts by regulating protein degradation. In the current model, four intracellular receptors TRANSPORT INHIBITOR RESPONSE 1 (TIR1) and AUXIN SIGNALLING F-BOX PROTEIN 1-3 (AFB1-3) [86-88] bind auxin and trigger the auxin response by inducing the degradation of AUXIN/INDOLE-3-ACETIC ACID (AUX/IAA) proteins, the repressors of auxin signalling. AUX/IAA proteins suppress the activity of AUXIN RESPONSE FACTORs (ARFs) by heterodimerisation under low auxin concentration. ARFs released from linkage with AUX/IAA regulate expression of auxin-responsive genes in a positive or negative manner [89-91].

The auxin-cytokinin interactions at the level of signalling pathways were discovered to be crucial for the specification and/or maintenance of both root and shoot apical meristem OCs.

In the dermatogen stage of *Arabidopsis* embryo development, a switch from the originally acropetal to basipetal auxin transport leads to auxin accumulation at the future root pole of the proembryo and in the suspensor [92]. Later on, the maximum auxin concentration is in the hypophysis, the uppermost cell of the suspensor that divides, leading to formation of basal and lens-shaped cells. The lens-shaped cell becomes an OC of the future root apical meristem, the quiescent centre (QC). Root-specific regulators such as homeodomain transcription factors encoding *WUSCHEL-RELATED HOMEOBOX (WOX)* genes, particularly *WOX5* [93] or *PLETHORA (PLT)* genes, are expressed there and interact with the *SCARECROW (SCR)* and *SHORTROOT (SHR)* pathways to control proper positioning of the QC and root meristem patterning [94].

Immediately after hypophysis division, the cytokinin signalling was found to be activated particularly in the lens-shaped cell, mirroring the auxin-response maximum in the basal cell [37]. The molecular mechanism of this mutual interaction seems to be based on the auxin-dependent regulation of cytokinin signalling. Auxin was shown to antagonize the output of cytokinin signalling in the hypophysis-derived basal cell lineage through up-regulation of two type-A ARRs, *ARR7* and *ARR15*, the cytokinin primary response genes and negative regulators of cytokinin signalling. Auxin directly activates transcription of *ARR7* and *ARR15* via a conserved TGTC sequence, thus interfering with the cytokinin-mediated feedback loop, which results in an auxin-mediated inhibition of cytokinin output specifically in the basal cell. Accordingly, RNAi-mediated down-regulation of *ARR7* in an *arr15* background led to defects in root patterning and organization of stem cell files that are associated with misexpression of *WOX5*, *SCR* and *PLT1* [37]. A similar effect was achieved via ectopic induction of cytokinin signalling in the embryonic basal cell. Therefore, it seems that control over spatiotemporal specificity of cytokinin and auxin response is critical for proper QC and root stem cell niche specification [37].

Regulations of an opposite type were identified, however, in the interaction of auxin with cytokinin signalling in the positioning of the shoot meristem OC, the expression domain of homeodomain transcription factor *WUSCHEL* (*WUS*). WUS acts cell non-autonomously via an as yet unknown signal as a positive regulator of the stem cell pool in the SAM [95]. The equilibrium between cell division and cell differentiation in the SAM

is maintained via feedback regulation between CLAVATA (CLV)-mediated signalling and WUS [96]. The CLV3 peptide is produced and processed by stem cells and binds to the heterodimer of leucine-rich repeat (LRR) receptor-like kinases CLV1 and CLV2, which lack the kinase domain. The interaction of CLV3 with CLV1/CLV2 triggers a signalling cascade that leads to inhibition of *WUS* expression (Fig. 2; reviewed in [97]). Expression of *WUS* has recently been found to be specified by the cytokinin-response domain that acts both through CLV-dependent and CLV-independent paths. Cytokinins were shown to negatively regulate expression of *CLV1*, the negative regulator of *WUS* that in turn represses several A-type RRs, the negative regulators of cytokinin signalling (Fig. 2 [98]). This self-potentiating and complex feedback regulatory loop, together with the gradient of *AHK4* expression, allows spatially delimited up-regulation of cytokinin signalling output. That contributes to the restricted expression of *WUS* and formation of SAM OC [39]. In contrast to the situation in the root, however, auxin response mediated by MONOPTEROS/AUXIN RESPONSE FACTOR 5 (MP/ARF5) negatively regulates the expression of *ARR7* and *ARR15* in the shoot [38]. Interestingly, in the shoot OC, auxin was shown to down-regulate *ARR7* and *ARR15* through the same AuxRE-like TGTC DNA motifs that were identified in the auxin-mediated up-regulation of the *ARR7* and *ARR15* in the QC specification, as mentioned above [37]. Thus, very probably, AuxRE-like motifs are recognized by different auxin responsive factors (ARFs), depending on the tissue context [38] (Fig. 2).

Establishment and maintenance of plant meristems is dependent on the balance between cell division and cell differentiation. The root meristem size seems to be controlled by equilibrium of the antagonistic effects between auxin and cytokinins. Cytokinins have been suggested to induce cell differentiation, while auxin has been considered a positive regulator of cell division [41]. Recently, the molecular mechanisms of this process have been revealed [40, 42]. AHK3/ARR1 and AHK3/ARR12 cytokinin signalling pathways were shown to transmit the cytokinin signal in the vascular tissues of the root meristem transition zone. This auxin/cytokinin interaction was found to occur through SHORT HYPOCOTYL 2 / INDOLE-3-ACETIC ACID 3 (SHY2/IAA3), an Aux/IAA auxin signalling repressor. The cytokinin signalling pathway mediated by AHK3 perception induces expression of the type-B response regulator *ARR1*. ARR1 binds directly to the *SHY2* promoter region and activates *SHY2* expression. SHY2 negatively regulates expression of auxin efflux carrier genes from the *PINFORMED* (*PIN*) family. That leads to redistribution of auxin from the transition zone and induction of cell differentiation. On the other hand, auxin induces SHY2 degradation, thus sustaining the *PIN* expression and auxin intercellular distribution. Taken together, all these mechanisms and mutual interactions contribute to the balance between cytokinin-induced cell differentiation and auxin-mediated cell division in the root transition zone, which results in the proper regulation of the meristem size [42, 99].

Another possible auxin/cytokinin interaction at the signalling level can be explained by auxin-mediated pH control. Cytokinins' association with their receptor depends on pH [100]. Auxin is known to influence pH in plant tissues through the induction of proton efflux from cells and acidification of the apoplast [101]. The acidification can significantly reduce the affinity of a receptor for cytokinins, by which it may contribute to the cytokinin-antagonistic activity of the auxin. Therefore, it seems that pH may contribute also to the cytokinin/ auxin crosstalk [100].

Regulations of gene expression, protein stability and transport

The importance of auxin-cytokinin crosstalk in postembryonic *de novo* organogenesis is a phenomenon that has long been known. Skoog and Miller showed that the auxin-to-cytokinin concentration ratio determines the identity of *de novo* formed organs *in vitro* [34]. The molecular nature of the underlying mechanisms was further revealed in experiments using *Arabidopsis* hypocotyl explants. Auxin was shown to induce *de novo* organogenesis while cytokinins were observed to modulate the morphogenetic response. Thus, the developmental output of auxin-induced *de novo* organogenesis seems to be dependent on spatial- and tissue-specific action of the cytokinin signalling pathway and changes in endogenous cytokinin levels. The cytokinin effect in this *in vitro* system is mediated via AHK2-4 and reflects the sum of both endogenous and exogenous cytokinins [14].

Further analysis identified cytokinin-mediated control of auxin transport as an important part of the cytokinin modulation of auxin-induced organogenic response. The molecular mechanism of this cytokinin-mediated modulation was identified to be concentration-dependent differential regulation of *PIN* genes expression [14]. This mode of auxin-cytokinins interaction seems to be generally valid in plant development. In roots with endogenous cytokinins depleted by overexpression of the *AtCKX* genes, changes in the local auxin maxima were associated with significant decrease in *PIN2* and *PIN4* mRNA levels, suggesting that endogenous cytokinin levels are important for proper expression of *PIN* genes and subsequent auxin maxima formation [14]. The aforementioned experimental evidence leads us to the formulation of a hypothetical model suggesting auxin accumulation as a trigger for organogenesis. According to our model, production of endogenous cytokinins is an intrinsic part of the auxin-induced organogenic response. The endogenous cytokinins in turn regulate auxin accumulation through regulation of auxin transport by cytokinin-mediated control of *PIN*s expression (Fig. 3).

The interaction of cytokinins and auxin at the level of *PIN* genes' expression was simultaneously published by two different research teams. Apart from the identification described above of cytokinin-regulated *PIN*s expression via modification of auxin signalling [42], quantitative RT-PCR showed fluctuating *PIN* genes' expression during the first 6 h after BA treatment [43].

However, cytokinins also seem to interfere with regulation of PIN-mediated auxin transport at the post-transcriptional level. While *PIN1* mRNA was nearly unaffected, PIN1-GFP internalized and gradually diminished with increasing kinetin concentration during *in vitro* organogenesis [14]. Similarly, decrease in the PIN1-RFP signal was detected also in BY-2 tobacco suspension cells treated by increasing BA concentration [43]. In root tips, long-term (24 or 48 h) BA application resulted in down-regulation of PIN1, PIN2 and PIN3 and up-regulation of PIN7 protein [43]. This suggests that cytokinins can differentially regulate the expression of *PIN* genes and/or of PIN proteins stability and/or localization.

Postembryonic lateral root (LR) formation represents a further example of the hormone-dependent developmental plasticity of plant cells. In *Arabidopsis thaliana,* the process of LR initiation has been reported to naturally occur in an acropetal pattern within a spatially defined "developmental window", a region close to the primary root meristem [102, 103]. The first LR can initiate its formation as early as 30 h after germination [10] by division of pericycle cell files adjacent to protoxylem poles [104]. Xylem-pole pericycle cell files are the only cell files of the differentiation zone that retain the capacity to progress through the cell cycle and are competent for LR formation. They are looked upon as "extended meristem" [105, 106]. Once initiated, LR primordia (LRP) progress through specific stages of development until they emerge from the primary root [107] or their growth may be arrested while having the potential to recontinue later [102].

In the light of recent studies, LR formation may be divided into several stages, including i) pre-initiation or what is called priming of the xylem-pole pericycle founder cells, ii) the first anticlinal division of the founder cells (LR initiation), iii) morphogenesis of LRP within the primary root, and iv) LRP emergence. These distinct phases are all regulated by auxin (reviewed in [108]). While auxin has been proven to be a key positive regulator of LR formation (reviewed in [109]), cytokinins have been reported to negatively affect this process (reviewed in [110-112]). The important question is whether these two hormonal pathways control particular phases of lateral root development independently of one another or if they interact. The aforementioned classification of LR development correlates well with data on auxin transport. In previous studies, LR initiation had been observed to be positively correlated with basipetal auxin transport (from the root tip to the root base [104]), while LR emergence had been shown to be dependent on functional primary root acropetal auxin transport via the phloem (originating in the shoot [104, 113]). Between these two stages, during LRP patterning, LRPs of 3–5 cell layers have been shown to temporarily acquire an independent auxin-autonomous status [114].

Recently, positive roles of root- and shoot-derived auxin in LR initiation and emergence, respectively, have been described in more detail. Basipetal auxin transport in the established root meristem [1, 115], controlled by auxin efflux carriers encoded by the *PIN* gene family (see above) and auxin influx carrier AUX1, has been proposed as controlling retainment of auxin's recycling flow in the root tip and LR initiation [1, 10]. A model has been hypothesized of AUX1-mediated auxin transport targeted from the apex to the base of the meristem along lateral root cap cells, which, together with PIN-mediated local auxin accumulation (the inverted fountain model), triggers pericycle cells adjacent to protoxylem cells for LR initiation. According to this model, the actual LR initiation occurs later, in the differentiation zone, when the previously primed xylem-pole pericycle cells receive an additional pulse of auxin, before the mitotic marker *cycB1:1::uidA* becomes expressed and the cell division occurs [10, 104, 106]. Under experimental conditions, every pericycle xylem-pole cell has the capacity to divide because of locally elevated auxin levels [11, 13]. Prior to pericycle cell division, auxin induces many cell-cycle-related genes [11, 116]. This supports the idea of a local cell-specific regulation of the cell cycle before LR initiation. In contrast to auxin's positive role, cytokinins have been proposed as inhibiting LR initiation through blocking pericycle founder cells at the G2 to M transition phase [33].

Benkova *et al.* (2003) [12] demonstrated the importance of polar auxin transport and establishment of the PIN-mediated, auxin-graded distribution during LRP development. Individual *pin* mutants exhibited changed frequencies of initiated LRPs and abnormal development of LRPs without established DR5 gradient [12, 117]. Exogenous cytokinin application, or endogenously elevated cytokinin levels due to tissue-specific or ectopic overexpression of the *IPT* gene [31] [32], resulted in increased frequencies of LRP with disturbed auxin-graded distribution and abnormal morphology. Do cytokinins negatively modulate polar auxin transport? At what stages of LR formation does this happen? Is it during priming of the LR founder cells, LR initiation or LRP morphogenesis? Based on the data of Laplaze *et al.* [31] the disturbed auxin maxima and abnormal patterning of LRP seem to result from cytokinin action prior to LR initiation, i.e. before the first anticlinal pericycle cell divisions. Xylem-pole pericycle cell-specific (J0121) and LRP-specific (J0192) GAL4-GFP enhancer trap lines were used to define the stage at which cytokinins act. LRP density of the J0121>>IPT plants was reduced by 42%, whereas that of the J0192>>IPT was not significantly changed. These results prove the direct effect of cytokinins on LR founder cells but not on proliferating cells in forming LRP from stage I to IV. Auxin did not rescue the J0121>>IPT LR phenotype. That is consistent with previous results of Li *et al.* [33] indicating that

auxin cannot rescue the cytokinin-mediated inhibition of LR initiation. Treatment with auxin (2,4-D) induced LRP formation along the entire length of the control root [31] whereas J0121>>IPT plants showed a strong phenotype of a continuous layer of cells in front of the xylem poles but no discrete primordia. Laplaze *et al.* [31] thus suggest that cytokinin accumulation in pericycle cells does not prevent the auxin-mediated activation of cell division but blocks the developmental program of LR initiation.. Cytokinins did not, however, perturb auxin perception in xylem-pole pericycle cells, thus excluding direct interaction with the molecular factors mediating auxin perception. Laplaze *et al.* [31] further demonstrated that, unlike primary root elongation, LR development is blocked by cytokinins independently of ethylene.

LRP of developmental stage III to V can form LRs even after their excision from the root, suggesting that they have developed autonomous promeristem. These excised LRPs feature the established DR5 gradient and they grow on media without auxin [12, 114]. Exogenously applied cytokinins [31] and their endogenously raised levels [32] result in the arrest of LRP at developmental phases IV to V, and this effect is dose-dependent. LRP of heterozygous *IPT*-expressing plants or plants growing on media with intermediate cytokinin concentration do not emerge, and the initiated LR founder cells progress through additional disorganized cell divisions leading to abnormal morphology and disturbed DR5 gradient. This suggests that enhanced cytokinin levels may shift the homeostatic balance of presumed auxin-induced cell division to cytokinin-stimulated premature cell differentiation. What cannot be excluded in this *in vivo* experimental system, however, is that the observed patterning defects of LRP may also be a result of the cytokinin-induced PINs misregulation [31] and disturbance of the DR5 gradient [31, 32] at stages of their development that include and follow LR initiation. Application of cytokinins to sections of the meristem/auxin-autonomous LRP grown *in vitro* within the experimental system of Laskowski *et al.* [114] might provide the answer.

Li *et al.* [118] have presented results of indirect cytokinin-auxin interaction during LR initiation but occurring through another hormonal pathway. They examined *brevis radix* (*brx-2)* mutants, defective in a protein that had been characterized as a regulator of cell proliferation and elongation in the root. BRX belongs to a five-member gene family and regulates expression of CONSTITUTIVE PHOTOMORPHOGENESIS AND DWARF (CPD), a rate-limiting enzyme in brassinosteroid biosynthesis [119] that is highly underexpressed in *brx-2* mutants. *brx-2* were insensitive to exogenous cytokinin-induced inhibition of LR initiation. The expression of cytokinin signalling genes (*AHKs*, *AHPs* and *ARRs*), *CKX*, *IPT* and *LOG* was not changed in *brx-2*, suggesting that cytokinin signalling and the biosynthesis pathway were not impaired in the mutant. The authors have also demonstrated that the cytokinin-insensitive LR phenotype is not directly dependent on brassinosteroid level. On the contrary, *brx-2* mutants exhibited altered auxin response (*IAA2::GUS*) and auxin-graded distribution (*DR5::GUS*) in LR founder cells and LRP. While cytokinin-treated wild-type roots exhibited down-regulated auxin response in presumptive LR founder cells compared with untreated wild-type roots, cytokinin-treated *brx-2* LR founder cells were positively stained as founder cells in untreated *brx-2* roots. These results support the general notion that cytokinin-mediated inhibition of LR initiation is due to loss or decrease of local auxin accumulation or sensitivity in LR founder cells.

Further results demonstrating that cytokinin signalling is repressed in xylem-pole pericycle cells [120], that increased cytokinins repress LR initiation [31-33], and that *CKX* genes are expressed in LRPs [54] indicate the importance of mechanisms suppressing cytokinin functioning during LRP initiation. Additional support for that view may be seen in the fact that double mutants in cytokinin sensor histidine kinase genes (*AHK* genes)

exhibit significantly increased number of the first- and second-order LRs [121]. On the other hand, the *IPT5* gene has been shown to be expressed both in pericycle cells and in developing LRPs [49]. That would mean that the expression of crucial genes involved in cytokinin and auxin metabolism, signalling or transport act in concert to keep balance between cytokinin and auxin levels, thereby ensuring proper cell patterning during LR development. This resembles, at least in part, what has been described in the main root, where a certain level of endogenous cytokinins was shown to be important for proper PINs expression and intercellular auxin distribution [14].

Conclusions and future prospects

Sequencing of *Arabidopsis* and other plant genomes together with establishment of several other molecular tools, in particular marker lines, allowing analysis of hormonal outputs at tissue, cellular or even subcellular levels, has led to a dramatic explosion in our knowledge about the molecular mechanisms of hormonal regulation during plant development. Consequently, this "molecular revolution" opens new horizons and raises many novel and exciting questions. Also, in spite of the fact that the dominant role of auxin maxima as a general trigger of organogenesis is being accepted [13, 14, 122], it is not yet clear what really are the determinants of the developmental fate of induced organs. Auxin maxima were shown to correlate with postembryonic *de novo* organogenesis in both root and shoot [8, 12]. Remaining to be answered, however, is the question of what the downstream molecular events are that differentiate organ identity. The possible role of cytokinins and their interaction with auxin in the process of determining developmental fate has been known for decades [34]. One of the possible clues allowing to identify underlying molecular determinants comes from the recent findings demonstrating the molecular mechanisms of cytokinin and auxin interactions. The differential regulation of repressors of cytokinin signalling ARR7 and ARR15 via identical DNA motif points towards one of the possible, simple and elegant molecular mechanisms via tissue-specific recognition of that motif by different ARFs. What are the putative molecular targets of these ARFs, however, remains to be identified.

Recently, we have found that differences between shoot and root occur at the level of proteome regulation (Žďárská *et al.*, manuscript in preparation) (Fig. 3). These differences might explain some of the aforementioned contradictory results regarding the analysis of auxin and cytokinin crosstalk, e.g. at the metabolism level. Thus, the tissue specificity and, as recently demonstrated in the case of QC determination, even the specificity of cytokinin signalling at the cellular level must be considered. In this context, however, the spatial specificity of the newly identified integration of cytokinins and auxin in the MP-dependent regulation of cytokinin signalling and *WUS* expression [38] is not clear and remains to be clarified.

Finally, one of the consequences of experimental efforts in the past decade has been to make evident the intense crosstalk and cross-regulation among different plant growth regulators. Thus, even in the narrow spectrum of cytokinin and auxin interactions, involvement of other regulators (e.g. brassinosteroids [118]) seems to be important and must be considered.

Acknowledgement

This work was supported by the Ministry of Education, Youth and Sports of the Czech Republic (grants MSM0021622415 and LC06034).

Figure legends

Figure 1. Putative model of mutual regulations of auxin and cytokinin pool. Exogenous auxin application [63, 65, 66] or IAA overproduction [64] leads to reduction of CK pool size. NAA, however, differentially regulates levels of iP and Z-type of cytokinins, suggesting certain level of specificity [72]. IBA was shown to up-regulate gene expression of cytokinin biosynthetic enzymes (IPTs) [49]. Gene expression of some cytokinin degradation enzymes (CKXs) is differentially regulated by IAA [67-70] and NAA [57]. *Vice versa*, the exogenous cytokinin application or cytokinin overproduction increases auxin content [75-77]. In contrast to that, decreased auxin levels were found in plants with increased cytokinins levels [64], suggesting spatiotemporal specificity of observed effects. For details see the text. AtCKX, *Arabidopsis thaliana* cytokinin oxidase/dehydrogenase; AtIPT, *Arabidopsis thaliana* ATP/ADP-isopentenyltransferase; CK, cytokinin; IAA, indole-3-acetic acid; IBA, indole-3-butyric acid; iP, N6-isopentenyl-adenine; NAA, 1-naphthaleneacetic acid; NPA, 1-naphthylphthalamic acid; Z, zeatin.

Figure 2. Cross-talk between cytokinins and auxin in determination of shoot and root apical meristem (SAM and RAM, respectively) organising centres (OC); SC, stem cells. Complex auxin/cytokinin interactions regulate OC positioning and maintenance in RAM and SAM, respectively. In SAM, cytokinins up-regulate *WUS* expression that in turn down-regulates expression of type-A *ARRs* (*ARR5, ARR7* and *ARR15*) the negative regulators of cytokinin signalling. This self-potentiating feedback regulatory loop is further enhanced by the auxin-mediated down-regulation of *ARR7* and *ARR15*. In contrast to that, in RAM auxin specifically down-regulates cytokinin signalling in lens-shaped cell via up-regulation of *ARR7* and *ARR15*, regulating thus expression of *WOX5* and proper positioning and organization of RAM OC.

Figure 3. Auxin/cytokinin interactions during postembryonic *de novo* organogenesis in plants. Based on ours' and other's data we propose a model in which auxin triggers organogenesis that is accompanied by endogenous cytokinins production. In turn, endogenous cytokinins control intercellular auxin distribution through ethylene-dependent or ethylene-independent regulation of auxin transport and biosynthesis.

References

[1] Blilou, I.; Xu, J.; Wildwater, M.; Willemsen, V.; Paponov, I.; Friml, J.; Heidstra, R.; Aida, M.; Palme, K.; Scheres, B. The PIN auxin efflux facilitator network controls growth and patterning in Arabidopsis roots. *Nature,* **2005,** *433*, 39-44.

[2] Friml, J.; Benkova, E.; Blilou, I.; Wisniewska, J.; Hamann, T.; Ljung, K.; Woody, S.; Sandberg, G.; Scheres, B.; Jurgens, G.; Palme, K. AtPIN4 mediates sink-driven auxin gradients and root patterning in Arabidopsis. *Cell,* **2002,** *108*, 661-73.

[3] Sabatini, S.; Beis, D.; Wolkenfelt, H.; Murfett, J.; Guilfoyle, T.; Malamy, J.; Benfey, P.; Leyser, O.; Bechtold, N.; Weisbeek, P.; Scheres, B. An auxin-dependent distal organizer of pattern and polarity in the Arabidopsis root. *Cell,* **1999,** *99*, 463-72.

[4] Pagnussat, G. C.; Alandete-Saez, M.; Bowman, J. L.; Sundaresan, V. Auxin-dependent patterning and gamete specification in the Arabidopsis female gametophyte. *Science,* **2009,** *324*, 1684-9.

[5] Sachs, T., *Pattern formation in plant tissues*. Cambridge University Press: 1991; p 246.

[6] Friml, J.; Wisniewska, J.; Benkova, E.; Mendgen, K.; Palme, K. Lateral relocation of auxin efflux regulator PIN3 mediates tropism in Arabidopsis. *Nature,* **2002,** *415*, 806-809.

[7] Lucas, M.; Godin, C.; Jay-Allemand, C.; Laplaze, L. Auxin fluxes in the root apex co-regulate gravitropism and lateral root initiation. *J Exp Bot,* **2008,** *59*, 55-66.

[8] Reinhardt, D.; Pesce, E. R.; Stieger, P.; Mandel, T.; Baltensperger, K.; Bennett, M.; Traas, J.; Friml, J.; Kuhlemeier, C. Regulation of phyllotaxis by polar auxin transport. *Nature,* **2003,** *426*, 255-60.

[9] Sachs, T. Integrating cellular and organismic aspects of vascular differentiation. *Plant Cell Physiol,* **2000,** *41*, 649-56.
[10] De Smet, I.; Tetsumura, T.; De Rybel, B.; Frey, N. F. D.; Laplaze, L.; Casimiro, I.; Swarup, R.; Naudts, M.; Vanneste, S.; Audenaert, D.; Inze, D.; Bennett, M. J.; Beeckman, T. Auxin-dependent regulation of lateral root positioning in the basal meristem of Arabidopsis. *Development,* **2007,** *134*, 681-690.
[11] Himanen, K.; Boucheron, E.; Vanneste, S.; de Almeida Engler, J.; Inze, D.; Beeckman, T. Auxin-mediated cell cycle activation during early lateral root initiation. *Plant Cell,* **2002,** *14*, 2339-51.
[12] Benkova, E.; Michniewicz, M.; Sauer, M.; Teichmann, T.; Seifertova, D.; Jurgens, G.; Friml, J. Local, efflux-dependent auxin gradients as a common module for plant organ formation. *Cell,* **2003,** *115*, 591-602.
[13] Dubrovsky, J. G.; Sauer, M.; Napsucialy-Mendivil, S.; Ivanchenko, M. G.; Friml, J.; Shishkova, S.; Celenza, J.; Benkova, E. Auxin acts as a local morphogenetic trigger to specify lateral root founder cells. *Proc Natl Acad Sci U S A,* **2008,** *105*, 8790-4.
[14] Pernisova, M.; Klima, P.; Horak, J.; Valkova, M.; Malbeck, J.; Soucek, P.; Reichman, P.; Hoyerova, K.; Dubova, J.; Friml, J.; Zazimalova, E.; Hejatko, J. Cytokinins modulate auxin-induced organogenesis in plants via regulation of the auxin efflux. *Proceedings of the National Academy of Sciences of the United States of America,* **2009,** *106*, 3609-3614.
[15] Che, P.; Lall, S.; Howell, S. H. Developmental steps in acquiring competence for shoot development in Arabidopsis tissue culture. *Planta,* **2007,** *226*, 1183-94.
[16] Miller, C. O.; Skoog, F.; Vonsaltza, M. H.; Strong, F. M. Kinetin, a Cell Division Factor from Deoxyribonucleic Acid. *Journal of the American Chemical Society,* **1955,** *77*, 1392-1392.
[17] Higuchi, M.; Pischke, M. S.; Mahonen, A. P.; Miyawaki, K.; Hashimoto, Y.; Seki, M.; Kobayashi, M.; Shinozaki, K.; Kato, T.; Tabata, S.; Helariutta, Y.; Sussman, M. R.; Kakimoto, T. In planta functions of the Arabidopsis cytokinin receptor family. *Proc Natl Acad Sci U S A,* **2004,** *101*, 8821-6.
[18] Kurakawa, T.; Ueda, N.; Maekawa, M.; Kobayashi, K.; Kojima, M.; Nagato, Y.; Sakakibara, H.; Kyozuka, J. Direct control of shoot meristem activity by a cytokinin-activating enzyme. *Nature,* **2007,** *445*, 652-5.
[19] Nishimura, C.; Ohashi, Y.; Sato, S.; Kato, T.; Tabata, S.; Ueguchi, C. Histidine kinase homologs that act as cytokinin receptors possess overlapping functions in the regulation of shoot and root growth in Arabidopsis. *Plant Cell,* **2004,** *16*, 1365-77.
[20] Kuroha, T.; Tokunaga, H.; Kojima, M.; Ueda, N.; Ishida, T.; Nagawa, S.; Fukuda, H.; Sugimoto, K.; Sakakibara, H. Functional analyses of LONELY GUY cytokinin-activating enzymes reveal the importance of the direct activation pathway in Arabidopsis. *Plant Cell,* **2009,** *21*, 3152-69.
[21] Medford, J. I.; Horgan, R.; El-Sawi, Z.; Klee, H. J. Alterations of Endogenous Cytokinins in Transgenic Plants Using a Chimeric Isopentenyl Transferase Gene. *Plant Cell,* **1989,** *1*, 403-413.
[22] Smigocki, A. C. Cytokinin content and tissue distribution in plants transformed by a reconstructed isopentenyl transferase gene. *Plant Mol Biol,* **1991,** *16*, 105-15.
[23] Sachs, T.; Thimann, V. Role of Auxins and Cytokinins in Release of Buds from Dominance. *American Journal of Botany,* **1967,** *54*, 136-&.
[24] Tanaka, H.; Dhonukshe, P.; Brewer, P. B.; Friml, J. Spatiotemporal asymmetric auxin distribution: a means to coordinate plant development. *Cell Mol Life Sci,* **2006,** *63*, 2738-54.
[25] Kim, H. J.; Ryu, H.; Hong, S. H.; Woo, H. R.; Lim, P. O.; Lee, I. C.; Sheen, J.; Nam, H. G.; Hwang, I. Cytokinin-mediated control of leaf longevity by AHK3 through phosphorylation of ARR2 in Arabidopsis. *Proc Natl Acad Sci U S A,* **2006,** *103*, 814-9.
[26] Hewelt, A.; Prinsen, E.; Schell, J.; Van Onckelen, H.; Schmulling, T. Promoter tagging with a promoterless ipt gene leads to cytokinin-induced phenotypic variability in transgenic tobacco plants:implications of gene dosage effects. *Plant J,* **1994,** *6*, 879-91.
[27] Tran, L. S.; Urao, T.; Qin, F.; Maruyama, K.; Kakimoto, T.; Shinozaki, K.; Yamaguchi-Shinozaki, K. Functional analysis of AHK1/ATHK1 and cytokinin receptor histidine kinases in response to abscisic acid, drought, and salt stress in Arabidopsis. *Proc Natl Acad Sci U S A,* **2007,** *104*, 20623-8.
[28] Hejatko, J.; Ryu, H.; Kim, G. T.; Dobesova, R.; Choi, S.; Choi, S. M.; Soucek, P.; Horak, J.; Pekarova, B.; Palme, K.; Brzobohaty, B.; Hwang, I. The Histidine Kinases CYTOKININ-INDEPENDENT1 and ARABIDOPSIS HISTIDINE KINASE2 and 3 Regulate Vascular Tissue Development in Arabidopsis Shoots. *Plant Cell,* **2009,** *21*, 2008-2021.
[29] Matsumoto-Kitano, M.; Kusumoto, T.; Tarkowski, P.; Kinoshita-Tsujimura, K.; Vaclavikova, K.; Miyawaki, K.; Kakimoto, T. Cytokinins are central regulators of cambial activity. *Proc Natl Acad Sci U S A,* **2008,** *105*, 20027-31.
[30] Nieminen, K.; Immanen, J.; Laxell, M.; Kauppinen, L.; Tarkowski, P.; Dolezal, K.; Tahtiharju, S.; Elo, A.; Decourteix, M.; Ljung, K.; Bhalerao, R.; Keinonen, K.; Albert, V. A.; Helariutta, Y. Cytokinin signaling regulates cambial development in poplar. *Proc Natl Acad Sci U S A,* **2008,** *105*, 20032-7.

[31] Laplaze, L.; Benkova, E.; Casimiro, I.; Maes, L.; Vanneste, S.; Swarup, R.; Weijers, D.; Calvo, V.; Parizot, B.; Herrera-Rodriguez, M. B.; Offringa, R.; Graham, N.; Doumas, P.; Friml, J.; Bogusz, D.; Beeckman, T.; Bennett, M. Cytokinins act directly on lateral root founder cells to inhibit root initiation. *Plant Cell,* **2007,** *19*, 3889-900.
[32] Kuderova, A.; Urbankova, I.; Valkova, M.; Malbeck, J.; Nemethova, D.; Hejatko, J. Effects of conditional IPT-dependent cytokinin overproduction on root architecture of Arabidopsis seedlings. *Plant Cell Physiol,* **2008,** *49*, 570-82.
[33] Li, X.; Mo, X.; Shou, H.; Wu, P. Cytokinin-mediated cell cycling arrest of pericycle founder cells in lateral root initiation of Arabidopsis. *Plant Cell Physiol,* **2006,** *47*, 1112-23.
[34] Skoog, F.; Miller, C. O. Chemical regulation of growth and organ formation in plant tissues cultured in vitro. *Symp Soc Exp Biol,* **1957,** *54*, 118-30.
[35] Gordon, S. P.; Heisler, M. G.; Reddy, G. V.; Ohno, C.; Das, P.; Meyerowitz, E. M. Pattern formation during de novo assembly of the Arabidopsis shoot meristem. *Development,* **2007,** *134*, 3539-48.
[36] Cary, A. J.; Che, P.; Howell, S. H. Developmental events and shoot apical meristem gene expression patterns during shoot development in Arabidopsis thaliana. *Plant J,* **2002,** *32*, 867-77.
[37] Muller, B.; Sheen, J. Cytokinin and auxin interaction in root stem-cell specification during early embryogenesis. *Nature,* **2008,** *453*, 1094-7.
[38] Zhao, Z.; Andersen, S. U.; Ljung, K.; Dolezal, K.; Miotk, A.; Schultheiss, S. J.; Lohmann, J. U. Hormonal control of the shoot stem-cell niche. *Nature,* **2010,** *465*, 1089-92.
[39] Gordon, S. P.; Chickarmane, V. S.; Ohno, C.; Meyerowitz, E. M. Multiple feedback loops through cytokinin signaling control stem cell number within the Arabidopsis shoot meristem. *Proc Natl Acad Sci U S A,* **2009,** *106*, 16529-34.
[40] Dello Ioio, R.; Linhares, F. S.; Scacchi, E.; Casamitjana-Martinez, E.; Heidstra, R.; Costantino, P.; Sabatini, S. Cytokinins determine Arabidopsis root-meristem size by controlling cell differentiation. *Curr Biol,* **2007,** *17*, 678-82.
[41] Beemster, G. T.; Baskin, T. I. Stunted plant 1 mediates effects of cytokinin, but not of auxin, on cell division and expansion in the root of Arabidopsis. *Plant Physiol,* **2000,** *124*, 1718-27.
[42] Dello Ioio, R.; Nakamura, K.; Moubayidin, L.; Perilli, S.; Taniguchi, M.; Morita, M. T.; Aoyama, T.; Costantino, P.; Sabatini, S. A genetic framework for the control of cell division and differentiation in the root meristem. *Science,* **2008,** *322*, 1380-4.
[43] Ruzicka, K.; Simaskova, M.; Duclercq, J.; Petrasek, J.; Zazimalova, E.; Simon, S.; Friml, J.; Van Montagu, M. C.; Benkova, E. Cytokinin regulates root meristem activity via modulation of the polar auxin transport. *Proc Natl Acad Sci U S A,* **2009,** *106*, 4284-9.
[44] Sugimoto, K.; Jiao, Y.; Meyerowitz, E. M. Arabidopsis regeneration from multiple tissues occurs via a root development pathway. *Dev Cell,* **2010,** *18*, 463-71.
[45] Sakakibara, H.; Kasahara, H.; Ueda, N.; Kojima, M.; Takei, K.; Hishiyama, S.; Asami, T.; Okada, K.; Kamiya, Y.; Yamaya, T.; Yamaguchi, S. Agrobacterium tumefaciens increases cytokinin production in plastids by modifying the biosynthetic pathway in the host plant. *Proceedings of the National Academy of Sciences of the United States of America,* **2005,** *102*, 9972-9977.
[46] Kakimoto, T. Identification of plant cytokinin biosynthetic enzymes as dimethylallyl diphosphate:ATP/ADP isopentenyltransferases. *Plant Cell Physiol,* **2001,** *42*, 677-85.
[47] Takei, K.; Sakakibara, H.; Sugiyama, T. Identification of genes encoding adenylate isopentenyltransferase, a cytokinin biosynthesis enzyme, in Arabidopsis thaliana. *J Biol Chem,* **2001,** *276*, 26405-10.
[48] Astot, C.; Dolezal, K.; Nordstrom, A.; Wang, Q.; Kunkel, T.; Moritz, T.; Chua, N. H.; Sandberg, G. An alternative cytokinin biosynthesis pathway. *Proceedings of the National Academy of Sciences of the United States of America,* **2000,** *97*, 14778-14783.
[49] Miyawaki, K.; Matsumoto-Kitano, M.; Kakimoto, T. Expression of cytokinin biosynthetic isopentenyltransferase genes in Arabidopsis: tissue specificity and regulation by auxin, cytokinin, and nitrate. *Plant J,* **2004,** *37*, 128-38.
[50] Takei, K.; Yamaya, T.; Sakakibara, H. Arabidopsis CYP735A1 and CYP735A2 encode cytokinin hydroxylases that catalyze the biosynthesis of trans-Zeatin. *Journal of Biological Chemistry,* **2004,** *279*, 41866-41872.
[51] Miyawaki, K.; Tarkowski, P.; Matsumoto-Kitano, M.; Kato, T.; Sato, S.; Tarkowska, D.; Tabata, S.; Sandberg, G.; Kakimoto, T. Roles of Arabidopsis ATP/ADP isopentenyltransferases and tRNA isopentenyltransferases in cytokinin biosynthesis. *Proc Natl Acad Sci U S A,* **2006,** *103*, 16598-603.
[52] Jones, R. J.; Schreiber, B. M. N. Role and function of cytokinin oxidase in plants. *Plant Growth Regulation,* **1997,** *23*, 123-134.
[53] Paces, V.; Werstiuk, E.; Hall, R. H. Conversion of N-(Delta-Isopentenyl)adenosine to Adenosine by Enzyme Activity in Tobacco Tissue. *Plant Physiol,* **1971,** *48*, 775-778.

[54] Werner, T.; Motyka, V.; Laucou, V.; Smets, R.; Van Onckelen, H.; Schmulling, T. Cytokinin-deficient transgenic Arabidopsis plants show multiple developmental alterations indicating opposite functions of cytokinins in the regulation of shoot and root meristem activity. *Plant Cell,* **2003,** *15*, 2532-50.
[55] Galuszka, P.; Popelkova, H.; Werner, T.; Frebortova, J.; Pospisilova, H.; Mik, V.; Kollmer, I.; Schmulling, T.; Frebort, I. Biochemical characterization of cytokinin Oxidases/Dehydrogenases from Arabidopsis thaliana expressed in Nicotiana tabacum L. *Journal of Plant Growth Regulation,* **2007,** *26*, 255-267.
[56] Frebortova, J.; Galuszka, P.; Werner, T.; Schmulling, T.; Frebort, I. Functional expression and purification of cytokinin dehydrogenase from Arabidopsis thaliana (AtCKX2) in Saccharomyces cerevisiae. *Biologia Plantarum,* **2007,** *51*, 673-682.
[57] Werner, T.; Kollmer, I.; Bartrina, I.; Holst, K.; Schmulling, T. New insights into the biology of cytokinin degradation. *Plant Biology,* **2006,** *8*, 371-381.
[58] Ljung, K.; Bhalerao, R. P.; Sandberg, G. Sites and homeostatic control of auxin biosynthesis in Arabidopsis during vegetative growth. *Plant J,* **2001,** *28*, 465-74.
[59] Woodward, A. W.; Bartel, B. Auxin: Regulation, action, and interaction. *Annals of Botany,* **2005,** *95*, 707-735.
[60] Normanly, J. Approaching cellular and molecular resolution of auxin biosynthesis and metabolism. *Cold Spring Harb Perspect Biol,* **2010,** *2*, a001594.
[61] Cohen, J. D.; Bandurski, R. S. Chemistry and Physiology of the Bound Auxins. *Annual Review of Plant Physiology and Plant Molecular Biology,* **1982,** *33*, 403-430.
[62] Bandurski, R. S.; Desrosiers, M. F.; Jensen, P.; Pawlak, M.; Schulze, A. Genetics, Chemistry, and Biochemical Physiology in the Study of Hormonal Homeostasis. *Progress in Plant Growth Regulation,* **1992,** *13*, 1-12.
[63] Hansen, C. E.; Meins, F.; Milani, A. Clonal and Physiological Variation in the Cytokinin Content of Tobacco-Cell Lines Differing in Cytokinin Requirement and Capacity for Neoplastic Growth. *Differentiation,* **1985,** *29*, 1-6.
[64] Eklof, S.; Astot, C.; Blackwell, J.; Moritz, T.; Olsson, O.; Sandberg, G. Auxin-cytokinin interactions in wild-type and transgenic tobacco. *Plant and Cell Physiology,* **1997,** *38*, 225-235.
[65] Palni, L. M. S.; Burch, L.; Horgan, R. The Effect of Auxin Concentration on Cytokinin Stability and Metabolism. *Planta,* **1988,** *174*, 231-234.
[66] Zhang, R.; Zhang, X.; Wang, J.; Letham, D. S.; Mckinney, S. A.; Higgins, T. J. V. The Effect of Auxin on Cytokinin Levels and Metabolism in Transgenic Tobacco Tissue Expressing an Ipt Gene. *Planta,* **1995,** *196*, 84-94.
[67] Rashotte, A. M.; Chae, H. S.; Maxwell, B. B.; Kieber, J. J. The interaction of cytokinin with other signals. *Physiologia Plantarum,* **2005,** *123*, 184-194.
[68] Goda, H.; Sawa, S.; Asami, T.; Fujioka, S.; Shimada, Y.; Yoshida, S. Comprehensive comparison of auxin-regulated and brassinosteroid-regulated genes in Arabidopsis. *Plant Physiol,* **2004,** *134*, 1555-73.
[69] Zimmermann, P.; Hirsch-Hoffmann, M.; Hennig, L.; Gruissem, W. GENEVESTIGATOR. Arabidopsis microarray database and analysis toolbox. *Plant Physiol,* **2004,** *136*, 2621-32.
[70] Redman, J. C.; Haas, B. J.; Tanimoto, G.; Town, C. D. Development and evaluation of an Arabidopsis whole genome Affymetrix probe array. *Plant J,* **2004,** *38*, 545-61.
[71] Carabelli, M.; Possenti, M.; Sessa, G.; Ciolfi, A.; Sassi, M.; Morelli, G.; Ruberti, I. Canopy shade causes a rapid and transient arrest in leaf development through auxin-induced cytokinin oxidase activity. *Genes Dev,* **2007,** *21*, 1863-8.
[72] Nordstrom, A.; Tarkowski, P.; Tarkowska, D.; Norbaek, R.; Astot, C.; Dolezal, K.; Sandberg, G. Auxin regulation of cytokinin biosynthesis in Arabidopsis thaliana: a factor of potential importance for auxin-cytokinin-regulated development. *Proc Natl Acad Sci U S A,* **2004,** *101*, 8039-44.
[73] Brzobohaty, B.; Moore, I.; Kristoffersen, P.; Bako, L.; Campos, N.; Schell, J.; Palme, K. Release of Active Cytokinin by a Beta-Glucosidase Localized to the Maize Root-Meristem. *Science,* **1993,** *262*, 1051-1054.
[74] Brzobohaty, B.; Moore, I.; Palme, K. Cytokinin metabolism: implications for regulation of plant growth and development. *Plant Mol Biol,* **1994,** *26*, 1483-97.
[75] Binns, A. N.; Labriola, J.; Black, R. C. Initiation of Auxin Autonomy in Nicotiana-Glutinosa Cells by the Cytokinin-Biosynthesis Gene from Agrobacterium-Tumefaciens. *Planta,* **1987,** *171*, 539-548.
[76] Bourquin, M.; Pilet, P. E. Effect of Zeatin on the Growth and Indolyl-3-Acetic Acid and Abscisic-Acid Levels in Maize Roots. *Physiologia Plantarum,* **1990,** *80*, 342-349.
[77] Bertell, G.; Eliasson, L. Cytokinin Effects on Root-Growth and Possible Interactions with Ethylene and Indole-3-Acetic-Acid. *Physiologia Plantarum,* **1992,** *84*, 255-261.
[78] Chae, H. S.; Faure, F.; Kieber, J. J. The eto1, eto2, and eto3 mutations and cytokinin treatment increase ethylene biosynthesis in Arabidopsis by increasing the stability of ACS protein. *Plant Cell,* **2003,** *15*, 545-59.
[79] Hansen, M.; Chae, H. S.; Kieber, J. J. Regulation of ACS protein stability by cytokinin and brassinosteroid. *Plant J,* **2009,** *57*, 606-14.

[80] Swarup, R.; Perry, P.; Hagenbeek, D.; Van Der Straeten, D.; Beemster, G. T.; Sandberg, G.; Bhalerao, R.; Ljung, K.; Bennett, M. J. Ethylene upregulates auxin biosynthesis in Arabidopsis seedlings to enhance inhibition of root cell elongation. *Plant Cell,* **2007,** *19*, 2186-96.
[81] Ruzicka, K.; Ljung, K.; Vanneste, S.; Podhorska, R.; Beeckman, T.; Friml, J.; Benkova, E. Ethylene regulates root growth through effects on auxin biosynthesis and transport-dependent auxin distribution. *Plant Cell,* **2007,** *19*, 2197-212.
[82] Stepanova, A. N.; Yun, J.; Likhacheva, A. V.; Alonso, J. M. Multilevel interactions between ethylene and auxin in Arabidopsis roots. *Plant Cell,* **2007,** *19*, 2169-85.
[83] Stepanova, A. N.; Robertson-Hoyt, J.; Yun, J.; Benavente, L. M.; Xie, D. Y.; Dolezal, K.; Schlereth, A.; Jurgens, G.; Alonso, J. M. TAA1-mediated auxin biosynthesis is essential for hormone crosstalk and plant development. *Cell,* **2008,** *133*, 177-91.
[84] Stock, A. M.; Robinson, V. L.; Goudreau, P. N. Two-component signal transduction. *Annual Review of Biochemistry,* **2000,** *69*, 183-215.
[85] To, J. P.; Kieber, J. J. Cytokinin signaling: two-components and more. *Trends Plant Sci,* **2008,** *13*, 85-92.
[86] Dharmasiri, N.; Dharmasiri, S.; Estelle, M. The F-box protein TIR1 is an auxin receptor. *Nature,* **2005,** *435*, 441-5.
[87] Dharmasiri, N.; Dharmasiri, S.; Weijers, D.; Lechner, E.; Yamada, M.; Hobbie, L.; Ehrismann, J. S.; Jurgens, G.; Estelle, M. Plant development is regulated by a family of auxin receptor F box proteins. *Dev Cell,* **2005,** *9*, 109-19.
[88] Kepinski, S.; Leyser, O. The Arabidopsis F-box protein TIR1 is an auxin receptor. *Nature,* **2005,** *435*, 446-451.
[89] Remington, D. L.; Vision, T. J.; Guilfoyle, T. J.; Reed, J. W. Contrasting modes of diversification in the Aux/IAA and ARF gene families. *Plant Physiol,* **2004,** *135*, 1738-52.
[90] Okushima, Y.; Overvoorde, P. J.; Arima, K.; Alonso, J. M.; Chan, A.; Chang, C.; Ecker, J. R.; Hughes, B.; Lui, A.; Nguyen, D.; Onodera, C.; Quach, H.; Smith, A.; Yu, G.; Theologis, A. Functional genomic analysis of the AUXIN RESPONSE FACTOR gene family members in Arabidopsis thaliana: unique and overlapping functions of ARF7 and ARF19. *Plant Cell,* **2005,** *17*, 444-63.
[91] Overvoorde, P. J.; Okushima, Y.; Alonso, J. M.; Chan, A.; Chang, C.; Ecker, J. R.; Hughes, B.; Liu, A.; Onodera, C.; Quach, H.; Smith, A.; Yu, G.; Theologis, A. Functional genomic analysis of the AUXIN/INDOLE-3-ACETIC ACID gene family members in Arabidopsis thaliana. *Plant Cell,* **2005,** *17*, 3282-300.
[92] Friml, J.; Vieten, A.; Sauer, M.; Weijers, D.; Schwarz, H.; Hamann, T.; Offringa, R.; Jurgens, G. Efflux-dependent auxin gradients establish the apical-basal axis of Arabidopsis. *Nature,* **2003,** *426*, 147-53.
[93] Haecker, A.; Gross-Hardt, R.; Geiges, B.; Sarkar, A.; Breuninger, H.; Herrmann, M.; Laux, T. Expression dynamics of WOX genes mark cell fate decisions during early embryonic patterning in Arabidopsis thaliana. *Development,* **2004,** *131*, 657-68.
[94] Aida, M.; Beis, D.; Heidstra, R.; Willemsen, V.; Blilou, I.; Galinha, C.; Nussaume, L.; Noh, Y. S.; Amasino, R.; Scheres, B. The PLETHORA genes mediate patterning of the Arabidopsis root stem cell niche. *Cell,* **2004,** *119*, 109-20.
[95] Mayer, K. F.; Schoof, H.; Haecker, A.; Lenhard, M.; Jurgens, G.; Laux, T. Role of WUSCHEL in regulating stem cell fate in the Arabidopsis shoot meristem. *Cell,* **1998,** *95*, 805-15.
[96] Fletcher, J. C.; Brand, U.; Running, M. P.; Simon, R.; Meyerowitz, E. M. Signaling of cell fate decisions by CLAVATA3 in Arabidopsis shoot meristems. *Science,* **1999,** *283*, 1911-4.
[97] Carles, C. C.; Fletcher, J. C. Shoot apical meristem maintenance: the art of a dynamic balance. *Trends Plant Sci,* **2003,** *8*, 394-401.
[98] Leibfried, A.; To, J. P.; Busch, W.; Stehling, S.; Kehle, A.; Demar, M.; Kieber, J. J.; Lohmann, J. U. WUSCHEL controls meristem function by direct regulation of cytokinin-inducible response regulators. *Nature,* **2005,** *438*, 1172-5.
[99] Moubayidin, L.; Di Mambro, R.; Sabatini, S. Cytokinin-auxin crosstalk. *Trends Plant Sci,* **2009,** *14*, 557-62.
[100] Romanov, G. A.; Lomin, S. N.; Schmulling, T. Biochemical characteristics and ligand-binding properties of Arabidopsis cytokinin receptor AHK3 compared to CRE1/AHK4 as revealed by a direct binding assay. *J Exp Bot,* **2006,** *57*, 4051-8.
[101] Cleland, R. E., Auxin and cell elongation. In *Plant hormones: biosynthesis, signal transduction, action!*, 3rd ed.; Davies, P. J., Ed. Kluwer Academic Publishers: Dordrecht/Boston/London, 2004; pp 204-220.
[102] Dubrovsky, J. G.; Gambetta, G. A.; Hernandez-Barrera, A.; Shishkova, S.; Gonzalez, I. Lateral root initiation in Arabidopsis: developmental window, spatial patterning, density and predictability. *Ann Bot,* **2006,** *97*, 903-15.
[103] Greenwood, M. S.; Xu, F. Y.; Hutchison, K. W. The role of auxin-induced peaks of alpha-expansin expression during lateral root primordium formation in Pinus taeda. *Physiologia Plantarum,* **2006,** *126*, 279-288.

[104] Casimiro, I.; Marchant, A.; Bhalerao, R. P.; Beeckman, T.; Dhooge, S.; Swarup, R.; Graham, N.; Inze, D.; Sandberg, G.; Casero, P. J.; Bennett, M. Auxin transport promotes Arabidopsis lateral root initiation. *Plant Cell,* **2001,** *13*, 843-852.
[105] Beeckman, T.; Burssens, S.; Inze, D. The peri-cell-cycle in Arabidopsis. *J Exp Bot,* **2001,** *52*, 403-11.
[106] Casimiro, I.; Beeckman, T.; Graham, N.; Bhalerao, R.; Zhang, H.; Casero, P.; Sandberg, G.; Bennett, M. J. Dissecting Arabidopsis lateral root development. *Trends Plant Sci,* **2003,** *8*, 165-71.
[107] Malamy, J. E.; Benfey, P. N. Organization and cell differentiation in lateral roots of Arabidopsis thaliana. *Development,* **1997,** *124*, 33-44.
[108] Peret, B.; De Rybel, B.; Casimiro, I.; Benkova, E.; Swarup, R.; Laplaze, L.; Beeckman, T.; Bennett, M. J. Arabidopsis lateral root development: an emerging story. *Trends Plant Sci,* **2009,** *14*, 399-408.
[109] Overvoorde, P.; Fukaki, H.; Beeckman, T. Auxin control of root development. *Cold Spring Harb Perspect Biol,* **2010,** *2*, a001537.
[110] Bishopp, A.; Help, H.; Helariutta, Y. Cytokinin signaling during root development. *Int Rev Cell Mol Biol,* **2009,** *276*, 1-48.
[111] Fukaki, H.; Tasaka, M. Hormone interactions during lateral root formation. *Plant Mol Biol,* **2009,** *69*, 437-49.
[112] Perilli, S.; Moubayidin, L.; Sabatini, S. The molecular basis of cytokinin function. *Curr Opin Plant Biol,* **2010,** *13*, 21-6.
[113] Reed, R. C.; Brady, S. R.; Muday, G. K. Inhibition of auxin movement from the shoot into the root inhibits lateral root development in Arabidopsis. *Plant Physiol,* **1998,** *118*, 1369-78.
[114] Laskowski, M. J.; Williams, M. E.; Nusbaum, H. C.; Sussex, I. M. Formation of lateral root meristems is a two-stage process. *Development,* **1995,** *121*, 3303-10.
[115] Petrasek, J.; Mravec, J.; Bouchard, R.; Blakeslee, J. J.; Abas, M.; Seifertova, D.; Wisniewska, J.; Tadele, Z.; Kubes, M.; Covanova, M.; Dhonukshe, P.; Skupa, P.; Benkova, E.; Perry, L.; Krecek, P.; Lee, O. R.; Fink, G. R.; Geisler, M.; Murphy, A. S.; Luschnig, C.; Zazimalova, E.; Friml, J. PIN proteins perform a rate-limiting function in cellular auxin efflux. *Science,* **2006,** *312*, 914-8.
[116] Himanen, K.; Vuylsteke, M.; Vanneste, S.; Vercruysse, S.; Boucheron, E.; Alard, P.; Chriqui, D.; Van Montagu, M.; Inze, D.; Beeckman, T. Transcript profiling of early lateral root initiation. *Proc Natl Acad Sci U S A,* **2004,** *101*, 5146-51.
[117] Ulmasov, T.; Murfett, J.; Hagen, G.; Guilfoyle, T. J. Aux/IAA proteins repress expression of reporter genes containing natural and highly active synthetic auxin response elements. *Plant Cell,* **1997,** *9*, 1963-71.
[118] Li, J.; Mo, X.; Wang, J.; Chen, N.; Fan, H.; Dai, C.; Wu, P. BREVIS RADIX is involved in cytokinin-mediated inhibition of lateral root initiation in Arabidopsis. *Planta,* **2009,** *229*, 593-603.
[119] Mouchel, C. F.; Osmont, K. S.; Hardtke, C. S. BRX mediates feedback between brassinosteroid levels and auxin signalling in root growth. *Nature,* **2006,** *443*, 458-61.
[120] Mahonen, A. P.; Bishopp, A.; Higuchi, M.; Nieminen, K. M.; Kinoshita, K.; Tormakangas, K.; Ikeda, Y.; Oka, A.; Kakimoto, T.; Helariutta, Y. Cytokinin signaling and its inhibitor AHP6 regulate cell fate during vascular development. *Science,* **2006,** *311*, 94-8.
[121] Riefler, M.; Novak, O.; Strnad, M.; Schmulling, T. Arabidopsis cytokinin receptor mutants reveal functions in shoot growth, leaf senescence, seed size, germination, root development, and cytokinin metabolism. *Plant Cell,* **2006,** *18*, 40-54.
[122] Benkova, E.; Ivanchenko, M. G.; Friml, J.; Shishkova, S.; Dubrovsky, J. G. A morphogenetic trigger: is there an emerging concept in plant developmental biology? *Trends in Plant Science,* **2009,** *14*, 189-193.

Pernisova et al., Figure 1.

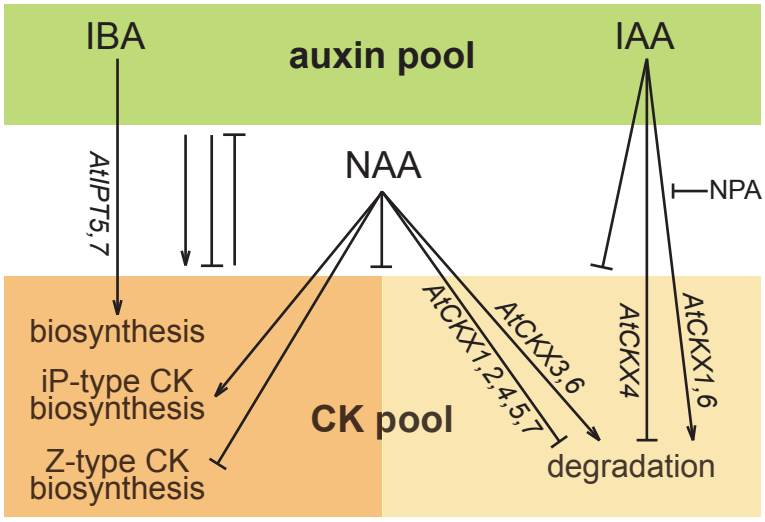

Pernisova et al., Figure 2.

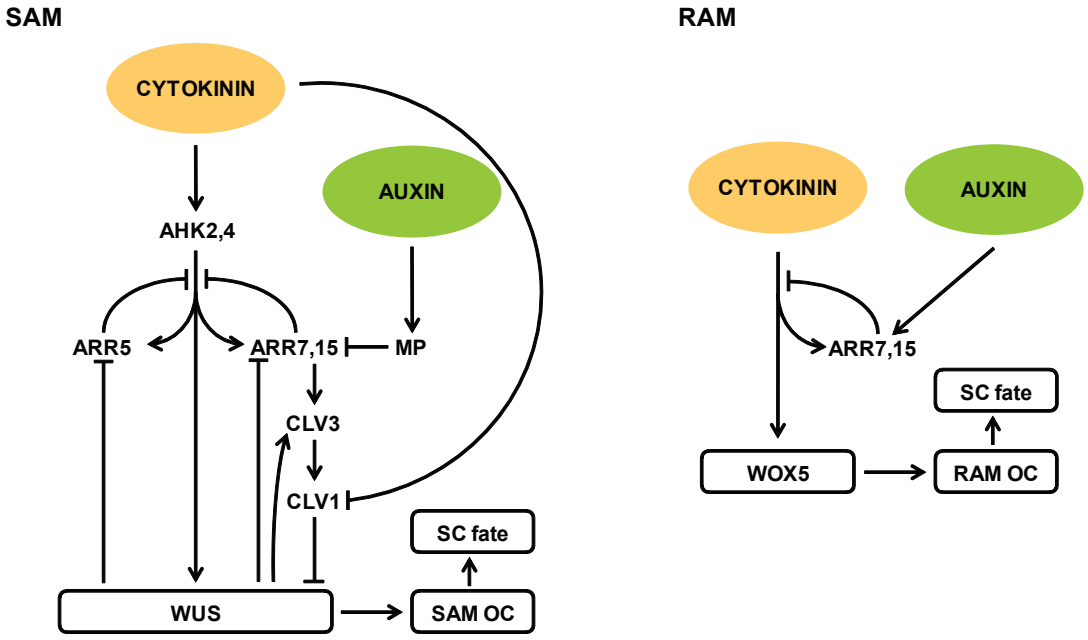

Pernisova et al., Figure 3.

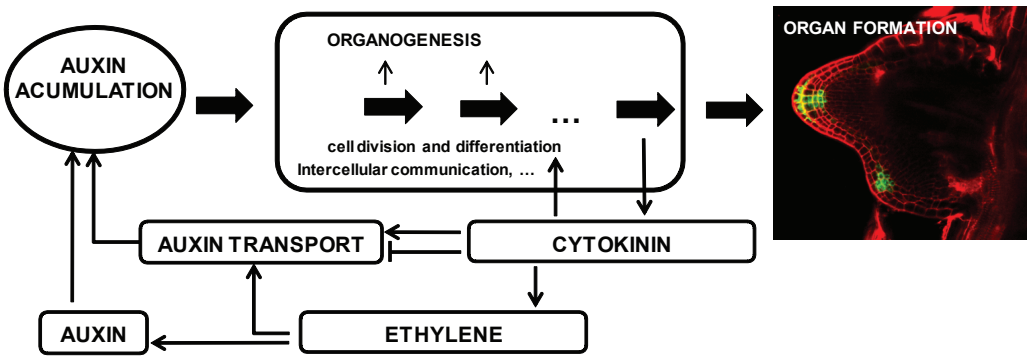

Enclosed Publication # 2

Horák, J., Janda, L., Pekárová, B. and **Hejátko, J.** (2011) Molecular mechanisms of the signalling specificity via phosphorelay pathways in *Arabidopsis*. *Current Protein & Peptide Science*, in press. IF_{2009} = 3,854

Molecular Mechanisms of the Signalling Specificity via Phosphorelay Pathways in *Arabidopsis*

Jakub Horák, Lubomír Janda, Blanka Pekárová and Jan Hejátko*

Laboratory of Molecular Plant Physiology, Division of Functional Genomics and Proteomics, Department of Experimental Biology, Faculty of Science, Masaryk University, Kotlářská 2, CZ-61137 Brno, Czech Republic

*Corresponding Author:

Jan Hejátko
Laboratory of Molecular Plant Physiology
Division of Functional Genomics and Proteomics, Department of Experimental Biology, Faculty of Science, Masaryk University
Kotlářská 2
CZ-61137 Brno
Czech Republic
e-mail: hejatko@sci.muni.cz
Phone: +420-549494165 FAX: +420-549492640

Abstract

Multistep phosphorelay (MSP) pathways mediate wide spectrum of adaptive responses in plants including hormonal and abiotic stress regulations. Recent genetic evidences suggest both, partial redundancy and possible functional crosstalk on one side and certain level of specificity on the other one. Here we discuss recent achievements in our understandings to possible molecular determinants of specificity in MSP. We consider certain evolutionary conservation of ancestral two-component signalling systems from bacteria in a process of molecular recognition that, as we have recently shown, could be applied to a certain level in case of plant MSP, too. Besides of that, we discuss possible role of kinase and phosphatase activities, kinetics of both of these enzymatic reactions and phosphorylation lifetime. We include also recent results on the expression specificity of individual members of MSP pathways and finally, as based on our recent findings, we speculate about possible role of magnesium in the regulation of MSP pathways in plants. All these mechanisms could significantly influence specificity and signalling output of the MSP pathways.

Key words

Arabidopsis thaliana, cytokinin, phosphorelay, plant hormone, signal integration, signal specificity, signalling pathway, two-component system,

The role of MSP signalling in plants: Straightforward highways or detours and crossroads?

Recognition of diverse signals via specific pathways belongs to one of the crucial developmental adaptations that evolved in all organisms. Two-component signalling (TCS) pathways mediate recognition of the wide spectrum of signals in bacteria and regulate adaptive responses ranging from basic metabolic regulations like nitrogen, oxygen and carbon usage or phosphate assimilation, through behavioural adaptations including e.g. chemotaxis, till the complex changes of developmental programmes of sporulation or virulence; for review see [1, 2]. Prototypical TCS system in bacteria consist of a pair of interacting molecules composed of a sensor histidine kinase (HK) that is recognized by its cognate partner, the response regulator (RR). Upon interaction of the respective signalling molecule with extracellular portion of the dimerized histidine kinase, the intracellular kinase domain is activated, which leads to the transphosphorylation of the conserved histidine residue by the selfinteracting kinase in the homodimer. The phosphorylated histidine subsequently serves as a target of the phosphotransfer activity mediated by the N-terminal regulatory or receiver domain of the response regulator that leads to the phosphorylation of its own conserved aspartate and activation of the output domain. In bacteria, the response regulators are mostly transcription factors and activation of their output domain leads to the regulation of target gene expression. However, bacterial response regulators are also involved in other processes, e.g. regulation of target effectors via protein-protein interactions, interactions with RNA or enzymatic regulations [1].

The TCS signalling systems were adopted by some of the mono- and multicellular eukaryotes like yeast (*Saccharomyces cerevisiae*, *Schizosaccharomyces pombe*, *Candida albicans*), fungi (*Neurospora crassa*), social amoeba (*Dictyostelium discoideum*), and plant organisms including algae and higher plants (Saito, 2001). In eukaryotic and in some of the bacterial signalling systems, however, specific modifications of the system evolved, leading to what is called multistep phosphorelay (MSP) (Fig. 1). In comparison to the prototypical bacterial TCS described above, the signal transduction in MSP contains two more signalling modules. First, the modified hybrid histidine kinase (hHK) contains additional, response regulator-like receiver domain and the first phosphotransfer reaction is thus intramolecular. Second, additional histidine-containing phosphotransfer protein (HPt) serves as a shuttle between (mostly) membrane-localized sensor histidine kinase and nucleus, where it allows phosphorylation of the terminal phosphate acceptor, the response regulator. Thus, in comparison to simple His-to-Asp phosphotransfer taking place in bacterial TCS systems, the above mentioned modifications lead to sequential His-to-Asp-to-His-to-Asp phosphorelay being employed by some bacteria and eukaryotes [3].

To better understand fundamental characteristic and advantages of MSP, which were decisive for adaptation of the ancient prokaryotic signalling modules by plant eukaryotic cell, it is important to consider the functional and structural changes occurring during evolution of phosphorelay signalling. Two-component system composed of the histidine kinase and response regulator proteins is a dominant signalling framework in prokaryotic cells. Most bacteria usually contain tens of TCS proteins with extreme number in *Myxococcus xanthus* TCS genes 278 (134 RR, 99 HK, 41 hHK, and 4 HPt) [5]. Beyond that, some bacteria and archebacteria are TCS-less; for review see [4, 5]. Bacterial cells usually possess 10-30 individual TCS signalling pathways, which respond to a variety of different stimuli. Most of the TCS system is simply composed of a specific couple of the sensor histidine kinase and its cognate response regulator, which are encoded by genes organized in a single operon. Therefore, TCS proteins passed mutual co-evolution. As a consequence of this co-evolution, high specificity between histidine kinase and cognate response regulator results into large reciprocal kinetic

preferences [6]. The signalling specificity of individual pathways in bacterial TCS is further enhanced by substrate competition and phosphatase activity of histidine kinases; for review see [7].

In prokaryotes, MSP representing the more complex versions of the TCSs are rarely present. Existence of this signalling framework relates to the regulation of developmental processes integrating multiple signals. The MSP-based global regulatory network controls differentiation of bacterial cells including capsule synthesis by *Escherichia coli* [8], asymmetric cell division by *Caulobacter crescentus* [9], sporulation by *Bacillus. subtilis* [10] or development of a nitrogen-fixing cell (heterocyst) by *Anabena sp*. [11]. The sophisticated lifestyle correlates with occurrence of hybrid histidine kinases and response regulators with complicated domain architecture where signals are integrated via one or few phosphate transmitters (HPt proteins) [5, 12]. Though substantial efforts to clarify the integration ability of MSP pathways, it still remains to be elucidated how the other signals from various cellular regulatory pathways are merged together with a single valued gene expression response.

Eukaryotic cells acquired MSP most probably from cyanobacterial ancestors, where MSP signalling is required for heterocyst maturation [13]. The major adaptive advantage provided by adoption of the MSP to plant eukaryotic system could be adaptation to an endomembranous cell compartmentalization and formation of the multicellular body [5]. The MSP in plants include wide spectrum of responses, including regulation of both intrinsic developmental programmes and physiological adaptations to changing environmental conditions (see later in the text). During evolutionary cooption of the MSP systems, the individual modules of bacterial MSP pathways were modified. For example, the cyanobacterial phytochrome is a light regulated histidine kinase that mediates red and far red reversible phosphorylation of Rcp1 response regulator [14]. Some of these histidine kinases altered their substrate specificity from histidine to serine kinase and later evolved into plant red/far red light receptors called phytochromes [15]. Additionally, apart from the plant MSP ancestors, the precursors of plant CHASE domain [16] or ethylene binding domain [17] are also found in the genome of cyanobacteria. These domains with different function in cyanobacteria were later linked with the hHKs and MSP signalling module to enable recognition of the new hormonal signals in higher plants [17, 18]. It was reported recently that TCS components encoded by both chloroplast and nuclear genes have been preserved in chloroplasts [19].

In spite of that the MSP network seems to be currently essential regulatory mechanism with important integrative property, the sequence of evolutionary events in plant MSP adoption is difficult to follow precisely. However, the increasing complexity and terrestrial life adaptation seem to correlate with the number of MSP genes. When focused on presumed cytokinin receptors containing the cytokinin binding CHASE domain and downstream signalling MSP elements, the genome of green algae *Chlamydomonas reinhardtii* contains 5 MSP genes (CHASE – 0; HPt – 1; RR – 4), the simple land plant *Physcomitrella patens* includes 19 MSP-related genes (CHASE – 3; HPt – 2; RR – 14) and 30 MSP genes (CHASE – 3, HPt – 5; RR – 22) were identified *A. thaliana* [20]. Next to the cytokinin receptors, other histidine kinases were, however, identified in the *Arabidopsis* genome suggesting that the downstream MSP signalling network could be under the control of many other environmental and hormonal stimuli as well and function in a highly integrative manner in higher plants. Therefore, the lessons taken from the evolutionary analysis of MSP signalling suggest that MSP proteins were multiplicated and modified during land expansion and differentiation of plant body. Such a process required more complex hormonal regulation and processing of a new set of abiotic stress factors [20]. Evolutionary renascence of vanishing signalling system in plant cells was started.

In *Arabidopsis thaliana*, the MSP systems were shown to mediate diverse developmental regulations. Hybrid histidine kinases AHK2, AHK3 and AHK4 are cytokinin receptors and trigger the cytokinin-regulated MSP-mediated responses during root and shoot development [21-25], vascular tissue formation [26-28], senescence [29], abiotic stress response [30] and postembryonic *de novo* organogenesis [23, 24, 31-33]. In addition to cytokinin, receptors of another phytohormone ethylene reveal similarity with the histidine kinases and the ethylene receptor ETR1 was proven to affect developmental responses in *Arabidopsis* via MSP, too [34-36]. In addition to hormonal regulation, the MSP in *Arabidopsis* mediates osmoregulation (AHK1) [30, 37, 38], stomatal signalling (AHK5) [39], root growth (AHK5) [40] and megagametogenesis (CKI1) [41-43].

Several independent evidences suggest signal integration being a dominant charateristic of MSP in *Arabidopsis*. Analysis of protein-protein interactions using combination of yeast two-hybrid and pull-down assay revealed that all HPt proteins in *Arabidopsis*, AHP1 to AHP5, interact with cytokinin receptors AHK2, AHK3 and AHK4 suggesting that AHP proteins might function as a signalling hub [44]. Similarly, each AHP protein is able to interact with several response regulators [37, 44-46], which implicates that MSP signalling pathways are highly redundant. Genetic analysis of MSP elements further substantiates these findings. Mutation in two out of the three cytokinin receptors is necessary to observe phenotypes linked with decreased cytokinin sensitivity [23-25]. Likewise, reduced sensitivity to cytokinin was observed only in higher-order *ahp* and type-B *arr* mutants [47, 48]. Creation of double and higher-order type-A *arr* mutants results in a progressively increased sensitivity to cytokinin as anticipated for their negative regulatory role in the cytokinin signalling [49]. Additionally, recent data indicate that integration and redundancy of MSP does not need to be limited only to cytokinin pathway. Histidine kinase CKI1 signals through the same downstream signalling elements as the cytokinin receptors. Five functional AHPs have to be knocked-out completely to achieve female gametophyte sterility as described for *cki1* mutants. Moreover, it is possible to bypass the female gametophyte sterility of *cki1* via ectopic expression of type-B response regulator ARR1, one of the key transcriptional regulators of cytokinin induced genes [41].

In contrast to findings which prefer integration and redundancy as a dominant concept for MSP network, considerable amount of evidences speaks also for a specific mode of signal transduction via MSP signalling pathway. Cytokinin receptors AHK2, AHK3 and AHK4 differ in the ligand binding specificity for various cytokinin and their glucosides [50, 51], and it is unlikely that a specificity evolved on a receptor level would not be evolutionary reflected also in downstream signalling events. In fact, when we trace the developmental processes into details, phenotypes coupled with the single gene mutations start to appear. Such specific phenotype examples could be traced back for all MSP gene families revealing the specific role of single MSP proteins. AHK3, for instance, plays a crucial role in the transition zone of the root meristem [21]. In the root meristem development, the specific role of type-B response regulator ARR1 and ARR12 was dissected. While ARR12 is important for balanced proliferation and differentiation in root meristem development during first five days after germination, ARR1 is necessary to maintain the proper meristem size in mature *Arabidopsis* root (Dello Ioio et al., 2007). Additionally, *Arabidopsis* HPt protein AHP4 regulates cell wall thickening and lignification in the endothecium of anthers during flower development [52]. AHK2 and AHK3 are necessary for a proper procambial activity in vascular bundles of inflorescence stem [26], while AHK4 specifically regulates cell differentiation in vascular tissue of the root [53, 54]. Finally, the type-A response regulators ARR7 and ARR15 are involved in developmental regulatory networks in the shoot and root apical meristems [55-57]. AHK2 and AHK4 were identified upstream of these response regulators in the shoot meristem [22, 58]; reviewed

in Pernisová *et al.*, this issue. Moreover, additional protein-protein interaction data using bimolecular fluorescence complementation and yeast two-hybrid assay probably with the different sensitivity threshold shows that CKI1 hybrid histidine kinase and type-C response regulator ARR22 prefer some interaction partners within the AHP family [59, 60]; unpublished data. Our data implicate that specific interaction preferences of the AHP proteins are common also to other hybrid histidine kinases and response regulators.

We are convinced that the redundancy, signal integration as well as signal specificity are the fundamental characteristic of plant MSP signalling network. It remains to be elucidated how much these properties are equilibrated in order to achieve appropriate and fine-tuned response to diverse environmental stimuli mediated via MSP signalling in plants. In our review we introduce several molecular mechanisms, which might significantly enhance signalling specificity of the MSP while keeping their integration capacity.

Molecular recognition establishes a fundamental framework for specificity of the phosphorelay pathways

Principal mechanism that is predominantly responsible for the rigid specificity of bacterial TCS systems is a molecular recognition of histidine kinase and its cognate response regulator. The molecular recognition is a prerequisite for the effective support of TCS specificity by other molecular mechanisms like phosphatase activity of bifunctional histidine kinases (see below) or substrate competition; for review see [7]. The molecular determinants of the protein surface recognition as well as those directly affecting the other protein kinetic parameters have been recently revealed in bacteria and appear as linked with the 3D structure of interacting proteins [8, 61, 62]. In MSP systems, a structure of Spo0B:Spo0F complex from *Bacillus subtilis* [62, 63] and YPD1:SLN1 from *Saccharomyces cerevisiae* [64, 65] were fundamental for understanding the interaction between the HPt protein and its cognate receiver domain.

In spite of several functional differences, the structure of the monomeric HPt protein resembles the dimerization histidine-containing phosphotransfer domain (DHpD) of the histidine kinases (Fig. 1); for review see [66]. Conserved histidine residue of the DHpD locates to the middle of a structure composed of two antiparallel α-helices, which form the four-helix bundle with the second identical subunit of its dimerization partner [67]. All HPt proteins follow this conserved up-and-down architecture of 4-helical core, which is stabilized by 2-3 additional α-helices in order to exist as a part of soluble monomeric protein (Fig. 2) [68, 69].

Receiver domains of both the hybrid histidine kinases and response regulators are structurally formed by five-stranded parallel β-sheet surrounded by five α-helices $(\alpha/\beta)_5$. Catalytical site of the receiver domain is characterized by an acidic pocket formed in the area of the loops L1, L3 and L5 surrounding the central β-sheet (Fig. 2). Phosphorelay activity of the receiver domain requires coordination of the Mg^{2+} metal ion into the catalytic site to enable phosphorylation of the conserved aspartate residue; for review see [66]. Plant receiver domains obviously follow the same $(\alpha/\beta)_5$ structural organization [70]. Thus, the interplay between the four-helix bundle of DHpD and HPt proteins on one side and $(\alpha/\beta)_5$ fold of hybrid histidine kinase or response regulator receiver domain on the other one represent the key-to-lock interaction, allowing proper signal transduction and signalling specificity (Fig. 1).

Resolving of the 3D structure of HPt protein in a complex with the receiver domain provided a platform for identification of molecular surfaces responsible for protein recognition in MSP systems. Protein structures of Spo0B:Spo0F [62] and YPD1:SLN1 [64] complexes revealed that in case of the HPt protein molecular contacts with the receiver domain take place mostly in the region around the conserved histidine residue at the α4 and at

the base of N-terminal part of α3 (Fig. 2). Receiver domain interacts with the HPt protein via amino acid residues along the α1 and loops L1 to L5 surrounding the active aspartate residue [62-65]. Therefore, it is reasonable to expect that amino acid residues responsible for the specific interaction between HPt proteins and receiver domains should appear in these regions. Recent experimental data support this hypothesis. Guided by the Spo0B:Spo0F-complex structure and a unique method for covariation analysis of co-evolution patterns, the amino acids responsible for specific recognition were identified. Change of four of these amino acid residues at the specific positions of *Escherichia coli* histidine kinase EnvZ resulted in a completely shifted specificity of this sensor towards a non-cognate response regulator [6]. Covariation analysis of cognate bacterial kinase-regulator pairs in bacteria revealed that α1 in the receiver domains is the most important for ensuring interaction specificity, although remaining regions could also significantly affect the interaction affinity [6]. Similarly to that, the residues in the α1 and loops surrounding the active aspartate were shown to be involved in the interprotein contacts in case of RcsD:RcsC in *Escherichia.coli* [8, 61] (see also bellow) and in YPD1:SLN1 in yeast [64]. Our results suggests that L3, possibly with the other loops, might be involved in a fine tuning of the interaction specificity of receiver domain in *Arabidopsis* histidine kinase CKI1 ($CKI1_{RD}$)[60].

In summary, it is reasonable to expect that also in the plant MSP systems, the differences in amino acid sequence and 3D structures are accompanied with the quantitative differences in interaction affinity. This determines the basic framework for MSP signalling, which might be further influenced by additional molecular mechanisms that possibly evolved in plants.

Kinase and phosphatase kinetics controls MSP signalling output

To ensure specific phosphorylation of the response regulator by its cognate histidine kinase and suppress the cross-regulation by histidine kinases of the other signalling pathways, many bacterial receptors adopted phosphatase activity, which enhances the control over the signalling output [7, 71]. The bifunctional histidine kinase receptor dephosphorylates its cognate response regulator in the absence of the signal and suppresses the effects of non-specific activation by other TCS pathways. As soon as the ligand is bound to the receptor, the bifunctional histidine kinase switches over to the kinase mode, which results in the phosphorylation of the cognate response regulator. Mathematical analysis on behaviour of various bacterial TCS proved that systems driven by bifunctional histidine kinases were indeed much more specific and effective in preventing cross-talk than those with monofunctional histidine kinases [72].

The same molecular mechanism might play very important role in plants. Out of the three cytokinin receptor in *Arabidopsis* – AHK2, AHK3, AHK4/CRE1 – only the hybrid histidine kinase AHK4 was proven to act as a bifunctional sensor. The AHK4 activity in phosphorelay was explored *in vitro* as well as in yeast and evidences were collected that AHK4 triggers phosphorelay in the presence of cytokinin, whereas in the absence of the ligand the receiver domain of AHK4 is involved in dephosphorylation of the AHP proteins [54]. These observations correlate well with the phenotypical analysis of different *ahk4* mutants. Null mutations in *AHK4* do not alter the root development due to functional overlaps with the other cytokinin receptors. In contrast, the gain-of-function class of mutations impairing AHK4 activation cause defects in root vascular tissue differentiation described as a *wol* phenotype [53, 54, 73]. AHK4 protein carrying the *wol* mutation is unable to bind cytokinins and exhibits negative effects towards cytokinin signalling, which are significant particularly in the root stele tissues where *AHK4* expression dominates over *AHK*2 and *AHK3*. Phosphatase activity of AHK4 and the total

equilibrium between HK-mediated kinase an phosphatase activities could therefore play a crucial role in establishing cytokinin responsiveness of the plant cells [54].

Bifunctional mode of action should be considered also for other hybrid histidine kinases in *Arabidopsis*. For instance, truncated CKI1 protein consisting only of the receiver domain shows phosphatase activity towards the AHP1 and AHP2 *in vitro* [74]. In contrast, full-length CKI1 protein reveals dominant histidine kinase activity, which upregulates cytokinin responsive reporter gene in the absence of cytokinin when assayed in mesophyll protoplast [75]. Functional analysis of CKI1 in *Arabidopsis* suggested, that CKI1 might act as a constitutively active histidine kinase via MSP elements common to cytokinin signalling pathway [26, 32, 41]. CKI1 was suggested to be involved in the regulation of the above mentioned equilibrium of kinase and phosphatase activities in the cytokinin signalling pathway [54]. Thus, as CKI1 signalling was shown to be cytokinin independent [26, 75], the factors regulating CKI1 expression or activity could be integrated in the regulation of cytokinin or in general MSP pathways. These factors, however, remain to be elucidated.

Dephosphorylation of signalling elements in His-to-Asp phosphorelay pathways occurs also in systems without bifunctional histidine kinases. Auxiliary phosphatases in bacteria similar to CheZ dephosphorylates response regulator by an acid/amid-mediated mechanism [76]. It was proposed that other phosphatase from Rap family, RapB, mediates dephosphorylation via direct protein-protein interaction, which promotes autophosphatase activity of the receiver domain [77]. Although similar proteins were not identified in plants so far, it is possible that some response regulator with strong autophosphatase activity carry out phosphatase function towards the MSP network in *Arabidopsis*. *In vitro* phosphorelay assay showed that a type-C response regulator ARR22 dephosphorylates AHP5 in a phosphorelay-dependent manner, but the radioactively labelled phosphate was not detected on the ARR22 protein [78]. In *Arabidopsis*, overexpression of ARR22 under the control of a strong and constitutive 35S promoter results in dwarfed plants, which are reminiscent to those with impaired cytokinin signalling. It was proposed that ARR22 act as a phosphatase and could create a phosphate sink within the MSP network in *Arabidopsis* [59, 78].

Taken together, experimental data suggests that phosphatase activity could determine both, the signalling specificity and signalling output of MSP network. Rates between kinase and phosphatase activity play an important role in the signal integration/specification and could represent a target for additional level of integration and regulation of cellular responses related to MSP signalling pathways in plants.

Receiver domains differ in phosphorylation lifetime

Another factor which should be considered as important for overall MSP signalling output is the phosphorylation lifetime of aspartate residue within the receiver domain. Though unstable in acid or alkaline conditions, acyl phosphates typically have a half-life of about 5 hours at pH7 [79]. To fit the times-scale requirements of the specific signalling systems in bacteria, the receiver domains carry out not only phosphorelay, but also hydrolysis of a phosphate bond in an autocatalytic reaction and both are absolutely Mg^{2+}-dependent [80]. Phosphorylation lifetime varies in the range from seconds to hours and is directly influenced by different amino acid residues at defined position within the receiver domain structure [81]. In some cases, the phospho-aspartate is stabilized far beyond that of typical acyl phosphate, in exceptional cases like SSK1 up to 2 days. Phosphorylated yeast response regulator SSK1 forms a stable complex with its HPt protein YPD1 that shields the phosphate group from hydrolysis [82]. Autocatalytical phosphate hydrolysis activity of the receiver domain

could be also controlled by an allosteric mechanism upon interaction with an auxiliary regulator protein such as RapB [77]. Comprehensive characterization of phosphorelay kinetic parameters together with the lifetime of the receiver domains could help to indentify new mechanism involved in regulation of the signalling pathway [83]. Regrettably, information on kinetic parameters and response regulator phosphorylation lifetime of plant MSP signalling elements are missing. On the other hand, phosphatase activity observed for CKI1 receiver domain [74], AHK4 bifunctional histidine kinase receptor for cytokinin [54] and type-C response regulator ARR22 [78] is carried out by conventional receivers and could be interpreted as an example of very short phosphorylation lifetime. Presence of response regulators with different phosphorylation lifetime in the cell at the same time might help to canalize phosphate flow into specific branches within the MSP signalling network**.** Characterization of phoshpho-aspartate stability within plant MSP elements should come to the focus of plant MSP signalling research soon.

In the context of presumed differences among plant response regulators regarding the phosphorylation lifetime it should be noted, that experimental work on several type-A ARR proteins revealed that these proteins differ significantly in protein stability/turnover. Moreover, some of the type-A ARR proteins were stabilized in phosphorylation dependent manner [84]. Regulation of protein stability is a mechanism broadly used in plant signalling pathways; for review see [85]. Future studies should elucidate the significance of protein turnovers in MSP signalling proteins including histidine kinases, HPt proteins and additional types of response regulators.

MSP signalling elements are differentially expressed in plant cells

Regulation of the gene expression directly influences intracellular protein concentration and could represent a potent mechanism to ensure signalling specificity in the plant MSP network. Signal transduction involves formation of the signalling complex via protein-protein interactions. Concentration of such a signalling complex in the plant cell grows with the decreasing dissociation constant (K_d), which reflects increasing interaction affinity of the two proteins as determined by their primary amino acid sequence and 3D protein structure. Equally, signalling complex concentration grows with increasing concentration of one or both interaction partners. Therefore, quantitative abundance of the different signalling complexes in the cell at certain time is determined by K_d of all interaction partners and their immediate concentration. Simply, if two proteins differ in the affinity towards the common interaction partner, twice lower K_d of one of the interaction partners could be compensated completely as soon as the protein characterized by lower affinity becomes twice more abundant in the cell. Resulting concentration of the two signalling complexes will be equal.

In *Arabidopsis*, multiple analysis of transcript levels using northern blotting, semi-quantitative or quantitative RT-PCR demonstrated that some MSP genes are differentially expressed in various tissues and developmental stages [23, 24, 86-89]. However, most of the MSP elements exhibit strongly overlapping expression profiles, which could explain high redundancy of the MSP genes. Therefore, construction of multiple mutants is often required to observe phenotypical differences between mutant and wild-type plants [25, 47, 49, 88]. Although RT-PCR expression profile of ethylene receptor proteins is largely overlapping, more detailed analysis of transgenic lines carrying reporter genes fusions under the control of native promoters revealed significant expression differences at the tissue levels. [86]. In many cases, appearance of a gene specific phenotype is accompanied with the specific expression profile, which cannot be fully compensated by homologous genes. *AHK4* is predominantly expressed in the central cylinder of the root meristem in contrast to

the *AHK2* and *AHK3*, which are expressed predominantly in the root tip and only slightly overlap with the *AHK4* expression domain. In result, AHK2 and AHK3 compensate *ahk4* null allele, but the AHK2 and AHK3 activity in the central cylinder is not sufficient to compensate the negative effects of *wol* allele towards the cytokinin effects on procambial differentiation [54]. The spatiotemporal-specific gene expression patterns were identified also in the root meristem transition zone. Cytokinin response in this region is mediated by AHK3 receptor histidine kinase and type-B response regulator ARR12 that is expressed in the first five days after germination. Later in the root development, ARR1 is expressed there and takes the control over the equilibrium between cell division and differentiation in the mature root meristem [21]. In contrast, AHK2 and AHK4 mediated cytokinin signalling upregulates *WUS* transcription in the shoot apical meristem [22].

Type-A response regulators might play the crucial role for modulation of the signal flow specificity in the MSP network. Transcription of these genes is controlled by the type-B response regulators and rapidly induced during primary cytokinin response; for review see [90]. Induction of these genes creates a feedback loop, which in turn represses cytokinin signalling probably by two parallel mechanisms. Firstly, induced type-A response regulators might compete with type-B response regulators for phosphorylated HPt proteins. Secondly, phosphorylated active forms of type-A response regulators could interact with yet unknown proteins, which attenuate cytokinin signalling. This would explain why $ARR5^{D87E}$ mutant resembling the activated ARR5 is able to partially rescue cytokinin hypersensitivity phenotype of multiple type-A *arr* mutant [84]. Another type-A response regulators ARR7 and ARR15 are expressed at the specific position, induced by auxin in the root apical meristem during embryogenesis, or *vice versa* downregulated by auxin in the shoot apical meristems. These two proteins help to establish feedback loops and integrate cytokinin and auxin signalling, which allows proper positioning and maintenance of shoot an root meristem organizing centers [22, 55-58]; for review see Pernisova *et al.*, this issue. It is very likely that induction of the type-A ARR proteins could represent a potent tool to specifically regulate ways of the phosphate flow through the MSP signalling network, particularly in combination with the other molecular mechanisms like molecular recognition and phosphorylation lifetime. Though technically rather difficult to address, closer look to the expression dynamic of MSP proteins in the tissues would help to elucidate many aspects of MSP regulated processes.

Magnesium (Mg^{2+}) dependent regulation of the receiver domain activity

The activity of wide range of the proteins is mediated and regulated by an ion metal binding. Many of the intracellular proteins are structurally changed by magnesium ion with the direct influence on their function and therefore sensitive on Mg^{2+} level or presence of the other metal ions. Receiver domain-containing proteins such as hybrid histidine kinases or response regulators require divalent metal ion in the active site to catalyze the phosphotransfer reaction and autocatalytical hydrolysis of phosphorylated aspartate. The necessity of divalent ions is not restricted only to magnesium because other divalent metal ions like Mn^{2+}, Zn^{2+} and Co^{2+} are also able to ensure phosphotransfer from bacterial CheA to CheY though the reaction kinetic might differ significantly [80]. In the presence of Mg^{2+}, Ca^{2+} reduces phosphotransfer activity of CheY response regulator presumably by competing with Mg^{2+} for CheY catalytic site resulting in the decreased phosphotransfer efficiency [80].

Metal binding site is localized in the acidic cleft on the surface of the receiver domain. Mg^{2+} binding is coordinated by carboxyl groups from two aspartic acids located at the N-terminus of the receiver domain and the catalytical aspartate, which undergoes phosphorylation. In the close proximity of the acidic cleft is located

strictly conserved lysine residue, which forms the salt bridge specifically with aspartic acid phosphorylation site and which helps to facilitate the formation and stabilization of the transition state during acyl-phosphate formation [65]. While histidine-containing domains represents exemplary conformational homogeneity without structural rearrangements after histidine phosphorylation, the conformations of receiver domains are flexible and provide an ideal platform for phosphorylation-dependent conformation changes regulating signalling output. Additionally, flexibility of the receiver domain could be regulatory target for metal ions as well. The most prominent Mg^{2+}-dependent structural change was shown to be a loss of internal dynamics and integrity within the active site, which is normally stabilized by magnesium ion [8, 60].

In bacterial systems, the magnesium-dependent phosphorylation of receiver domain plays a crucial role in interaction with its cognate partner. In *Escherichia coli*, the signalling between RcsC receiver domain and RcsD HPt protein regulates capsule synthesis. Mg^{2+}-dependent BeF_3^--mediated activation of RcsC which mimicks RcsC phosphorylation on the conserved aspartate residue, increased 5-10 times the interaction affinity of RcsC to RcsD [8]. Similarly, the phosphorylation-mediated structural changes were reported for other bacterial response regulators like FixJ and Spo0A, too [91, 92]. In contrast to that, in case of *Arabidopsis* $CKI1_{RD}$, the presence of Mg^{2+} dominantly contributed to observed structural changes, while addition of BeF_3^- resulted only in minor modifications of $CKI1_{RD}$ structure [60]. Therefore, in comparison to bacteria, it seems that the structure of *Arabidopsis* histidine kinase CKI1 is more sensitive to magnesium then to the magnesium-dependent phosphorylation. Whether this could be generalized to other plant histidine kinases, however, remains to be identified.

In regard to this, it is important to consider that the intracellular Mg^{2+} concentration varies between different cell types in the range of 0.23 – 3.8 mM [93]. Our results suggest that magnesium dissociation constant falls into this range in case of $CKI1_{RD}$ [60]. These findings are in agreement with Mg^{2+} dissociation constant of bacterial CheY (0.5 mM) [80] and implicate that at the physiological conditions, receiver domains might remain not completely saturated with Mg^{2+}. Consequently, this could significantly impact their interaction affinities, phosphorelay kinetic constants and/or phosphatase activity. Concentration changes in intracellular concentrations of free Mg^{2+} could therefore represent important regulatory checkpoint in regulation of MSP specificity and signalling output in plants.

Auxiliary regulators control MSP signalling

In addition to molecular mechanisms described above, MSP signalling pathways might be influenced by other proteins, which are called auxiliary regulators. One group of these proteins modulates phosphorelay by acting on histidine kinases. They influence their histidine kinase activity by interaction with its ATP-binding catalytic domain or they physically bind to DHpD domain of histidine kinase, the site of phosphorylation, and thus block transduction mechanisms. Next group of auxiliary proteins are phosphatases that catalyze response regulator dephosphorylation. Auxiliary proteins are also those that regulate nucleocytoplasmic transport or mediate interaction with other proteins of phosphorelay pathways (e.g. transcription factors).

The best characterized example of regulated MSP is the initiation of the sporulation developmental pathway in *Bacillus subtilis* where multiple auxiliary regulators are involved in the control of MSP signalling output; for review see [12, 94]. Core MSP signalling pathway consists of KinA histidine kinase, a single domain response regulator Spo0F, a HPt protein Spo0B, and finally response regulator Spo0A, which is the transcription

activator of sporulation genes [95]. This signalling pathway is negatively regulated by both types of auxiliary proteins, which attenuate histidine kinase activity and auxiliary phosphatases, regulating thus a lifetime of phosphorylated response regulators. Protein KipI influences KinA activity through interactions with the catalytic domain of the histidine kinase and affects the ATP/ADP reactions, which in turn results in the inhibition of KinA histidine kinase activity [17]. Sda auxiliary protein interacts with the KinA HPt domain to block autophosphorylation and phosphotransfer to the response regulator Spo0F [96]. Functions of Spo0F and Spo0A response regulators are controlled by two families of auxiliary phosphatases. Spo0E phosphatase catalyzes the dephosphorylation of Spo0A using acid/amid-mediated mechanism, which was described in detail for CheZ modulator of CheA-CheY chemotaxis regulating TCS in *Escherichia coli*; for review see [76]. The other family of phosphatases (RapA, RapB, RapE, and RapH) catalyzes dephosphorylation of Spo0F, nevertheless the mechanism of the dephosphorylation reaction was not elucidated yet. Experiments carried out with RapB suggest that RapB binds directly to the surface of Spo0F and increases autocatalytical dephosphorylation via allosteric mechanism [77].

The only described auxiliary protein from yeast is MOG1, which is involved in the nuclear-protein import [97]. Additionally, MOG1 modulates SLN1-YPD1-SKN7 phosphorelay branch of osmosensing pathway in *Saccharomyces cerevisiae*. The interaction studies showed that MOG1 protein physically interacts with all three members of this MSP phosphorelay branch and is required for SKN7 nuclear localization. Subsequent studies also suggested that the MOG1 promotes binding of SKN7 to the promoters of osmotic stress target genes [98]. Furthermore, the way of MOG1 interaction with all three MSP elements and the fact that MOG1 shares some features with scaffold proteins, the question have arisen whether MOG1 could promote formation of SLN1-SKN7 signalosome [98].

In plants, so far only one protein was identified, which shares some feature with auxiliary regulators described above. TCP10 protein, which interacts with AHP2, AHP3, and weakly with AHP1 was discovered in yeast two-hybrid screen using AHP2 as a bait. Although TCP10 is homologous to some proteins containing similar structural motives, its function in *Arabidopsis* remains unclear [99]. However, recent findings revealed that AHP proteins maintain a nuclear/cytosolic distribution via active transport into and out of the nucleus [100]. We can assume that proteins regulating this process will be discovered in plants. Similarly, seeking for the molecular mechanisms described in *Bacillus subtilis* will answer the question, whether these mechanisms have evolved also in plants.

Conclusions and future prospect

MSP represents a signalling system of critical importance in the plant development. Recently published results suggest the role of MSP in the integration of multiple signalling pathways. Besides integration of the above described hormonal signalling inputs of auxin [21, 56, 57, 101], abscisic acid [30], cytokinin [23-25, 31] and ethylene [34-36], MSP mediate sensing of environmental signals, like osmoregulation [30, 37-39] or phosphate availability [102]. This implies that crosstalk and crossregulation together with the signalling specificity of individual pathways would be included in the complex developmental control mediated by MSP pathways. Here we have summarized a current status of the knowledge of possible molecular mechanisms, which might probably contribute to the specificity of signal transduction through the MSP-based signalling in plants. We believe that a combination of biochemical and molecular approaches together with structural and

protein interaction studies will be necessary for our understanding to the biological codes included in the structure of MSP regulatory proteins. Together with that, the comprehensive tools of systems biology, employing analysis of large transcriptome and proteome data sets would be critical in the understanding of complex mutual interactions involved (not only) in MSP-mediated adaptive responses. For that, the proper biostatistical tools and computational modelling will allow us to predict the non-intuitive conclusions and hypothesis. A good example represents the recently identified integration of MSP with previously identified molecular mechanisms of control over positioning of shoot apical meristem organizing centre, one of the principal questions of the plant developmental biology [22]. Further important discoveries in that direction are on the way in our and other laboratories. Finally, recent findings suggest the direct role of MSP in the regulation of plant growth during both vegetative [23-28] and generative phases [26, 41, 43]. We believe that our understanding to the molecular determinants of MSP specificity will provide us with tools for targeted improvements of plant growth and crop yield that will allow feed the exponentially growing human population and improve our life quality on the Earth.

Acknowledgements

The work was supported by Ministry of Education, Youth and Sports (grant Nos. MSM0021622415 and LC06034) and the Czech Science Foundation (grant No. 521/09/1699). We are thankful to Tomáš Klumpler for assistance during figure preparation.

Figure legends

Figure 1. Basic scheme of the multistep phosphorelay signal transduction pathway supplemented with the schematic structural models of individual domains participating in phosphate transfer. Signal molecule binds to the input domain (ID) of the histidine kinase and triggers transautophosphorylation of a conserved histidine residue within the dimerization histidine-containing phosphotransfer domain (DHpD). ATP to ADP hydrolysis mediated by catalytic ATP-binding domain (CAD) provides energized phosphate for histidine phoshorylation. The phosphate is intramolecularly transferred to the aspartate within the C-terminal receiver domain (RD)and subsequently to the histidine residue on the protein consiting of the histidine-containing phosphotransfer domain (HPtD). Finally, phosphorylated HPtD serve as a phoshphohistidine substrate in the phosphorelay reaction, which results in phosphorylation of the response regulator RD on the conserved aspartate residue. Output domain (OD) is attached in most cases to the RD of the response regulator protein and mediate transcription of target genes in response to RD phosphorylation. H, conserved histidine residue; N G1 F G2, highly conserved motif; D, catalytic aspartate residue; P, phosphoryl group. In the structural models cylinders represent α-helices and pentagons represent β-sheets.

Figure 2. Complex of the histidine-containing phosphotransfer protein (HPt, left) and receiver domain (right) created with UCSF Chimera visualization system [103] according to the available 3D structures deposited in the PDB. HPt protein consists of helices α1 to α6. Helices α3,4,5,6 forms structural core, which resemble to dimerization histidine-containing phosphotransfer domain of the histidine kinase receptor dimer. Residues involved in the specific interaction lie at base of α3 and α4. Receiver domain consists of parallel β sheets (β1-5) surrounded by helices α1 to α5 and with the catalytical acidic pocket on the top. Residues within the α1 and

loops L1 to L5 arround the active site contributes to specific interaction with the HPt protein. The histidine (H) and aspartate (D) residues that become phosphorylated are shown in the ball-and-stick representation.

References

[1] Gao, R.; Mack, T. R.; Stock, A. M. Bacterial response regulators: versatile regulatory strategies from common domains. *Trends Biochem Sci,* **2007,** *32*, 225-34.

[2] Stock, J. B.; Ninfa, A. J.; Stock, A. M. Protein phosphorylation and regulation of adaptive responses in bacteria. *Microbiol Rev,* **1989,** *53*, 450-90.

[3] Chang, C.; Stewart, R. C. The two-component system. Regulation of diverse signaling pathways in prokaryotes and eukaryotes. *Plant Physiol,* **1998,** *117*, 723-31.

[4] Robinson, V. L.; Buckler, D. R.; Stock, A. M. A tale of two components: a novel kinase and a regulatory switch. *Nat Struct Biol,* **2000,** *7*, 626-33.

[5] Whitworth, D. E.; Cock, P. J. Two-component systems of the myxobacteria: structure, diversity and evolutionary relationships. *Microbiology,* **2008,** *154*, 360-72.

[6] Skerker, J. M.; Perchuk, B. S.; Siryaporn, A.; Lubin, E. A.; Ashenberg, O.; Goulian, M.; Laub, M. T. Rewiring the specificity of two-component signal transduction systems. *Cell,* **2008,** *133*, 1043-54.

[7] Laub, M. T.; Goulian, M. Specificity in two-component signal transduction pathways. *Annu Rev Genet,* **2007,** *41*, 121-45.

[8] Rogov, V. V.; Schmoe, K.; Lohr, F.; Rogova, N. Y.; Bernhard, F.; Dotsch, V. Modulation of the Rcs-mediated signal transfer by conformational flexibility. *Biochem Soc Trans,* **2008,** *36*, 1427-32.

[9] Thanbichler, M. Spatial regulation in Caulobacter crescentus. *Curr Opin Microbiol,* **2009,** *12*, 715-21.

[10] Piggot, P. J.; Hilbert, D. W. Sporulation of Bacillus subtilis. *Curr Opin Microbiol,* **2004,** *7*, 579-86.

[11] Ning, D. G.; Xu, X. D. alr0117, a two-component histidine kinase gene, is involved in heterocyst development in Anabaena sp PCC 7120. *Microbiology-Sgm,* **2004,** *150*, 447-453.

[12] Buelow, D. R.; Raivio, T. L. Three (and more) component regulatory systems - auxiliary regulators of bacterial histidine kinases. *Mol Microbiol,* **2010,** *75*, 547-66.

[13] Fan, Q.; Lechno-Yossef, S.; Ehira, S.; Kaneko, T.; Ohmori, M.; Sato, N.; Tabata, S.; Wolk, C. P. Signal transduction genes required for heterocyst maturation in Anabaena sp. strain PCC 7120. *J Bacteriol,* **2006,** *188*, 6688-93.

[14] Yeh, K. C.; Wu, S. H.; Murphy, J. T.; Lagarias, J. C. A cyanobacterial phytochrome two-component light sensory system. *Science,* **1997,** *277*, 1505-8.

[15] Elich, T. D.; Chory, J. Phytochrome: if it looks and smells like a histidine kinase, is it a histidine kinase? *Cell,* **1997,** *91*, 713-6.

[16] Pas, J.; von Grotthuss, M.; Wyrwicz, L. S.; Rychlewski, L.; Barciszewski, J. Structure prediction, evolution and ligand interaction of CHASE domain. *FEBS Lett,* **2004,** *576*, 287-90.

[17] Wang, L.; Grau, R.; Perego, M.; Hoch, J. A. A novel histidine kinase inhibitor regulating development in Bacillus subtilis. *Genes Dev,* **1997,** *11*, 2569-79.

[18] Pao, G. M.; Saier, M. H., Jr. Nonplastid eukaryotic response regulators have a monophyletic origin and evolved from their bacterial precursors in parallel with their cognate sensor kinases. *J Mol Evol,* **1997,** *44*, 605-13.

[19] Puthiyaveetil, S.; Allen, J. F. Chloroplast two-component systems: evolution of the link between photosynthesis and gene expression. *Proc Biol Sci,* **2009,** *276*, 2133-45.

[20] Pils, B.; Heyl, A. Unraveling the evolution of cytokinin signaling. *Plant Physiol,* **2009,** *151*, 782-91.

[21] Dello Ioio, R.; Linhares, F. S.; Scacchi, E.; Casamitjana-Martinez, E.; Heidstra, R.; Costantino, P.; Sabatini, S. Cytokinins determine Arabidopsis root-meristem size by controlling cell differentiation. *Curr Biol,* **2007,** *17*, 678-82.

[22] Gordon, S. P.; Chickarmane, V. S.; Ohno, C.; Meyerowitz, E. M. Multiple feedback loops through cytokinin signaling control stem cell number within the Arabidopsis shoot meristem. *Proc Natl Acad Sci U S A,* **2009,** *106*, 16529-34.

[23] Higuchi, M.; Pischke, M. S.; Mahonen, A. P.; Miyawaki, K.; Hashimoto, Y.; Seki, M.; Kobayashi, M.; Shinozaki, K.; Kato, T.; Tabata, S.; Helariutta, Y.; Sussman, M. R.; Kakimoto, T. In planta functions of the Arabidopsis cytokinin receptor family. *Proc Natl Acad Sci U S A,* **2004,** *101*, 8821-6.

[24] Nishimura, C.; Ohashi, Y.; Sato, S.; Kato, T.; Tabata, S.; Ueguchi, C. Histidine kinase homologs that act as cytokinin receptors possess overlapping functions in the regulation of shoot and root growth in Arabidopsis. *Plant Cell,* **2004,** *16*, 1365-77.

[25] Riefler, M.; Novak, O.; Strnad, M.; Schmulling, T. Arabidopsis cytokinin receptor mutants reveal functions in shoot growth, leaf senescence, seed size, germination, root development, and cytokinin metabolism. *Plant Cell,* **2006,** *18*, 40-54.

[26] Hejatko, J.; Ryu, H.; Kim, G. T.; Dobesova, R.; Choi, S.; Choi, S. M.; Soucek, P.; Horak, J.; Pekarova, B.; Palme, K.; Brzobohaty, B.; Hwang, I. The histidine kinases CYTOKININ-INDEPENDENT1 and ARABIDOPSIS HISTIDINE KINASE2 and 3 regulate vascular tissue development in Arabidopsis shoots. *Plant Cell,* **2009,** *21*, 2008-21.

[27] Matsumoto-Kitano, M.; Kusumoto, T.; Tarkowski, P.; Kinoshita-Tsujimura, K.; Vaclavikova, K.; Miyawaki, K.; Kakimoto, T. Cytokinins are central regulators of cambial activity. *Proc Natl Acad Sci U S A,* **2008,** *105*, 20027-31.

[28] Nieminen, K.; Immanen, J.; Laxell, M.; Kauppinen, L.; Tarkowski, P.; Dolezal, K.; Tahtiharju, S.; Elo, A.; Decourteix, M.; Ljung, K.; Bhalerao, R.; Keinonen, K.; Albert, V. A.; Helariutta, Y. Cytokinin signaling regulates cambial development in poplar. *Proc Natl Acad Sci U S A,* **2008,** *105*, 20032-7.

[29] Kim, H. J.; Ryu, H.; Hong, S. H.; Woo, H. R.; Lim, P. O.; Lee, I. C.; Sheen, J.; Nam, H. G.; Hwang, I. Cytokinin-mediated control of leaf longevity by AHK3 through phosphorylation of ARR2 in Arabidopsis. *Proc Natl Acad Sci U S A,* **2006,** *103*, 814-9.

[30] Tran, L. S.; Urao, T.; Qin, F.; Maruyama, K.; Kakimoto, T.; Shinozaki, K.; Yamaguchi-Shinozaki, K. Functional analysis of AHK1/ATHK1 and cytokinin receptor histidine kinases in response to abscisic acid, drought, and salt stress in Arabidopsis. *Proc Natl Acad Sci U S A,* **2007,** *104*, 20623-8.

[31] Inoue, T.; Higuchi, M.; Hashimoto, Y.; Seki, M.; Kobayashi, M.; Kato, T.; Tabata, S.; Shinozaki, K.; Kakimoto, T. Identification of CRE1 as a cytokinin receptor from Arabidopsis. *Nature,* **2001,** *409*, 1060-3.

[32] Kakimoto, T. CKI1, a histidine kinase homolog implicated in cytokinin signal transduction. *Science,* **1996,** *274*, 982-5.

[33] Pernisova, M.; Klima, P.; Horak, J.; Valkova, M.; Malbeck, J.; Soucek, P.; Reichman, P.; Hoyerova, K.; Dubova, J.; Friml, J.; Zazimalova, E.; Hejatko, J. Cytokinins modulate auxin-induced organogenesis in plants via regulation of the auxin efflux. *Proc Natl Acad Sci U S A,* **2009,** *106*, 3609-14.

[34] Hass, C.; Lohrmann, J.; Albrecht, V.; Sweere, U.; Hummel, F.; Yoo, S. D.; Hwang, I.; Zhu, T.; Schafer, E.; Kudla, J.; Harter, K. The response regulator 2 mediates ethylene signalling and hormone signal integration in Arabidopsis. *EMBO J,* **2004,** *23*, 3290-302.

[35] Scharein, B.; Voet-van-Vormizeele, J.; Harter, K.; Groth, G. Ethylene signaling: identification of a putative ETR1-AHP1 phosphorelay complex by fluorescence spectroscopy. *Anal Biochem,* **2008,** *377*, 72-6.

[36] Voet-van-Vormizeele, J.; Groth, G. Ethylene controls autophosphorylation of the histidine kinase domain in ethylene receptor ETR1. *Molecular Plant,* **2008,** *1*, 380-387.

[37] Urao, T.; Miyata, S.; Yamaguchi-Shinozaki, K.; Shinozaki, K. Possible His to Asp phosphorelay signaling in an Arabidopsis two-component system. *FEBS Lett,* **2000,** *478*, 227-32.

[38] Urao, T.; Yakubov, B.; Satoh, R.; Yamaguchi-Shinozaki, K.; Seki, M.; Hirayama, T.; Shinozaki, K. A transmembrane hybrid-type histidine kinase in Arabidopsis functions as an osmosensor. *Plant Cell,* **1999,** *11*, 1743-54.

[39] Desikan, R.; Horak, J.; Chaban, C.; Mira-Rodado, V.; Witthoft, J.; Elgass, K.; Grefen, C.; Cheung, M. K.; Meixner, A. J.; Hooley, R.; Neill, S. J.; Hancock, J. T.; Harter, K. The histidine kinase AHK5 integrates endogenous and environmental signals in Arabidopsis guard cells. *PLoS One,* **2008,** *3*, e2491.

[40] Iwama, A.; Yamashino, T.; Tanaka, Y.; Sakakibara, H.; Kakimoto, T.; Sato, S.; Kato, T.; Tabata, S.; Nagatani, A.; Mizuno, T. AHK5 histidine kinase regulates root elongation through an ETR1-dependent abscisic acid and ethylene signaling pathway in Arabidopsis thaliana. *Plant Cell Physiol,* **2007,** *48*, 375-80.

[41] Deng, Y.; Dong, H.; Mu, J.; Ren, B.; Zheng, B.; Ji, Z.; Yang, W. C.; Liang, Y.; Zuo, J. Arabidopsis histidine kinase CKI1 acts upstream of histidine phosphotransfer proteins to regulate female gametophyte development and vegetative growth. *Plant Cell,* **2010,** *22*, 1232-48.

[42] Hejatko, J.; Pernisova, M.; Eneva, T.; Palme, K.; Brzobohaty, B. The putative sensor histidine kinase CKI1 is involved in female gametophyte development in Arabidopsis. *Mol Genet Genomics,* **2003,** *269*, 443-53.

[43] Pischke, M. S.; Jones, L. G.; Otsuga, D.; Fernandez, D. E.; Drews, G. N.; Sussman, M. R. An Arabidopsis histidine kinase is essential for megagametogenesis. *Proc Natl Acad Sci U S A,* **2002,** *99*, 15800-5.

[44] Dortay, H.; Mehnert, N.; Burkle, L.; Schmulling, T.; Heyl, A. Analysis of protein interactions within the cytokinin-signaling pathway of Arabidopsis thaliana. *FEBS J,* **2006,** *273*, 4631-44.

[45] Imamura, A.; Hanaki, N.; Nakamura, A.; Suzuki, T.; Taniguchi, M.; Kiba, T.; Ueguchi, C.; Sugiyama, T.; Mizuno, T. Compilation and characterization of Arabidopsis thaliana response regulators implicated in His-Asp phosphorelay signal transduction. *Plant Cell Physiol,* **1999,** *40*, 733-42.

[46] Suzuki, T.; Miwa, K.; Ishikawa, K.; Yamada, H.; Aiba, H.; Mizuno, T. The Arabidopsis sensor His-kinase, AHk4, can respond to cytokinins. *Plant Cell Physiol,* **2001,** *42*, 107-13.

[47] Hutchison, C. E.; Li, J.; Argueso, C.; Gonzalez, M.; Lee, E.; Lewis, M. W.; Maxwell, B. B.; Perdue, T. D.; Schaller, G. E.; Alonso, J. M.; Ecker, J. R.; Kieber, J. J. The Arabidopsis histidine phosphotransfer proteins are redundant positive regulators of cytokinin signaling. *Plant Cell,* **2006,** *18*, 3073-87.

[48] Mason, M. G.; Mathews, D. E.; Argyros, D. A.; Maxwell, B. B.; Kieber, J. J.; Alonso, J. M.; Ecker, J. R.; Schaller, G. E. Multiple type-B response regulators mediate cytokinin signal transduction in Arabidopsis. *Plant Cell,* **2005,** *17*, 3007-18.

[49] To, J. P.; Haberer, G.; Ferreira, F. J.; Deruere, J.; Mason, M. G.; Schaller, G. E.; Alonso, J. M.; Ecker, J. R.; Kieber, J. J. Type-A Arabidopsis response regulators are partially redundant negative regulators of cytokinin signaling. *Plant Cell,* **2004,** *16*, 658-71.

[50] Romanov, G. A.; Lomin, S. N.; Schmulling, T. Biochemical characteristics and ligand-binding properties of Arabidopsis cytokinin receptor AHK3 compared to CRE1/AHK4 as revealed by a direct binding assay. *J Exp Bot,* **2006,** *57*, 4051-8.

[51] Spichal, L.; Rakova, N. Y.; Riefler, M.; Mizuno, T.; Romanov, G. A.; Strnad, M.; Schmulling, T. Two cytokinin receptors of Arabidopsis thaliana, CRE1/AHK4 and AHK3, differ in their ligand specificity in a bacterial assay. *Plant Cell Physiol,* **2004,** *45*, 1299-305.

[52] Jung, K. W.; Oh, S. I.; Kim, Y. Y.; Yoo, K. S.; Cui, M. H.; Shin, J. S. Arabidopsis histidine-containing phosphotransfer factor 4 (AHP4) negatively regulates secondary wall thickening of the anther endothecium during flowering. *Mol Cells,* **2008,** *25*, 294-300.

[53] Mahonen, A. P.; Bonke, M.; Kauppinen, L.; Riikonen, M.; Benfey, P. N.; Helariutta, Y. A novel two-component hybrid molecule regulates vascular morphogenesis of the Arabidopsis root. *Genes Dev,* **2000,** *14*, 2938-43.

[54] Mahonen, A. P.; Higuchi, M.; Tormakangas, K.; Miyawaki, K.; Pischke, M. S.; Sussman, M. R.; Helariutta, Y.; Kakimoto, T. Cytokinins regulate a bidirectional phosphorelay network in Arabidopsis. *Curr Biol,* **2006a,** *16*, 1116-22.

[55] Leibfried, A.; To, J. P.; Busch, W.; Stehling, S.; Kehle, A.; Demar, M.; Kieber, J. J.; Lohmann, J. U. WUSCHEL controls meristem function by direct regulation of cytokinin-inducible response regulators. *Nature,* **2005,** *438*, 1172-5.

[56] Muller, B.; Sheen, J. Cytokinin and auxin interaction in root stem-cell specification during early embryogenesis. *Nature,* **2008,** *453*, 1094-7.

[57] Zhao, Z.; Andersen, S. U.; Ljung, K.; Dolezal, K.; Miotk, A.; Schultheiss, S. J.; Lohmann, J. U. Hormonal control of the shoot stem-cell niche. *Nature,* **2010,** *465*, 1089-92.

[58] Buechel, S.; Leibfried, A.; To, J. P.; Zhao, Z.; Andersen, S. U.; Kieber, J. J.; Lohmann, J. U. Role of A-type ARABIDOPSIS RESPONSE REGULATORS in meristem maintenance and regeneration. *Eur J Cell Biol,* **2010,** *89*, 279-84.

[59] Horak, J.; Grefen, C.; Berendzen, K. W.; Hahn, A.; Stierhof, Y. D.; Stadelhofer, B.; Stahl, M.; Koncz, C.; Harter, K. The Arabidopsis thaliana response regulator ARR22 is a putative AHP phospho-histidine phosphatase expressed in the chalaza of developing seeds. *BMC Plant Biol,* **2008,** *8*, 77.

[60] Pekarova, B.; Klumpler, T.; Triskova, O.; Horak, J.; Jansen, S.; Dopitova, R.; Motackova, V.; Nejedla, E.; Zidek, L.; Marek, J.; Sklenar, V.; Hejatko, J.; Janda, L. Dynamic structure and binding specificity of the receiver domain of sensor histidine kinase CKI1 from Arabidopsis thaliana. *submitted*, **2010**.

[61] Rogov, V. V.; Rogova, N. Y.; Bernhard, F.; Koglin, A.; Lohr, F.; Dotsch, V. A new structural domain in the Escherichia coli RcsC hybrid sensor kinase connects histidine kinase and phosphoreceiver domains. *J Mol Biol,* **2006,** *364*, 68-79.

[62] Zapf, J.; Sen, U.; Madhusudan; Hoch, J. A.; Varughese, K. I. A transient interaction between two phosphorelay proteins trapped in a crystal lattice reveals the mechanism of molecular recognition and phosphotransfer in signal transduction. *Structure,* **2000,** *8*, 851-62.

[63] Varughese, K. I.; Tsigelny, I.; Zhao, H. The crystal structure of beryllofluoride Spo0F in complex with the phosphotransferase Spo0B represents a phosphotransfer pretransition state. *J Bacteriol,* **2006,** *188*, 4970-7.

[64] Xu, Q.; Porter, S. W.; West, A. H. The yeast YPD1/SLN1 complex: insights into molecular recognition in two-component signaling systems. *Structure,* **2003,** *11*, 1569-81.

[65] Zhao, X.; Copeland, D. M.; Soares, A. S.; West, A. H. Crystal structure of a complex between the phosphorelay protein YPD1 and the response regulator domain of SLN1 bound to a phosphoryl analog. *J Mol Biol,* **2008,** *375*, 1141-51.

[66] West, A. H.; Stock, A. M. Histidine kinases and response regulator proteins in two-component signaling systems. *Trends Biochem Sci,* **2001,** *26*, 369-76.

[67] Marina, A.; Waldburger, C. D.; Hendrickson, W. A. Structure of the entire cytoplasmic portion of a sensor histidine-kinase protein. *EMBO J,* **2005,** *24*, 4247-59.

[68] Sugawara, H.; Kawano, Y.; Hatakeyama, T.; Yamaya, T.; Kamiya, N.; Sakakibara, H. Crystal structure of the histidine-containing phosphotransfer protein ZmHP2 from maize. *Protein Sci,* **2005,** *14*, 202-8.

[69] Xu, Q.; West, A. H. Conservation of structure and function among histidine-containing phosphotransfer (HPt) domains as revealed by the crystal structure of YPD1. *J Mol Biol,* **1999,** *292*, 1039-50.

[70] Muller-Dieckmann, H. J.; Grantz, A. A.; Kim, S. H. The structure of the signal receiver domain of the Arabidopsis thaliana ethylene receptor ETR1. *Structure,* **1999,** *7*, 1547-56.

[71] Kenney, L. J. How important is the phosphatase activity of sensor kinases? *Curr Opin Microbiol, 13*, 168-76.

[72] Alves, R.; Savageau, M. A. Comparative analysis of prototype two-component systems with either bifunctional or monofunctional sensors: differences in molecular structure and physiological function. *Mol Microbiol,* **2003,** *48*, 25-51.

[73] Scheres, B.; Dilaurenzio, L.; Willemsen, V.; Hauser, M. T.; Janmaat, K.; Weisbeek, P.; Benfey, P. N. Mutations Affecting the Radial Organization of the Arabidopsis Root Display Specific Defects Throughout the Embryonic Axis. *Development,* **1995,** *121*, 53-62.

[74] Nakamura, A.; Kakimoto, T.; Imamura, A.; Suzuki, T.; Ueguchi, C.; Mizuno, T. Biochemical characterization of a putative cytokinin-responsive His-kinase, CKI1, from Arabidopsis thaliana. *Biosci Biotechnol Biochem,* **1999,** *63*, 1627-30.

[75] Hwang, I.; Sheen, J. Two-component circuitry in Arabidopsis cytokinin signal transduction. *Nature,* **2001,** *413*, 383-9.

[76] Silversmith, R. E. Auxiliary phosphatases in two-component signal transduction. *Curr Opin Microbiol,* **2010,** *13*, 177-83.

[77] Tzeng, Y. L.; Feher, V. A.; Cavanagh, J.; Perego, M.; Hoch, J. A. Characterization of interactions between a two-component response regulator, Spo0F, and its phosphatase, RapB. *Biochemistry,* **1998,** *37*, 16538-45.

[78] Kiba, T.; Aoki, K.; Sakakibara, H.; Mizuno, T. Arabidopsis response regulator, ARR22, ectopic expression of which results in phenotypes similar to the wol cytokinin-receptor mutant. *Plant Cell Physiol,* **2004,** *45*, 1063-77.

[79] Post, R. L.; Kume, S. Evidence for an aspartyl phosphate residue at the active site of sodium and potassium ion transport adenosine triphosphatase. *J Biol Chem,* **1973,** *248*, 6993-7000.

[80] Lukat, G. S.; Stock, A. M.; Stock, J. B. Divalent metal ion binding to the CheY protein and its significance to phosphotransfer in bacterial chemotaxis. *Biochemistry,* **1990,** *29*, 5436-42.

[81] Pazy, Y.; Motaleb, M. A.; Guarnieri, M. T.; Charon, N. W.; Zhao, R.; Silversmith, R. E. Identical phosphatase mechanisms achieved through distinct modes of binding phosphoprotein substrate. *Proc Natl Acad Sci U S A,* **2010,** *107*, 1924-9.

[82] Janiak-Spens, F.; Sparling, D. P.; West, A. H. Novel role for an HPt domain in stabilizing the phosphorylated state of a response regulator domain. *J Bacteriol,* **2000,** *182*, 6673-8.

[83] Kaserer, A. O.; Andi, B.; Cook, P. F.; West, A. H. Effects of osmolytes on the SLN1-YPD1-SSK1 phosphorelay system from Saccharomyces cerevisiae. *Biochemistry,* **2009,** *48*, 8044-50.

[84] To, J. P.; Deruere, J.; Maxwell, B. B.; Morris, V. F.; Hutchison, C. E.; Ferreira, F. J.; Schaller, G. E.; Kieber, J. J. Cytokinin regulates type-A Arabidopsis Response Regulator activity and protein stability via two-component phosphorelay. *Plant Cell,* **2007,** *19*, 3901-14.

[85] Santner, A.; Estelle, M. The ubiquitin-proteasome system regulates plant hormone signaling. *Plant J,* **2010,** *61*, 1029-40.

[86] Grefen, C.; Stadele, K.; Ruzicka, K.; Obrdlik, P.; Harter, K.; Horak, J. Subcellular localization and in vivo interactions of the Arabidopsis thaliana ethylene receptor family members. *Mol Plant,* **2008,** *1*, 308-20.

[87] Hradilova, J.; Brzobohaty, B. Expression pattern of the AHP gene family from Arabidopsis thaliana and organ specific alternative splicing in the AHP5 gene. *Biologia Plantarum,* **2007,** *51*, 257-267.

[88] Mason, M. G.; Li, J.; Mathews, D. E.; Kieber, J. J.; Schaller, G. E. Type-B response regulators display overlapping expression patterns in Arabidopsis. *Plant Physiol,* **2004,** *135*, 927-37.

[89] Tanaka, Y.; Suzuki, T.; Yamashino, T.; Mizuno, T. Comparative studies of the AHP histidine-containing phosphotransmitters implicated in His-to-Asp phosphorelay in Arabidopsis thaliana. *Biosci Biotechnol Biochem,* **2004,** *68*, 462-5.

[90] To, J. P.; Kieber, J. J. Cytokinin signaling: two-components and more. *Trends Plant Sci,* **2008,** *13*, 85-92.

[91] Birck, C.; Mourey, L.; Gouet, P.; Fabry, B.; Schumacher, J.; Rousseau, P.; Kahn, D.; Samama, J. P. Conformational changes induced by phosphorylation of the FixJ receiver domain. *Structure,* **1999,** *7*, 1505-15.

[92] Lewis, R. J.; Brannigan, J. A.; Muchova, K.; Barak, I.; Wilkinson, A. J. Phosphorylated aspartate in the structure of a response regulator protein. *J Mol Biol,* **1999,** *294*, 9-15.

[93] Gunther, T. Concentration, compartmentation and metabolic function of intracellular free Mg2+. *Magnes Res,* **2006,** *19*, 225-36.

[94] Perego, M. A new family of aspartyl phosphate phosphatases targeting the sporulation transcription factor Spo0A of Bacillus subtilis. *Mol Microbiol,* **2001b,** *42*, 133-43.

[95] Burbulys, D.; Trach, K. A.; Hoch, J. A. Initiation of sporulation in B. subtilis is controlled by a multicomponent phosphorelay. *Cell,* **1991,** *64*, 545-52.

[96] Burkholder, W. F.; Kurtser, I.; Grossman, A. D. Replication initiation proteins regulate a developmental checkpoint in Bacillus subtilis. *Cell,* **2001,** *104*, 269-79.

[97] Oki, M.; Nishimoto, T. A protein required for nuclear-protein import, Mog1p, directly interacts with GTP-Gsp1p, the Saccharomyces cerevisiae ran homologue. *Proc Natl Acad Sci U S A,* **1998,** *95*, 15388-93.

[98] Lu, J. M.; Deschenes, R. J.; Fassler, J. S. Role for the Ran binding protein, Mog1p, in Saccharomyces cerevisiae SLN1-SKN7 signal transduction. *Eukaryot Cell,* **2004,** *3*, 1544-56.

[99] Suzuki, T.; Sakurai, K.; Ueguchi, C.; Mizuno, T. Two types of putative nuclear factors that physically interact with histidine-containing phosphotransfer (Hpt) domains, signaling mediators in His-to-Asp phosphorelay, in Arabidopsis thaliana. *Plant Cell Physiol,* **2001,** *42*, 37-45.

[100] Punwani, J. A.; Hutchison, C. E.; Schaller, G. E.; Kieber, J. J. The subcellular distribution of the Arabidopsis histidine phosphotransfer proteins is independent of cytokinin signaling. *Plant J,* **2010,** *62*, 473-82.

[101] Dello Ioio, R.; Nakamura, K.; Moubayidin, L.; Perilli, S.; Taniguchi, M.; Morita, M. T.; Aoyama, T.; Costantino, P.; Sabatini, S. A genetic framework for the control of cell division and differentiation in the root meristem. *Science,* **2008,** *322*, 1380-4.

[102] Franco-Zorrilla, J. M.; Martin, A. C.; Leyva, A.; Paz-Ares, J. Interaction between phosphate-starvation, sugar, and cytokinin signaling in Arabidopsis and the roles of cytokinin receptors CRE1/AHK4 and AHK3. *Plant Physiol,* **2005,** *138*, 847-57.

[103] Pettersen, E. F.; Goddard, T. D.; Huang, C. C.; Couch, G. S.; Greenblatt, D. M.; Meng, E. C.; Ferrin, T. E. UCSF Chimera--a visualization system for exploratory research and analysis. *J Comput Chem,* **2004,** *25*, 1605-12.

Horak et al., Figure 1.

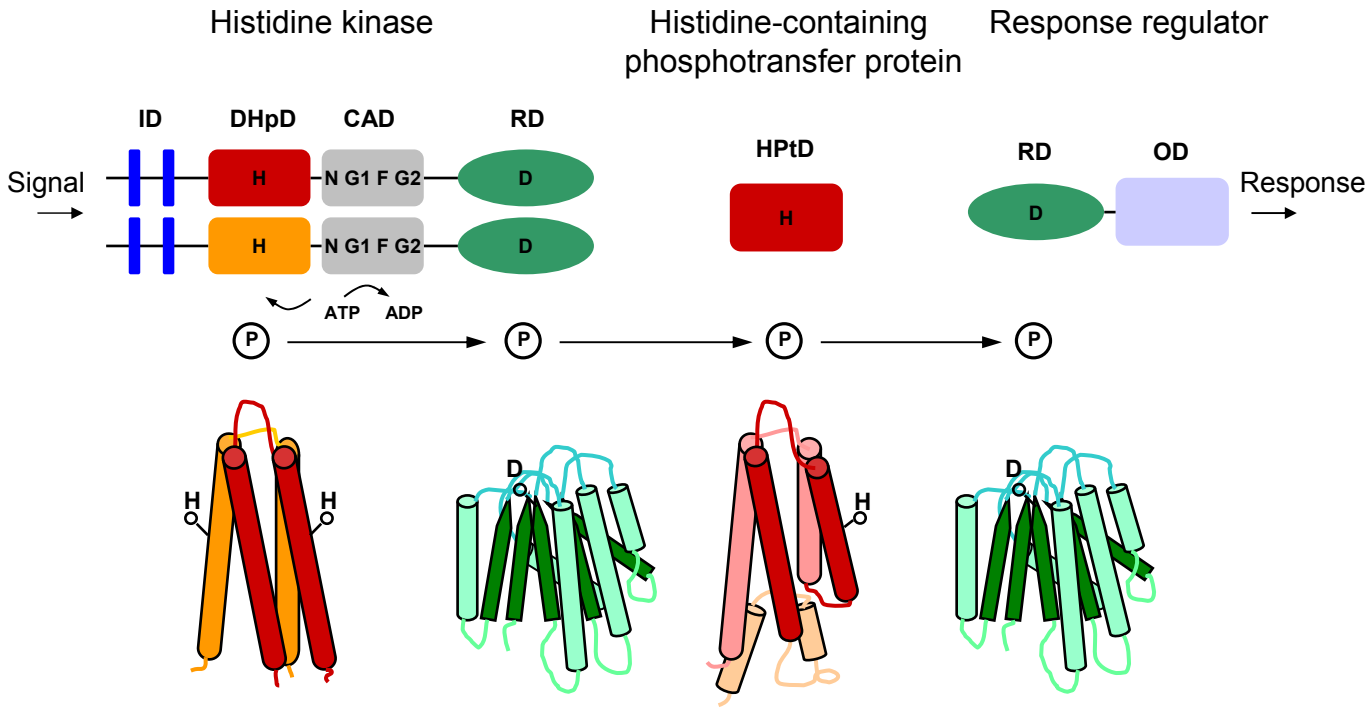

Horak et al., Figure 2.

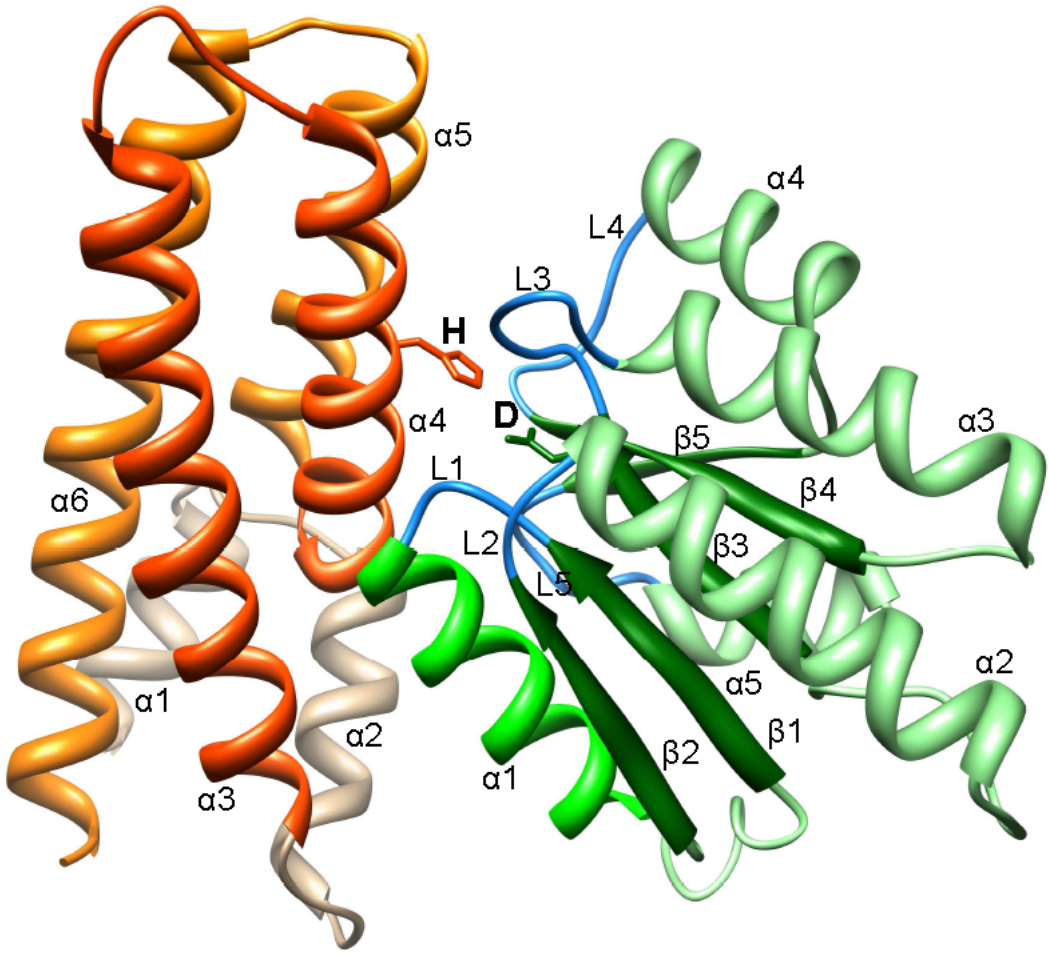

Enclosed Publication # 3

Hejátko, J., Pernisová, M., Eneva, T., Palme, K. and Brzobohatý, B. (2003) The putative sensor histidine kinase CKI1 is involved in female gametophyte development in *Arabidopsis*. *Molecular Genetics and Genomics*, **269**, 443-453. IF_{2008}=2.838

Mol Gen Genomics (2003) 269: 443–453
DOI 10.1007/s00438-003-0858-7

ORIGINAL PAPER

J. Hejátko · M. Pernisová · T. Eneva · K. Palme
B. Brzobohatý

The putative sensor histidine kinase CKI1 is involved in female gametophyte development in *Arabidopsis*

Received: 20 January 2003 / Accepted: 28 April 2003 / Published online: 28 May 2003
© Springer-Verlag 2003

Abstract Embryo sac formation is a fundamental step in sexual reproduction in plants. However, the key players involved in the development of the female gametophyte remain elusive. We present data indicating that a two-component sensor histidine kinase, CKI1, originally implicated in cytokinin perception, is required for completion of megagametogenesis in *Arabidopsis*. We isolated a loss-of-function mutation in *CKI1* resulting from an insertion of the *En-1* transposon into the *CKI1* coding sequence. Genetic analysis revealed that the mutant allele, *cki1-i*, could not be transmitted through the female germ line. Confocal laser scanning microscopy identified a block in megagametogenesis, characterized by the abortion of the central vacuole in mutant embryo sacs, and degradation of the developing female gametophyte after completion of all mitotic divisions. The recovery of two independent stable alleles and one revertant wild-type allele resulting from *En-1* excision confirmed unambiguously the causal link between the *cki1-i* mutation and the abnormal phenotype. In situ localization of *CKI1* mRNA and histochemical analysis of stable transformants harboring the *uidA* gene under the control of *CKI1* promoter revealed that expression of *CKI1* starts at the very beginning of female gametophyte development, and continues until fertilization. This suggests that the developing embryo sac may remain sensitive to signals recognized by CKI1 throughout megagametogenesis. Furthermore, expression of the paternally transmitted *CKI1* was detected early after fertilization. The results indicate a role for a two-component signaling system during female gametophyte development, and provide the first evidence that gametophytic expression of a sensor-like molecule is essential for specific processes during megagametogenesis.

Keywords Female gametophyte development · Two-component signaling · Sensor histidine kinase · Early seed development · Genomic imprinting

Communicated by G. Jürgens

J. Hejátko · B. Brzobohatý (✉)
Institute of Biophysics, Academy of Sciences of the Czech Republic, Královopolská 135, 61265 Brno, Czech Republic
E-mail: brzoboha@ibp.cz
Tel.: +42-541-517184
Fax: +42-541-211293

J. Hejátko · M. Pernisová · B. Brzobohatý
Department of Functional Genomics and Proteomics, Masaryk University, Kotlářská 2, 61137 Brno, Czech Republic

J. Hejátko · K. Palme
Max-Delbrück-Laboratorium in der Max-Planck-Gesellschaft, Carl-von-Linné Weg 10, 50829 Köln, Germany

T. Eneva · K. Palme
Institut für Biologie II, Albert-Ludwigs-Universität Freiburg, Schänzlestr. 1, 79104 Freiburg, Germany

Introduction

During its life cycle, the plant body passes through two extreme forms, the highly organized multicellular form and the single-celled zygote. Identification of the mechanisms that guide formation of the complex plant body from a single cell represents one of the most intriguing challenges in plant developmental biology. In angiosperms the formation of the female gametophyte, which harbors pre-programmed cell lineages and a putative position-specific distribution of morphogenetic factors (Reiser and Fischer 1993; Brown et al. 1999; Chaudhury et al. 2001; Drews and Yadegari 2002), represents a fundamental step in plant sexual reproduction. Characterization of the factors that drive the formation of the complex structure of the female gametophyte in angiosperms promises to provide us with deeper insights into the mechanisms of early embryo and seed development. However, despite the crucial importance of the megagametogenesis in the plant life cycle, our current understanding of its molecular aspects remains fragmentary. Nevertheless, detailed morphological analysis has defined several steps in the formation of the embryo sac, the female gametophyte of angiosperms. After

initiation of the ovule primordia, an archesporial cell line is established, resulting in megaspore mother cell differentiation. Following meiosis, the most proximal megaspore survives in *Arabidopsis* (Reiser and Fischer 1993; Christensen et al. 1997). In 70% of the plant species studied so far, including *Arabidopsis*, a *Polygonum* -type of megagametogenesis follows (Christensen et al. 1997, 1998, and references therein). Though several mutations that have an impact on both ovule sporophyte and female gametophyte tissue have been described (Christensen et al. 1998; Drews et al. 1998; Gasser et al. 1998; Grossniklaus and Schneitz 1998; Drews and Yadegari 2002), the molecular mechanisms guiding female gametophyte development remain to be identified.

In contrast to the naked, non-polarized, female gametes of fucoid algae (Hable and Kropf 2000, and references therein), the female gametophyte of angiosperms, which is completely surrounded by maternal tissue, represents a highly organized and polar structure. Current data suggest tight genetic control of interregional interactions between the developing female gametophyte and the surrounding sporophytic tissue, which seems to be crucial for proper embryo sac assembly and development (Gasser et al. 1998; Western and Haughn 1999; Chaudhury and Berger 2001). Some authors (Reiser and Fischer 1993; Grossniklaus and Schneitz 1998) invoke a role for positional cues transmitted by the sporophytic tissue adjacent to the developing embryo sac. However, the molecular evidence for such information exchange, including identification of the signaling molecules involved, is sparse. Recently, Hecht et al. (2001) described *AtSERK1*, which encodes a receptor-like kinase that is expressed throughout female gametophyte development and in the early embryo. Nevertheless, the possible role of this sensor-like molecule during embryo sac formation is unclear, as genetic data are lacking. Hence, the key players that control female gametophyte development remain elusive.

Two-component signal transduction systems, consisting of sensor histidine kinases coupled with effector response regulators, were originally found to mediate the regulation of a broad spectrum of adaptive responses in bacteria (Parkinson and Kofoid 1992). In the last decade, homologues of the bacterial two-component systems have also been recognized in plants (for a review, see Urao et al. 2000a). In *Arabidopsis*, genes for 11 suspected sensor histidine kinases have been identified. Some of these have been shown to mediate perception and transduction of environmental variables (e.g. osmosensing) and developmental stimuli (e.g. ethylene and cytokinins; for review, see Urao et al. 2001). One of the putative *Arabidopsis* sensor histidine kinases, CYTOKININ INDEPENDENT 1 (CKI1), was originally classified as a candidate cytokinin receptor, based on the fact that overexpression of *CKI1* in *Arabidopsis* hypocotyl segments resulted in callus proliferation and shoot differentiation in the absence of exogenously supplied cytokinin and auxin (Kakimoto 1996). CKI1 was also shown to complement a mutation in the gene for the homologous bacterial sensor histidine kinase RcsC (Yamada et al. 2001). In the yeast two-hybrid system CKI1 interacts with the histidine-containing phosphotransmitters (HPt proteins) AHP2 and AHP3, which are thought to be downstream partners of sensor histidine kinases (Urao et al. 2000b). The C-terminal part of CKI1, which displays similarities to prokaryotic signal receiver domains, was also shown to dephosphorylate the *Arabidopsis* HPt proteins AHP1 and AHP2 in vitro (Nakamura et al. 1999). Finally, conserved amino acid residues implicated in the deduced histidine kinase and phosphoryl transfer activities of CKI1 have been shown to be involved in the CKI1-mediated constitutive activation of a cytokinin-responsive promoter in *Arabidopsis* protoplasts (Hwang and Sheen 2001). Taken together, these results suggest a role for CKI1 as a sensor histidine kinase in *Arabidopsis*. However, neither the endogenous ligand nor the biological function of CKI1 has been identified.

To investigate the involvement of CKI1 in *Arabidopsis* development, we employed an approach that relies on the phenotypic analysis of loss-of-function mutants. Here we report the identification of an allele of *CKI1*, *cki1-i* , which resulted from the insertion of an *En-1* transposon into *CKI1*, and show that the mutation causes a block in embryo sac formation. Furthermore, we show that *CKI1* is expressed throughout embryo sac development, and is switched on transiently during early seed development. These results, together with data published independently by Pischke et al. (2002), demonstrate for the first time that gametophytic expression of a sensor-like molecule is essential for specific processes during megagametogenesis in *Arabidopsis*.

Materials and methods

Screening primers

An *En-1* mutagenized population of *Arabidopsis thaliana* (ecotype Columbia 0) was screened by PCR as previously described (Baumann et al. 1998). A positive signal was obtained using the primers 1262-3 (5′-CATCATAAACCACACAAACCATA-3′) and 67Xho (5′-CCGCTCGAGCTTTTTAGGGTTTATCATTCTC-C-3′), which are specific for the CKI1 cDNA, in combination with the *En-1* specific primers EN205 (5′-AGAAGCACG-ACGGCTGTAGAATAGGA-3′) and EN8130 (5′-GAGCGT-CGGTCCCCACACTTCTATAC-3′), respectively. The *En-1* insertion-specific primers 1262-3 and EN205 were used to screen *CKI1* / *cki1-i* segregating populations. Primers specific for the stable alleles *cki1-s1* (5′-TTCCTCGTCGAATTCAAGTCGTAC-3′) and *cki1-s2* (5′-CTCGTCGAATTCAAGTCGCG-3′) were then designed and used in combination with a universal primer (5′-GCATCATAAACCACACAAACCATA-3′) in PCR screens of families harboring the respective stable mutant alleles.

Microscopy and image analysis

For scanning electron microscope analysis, both mutant (*CKI1*/*cki1-i*) and wild-type (*CKI1*/*CKI1*) siliques were carefully slit under a stereomicroscope using a sharp scalpel, and fixed immediately in 3% glutaraldehyde in 0.1 M sodium phosphate (Na-Pi) buffer

(pH 7.1) overnight at 4°C. The tissue was impregnated with osmium tetroxide (1% in the same Na-Pi buffer) for 2 h on ice, dehydrated through an ethanol series and critical-point dried in a CO_2 atmosphere. The dried tissue was then gold coated and examined at 10 kV using a DSM 940 scanning electron microscope (Zeiss). Confocal microscopy was performed as previously described (Christensen et al. 1997) using the upright confocal laser scanning microscope Sarastro 2000 (Molecular Dynamics). The confocal images were processed using ImageSpace (Molecular Dynamics) and Adobe Photoshop (Adobe Systems) software. Observations on GUS-stained ovules were performed using DIC optics with a Leica DM R microscope.

Expression analysis

In situ mRNA analysis was performed as previously described (Hartmann et al. 2000). The *CKI1* specific probe was generated by in vitro transcription of *CKI1* cDNA subcloned into the pBluescript (Stratagene) vector (a generous gift from T. Kakimoto). As a control, a sense RNA probe was prepared from the same template. GUS staining of dissected pistils with 0.2% 5-bromo-4-chloro-3-indolyl β-D-glucuronide (X-gluc; Roth) and tissue clearing was performed as previously described (Malamy and Benfey 1997).

Cloning techniques

The primers SII-ckpr (5′-GTAACCGCGGGAGGAGGCACAAAATGACGAA-3′) and B-ckpr (5′-GCTGGGATCCTCATATTATCTTCTTCCTCGGAGC-3′) were used for PCR amplification of the putative promoter region of *CKI1*, and the resulting PCR fragment was subcloned into the *Sac* II/*Bam*HI sites in pBluescript. After verification by sequencing, the amplified promoter region was cloned into the *Sst* I/*Bam*HI sites upstream of the *uidA* reporter gene in the binary vector pVKH*35SGUSpA* (Reintanz et al. 2001).

Results

Mutations in *CKI1* cannot be obtained in the homozygous state

We screened a collection of *Arabidopsis* lines (*A. thaliana*, ecotype Col-0) that had been mutagenized with the maize autonomous transposable element *En-1* for a *CKI1* knockout using a PCR-based method (Baumann et al. 1998; Wisman et al. 1998). We identified a line carrying a single *En-1* insertion in *CKI1* and designated the mutant allele as *cki1-i*. The insertion is located in exon 6, upstream of the deduced histidine kinase catalytic center (Fig. 1 *i*), suggesting that *cki1-i* is a loss-of-function mutation. In the progeny of *CKI1*/*cki1-i* plants the expected 1:2:1 ratio of *CKI1*/*CKI1, CKI1*/*cki1-i* and *cki1-i*/*cki1-i* genotypes was distorted, as determined by Southern hybridization with a probe specific for the *CKI1* genomic sequence (data not shown). In a population of 36 plants analyzed, 25 were homozygous for the wild-type allele (*CKI1*/ *CKI1*) and the remaining 11 plants were heterozygous for the mutant allele (*CKI1*/*cki1-i*), as indicated by the shift in the size of the genomic fragment containing the *En-1* insertion on Southern blots, and confirmed by PCR using insertion-specific primers (see Materials and methods). Hence we were unable to detect any *cki1-i* homozygotes in the population analyzed.

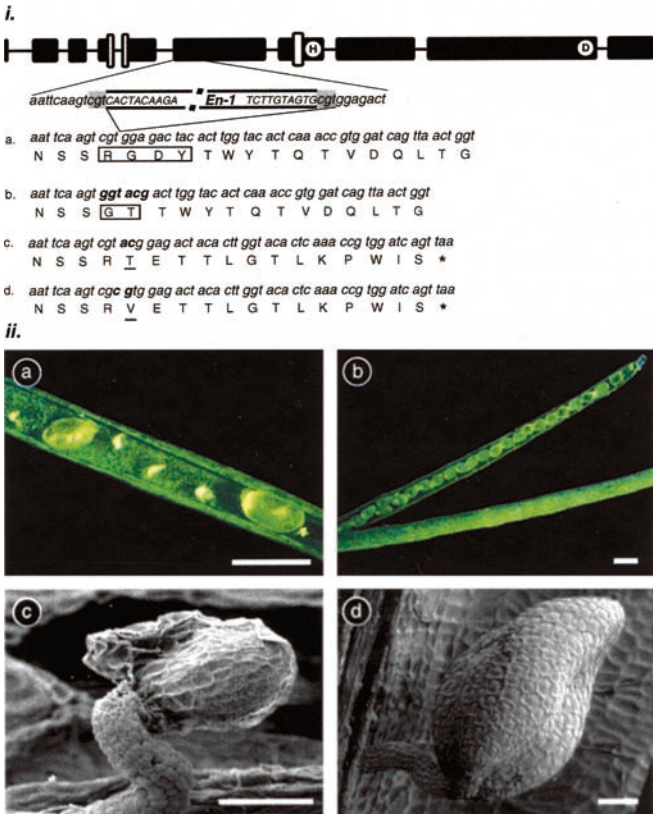

Fig. 1 Panel *i*. Mutant alleles of *CKI1* identified. Schematic representation of the *CKI1* genomic sequence, showing the exact position of the *En-1* insertion in exon 6. Exons (*black boxes*), introns (*lines*) and the locations of putative transmembrane regions in the gene product (*empty boxes*) are indicated at the *top*. The positions of nucleotides encoding conserved His (H) and Asp (D) residues proposed to be involved in His-kinase and phospohorelay activities of CKI1, respectively, are shown. The *En-1* sequence is given in *upper case*; the 3-bp duplication resulting from *En-1* insertion is *shaded* . a–d. DNA and predicted amino acid sequences encoded by the wild-type *CKI1* and mutant *cki1* alleles generated by imperfect excision of *En-1* from the *cki1-i* (*cki1::En-1*) allele. a. *CKI1* wild-type allele. b. *cki1-r*, the wild-type revertant sequence; the substituted amino acids in products of both *CKI1* and *cki1-r* are *boxed*, the footprint DNA sequence is shown in *bold*. c, d. Stable mutant alleles (*cki1-s1*and *cki1-s2*, respectively) resulting from 2-bp insertions (in *bold*) associated with imperfect *En-1* excisions; the unique amino acid residues that distinguish the two alleles are *underlined*, and the premature termination codons arising from the frameshift are represented by *asterisks*. Panel *ii*. Morphological analysis of the *cki1-i* phenotype by light microscopy (a, b) and scanning electron microscopy (c, d). a. Semi-sterile siliques found in *CKI1*/*cki1-i* plants. b. Siliques of a *CKI1*/*CKI1* plant (sibling from the same segregating family as in a). *Scale bars* 500 μm (a) and 1 mm (b). c. Desiccated arrested ovule in *CKI1*/*cki1-i* silique. d. A normally developing seed from the same silique. *Scale bars* 50 μm

The *cki1-i* allele cannot be transmitted through the female germ line

Detailed inspection of siliques in plants heterozygzous for *cki1-i* revealed the presence of arrested and

desiccated ovules, while no obvious defect was found in the ovule sporophytic tissue (Fig. 1 *ii*, c). In *CKI1*/*cki1-i* plants, the average total number of developed seeds per silique was reduced by half compared to that in *CKI1*/*CKI1* siblings (22.2 ± 1.3 and 44.6 ± 2.4, respectively). Silique lengths were similar in the two genotypes (11.1 ± 0.5 mm and 11.7 ± 0.3 mm in the mutant and wild type, respectively; the 95% confidence intervals are given for both values). The phenotype cosegregated with *cki1-i* based on both Southern hybridization and PCR analysis (data not shown). We observed no other phenotypic deviations linked with the *CKI1*/*cki1-i* genotype.

To analyze the transmission of *cki1-i* through the male and female germ lines a series of reciprocal backcrosses was performed, and the presence of *cki1-i* in the progeny was traced by PCR. In B1 populations resulting from pollination of wild-type (Col-0) plants with pollen from lines heterozygous for *cki1-i,* the frequency of plants harboring *cki1-i* was 0.4 (53/131). However, when lines heterozygous for *cki1-i* were used as the female parents and were pollinated with wild-type (Col-0) pollen, no individual harboring *cki1-i* could be identified in a screen of 88 of the resulting progeny (data not shown).

Mutations in *CKI1* disrupt female gametophyte development

The development of the female gametophyte in *Arabidopsis* has been divided into seven distinct stages (FG1–FG7; Fig. 2 *ii*) based mainly on confocal laser scanning microscopy (CLSM) analysis of wild-type ovules and recently identified mutants (Christensen et al. 1997, 1998, 2002). To investigate the nature of the defects in *cki1-i* female gametophyte development and/or function at the cellular level, the mutants were double backcrossed and developing ovules were examined in the pistils of *CKI1*/*cki-i* plants (identified by PCR) using CLSM. No abnormal ovules (scored by number and position of nuclei, and formation of a central vacuole) were identified until FG4 (Fig. 2 *i*, a–d and Table 1). However, in late FG5 (FG5 *III* in Fig. 2 *ii*), two populations of ovules were found in the pistils of *CKI1*/*cki-i* plants. In comparison with wild type (Fig. 2 *i*, e), the central vacuole was distorted in mutant ovules (Fig. 2 *i*, f) and cellularization was hampered, as indicated by the diffuse structure of the cells. In addition, the antipodal-like nuclei were improperly positioned in some of the mutant ovules (Fig. 2 *i*, f and the corresponding legend). To analyze the terminal phenotype of the mutant ovules, flowers were emasculated and the ovule phenotype was analyzed 24 and 48 h after emasculation (HAE). At 24 HAE, wild-type ovules were found in FG6 and FG7 (data not shown). The mutant ovules still had not completed the transition from FG5 to FG6, and displayed varying degrees of embryo sac degradation. In the least degraded embryo sacs (classified as phenotype I, Fig. 2 *i*, g), the localization and morphology of

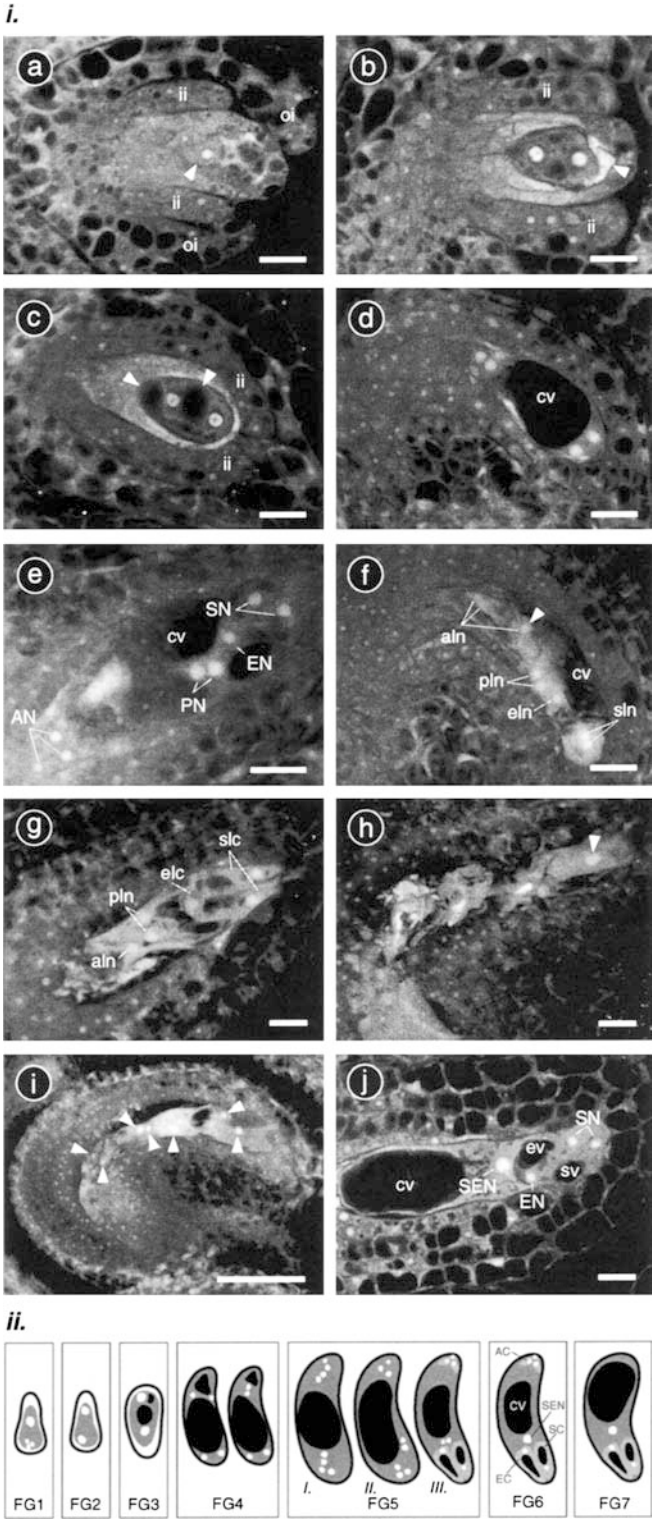

synergids and egg cell were almost as expected for wild type at late FG5 and/or FG6. However, the polar nuclei were not fused, indicating arrest at FG5. Furthermore, one of the antipodal-like nuclei was adjacent to the polar nuclei. In a minor proportion of the mutant ovules analyzed, a higher degree of embryo sac degradation was observed (phenotype II, Fig. 2 *i*, h). Within these

Fig. 2 Panel *i*. Analysis of female gametophyte development in *CKI1/cki1-i* plants by confocal laser scanning microscopy. a. The embryo sac at the 1-nucleus stage (FG1) that defines the start of female gametophyte development (megagametogenesis). The functional megaspore is differentiated (*arrowhead*). Both inner and outer integuments are developed, inner integuments surround approximately two-thirds of the nucellus. The bright fluorescence corresponds to nucleoli, which are referred to as nuclei for simplicity. b. Female gametophyte at stage FG2. At the distal pole the highly fluorescent remnants of degenerating megaspores are still apparent (*arrowhead*), inner integuments almost completely surround the nucellus. c. Stage FG3. The central and chalazal vacuoles have formed (*arrowheads*), the inner integuments cover the nucellus completely. d. FG4. The central vacuole is fully developed. Panels a–c are single 1.5-μm optical sections, panel d shows a stack of three 1.5 μm CLSM images. e. Stack of five 1.5 μm optical sections, showing the wild-type phenotype at late FG5 in *CKI1/cki1-i* pistils (compare with Panel *ii*, FG5 *III*). f. Mutant embryo sac at late FG5. Note the fuzzy structure of the cells, one of the antipodal-like nuclei migrates towards the micropylar pole (*arrowhead*); the central vacuole starts to degenerate. Five optical sections (1.5 μm) were superimposed. g. Morphology of the least degraded *cki1-i* embryo sacs (phenotype I) at 24 HAE (two 1.5 μm optical sections). h. The highly degraded *cki1-i* embryo sac (phenotype II) at 24 HAE (four 1.5 μm optical sections). At the micropylar pole, degenerating synergid nuclei can be seen (*arrowhead*). i. The *cki1-i* embryo sac (phenotype I) in the terminal stages of development at 48 HAE (five 1.5 μm CLSM sections). Seven nuclei (*arrowheads*) are distinguishable. j. A single CLSM section (1.5 μm) showing the mature wild-type embryo sac at stage FG7. Abbreviations: ii, inner integuments; oi, outer integuments; cv, central vacuole; SN, synergid nuclei; EN, egg nucleus; PN, polar nuclei; AN, antipodal nuclei; aln, antipodal-like nuclei; pln, polar-like nuclei; eln, egg-like nucleus; sln, synergid-like nuclei; slc, synergid-like cells; elc, egg-like cell; SEN, secondary endosperm nucleus; EN, egg nucleus; SN, synergid nuclei; ev, egg cell vacuole; sv, synergid cell vacuole. The *scale bars* correspond to 10 μm (a–h, j) and 50 μm (i). In all the micrographs, the embryo sacs are oriented with the micropylar pole to the *right* and the chalazal pole to the *left*. In a–d, f, h and i the optical sections were taken in the longitudinal plane and oblique to that in j. In e and g optical sectioning was performed in the plane perpendicular to the longitudinal one (abaxial to adaxial side view). Panel *ii*. Schematic drawings representing the seven stages of female gametophyte development (based on data presented by Christensen et al. 1997, and the data in this paper). The nuclei are depicted in *white*, vacuoles in *black* and cytoplasm in *grey*. FG1, female gametophyte at stage 1. Four nuclei, the products of megaspore mother cell meiosis, are present. Three of these later degenerate. During the next few stages (FG2 to early FG5) the most proximal nucleus (the functional megaspore) undergoes three rounds of mitotic divisions, forming the eight-nuclei of the embryo sac. The central vacuole and usually another smaller vacuole at the chalazal pole are formed during FG3. During late FG4, the two chalazal nuclei are reoriented parallel to the chalazal-micropylar axis. For FG1–FG4 compare with micrographs a–d. In the course of FG5, the nuclei (originally four at each pole; FG5 *I*. in our classification) undergo dramatic movements. Groups of three nuclei are formed at each pole, and the polar nuclei migrate asymmetrically to the position where they later fuse (FG5 *II*.). Cellularization and cell differentiation start, resulting in the seven-celled embryo sac. Two synergid cells surrounding an egg cell at the micropylar pole (here, only one synergid is shown) are separated from the three antipodal cells at the chalazal pole by the central cell with two polar nuclei and a large vacuole (FG5 *III*, see micrograph e). The polar nuclei fuse and form a diploid central cell nucleus (secondary endosperm nucleus) during FG6. The antipodal cells then degenerate and a four-celled embryo sac is finally established in FG7 (see micrograph j). In the drawings the developing embryo sacs are oriented with the chalazal (proximal) pole at the *top* and the micropylar (distal) pole at the *bottom*, with the abaxial (posterior) side on the *left* and the adaxial (anterior) side on the *right*. The gradual bending of the developing embryo sac is shown schematically. Abbreviations: SEN, secondary endosperm nucleus; CV, central vacuole; EC, egg cell; SC, synergid cell; AC, antipodal cells

Table 1 Phenotypic analysis of embryo sac development in pistils of *CKI1/cki1-i* plants

Developmental stage	Number of ovules scored				
	Wild type	Mutant phenotype I	Mutant phenotype II	Mutant phenotype III	Total number of mutants
FG1	37	–	–	–	0
FG2	14[b]	–	–	–	0
FG3	52	–	–	–	0
FG4	46	–	–	–	0
FG5[a]	21	5	1	–	6
24 HAE	16	10	3	1	14
48 HAE	31	17	8	4	29

[a]Female gametophytes in the terminal FG5 (stage FG5 *III*, see Fig. 2 *ii*)
[b]The small number of ovules identified at FG2 reflects the rapidity of the transition from stage FG2 to FG3 (see also Christensen et al. 1997)

embryo sacs individual cells could not be identified and only a few nuclei could sometimes be distinguished. The central vacuole was completely missing in these mutant ovules. In a small percentage of ovules from *CKI1/cki1-i* pistils (phenotype III, see Table 1) 10–14 nuclei were identified (data not shown). All the above-mentioned features of the mutant phenotype (i.e. absence of the central vacuole and cellularization defects) were also present. At 48 HAE, all wild-type ovules (approximately half the total; a goodness-of-fit test confirmed a 1:1 ratio of mutant to wild-type ovules at $\alpha \sim 0.8$, see Table 1) reached the terminal stage of development (FG7) with fully developed and mature embryo sacs (Fig. 2 *i*, j). In the other ovules, embryo sacs with a mutant phenotype were found. This indicates normal (Mendelian) segregation of the *cki1-i* trait, and is in a good agreement with the genetic data, suggesting complete phenotypic penetrance of the *cki1-i* allele (see previous section). Also the mutants at 48 HAE displayed two major classes of phenotype (Table 1) resembling those previously

described (see above). In mutants of class I a slightly higher degree of embryo sac degradation was identified, as revealed by the more pronounced changes in the position of nuclei and the degree of disruption of cell structure; in these cases, the central vacuole could not be identified unambiguously (Fig. 2 *i*, i). In the *CKI1*/*CKI1* siblings of *CKI1*/*cki-i* none of the 48 ovules inspected at 48 HAE (three sibling lines) revealed any abnormalities compared to the mature wild-type embryo sac.

Novel alleles of *CKI1* confirm a causal link between the *cki1-i* mutation and the block in female gametophyte development

The *cki1-i* allele and the semi-sterile silique phenotype were originally identified in a plant that harbored multiple *En-1* insertions. To exclude the possibility that the phenotype is caused by an *En-1* insertion in another gene, the co-segregation of the phenotype with individual *En-1* elements was analyzed by Southern hybridization using an *En-1* specific probe (data not shown). The results clearly showed that only the *En-1* element inserted in *CKI1* co-segregated with the phenotype, thus demonstrating that *cki1-i* and the semi-sterile silique phenotype are genetically linked.

To prove a causal link between the *En-1* insertion in *CKI1* and the phenotype, we used the instability of the *En-1* element in *CKI1*, as this often results in imperfect excisions leading to novel mutant alleles.

An *En-1* excision that restores the *CKI1* ORF rescues the wild-type phenotype

In a population of 90 *CKI1*/*cki1-i* plants (identified by PCR), two individuals were identified that yielded both wild-type and semi-sterile siliques. Seeds from the wild-type siliques were harvested, and twelve plants from each line were analyzed. The absence of *En-1* in *CKI1* was confirmed by PCR, and a genomic fragment encompassing the original *En-1* integration site in the *CKI1* gene was amplified, sub-cloned and sequenced. In one of the two wild-type revertant lines (E5), sequence analysis revealed a footprint resulting in conversion of the putative amino acid sequence RGDY to GT, but otherwise restoring the *CKI1* ORF (Fig. 1 *i,* b). Plants homozygous for this allele, designated *cki1-r*, were identified among the progeny of E5. In *cki1-r*/*cki1-r* progeny (54 individuals), no plants with semi-sterile siliques were found. Thus, the reconstitution of *CKI1* ORF after *En-1* excision is sufficient to restore the wild-type phenotype. Hence, the block in female gametophyte development cannot be caused by a stable mutation that might have been generated, for example, by an earlier *En-1* integration/excision event in a locus genetically linked to *CKI1*.

Excisions of *En-1* that result in frameshifts in *CKI1* retain the mutant phenotype

Genotype analysis of the progeny of self-pollinated plants heterozygous for the *cki1-i* allele was used to look for frameshift mutations caused by imperfect *En-1* excision from *cki1-i*. The first screen included 54 plants, of which 18 displayed the semi-sterile silique phenotype characteristic of the *cki1-i* allele. However, one of these plants lacked the *En-1* insertion in *CKI1*, as revealed by PCR analysis. Sequence analysis (as outlined above) revealed an *En-1* footprint that results in a premature termination codon in the *CKI1* ORF (Fig. 1 *i*, c). A second, independent mutation was identified in a similar screen (Fig. 1 *i*, d). The alleles were designated *cki1-s1* and *cki1-s2*, respectively, and were found to co-segregate with the semi-sterile silique phenotype using footprint specific primers (data not shown).

Inspection of the embryo sacs in a line that was heterozygous for one of the stable mutant alleles (*CKI1*/*cki1-s1*) by CLSM to examine the terminal phenotype at 24 and 48 HAE yielded results similar to those for *cki1-i* (see previous section). However, the phenotype of *cki1-s1* embryo sacs was characterized by a higher degree of degradation (similar to the less frequent phenotype II of *cki1-i*, Fig. 2 *i,* h), which suggests that the *cki1-s1* allele has a somewhat greater effect (data not shown). Also, in *CKI1*/*CKI1* siblings of *CKI1*/*cki1-s1* plants, none of the 40 ovules inspected at 48 HAE (two lines) revealed any deviations from the wild type.

Taken together, the results of these studies with the newly derived *cki1-r*, *cki1-s1* and *cki1-s2* alleles provide unambiguous proof of a causal link between the interruption of the *CKI1* ORF and the block in female gametophyte development.

CKI1 is expressed during ovule development

The expression of *CKI1* was examined during female gametophyte development in order to establish a correlation with the mutant phenotype. In situ localization of *CKI1* mRNA was performed on paraffin sections using a gene specific antisense RNA probe (Fig. 3b, d, f, h). A weak but specific signal was detectable throughout female gametophyte development, starting at FG1 and continuing up to FG7. To obtain independent data supporting *CKI1* expression throughout embryo sac formation, the transcriptional activity of the putative *CKI1* promoter was assayed using the reporter gene *uidA*, which codes for bacterial β-glucuronidase (GUS). The reporter gene was placed under the control of a 2.7-kb region located upstream of the putative transcriptional start, which is assumed to include the promoter region of *CKI1*. As a short peptide (MKRAF) encoded by the 5′ UTR of *CKI1* mRNA might be involved in regulating the expression pattern by translational repression (Wang and Wessler 1998), the GUS coding sequence was fused with the putative translation

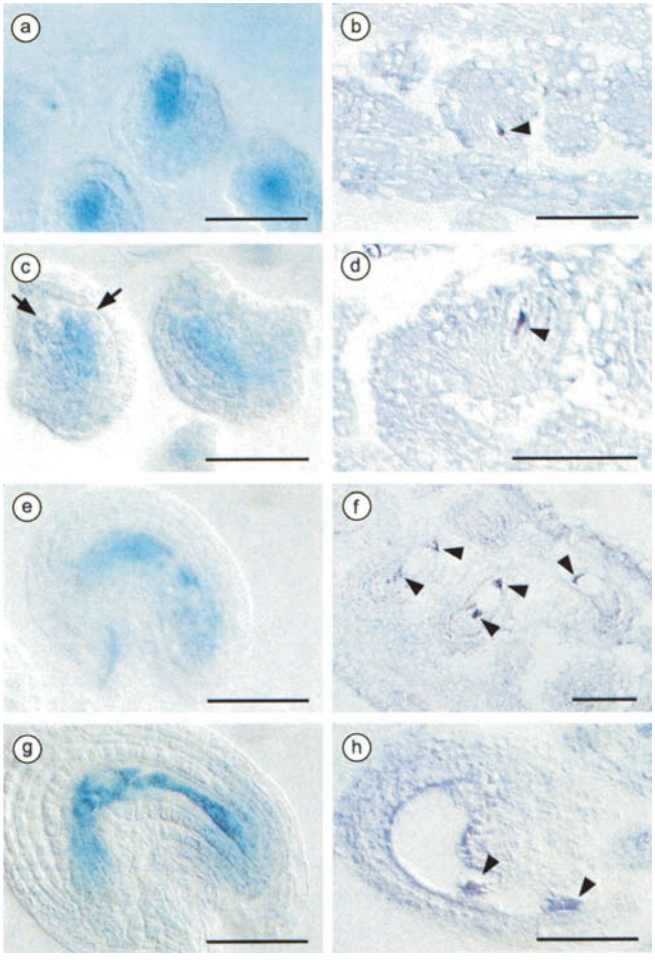

Fig. 3 Analysis of *CKI1* expression during female gametophyte development. Histochemical analysis of GUS activity in stable p*CKI1::uidA* transformants (a, c, e, g) and in situ localization of *CKI1* mRNA (b, d, f, h). The relatively higher level of background signal in the in situ hybridizations is due to the long exposure times needed to visualize very low levels of *CKI1* mRNA. a, b. Expression of *CKI1* during the transition from later 2-V to the early 3-I stage of ovule development (corresponding to stages FG0 to FG1 of female gametophyte development). The inner integuments surround approximately two-thirds of the nucellus (compare with Fig. 2 *i,* a). Stage 3-I defines the start of female gametophyte development (megagametogenesis, stage FG1). c, d. Transition from late stage 3-II (FG2) to early 3-III (FG3), compare with Fig. 2 *i,* b and c. The *arrows* point to inner integuments. e, f. Stage 3-IV (FG4) to 3-V (FG5). g, h. The four-celled mature female gametophyte (3-VI, FG7), 5 days (g) and 24 h (h) after flower emasculation. *Scale bars* 50 μm. Ovule development stages according to Schneitz et al. (1995); the *arrowheads* indicate the *CKI1* mRNA signal

initiation site at the ATG codon of the short peptide MKRAF. A binary vector construct (p*CKI1*::*uidA*) was used to transform wild-type *Arabidopsis* plants. To exclude possible positional effects, a number of stably transformed lines were assayed for GUS activity, and gave consistent results. A detailed analysis of *uidA* expression in developing ovules was performed on two independent transformants, both of which yielded similar results, differing only in the intensity of the GUS staining. GUS activity in developing ovules was detected as early as FG1 and remained detectable until the female gametophyte was mature (Fig. 3a, c, e, g). Minor inconsistencies between the mRNA localization and the GUS histochemical assay (the localization of the RNA was more restricted than the GUS staining) may result from diffusion of the reaction product in GUS assays and/or differences in substrate accessibility in the two methods used (i.e. paraffin sections versus whole mounts). Weak GUS activity was also detected in developing anthers, specifically in the tapetum (data not shown).

Expression of *CKI1* in the developing seed

The *CKI1* expression pattern and the phenotype of *cki1-i* indicate a requirement for CKI1 during female gametophyte development. Analysis of *CKI1* expression in the mature embryo sac, in which GUS activity was detectable 5 days after emasculation (Fig. 3g, h) might suggest a role for CKI1 in (1) the maintenance of embryo sac integrity, (2) the acquisition of competence for fertilization and/or (3) subsequent events during early stages of seed development. To determine whether the *CKI1* gene is expressed in the newly formed sporophyte (i.e. embryo and endosperm), the transcriptional activity of the *CKI1* promoter was assayed during the early stages of seed development. To prevent interference caused by the detection of persistent GUS activity originating from *CKI1* promoter activity in the mature embryo sac before fertilization, wild-type flowers were emasculated, and the pistils were pollinated using pollen from p*CKI1*::*uidA* plants 36–48 h later (three experiments using three independent lines). GUS activity was examined in dissected pistils 10, 12, 24, 48 and 72 h after pollination (HAP). At 10 HAP only weak GUS activity was detectable (data not shown). Between 10 and 12 HAP, a sharp increase in GUS staining was detected (Fig. 4a) and from 12 to 24 HAP *uidA* expression reached its maximum (Fig. 4b, c). The transcriptional activity of *CKI1* after fertilization was confirmed using in situ localization of *CKI1* mRNA at 24 HAP (Fig. 4f). Weak and probably only residual GUS activity spread over most of the endosperm at 48 HAP (Fig. 4d), and at 72 HAP activity was no longer detectable (Fig. 4e). No GUS staining was observed in the developing embryo, indicating that *CKI1* expression during the early stages of seed development is specific to the endosperm.

Discussion

We report the isolation of a mutation in a gene for a putative sensor histidine kinase, *CKI1*, that resulted from the insertion of an *En-1* transposon into the *CKI1* coding sequence. We failed to identify the mutant allele *cki1-i* in the homozygous state, and subsequently found that it could not be transmitted through the female germ line. Furthermore, in *CKI1*/*cki1-i* pistils, embryo sacs

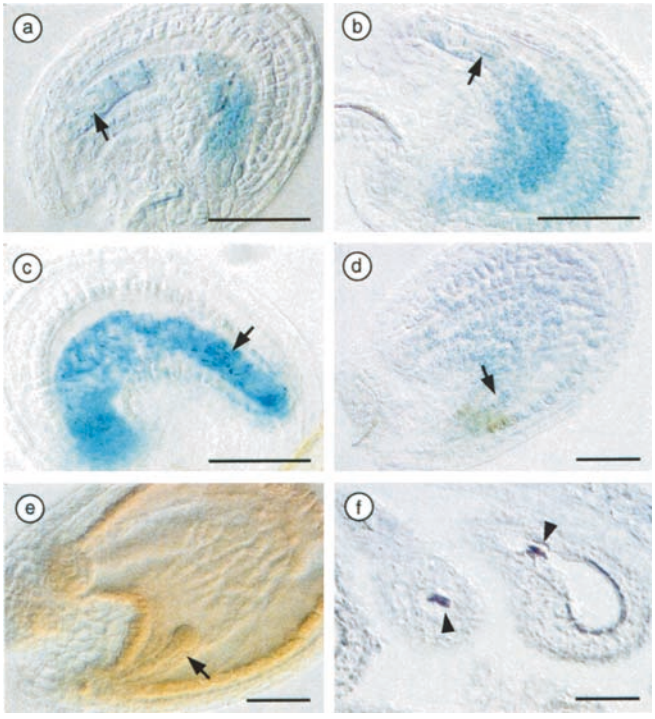

Fig. 4 Expression of *CKI1* after fertilization. a–e. Histochemical detection of GUS activity in ovules after pollination of wild-type pistils with pollen from stable p*CKI1::uidA* transformants. a. 12 h after pollination (HAP). b, c. 24 HAP. Despite the low resolution of GUS staining at the micropyle over the zygote, the zygote itself does not appear to be stained. d. 48 HAP. e. 72 HAP. The brownish color is due to changes in seed composition during development. f. In situ localization of *CKI1* mRNA (*arrowheads*) in wild-type ovules at 24 HAP. The *arrows* indicate the elongating zygote and early embryo. *Scale bars* 50 μm

with a mutant phenotype were found in one half of the ovules, using CLSM analysis. *CKI1* expression was detected in the developing female gametophyte, supporting a role for CKI1 in megagametogenesis. A causal link between the *cki1-i* mutation and the block in female gametophyte development was confirmed by the isolation of (1) an *En-1* excision that restores the *CKI1* ORF and simultaneously rescues the wild-type phenotype, and (2) two stable mutant alleles, *cki1-s1* and *cki1-s2*, resulting from frameshifts caused by imprecise *En-1* excisions. While our manuscript was in preparation, a paper by Pischke et al. (2002) reporting similar, but not identical, results based on the analysis of independent mutant alleles of *CKI1* (*cki1-5*and *cki1-6*) in *A. thaliana* (ecotype Wassilewskija), was published. In the following sections, we discuss our data together with those of Pischke et al. (2002).

The *cki1-i* allele cannot be transmitted through the female germ line

The distorted genotype ratios in the progeny of self-pollinated *CKI1*/*cki1-i* plants, together with the reduced seed set, was consistent with a possible defect in the function of either male or female gametes carrying the mutation (Feldmann et al. 1997; Drews et al. 2002). This hypothesis was confirmed at the genetic level by reciprocal backcrosses. The absence of the mutant alleles in the progeny obtained after pollination of mutant *CKI1*/*cki1-i* plants with wild-type pollen indicates complete penetrance of the lethal *cki1-i* phenotype in the female germ line. The frequency of plants carrying the mutation in the B1 populations resulting from backcrosses in which the *CKI1*/*cki-i* plants were used as the male parent (0.4, 53/131) suggested the possibility of reduced transmission of the *cki1-i* through the male germ line. However, the statistical significance of the difference (compared to the expected frequency 0.5) was found to be at the lowest limit of acceptance (the α value calculated using a goodness-of-fit test was between 0.05 and 0.02). Thus, additional experiments were necessary to justify our conclusions. In progeny of twice backcrossed, self-pollinated *CKI1*/*cki1-i* plants the goodness-of fit-test confirmed that the frequency of *CKI1*/*cki1-i* plants (0.45, 25/56) was compatible with a model predicting equal proportions of *CKI1*/*CKI1* and *CKI1*/*cki1-i* individuals ($0.3 < \alpha < 0.5$). Furthermore, in back crosses using pollen from the *CKI1*/*cki1-s1* plants, we found the frequency of the paternally transmitted stable mutant allele to be 0.5 (41/80). Taken together, these data indicate that the presence of functional CKI1 is not likely to be crucial for the formation of functional male gametes. The slightly reduced frequency of the *CKI1*/*cki1-i* plants in the case of B1 populations could be the result of incomplete emasculation and/or lower accuracy of PCR analysis. Similar results have also been reported for the *cki1-5* and *cki1-6* alleles by Pischke et al. (2003). However, given our detection of weak expression of *CKI1* in the tapetum (not shown), a more detailed investigation of the possible involvement of CKI1 in processes associated with pollen formation appears warranted.

CKI1 is essential for the transition from FG5 to FG6 in the course of megagametogenesis

In the pistils of *CKI1*/*cki1-i* plants, mutant ovules were first identified by CLSM analysis in late FG5, based on distorted central vacuoles, the fuzzy structure of the cells and mislocated antipodal nuclei (phenotype I, Fig. 2 *i*, f, g). As indicated by the unfused polar nuclei, the mutant ovules had not completed the transition from FG5 to FG6 even at 48 HAE, when all wild-type ovules had reached the terminal developmental stage, FG7 (Fig. 2 *i,* j). At the terminal stage, a minor proportion of the mutant ovules, which completely lacked the central vacuole, displayed signs of a higher degree of embryo sac degradation (phenotype II, Fig. 2 *i,* h): individual cells of the embryo sac could not be identified and only a few nuclei could sometimes be distinguished. The least frequently encountered phenotype III was characterized by the presence of 10–14 nuclei in an embryo sac lacking the

central vacuole and displaying signs of partial degradation (data not shown). In *cki1-5* and *cki1-6* mutant ovules, phenotypic abnormalities were already detectable at stage FG4, and the mutant phenotype became fully penetrant at stage FG5 (Pischke et al. 2002). The *cki1-5(6)* mutant female gametophytes fell into two phenotypic categories. In the first (more frequent) category, female gametophytes appeared to be in various stages of degeneration ranging from partial to complete. The embryo sac cavity of partially degenerated female gametophytes was collapsed, but displayed evidence of cellularization. The embryo sac cavity of completely degenerated female gametophytes was collapsed and filled with brightly fluorescent material. In the second phenotypic category, the embryo sac cavity was filled with a matrix of cytoplasmic strands connecting many small vacuoles, as well as a larger than normal number of nuclei (≥16). Thus, the first and second phenotypic categories resemble the phenotypes II and III, respectively, found in *cki1-i* and *cki1-s1*. The absence of an equivalent of phenotype I and the detection of a mutant phenotype in FG4 may indicate that *cki1-5* and *cki1-6* represent alleles that are stronger than *cki1-i*.

Consequently, in spite of the partial cellularization found in the less degenerated *cki1-5(6)* embryo sacs, the pleiotropic nature of the defect did not allow Pischke et al. (2002) to limit the CKI1 function primarily to any one of the processes required for the completion of stages FG4 and FG5. These processes include a final round of mitosis, cellularization, vacuole formation, and the establishment of cell identities. In contrast, the nature of the *cki1-i* mutant phenotype I, first detected in late FG5, suggests that CKI1 function is not directly required for the completion of mitotic divisions, proper nuclei positioning and probably not for the acquisition of cell identity (Fig. 2 *i,* f, g). Comparison of the frequencies of the mutant phenotypes at late FG5 (0.3) and 48 HAE (0.5, see Table 1) indicates that at late FG5 a fraction of the *cki1-i* embryo sacs remains morphologically indistinguishable from the wild type. Also the structure of the mutant female gametophyte at 24 HAE suggests that cellularization is essentially unaffected in *cki1-i* embryo sacs (Fig. 2 *i*, g). The subsequent changes in nuclear positions and overall cell morphology (Fig. 2 *i*, i, and phenotype II in Fig. 2 *i*, h) appear to result from progressive degradation of the embryo sac due to collapse of the central vacuole, which seems to be one of the first morphologically detectable abnormalities in the mutant embryo sacs (Fig. 2 *i,* f). The identification of phenotype III suggests that the *cki1-i* mutation has pleiotropic effects on embryo sac development after FG5, as some nuclei can apparently undergo additional mitotic divisions. These data, together with the fact that the positions of nuclei were changed following the collapse of the central vacuole (Fig. 2 *i,* g, i), may imply that the integrity of the central vacuole is important for the timing and spatial distribution of specific cellular events (e.g. mitosis) during female gametophyte development.

The block in the development of *cki1-i* embryo sacs may occur very early in megagametogenesis

The embryo sac may become sensitive to a signal picked up by CKI1 starting near the completion of megaspore differentiation, as indicated by the very weak but distinct transcriptional activity of *CKI1* throughout female gametophyte development (Fig. 3). However, the earliest morphologically distinguishable consequences of the defect in the *cki1* mutants are observed only at FG4 (Pischke et al. 2002). Therefore, the immediate effects of the absence of functional CKI1 may only become morphologically manifest at FG4, or the signaling molecule perceived by CKI1 might appear only just before or concomitantly with FG4. As Pischke et al. (2002) were unable to detect any *CKI1* expression in developing embryo sacs at stages prior to FG7, no conclusion regarding the stage at which CKI1 becomes critical could be drawn from their data. The results of our analysis of *CKI1* expression are consistent with the idea that the initial block in the *cki1* female gametophyte occurs in FG4. This represents a starting point for future identification of the exact stage at which CKI1 becomes crucial for the successful completion of embryo sac development.

Recently, a number of *Arabidopsis* mutants defective in female gametophyte development have been described (Christensen et al. 1998, 2002). In the female gametophyte-specific mutant *fem1*, defects in embryo sac development resembling those found in *cki1-i* were reported. Fusion of polar nuclei is blocked during FG5/FG6 in developing *fem1* embryo sacs. Subsequent degradation of the central vacuole was hypothesized to yield the highly fluorescent material detectable in the central cavity (Christensen et al. 1998) that is the most striking phenotypic feature of the terminal stage of *fem1* embryo sac development. Though *fem1* was shown not to be allelic to *cki1-5(6)* (Pischke et al. 2002), based on the phenotypic analysis of *cki1-i*, FEM1 and CKI1 seem to affect similar aspects of embryo sac development.

The mutants affecting female gametophyte development that have been identified so far have been classified into five phenotypic categories (Drews and Yadegari 2002). However, the *cki1-i* (like the *fem1*) phenotype does not seem to fit the phenotypic criteria for any of these five categories. The most similar category (4) comprises mutants with defects in polar nuclei fusion (*gfa2, gfa3*, *maa1* and *maa3*). However, only the *gfa2* and *gfa3* mutants have been subjected to detailed phenotypic inspection by CLSM (Christensen et al. 1998). In *gfa2*, a specific block in the fusion of polar nuclei was found. Interestingly, in *gfa3*, the incompletely penetrant mutant phenotype appears as early as FG4, leading to pleiotropic defects, with the majority of mutant embryo sacs displaying a block in fusion of the polar nuclei during FG6 (Christensen et al. 1998). Thus, the fusion of polar nuclei might reflect the successful progression and/or completion of other processes involved in megaga-

metogenesis prior to FG5/FG6, as is also implied by the *cki1-i* phenotype.

CKI1 was originally implicated in the perception of the plant hormone cytokinin (Kakimoto 1996). Our data provide experimental evidence indicating that the putative sensor histidine kinase, CKI1 is a key player in processes leading to embryo sac formation. Several reports suggest the involvement of the plant growth regulators auxin (Hardtke and Berleth 1998), ethylene (Kieber and Ecker 1994; De Martinis and Mariani 1999) and cytokinin (Blintsov et al. 2000) in ovule and early seed development. However, there is no evidence for the direct interaction of CKI1 with cytokinins, or for cytokinin-dependent signal transduction via CKI1 (Hwang and Sheen 2001; Yamada et al. 2001). Thus, the putative signaling molecule that interacts with CKI1 in the regulation of female gametophyte development remains to be identified.

CKI1 is switched on temporarily after fertilization

The histochemical analysis of wild-type ovules fertilized with pollen from p*CKI1*::*uidA* transgenic lines suggests that *CKI1* expression is not solely restricted to gametophytic tissues. The first traces of transcriptional activity of *CKI1* during early endosperm development were detected at 10 HAP. By 12 HAP GUS activity was obvious (Fig. 4a), suggesting early activation of the paternally transmitted *CKI1* promoter. Recently, it has been proposed that activation of the whole paternal genome after fertilization is delayed (Vielle-Calzada et al. 2000). The delay in *CKI1* expression from the paternal chromosome after fertilization was estimated based on the recent data of Faure et al. (2002). Pollen tube penetration of the ovule was detected by 4.5 HAP, and karyogamy of the central and sperm nuclei was detected at 6–7 HAP. *CKI1* promoter-driven expression of *uidA* (Fig. 4a) is detectable by 5–6 h after central cell fertilization, hence suggesting very early activation of the paternally transmitted *CKI1* promoter in the developing endosperm. Thus, although we cannot rule out a lack of potential imprinting sites in the promoter region used to drive *uidA* in our experiments, the results rather suggest a need to reconsider the concept of genome-wide male imprinting during early seed development. Based on the current debate it seems that even though large genome fragments may be targets for genomic imprinting (Grossniklaus et al. 1998; Luo et al. 2000), silencing of the plant paternal genome during early embryo development is not a general rule (Weijers et al. 2001). Taking into account the random nature of T-DNA integration in the plant genome, one could hypothesize that sequence specificity is a significant if not decisive criterion for parent-specific regulation of gene expression in *Arabidopsis*.

Using in situ localization of mRNA, Pischke et al. (2002) detected the expression of *CKI1* in the developing endosperm 24–48 h after fertilization. In addition, our data suggest subsequent down regulation of *CKI1* transcription. The absence of detectable GUS activity at 72 HAP (Fig. 4e) suggests that *CKI1* promoter becomes inactive between 48 and 72 HAP. However, as the stability of GUS activity in the tissue is unknown, the precise time at which the *CKI1* promoter is switched-off cannot be inferred; it is possible that transcription could cease even before 48 HAP.

The endosperm-specific expression of *CKI1* early after central cell fertilization might indicate that the tissue becomes transiently sensitive to the CKI1 ligand for a short period when endosperm development is initiated. To elucidate the potential role of CKI1 in early seed development, the use of antisense and/or post-translational gene silencing (RNA interference) approaches will be necessary, as the mutant *cki1* alleles cannot be obtained in the homozygous state.

Acknowledgements We wish to thank Jiří Široký and Peter Huijser for their help and for an introduction to microscopy techniques (CLSM and scanning electron microscopy, respectively). Furthermore, we thank Tatsuo Kakimoto for the gift of *CKI1* cDNA. We also thank Jana Klánová, Hana Konečná and the ADIS Service Group for DNA sequencing and synthesis, and ZIGIA (The Centre for Functional Genomics in *Arabidopsis*, Köln). We are also grateful to Ellen Wisman for help. We are grateful to Nagavalli S. Kiran and Laura Zonia for their careful and critical reading of the manuscript. This work was supported by the Ministry of Education of the Czech Republic (Grants VS96096, MSM143100008 and LN00A081), by the INCO-Copernicus Program (Grant ERB3512-PL966135), the DFG (SPP "Molekulare Analyse der Phytohormonwirkung"), and the European Communities Biotech Program (QLRT-2000-0020). J.H. was supported by the DAAD.

References

Baumann E, Lewald J, Saedler H, Schulz B, Wisman E (1998) Successful PCR based reverse genetic screens using an *En-1* mutagenised *Arabidopsis thaliana* population generated via single-seed descent. Theor Appl Genet 97:729–734

Blintsov AN, Gussakovskaya MA, Yermakov IP (2000) Changes in the hormonal status of the *Taraxacum officinale* Web. ovary at early stages of embryogenesis. Biochemistry (Moscow) 65:192–197

Brown RC, Lemmon BE, Nguyen H, Olsen OA (1999) Development of endosperm in *Arabidopsis thaliana*. Sex Plant Reprod 12:32–42

Chaudhury AM, Berger F (2001) Maternal control of seed development. Semin Cell Dev Biol 12:381–386

Chaudhury AM., Koltunow A, Payne T, Luo M, Tucker MR, Dennis ES, Peacock WJ (2001) Control of early seed development. Annu Rev Cell Dev Biol 17:677–699

Christensen CA, King EJ, Jordan JR, Drews GN (1997) Megagametogenesis in *Arabidopsis* wild type and the Gf mutant. Sex Plant Reprod 10:49–64

Christensen CA, Subramanian S, Drews GN (1998) Identification of gametophytic mutations affecting female gametophyte development in *Arabidopsis*. Dev Biol 202:136–151

Christensen CA, Gorsich SW, Brown RH, Jones LG, Brown J, Shaw JM, Drews GN (2002) Mitochondrial GFA2 is required for synergid cell death in *Arabidopsis*. Plant Cell 14:2215–2232

De Martinis D, Mariani C (1999) Silencing gene expression of the ethylene-forming enzyme results in a reversible inhibition of

ovule development in transgenic tobacco plants. Plant Cell 11:1061–1072
Drews GN, Yadegari R (2002) Development and function of the angiosperm female gametophyte. Annu Rev Genet 36:99–124
Drews GN, Lee D, Christensen CA (1998) Genetic analysis of female gametophyte development and function. Plant Cell 10:5-17
Faure JE, Rotman N, Fortune P, Dumas C (2002) Fertilization in *Arabidopsis thaliana* wild type: developmental stages and time course. Plant J 30:481–488
Feldmann KA, Coury DA, Christianson ML (1997) Exceptional segregation of a selectable marker (Kan^R) in *Arabidopsis* identifies genes important for gametophytic growth and development. Genetics 147:1411–1422
Gasser CS, Broadhvest J, Hauser BA (1998) Genetic analysis of ovule development. Annu Rev Plant Physiol Plant Mol Biol 49:1–24
Grossniklaus U, Schneitz K (1998) The molecular and genetic basis of ovule and megagametophyte development. Semin Cell Dev Biol 9:227–238
Grossniklaus U, Vielle-Calzada JP, Hoepner MA, Gagliano WB (1998) Maternal control of embryogenesis by *MEDEA*, a *Polycomb* group gene in *Arabidopsis*. Science 280:446–450
Hable WE, Kropf DL (2000) Sperm entry induces polarity in fucoid zygotes. Development 127:493–501
Hardtke SC, Berleth T (1998) The *Arabidopsis* gene *MONOPTEROS* encodes a transcription factor mediating embryo axis formation and vascular development. EMBO J 17:1405–1411
Hartmann U, Hoehmann S, Nettesheim K, Wisman E, Saedler H, Huijser P (2000) Molecular cloning of *SVP*: a negative regulator of the floral transition in *Arabidopsis*. Plant J 21:351–360
Hecht V, Vielle-Calzada JP, Hartog MV, Schmidt EDL, Boutilier K, Grossniklaus U, de Vries SC (2001) The *Arabidopsis SOMATIC EMBRYOGENESIS RECEPTOR KINASE 1* gene is expressed in developing ovules and embryos and enhances embryogenic competence in culture. Plant Physiol 127:803–816
Hwang I, Sheen J (2001) Two-component circuitry in *Arabidopsis* cytokinin signal transduction. Nature 413:383–388
Kakimoto T (1996) CKI1, a histidine kinase homolog implicated in cytokinin signal transduction. Science 274:982–985
Kieber JJ, Ecker JR (1994) Molecular and genetic analysis of the constitutive ethylene response mutation *ctr1*. In: Coruzzi G, Puigdomenech P (eds) Plant molecular biology: molecular genetic analysis of plant development and metabolism. Springer-Verlag, Berlin, pp 193–201
Luo M, Bilodeau P, Tennis ES, Peacock WJ, Chaudhury A (2000) Expression and parent-of-origin effects for *FIS2*, *MEA* and *FIE* in the endosperm and embryo of developing *Arabidopsis* seeds. Proc Natl Acad Sci USA 97:10637–10642
Malamy JE, Benfey PN (1997) Organization and cell differentiation in lateral roots of *Arabidopsis thaliana*. Development 124:33–44
Nakamura A, Kakimoto T, Imamura A, Suzuki T, Ueguchi C, Mizuno T (1999) Biochemical characterization of a putative cytokinin-responsive His-kinase, CKI1, from *Arabidopsis thaliana*. Biosci Biotechnol Biochem 63:1627–1630
Parkinson JS, Kofoid EC (1992) Communication modules in bacteria signalling proteins. Annu Rev Genet 26:71–112
Pischke MS, Jones LG, Otsuga D, Fernandez D, Drews G, Sussman MR (2002) An Arabidopsis histidine kinase is essential for megagametogenesis. Proc Natl Acad Sci USA 99:15800–15805
Reintanz B, Lehnen M, Reichelt M, Gershenzon J, Kowalczyk M, Sandberg G, Godde M, Uhl R, Palme K (2001) *bus*, a bushy *Arabidopsis CYP79F1* knockout mutant with abolished synthesis of short-chain aliphatic glucosinolates. Plant Cell 13:351–367
Reiser L, Fischer RL (1993) The ovule and the embryo sac. Plant Cell 5:1291–1301
Schneitz K, Hülskamp M, Pruitt RE (1995) Wild type ovule development in *Arabidopsis thaliana*: a light microscope study of cleared whole-mount tissue. Plant J 7:731–749
Urao T, Yamaguchi-Shinozaki K, Shinozaki K (2000a) Two-component systems in plant signal transduction. Trends Plant Sci 5:67–74
Urao T, Shinichi M, Yamaguchi-Shinozaki K, Shinozaki K (2000b) Possible His to Asp phosphorelay signaling in an *Arabidopsis* two-component system. FEBS Lett 478:227–232
Urao T, Yamaguchi-Shinozaki K, Shinozaki K (2001) Plant histidine kinases: an emerging picture of two-component signal transduction in hormone and environmental responses. Sci STKE 20:RE18
Vielle-Calzada JP, Baskar R, Grossniklaus U (2000) Delayed activation of the paternal genome during seed development. Nature 404:91–94
Wang L, Wessler SR (1998) Inefficient reinitiation is responsible for upstream open reading frame-mediated translational repression of the maize *R* gene. Plant Cell 10:1733–1745
Weijers D, Geldner N, Offringa R, Jürgens G (2001) Seed development: early paternal gene activity in *Arabidopsis*. Nature 414:709–710
Western TL, Haughn G (1999) *BELL1* and *AGAMOUS* genes promote ovule identity in *Arabidopsis thaliana*. Plant J 18:329–336
Wisman E, Cardon GH, Fransz P, Saedler H (1998) The behaviour of the maize autonomous transposable element *En*/*Spm* in *Arabidopsis thaliana* allows efficient mutagenesis. Plant Mol Biol 37:989–999
Yamada H, Suzuki T, Terada K, Takei K, Ishikawa K, Miwa K, Yamashino T, Mizuno T (2001) The *Arabidopsis* AHK4 histidine kinase is a cytokinin-binding receptor that transduces cytokinin signals across the membrane. Plant Cell Physiol 42:1017–1023

Enclosed Publication # 4

Hejátko, J., Blilou, I., Brewer, P.B., Friml, J., Scheres, B. and Benková, E. (2006) *In situ* hybridisation technique for mRNA detection in whole mount *Arabidopsis* samples. *Nature Protocols*, **1**, 1939 – 1946. IF_{2008}= 4.170

In situ hybridization technique for mRNA detection in whole mount *Arabidopsis* samples

Jan Hejátko[1], Ikram Blilou[2], Philip B Brewer[3], Jiří Friml[1,3], Ben Scheres[2] and Eva Benková[3]

[1]Masaryk University, Department of Functional Genomics and Proteomics, Laboratory of Molecular Plant Physiology, Kamenice 5, 625 00 Brno, Czech Republic. [2]Department of Molecular Genetics, Utrecht University, 3584 CH Utrecht, The Netherlands. [3]Centre for Plant Molecular Biology, Tübingen University, 72076 Tübingen, Germany. Correspondence should be addressed to E.B. (eva.benkova@zmbp.uni-tuebingen.de)

Published online 22 November 2006; doi:10.1038/nprot.2006.333

© 2006 Nature Publishing Group http://www.nature.com/natureprotocols

High throughput microarray transcription analyses provide us with the expression profiles for large amounts of plant genes. However, their tissue and cellular resolution is limited. Thus, for detailed functional analysis, it is still necessary to examine the expression pattern of selected candidate genes at a cellular level. Here, we present an *in situ* mRNA hybridization method that is routinely used for the analysis of plant gene expression patterns. The protocol is optimized for whole mount mRNA localizations in *Arabidopsis* seedling tissues including embryos, roots, hypocotyls and young primary leaves. It can also be used for comparable tissues in other species. Part of the protocol can also be automated and performed by a liquid handling robot. Here we present a detailed protocol, recommended controls and troubleshooting, along with examples of several applications. The total time to carry out the entire procedure is ~7 d, depending on the tissue used.

INTRODUCTION

The analysis of the expression patterns of genes during plant development and after environmental or chemical treatments or in mutant background is a standard approach to investigate gene functions and genetic pathways. Several methods have been routinely used to examine the expression pattern of candidate genes. These include the use of transgenic reporter genes encoding easily detectable products, such as BETA-GLUCURONIDASE (*uidA*), GREEN FLUORESCENT PROTEIN (*GFP*) and LUCIFERASE (*LUC*), each of which can be placed under the transcriptional control of gene specific promoters; Northern blot hybridization; reverse transcriptase and PCR on isolated RNA; and ever more frequently, gene chip technology. However, these methods often fail to provide enough resolution or certainty and more reliable methods, such as immunocytochemical techniques for protein detection and *in situ* mRNA hybridization, remain necessary. Each of these above mentioned techniques has advantages and disadvantages, and mostly a combination of several of them provides a reliable picture of gene expression and its regulation on transcriptional and/or post-transcriptional levels, respectively.

Classical techniques for mRNA or protein *in situ* localization use sections of biological material. This allows better accessibility of the probe to specific, usually deeply embedded cell types and tissues. However, making quality sections is a time consuming and expensive process, demanding considerable experience and specific instrumentation. Therefore, to simplify and speed-up the entire procedure, whole mount techniques were developed. Originally, a whole mount *in situ* hybridization method was introduced and optimised for localization of transcripts in *Drosophila* embryos[1]. In animal systems, whole mount methods generally work effectively. However, their adaptation to plants was hindered by several problems resulting mostly from the poor permeability of reagents through cell walls. Previously described whole mount *in situ* hybridization techniques for plants[2–4] were successfully used for the localization of abundant mRNAs. In order to improve the limiting signal-to-background ratio and to increase the sensitivity sufficient for analysis of weakly expressed genes, we adopted these protocols, including those used for mRNA localization in *Drosophila* embryos[1] and hydras[5], and developed a functional and reproducible procedure for whole mount mRNA *in situ* hybridization in plants. The protocol is designed for easily permeable plant tissues like *Arabidopsis thaliana* root tips, lateral roots, embryos, young primary leaves, young meristems and hypocotyls. Here, we would like to stress three critical steps: (i) probe synthesis, (ii) tissue fixation and permeation (including some specific aspects of the plant tissue handling), and (iii) signal detection. Further we provide brief instructions for (iv) automation of the method using liquid handling robots and (v) experimental setup, which provides a short overview of the procedure and tissue handling to facilitate comfortable and errorless planning of the experiment. If not otherwise stated, all steps are performed under room temperature (RT, usually considered in the range 20–25 °C).

Probe synthesis

For hybridization, probes such as digoxigenin-labelled antisense RNAs can be used. There are two possibilities to generate templates for the *in vitro* transcription to prepare gene-specific, labelled ssRNA probe. (1) The DNA to be transcribed is cloned into a polylinker site of a transcription vector, which contains a promoter for T3, T7 or SP6 RNA polymerase (e.g., pBluescript, Stratagene). To synthesize the "run-off" transcript, a restriction enzyme that creates either a 5′-overhang or a blunt end is used to linearise the template before transcription. It is important to never use a restriction enzyme that produces a 3′-overhang. When the linearised DNA template has a 3′-overhang then RNA polymerase can initiate the reaction from this 3′-overhang, thus transcribing the complementary (and non-desired) strand. (2) Optionally, PCR can be used to introduce the RNA promoter sequence to a 5′end of amplified cDNA fragment (see PROCEDURE for details). Template prepared by one of the above methods is used for a labelled ssRNA probe synthesis using *in vitro* transcription in the presence of digoxigenin-11-UTP. Routinely, we test the quality of probes on agarose gels (both before and after hydrolysis, see the

PROCEDURE). Specific activity of labelled probes can be tested using dot-blot as described[6]. Once the active, labelled and RNase-free ssRNA probe is prepared, a hydrolysis step ensures the generation of short probe fragments, allowing better tissue penetration. This is particularly important when long DNA (i.e., >0.5 kb) templates are used for the *in vitro* transcription. However, we should note here that based on our experience, for localization of most mRNAs the hydrolysis step is not critical and might be omitted. Careful probe precipitation after hydrolysis and re-association in water under RNase-free conditions is critical to avoid excessive probe loss or RNase contamination.

The probe quality is of critical importance for successful *in situ* mRNA hybridization. In contrast to DNases, ubiquitous RNases do not require any cofactor for its action and RNase contamination represents one of the most severe problems during probe handling and most often hampers all experimental effort. Until the hybridization step, all solutions made from dry chemicals must be RNase free. One can ensure this by autoclaving solutions with the optional addition of 1 ml l^{-1} DEPC. Because commonly used chemicals are readily susceptible to RNase contamination, it is beneficial to store equipment, stock chemicals, prepared solutions and RNase free aliquots separately in the laboratory, only for use with RNA. Where water is mentioned, RNase-free (DEPC-treated), sterile and pure water is required (e.g. Milli-Q (Millipore) produced water, resistance ~18.2 MΩ cm at 25 °C).

Tissue fixation and permeation

Most *in situ* hybridization protocols, including ours, start with a fixation step using cross-linking by an aldehyde. The fixation time is critical, as the tissue must be properly fixed to avoid artefacts resulting from mRNA degradation and post-fixation changes in mRNA location. On the other hand, over-fixed tissue can not be properly permeated to ensure efficient probe interaction with target mRNA, which leads to a weak or no signal and could be critical mainly in cases of weak gene expression (see also TROUBLESHOOTING).

In our protocol, tissue fixation is performed in plastic tubes, routinely 50 ml Falcon tubes. The first step is infiltration of the collected material by fixation solution. Fixation for good penetrable tissues like root tips, hypocotyls and leaves is performed under shaking at RT. In case of poorly penetrable material like embryos, use of a vacuum for ~10 min is recommended. If the material sinks, this indicates proper material infiltration. Some tissues may keep floating, which is not critical for proper fixation; however, we recommend increasing the time of tissue fixation in these cases. Proper sample infiltration also facilitates later solution exchange via decantation. Home-made metal sieves, adopted to fit Falcon tubes, can be used to avoid material loss during solution exchange.

Fixation is followed by degradation of proteins bound to mRNA so that the RNA is free to interact with a labelled probe; this is usually achieved via treatment with proteinase K. While this step can be fully replaced by a brief heat denaturation, as it has been described for specimens of animal origin[5], the use of proteinase K is advantageous because it can degrade RNases potentially present in the tissue.

Because of specific properties of plant material, namely the presence of cell walls and a waxy layer on the surface of most of the plant body, additional permeation steps have to be included. These include a heptane treatment during material fixation; an alcohol stage, which also removes chlorophyll and other pigments; and finally a xylene (or a xylene substitute, e.g. Histo-Clear®) treatment. In case of persisting penetration problems, duration of these treatments can simply be prolonged according to the type of plant material. Also, prolonging the proteinase K step improves permeability of the tissue.

Signal detection

After hybridization, immunostaining reactions using Anti-Digoxigenin-AP, Fab-fragments (see REAGENTS) are used to identify specifically bound probes. Washes under restrictive conditions are critical to ensure specificity of target mRNA location. Also, the specific activity of the probe used might be critical, as too much probe leads to unspecific binding and insufficient amounts of labelled probe will reduce the signal; this is important particularly in the case of weak gene expression (see TROUBLESHOOTING). The staining time is gene- (or rather probe-) and tissue-specific and must be optimized for each probe and tissue used. A good criterion is the time when the first traces of dye appear in the control specimen when using a sense probe or no probe. Staining in the control might be used to estimate the maximum time interval of the staining, as this means that non-specific signal (e.g., resulting from unspecific antibody binding, etc.) appears. That might be critical particularly in the case of weak gene expression.

It is crucial to ensure that the observed signals specifically reflect the localization pattern of RNA of interest in every *in situ* hybridization protocol. This is particularly important for whole mount techniques because, with most probes, after a sufficiently long staining time, unspecific signals can almost always be obtained, especially in the meristematic regions. Usually, such background staining will also be observed with the sense probe controls. However, one can also validate results obtained by *in situ* detection with a parallel experiment using a corresponding knock-out mutant. If this is not available or is uninformative (e.g., due to lethality or genetic redundancy), the simultaneous use of a probe with a known staining pattern as a positive control and a non-plant RNA probe as a negative control could also be helpful to ensure that the observed experimental staining is not an artefact.

Automation of the method

Most of the described protocol consists of solution exchange under different treatment conditions (i.e., temperature). The use of suitable robotics (i.e., use of special histological robots and/or adaptation of universal liquid handling robots) is extremely advantageous. Besides human labor saving, one of the major advantages is maximal tissue protection against mechanical damage during the procedure via either vacuum or air-pressure based solution exchange applied in the liquid handling robots.

Our protocol was adopted for automation using an *in situ* dedicated robot "InSitu Pro" from Intavis[7] (http://www.intavis.com). To create a program to perform the procedure according to our protocol is rather simple as the manufacturer provides instructions for very intuitive and user friendly programming of the automate. Using this robot, Steps 23–44 (tissue permeabilization, hybridization, and washing steps until detection) — with the exception of Step 41 (preadsorbing of antibodies with plant extract) — can be performed.

© 2006 Nature Publishing Group http://www.nature.com/natureprotocols

© 2006 Nature Publishing Group http://www.nature.com/natureprotocols

Experimental setup

The first step in the entire procedure is RNA probe synthesis. As already mentioned, the probe quality and its specific activity are of critical importance. Thus, the probe synthesis should be done in advance and one should start with the rest of the procedure after the probe is successfully prepared and stored in the freezer. The next steps (i.e., tissue fixation and permeation, washing, hybridization and detection) should be done consecutively using the timeline below, which in most cases fits the working week (~5 days). It is strongly recommended to prepare all the needed solutions and equipment in advance because of the time limitations during the procedure. The above timeline is the best option; however, if necessary due to time constraints, tissue fixation could be done in advance and stored at –20 °C in ethanol.

Our protocol was optimised for *Arabidopsis* seedlings, specifically root tips, lateral roots, young primary leaves, meristems and hypocotyls and *Arabidopsis* embryos. In the case of *Arabidopsis* seedlings, we usually use 5–8-day old seedlings, grown on Murashige & Skoog (MS) medium. Seedlings are harvested into Eppendorf tubes or multi-well cell culture plates, where fixation and chlorophyll removal could easily be performed. If using a robot, after fixation and chlorophyll removal seedlings are transferred into special vials for the next part of the procedure and removed back into multi-well cell culture plates or Eppendorf tubes for the detection step. Stained seedlings are cleared or directly mounted into 50% (v/v) glycerol and inspected using bright field and/or (preferred) Nomarski (Differential Interference Contrast, DIC) optics when using 5-bromo-4-chloro-3-indolyl phosphate (BCIP) / nitroblue tetrazolium chloride (NBT) or using a confocal and/or fluorescent microscope with appropriate filter sets when using fluorescent alkaline phosphatase (AP) substrate. During all procedure from harvesting until specimen preparation, seedlings are manipulated carefully with fine tweezers.

For embryos, siliques are collected on double-sided tape, opened and embryos are carefully extruded from developing seeds under a stereomicroscope using fine tweezers, and transferred into small Petri dishes with fixative solution. Embryos are very fragile so they have to be handled with a lot of care. Even very young embryos (younger globular stage) can be extruded from developing seeds and handled in the strainers during the whole procedure. After fixation, embryos are transferred into cell strainers (40 µm diameter) by pipetting with 1 ml micropipette and handled in the strainers during the entire procedure. Once the signal is detected the reaction is stopped by 100% ethanol for 2–5 min and embryos are transferred to 50% (v/v) ethanol for 2–5 min. 50% (v/v) glycerol is added to the samples, and then they can be finally transferred to slides by pipetting using a cut 200 µl (yellow) tip. When using this protocol for other tissues, some modifications might be necessary, mainly with regard to the tissue fixation and permeation as already described for developing embryo sacs and seeds[8], and floral meristems[9].

MATERIALS

REAGENTS

- Suitable restriction endonuclease enzyme, producing 5′-overhang or blunt end
- Suitable restriction enzyme buffer
- QIAquick PCR Purification Kit (Qiagen, cat. no. 28104)
- Water, RNase-free (DEPC treated), sterile
- Usual PCR chemicals (optional)
- 10× RNA labelling mix containing 10 mM ATP, 10 mM CTP, 10 mM GTP, 6.5 mM UTP and 3.5 mM digoxigenin-11-UTP (DIG-UTP mix; Roche, cat. no. 1 277 073)
- RNase inhibitor (RNasin, 20 U μl^{-1}), 20 U per reaction (Roche, cat. no. 3335399)
- T7/T3 RNA polymerase, supplied with 10× transcription buffer (10 U μl^{-1}), 10 U per reaction (Roche, T7 RNA polymerase cat. no. 881 767, T3 RNA polymerase cat.no. 1 031 163)
- tRNA, from backer's yeast (20 mg ml^{-1}; Roche, cat. no. 109 495)
- DNase I (1 U μl^{-1}), 1 U per reaction (Fermentas, cat. no. EN 0521; RNase free)
- EDTA, 0.2 M, pH 8.0 (Carl Roth, cat. no. 8043.2)
- Lithium chloride (LiCl), 4 M (Sigma, cat. no. 21323-3)
- Ethanol, 80% (v/v) in DEPC water, 25% and 50% (v/v) in PBS buffer, 75% (v/v) in water and 100% ethanol (Merck, cat. no. 108543)
- 2× hydrolysis buffer (see REAGENT SETUP)
- Sodium acetate (NaOAc), 3 M, pH 6.0 (Sigma, cat. no. 71183)
- Acetic acid (HOAc; Sigma, cat. no. 537020)
- Polyadenylic acid (poly(A); 10 mg ml^{-1}; Roche, cat. no. 108 626)
- Isopropanol (Merck, cat. no. 109634)
- Fixative (see REAGENT SETUP)
- Histo-Clear® (National Diagnostics, cat. no. HS-200)
- n-Heptane (Merck, cat. no. 104379)
- Methanol, 100% (Carl Roth, cat. no. 7342.1)
- 10× PBS buffer (see REAGENT SETUP)
- Tween-20, 0.1% (v/v) in PBS (Sigma, cat. no. P9416)
- Fixative without heptane (see REAGENT SETUP)
- Proteinase K, stock 25 mg ml^{-1} (Roche, cat. no. 3115887)
- Glycine, 2 mg ml^{-1} in PBS (Sigma, cat. no. G7403)
- Hybridization solution (see REAGENT SETUP)
- 20× SSC (see REAGENT SETUP)
- Complete hybridization solution (see REAGENT SETUP)
- Formamide (deionized; Sigma, cat. no. F7503; see REAGENT SETUP)
- 2× SSC, and 0.2× SSC supplemented with 0.1% (v/v) Tween-20
- PBS, supplemented with 0.1% (v/v) Tween-20, and with or without 1% (w/v) BSA (Serva, cat. no. 11930; see REAGENT SETUP)
- Plant extract (see REAGENT SETUP)
- Anti-Digoxigenin-AP, Fab-fragments (Roche, cat. no. 11 093 274 910)
- ALP buffer (see REAGENT SETUP)
- Levamisol, used as 2 mM in ALP buffer (Sigma, cat. no. L9756)
- NBT, stock 50 mg ml^{-1} (Roche, cat. no. 1 383 213) in 70% (v/v) N,N dimethylformamid (DMF) (Merck, cat. no 103034)
- BCIP, stock 50 mg ml^{-1} in DMF (Roche, cat. no. 1 383 221)
- Chloral hydrate clearing solution (see REAGENT SETUP)
- Glycerol, 50% (v/v) in water (Carl Roth, cat. no. 3783.1)

EQUIPMENT

- Sieves (cell strainer 70 µm for seedlings and 40 µm for embryos; VWR/BD Falcon, cat. no. 352340)
- Vacuum pump (water jet type or comparable with desiccator; e.g. Savant)
- Microscope (DIC, epifluorescence and/or confocal laser scanning; e.g. Leica or Olympus)
- DNA electrophoresis equipment (e.g. Biometra)
- Thermocycler (e.g. Perkin Elmer)
- Thermoblock (e.g. Eppendorf), required temperatures 37 °C, 40 °C, 55 °C, 70 °C and 94 °C
- Cuvettes or multiple-well plates (e.g. cell culture plates) (e.g. IWAKI)
- Standard plastic labware, glass and instrumentation (Eppendorf and Falcon tubes, cylinders, beakers, vacuum concentrator (e.g. SpeedVac, Savant; optional), rotary shaker (or similar), spectrophotometer, etc.)
- Liquid handling robot (e.g. InSitu Pro, Intavis; optional)

! CAUTION Carefully clean all instruments, such as forceps, pipettes, etc., by dipping in 100% ethanol. If necessary, laboratory glass and metal parts can also be autoclaved or baked at 180 °C for 3 h to degrade RNases. Alternatively, washing in 0.4 M NaOH (Carl Roth, cat. no. 6771.2) with

subsequent rinsing in sterile, RNase-free water also reduces a risk of possible RNase contamination.

REAGENT SETUP

RNase-free water Add 1 ml l^{-1} DEPC (Sigma, cat. no. D5758), shake vigorously to get DEPC into solution, incubate for ~2 h or overnight and autoclave properly to inactivate remaining DEPC. ! CAUTION DEPC is a suspected carcinogen; wear gloves and work in a fume hood while handling DEPC. ▲ CRITICAL DEPC cannot be added to chemicals containing amino groups, e.g. Tris (Tris inactivates DEPC in the concentration usually used, i.e. 0.1% (v/v)).

2× hydrolysis buffer (pH 10.2) For 1 ml 2× hydrolysis buffer mix 240 µl 0.5 M Na_2CO_3 (Carl Roth, cat. no. 6885.1), 160 µl 0.5 M $NaHCO_3$ (Carl Roth, cat. no. A135.1) and 600 µl H_2O.

Fixative 4% (w/v) paraformaldehyde (Sigma, cat. no. P6148), 15% (v/v) DMSO (Carl Roth, cat. no. 4720.1) and 0.1% (v/v) Tween-20 in PBS. 10% (w/v) paraformaldehyde in water is prepared as follows: 10 g of paraformaldehyde powder is dissolved in 100 ml of water by heating to 60–70 °C (use glass beaker covered with aluminum foil) and continuous stirring. One or two drops of 1 N NaOH are added until the solution becomes clear. The solution is cooled down before use. Best results are achieved with freshly prepared paraformaldehyde. ! CAUTION Carefully prepare and use paraformaldehyde in a fume hood; take care handling DMSO as it readily penetrates cellular membranes.

10× PBS buffer 1.3 M NaCl (Carl Roth, cat. no. 3957.2), 70 mM Na_2HPO_4 (Carl Roth, cat. no. 4984.1), 30 mM NaH_2PO_4 (Carl Roth, cat. no. 2370), pH 7.4.

Hybridization solution 50% (v/v) formamide in 5× SSC, 0.1% (v/v) Tween-20 and 0.1 mg ml^{-1} of heparin (Sigma, cat. no. H4784).

20× SSC 3 M NaCl, 300 mM sodium citrate (Na_3 citrate; Carl Roth, cat. no. 3580.2), pH adjusted to 7.0 with 1 M HCl (Carl Roth, cat. no. 4625.2). Other SSC dilutions needed 5×, 2× and 0.2×.

Complete hybridization solution Hybridization solution supplemented with 1 mg ml^{-1} of denatured Herring sperm DNA (94 °C for 5 min, then quickly cooled down on ice; Roche, cat. no. 223646). Optionally use 150 µg ml^{-1} tRNA and 500 µg ml^{-1} poly(A) instead.

50% (v/v) formamide 50% (v/v) formamide in 2× SSC, 0.1% (v/v) Tween-20.

Plant extract Prepared from wild-type seedlings. As a lot of material is needed, seedlings are either grown in liquid medium (1.5 ml of *Arabidopsis* seeds grown in 500 ml of 1/2 GM medium for 11 days), or germinated on ~ 5 plates (12 cm × 12 cm) for 4 d. Advantage of cultivation in liquid medium is that you will get more material and it is easier to harvest. Seedlings are fixed in a fixative solution (without heptane), dried with tissue paper and frozen in liquid nitrogen. After grinding them in a mortar they are homogenized with 5 to 10 ml of 80% (v/v) acetone (per mortar, you can add more acetone until you have a liquid solution), then vortexed vigorously and left shaking overnight (ON) at 4 °C. Spin-down at 13,000*g* for 5 min at 4 °C, remove the supernatant and air dry in the desiccator. The powder can be stored at –20 °C for 2–3 months.

ALP buffer 0.1 M Tris-HCl, pH 9.5 (USB, cat. no. 22676), 0.1 M NaCl, 50 mM $MgCl_2$ (J.T. Baker, cat. no. 0162), 0.1% (v/v) Tween-20. ! CAUTION Because of its instability, always add freshly prepared $MgCl_2$.

Chloral hydrate clearing solution 240 g chloral hydrate (Sigma, cat. no. C8383), 23.8 ml glycerol (Carl Roth, cat. no. 3783.1) and 90 ml H_2O.

1/2 GM 0.5× MS salt mixture (Duchefa Biochemie, cat. no. M0221.0005), 1% (w/v) saccharose (Carl Roth, cat. no. 4621.2), 0,5g l^{-1} 2-[N-morpholino]ethanesulfonic acid (MES; Sigma, cat. no. M8250)

EQUIPMENT SETUP

Hybridization and liquid handling Hybridization of seedlings might be done in Eppendorf tubes; however, we prefer multi-well cell culture plates (usually we use 12-well plates), as these are most suitable for specimen handling, particularly for embryos and young seedlings, and ensures minimal specimen damage during solution exchange by pipetting. When pipetting, take care to avoid aspirating or damaging the material, which is very soft and fragile, particularly after permeabilization. Use of a liquid handling robot that uses vacuum and/or air pressure to exchange solutions (e.g. Intavis InSitu Pro, more details at http://www.intavis.com) overcomes this problem. Hybridization under restrictive conditions (i.e. mainly proper temperature) is important for the specific probe binding and might be an issue of optimization.

PROCEDURE

Preparation of a DIG labelled probe

1| Digest 10 µg of plasmid carrying cDNA of your gene (or its part) under T3 or T7 promoter (see INTRODUCTION) with the appropriate restriction enzyme (5′-overhang or blunt end, 10 U $µg^{-1}$ DNA, usually at 37 °C for ~ 2–3 h).
▲ CRITICAL STEP It is important to never use a restriction enzyme that produces a 3′-overhang. See INTRODUCTION for more details.

2| Use QIAquick PCR Purification Kit according to the manufacturer's instructions to purify the DNA template. Take care to obtain an RNase-free sample.
▲ CRITICAL STEP Use RNase-free water (usually 2 × 50 µl) to elute DNA and a vacuum concentrator to reach the desired DNA concentration (optimal at least 100 ng $µl^{-1}$, estimated by spectrophotometer at 260/280 nm). Optional: Use PCR to introduce the RNA promoter sequence to a 5′ end of amplified cDNA fragment, see **Box 1**.

3| Mix the following (use RNase-free solutions), add x µl of DNA template and water according to used DNA concentration to a final volume of 25 µl:

0.5–1 µg DNA template	x	µl
H_2O	x	µl
10× transcription buffer	2.5	µl
DIG-UTP mix	2.5	µl
RNasin (20 U $µl^{-1}$)	1	µl
T7/T3 RNA polymerase (10 U $µl^{-1}$)	1	µl
Total volume	25	µl

4| Incubate for 2 h at 37 °C. If using SP6 RNA polymerase incubate at 40 °C.

5| Add 2 µl yeast tRNA (20 mg ml^{-1}) and 1 µl DNase I (1 U $µl^{-1}$, RNase-free).

6| Incubate for 15 min at 37 °C.

© 2006 Nature Publishing Group http://www.nature.com/natureprotocols

BOX 1 | PCR-BASED GENERATION OF TEMPLATE FOR RNA PROBE SYNTHESIS

1. Design a 5′- (upper) primer with the following extension (for T7 RNA polymerase): 5′- CCA AGC TTC TAA TAC GAC TCA CTA TAG GGA GA/.-3′ followed with a gene specific sequence of ~18 bp length and a 3′- (lower) gene specific primer without any extension.
2. Perform PCR; in the first four cycles use an annealing temperature (a.t.) of ~2–3 °C lower then a.t. calculated for the respective pair of primers.
3. Check PCR-product on an agarose gel. Purify PCR-product using QIAquick PCR Purification Kit and elute in 50 µl 10 mM Tris-HCL, pH 8.0 or water.
4. Estimate DNA concentration on an agarose gel or with a spectrophotometer at 260/280 nm. The PCR product can directly be used without further processing as a template for the *in vitro* transcription using T7 RNA polymerase.

© 2006 Nature Publishing Group http://www.nature.com/natureprotocols

7| Put on ice and add 2 µl EDTA (0.2 M, pH 8.0), 2.5 µl LiCl (4 M) and 75 µl ethanol.

8| Precipitate for at least 30 min at –70 °C (or >2 h at –20 °C).

9| Spin-down in a centrifuge (30 min, 13 k.r.p.m. at 4 °C).

10| Wash the pellet twice with 80% (v/v in DEPC water) ethanol.

11| After drying (~ 5 min in the SpeedVac or in the laminar box at RT until any liquid disappears), dissolve the pellet in 100 µl RNase-free water.

12| Check 5 µl of the probe on a 1% agarose mini gel. A single band should be visible. A slight smear usually appears as a result of the tRNA addition during co-precipitation.
■ **PAUSE POINT** Labelled probe can be stored at –80 °C for up to one year; aliquot probe and avoid repeated freezing and thawing.

13| Add 95 µl of RNA solution (labelled probe) to 95 µl of 2× hydrolysis buffer.

14| Incubate at 60 °C to get RNA fragments with an average length of 100–200 nts.
▲ **CRITICAL STEP** Hydrolysis time is calculated from the formula: $t = (L_0 - L_f) / (k \times L_0 \times L_f)$, where t = time in min, L_0 = initial fragment length in kb, L_f = final fragment length in kb, and k = rate constant (~ 0.11 kb min^{-1}) (ref. 10).

15| Put on ice and immediately add the following:

HOAc	1 µl	(final conc. 0.5%, v/v)
NaOAc (3 M; pH 6)	7 µl	(final conc. 0.1 M)
tRNA (yeast; 20 mg ml^{-1})	1 µl	(final conc. 100 µg ml^{-1})
poly(A) (10 mg ml^{-1})	1 µl	(final conc. 50 µg ml^{-1})

16| Precipitate with 210 µl (= 1 volume) isopropanol for at least 1 h at –20 °C.

17| Pellet RNA by centrifugation (45 min, 13 k.r.p.m. at 4 °C).

18| Wash the pellet carefully two times with cold 80% (v/v in DEPC water) ethanol.

19| After drying, dissolve pellet in 100 µl H_2O. Specific activity can be determined by dot blotting if required.

Plant material fixation and chlorophyll removal

20| Fix whole seedlings in a 1:1 mixture of fixative and heptane, for 45 min on a rotary shaker at room temperature. Shake the mixture vigorously for at least 15 min immediately prior to use.
▲ **CRITICAL STEP** Fixation times of other tissue must be optimised (see INTRODUCTION). In case of probing embryos, they have to be dissected from ovules in fixative without heptane and then fixed under vacuum for 1–3 h. After fixation, embryos are transferred to 40 µm Falcon cell strainer.
▲ **CRITICAL STEP** Fixation must be done immediately after material dissection to avoid mRNA degradation and delocalization in the analysed plant tissue.

21| Remove chlorophyll by incubation for 2× 5 min in methanol and 3× 5 min in ethanol.

22| Store in 100% ethanol overnight at –20 °C.
■ **PAUSE POINT** Under these conditions, material can be stored for up to several days.

Permeabilization and hybridization

23| Permeabilize samples by incubation for 30 min in a 1:1 mixture of ethanol and Histo-Clear®.

24| Wash twice for 5 min in ethanol.

25| Rehydrate in 75% ethanol (v/v in water), 50% ethanol (v/v in PBS) and 25% ethanol (v/v in PBS) for 10 min each.

26| Refix samples in fixative (without heptane) for 20 min at RT.

27| Wash twice for 10 min in 0.1% (v/v) Tween-20 in PBS.

28| Digest with proteinase K for 15 min (use final concentration 125 μg ml^{-1} in water).
▲ **CRITICAL STEP** Working concentration of proteinase K is a matter of optimization and might vary substantially (ranging from ~10 to 150 μg ml^{-1}).

29| Stop the digest with glycine (2 mg ml^{-1}) in PBS for 5 min.

30| Wash twice for 10 min in 0.1% (v/v) Tween-20 in PBS.

31| Refix material in fixative (without heptane) for 20 min at RT.

32| Wash twice for 10 min in 0.1% (v/v) Tween-20 in PBS.

33| Wash for 10 min in hybridization solution.

34| Pre-hybridize for 1 h at 55 °C in hybridization solution with gentle shaking.

35| Hybridize for 16 h at 55 °C in complete hybridization solution (supplemented with the denatured Herring sperm) and containing 20–100 ng denatured probe per ml of the hybridization solution (denature probe by incubating the hybridization mix at 70 °C for 10 min just before hybridization).
▲ **CRITICAL STEP** Concentration of probe requires certain optimization.
? TROUBLESHOOTING

Washing

36| Wash samples three times (10 min, 60 min and 20 min) in 50% (v/v) formamide, 2× SSC, 0.1% (v/v) Tween-20 at 55 °C.

37| Wash samples for 20 min in 2× SSC, 0.1% (v/v) Tween-20 at 55 °C.

38| Wash samples twice for 20 min in 0.2× SSC, 0.1% (v/v) Tween-20 at 55 °C.

39| Wash samples three times for 10 min in PBS, 0.1% (v/v) Tween-20 at RT.

40| Preincubate samples in PBS, 0.1% (v/v) Tween-20 with 1% (w/v) BSA for 90 min at RT.

41| Preabsorb the 1:2,000 diluted Anti-Digoxigenin-AP, Fab-fragments in 5 ml per sample of PBS, 0.1% (v/v) Tween-20 with 1% (w/v) BSA, supplemented with 3 mg plant extract for at least 3 h at 4 °C.

42| Incubate samples ON in the above solution (preabsorbed anti-DIG-AP antibody) in the dark at RT.

Washing and detection

43| Wash eight times for 20 min in PBS, 0.1% (v/v) Tween-20.

44| Incubate twice for 10 min in ALP buffer with (freshly added) 50 mM $MgCl_2$.

45| Perform the AP staining reaction in the dark at RT in ALP buffer containing 2 mM levamisole, 2.25 μl NBT and 1.75 μl BCIP per ml (in case of embryos, double the concentration of BCIP and NBT). Alternatively, for the detection of the probe (secondary antibody), a fluorescent AP substrate could be used (e.g. HNPP Fluorescent Detection Set; Roche, cat. no. 1 758 888; use according to the manufacturer's instructions). The sensitivity is slightly lower in comparison to the BCIP/NBT substrate;

© 2006 Nature Publishing Group http://www.nature.com/natureprotocols

however, confocal microscopy could be used for the observation of the resulting fluorescent precipitate that allows detailed analysis with cellular resolution.

46| Inspect the material every 30 min, stop staining briefly with 100% ethanol and keep in 50% ethanol (v/v) for ~ 15 min.
▲ **CRITICAL STEP** Stopping of reaction in water is not sufficient, particularly in case of longer storage of slides before microscopy.
Optionally, use a negative control (samples without probe or with sense probe) to estimate a time of the staining reaction (stop the reaction as the first traits of the dye will appear in the negative control).

47| Mount tissue in 50% (v/v) glycerol and proceed with microscope analysis.
■ **PAUSE POINT** Specimens mounted in glycerol could be stored at 4 °C before microscopy analysis; however, minimal delay in the microscopy analysis is preferred.
Optional: If Nomarski (DIC) optics is used for inspection of specimens, tissue clearing is recommended by (i) mounting specimen into chloral hydrate clearing solution or (ii) using the tissue clearing protocol in ref. 11.

● **TIMING**
Steps 1–2, Template generation: 5 h – 1 d
Steps 3–12, Synthesis of DIG labelled ssRNA: 5 h
Steps 13–19, Hydrolysis of ssRNA: 3 h
Steps 20–22, Fixation and chlorophyll removal: 3 h – 2 d
Steps 23–35, Permeabilization and hybridization: 1 d
Steps 36–42, Washing: 1 d
Steps 43–47, Washing and detection: 1 d

? TROUBLESHOOTING
See **Table 1** for troubleshooting advice.

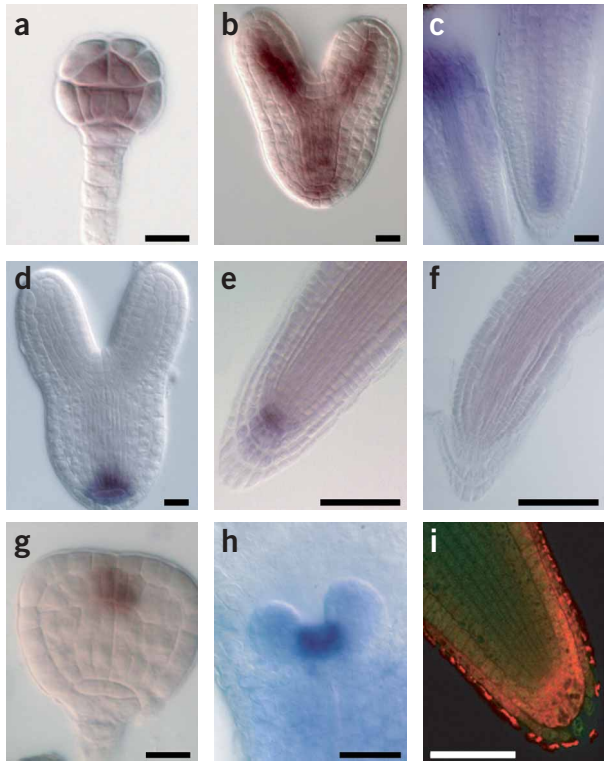

Figure 1 | Examples of various whole-mount *in situ* mRNA localizations in different plant tissues. *MONOPTEROS* mRNA in 16-cell (**a**) and heart (**b**) stage embryos confirming results from tissue sections[12]. *PIN1* (**c**), *PIN4* (**d**,**e**) and *PIN4* sense control (**f**), mRNA localization in torpedo stage embryo (**d**) and *Arabidopsis* seedling root tips (**c**,**e**,**f**) as described previously[13]. *SHOOT MERISTEMLESS1* mRNA in triangular stage embryo (**g**) and seedling shoot apical meristem (**h**) as shown previously[14]. (**i**) *CKI1* mRNA in the root tip of 1-d old seedlings as visualized by red fluorescence, using confocal microscope. Detection is with HNPP Fluorescent Detection Set. Scale bars, 10 μm (**a**,**b**,**d**,**g**), 25 μm (**c**,**e**,**f**,**i**) and 50 μm (**h**).

TABLE 1 | Troubleshooting table.

Problem	Reason	Possible steps affected	Possible solution
Low yield or no probe synthesized	RNase contamination	1–19	Check all the chemicals for RNase contamination. Use freshly prepared, RNase-free chemicals
			Work carefully, wear gloves while handling RNA and RNase free chemicals.
			Use RNase free labware
			Avoid dust and excessive air circulation in the lab
	Low quality of the template DNA	1–2	Check the DNA template and its purity, use Qiagen columns to purify it
No or weak signal	Low gene expression		Use PCR product from an entire cDNA (if still specific)
			Extend the AP staining interval during immunodetection
			Use less stringent washing conditions or omit the last washing step. However, it can lead to increased unspecific background signal
			Perform the probe hydrolysis step, if omitted

© 2006 Nature Publishing Group http://www.nature.com/natureprotocols

TABLE 1 | Troubleshooting table (continued).

Problem	Reason	Possible steps affected	Possible solution
	Conditional gene expression		Check available expression profiling databases and/or use RT-PCR to identify the tissue(s) and condition(s), when your gene is expressed
	Over-fixed tissue	20	Lower the time of fixation, fix the tissue at 4 °C
			Extend the proteinase K treatment; however, consider that extended proteinase K might lead to higher background and there is a trade-off between longer proteinase K treatment and quality preservation of the tissue
	Not efficiently fixed tissue or RNA degradation before fixation	20	Be sure that your fixative is fresh and of correct pH
			Increase the time of fixation, fix the tissue at RT
			Fix the tissue immediately after dissection
	Probe degraded	1–19	Avoid possible RNase contamination
	Probe not efficiently labelled	3–4	Check the probe by a dot-blot
			Repeat the labelling with fresh (new) chemicals
	Immunodetection failed	40–42	Check the chemicals for immunodetection by a dot-blot Repeat the immunodetection with freshly prepared (new) chemicals (including dilution buffers)
High background	Probe concentration too high	35	Decrease the amount of the probe
	Highly transcriptionally active tissue (e.g., meristems)		Decrease the staining time
			Prolong the washing times or use more stringent washing conditions
			Lower the concentration of both the primary and secondary antibodies
Unspecific signal	Sequence similarity of the probe		Select a more specific probe from the sequence of your gene

ANTICIPATED RESULTS

Figure 1 shows typical staining results of the whole mount *in situ* hybridization technique for mRNA detection in three different organs: embryos of different developmental stages (**Fig. 1a,b,d,g**), seedling root tips (**Fig. 1c,e,f,i**) and seedling shoot meristem (**Fig. 1h**). Signals are observed by light microscope either using DIC (**Fig. 1 a–h**) or confocal microscope (**Fig. 1i**).

ACKNOWLEDGMENTS J.H. was supported by the Ministry of Education of the Czech Republic (LC06034, MSM0021622415); P.B. and J.F. by the VolkswagenStiftung and the EMBO Young Investigator Program; E.B. by the Margarete von Wrangell-Habilitations program.

COMPETING INTERESTS STATEMENT The authors declare that they have no competing financial interests.

Published online at http://www.natureprotocols.com
Reprints and permissions information is available online at http://npg.nature.com/reprintsandpermissions

1. Tautz, D. & Pfeifle, C. A non-radioactive *in situ* hybridization method for the localization of specific RNAs in *Drosophila* embryos reveals translational control of the segmentation gene hunchback. *Chromosoma* **98**, 81–85 (1989).
2. de Almeid Engler, J., Van Montagu, M. & Engler, G. Whole-mount *in situ* hybridization in plants. *Methods Mol. Biol.* **82**, 373–384 (1998).
3. Bennett, M.J. *et al.* *Arabidopsis* AUX1 gene: a permease-like regulator of root gravitropism. *Science* **273**, 948–950 (1996).
4. Ludevid, D., Hofte, H., Himelblau, E. & Chrispeels, M.J. The expression pattern of the tonoplast intrinsic protein gamma-TIP in *Arabidopsis thaliana* is correlated with cell enlargement. *Plant Physiol.* **100**, 1633–1639 (1992).
5. Plickert, G., Gajewski, M., Gehrke, G., Gausepohl, H., Schlossherr, J. & Ibrahim, H. Automated *in situ* detection (AISD) of biomolecules. *Dev. Genes Evol.* **207**, 362–367 (1997).
6. *Nonradioactive In Situ Hybridisation Application Manual,* 2nd edition, 51–56 (Boehringer Manheim 1996).
7. Friml, J., Benková, E., Mayer, U., Palme, K. & Muster, G. Automated whole-mount localization techniques for plant seedlings. *Plant J.* **34**, 115–124 (2003).
8. García-Aguilar, M., Dorantes-Acosta, A., Pérez-España, V. & Vielle-Calzada, J.P. Whole-mount *in situ* mRNA localization in developing ovules and seeds of *Arabidopsis*. *Plant Mol. Biol. Reporter* **23**, 279–289 (2005).
9. Zachgo, S., Perbal, M.C., Saedler, H. & Schwarz-Sommer, Z. *In situ* analysis of RNA and protein expression in whole mounts facilitates detection of floral gene expression dynamics. *Plant J.* **23**, 697–702 (2000).
10. Fisher, H.W. & Williams, R.C. Electron microscopic visualization of nucleic acids and of their complexes with proteins. *Annu. Rev. Biochem.* **48**, 649–679 (1979).
11. Malamy, J.E. & Benfey, P.N. Organization and cell differentiation in lateral roots of *Arabidopsis thaliana*. *Development,* **124**, 33–44 (1997).
12. Hamann, T., Benková, E., Bäurle, I., Kientz, M. & Jürgens, G. The *Arabidopsis BODENLOS* gene encodes an auxin response protein inhibiting MONOPTEROS-mediated embryo patterning. *Genes & Dev.* **16**, 1610–1615 (2002).
13. Friml, J. *et al.* AtPIN4 mediates sink driven auxin gradients and patterning in *Arabidopsis* roots. *Cell,* **108**, 661–673 (2002).
14. Blilou, I. *et al.* The PIN auxin efflux facilitator network controls growth and patterning in *Arabidopsis* roots. *Nature,* **433**, 39–44 (2005).

© 2006 Nature Publishing Group http://www.nature.com/natureprotocols

Enclosed Publication # 5

Hejátko, J., Ryu, H., Kim, G.T., Dobešová, R., Choi, S., Choi, S.M., Souček, P., Horák, J., Pekárová, B., Palme, K., Brzobohatý, B. and Hwang, I. (2009) The histidine kinases CYTOKININ-INDEPENDENT1 and ARABIDOPSIS HISTIDINE KINASE2 and 3 regulate vascular tissue development in *Arabidopsis* shoots. *Plant Cell*, **21**, 2008-2021. IF_{2008}= 9.296

The Plant Cell, Vol. 21: 2008–2021, July 2009, www.plantcell.org © 2009 American Society of Plant Biologists

The Histidine Kinases CYTOKININ-INDEPENDENT1 and ARABIDOPSIS HISTIDINE KINASE2 and 3 Regulate Vascular Tissue Development in *Arabidopsis* Shoots [W]

Jan Hejátko,[a,1,2] Hojin Ryu,[b,1] Gyung-Tae Kim,[c,d] Romana Dobešová,[a] Sunhwa Choi,[b] Sang Mi Choi,[b] Přemysl Souček,[e,f] Jakub Horák,[a] Blanka Pekárová,[a] Klaus Palme,[g] Břetislav Brzobohatý,[e,f] and Ildoo Hwang[b,2,3]

[a] Department of Functional Genomics and Proteomics, Institute of Experimental Biology, Faculty of Science, Masaryk University, CZ-61137, Brno, Czech Republic

[b] Department of Life Sciences and Functional Genomics Center, Pohang University of Science and Technology, Pohang 790-784, Korea

[c] Department of Molecular Biotechnology, Dong-A University, Busan 604-714, Korea

[d] Environmental Biotechnology National Core Research Center, Gyeongsang National University, Jinju 660-701, Korea

[e] Institute of Biophysics AS CR, CZ-612 65, Brno, Czech Republic

[f] Mendel University of Agriculture and Forestry in Brno, CZ-613 00, Brno, Czech Republic

[g] Institut für Biologie II/Botany, Freiburg Institute of Advances Studies, Centre of Biological Signaling Studies, Faculty of Biology, University of Freiburg, D-79104 Freiburg, Germany

The development and activity of the procambium and cambium, which ensure vascular tissue formation, is critical for overall plant architecture and growth. However, little is known about the molecular factors affecting the activity of vascular meristems and vascular tissue formation. Here, we show that the His kinase CYTOKININ-INDEPENDENT1 (CKI1) and the cytokinin receptors ARABIOPSIS HISTIDINE KINASE2 (AHK2) and AHK3 are important regulators of vascular tissue development in *Arabidopsis thaliana* shoots. Genetic modifications of CKI1 activity in *Arabidopsis* cause dysfunction of the two-component signaling pathway and defects in procambial cell maintenance. *CKI1* overexpression in protoplasts leads to cytokinin-independent activation of the two-component phosphorelay, and intracellular domains are responsible for the cytokinin-independent activity of CKI1. *CKI1* expression is observed in vascular tissues of inflorescence stems, and CKI1 forms homodimers both in vitro and in planta. Loss-of-function *ahk2* and *ahk3* mutants and plants with reduced levels of endogenous cytokinins show defects in procambium proliferation and an absence of secondary growth. CKI1 overexpression partially rescues *ahk2 ahk3* phenotypes in vascular tissue, while the negative mutation CKI1^{H405Q} further accentuates mutant phenotypes. These results indicate that the cytokinin-independent activity of CKI1 and cytokinin-induced AHK2 and AHK3 are important for vascular bundle formation in *Arabidopsis*.

INTRODUCTION

Vascular tissue formation in plants is a process with broad developmental and physiological consequences. Factors regulating the proper formation of vascular tissue affect important developmental processes in plants, including the establishment of apical/basal symmetry during embryogenesis (Friml et al., 2003), organogenesis (Scheres et al., 1995; Mähönen et al., 2000), adaxial/abaxial cell fate determination (Emery et al., 2003; Prigge et al., 2005), and cell elongation and differentiation (Szekeres et al., 1996; Cano-Delgado et al., 2004).

Development of vascular tissue entails the differentiation of primary phloem and xylem from procambium, which contains vascular stem cells. Secondary vascular growth is characterized by vascular cambium originating from procambium and interfascicular cambium differentiating from phloem parenchyma and starch sheath cells (Altamura et al., 2001). The mitotic activity and differentiation of vascular and interfascicular cambial cells leads to the formation of secondary xylem and secondary phloem (Altamura et al., 2001; Ye et al., 2002).

Phytohormones appear to be regulatory factors of both primary and secondary vascular growth. Polar auxin transport is presumed to be necessary for the continuity of procambium (Jacobs, 1952; Sachs, 2000), and gibberellins are positive regulators of biomass production in hybrid aspen (*Populus tremula* × *Populus tremuloides*; Eriksson et al., 2000). Cytokinins have been suggested to be important regulators of primary vascular growth (Aloni, 1987; Medford et al., 1989), but their role in the regulation of procambium is just starting to emerge. Two-component signaling, wherein a His kinase receptor transfers a phosphate to downstream response regulators, is key for the

[1] These authors contributed equally to this work.
[2] These authors contributed equally to this work.
[3] Address correspondence to ihwang@postech.ac.kr.
The authors responsible for distribution of materials integral to the findings presented in this article in accordance with the policy described in the Instructions for Authors (www.plantcell.org) are: Jan Hejátko (hejátko@sci.muni.cz) and Ildoo Hwang (ihwang@postech.ac.kr).
[W] Online version contains Web-only data.
www.plantcell.org/cgi/doi/10.1105/tpc.109.066696

cytokinin response (Hwang and Sheen, 2001; Kim et al., 2006). Cytokinin-induced signaling via its receptor ARABIOPSIS HISTIDINE KINASE4 (AHK4) and the type-B response regulators ARR1, ARR10, and ARR12 is necessary for procambium formation in *Arabidopsis thaliana* roots (Scheres et al., 1995; Mähönen et al., 2000; Yokoyama et al., 2007). Reduction of endogenous cytokinins by ectopic overexpression of *CYTOKININ OXIDASE/DEHYDROGENASE1* (*CKX1*) or *CKX2* results in the exclusive formation of protoxylem in root vascular bundles (VBs) (Mähönen et al., 2000, 2006a). The role of cytokinin in vascular tissue formation is further suggested by the vascular tissue-specific expression of genes involved in cytokinin biosynthesis (Miyawaki et al., 2004; Zhao et al., 2005) and transport (Hirose et al., 2005, 2008). Factors involved in cytokinin signaling in poplar (*Populus* spp; Nieminen et al., 2008) and cytokinin biosynthesis in *Arabidopsis* (Matsumoto-Kitano et al., 2008) were shown to be principal regulators of the cambium activity and positive regulators of the radial growth via secondary thickening. Nonetheless, the nature of cytokinin action in the primary vascular meristems of shoots, which supply the majority of economically useful plant biomass, is still largely unknown. In addition to hormonal regulations, recent studies of dodeca-peptides, *CLV3/ESR-related41* (*CLE41*) and *CLE44*, and their receptor, *PHLOEM INTERCALTED WITH XYLEM*, showed that non-cell-autonomous communication between phloem and procambium is essential for procambium proliferation and polarity as well as xylem differentiation in the VB development (Fisher and Turner, 2007; Hirakawa et al., 2008). However, although few molecular factors regulating individual processes during vascular tissue formation and differentiation have been identified (Fukuda, 2004; Carlsbecker and Helariutta, 2005; Baucher et al., 2007), our knowledge of the molecular regulators of procambium and vascular cambium is still fragmentary.

Here, we report that the His kinase CYTOKININ-INDEPENDENT1 (CKI1) is important for vascular development via the regulation of procambium proliferation and/or the maintenance of its identity. Genetic manipulation of CKI1 activity leads to abnormal two-component signaling and defects in vascular tissue formation in *Arabidopsis* shoots. Cytokinin depletion and mutations in the cytokinin receptors *AHK2* and *AHK3* result in defects in vascular tissue formation in the inflorescence stem. Collectively, these results suggest that the two-component phosphorelay system is a key regulatory pathway for VB development in *Arabidopsis* shoots.

RESULTS

CKI1 Is Expressed in Specific Cell Types of VBs in *Arabidopsis* Inflorescences

To investigate the physiological function of the putative sensor His kinase CKI1 in *Arabidopsis* sporophyte development, we first determined the transcriptional activity of *CKI1* in *ProCKI1:uidA* and *ProCKI1:R12-uidA* transgenic lines that carry the *uidA* marker gene under the control of the *CKI1* promoter (Hejátko et al., 2003; Figure 1A; see Supplemental Figure 1 online). In *ProCKI1:uidA* and *ProCKI1:R12-uidA* plants (see Methods), β-glucuronidase (GUS) activity was mostly detected in the vascular tissue of all floral organs, the top of the inflorescence stem and flower pedicels, and in the branching points adjacent to axillary meristems (Figures 1Aa to 1Ac and 1Ae). Weak but distinct GUS activity was also detectable in male sporogenous tissue (Figure 1Ad). In transverse sections of inflorescence stems, GUS activity was limited to specific cell types of VBs (Figure 1Ba).

To confirm the relevance of the GUS data with *CKI1* expression, the localization of *CKI1* mRNA and CKI1 protein was determined in situ on cross sections of inflorescence stems (Figure 1B). Similar to what was seen for GUS activity, *CKI1* mRNA was detected in differentiating xylem cells and in VB sheath cells (Figure 1Bb). Antibodies raised against the extracellular domain of CKI1 ($\alpha CKI1_{ED}$) identified the protein in the procambium of VBs, with the most intense signals in the VB sheath cells located at the lateral procambium borders (Figures 1Bc and 1Bd). Weak CKI1 signals were also distinguishable in the xylem (Figure 1B; for the specificity of αCKI_{ED}, see Supplemental Figure 2 online). The absence of *CKI1* promoter activity and *CKI1* mRNA in the procambium suggests the presence of a signal for procambial CKI1 localization. This was confirmed by immunolocalization of CKI1 in *CKI1*-overexpressing (*Pro35S:CKI1*) lines. Similar to wild-type plants, in *Pro35S:CKI1* lines, the CKI1 protein localized predominantly to procambial cells (Figures 1Bg and 1Bh). Collectively, these data suggest that CKI1 may be involved in growth and development of VB, particularly in procambium development. Weak expression of *CKI1* in the cortex (Figure 1B) might account for an additional role of CKI1 in other aspects of inflorescence stem growth.

CKI1 Is Involved in Controlling Meristematic Activity and Vascular Tissue Formation

To further assess the role of CKI1 in the sporophyte development of *Arabidopsis*, we employed a gain-of-function approach, as mutants completely lacking *CKI1* cannot be obtained due to the infertility of female gametes carrying *cki1* insertion alleles (Pischke et al., 2002; Hejátko et al., 2003). Ectopic overexpression of *CKI1* caused pleiotropic developmental changes (Figures 2A and 2B). *Pro35S:CKI1* transgenic lines were found to be partially or almost completely sterile and to have dramatically shorter siliques. Immunoblot analysis showed that sterility correlated well with *CKI1* expression levels (Figures 2A and 2B). *Pro35S:CKI1* lines also had unusually thick fasciated inflorescence stems, along with changes in overall VB architecture (Figure 2C). Ectopic formation of increased numbers of VBs was observed in transverse sections of inflorescence stems, which suggests higher mitotic activity and abnormal differentiation (Figure 2E). The overall number of cells in transgenic stems was dramatically increased compared with wild-type stems, as seen in transverse sections of inflorescence stems (Figures 2Ea and 2Ed). *CKI1*-overexpressing plants also developed additional inflorescence branches that were initiated from axillary meristems (Figures 2D and 2F). Longitudinal sections of axillary buds revealed additional meristematic tissues bearing many smaller cells (Figure 2Fb, arrow). These findings further suggest that CKI1 might be involved in the regulation of cell division in vascular and meristematic tissues and in their development.

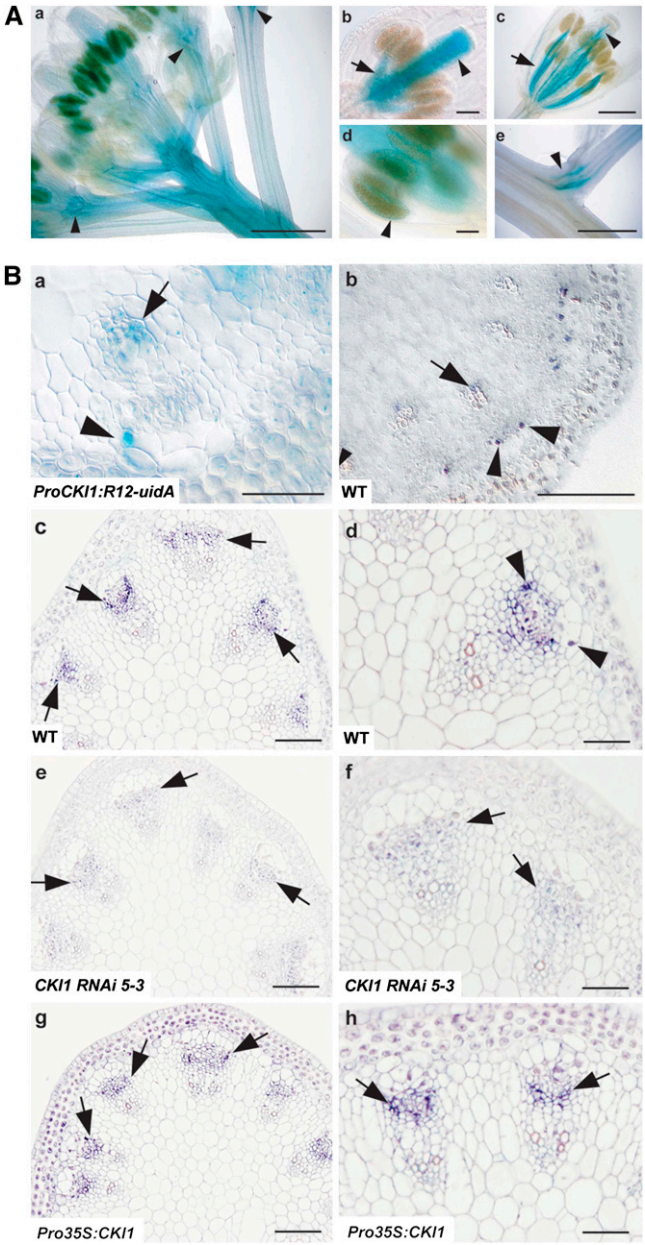

Figure 1. Expression of *CKI1* in VBs.

(A) GUS activity in flowering transgenic plants harboring *ProCKI1:R12-uidA* (**[a]** and **[c]** to **[e]**) or *ProCKI1:uidA* **(b)**. **(a)** Top of the *Arabidopsis* inflorescence. Note the intensity of the signal in the subapical region of the inflorescence stem, vascular tissues of floral organs, and floral pedicels (arrowheads). **(b)** and **(c)** Floral organs before **(b)** and at/just after anthesis **(c)**. Note the predominant GUS staining in the pistil in the flowers before anthesis (**[b]**; arowhead); conversely, the signal in the vascular tissue of stamens is stronger in flowers at/just after anthesis (**[c]**; arrow). **(d)** Male sporophytic tissue (arrowhead). **(e)** Axillary meristem. Bars = 500 μm in **(a)**, **(c)**, and **(e)** and 100 μm in **(b)** and **(d)**.

(B) *CKI1* expression in VBs of the inflorescence stem. **(a)** GUS staining in a cross section of the inflorescence stem of a *ProCKI1:R12-uidA* plant. GUS activity is seen in cells of the VB sheath located at the lateral (outer) borders of the VB (arrowhead) and xylem (arrows; see also **[b]**). **(b)** In situ localization of *CKI1* mRNA. **(c)** to **(h)** In situ immunolocalization of CKI1 using $\alpha CKI1_{ED}$ polyclonal antibodies in the cambium of VBs (deep-purple signal, arrows) on cross sections of inflorescence stems of wild-type (**[c]** and **[d]**), CKI1RNAi (**[e]** and **[f]**), and *Pro35S:CKI1* plants (**[g]** and **[h]**). px, protoxylem; mx, metaxylem; arrowheads point to the strongest signal, located in cells on the outer border of the VB (cf. with **[a]** and **[b]**; arrowheads). Note the procambial localization of CKI1 even in the *Pro35S:CKI1* line. Bars = 100 μm in **(b)**, **(c)**, **(e)**, and **(g)** and 50 μm in **(a)**, **(d)**, **(f)**, and **(h)**.

To examine CKI1 action in vascular development and to avoid possible artifacts due to *CKI1* overexpression, we employed RNA interference (RNAi) to knock down the level of *CKI1*. The relative amounts of *CKI1* transcripts and proteins in RNAi transgenic plants were determined by immunostaining and quantitative real-time PCR (Figure 1B; see Supplemental Figure 3A online). Wild-type and transgenic plants were grown under long-day conditions to the stage at which the first silique is formed on the inflorescence. We found that in comparison to wild-type plants, the procambial cell file layers of RNAi lines were decreased (Figures 3Ac, 3Ad, and 3Ag). By contrast, the number of procambial cells in VBs of inflorescence stems in *Pro35S:CKI1* plants (122.8 ± 25, $n = 6$; mean ± SE) was increased compared with wild-type plants (77.6 ± 6.1, $n = 8$) (Figures 3Ae and 3Af; see Supplemental Figure 4B online; for an example of quantification of procambial cells, see Supplemental Figure 4A online). *CKI1* expression in analyzed RNAi lines was not completely absent, as shown by both RNA and protein levels (Figure 1B; see Supplemental Figure 3A online), suggesting that even a partial reduction of *CKI1* expression might lead to phenotypic changes. We therefore analyzed two independent T-DNA insertion mutants in *CKI1*, *cki1-5/CKI1* and *cki1-6/CKI1* (Pischke et al., 2002). *CKI1* transcripts in heterozygous plants of both lines were reduced up to 50% of the wild-type level (see Supplemental Figure 3B online). Defects similar to, but not identical, those identified in the *CKI1* RNAi plants (i.e., reduction of procambium and abnormal cell shape) were observed in heterozygous *cki1-6* plants (Figure 3B; see Supplemental Figures 4A and 4B online). The number of procambial cells in VBs of inflorescence stems in *cki1* heterozygotes (51.1 ± 5, $n = 14$) was significantly lower than in wild-type plants (84.9 ± 5.7, $n = 12$). These results suggest that quantitative changes in the *CKI1* activity result in a mutant phenotype and, furthermore, indicate that CKI1 is important for the maintenance of mitotic activity and/or the identity of procambial cells during VB development in *Arabidopsis*.

CKI1 Acts through the Two-Component Signaling Pathway

CKI1 shares similarity with members of the His kinase family, and CKI1 His kinase activity has been reported in heterologous and *Arabidopsis* protoplast systems (Hwang and Sheen, 2001; Yamada et al., 2001; Mähönen et al., 2006a). To understand the mechanism by which CKI1 affects vascular tissue development, we inspected the His kinase activity of CKI1 in a two-component signaling network by measuring both the activity of the cytokinin-responsive *ARR6* promoter fused to a luciferase (*LUC*) reporter gene and measuring cytokinin-dependent ARR2

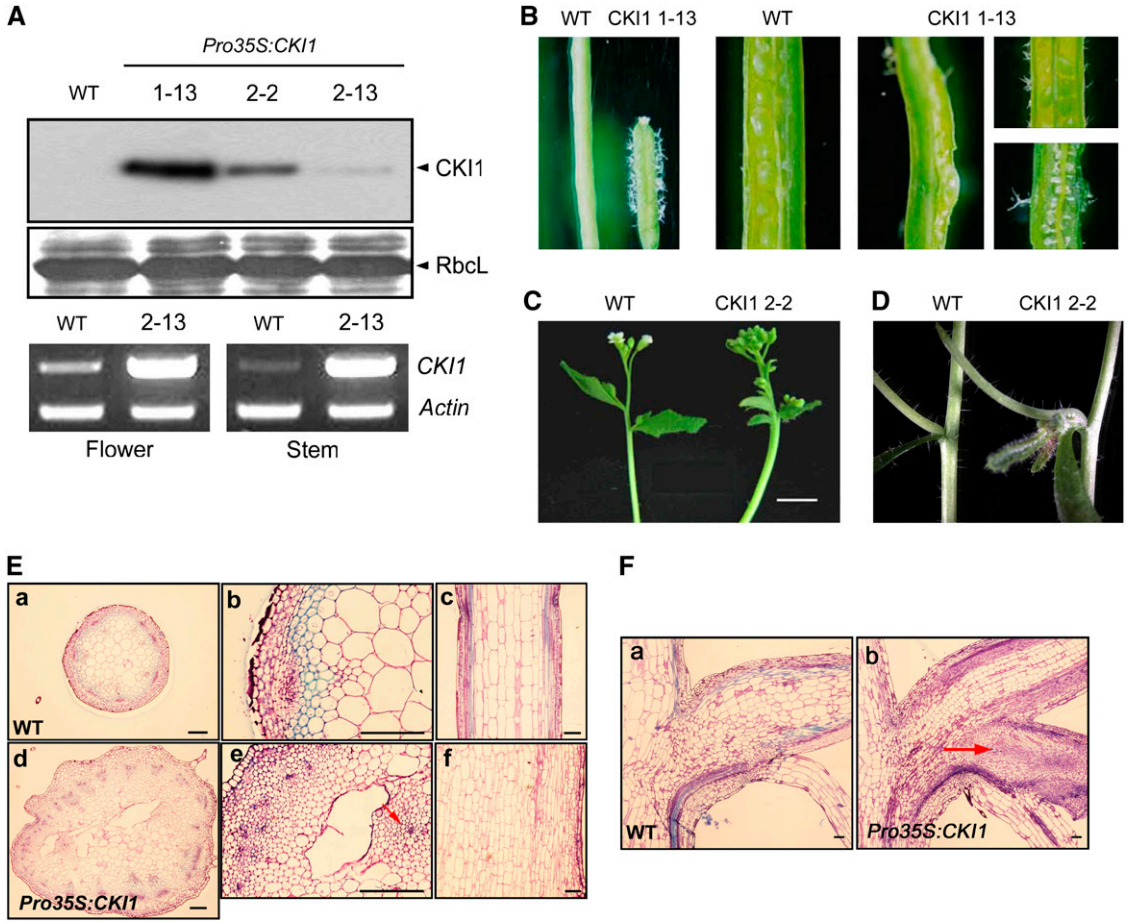

Figure 2. Phenotype Analysis of *CKI1*-Overexpressing Plants.

(A) Expression analysis of *Pro35S:CKI1-HA* transgenic lines. Total protein and RNA from 2-week-old wild-type and transgenic plants were subjected to an immunoblot assay (top) and RT-PCR assay (bottom). RbcL and *actin* serve as input controls in the two assays.
(B) and **(C)** Ectopic expression of CKI1 leads to sterility, many trichomes **(B)**, and thick fasciated inflorescence stems **(C)**.
(D) Ectopic expression of *CKI1* leads to additional vegetative tissues initiated from lateral meristems.
(E) The architecture of VBs in *Pro35S:CKI1* transgenic plants. Transverse sections (**[a]**, **[b]**, **[d]**, and **[e]**) and longitudinal sections (**[c]** and **[f]**) of the inflorescence stems of wild-type (top) and *Pro35S:CKI1* transgenic plants (bottom). The arrows indicate ectopically formed VBs.
(F) The node structures of wild-type and *Pro35S:CKI1* transgenic plants. Longitudinal sections of wild-type **(a)** and *Pro35S:CKI1* transgenic nodes **(b)**. The arrow indicates an ectopic axillary bud in a *Pro35S:CKI1* transgenic plant.
Bars = 100 μm.

phosphorylation; both of these approaches have proved to be reliable indicators of two-component signaling outputs (Hwang and Sheen, 2001; Kim et al., 2006). CKI1 induced *ARR6-LUC* activity in both the presence and absence of cytokinin, as previously shown (Hwang and Sheen, 2001; see Supplemental Figure 5A online). However, CKI1 did not affect expression of the abscisic acid–responsive *RD29A* or auxin-responsive *GH3* promoters, suggesting a specificity of CKI1-mediated responses to the two-component phosphorelay (see Supplemental Figure 5A online). Then we tested whether CKI1 could initiate a phosphorelay to ARR2, a type-B response regulator that is involved in cytokinin-mediated two-component responses (Hwang and Sheen, 2001). As previously demonstrated (Kim et al., 2006), the ARR2 protein was phosphorylated in a cytokinin-dependent manner, resulting in a gel band shift. By contrast, cytokinin-dependent phosphorylation of ARR2 was abolished in protoplasts prepared from the loss-of-function *ahk2 ahk3* mutants (Figure 4A). When *CKI1* was expressed in *ahk2 ahk3* cells, ARR2 phosphorylation was restored regardless of cytokinin treatment. However, overexpression of $CKI1^{H405Q}$ carrying a mutation in the conserved functional His residue could not induce ARR2 phosphorylation in the double mutant (Figure 4A). These results suggest that CKI1 has cytokinin-independent His kinase activity in the two-component phosphorelay system.

The His residue at position 405 of CKI1 amino acid sequence is reported to be a primary target of His kinase activity in the two-component phosphorelay (Hwang and Sheen, 2001). We previously showed that the $CKI1^{H405Q}$ mutation diminishes the

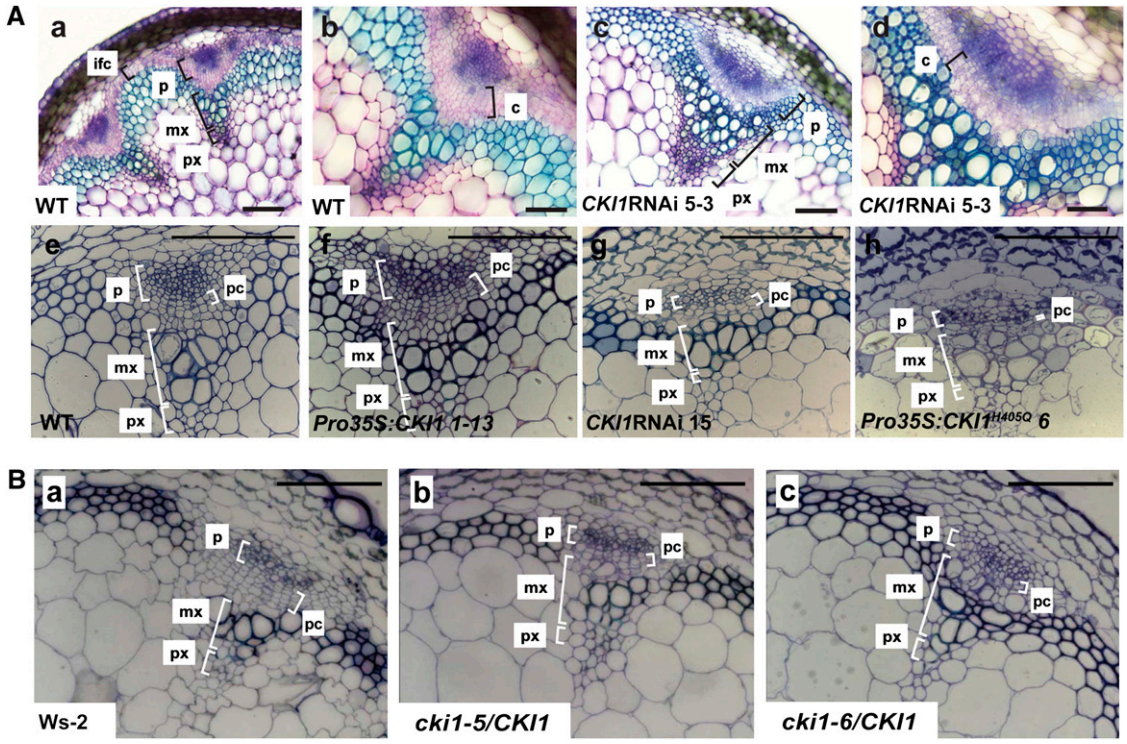

Figure 3. CKI1 Is Involved in the VB Development of Inflorescence Stems.

(A) Suppression of CKI1 activity in *CKI1* RNAi lines (**[c]**, **[d]**, and **[g]**) results in reduced and disorganized files of cambial cells. Conversely, the overexpression of *CKI1* **(f)** results in an increase in the number of cambium layers. Note the presence of interfascicular cambium in toluidine blue staining of native tissue (**[a]** to **[d]**), suggesting the onset of secondary growth and, thus, cambium formation. Fixed material was subjected to phenotypic analysis before the onset of secondary growth, providing evidence for the role of CKI1 in procambium development (**[e]** to **[h]**). Overexpression of the negative allele $CKI1^{H405Q}$ leads to a dramatic reduction in procambium formation. Native staining of handmade sections (**[a]** to **[d]**) with toluidine blue and thin sections made from fixed and embedded material (**[e]** to **[h]**). With native toluidine blue staining, the phloem appears as blue, the undifferentiated cambial zone as pink, metaxylem as blue-green, and protoxylem as purple. c, cambium; ic, interfascicular cambium; pc, procambium; mx, metaxylem; p, phloem. Bars = 100 μm in **(a)**, **(c)**, and **(e)** to **(h)** and 50 μm in **(b)** and **(d)**.

(B) The phenotypes conferred by reducing *CKI1* expression by T-DNA insertion resemble those of *CKI1RNAi* plants. Transverse sections of the inflorescence stems of wild-type plants (Ws-2; **[a]**) and the heterozygous *CKI1* T-DNA insertion lines *cki1-5/CKI1* **(b)** and *cki1-6/CKI1* **(c)**. Bars = 100 μm.

cytokinin-dependent activation of the *ARR6* promoter in wild-type protoplasts (Hwang and Sheen, 2001), suggesting that this mutation might act in a dominant-negative manner in AHK2-, AHK3-, and AHK4-mediated cytokinin signaling pathway.

To determine the mechanism for this negative regulation, wild-type protoplasts were transfected with $CKI1^{H405Q}$ and *ARR6-LUC* along with the His kinases *AHK2*, *AHK3*, or *AHK4* and treated with cytokinin. Interestingly, $CKI1^{H405Q}$ suppressed the AHK2-, AHK3-, and AHK4-mediated *ARR6-LUC* activation that was induced by exogenous cytokinins (Figure 4B; see Supplemental Figure 5B online). Accordingly, when wild-type protoplasts were transfected with $AHK2^{H597Q}$, $AHK3^{H460Q}$, or $AHK4^{H459Q}$ carrying mutation in the conserved His residue along with wild-type *CKI1* and the *ARR6-LUC* reporter gene, the CKI1-mediated activation of the *ARR6* promoter was also blocked (Figure 4B; see Supplemental Figure 5B online). These data indicate that CKI1 is connected to the two-component signal transduction pathway via its His kinase activity and that the negative effect of the $CKI1^{H405Q}$ protein is exerted via its interference with signaling mediated by the other His kinases AHK2, AHK3, or AHK4. Moreover, $Pro35S{:}CKI1^{H405Q}$ transgenic lines displayed defects in VBs (Figure 3Ah). Notably, these lines exhibited abnormal cell morphology with irregularly sized cells in both the xylem and phloem. These results provide additional experimental evidence for the functional importance of two-component mediated signaling in proper VB formation in *Arabidopsis*.

Dimerization of His kinases in plants and bacteria was previously demonstrated (Schaller et al., 1995; Surette et al., 1996; Tomomori et al., 1999; Gao et al., 2008; Grefen et al., 2008). Thus, we tested whether CKI1 directly interacts with other His kinases in *Arabidopsis* two-component signaling. To do this, myc-tagged *CKI1* was cotransfected with HA-tagged *CKI1*, *AHK3*, or *AHK4* in *Arabidopsis* protoplasts. When whole protoplast lysates were immunoprecipitated with an anti-myc antibody, CKI1-HA but not AHK3-HA or AHK4-HA was pulled down together with CKI1-myc, either in the presence or absence of exogenous cytokinins (Figure 4C). Wild-type CKI1 protein still interacted with the

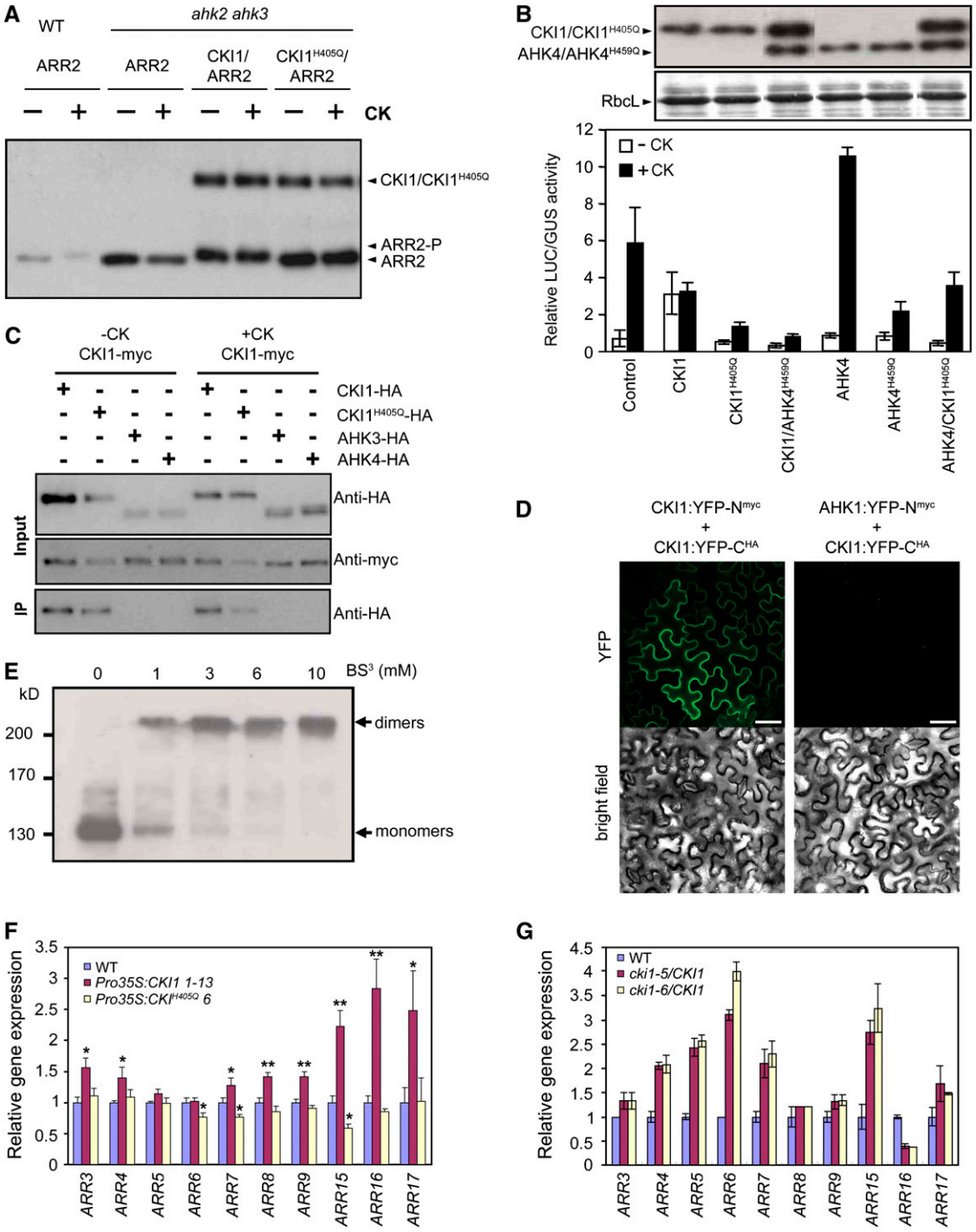

Figure 4. CKI1-Mediated Signaling Is Connected to the Two-Component Signal Transduction Pathway.

(A) CKI1 induces cytokinin-independent ARR2 phosphorylation. Protoplasts from *ahk2 ahk3* plants were cotransfected with *ARR2-HA* along with *CKI1-HA* or *CKI1*^{H405Q}*-HA*, incubated for 6 h, and treated with 100 nM t-zeatin (cytokinin) in the presence of 100 μM cycloheximide for 1 h. Wild-type protoplasts transfected with *ARR2* served as a control. The mobility shift of ARR2 induced by phosphorylation was detected with an anti-HA antibody. Equal amounts of protein were loaded on each lane.

(B) A negative form of CKI1 protein represses the AHK4-mediated induction of *ARR6*. Protoplasts from wild-type plants were transfected with *ARR6-LUC* alone, wild-type *AHK4*, wild-type *AHK4* plus mutant *CKI1*, wild-type *CKI1*, or wild-type *CKI1* plus mutant *AHK4*. Error bars indicate SE (n = 2). *CKI1*^{H405Q} and *AHK4*^{H459Q} are negative versions of *CKI1* and *AHK4*, respectively. Rubisco large subunit (RbcL) stained by Coomassie blue was used as a protein loading control.

CKI1^{H405Q} mutant protein (Figure 4C), suggesting that the His kinase and phosphoryl transfer activities of CKI1 are not required for its dimerization. The self-interaction of CKI1 in planta was confirmed using a bimolecular fluorescence complementation system (Walter et al., 2004). Coexpressed CKI1-cYFP and CKI1-nYFP, but not CKI1-cYFP and AHK1-nYFP, produced strong yellow fluorescent protein (YFP) fluorescence at the plasma membrane in tobacco (*Nicotiana tabacum*) leaf cells (Figure 4D). To determine whether CKI1 forms a dimer or a higher-order multimer, detergent-solubilized proteins from protoplasts expressing *CKI1-HA* were treated with the cross-linker bis-sulfosuccinimidyl suberate (BS^3) (Figure 4E). The intensity of immunoreactive bands corresponding to the approximate size of the CKI1 monomer was gradually reduced as the BS^3 concentration increased, while the intensity of a higher band with the approximate predicted size of a CKI1 dimer was concomitantly increased. Taken together, these results indicate that CKI1 forms homodimers both in vitro and in planta. However, in contrast with sensor His kinases involved in ethylene signaling, which form heterodimers (Gao et al., 2008; Grefen et al., 2008), CKI1 does not form heterodimers with any of the tested His kinases.

To confirm the His kinase activity of CKI1 in planta, we examined the expression of type-A *ARR* genes, the cytokinin primary response genes (D'Agostino et al., 2000), in *Pro35S:CKI1*, *Pro35S:CKI1^{H405Q}*, and *CKI1* knockdown lines. The ectopic expression of *CKI1* induced the expression of a subset of type-A response regulators, including *ARR3*, *4*, *7*, *8*, *9*, *15*, *16*, and *17* (Figure 4F). By contrast, overexpression of *CKI1^{H405Q}* significantly reduced the expression of *ARR6*, *7*, and *15* (Figure 4F), thus confirming the negative regulatory role of CKI1^{H405Q} in the two-component phosphorelay. Moreover, in heterozygous *cki1-5* and *cki1-6* lines, the expression of most of the inspected *ARR* genes was upregulated (Figure 4G), further demonstrating that CKI1 exerts its action through the two-component signal transduction pathway in planta. Furthermore, these results imply that changing CKI1 activity via site-directed mutagenesis and/or deregulation of endogenous *CKI1* expression leads to differential changes in expression of individual *ARRs*, suggesting a disturbance of the two-component phosphorelay.

The Cytoplasmic CKI1 Domain Is Necessary for Its His Kinase Activity

Our data suggested that CKI1 can activate the two-component phosphorelay via its His kinase activity, which is independent of exogenously added cytokinins. To unravel the potential importance of extracellular and intracellular CKI1 domains in CKI1-mediated signaling, we constructed chimeric receptors composed of CKI1 and AHK4 (CKI1-AHK4 and AHK4-CKI1) along with truncated forms of CKI1 (see Supplemental Figure 5C online). AHK4-CKI1, which consists of the extracellular and transmembrane domains of AHK4 fused to the kinase and receiver domains of CKI1, could activate the *ARR6* promoter as efficiently as wild-type CKI1, either in the presence or absence of cytokinins (see Supplemental Figure 5D online). However, CKI1-AHK4, which consists of the extracellular and transmembrane domains of CKI1 fused to the intracellular domain of AHK4, could not enhance the activity of the *ARR6* promoter, regardless of the presence or absence of cytokinins. Moreover, CKI1ΔN, which lacks the extracellular domain of CKI1, still constitutively activated *ARR6-LUC*, unlike CKI1ΔC, which consists of the extracellular and transmembrane domains of CKI1 (see Supplemental Figure 5D online). *Pro35S:AHK4-CKI1* transgenic lines displayed similar *CKI1*-overexpressing phenotypes with reduced fertility, shorter siliques, and additional inflorescence branches (see Supplemental Figures 6A and 6B online). They also had thick fasciated inflorescence stems with increased mitotic activity (see Supplemental Figure 6C online). Thus, the cytoplasmic kinase domain of CKI1 is sufficient for CKI1 cytokinin-independent His kinase activity in two-component signaling.

Cytokinins Regulate VB Development of *Arabidopsis* Inflorescence Stems via the AHK2 and AHK3 Signaling Pathway

Our data suggest that CKI1 regulates the development of vascular tissue in shoots via its His kinase activity. Proteins involved in the cytokinin-regulated two-component signaling pathway are known to regulate vascular tissue formation in *Arabidopsis* roots (Mähönen et al., 2000, 2006b; Hutchison et al., 2006). In addition,

Figure 4. (continued).

(C) CKI1-HA but none of the tested AHKs-HA proteins c-immunoprecipitate with myc-tagged CKI1. Mesophyll protoplasts from wild-type plants were transfected with *CKI1-HA*, *CKI1^{H405Q}-HA*, *AHK3-HA*, or *AHK4-HA*, with or without *CKI1-myc*, incubated for 6 h, and then immunoprecipitated with anti-myc antibodies. CKI1 proteins were detected with an anti-HA antibody.

(D) CKI1 forms homodimers in tobacco leaf cells. Confocal images of abaxial epidermal tobacco leaf cells expressing the indicated YFP-N and YFP-C fusion proteins demonstrate YFP fluorophore reconstitution due to protein–protein interaction of the tested proteins (top row). The bottom row shows the corresponding bright-field images of the transiently transformed cells. Bars = 50 μm.

(E) CKI1 forms dimers. Protoplasts expressing *CKI1-HA* were solubilized with Triton X-100. Total protein was treated with increasing amounts of the cross-linker BS^3 and subjected to SDS-PAGE. Two bands corresponding to the predicted sizes of the CKI1 monomer and dimer were detected with the anti-HA antibody.

(F) and **(G)** Genetic manipulation of CKI1 activity affects two-component signaling in planta. Transgenic plants overexpressing CKI1 or CKI1^{H405Q} **(F)** or CKI1 T-DNA insertion lines **(G)** show changes in the expression of specific type-A *ARRs*. Quantitative RT-PCR was performed with total RNA extracted from 3-week-old seedlings **(F)** or inflorescence stems **(G)** using gene-specific primers for type-A *ARRs* (see Supplemental Table 1 online for primer sequences). Error bars indicate SE (n = 8 **[F]** and 3 **[G]**). Asterisks indicate statistically significant differences from wild-type transgenic plants analyzed by Student's t test (*P < 0.05; ** P < 0.01).

the role of cytokinins in the cambium growth activity was recently identified (Matsumoto-Kitano et al., 2008; Nieminen et al., 2008). These results raised the possibility that two-component signaling cascades initiated by cytokinins as well as by CKI1 are also involved in the regulation of VB formation in shoots. Thus, we examined vascular tissue morphology in the inflorescence stems of plants with mutations in individual cytokinin receptors and in double mutants. In the *ahk2* mutant, the number of cell layers in the procambial region was decreased (Figures 5Ab, 5Ag, and 5Al). A weaker phenotype was identifiable in the *ahk3* line (Figures 5Ac, 5Ah, and 5Am). In the *ahk2 ahk3* double mutant, reduction of the procambium and in the size of VBs was more pronounced than in either single mutant (Figures 5Ad, 5Ai, and 5An). A similar phenotype was also observed as a result of endogenous cytokinin depletion in *Pro35S:CKX3* and *Pro35S:CKX1* lines (Figures 5Ae, 5Aj, and 5Ao, respectively). In *ahk2 ahk3* plants and in lines with decreased endogenous cytokinin, we further observed that interfascicular cambium failed to form when compared with the wild type in Figure 5Aa, suggesting defects in the onset of secondary growth. Taken together, AHK2 and AHK3 together with CKI1 play important roles in proper VB development, especially in the maintenance of procambial cell identity and/or regulation of procambial cell proliferation.

To confirm that CKI1 can affect vascular tissue development via the AHK2/3 signaling pathway, we ectopically expressed *CKI1* or *CKI1*^{H405Q} in *ahk2 ahk3* mutants. Ectopic expression of *CKI1* partially rescued the growth defects of these mutants (Figures 5B and 5C). The rosette leaves and petioles of *ahk2 ahk3*/*Pro35S:CKI1* transgenic plants were similar to those of wild-type plants (Figure 5B). Overexpression of *CKI1* in the *ahk2 ahk3* background resulted in an increase of cambial layers, with a two- to threefold increase in the diameter of inflorescence stems compared with *ahk2 ahk3* (Figure 5D). In addition, a reduced number of cells with the irregular size of *ahk2 ahk3* in the xylem, phloem, and cambial layers were partially restored in these transgenic lines (Figure 5E). As a result, the radial growth was rescued, manifested by almost, but still partially, wild-type-like diameter of the inflorescence stem in *Pro35S:CKI1/ahk2 ahk3* (Figure 5E). By contrast, ectopic expression of the dominant-negative mutation *CKI1*^{H405Q} further accentuated the mutant phenotypes of *ahk2 ahk3* plants. In comparison to the *ahk2 ahk3* mother line, the aerial parts and diameters of inflorescence stems of *ahk2 ahk3*/*Pro35S:CKI1*^{H405Q} plants were much smaller (Figures 5B and 5D). The cambial cell layers were unidentifiable, and vascular tissue differentiation was nearly abolished (Figure 5E). Collectively, these results suggest that CKI1 is functionally conserved with AHK2 and AHK3 in VB development but that it still has its own specificity in the regulation of vascular tissue development.

DISCUSSION

Cytokinin-Independent CKI1 Regulates Two-Component Phosphorelay in *Arabidopsis*

CKI1 was the first His kinase implicated in the perception of cytokinins (Kakimoto, 1996). However, CKI1 does not contain the cytokinin binding CHASE domain and does not bind cytokinins in vitro (Yamada et al., 2001). Defects in megagametogenesis conferred by a *cki1* loss-of-function allele, together with observations of *CKI1* expression in the ovule and endosperm, show that CKI1 is critical in female gametophyte development (Pischke et al., 2002; Hejátko et al., 2003). However, the mechanisms underlying the involvement and action of CKI1 signaling in specific biological processes during *Arabidopsis* gametophyte and/or sporophyte development remain largely unknown. Furthermore, when overexpressed in plants, calli, or protoplasts, *CKI1* induces typical cytokinin responses, including shoot regeneration, delay of leaf senescence, and activation of the cytokinin-responsive *ARR6* promoter in the absence of exogenously applied cytokinins (Kakimoto, 1996; Hwang and Sheen, 2001). It was suggested that ectopic expression of *CKI1* allows the expressing cells to sense low concentrations of endogenous cytokinins that are otherwise unable to trigger shoot formation (Kakimoto, 1996). Here, we have shown that CKI1 can mediate cytokinin-independent regulation of the two-component signaling pathway. Thus, rather than recognition of endogenous cytokinin levels as suggested previously (Hwang and Sheen, 2001), the cytokinin-independent His kinase activity of CKI1 probably leads to the cytokinin-like phenotype in calli overexpressing *CKI1* (Kakimoto, 1996). However, the possibility that the extracellular domain of CKI1 allows another mode of cytokinin-independent regulation of its His kinase activity cannot be excluded.

We found here that CKI1 shares at least some of the signaling proteins with the two-component phosphorelay system in the cytokinin signaling pathway. Based on our results, and of studies showing dephosphorylation of AHP1 and AHP2 by CKI1 in vitro (Nakamura et al., 1999), functional complementation of bacterial and yeast His kinase mutants by CKI1 (Yamada et al., 2001), and CKI1 interaction with AHP proteins in a yeast two-hybrid system (Dortay et al., 2006), we conclude that CKI1 can activate the two-component phosphorelay in *Arabidopsis* via proteins involved in the cytokinin signaling pathway. Whether CKI1 activity directly affects cytokinin signaling and/or other adaptive responses mediated by the two-component phosphorelay (e.g., osmosensing or abscisic acid responses), however, remains to be determined. *CKI1* overexpression activated *ProARR6:LUC*, a marker for two-component signaling in protoplasts, but we could not observe similar activation of *ARR6* in a late developmental stage of *CKI1*-overexpressing plants. This result implies that a single cell system may not always reflect different developmental stages at which multiple cells incorporate diverse external and/or internal signals to properly execute growth and development programs (Figure 4; see Supplemental Figure 5 online).

The output of the two-component phosphorelay was proposed to be a result of interactions of multiple His kinases and their kinase and phosphatase activities (Mähönen et al., 2006a). In this model, the final output of the two-component phosphorelay also depends on the expression levels of cytokinin binding and cytokinin nonbinding His kinases, including CKI1. The phosphatase activity of the receiver domain of CKI1 has been demonstrated (Nakamura et al., 1999), suggesting that CKI1 might contribute to two-component phosphorelay regulation via both kinase and phosphatase activities. Here, we have shown that both overexpression and downregulation of CKI1 affects the

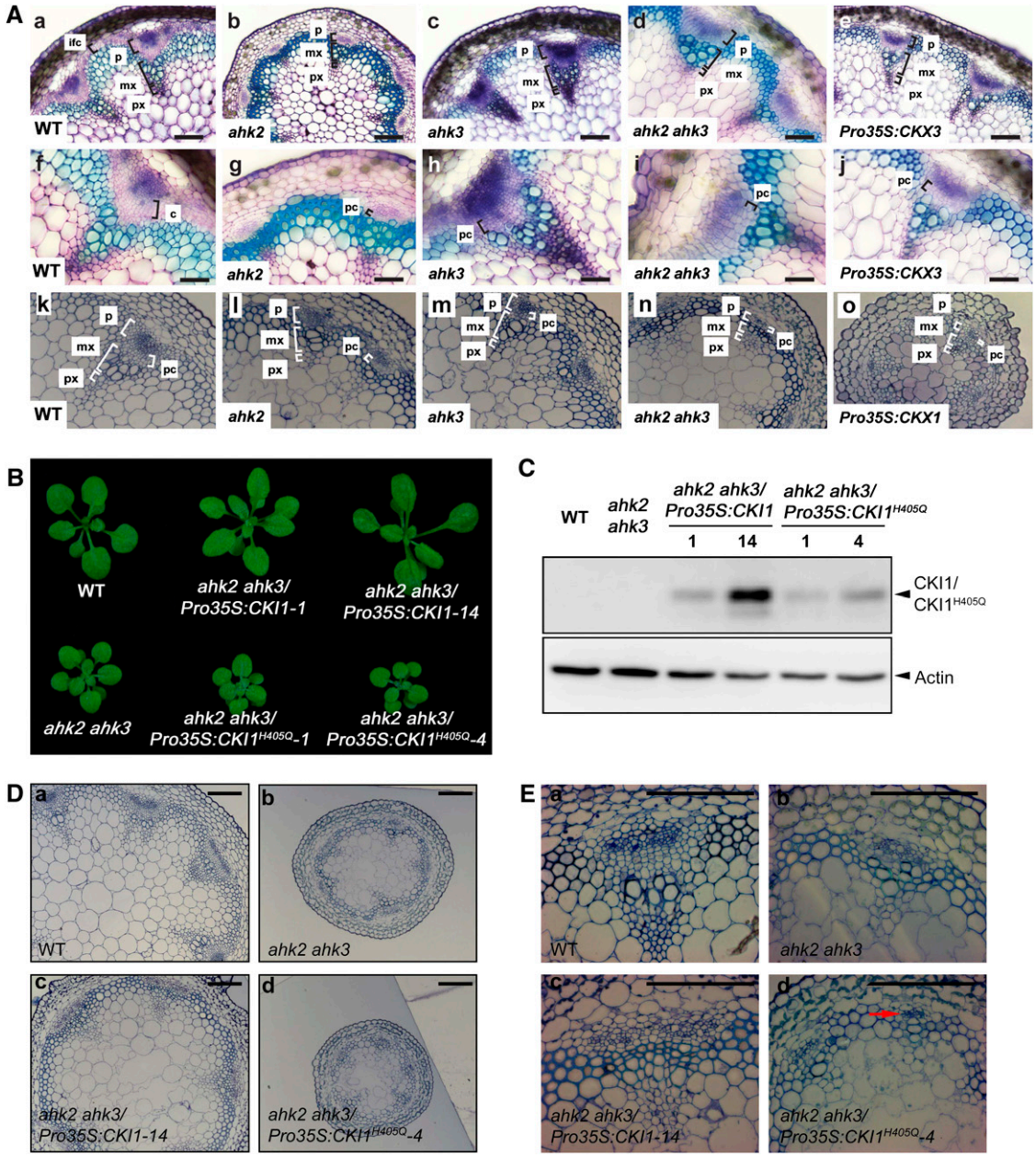

Figure 5. Cytokinin Regulates VB Formation via AHK2 and AHK3 Phosphorelay.

(A) Transverse sections of the inflorescence stems of wild-type (Columbia-0 [Col-0]) ([**a**], [**f**], and [**k**]), *ahk2* ([**b**], [**g**], and [**l**]), *ahk3* ([**c**], [**h**], and [**m**]), *ahk2* and *ahk3* ([**d**], [**i**], and [**n**]), and *Pro35S:CKX* ([**e**], [**j**], and [**o**]) lines. Note the reduction of procambial layers in *ahk2* and *ahk3* plants and particularly in *ahk2 ahk3* double mutants. The overall reduction in VB size is apparent in *ahk2 ahk3* and in *Pro35S:CKX* lines, suggesting positive regulation of cytokinin signaling via the *AHK2*/*AHK3* pathway in VB development in *Arabidopsis* inflorescence stems. Staining of handmade sections ([**a**] to [**j**]) with toluidine blue and thin sections made from fixed and embedded material ([**k**] to [**o**]). c, cambium; ic, interfascicular cambium; pc, procambium; mx, metaxylem; p, phloem. Bars = 100 μm in **(a)** to **(e)** and **(k)** to **(o)** and 50 μm in **(f)** to **(j)**.

(B) The dwarfism resulting from deletion of *ahk2 ahk3* is rescued in the presence of CKI1. Three-week-old wild-type (Col-0) and transgenic plants expressing *Pro35S:CKI1-HA* or *Pro35S:CKI1*^{H405Q}*-HA* in the *ahk2 ahk3* background were used for phenotypic analysis.

(C) Expression analysis of HA-tagged CKI1 and CKI1^{H405Q} proteins under the control of the *Pro35S* promoter in transgenic lines. Total proteins from 3-week-old plants of each designated line were subjected to 7.5% SDS-PAGE. Actin proteins detected by immunoblotting serve as input controls.

(D) and **(E)** Ectopic expression of *CKI1* rescues the abnormal vasculature of the *ahk2 ahk3* mutant. Microscopy images of transverse sections of the inflorescence stems of wild-type **(a)**, *ahk2 ahk3* **(b)**, *Pro35S:CKI1-HA*/ *ahk2 ahk3* **(c)**, and *Pro35S:CKI1*^{H405Q}*-HA*/ *ahk2 ahk3* **(d)** plants. The arrow indicates extensively reduced VB. Bars = 100 μm.

output of the two-component signaling pathway, as measured by regulation of the expression of *ARRs*. This observation accords well with the above-described model proposed by Mähönen et al. (2006a) and suggests that an equilibrium of individual inputs into the two-component pathway is critical for proper vascular tissue development in *Arabidopsis* shoots. Type-A *ARR* genes have been identified as negative regulators of cytokinin signaling (To et al., 2004). Auxin-induced regulation of *ARR7* and *ARR15* was recently identified as a mechanism of auxin-dependent spatial-specific attenuation of cytokinin signaling during stem cell niche formation in *Arabidopsis* roots (Müller and Sheen, 2008). Thus, upregulation of negative type-A *ARRs* in knockdown *CKI1* lines might disrupt the proper regulation of two-component signaling in procambial development; therefore, these lines may partially phenocopy plants deficient in cytokinin signaling. However, whether CKI1-regulated expression of *ARR* genes represents another cytokinin-independent mechanism for regulation of the cytokinin two-component pathway remains to be determined. Furthermore, it is still uncertain if cytokinin-responsive *ARR* genes are direct regulators required for cambial development, although it is evident that perturbation of cytokinin homeostasis affects cambial activity in shoots and roots (Matsumoto-Kitano et al., 2008; Nieminen et al., 2008).

CKI1 Together with AHK2/AHK3 Is Involved in the Maintenance of Procambial Activity during VB Development in *Arabidopsis* Shoots

Vascular development in *Arabidopsis* can be divided into three major steps: (1) initiation and maintenance of (pro)cambium, (2) asymmetric cell patterning and differentiation into xylem and phloem precursor cells, and (3) their final specification into distinct xylem and phloem cell types. While auxin initiates and maintains continuous vascular pattern formation of procambial cells via polar auxin transport (Fukuda, 2004; Friml et al., 2004), cytokinin signaling mediated by AHK2/3 is unlikely to be involved in the initiation of procambial cell files as knockout lines still contain functional VBs (Figure 5). Rather, our results suggest that CKI1 and AHK2/3 are required for the proliferation and maintenance of procambial cells and vascular stem cells, which give rise to primary vascular tissues and vascular cambium.

Besides the procambium activity, the activity of the shoot apical meristem (SAM) seems to be genetically linked with the regulation of vascular tissue development (Baucher et al., 2007). Cytokinins were shown to be positive regulators of the shoot meristem size (Higuchi et al., 2004; Nishimura et al., 2004; Kurakawa et al., 2007). Thus, the downregulation of the diameter of the inflorescence stem and the size of VBs in *ahk2 ahk3* mutants might be at least partially due to the defects in the SAM activity during procambium initiation. Accordingly, formation of enlarged and fasciated inflorescence stems in *Pro35S:CKI1* lines could be affected by the increased mitotic activity in the SAM upon *CKI1* overexpression. However, we could not observe any quantitatively significant change of the SAM size in the transgenic lines overexpressing *CKI1* (see Supplemental Figure 8A online). In addition, we have analyzed the VB phenotype at the very base of the first internodium and, thus, in a position spatially and developmentally well dissected from the shoot apical meristem. The analysis was performed at the stage when the first silique was formed on the inflorescence. This stage corresponds to the end of the primary growth, which is primarily governed by the procambial activity (Altamura et al., 2001). Taken together, although we cannot completely exclude the possibility that some of the observed phenotype changes originate in the SAM, the defects in the procambium activity due to impaired cytokinin signaling seem to be at least one of the substantial contributions to the observed defects in the primary radial growth of *ahk2 ahk3* and *Pro35S:CKX1(2)* lines.

Interestingly, AHK2/3-mediated cytokinin signaling seems to be also involved in secondary VB development. Formation of interfascicular cambium is one of the anatomically well distinguishable markers of the secondary growth initiation in *Arabidopsis* (Altamura et al., 2001). We observed that the formation of interfascicular cambium was absent and/or substantially reduced in the *ahk2 ahk3* double mutant and in *Pro35S:CKX1(2)* lines, which suggests possible defects in the onset of the secondary thickening. It is possible that CKI1 maintains the basal meristematic activity of procambial cells and that AHK2/3 fine-tunes (pro)cambial activity following environmental and/or developmental cues that regulate endogenous cytokinin levels (Samuelson et al., 1992; Yang et al., 2001; Takei et al., 2004; Werner et al., 2006; Matsumoto-Kitano et al., 2008). Recently, results showing the involvement of cytokinin in the regulation of cambium in *Arabidopsis* and poplar were published (Matsumoto-Kitano et al., 2008; Nieminen et al., 2008). A reduction of cytokinins in null mutants of the *Arabidopsis* cytokinin biosynthetic genes *ipt1,3,5,7* and in transgenic poplar trees overexpressing *Arabidopsis CYTOKININ OXIDASE/DEHYDROGENASE2* resulted in impaired cambial formation, indicating that cytokinins are important regulators of vascular cambium. These results are consistent and complementary with our findings of a role for His kinase–mediated two-component signaling in vascular tissue formation of *Arabidopsis* shoots.

However, it should be emphasized here that in addition to hormonal regulations, other signals (e.g., weight of the produced biomass of the plant body) (Ko et al., 2004) are also integrated in the regulation of the secondary thickening. Thus, this type of signal might contribute to the observed defects in the onset of secondary thickening in *ahk2 ahk3* and cytokinin-deficient plants, both of which are deficient in radial growth, thus revealing lowered production of the shoot biomass.

It has long been known that roots and shoots respond differently to cytokinins in *Arabidopsis* (Werner et al., 2003). In *Arabidopsis* roots, cytokinins have been shown to be necessary for the periclinal procambial cell divisions required for the proliferation of vascular cell files (Scheres et al., 1995; Mähönen et al., 2000, 2006b). Similar to what we have found, this suggests a positive role of cytokinins for procambium proliferation and/or maintenance. However, CKX1(2)-mediated depletion of cytokinins in *Arabidopsis* roots leads to the formation of abnormal vascular tissue that is devoid of phloem but which exhibits abundant protoxylem formation (Mähönen et al., 2006b). This is apparently not the case in the inflorescence stem, where CKX1 (3)-mediated cytokinin depletion led to the formation of VBs of reduced size; however, all cell types (i.e., protoxylem, metaxylem, and phloem) still could be detected (Figure 5C). Accordingly,

we did not observe specific phenotypic changes in root and hypocotyl vascular development in *CKI1* knockdown lines (see Supplemental Figures 8B and 8C online). This could be explained by a lower sensitivity of the inflorescence stem to cytokinin depletion and by the specificity of CKI1 and AHK2/3 signaling. CKI1-driven, cytokinin-independent regulation of VB development could contribute to the lower sensitivity and resulting phenotype in *Pro35S:CKX1(3)* inflorescence stems. Alternatively, modified developmental pathways might operate in root and shoot vascular tissue development.

Here, we have shown that His kinases in *Arabidopsis* regulate vascular tissue formation in shoots via the regulation of procambium activity (see Supplemental Figure 9 online). This is of great economic importance as procambium and vascular cambium activities regulate biomass production in plants. Thus, regulation of the activity of individual His kinases by means of genetic engineering might be used to regulate biomass production in plants and might help us to lower our dependence on other, mostly nonrenewable, energy resources.

METHODS

Plant Materials

The *Arabidopsis thaliana* Col-0 ecotype and the mutant carrying the *ahk2-1* and *ahk3-1* mutant alleles (Higuchi et al., 2004), both in the Col-0 background, were used. Wild-type and mutant plants were grown in an environmentally controlled room at 23°C under white light with 14-h-light/10-h-dark cycles.

Transient Expression in *Arabidopsis* Protoplasts

Transient expression in protoplasts was performed as previously described (Hwang and Sheen, 2001). Typically, 2×10^4 protoplasts were transfected with 20 μg total plasmid DNA consisting of different combinations of the reporter, effectors, and internal control. Transfected protoplasts were incubated at 10^4 cells per mL with or without 100 nM t-zeatin (Sigma-Aldrich) for 6 h. As an internal control, the *GUS* reporter gene fused to the *Arabidopsis* ubiquitin promoter (*UBI10−GUS*) was used. The results shown are the means and error bars of relative LUC activities obtained from duplicate samples. All assays were performed at least three times, and similar results were obtained in all experiments.

Plasmid Constructs and Generation of Transgenic Plants

Full-length and truncated *CKI1* were amplified by PCR from genomic *Arabidopsis* DNA. Full-length *AHK4* was obtained by PCR from an *Arabidopsis* cDNA library. Chimeric *AHK4-CKI1* and *CKI1-AHK4* constructs were generated by overlap extension PCR using the overlapping primers 5′-CATCTCTCTCCTTGTTGCTTGAGCTGCACCATACAGTATATA-3′ and 5′-CTTCGACTTTTACTATGTGCATCATAAACCACACAAACCATAC-3′, respectively. The coding regions of all proteins were tagged with either two copies of the hemagglutinin epitope (HA), the myc epitope, or green fluorescent protein and inserted into a plant expression vector containing the *35SC4PPDK* promoter and the *NOS* terminator (Hwang and Sheen, 2001). Transgenic *Arabidopsis* plants expressing *CKI1-HA* under the control of the *35SC4PPDK* promoter were generated by the floral dip method and BASTA selection as described (Clough and Bent, 1998). *Pro35S:CKX2* and *Pro35S:CKX3* lines were generated as described (Pernisova et al., 2009). The ectopic expression of *CKI1* was tested by RT-PCR and immunoblot analysis. Phenotypic analyses of transgenic lines were performed with homozygous T3 plants. All mutants were generated by site-directed mutagenesis using the QuikChange site-directed mutagenesis kit (Stratagene) according to the manufacturer's instructions. All constructs were confirmed by sequencing. To analyze the specificity of the *CKI1* promoter, two different constructs were made and introduced into *Arabidopsis* ecotype Col-0. The first construct, *ProCKI1:uidA*, contains a 2.7-kb fragment of upstream genomic DNA that includes the putative translational start site of the short open reading frame (MKRAF) in the 5′ untranslated region of the *CKI1* mRNA. The primers SII-ckpr (5′-GTAACCGCGGGAGGAGGCACAAAATGACGAA-3′) and B-ckpr (5′-GCTGGGATCCTCATATTATCTTCTTCCTCGGAGC-3′) were used for PCR amplification of the putative promoter region of CKI1; this fragment is translationally fused with the *uidA* coding sequence (Hejátko et al., 2003). The second construct, *ProCKI1:R12-uidA*, also contains a translational fusion of *uidA* with the same genomic fragment described above; however, the 3′ end of this fragment was extended to include the CGT codon that encodes the R12 residue of CKI1 (see Supplemental Figure 1 online). Multiple independent transgenic lines were inspected in both cases, and no apparent differences in the resulting distribution of GUS activity were detectable.

Expression Analysis

In situ mRNA and GUS staining were performed as previously described (Hartmann et al., 2000; Hejátko et al., 2003; Brewer et al., 2006). Polyclonal rabbit anti-CKI1 antibody was prepared against the peptide from the CKI1 extracellular domain (GATRIKHQAEKAKYQC, αCKI_{ED}; Sigma-Genosys) and used for indirect immunolocalization on Steedman's wax sections as described (Vitha et al., 2000). Two batches of polyclonal sera (anti-$CKI1_{ED}$120 and anti-$CKI1_{ED}$121) isolated from two independently immunized rabbits were tested (see Supplemental Figure 2 online). If not otherwise mentioned, anti-$CKI1_{ED}$121 was used. The alkaline phosphatase–conjugated secondary antibody was visualized by 5-bromo-4-chloro-3-indol phosphate (BCIP)/*p*-Nitro-Blue tetrazolium chloride (NBT) staining. Antibody specificity was characterized on immunoblots using recombinant proteins expressed in *Escherichia coli* and on immunoblot using plant protein extracts (see Supplemental Figure 2 online). Preimmune serum was used as a negative control in immunolocalizations of CKI1 on sections, and no signal was obtained.

RT-PCR and Quantitative Real-Time PCR Analysis

Total RNA was isolated using Trizol reagent (Invitrogen) according to the manufacturer's instructions. For RT-PCR, first-strand cDNA was synthesized from 1 μg RNA with oligo(dT) primers and ImProm-II reverse transcriptase (Promega). The expression of *CKI1* was verified with 30 cycles using a gene-specific primer set, CKI1fwd (5′-AACAGCTCAAGGACACCAAG-3′) and CKI1rev (5′-GCGTTCTTCATTTTTCAATA-3′), and *actin* gene as a control using ACTfwd (5′-GTACAACTATGTTCTCAGGT-3′) and ACTrev (5′-GAAGCATTTTCTGTGGACAA-3′) primers. For quantitative real-time RT-PCR, first-strand cDNA was prepared with SuperScript II reverse transcriptase (Invitrogen) and the ACT-L and rCKI1rt primers. The subsequent quantitative PCR was performed in a Light Cycler 2.0 (Roche) with SYBR Premix ExTaq system (Takara) as a fluorescent dye that monitors DNA content. To amplify gene-specific products, the following primers were used: fACTrt (5′-CAGTGTCTGGATCGGAGGAT-3′), rACTrt (5′-TGAACAATCGATGGACCTGA-3′), fCKI1rt (5′-CTATTGGGAACCCAGAGGACG-3′), rCKI1rt (5′- AAGCTTCTTTCCCACTGTCGC-3′), and type-A *ARR*s (see Supplemental Table 1 online). The steady state levels of the transcripts were determined by standard curve quantitation. All quantitative RT-PCR experiments were performed with biologically independent samples at least three times.

Coimmunoprecipitation and Immunoblot Analysis

Protoplasts were transfected with either HA- or myc-tagged *CKI1*, *AHK3*, *AHK4*, *CKI1*^{H405Q}, or *AHK4* and then incubated for 6 h to allow protein expression. Total protein was extracted from the transfected protoplasts in IP buffer (50 mM Tris, pH 7.5, 150 mM NaCl, 5 mM EDTA, 1% Triton X-100, protease inhibitor cocktail [Roche], and 1 mM DTT) and incubated with a monoclonal anti-HA antibody (Roche) or a monoclonal anti-c-myc antibody (Cell Signaling). The protein-antibody complex was precipitated with protein A/G plus-agarose beads (Calbiochem). For cross-linking experiments, protoplasts transfected with *CKI1-HA* were incubated for 6 h and lysed with protein extraction buffer (50 mM sodium phosphate, pH 7.4, 5 mM EDTA, 1% Triton X-100, 1 mM DTT, and protease inhibitor cocktail). Total protein extracts were incubated with different concentrations of the cross-linker BS^3 (Pierce) for 1 h at 4°C before being quenched with 25 mM Tris-HCl, pH 7.5, for 30 min. Immunoprecipitated proteins and total proteins were subjected to 7.5 or 10% SDS-PAGE and blotted onto Immunobilon-P membranes (Millipore). The blots were probed with a peroxidase-conjugated anti-HA antibody (Roche) or a monoclonal anti-myc antibody. Extracellular domains of AHK4 ($AHK4_{ED}$, D127-P395) and CKI1 ($CKI1_{ED}$, E28-Q345) were cloned into *E. coli* expression vector pDEST17 and expressed as a recombinant protein in a translational fusion with His-Tag. One hundred micrograms of the total protein (bacterial lysate) was separated using 15% SDS-PAGE, blotted on polyvinylidene fluoride (PVDF) membrane, and immunodetected using monoclonal anti-polyHistidine (Sigma-Aldrich) or polyclonal anti-$CKI1_{ED}$ 1:10,000 in blocking buffer (5% milk in 10 mM Tris-HCl, pH 7.5, 150 mM NaCl, and 0.1% Tween-20). The detection was performed using alkaline phosphatase–conjugated goat anti-rabbit secondary antibodies (Sigma-Aldrich) diluted 1: 30,000 in blocking buffer and anti-mouse-AP antibodies (Sigma-Aldrich) diluted 1:20,000 in a blocking buffer with BCIP/NBT substrate for 10 min, within the linear range of signal development. All experiments were performed at least three times.

Analysis of CKI1 Dimerization Using Bimolecular Fluorescence Complementation

Entry clones containing *CKI1* and *AHK1* cDNA were prepared according to the manual for Gateway technology in pDONR207 (Invitrogen), verified by sequencing, and subsequently recombined via the LR reaction into pSPYNE-35S and pSPYCE-35S (Walter et al., 2004). Transient transformation of tobacco (*Nicotiana tabacum*) leaves and immunodetection of fusion proteins were performed as previously described (Horak et al., 2008). Confocal laser scanning microscopy was performed using an Olympus IX81 microscope equipped with a Fluoview 500 confocal unit at a setup recommended by the manufacturer for YFP fluorescence detection.

Histological Analysis

Tissue samples were fixed for 24 h in 3% glutaraldehyde and 4% paraformaldehyde in 0.1 M phosphate buffer, pH 7.2, or in FAA containing 5% acetic acid, 45% ethanol, and 5% formaldehyde. The fixed samples were then rinsed with 0.1 M phosphate buffer, pH 7.2, and dehydrated through a graded ethanol series. The specimens were infiltrated and embedded in Spurr's resin (Ted Pella) or Technovit resin (Kulzer and Co.) for 48 h at 65°C. Sections (0.5 or 4 μm) were made using an MT-X ultramicrotome (RMC), stained in 0.1% toluidine blue, and photographed with a Zeiss Axioplan2 microscope. For native staining, handmade sections were prepared with a razor blade from the base of the inflorescence stems when the first silique appeared. Sections were stained with toluidine blue (0.05% [w/v] solution in water) for 1 min, destained in distilled water for 30 seconds, mounted in 50% glycerol, and observed with a microscope (Olympus BX 61) using differential interference contrast microscopy.

Accession Numbers

Sequence data from this article can be found in the Arabidopsis Genome Initiative or GenBank/EMBL databases under the following accession numbers: *CKI1* (AT2G47430), *AHK1* (AT2G17820), *AHK2* (AT5G35750), *AHK3* (AT1G27320), *AHK4* (AT2G01830), *ARR2* (AT4G16110), *CKX1* (AT2G41510), *CKX2* (AT2G19500), and *CKX3* (AT5G56970). Germplasm identification numbers from this article are as follows: *cki1-5* (CS6360) and *cki1-6* (CS6361).

Supplemental Data

The following materials are available in the online version of this article.

Supplemental Figure 1. Schematic Representation of the *ProCKI1:uidA* (Up) and *ProCKI1:R12-uidA* (Down) Constructs Used in Analysis of the Transcriptional Specificity of the *CKI1* Promoter.

Supplemental Figure 2. Anti-$CKI1_{ED}$ Antibody ($\alpha CKI1_{ED}$) Specifically Recognizes the Extracellular Domain of CKI1.

Supplemental Figure 3. Transcript Levels of *CKI1* in RNAi Lines and T-DNA Insertion Heterozygous Lines.

Supplemental Figure 4. CKI1 Regulates the Number of Procambial Cells.

Supplemental Figure 5. CKI1 Specifically Enhances the Activity of the Two-Component, Cytokinin-Responsive *ARR6* Promoter in a Cytokinin-Independent Manner.

Supplemental Figure 6. The Ectopic Expression of *CKI1* or *AHK4-CKI1* Leads to Sterility and Formation of Short Siliques and to Additional Vegetative Tissues Initiated from Lateral Meristems.

Supplemental Figure 7. Expression of Individual Constructs Used in the BiFC Assay in Figure 5B Was Determined by Immunostaining and Ponceau S Staining to Prove Equal Protein Loading (Red Bands).

Supplemental Figure 8. CKI1 Activity Does Not Affect Either the SAM Activity or the Vascular Bundle Development in Hypocotyl and Root.

Supplemental Figure 9. A Proposed Model for CKI1 and Cytokinin Action Mechanism in the Vascular Bundle Development of Inflorescence Stems.

Supplemental Table 1. Gene-Specific Primers for Type-A *ARRs*.

ACKNOWLEDGMENTS

We thank Filip Rolland and Jiří Friml for critically reading the manuscript, Thomas Schumülling for *Pro35S:CKX1* and *Pro35S:CKX2* seeds, and Chiharu Ueguchi and Yka Helariutta for *ahk* mutant seeds. This work was supported by grants to I.H. from the Plant Diversity Research Center of MOST, the Plant Signaling Network Research Center, and Technology Development Program for Agriculture and Forestry (309017-5) and, in part, by a grant to G.-T.K. from the Environmental Biotechnology National Core Research Center of MOST. The work was also supported by the Ministry of Education of the Czech Republic (LN00A081, LC06034, and MSM0021622415), the Academy of Sciences of the Czech Republic (IAA600380507), the Bundesministerium für Bildung und Forschung, and Fonds of Chemical Industry. J.H. was supported by the Deutscher Akademischer Austausch Dienst. S.M.C. was a recipient of a Brain Korea 21 fellowship.

Received March 3, 2009; revised June 16, 2009; accepted June 30, 2009; published July 21, 2009.

REFERENCES

Aloni, R. (1987). Differentiation of vascular tissues. Annu. Rev. Plant Physiol. Plant Mol. Biol. **38:** 179–204.

Altamura, M.M., Possenti, M., Matteucci, A., Baima, S., Ruberti, I., and Morelli, G. (2001). Development of the vascular system in the inflorescence stem of Arabidopsis. New Phytol. **151:** 381–389.

Baucher, M., El Jaziri, M., and Vandeputte, O. (2007). From primary to secondary growth: Origin and development of the vascular system. J. Exp. Bot. **58:** 3485–3501.

Brewer, P.B., Heisler, M.G., Hejátko, J., Friml, J., and Benkova, E. (2006). In situ hybridization for mRNA detection in Arabidopsis tissue sections. Nat. Protocols **1:** 1462–1467.

Cano-Delgado, A., Yin, Y., Yu, C., Vafeados, D., Mora-Garcia, S., Cheng, J.C., Nam, K.H., Li, J., and Chory, J. (2004). BRL1 and BRL3 are novel brassinosteroid receptors that function in vascular differentiation in Arabidopsis. Development **131:** 5341–5351.

Carlsbecker, A., and Helariutta, Y. (2005). Phloem and xylem specification: pieces of the puzzle emerge. Curr. Opin. Plant Biol. **8:** 512–517.

Clough, S.J., and Bent, A.F. (1998). Floral dip: A simplified method for Agrobacterium-mediated transformation of *Arabidopsis thaliana*. Plant J. **16:** 735–743.

D'Agostino, I.B., Deruere, J., and Kieber, J.J. (2000). Characterization of the response of the Arabidopsis response regulator gene family to cytokinin. Plant Physiol. **124:** 1706–1717.

Dortay, H., Mehnert, N., Burkle, L., Schmulling, T., and Heyl, A. (2006). Analysis of protein interactions within the cytokinin-signaling pathway of *Arabidopsis thaliana*. FEBS J. **273:** 4631–4644.

Emery, J.F., Floyd, S.K., Alvarez, J., Eshed, Y., Hawker, N.P., Izhaki, A., Baum, S.F., and Bowman, J.L. (2003). Radial patterning of Arabidopsis shoots by class III HD-ZIP and KANADI genes. Curr. Biol. **13:** 1768–1774.

Eriksson, M.E., Israelsson, M., Olsson, O., and Moritz, T. (2000). Increased gibberellin biosynthesis in transgenic trees promotes growth, biomass production and xylem fiber length. Nat. Biotechnol. **18:** 784–788.

Fisher, K., and Turner, S. (2007). PXY, a receptor-like kinase essential for maintaining polarity during plant vascular-tissue development. Curr. Biol. **17:** 1061–1066.

Friml, J., Vieten, A., Sauer, M., Weijers, D., Schwarz, H., Hamann, T., Offringa, R., and Jurgens, G. (2003). Efflux-dependent auxin gradients establish the apical-basal axis of Arabidopsis. Nature **426:** 147–153.

Friml, J., et al. (2004). A PINOID-dependent binary switch in apical-basal PIN polar targeting directs auxin efflux. Science **306:** 862–865.

Fukuda, H. (2004). Signals that control plant vascular cell differentiation. Nat. Rev. Mol. Cell Biol. **5:** 379–391.

Gao, Z., Wen, C.K., Binder, B.M., Chen, Y.F., Chang, J., Chiang, Y.H., Kerris III, R.J., Chang, C., and Schaller, G.E. (2008). Heteromeric interactions among ethylene receptors mediate signaling in Arabidopsis. J. Biol. Chem. **283:** 23801–23810.

Grefen, C., Städele, K., Ruzicka, K., Obrdlik, P., Harter, K., and Horák, J. (2008). Subcellular localization and in vivo interactions of the *Arabidopsis thaliana* ethylene receptor family members. Mol. Plant **1:** 308–320.

Hartmann, U., Hohmann, S., Nettesheim, K., Wisman, E., Saedler, H., and Huijser, P. (2000). Molecular cloning of SVP: A negative regulator of the floral transition in Arabidopsis. Plant J. **21:** 351–360.

Hejátko, J., Pernisova, M., Eneva, T., Palme, K., and Brzobohaty, B. (2003). The putative sensor histidine kinase CKI1 is involved in female gametophyte development in Arabidopsis. Mol. Genet. Genomics **269:** 443–453.

Higuchi, M., et al. (2004). In planta functions of the Arabidopsis cytokinin receptor family. Proc. Natl. Acad. Sci. USA **101:** 8821–8826.

Hirakawa, Y., Shinohara, H., Kondo, Y., Inoue, A., Nakanomyo, I., Ogawa, M., Sawa, S., Ohashi-Ito, K., Matsubayashi, Y., and Fukuda, H. (2008). Non-cell-autonomous control of vascular stem cell fate by a CLE peptide/receptor system. Proc. Natl. Acad. Sci. USA **105:** 15208–15213.

Hirose, N., Makita, N., Yamaya, T., and Sakakibara, H. (2005). Functional characterization and expression analysis of a gene, OsENT2, encoding an equilibrative nucleoside transporter in rice suggest a function in cytokinin transport. Plant Physiol. **138:** 196–206.

Hirose, N., Takei, K., Kuroha, T., Kamada-Nobusada, T., Hayashi, H., and Sakakibara, H. (2008). Regulation of cytokinin biosynthesis, compartmentalization and translocation. J. Exp. Bot. **59:** 75–83.

Horak, J., Grefen, C., Berendzen, K.W., Hahn, A., Stierhof, Y.D., Stadelhofer, B., Stahl, M., Koncz, C., and Harter, K. (2008). The *Arabidopsis thaliana* response regulator ARR22 is a putative AHP phospho-histidine phosphatase expressed in the chalaza of developing seeds. BMC Plant Biol. **8:** 77.

Hutchison, C.E., Li, J., Argueso, C., Gonzalez, M., Lee, E., Lewis, M. W., Maxwell, B.B., Perdue, T.D., Schaller, G.E., Alonso, J.M., Ecker, J.R., and Kieber, J.J. (2006). The *Arabidopsis* histidine phosphotransfer proteins are redundant positive regulators of cytokinin signaling. Plant Cell **18:** 3073–3087.

Hwang, I., and Sheen, J. (2001). Two-component circuitry in Arabidopsis cytokinin signal transduction. Nature **413:** 383–389.

Jacobs, W.P. (1952). The role of auxin in differentiation of xylem around a wound. Am. J. Bot. **39:** 301–309.

Kakimoto, T. (1996). CKI1, a histidine kinase homolog implicated in cytokinin signal transduction. Science **274:** 982–985.

Kim, H.J., Ryu, H., Hong, S.H., Woo, H.R., Lim, P.O., Lee, I.C., Sheen, J., Nam, H.G., and Hwang, I. (2006). Cytokinin-mediated control of leaf longevity by AHK3 through phosphorylation of ARR2 in Arabidopsis. Proc. Natl. Acad. Sci. USA **103:** 814–819.

Ko, J.H., Han, K.H., Park, S., and Yang, J. (2004). Plant body weight-induced secondary growth in Arabidopsis and its transcription phenotype revealed by whole-transcriptome profiling. Plant Physiol. **135:** 1069–1083.

Kurakawa, T., Ueda, N., Maekawa, M., Kobayashi, K., Kojima, M., Nagato, Y., Sakakibara, H., and Kyozuka, J. (2007). Direct control of shoot meristem activity by a cytokinin-activating enzyme. Nature **445:** 652–655.

Mähönen, A.P., Bishopp, A., Higuchi, M., Nieminen, K.M., Kinoshita, K., Tormakangas, K., Ikeda, Y., Oka, A., Kakimoto, T., and Helariutta, Y. (2006b). Cytokinin signaling and its inhibitor AHP6 regulate cell fate during vascular development. Science **311:** 94–98.

Mähönen, A.P., Bonke, M., Kauppinen, L., Riikonen, M., Benfey, P. N., and Helariutta, Y. (2000). A novel two-component hybrid molecule regulates vascular morphogenesis of the Arabidopsis root. Genes Dev. **14:** 2938–2943.

Mähönen, A.P., Higuchi, M., Tormakangas, K., Miyawaki, K., Pischke, M.S., Sussman, M.R., Helariutta, Y., and Kakimoto, T. (2006a). Cytokinins regulate a bidirectional phosphorelay network in Arabidopsis. Curr. Biol. **16:** 1116–1122.

Matsumoto-Kitano, M., Kusumoto, T., Tarkowski, P., Kinoshita-Tsujimura, K., Vaclavikova, K., Miyawaki, K., and Kakimoto, T. (2008). Cytokinins are central regulators of cambial activity. Proc. Natl. Acad. Sci. USA **105:** 20027–20031.

Medford, J.I., Horgan, R., El-Sawi, Z., and Klee, H.J. (1989). Alterations of endogenous cytokinins in transgenic plants using a chimeric isopentenyl transferase gene. Plant Cell **1:** 403–413.

Miyawaki, K., Matsumoto-Kitano, M., and Kakimoto, T. (2004). Expression of cytokinin biosynthetic isopentenyltransferase genes in

Arabidopsis: Tissue specificity and regulation by auxin, cytokinin, and nitrate. Plant J. **37:** 128–138.

Müller, B., and Sheen, J. (2008). Cytokinin and auxin interaction in root stem-cell specification during early embryogenesis. Nature **453:** 1094–1097.

Nakamura, A., Kakimoto, T., Imamura, A., Suzuki, T., Ueguchi, C., and Mizuno, T. (1999). Biochemical characterization of a putative cytokinin-responsive His-kinase, CKI1, from *Arabidopsis thaliana*. Biosci. Biotechnol. Biochem. **63:** 1627–1630.

Nieminen, K., et al. (2008). Cytokinin signaling regulates cambial development in poplar. Proc. Natl. Acad. Sci. USA **105:** 20032–20037.

Nishimura, C., Ohashi, Y., Sato, S., Kato, T., Tabata, S., and Ueguchi, C. (2004). Histidine kinase homologs that act as cytokinin receptors possess overlapping functions in the regulation of shoot and root growth in *Arabidopsis*. Plant Cell **16:** 1365–1377.

Pernisova, M., Klima, P., Horak, J., Valkova, M., Malbeck, J., Soucek, P., Reichman, P., Hoyerova, K., Dubova, J., Friml, J., Zazimalova, E., and Hejatko, J. (2009). Cytokinins modulate auxin-induced organogenesis in plants via regulation of the auxin efflux. Proc. Natl. Acad. Sci. USA **106:** 3609–3614.

Pischke, M.S., Jones, L.G., Otsuga, D., Fernandez, D.E., Drews, G. N., and Sussman, M.R. (2002). An Arabidopsis histidine kinase is essential for megagametogenesis. Proc. Natl. Acad. Sci. USA **99:** 15800–15805.

Prigge, M.J., Otsuga, D., Alonso, J.M., Ecker, J.R., Drews, G.N., and Clark, S.E. (2005). Class III homeodomain-leucine zipper gene family members have overlapping, antagonistic, and distinct roles in *Arabidopsis* development. Plant Cell **17:** 61–76.

Sachs, T. (2000). Integrating cellular and organismic aspects of vascular differentiation. Plant Cell Physiol. **41:** 649–656.

Samuelson, M.E., Eliasson, L., and Larsson, C.M. (1992). Nitrate-regulated growth and cytokinin responses in seminal roots of barley. Plant Physiol. **98:** 309–315.

Schaller, G.E., Ladd, A.N., Lanahan, M.B., Spanbauer, J.M., and Bleecker, A.B. (1995). The ethylene response mediator ETR1 from Arabidopsis forms a disulfide-linked dimer. J. Biol. Chem. **270:** 12526–12530.

Scheres, B., Dilaurenzio, L., Willemsen, V., Hauser, M.T., Janmaat, K., Weisbeek, P., and Benfey, P.N. (1995). Mutations affecting the radial organization of the Arabidopsis root display specific defects throughout the embryonic axis. Development **121:** 53–62.

Surette, M.G., Levit, M., Liu, Y., Lukat, G., Ninfa, E.G., Ninfa, A., and Stock, J.B. (1996). Dimerization is required for the activity of the protein histidine kinase CheA that mediates signal transduction in bacterial chemotaxis. J. Biol. Chem. **271:** 939–945.

Szekeres, M., Nemeth, K., Koncz-Kalman, Z., Mathur, J., Kauschmann, A., Altmann, T., Redei, G.P., Nagy, F., Schell, J., and Koncz, C. (1996). Brassinosteroids rescue the deficiency of CYP90, a cytochrome P450, controlling cell elongation and de-etiolation in Arabidopsis. Cell **85:** 171–182.

Takei, K., Ueda, N., Aoki, K., Kuromori, T., Hirayama, T., Shinozaki, K., Yamaya, T., and Sakakibara, H. (2004). AtIPT3 is a key determinant of nitrate-dependent cytokinin biosynthesis in Arabidopsis. Plant Cell Physiol. **45:** 1053–1062.

To, J.P., Haberer, G., Ferreira, F.J., Deruere, J., Mason, M.G., Schaller, G.E., Alonso, J.M., Ecker, J.R., and Kieber, J.J. (2004). Type-A Arabidopsis response regulators are partially redundant negative regulators of cytokinin signaling. Plant Cell **16:** 658–671.

Tomomori, C., et al. (1999). Solution structure of the homodimeric core domain of *Escherichia coli* histidine kinase EnvZ. Nat. Struct. Biol. **6:** 729–734.

Vitha, S., Baluska, F., Braun, M., Samaj, J., Volkmann, D., and Barlow, P.W. (2000). Comparison of cryofixation and aldehyde fixation for plant actin immunocytochemistry: Aldehydes do not destroy F-actin. Histochem. J. **32:** 457–466.

Walter, M., Chaban, C., Schutze, K., Batistic, O., Weckermann, K., Nake, C., Blazevic, D., Grefen, C., Schumacher, K., Oecking, C., Harter, K., and Kudla, J. (2004). Visualization of protein interactions in living plant cells using bimolecular fluorescence complementation. Plant J. **40:** 428–438.

Werner, T., Kollmer, I., Bartrina, I., Holst, K., and Schmulling, T. (2006). New insights into the biology of cytokinin degradation. Plant Biol. **8:** 371–381.

Werner, T., Motyka, V., Laucou, V., Smets, R., Van Onckelen, H., and Schmulling, T. (2003). Cytokinin-deficient transgenic *Arabidopsis* plants show multiple developmental alterations indicating opposite functions of cytokinins in the regulation of shoot and root meristem activity. Plant Cell **15:** 2532–2550.

Yamada, H., Suzuki, T., Terada, K., Takei, K., Ishikawa, K., Miwa, K., Yamashino, T., and Mizuno, T. (2001). The Arabidopsis AHK4 histidine kinase is a cytokinin-binding receptor that transduces cytokinin signals across the membrane. Plant Cell Physiol. **42:** 1017–1023.

Yang, J., Zhang, J., Wang, Z., Zhu, Q., and Wang, W. (2001). Hormonal changes in the grains of rice subjected to water stress during grain filling. Plant Physiol. **127:** 315–323.

Ye, Z.H., Freshour, G., Hahn, M.G., Burk, D.H., and Zhong, R. (2002). Vascular development in Arabidopsis. Int. Rev. Cytol. **220:** 225–256.

Yokoyama, A., Yamashino, T., Amano, Y., Tajima, Y., Imamura, A., Sakakibara, H., and Mizuno, T. (2007). Type-B ARR transcription factors, ARR10 and ARR12, are implicated in cytokinin-mediated regulation of protoxylem differentiation in roots of *Arabidopsis thaliana*. Plant Cell Physiol. **48:** 84–96.

Zhao, C., Craig, J.C., Petzold, H.E., Dickerman, A.W., and Beers, E.P. (2005). The xylem and phloem transcriptomes from secondary tissues of the Arabidopsis root-hypocotyl. Plant Physiol. **138:** 803–818.

The Histidine Kinases CYTOKININ-INDEPENDENT1 and ARABIDOPSIS HISTIDINE KINASE2 and 3 Regulate Vascular Tissue Development in Arabidopsis Shoots
Jan Hejátko, Hojin Ryu, Gyung-Tae Kim, Romana Dobesová, Sunhwa Choi, Sang Mi Choi, Premysl Soucek, Jakub Horák, Blanka Pekárová, Klaus Palme, Bretislav Brzobohaty and Ildoo Hwang
PLANT CELL 2009;21;2008-2021; originally published online Jul 21, 2009;
DOI: 10.1105/tpc.109.066696

This information is current as of September 11, 2009

Supplemental Data	http://www.plantcell.org/cgi/content/full/tpc.109.066696/DC1
References	This article cites 62 articles, 35 of which you can access for free at: http://www.plantcell.org/cgi/content/full/21/7/2008#BIBL
Permissions	https://www.copyright.com/ccc/openurl.do?sid=pd_hw1532298X&issn=1532298X&WT.mc_id=pd_hw1532298X
eTOCs	Sign up for eTOCs for *THE PLANT CELL* at: http://www.plantcell.org/subscriptions/etoc.shtml
CiteTrack Alerts	Sign up for CiteTrack Alerts for *Plant Cell* at: http://www.plantcell.org/cgi/alerts/ctmain
Subscription Information	Subscription information for *The Plant Cell* and *Plant Physiology* is available at: http://www.aspb.org/publications/subscriptions.cfm

© American Society of Plant Biologists

ADVANCING THE SCIENCE OF PLANT BIOLOGY

Supplemental Data. Hejátko et al. (2009). The histidine kinases CYTOKININ INDEPENDENT 1 and ARABIDOPSIS HISTIDINE KINASE 2 and 3 regulate vascular tissue development in *Arabidopsis* shoots.

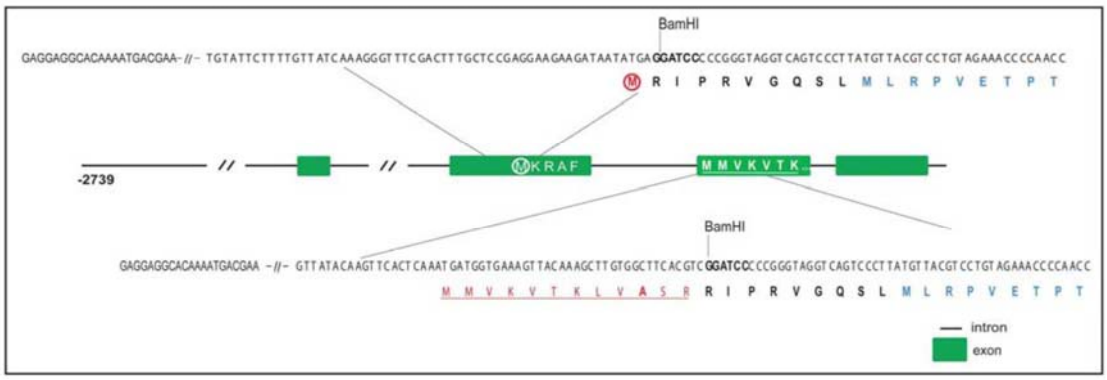

Supplemental Figure 1. Schematic representation of the *ProCKI1:uidA* (up) and *ProCKI1:R12-uidA* (down) constructs used in analysis of the transcriptional specificity of the *CKI1* promoter. Exons are depicted as green boxes; amino acid sequences of CKI1 and a small ORF identified in the 5' UTR of the *CKI1* cDNA are shown.

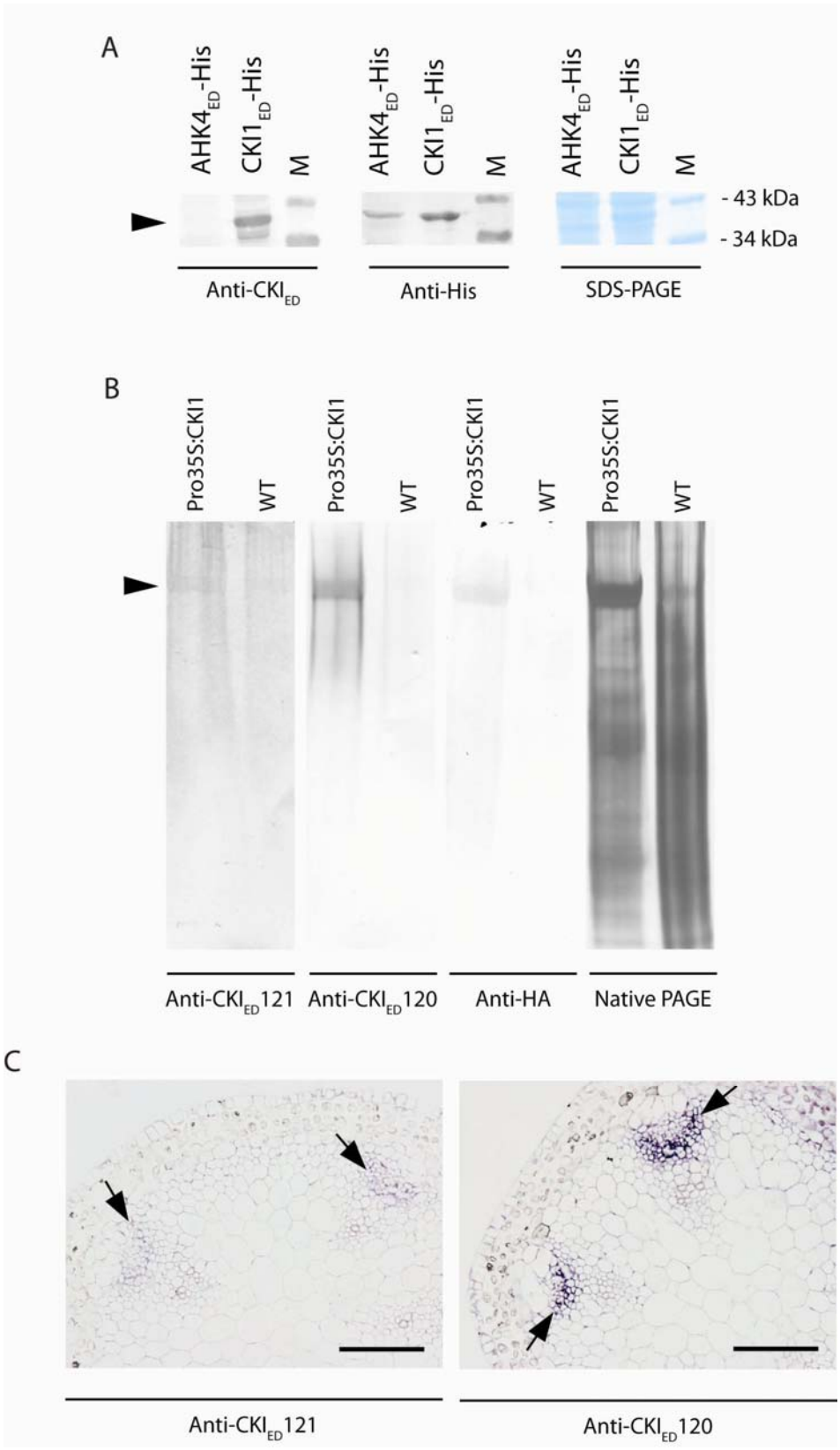
A
AHK4ED-His
CKI1ED-His
M
AHK4ED-His
CKI1ED-His
M
AHK4ED-His
CKI1ED-His
M
- 43 kDa
- 34 kDa
Anti-CKIED
Anti-His
SDS-PAGE
B
Pro35S:CKI1
WT
Pro35S:CKI1
WT
Pro35S:CKI1
WT
Pro35S:CKI1
WT
Anti-CKIED121
Anti-CKIED120
Anti-HA
Native PAGE
C
Anti-CKIED121
Anti-CKIED120

Supplemental Figure 2. A. Anti-CKI1$_{ED}$ (αCKI1$_{ED}$) distinctively recognizes the extracellular domain of CKI1. Recombinant proteins containing extracellular domains of CKI1 (CKI1$_{ED}$, E28-Q345, 42 kDa) and AHK4 (AHK4$_{ED}$, D127- P395, 37 kDa) were expressed in *E. coli* as a translational fusion with His-Tag. Both proteins were immunodetected using anti-polyHistidine (anti-His) and αCKI1$_{ED}$ antibodies. The arrowhead shows the position of the specific signals; M is for molecular weight markers. **B.** Anti-CKI1$_{ED}$ recognizes specifically CKI1 in the protein extract from inflorescence stems on immuno blots from native-PAGE; 80 µg of the total protein was loaded in each lane. WT and *Pro35S:CKI1* plants were used for protein isolation. Two batches of polyclonal sera (Anti-CKI1$_{ED}$120 [dilution 1:5,000] and Anti-CKI1$_{ED}$121 [1:2,000]) isolated from two independently immunized rabbits were tested. Position of CKI1-HA proteins from *Pro35S:CKI1* line was verified by anti-HA antibody. The silver-stained gel after native-PAGE is shown as a loading control. **C.** Both batches of Anti-CKI1$_{ED}$ recognize CKI1 *in situ* with different efficiency. Both antibodies (dilution 1:1,000) were used for *in situ* CKI1 localization on sections of WT inflorescence stems; the arrows point to the signal. Note the apparently lower signal intensity of Anti-CKI1$_{ED}$121 that reflects its lower efficiency on immuno blots (Fig. S2B). Scale bars 100 µm.

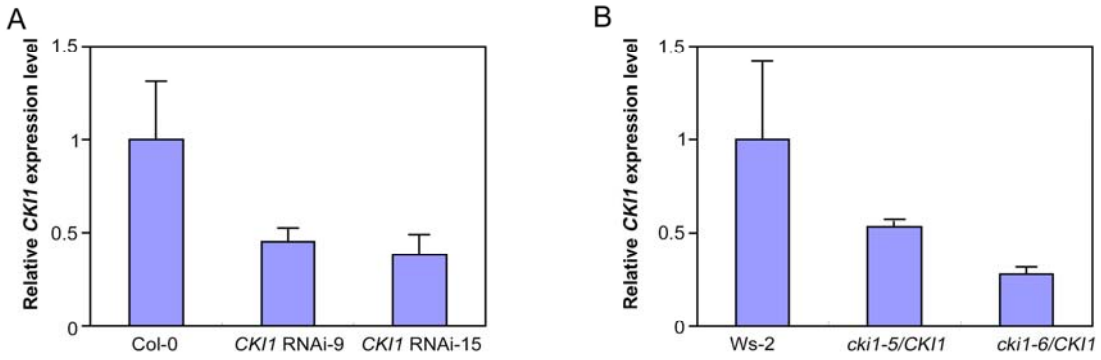

Supplemental Figure 3. Transcript levels of *CKI1* in RNAi lines (A) and T-DNA insertion heterozygous lines (B). Quantitative real time PCR was performed with total RNA extracted from inflorescence stems of WT (Col-0 and WS-2), *CKI1* RNAi, *cki1-5/CKI1* and *cki1-6/CKI1* transgenic plants and gene-specific primers for *CKI1*. Error bars indicate SE (n=3).

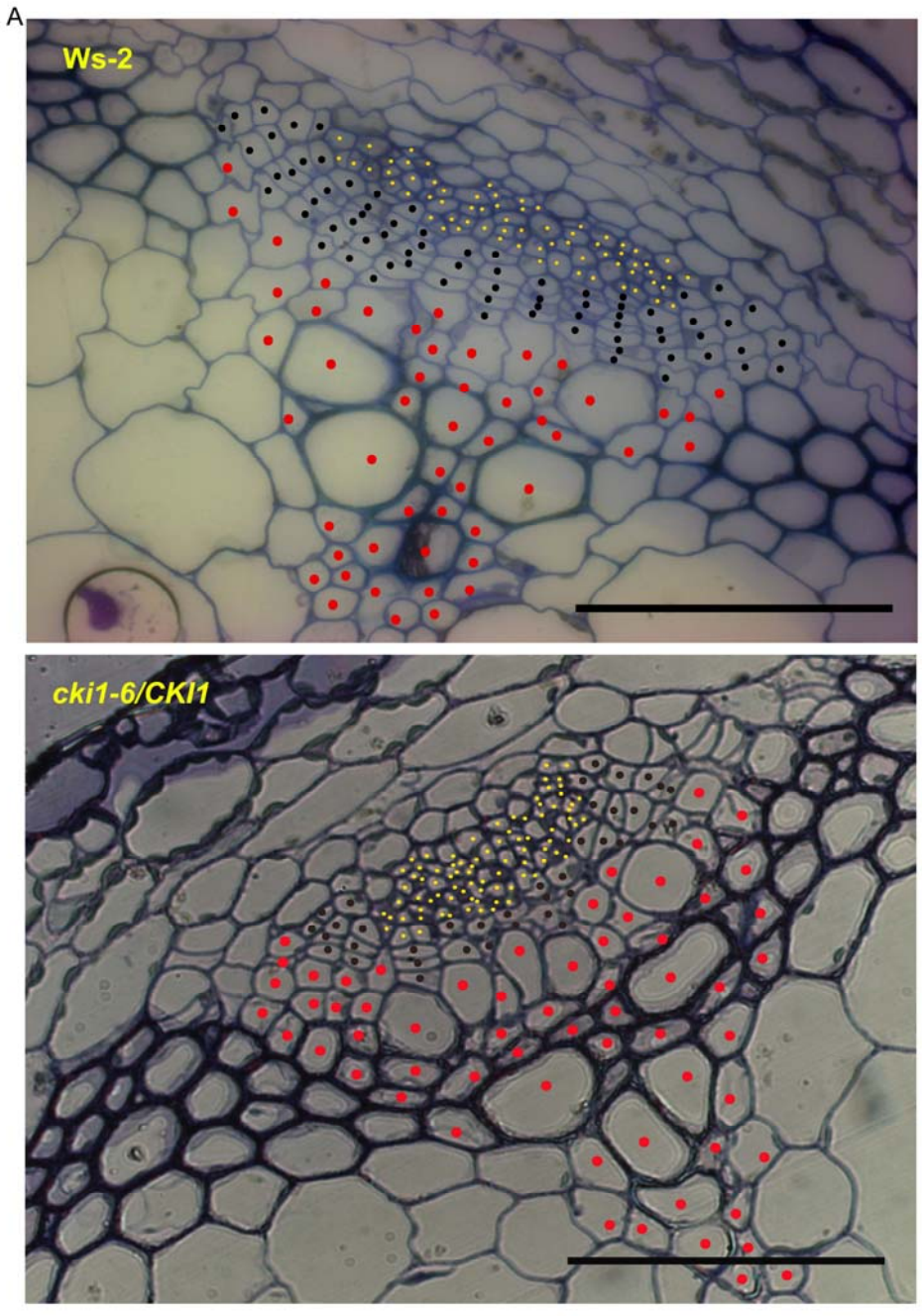
A
Ws-2
cki1-6/CKI1
B
Number of cambial cells
175
150
100
50
0
Col-0
Pro35S:
CKI1 1-13
Ws-2
cki1-6/CKI1

Supplemental Figure 4. CKI1 regulates the number of procambial cells. **A.** Examples of cell counting in an inflorescence stem section of WT (Ws-2) and *cki1-6/CKI1* plant. The cells marked with black dots, yellow dots, and red dots are indicated as procambia, phloem, and xylem cells, respectively. Scale bars, 100 μm. **B.** The number of cells in WT, *Pro35S:CKI1* and *cki1-6/CKI1* sections. Error bars indicate SE; Col-0 (n=8), Ws-2 (n=12), *Pro35S:CKI1*1-13 (n=6), and *cki1-6/CKI1* (n=14).

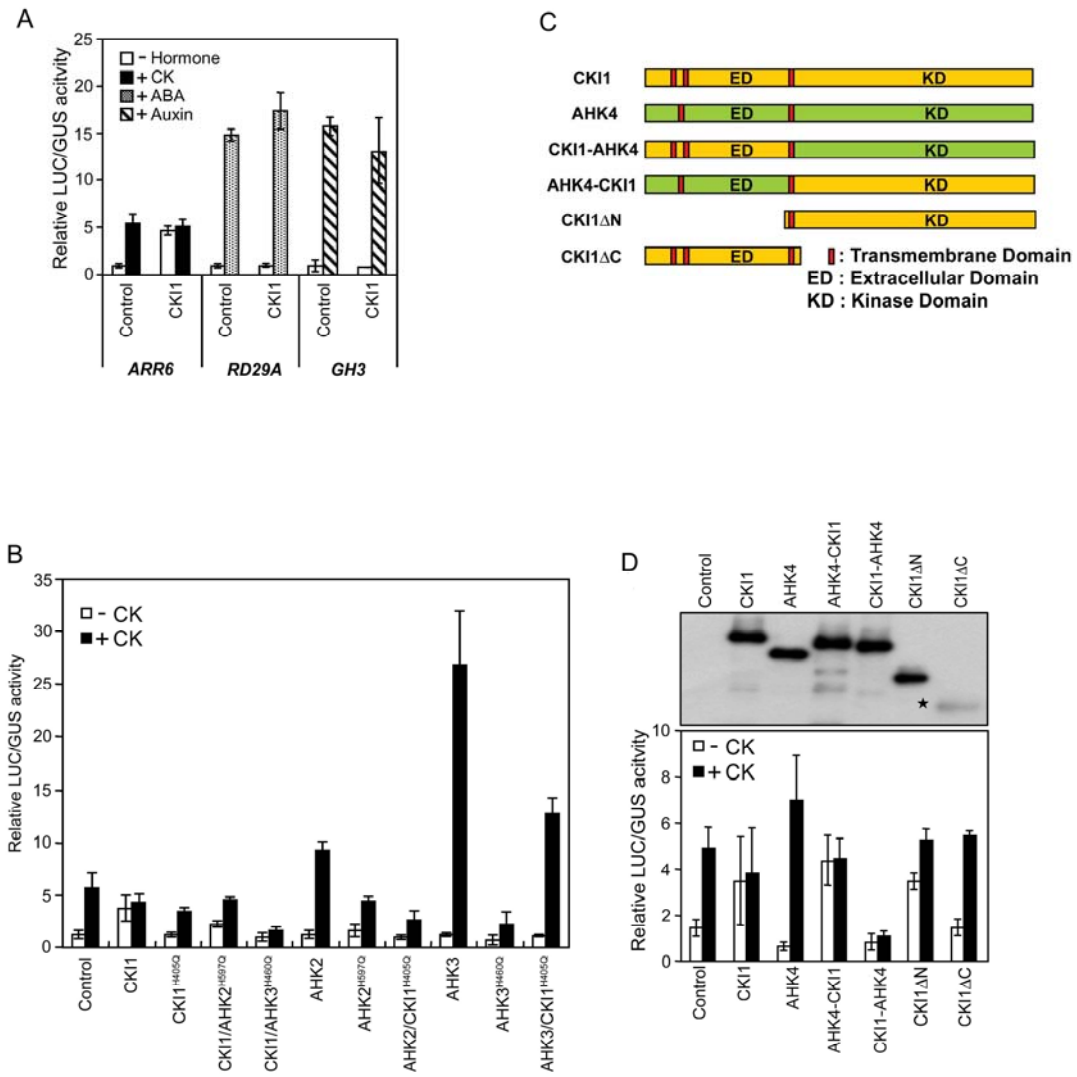

Supplemental Figure 5. **A**. CKI1 specifically enhances the activity of the two-component, cytokinin-responsive *ARR6* promoter in a cytokinin-independent manner. Protoplasts were co-transfected with *CKI1*, *UBQ10-GUS* (internal control) and *ARR6-LUC (ARR6), RD29A-LUC (RD29A),* or *GH3-LUC (GH3)*. Vector DNA served as a transfection control. Protoplasts transfected with *ARR6, RD29A,* and *GH3* were treated with 100 nM t-zeatin (cytokinin), 1 μM indole acetic acid, and 100 μM abscisic acid, respectively. Error bars indicate SE (n=2) **B**. A negative form of CKI1 proteins represses cytokinin receptor-mediated

induction of *ARR6*. Protoplasts from WT plants were transfected with *ARR6-LUC* alone, WT *AHK2* and *AHK3*, WT *AHK2* and *AHK3* plus mutant *CKI1*, WT *CKI1*, or WT *CKI1* plus mutant *AHK2* and *AHK3*. $CKI1^{H405Q}$, $AHK2^{H597Q}$, and $AHK3^{H460Q}$ are negative versions of CKI1, AHK2, and AHK3 respectively. Error bars indicate SE (n=2). **C**. Schematic depiction of full-length *CKI1*, *AHK4*, various *CKI1* deletion constructs and chimeric constructs composed of different domains of *AHK4* and *CKI1*. **D**. The C-terminal kinase domain of CKI1 is essential for its cytokinin-independent histidine kinase activity. Protoplasts from WT plants were transfected with *ARR6-LUC* and one of the following: *CKI1*, *AHK4*, *AHK4-CKI1*, *CKI1-AHK4*, *CKI1ΔN*, or *CKI1ΔC*. All of these constructs, except for CKI1ΔN (indicated by an asterisk), were expressed at comparable levels (top panel). The transfected protoplasts were incubated with or without 100 nM t-zeatin. *UBQ10-GUS* served as an internal control. Error bars indicate SE (n=2).

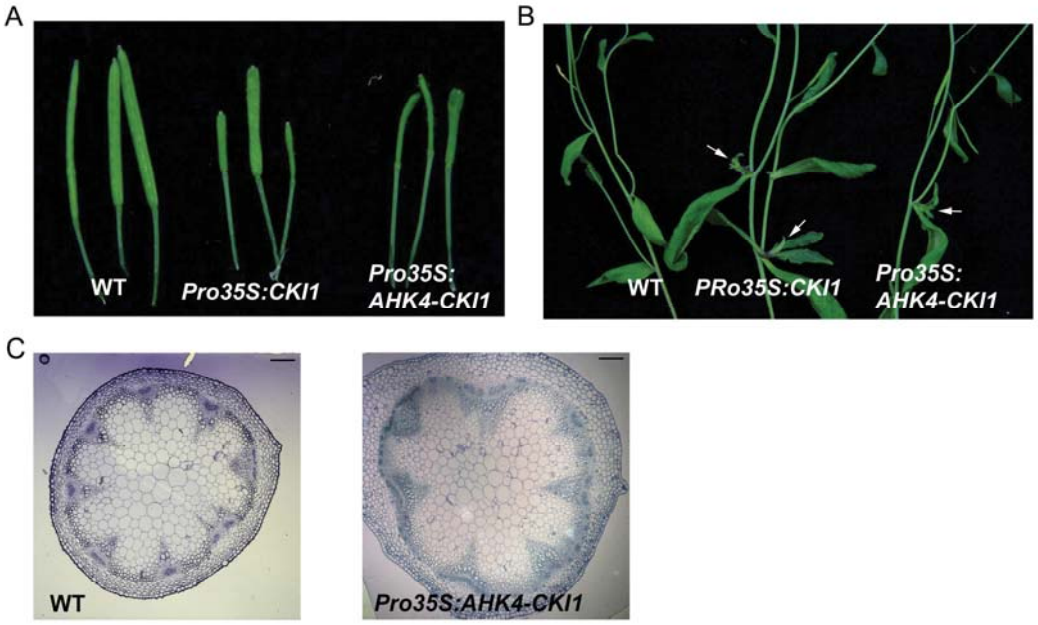

Supplemental Figure 6. **A, B.** The ectopic expression of both CKI1 and AHK4-CKI1 leads to sterility and short fascinated siliques (A) and to additional vegetative tissues initiated from lateral meristems (B). The arrow indicates these tissues in *Pro35S:CKI1* and *Pro35S:AHK4-CKI1* transgenic plants. **C.** Overexpression of AHK4-CKI1 leads to the changes in VB formation. Transverse sections of the inflorescence stems of WT (Col-0) and *Pro35S:AHK4-CKI1* transgenic plants. Scale bars, 100 μm.

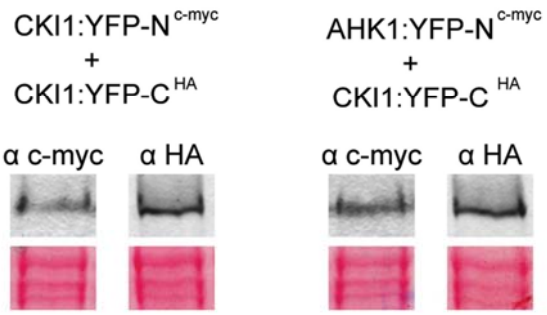

Supplemental Figure 7. The expression of individual constructs used in BiFC assay in Figure 5B was determined by immunostaining; Ponceau S staining was used to prove equal protein loading (red bands).

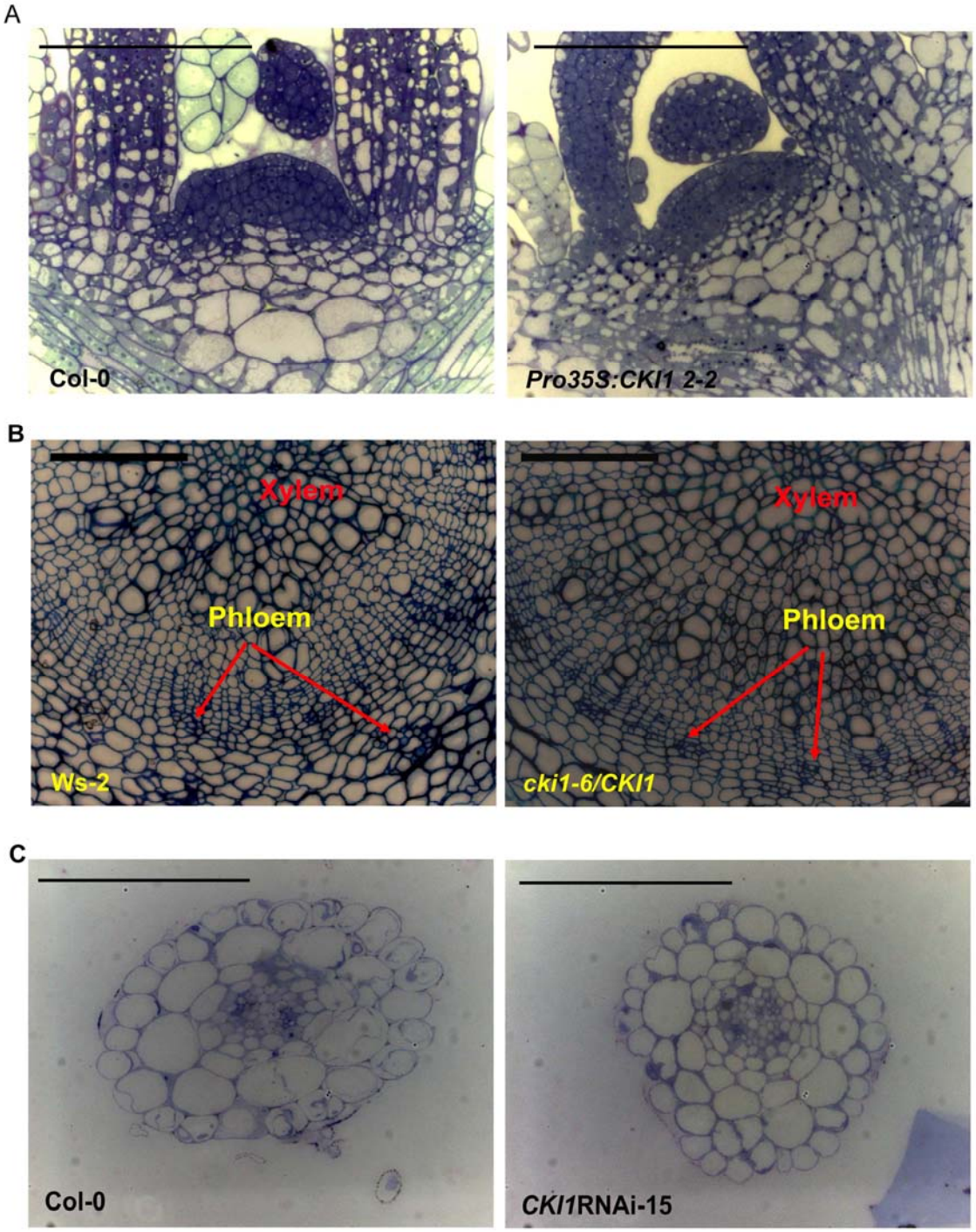

Supplemental Figure 8. CKI1 activity does not affect either the SAM activity or the vascular bundle development in hypocotyl and root. **A.** Transverse section of 7-day-old seedling of *Pro35S:CKI1 2-2* lines and WT (Col-0). Scale bars, 100

μm. **B.** Cross section of 25-day-old hypocotyl of *cki1-6/CKI1* and WT (Ws-2). Scale bars, 100 μm. **C.** Cross section of 7-day-old root of CKI1RNAi and WT (Col-0). Scale bars, 100 μm.

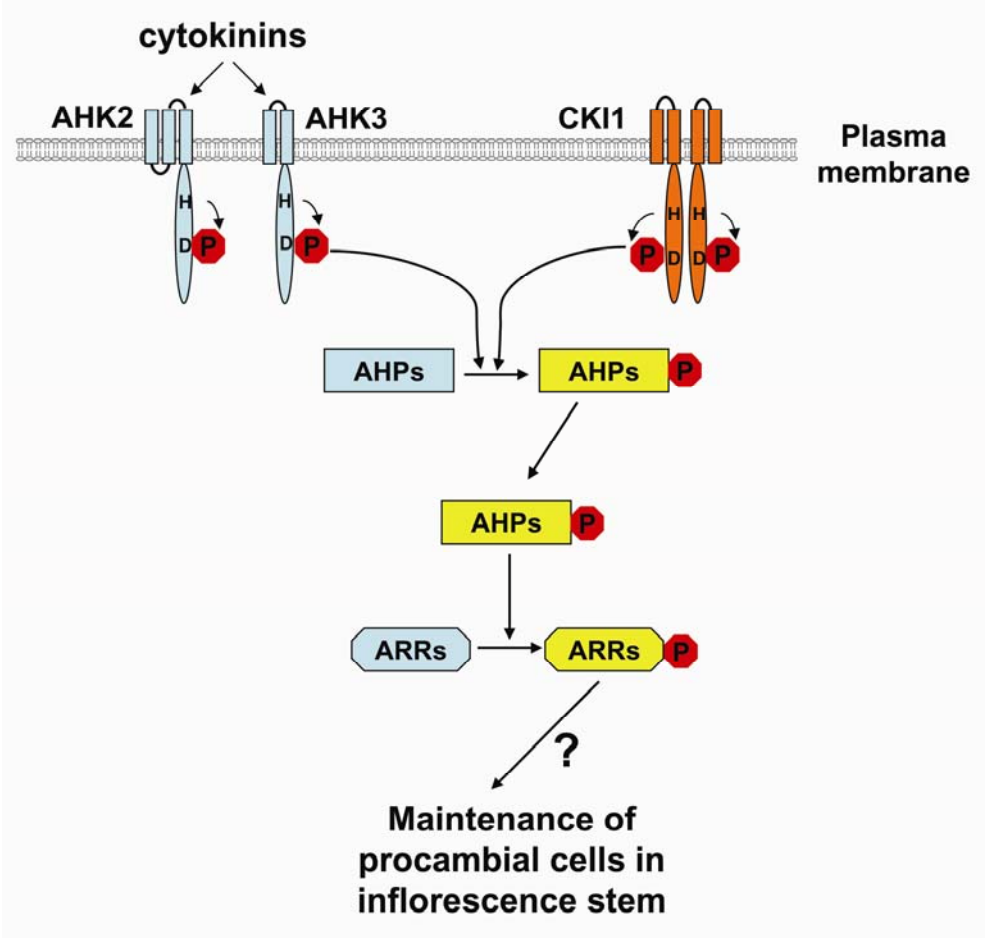

Supplemental Figure 9. A proposed model for CKI1 and cytokinin action mechanism in the vascular bundle development of inflorescence stems. We here propose that the histidine kinase activities from cytokinin-independent CKI1 and cytokinin-induced AHK2 and AHK3 are important for the vascular bundle development. CKI1, AHK2 and AHK3 are involved in the regulation of procambium proliferation and/or the maintenance of its identity in *Arabidopsis* inflorescence stems. However, the functional roles of phosphorelay to ARRs via AHPs in this developmental process are remained to be explored.

Supplemental Table 1. Gene-specific primers for type-A *ARR*s

Gene	Primer sequences
ARR3	F:ACGAGAGACGTTAAAGTCGC R:CTAAGCTAATCCGGGACTCC
ARR4	F:TCCACCGTCACCTCCGTTGA R:ATCTAATCCGGGACTCCTCA
ARR5	F:GTATCGATAGATGTCTTGAA R:CAGCTATGTATCTGTAGCAAT
ARR6	F:CGAGAACATTTTGCCTCGTA R:CAGCTCAAACGCGCAAAGATC
ARR7	F:TCTTGTTGAAACCGGTGAAG R:CAAAGTAGAGAAAAAAGGTT
ARR8	F:TACCAAGTTGAAACCTCATA R:GACCGAGGTTGTGATATCAT
ARR9	F:TGGAGTCCCCACTGCAGTAG R:GACAGCGGTTGCGATACCGT
ARR15	F:AATTAGCTGATGTGAAGCGT R:CCCCTAGACTCTAATTTGAT
ARR16	F:ATCACCGATTACTGTATGCC R:GCTTCTGCAGTTCATGAGAT
ARR17	F:GTATGCCAGGAATGACAGGT R:GCTTCTGCAATTTAAAAGAT

Enclosed Publication # 6

Klumpler, T., Pekárová, B., Marek, J., Borkovcová, P., Janda, L. and **Hejátko, J.** (2009) Cloning, purification, crystallization and preliminary X-ray analysis of the receiver domain of the histidine kinase CKI1 from *Arabidopsis thaliana*. *Acta Crystallographica Section F*, **F65**, 478-481. IF_{2008}= 0.606

electronic reprint

Acta Crystallographica Section F
Structural Biology and Crystallization Communications
ISSN 1744-3091
Editors: **H. M. Einspahr and M. S. Weiss**

Cloning, purification, crystallization and preliminary X-ray analysis of the receiver domain of the histidine kinase CKI1 from *Arabidopsis thaliana*

Tomáš Klumpler, Blanka Pekárová, Jaromír Marek, Petra Borkovcová, Lubomír Janda and Jan Hejátko

Acta Cryst. (2009). F**65**, 478–481

Copyright © International Union of Crystallography

Author(s) of this paper may load this reprint on their own web site or institutional repository provided that this cover page is retained. Republication of this article or its storage in electronic databases other than as specified above is not permitted without prior permission in writing from the IUCr.

For further information see http://journals.iucr.org/services/authorrights.html

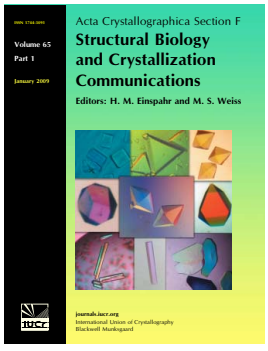

Acta Crystallographica Section F: Structural Biology and Crystallization Communications is a rapid all-electronic journal, which provides a home for short communications on the crystallization and structure of biological macromolecules. It includes four categories of publication: protein structure communications; nucleic acid structure communications; structural genomics communications; and crystallization communications. Structures determined through structural genomics initiatives or from iterative studies such as those used in the pharmaceutical industry are particularly welcomed. *Section F* is essential for all those interested in structural biology including molecular biologists, biochemists, crystallization specialists, structural biologists, biophysicists, pharmacologists and other life scientists.

Crystallography Journals Online is available from **journals.iucr.org**

Acta Crystallographica Section F
Structural Biology and Crystallization Communications
ISSN 1744-3091

Cloning, purification, crystallization and preliminary X-ray analysis of the receiver domain of the histidine kinase CKI1 from *Arabidopsis thaliana*

Tomáš Klumpler, Blanka Pekárová, Jaromír Marek,* Petra Borkovcová, Lubomír Janda and Jan Hejátko

Laboratory of Molecular Plant Physiology, Department of Functional Genomics and Proteomics, Institute of Experimental Biology, Faculty of Science, Masaryk University, Kamenice 5/A2, CZ-625 00 Brno, Czech Republic

Correspondence e-mail: marek@chemi.muni.cz

Received 15 January 2009
Accepted 31 March 2009

The receiver domain (RD) of a sensor histidine kinase (HK) catalyses the transphosphorylation reaction during the action of HKs in hormonal and abiotic signalling in plants. Crystals of the recombinant RD of the *Arabidopsis thaliana* HK CYTOKININ-INDEPENDENT1 ($CKI1_{RD}$) have been obtained by the hanging-drop vapour-diffusion method using ammonium sulfate as a precipitant and glycerol as a cryoprotectant. The crystals diffracted to approximately 2.4 Å resolution on beamline BW7B of the DORIS-III storage ring. The diffraction improved significantly after the use of a non-aqueous cryoprotectant. Crystals soaked in Paratone-N diffracted to at least 2.0 Å resolution on beamline BW7B and their mosaicity decreased more than tenfold. The crystals belonged to space group $C222_1$, with unit-cell parameters a = 54.46, b = 99.82, c = 79.94 Å. Assuming the presence of one molecule of the protein in the asymmetric unit gives a Matthews coefficient V_M of 2.33 Å^3 Da^{-1}. A molecular-replacement solution has been obtained and structure refinement is in progress.

1. Introduction

Sensor histidine kinases (HKs) are members of the two-component (TC) signalling systems that mediate signal transduction in a broad spectrum of adaptive responses in bacteria (Calva & Oropeza, 2006; Hoch, 2000). A modified version of bacterial TC signalling has been adapted by yeast and plants (Chang & Stewart, 1998): as a so-called two-component phosphorelay (Hoch, 2000). In TC signalling in plants, the membrane-associated sensor HK interacts with a signalling molecule, which activates an intracellular HK domain and leads to autophosphorylation of its conserved histidine moiety. The downstream phosphorelay is initiated by a receiver domain (RD) of the HK. The RD transfers phosphate from a His to its own Asp and further transmits the signal *via* transphosphorylation to the His of a histidine-containing phosphotransfer (HPt) domain. The HPt proteins translocate the signal to the nucleus, where the phosphorylated histidine serves as a donor for the phosphorylation of a final phosphate acceptor, the Asp residue of the response regulator (To & Kieber, 2008; Mizuno, 2005).

The receiver domain of sensor HKs seems to mediate the limiting steps in the above-described phosphorelay and thus signal transduction. In addtion to its catalytic activity, which triggers the phosphorelay, the RD is also supposed to be involved in specific protein–protein interactions with its downstream signalling partners. The amino-acid residues in the C-terminal domains of the sensor HKs have recently been shown to be responsible for the specificity of the signal transduction to their downstream signalling proteins in bacteria (Skerker *et al.*, 2008). Moreover, the amino acids predicted, using covariant analysis, to be important for the specific protein–protein interactions were located close to the physical interface of both interaction partners (Skerker *et al.*, 2008). This suggests that the structure of the RD might contribute to the recognition of its interaction partner(s).

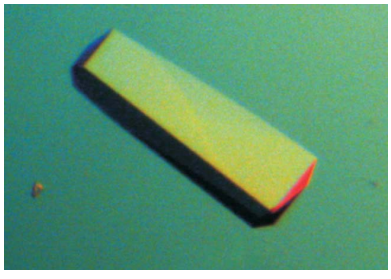

© 2009 International Union of Crystallography
All rights reserved

electronic reprint

In the *Arabidopsis thaliana* genome, genes encoding 11 HKs, six HPt proteins and 23 response regulators have been identified. *A. thaliana* HKs mediate discrete responses to various phytohormones (ethylene, cytokinin and abscisic acid) and abiotic stress (osmosensing) (Mizuno, 2005; Tran *et al.*, 2007). Based on the mechanism of the above-described bacterial TC signalling, protein–protein interactions of the RD domains of individual histidine kinases and HPt proteins will presumably be involved in determination of the specificity of the individual signalling pathways and/or their crosstalk in plants. However, the mechanisms discriminating this specificity at the protein level, which are likely to depend on differential tertiary structures of the interacting partners, have not yet been characterized. Thus, knowledge of the structure of individual RDs and their interaction partners seems to be critical to our understanding of the molecular mechanism of these specific interactions. To date, the structures of many bacterial RDs belonging to a family of phosphatases and phosphate carrier proteins have been determined, *e.g.* CheY (Stock *et al.*, 1989) and PhoB (Sola *et al.*, 1999). However, the RD of ethylene receptor ETR1 is the only receiver domain from a plant for which the structure has been solved (Muller-Dieckmann *et al.*, 1999).

The sensor histidine kinase CKI1 was identified as an activator of a cytokinin-like response when overexpressed in hypocotyl explants of *A. thaliana* (Kakimoto, 1996). However, in contrast to the genuine cytokinin receptors of *A. thaliana*, AHK2, AHK3 and AHK4, CKI1 was found to be constitutively active in bacteria and yeast or *A. thaliana* protoplasts (Yamada *et al.*, 2001; Hwang & Sheen, 2001). Thus, the specificity and the role of CKI1 in the TC signalling in *A. thaliana* remain unclear. Our recent data suggest that $CKI1_{RD}$ is responsible for a specific interaction with individual HPt proteins in *A. thaliana* (Pekárová *et al.*, manuscript in preparation). Here, we describe the cloning, protein overproduction, purification, crystallization and preliminary X-ray diffraction analysis of $CKI1_{RD}$ from *A. thaliana*.

2. Materials and methods

2.1. Cloning and protein overproduction

A plasmid containing a DNA fragment encoding the receiver domain of CKI1 ($CKI1_{RD}$) was generated by PCR using *CKI1* cDNA (provided by T. Kakimoto, Osaka University, Japan) as a template and primers 5′-TAA TG**G CTA GC**A CAG ATT CAG AGA GT-3′ (*Nhe*I restriction site in bold) and 5′-TAT AC**C TCG AG**A GTG ACG TTT GCT TTC GAT TTC TC-3′ (*Xho*I restriction site in bold).

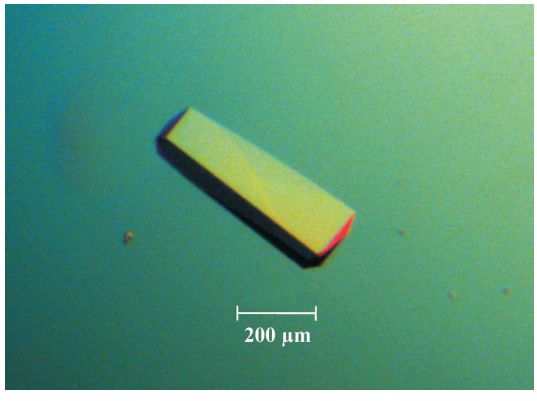

Figure 1
An example of a typical crystal of $CKI1_{RD}$.

The amplified DNA fragment was purified on agarose gel, digested with *Nhe*I and *Xho*I, ligated into the vector pET28a(+) (Novagen) and transformed into *Escherichia coli* strain DH10β and finally into *E. coli* strain BL21(DE3)pLysS. The cells carrying the expression plasmid were cultured with shaking in TB medium pH 7.5 at 310 K until an OD_{600} of 0.8 was reached. At this point, the expression of $CKI1_{RD}$ was induced by adding isopropyl β-D-1-thiogalactopyranoside to a final concentration of 0.42 m*M*. After 3 h incubation at 301 K, the cells were harvested by centrifugation at 3500*g* for 20 min at 277 K.

2.2. Purification

The cells expressing $CKI1_{RD}$ were resuspended in a buffer containing 20 m*M* Tris–HCl pH 7.9, 500 m*M* NaCl, 0.1% Triton X-100 and disintegrated by sonication. After centrifugation at 48 500*g* for 40 min at 277 K, the supernatant was applied onto a HiTrap Chelating HP column (Amersham Biosciences, ÄKTA FPLC system) charged with Zn^{2+} ions and equilibrated in 50 m*M* Tris–HCl pH 7.0, 1 *M* NaCl, 20 m*M* imidazole. The protein was eluted with a linear gradient of imidazole (20–150 m*M*) and pH (7.0–4.5).

The final purification was achieved by gel filtration with a HiLoad 16/60 Superdex 75 prep-grade column (Amersham Biosciences, ÄKTA FPLC system) equilibrated in 50 m*M* Tris–HCl pH 7.5, 150 m*M* NaCl, 10 m*M* EDTA. The collected fractions were analysed on polyacrylamide gels. SDS–PAGE and native PAGE were performed according to Laemmli (1970) using 15%(*w*/*v*) separation gels. Pure fractions (≥95%, Densitometer GS-800, *Quantity One 1-D* analysis software; Bio-Rad) were concentrated to a final concentration of 10 mg ml^{-1} using an Amicon Ultra system (Millipore) with a molecular-weight cutoff of 10 kDa. The protein concentration was determined according to Bradford (1976) using BSA as a standard. The purified protein was stored at 277 K temporarily and at 193 K for long-term storage.

2.3. Crystallization

Preliminary screening of crystallization conditions was carried out by the sitting-drop (100 nl protein solution mixed with 100 nl reservoir solution equilibrated against 100 µl reservoir solution) vapour-diffusion method at 293 K in 96-well plates using an automated nanolitre liquid-handling system (Mosquito, TTP LabTech) and Structure Screen I + II HT-96, MemStart + MemSys HT-96 and PACT Premier HT-96 (all screens were from Molecular Dimensions). Promising microcrystals were obtained after a few days from condition A5 of the MemStart + MemSys screen (0.1 *M* sodium acetate buffer pH 4.6, 2.0 *M* ammonium sulfate). The gradual optimization of the identified conditions was focused on increasing the drop and crystal size, improvement of crystal quality and the use of cryoprotectant. The optimization yielded an optimized composition of the reservoir solution consisting of 2.54 *M* ammonium sulfate, 15.9%(*v*/*v*) glycerol and 0.1 *M* MES buffer pH 5.05. Crystals (Fig. 1) of maximum dimensions of up to 800 × 250 × 50 µm were obtained within 2–3 d in 24-well plates using the hanging-drop vapour-diffusion method with drops containing 1 µl protein solution mixed with 1 µl reservoir solution and equilibrated against 1000 µl reservoir solution at 293 K.

2.4. Data collection and processing

For the collection of the first data set, the crystals were transferred from mother liquor containing 16%(*v*/*v*) glycerol directly into a cold nitrogen stream (100 K) on beamline BW7B of the DORIS-III storage ring at EMBL/DESY (Hamburg, Germany). For the collec-

electronic reprint

Table 1
Data-collection statistics.

Values in parentheses are for the highest resolution shell. Observed reflections are those for which $I > 2\sigma(I)$.

Cryoprotectant	Glycerol	Glycerol + Paratone-N
Mosaicity (°)	0.577	0.04
Resolution range (Å)	19.3–2.24 (2.37–2.24)	19.4–2.00 (2.07–2.00)
Completeness (all/observed) (%)	98.3/75.8 (97.7/54.7)	99.8/90.7 (99.9/76.9)
Reflections (all/observed)	71472/55981 (9554/5523)	167628/156406 (10541/8238)
Unique reflections (all/observed)	10396/8016 (1578/884)	15054/13674 (1439/1107)
$I/\sigma(I)$ (all/observed)	15.8/20.5 (4.2/7.3)	20.6/22.6 (7.2/9.2)
$R_{\rm merge}$† (all/observed) (%)	9.2/7.6 (48.9/30.3)	9.5/9.2 (32.3/26.2)

† $R_{\rm merge} = \sum_{hkl}\sum_i |I_i(hkl) - \langle I(hkl)\rangle| / \sum_{hkl}\sum_i I_i(hkl)$, where $I_i(hkl)$ is the intensity of reflection hkl and $\sum_i$ is the sum over all i measurements of reflection hkl.

tion of the second data set, the crystals were flash-cooled to 100 K after soaking in the cryoprotectant Paratone-N (Molecular Dimensions). All data frames were collected at a wavelength of 0.8423 Å using a MAR345 image-plate detector (MAR Research) in dose mode with an oscillation angle of 1.0°. Data for the second set with Paratone-N were recorded in two sweeps at different distances and doses in order to accurately record both the strongest low-resolution and the weakest high-resolution diffraction intensities. A total of 180 images were collected during each of the sweeps. All data were processed and merged using the *XDS* system (Kabsch, 1993). The data-collection statistics are summarized in Table 1.

3. Results and discussion

As shown in Fig. 2(*a*) and Table 1, the diffraction images of the crystal of $CKI1_{RD}$ with the 'natural' cryoprotectant glycerol showed significant widening (the *XDS* package interpreted this widening as a mosaicity of 0.6°) and a corresponding attenuation of the diffraction spots around 3.0 Å resolution. The diffraction images changed dramatically after the use of the non-aqueous cryoprotectant Paratone-N. The widening of the spots disappeared (see Fig. 2*b*), the mosaicity decreased more than tenfold (to a value of 0.04° in *XDS*) and the resolution of the data increased to at least 2.0 Å.

The crystal of $CKI1_{RD}$ belonged to the orthorhombic *C*-centric space group $C222_1$, with unit-cell parameters a = 54.46, b = 99.82, c = 79.94 Å. Assuming that the asymmetric unit contains one molecule of the protein gives a Matthews coefficient V_M of 2.33 Å^3 Da^{-1} (Matthews, 1968); the estimated solvent content is then approximately 47.3%.

The structure of $CKI1_{RD}$ was determined by molecular replacement using an automated scheme for molecular replacement as implemented in *MrBUMP* v.0.4.1 (Keegan & Winn, 2007) in conjunction with the multiple sequence-alignment program *T-Coffee* (Notredame *et al.*, 2000), with *Phaser* (McCoy *et al.*, 2007) as the molecular-replacement engine and *REFMAC* (Murshudov *et al.*, 1997) as the refinement program. An unambiguous solution was found using the bacterial response-regulator protein CheY (PDB entry 1ab5; Wilcock *et al.*, 1998) as a search model. It gave an initial R value of 0.54, which decreased to R = 0.413 and $R_{\rm free}$ = 0.426 after 30 cycles of *REFMAC* refinement. The quality of the $2F_o - F_c$ map generated with this result was good enough to allow successful application of the autobuild regime of *ARP*/*wARP* (v.7.0.1; Cohen *et al.*, 2008). Model improvement and refinement based on both X-ray and NMR data (Pekárová *et al.*, unpublished data) is in progress.

This work was supported by the Ministry of Education, Youth and Sports of the Czech Republic (grant Nos. MSM0021622415 and LC06034). We wish to thank the staff at EMBL Hamburg for their assistance with data collection on beamline BW7B of the DORIS-III storage ring at DESY Hamburg, the EMBL/DESY Hamburg for

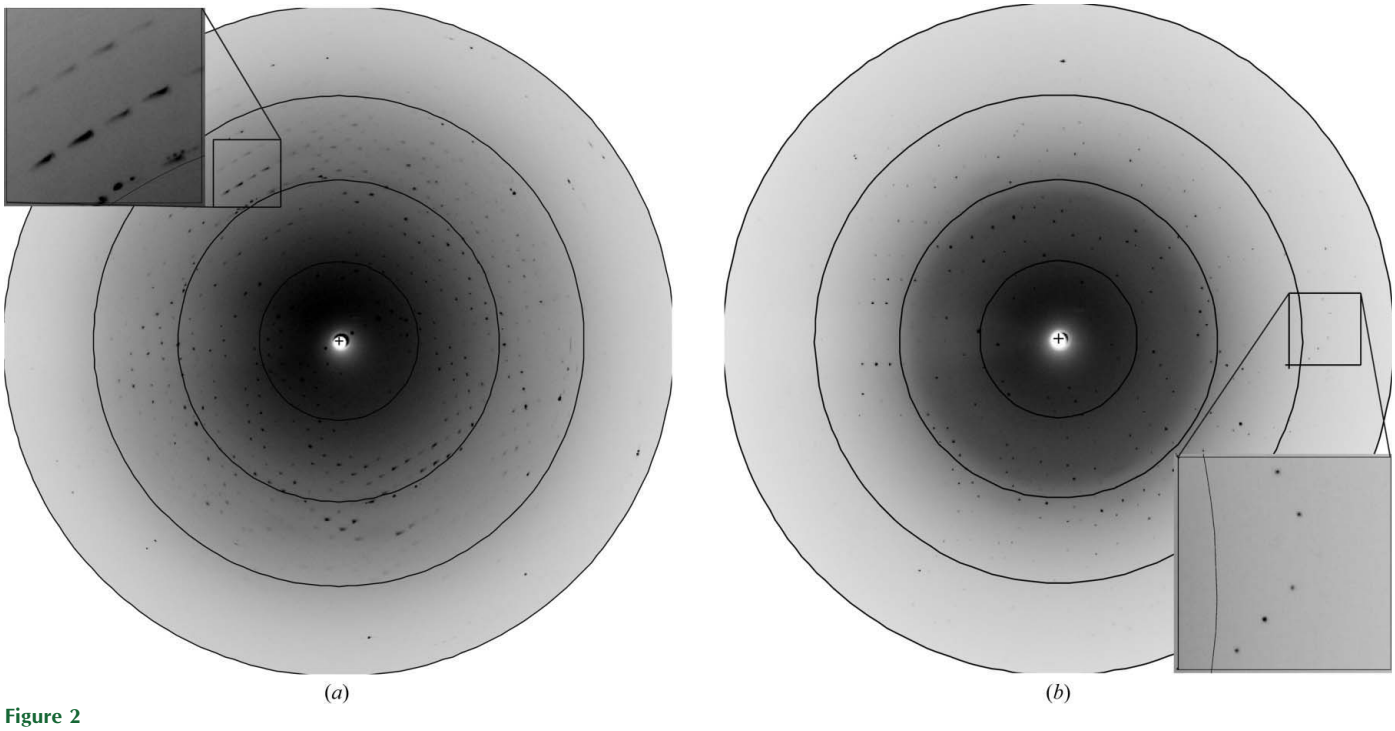

Figure 2
Representative 1.0° oscillation images of the data collected from a $CKI1_{RD}$ crystal using a MAR345 image-plate detector on station BW7B of the DORIS-III storage ring at DESY Hamburg. (*a*) An image from an unsoaked crystal of $CKI1_{RD}$. The magnified rectangle shows a typical example of the widening of the diffraction spots around 3.0 Å resolution. The resolution rings are at 8.8, 4.4, 2.9 and 2.2 Å. (*b*) An image from a crystal of $CKI1_{RD}$ soaked in Paratone-N. The magnified rectangle shows sharp unwidened diffraction spots at a resolution below 2.6 Å. The resolution rings are at 7.9, 3.9, 2.6 and 2.0 Å.

electronic reprint

providing us with synchrotron facilities and European Community for support through the Research Infrastructure Action under the FP6 (contract No. RII3/CT/2004/5060008).

References

Bradford, M. M. (1976). *Anal. Biochem.* **72**, 248–254.
Calva, E. & Oropeza, R. (2006). *Microb. Ecol.* **51**, 166–176.
Chang, C. & Stewart, R. C. (1998). *Plant Physiol.* **117**, 723–731.
Cohen, S. X., Ben Jelloul, M., Long, F., Vagin, A., Knipscheer, P., Lebbink, J., Sixma, T. K., Lamzin, V. S., Murshudov, G. N. & Perrakis, A. (2008). *Acta Cryst.* D**64**, 49–60.
Hwang, I. & Sheen, J. (2001). *Nature (London)*, **413**, 383–389.
Hoch, J. A. (2000). *Curr. Opin. Microbiol.* **3**, 165–170.
Kabsch, W. (1993). *J. Appl. Cryst.* **26**, 795–800.
Kakimoto, T. (1996). *Science*, **274**, 982–985.
Keegan, R. M. & Winn, M. D. (2007). *Acta Cryst.* D**63**, 447–457.
Laemmli, U. K. (1970). *Nature (London)*, **227**, 680–685.
Matthews, B. W. (1968). *J. Mol. Biol.* **33**, 491–497.
McCoy, A. J., Grosse-Kunstleve, R. W., Adams, P. D., Winn, M. D., Storoni, L. C. & Read, R. J. (2007). *J. Appl. Cryst.* **40**, 658–674.
Mizuno, T. (2005). *Biosci. Biotechnol. Biochem.* **69**, 2263–2276.
Muller-Dieckmann, H. J., Grantz, A. A. & Kim, S.-H. (1999). *Structure*, **7**, 1547–1556.
Murshudov, G. N., Vagin, A. A. & Dodson, E. J. (1997). *Acta Cryst.* D**53**, 240–255.
Notredame, C., Higgins, D. & Heringa, J. (2000). *J. Mol. Biol.* **302**, 205–217.
Skerker, J. M., Perchuk, B. S., Siryaporn, A., Lubin, E. A., Ashenberg, O., Goulian, M. & Laub, M. T. (2008). *Cell*, **133**, 1043–1054.
Sola, M., Gomis-Ruth, F. X., Serrano, L., Gonzalez, A. & Coll, M. (1999). *J. Mol. Biol.* **285**, 675–687.
Stock, A. M., Mottonen, J. M., Stock, J. B. & Schutt, C. E. (1989). *Nature (London)*, **337**, 745–749.
To, J. P. & Kieber, J. J. (2008). *Trends Plant Sci.* **13**, 85–92.
Tran, L. S., Urao, T., Qin, F., Maruyama, K., Kakimoto, T., Shinozaki, K. & Yamaguchi-Shinozaki, K. (2007). *Proc. Natl Acad. Sci. USA*, **104**, 20623–20628.
Wilcock, D., Pisabarro, M. T., López-Hernandez, E., Serrano, L. & Coll, M. (1998). *Acta Cryst.* D**54**, 378–385.
Yamada, H., Suzuki, T., Terada, K., Takei, K., Ishikawa, K., Miwa, K., Yamashino, T. & Mizuno, T. (2001). *Plant Cell Physiol.* **42**, 1017–1023.

electronic reprint

Enclosed Publication # 7

Pekárová, B., Klumpler, T., Třísková, O., Horák, J., Jansen, S., Dopitová, R., Papoušková, V., Nejedlá, E., Žídek, L., Sklenář, V., Marek, J., **Hejátko, J.**, Janda, L. Dynamic structure and binding specificity of the receiver domain of sensor histidine kinase CKI1 from *Arabidopsis thaliana*. Submitted.

Dynamic structure and binding specificity of the receiver domain of sensor histidine kinase CKI1 from *Arabidopsis thaliana*

Blanka Pekárová[1,3,*], Tomáš Klumpler[1,3,*], Olga Třísková[2], Jakub Horák[1,3], Severine Jansen[1], Radka Dopitová[1,3], Veronika Papoušková[2], Eliška Nejedlá[1,3], Lukáš Žídek[2], Vladimír Sklenář[2], Jaromír Marek[1,3], Jan Hejátko[1,3], Lubomír Janda[1,3]

From Department of Functional Genomics and Proteomics[1] and National Centre for Biomolecular Research[2], Masaryk University, Kotlářská 2, 611 37 Brno, Czech Republic;
CEITEC, Masaryk University, Zerotinovo nam. 9, CZ-60177 Brno, Czech Republic[3]

Running head: Dynamic structure of the receiver domain of CKI1

*These authors contributed equally to this work.
Address correspondence to: Jan Hejátko, Kamenice 5/A2, 625 00 Brno, Czech Republic. Telephone: +420 5 4949 4165; Fax: +420 5 4949 2640; E-mail: hejatko@sci.muni.cz.

In *Arabidopsis* multistep phosphorelay (MSP) signaling, the signal is transferred from sensor histidine kinase (HK) via histidine-containing phosphotransfer proteins (AHP1-5) to nuclear response regulators. In contrast to bacteria, two-component signaling (TCS) protein interactions in plants are supposed to be rather nonspecific. Using both *in vivo* and *in vitro* assays, we found that the C-terminal receiver domain of HK CKI1 ($CKI1_{RD}$) interacts with AHP2, AHP3, and AHP5 with different affinities. We determined the crystal structure of free $CKI1_{RD}$ and $CKI1_{RD}$ in a complex with Mg^{2+}, the cofactor necessary for MSP phosphorelay. Dynamics of $CKI1_{RD}$ structure in solution were studied by NMR in the absence or presence of Mg^{2+} and phosphorylation-mimicking BeF_3^-. We found that $CKI1_{RD}$ shares similarity with the only known structure of plant HK, $ETR1_{RD}$, with the main differences being in the loop L3. Using indirect ELISA, we found that presence of Mg^{2+} affects the interaction of $CKI1_{RD}$ with its downstream signaling partners and may thus contribute to a fine-tuning of the AHP binding specificity in MSP in plants.

Two-component signaling (TCS) systems mediate magnesium-dependent phosphoryl transfer leading to a wide spectrum of signaling events and adaptive responses mostly in bacteria and yeast (1). It has been recognized in the last decade, however, that TCS systems were adopted also by multicellular organisms (2). In plants, two-component-based signaling pathways are involved in several environmental and developmental regulatory pathways and are critical for hormonal regulation, namely for cytokinin signaling (for review, see 3).

In plants, TCS is mediated via a modified system known as multistep phosphorelay (MSP) (3). In contrast to a simple His-to-Asp phosphotransfer occurring in most bacterial TCS, the multistep system includes additional signaling domains and leads to a multicomponent His-to-Asp-to-His-to-Asp phosphorelay. In plants, the MSP system is composed of three types of signaling molecules: a (mostly) membrane-bound sensor histidine kinase (HK), a histidine phosphotransfer protein (HPt), and a response regulator. The pathway is usually triggered by an interaction of a signal molecule with the N-terminal extracellular sensory domain of HK and leading to autophosphorylation of the conserved histidine residue in a central cytoplasmic HK domain. The phosphoryl group is subsequently transferred intramolecularly to an aspartate moiety in a C-terminal response regulator-like receiver domain (RD). The RD initiates the downstream transfer of phosphate to specific histidine residues in HPt proteins. HPt proteins further transmit the phosphoryl group to a final phosphate acceptor – aspartate residues in receiver domains of response regulator proteins – located mainly in the nucleus. The phosphorylation of the response regulator results in activation of either associated effector

domains or downstream signaling partners to evoke the desired response (3-5).

The described MSP signaling system often involves complicated protein-protein interaction networks allowing possible cross-talk, cross-regulations or existence of branched signaling pathways (6). Bacteria have evolved several mechanisms that prevent unwanted cross-talk among different pathways. These include, e.g., the presence of bifunctional HKs, which ensure the necessary selectivity via specific phosphatase activity of HKs directed toward their cognate interaction partners. Alternatively, kinetic preferences of histidine kinases and their cognate response regulators have been described in several bacterial signaling pathways (for review, see 6). However, all of these mechanisms assume molecular recognition of cognate partners in the respective signaling cascade.

The mechanisms driving the molecular recognition in TCS have recently begun to be elucidated. There are several studies showing at molecular level that the C-terminal RD of hybrid sensor HK is directly involved in the specific interaction with its downstream signaling partners, HPt proteins, and it is likely to control the interaction with sufficient specificity. One example is the crystal structure of the $SLN1_{RD}$-YPD1 complex from *Saccharomyces cerevisiae* (7), while another is an NMR titration study of interaction between a phosphoreceiver domain of RcsC and an HPt domain of RcsD from *E. coli* (8). The studies demonstrate that obtaining knowledge of the RD structures and identifying amino acids responsible for the interaction specificity are two important steps toward a detailed understanding of the mechanism of signal transduction from the receiver domain to the downstream HPt proteins.

In the genome of the model plant *Arabidopsis thaliana*, three cytokinin receptors, AHK2, AHK3, and AHK4/CRE1 (9-11), one putative osmosensing HK, AtHK1 (12-14), and two cytokinin independent histidine kinases, CKI1 (15-19) and CKI2/AHK5 (15,20,21), are supposed to mediate phosphate transfer via five downstream HPt proteins (AHP1-5) to 11 B-type response regulators (ARRs) (for review, see 3). In addition, a member of the ethylene receptor family, ETR1, also has been shown to be involved in MSP (22,23).

The histidine kinase CKI1 has been identified as an activator of cytokinin-like response when overexpressed in hypocotyl explants of *Arabidopsis* (15), and it is essential for female gametophyte development (16,17). No cytokinin binding to CKI1 has been detected, however, and, in contrast to genuine cytokinin receptors, CKI1 has been found to be constitutively active in bacteria or *Arabidopsis* protoplasts (18,24,25). Little is known about downstream phosphorelay targets of CKI1. Previous studies have demonstrated that CKI1 interacts with AHP2, and AHP3 proteins in a yeast two-hybrid assay (13) and *in vitro* phosphorylates AHP1, AHP2, AHP3, and AHP5 (26). Finally, recent genetic data further support the role of CKI1 in the AHP-mediated MSP *in planta* (18,19).

The current model of TCS in plants assumes a rather intense cross-talk between individual pathways, as implied in particular by numerous protein-protein cross-interactions identified using yeast two-hybrid and pull-down assays (27,28). Genetic data also suggest at least partial redundancy of individual members of *Arabidopsis* MSP in the case of receptor hybrid histidine kinases (9,10,11), HPt proteins (29), or response regulators (30,31). Thus, it is not clear whether there is any specificity in the MSP signaling pathways in *Arabidopsis* as identified in bacterial systems and nothing is known about potential molecular determinants of such specificity.

Here, we present data showing that sensor histidine kinase CKI1 preferentially interacts with AHP2, with AHP3, and only weakly with AHP5. We identified the receiver domain of CKI1 ($CKI1_{RD}$) as a sufficient and necessary factor determining the specificity of CKI1 interaction with HPt proteins *in vivo*. Further, we employed indirect ELISA to quantify the identified binding of AHP proteins to $CKI1_{RD}$ *in vitro*. We also investigated effects of Mg^{2+}, the cofactor that is necessary for HK-mediated phosphorelay in MSP signaling and BeF_3^-, the isomorphous stable phosphate analogue, on $CKI1_{RD}$ by multidimensional NMR spectroscopy and solved three-dimensional structures of $CKI1_{RD}$ in its free and Mg^{2+}-bound forms. Our results represent a

first step in identifying molecular determinants involved in the specific recognition of downstream signaling partners in MSP pathways in plants.

Experimental procedures

Proteins – $CKI1_{RD}$ protein was prepared as previously described (32). D1050A mutation was introduced using QuikChange Multi Site-Directed Mutagenesis kit (Stratagene) with mutagenic primer 5‘ GCA TTTGGCA**CGC**CATGAATATGTAGTCAAAC GG 3‘ (changed nucleotides are underlined). Mutation was verified by sequencing using an ABI 310 genetic analyzer (Perkin Elmer). For producing AHP proteins, the AHP coding sequences were amplified from the *Arabidopsis* suspension culture cDNA library using appropriate pairs of primers containing *EcoRI* restriction sites. The sequences of the primers were as follow: for AHP2, 5´-CCG GAA TTC ATG GAC GCT CTC ATT GCT CAG-3´ and 5´- CCG GAA TTC TTA GTT AAT ATC CAC TTG AGG-3´; for AHP3, 5´-CCG GAA TTC ATG GAC ACA CTC ATT GCT CAG-3´and 5´-CCG GAA TTC TTA TAT ATC CAC TTG AGG GAT-3´; and for AHP5, 5´-ATA GAA TTC ATG AAC ACC ATC GTC GTT GCT-3´ and 5´- CCG GAA TTC CTA ATT TAT ATC CAC TTG AGG-3´ *(EcoRI* restriction sites are underlined). The *EcoRI* fragments of amplified sequences were ligated into pRSET B expression plasmid (Invitrogen) and verified by sequencing using an ABI 310 genetic analyzer (Perkin Elmer). The *E. coli* strain BL21(DE3)pLysS (Novagen) carrying individual expression plasmids was cultured in Terrific broth (TB) medium at pH 7.5 and supplemented with ampicillin (100 µg/ml) and 1% glucose at 22 °C. When OD_{600} reached 0.8, expression was induced by addition of 0.4 mM isopropyl β-D-1-thiogalactopyranoside (IPTG). Three hours after induction at 22 °C, cells were harvested by centrifugation at 3220 x g for 20 min at 4 °C. The cell pellets were resuspended in extraction buffer (50 mM Tris-Cl pH 7.9, 300 mM NaCl, 20 mM imidazol, 10% glycerol, 3.5 mM mercaptoethanol, 0.1% TritonX-100) and broken by sonication. Cell debris was removed by centrifugation at 47 448 x g for 30 min at 4 °C. The supernatant was applied onto a HisTRAP HP (5ml) column (GE Healthcare) equilibrated in buffer containing 50 mM Tris-Cl pH 7.9, 300 mM NaCl, 20 mM imidazol, 10% glycerol and 3.5 mM mercaptoethanol. Bounded proteins were eluted by gradient from 20 mM to 500 mM imidazol. The fractions containing AHP proteins were collected, concentrated using an Amicon Ultra-4 ultrafiltration cell with 3 kDa cutoff (Millipore), and diluted in 20 mM Tris-Cl pH 7.9. The protein sample was further purified by anion exchange using a Resource Q column (GE Healthcare) equilibrated in 20 mM Tris-Cl pH 7.9. Adsorbed proteins were eluted using a gradient of 0-2 M NaCl. The fractions containing AHPs were concentrated using an Amicon Ultra-4 ultrafiltration cell with 3 kDa cutoff (Millipore). Protein concentration was determined according to Bradford protein assay (33), and bovine serum albumin was used as a standard. The protein purity was determined by SDS-PAGE followed by Coomassie Brilliant blue staining.

Protein-protein interactions in vivo – DNA constructs for expression of appropriate fusion proteins were prepared by means of Gateway® technology (Invitrogen) according to the manufacturer’s instructions. Destination vectors pSPYCE-35S and pSPYNE-35S were used for bimolecular fluorescence complementation (BiFC) (34). For yeast, two-hybrid destination vectors pGBKT7-DEST and pGADT7-DEST were derived from the Matchmaker™ system (Clontech) (35). All procedures required for *in vivo* interaction experiments, such as tobacco infiltration, confocal laser-scanning microscopy, yeast transformation, growth assay or western blotting were identical to those described elsewhere (35).

ELISA – The equilibrium dissociation constant (K_d) of $CKI1_{RD}$-AHP complex in solution was determined by ELISA. The surfaces of Maxisorp 96-microtitre plate wells (Nalge Nunc Internacional) were coated with 100 µl of purified $CKI1_{RD}$ diluted in bicarbonate buffer, pH 9.6, to concentration 170 nM overnight at 4 °C and thereafter washed three times with the wash buffer PBST (phosphate-buffed saline, PBS, pH 7.2, with 0.05% Tween) to wash away the unbound protein. Wells were then blocked with 150 µl of blocking

buffer (PBST with 1% BSA) for 1 h at 37 °C. After washing three times with the wash buffer, 100 µl of interaction buffer containing different concentrations of AHP proteins was added to the wells and left to react for 2 h at RT with shaking at 300 rpm. Three interaction buffers were used: buffer A: PBST; buffer B: PBST supplemented with 5 mM $MgCl_2$; and finally buffer C: PBST supplemented with 5 mM $MgCl_2$, 3 mM NaF and 0.6 mM $BeCl_2$. Wells were washed three times with the washing buffer and 100 µl of blocking buffer containing 33 ng/ml of a primary monoclonal antibody anti-AHP2 (for AHP2 and AHP3 detections) or 100 ng/ml of anti-AHP5 mAb were added and incubated for 1 h at 37 °C, 300 rpm. Both mAbs were raised against recombinant proteins. Peroxidase conjugated anti-mouse secondary antibody and 3,3',5,5'–tetramethylbenzidine substrate were used for detection at 450 nm. Binding curves were calculated using SigmaPlot software (version 10, Systat Software Inc., USA) to determine the dissociation constants using a simple hyperbole fit.

X-ray crystallography – Crystallization and structure determination of the magnesium-free form of $CKI1_{RD}$ were described previously (32). Crystallization of the magnesium-bound form of $CKI1_{RD}$ was performed similarly: we added 21 mM $MgCl_2$, 5.3 mM $BeCl_2$, and 35 mM NaF into the 0.5 mM protein solution and the crystallization conditions remained the same, with 2.5 M ammonium sulfate used as a precipitant. Crystals of maximum dimensions up to 500x200x50 µm were obtained within 2–3 days in a 24-well EasyXtal DG-Tool (Qiagene) using the hanging drop vapor-diffusion method with drops containing 1 µl of the protein solution mixed with 1 µl of reservoir solution and equilibrated against 1000 µl of reservoir solution at 293 K. Prior to the diffraction experiment, the crystals were flash-cooled to 100 K in a nitrogen stream after soaking in the cryoprotectant Paratone-N (Molecular Dimensions). For collection of the $CKI1_{RD}$ Mg^{2+} diffraction data, we used beamline X13 of the DORIS-III storage ring at EMBL/DESY (Hamburg, Germany). All data were processed and merged using the *XDS* system (36). The structure of $CKI1_{RD}$ Mg^{2+} was determined by molecular replacement method with *MOLREP* (37) using coordinates of metal-free $CKI1_{RD}$ as a search model. The quality of electron density maps allows successful application of the autobuild regime of *ARP/wARP* (38). Final refinement of models of Mg^{2+}-free and Mg^{2+}-bound forms of $CKI1_{RD}$ was performed using restrained refinement with the maximum likelihood method of *REFMAC* (39). Manual fine-tuning of both structures was performed with *Coot* (40). Data collection and refinement statistics for both structures are summarized in Table 1. Molecular graphics images were produced using the *UCSF Chimera* (41). The refined structures were deposited in the Protein Data Bank under accession codes 3MM4 and 3MMN.

NMR measurements – Uniformly ^{13}C-labeled and/or ^{15}N-labeled $CKI1_{RD}$ was produced in M9 minimal medium supplemented with trace metals, vitamins and with 2 g/l ^{13}C-glucose as a carbon source and/or 0.5 g/l $^{15}NH_4Cl$ as a sole nitrogen source. Cells were grown at 37 °C to OD_{600} of 0.8, and expression was induced by the addition of 0.42 mM IPTG. Growth was continued for 16 h at 25 °C until harvest. $CKI1_{RD}$ was purified by a combination of affinity and size exclusion chromatography as described earlier (32). Finally, recombinant $CKI1_{RD}$ was concentrated by Amicon filtration to 0.5 mM in 50 mM Tris/HCl buffer, pH 7.5, containing 150 mM NaCl. $CKI1_{RD}$ selectively labeled with ^{15}N-Met was expressed according to a procedure described previously (42). One liter of M9 medium containing 0.2% glucose was inoculated with 1.2 ml of frozen stock solution. When the OD_{600} reached 0.8, lysine, phenylalanine, threonine (100 mg/l), isoleucine, leucine, valine (50 mg/l) and ^{15}N-methionine (60 mg/l) were added to the medium and it was incubated 15 min at 25 °C. Expression was then induced with 1 mM IPTG, and the protein was expressed at 25 °C for 16 hours and purified as described above. All NMR spectra were measured at 25 °C on a Bruker Avance 600 MHz spectrometer equipped with the cryogenic H/C/N TCI probe head. A sample consisting of 340 µl 1.0 mM uniformly ^{13}C, ^{15}N-labeled $CKI1_{RD}$ in 20 mM sodium phosphate buffer, pH 7.5, containing 150 mM sodium chloride, 1 mM ethylenediamine tetraacetic acid (EDTA), 0.05% sodium azide, and 10% deuterium oxide, placed in a Shigemi tube,

was used for the resonance assignment. The sequential assignment was obtained using a standard set of triple resonance experiments: amide proton and nitrogen to C^{α} carbon correlation experiment (HNCA), amide proton and nitrogen to C^{α} via carbonyl carbon correlation experiment (HN(CO)CA), amide proton and nitrogen to C^{α} and C^{β} carbon correlation experiment (HNCACB), and C^{β} and C^{α} carbon to amide nitrogen and proton *via* carbonyl carbon correlation experiment (CBCA(CO)NH) (43). The same sample was used for titration with magnesium chloride aliquots, corresponding to 1.5, 2.5, 8, 25, and 48 mM Mg^{2+} concentrations (corrected for the amount bound to EDTA). The HNCACB and CBCA(CO)NH spectra were measured on the sample containing 25 mM Mg^{2+} in order to assign the resonances of the Mg^{2+}-bound $CKI1_{RD}$ form. The titration was repeated with 15 magnesium chloride aliquots, covering a concentration range up to 30 mM, on a sample of 0.6 mM uniformly ^{15}N-labeled $CKI1_{RD}$ in 20 mM Tris buffer, pH 7.5, containing 150 mM sodium chloride, and 10% deuterium oxide, placed in a round-bottom NMR tube. The dissociation constant was obtained from this series of experiments by a nonlinear least square fitting the compound chemical shift changes (44) to a two-state interaction model. As the presence of EDTA in the sample was needed in long-term studies to prevent the protein from proteolysis, the effect of EDTA on the spectra was checked by repeating the Mg^{2+} binding experiment on a 0.5 mM uniformly ^{15}N-labeled sample prepared in the same buffer, but in the presence of 10 mM EDTA. No differences in the $CKI1_{RD}$ ^{1}H or ^{15}N frequencies were observed. The Mg^{2+}-bound protein for the beryllofluoridation study was prepared by addition of 18 µl 0.5 M magnesium chloride and 6 µl 0.3 M sodium fluoride to 660 µl of the ^{15}N-labeled sample as described above. Beryllofluoridation was monitored by adding aliquots of sodium fluoride and beryllium chloride (in 3:1 molar ratio), corresponding to 0.17, 0.34, 0.51, 0.68, and 1.0 mM beryllium concentrations. A heteronuclear single-quantum coherence (^{1}H-^{15}N HSQC) spectrum was recorded at every beryllium concentration. The Mg^{2+} binding and beryllofluoridation experiments were also performed with samples of 0.6 mM $CKI1_{RD}$ selectively ^{15}N-labeled at methionines. All NMR spectra were processed using NMRPIPE (45) and analyzed using the SPARKY program (46). The assigned chemical shifts and measured relaxation data were stored in the BioMagResBank database with accession numbers 16917 (free) and 16918 (Mg^{2+}-bound).

Results

CKI1 specifically recognizes a subset of AHPs via its receiver domain. To identify potential specificity of the CKI1-mediated MSP we performed extensive *in vivo* protein-protein interaction studies using BiFC in plant cells (34). We generated 35S promoter-driven BiFC constructs expressing a full-length CKI1 protein or the C-terminal receiver domain, $CKI1_{RD}$, in fusion with the C-terminal YFP fragment (YFP-C) and all six HPt proteins from *Arabidopsis* (AHP1-6) in fusion with the N-terminal YFP fragment (YFP-N). Using these constructs, the BiFC interaction assay was performed as described previously (34).

As shown in Fig. 1A, when the full-length CKI1 protein was co-expressed with AHPs, the strong BiFC signal indicating interaction of $CKI1_{RD}$ with HPt proteins was observed for AHP2, AHP3, and AHP5. A weak YFP fluorescence signal was scored for AHP1, while no detectable interaction occurred with AHP4 and AHP6. Similar fluorescence patterns were observed for co-expression of individual AHPs with the receiver domain $CKI1_{RD}$ alone (Fig. 1B). In case of the full-length CKI1, the BiFC fluorescence outlined the epidermal cells that corresponded to the expected subcellular localization of CKI1 into the cytoplasmic membrane (Fig. 1A). In contrast to that, interaction with $CKI1_{RD}$ lacking the transmembrane domains occurred in both the cytosol and nucleus (Fig. 1B). The fluorescence signal appears stronger with $CKI1_{RD}$, as the volume of the fluorescence layer is much higher compared to the cells expressing the full-length CKI1 protein localized in the cytoplasmic membrane. The interaction patterns in terms of their specificity, however, are the same for both proteins, suggesting that the receiver domain of

CKI1 is required and sufficient for selective interaction of CKI1 with a subset of *Arabidopsis* phosphotransfer proteins AHP2, AHP3, and AHP5. Moreover, these results show that membrane localization of $CKI1_{RD}$ is not required for interaction with AHP proteins.

To further substantiate CKI1 interactions observed in plants, we studied protein-protein interactions using a yeast two-hybrid assay. As membrane-localized proteins cannot be used in this type of assay, we omitted the full length CKI1 from the analysis. The $CKI1_{RD}$ was used as a "bait," while the six tested AHP proteins were cloned in the "prey" vector. Although all fusion proteins were expressed at comparable levels, we found that $CKI1_{RD}$ interacts only with AHP2, AHP3, and AHP5 (Fig. 1C). When compared to AHP2 and AHP3, the growth of isolated colonies in the case of AHP5 indicated that this interaction might be weaker. Thus, similarly to our result from the *in planta* fluorescent assay, these data indicate that specific interaction of CKI1 with AHP2, AHP3, and AHP5 is mediated by $CKI1_{RD}$.

Three standard methods – surface plasmon resonance (SPR), isothermal titration calorimetry (ITC), and indirect ELISA – were employed to quantify the identified binding of AHP2, AHP3, and AHP5 to $CKI1_{RD}$ *in vitro*. As the AHP proteins tend to aggregate at concentrations above ~20 μg/ml, apparent kinetic data were measured by ELISA that was more sensitive to low concentrations of interacting AHP proteins than SPR and ITC. The obtained dissociation constants showed that AHP2 and AHP3 bound with similar affinities to $CKI1_{RD}$, and these affinities are ~10-fold higher than the affinity of $CKI1_{RD}$ to AHP5 (Fig. 2, Table 2). These data are in agreement with the *in vivo* data determined by BiFC and Y2H techniques (Fig. 1), suggesting a sufficient specificity of our *in vitro* assay.

Taken together, using three independent assays, both *in vitro* and *in vivo*, we have found that the receiver domain of CKI1 is necessary and sufficient for specific interactions of CKI1 with its downstream signaling partners, the HPt proteins. Importantly, we have found that there is a specificity of the interactions resulting in preferential interaction of $CKI1_{RD}$ with AHP2 and AHP3 compared to the weaker interaction of $CKI1_{RD}$ with AHP5.

Crystal structure of $CKI1_{RD}$ and its magnesium co-crystal. To study structural details of the receiver domain of CKI1 at the atomic level, $CKI1_{RD}$ was expressed in *E. coli,* purified and crystallized (32,47), then its three-dimensional structure was determined using X-ray diffraction. The crystal structure of $CKI1_{RD}$ shows the conformational conservation of receiver domains belonging to the CheY-like protein superfamily (48). $CKI1_{RD}$ was found to be folded in an $(\alpha/\beta)_5$ manner with the central β-sheet formed from five parallel β-strands (β2-β1-β3-β4-β5), surrounded on both sides by two (α1, α5) and three (α2, α3, α4), α-helices. Secondary structure elements are connected with five loops, L1–L5, on the face side of the domain and by four loops ℓ1–ℓ4 on the opposite side (Fig. 3A). The purified protein consists of 207 amino acids, 179 of which are encoded by the *CKI1* gene (944–1122) and are well-defined in the model. The remaining amino acids are encoded by the vector and, of these, only residues 936–939 are defined in the crystal electron density. Residues 936 and 937 form a β-strand antiparallely bonded to β5 of the central β-sheet.

To identify the actual structural changes upon Mg^{2+} and BeF_3^- binding, we analyzed the structure of a co-crystal of $CKI1_{RD}$ with Mg^{2+} and BeF_3^-. The presence of magnesium in the co-crystals was confirmed by inductively coupled plasma mass spectrometry. However, we were not able to confirm presence of BeF_3^- in the crystal. Thus, the beryllfluoridation of $CKI1_{RD}$ was unstable during crystal formation, most probably because of high concentration of ammonium sulfate in the crystallization buffer (32). The crystals of Mg^{2+}-bound $CKI1_{RD}$ belong to the same orthorhombic space group C2221 as does the crystal of the Mg^{2+}-free protein, but their unit-cell parameters slightly differ (a = 54.14, b = 100.92, c = 80.14 Å). The final modeling of $CKI1_{RD}$ with Mg^{2+} refinement was performed using *Coot* in combination with *REFMAC* and it gave the final R=0.177 and R_{free}=0.239 (Table 1).

The secondary structure of the Mg^{2+} complex of $CKI1_{RD}$ in comparison to the free structure (without Mg^{2+}) is only slightly affected and the

overall root mean square deviation is only 0.25 Å for 140 equivalent C^{α} atom pairs (data not shown). Maximum change in C^{α} atoms positions after Mg^{2+} binding is located in the N-terminal part of loop L5, where conserved K1105 is located (with shift of 0.4 Å for C^{α} pair of K1105; Fig. 4). The main effect caused by Mg^{2+} binding is the chi angle change of the D1050 side chain (C-terminal part of strand β3). Upon magnesium binding, the side chain of D1050 rotates by 90° toward the divalent cation. The connection via a salt bridge between D1050 and K1105 induces rotation of K1105, whereas the salt bridge remains established (Fig. 4). This change induces a 3.4 Å shift of N^{ζ} (K1105) and 2 Å of O^{δ} (D1050), resulting in appropriate geometry in the acidic pocket required for acceptance of the phosphate group. No significant structural changes were found in C^{α} atom positions in loops L3, L4, and L5 and only minor structural changes (less than 0.5 Å) were determined in terminal atoms of the side chain of appropriate amino acids residues (except D1085 – 0.537 Å). The only two residues that remain shifted in terminal side chains atoms are N^{ζ} (K1105) and O^{δ} (D1050).

Both residues belong to the active site for catalysis of magnesium-dependent phosphoryl transfer that is highly conserved among receiver domains of several bacterial and eukaryotic histidine kinases belonging to the CheY-like superfamily. Here, the active site is formed (according to CheY numbering) by D12, D13, D57, N59, T87, and K109 (49,50). Based on the high level of conservation, we have located the Mg^{2+} binding site in the structure of $CKI1_{RD}$. The active site of $CKI1_{RD}$ with the phosphoacceptor D1050 (equivalent to D57 in CheY) and with the Mg^{2+} binding site is located on the C-terminus of the central β3-strand in a pocket delimited by loops L1, L3, and L5. A highly conserved triad of carboxyl oxygens formed by D1050 together with D992 (equivalent to D12 in CheY), D993 (equivalent to D13 in CheY), and carbonyl oxygen of Q1052 (equivalent to N59 in CheY) give the active site an acidic character. Mg^{2+} is approximately octahedrally coordinated with carboxyl oxygens of D993 and D1050, carbonyl oxygen of Q1052, and one water molecule that forms a hydrogen bridge to carboxyl oxygen of D992 (Fig. 4).

Mg^{2+} binding induces structural changes in the active site of $CKI1_{RD}$ in solution. To analyze structural changes upon binding of Mg^{2+} and phosphorylation (mimicked by beryllofluoridation) in solution, a ^{13}C, ^{15}N-labelled $CKI1_{RD}$ sample was prepared. Backbone amide as well as $^{13}C^{\alpha}$ and $^{13}C^{\beta}$ resonances were assigned using standard triple resonance NMR experiments. The assignment was obtained for 147 (91%) residues in a region of the whole construct between P964 and E1124 (amino acid residue numbering according to the full length CKI1 sequence) and for an additional 15 residues of the N-terminal region (Fig. 5, in green). With the exception of a few residues (F995, E1035, K1041, L1042), the missing assignment in the receiver domain (R984–I1114) corresponds to residues C1051–E1060 (Fig. 6). The residues follow active site D1050 in the sequence and constitute the loop L3 in the crystal structure (Fig. 3). Therefore, conformational dynamics of L3 in solution may account for the missing signals in the NMR spectra.

Structural effects of Mg^{2+} ions were investigated in titration experiments monitored by running ^{1}H-^{15}N HSQC NMR spectra. During titration of a 0.5 mM $CKI1_{RD}$ sample with magnesium chloride aliquots, large changes of ^{1}H and ^{15}N chemical shifts of some signals were observed (Figs. 5 and 6A). As some peaks moved significantly upon Mg^{2+} binding, HNCACB and CBCA(CO)NH spectra were recorded at 15 mM Mg^{2+} concentration in order to verify the sequential assignment. Most peaks exhibited fast exchange during titration, but notable line broadening was observed in some cases, including well-resolved peaks of D993, N994, S997, and G1019. The dissociation constant estimated from the compound chemical shifts was 0.43 ± 0.06 mM. The most shifted peaks upon the Mg^{2+} binding corresponded to backbone NH groups of D993, N994, R998, and A1001, i.e., the residues identical with or in close proximity to D992 and D993 in loop L1, which bind the Mg^{2+} ion in the crystal structure. Other peaks with large resonance frequency changes corresponded to residues around loops L4 and L5 and to two residues directly preceding the unassigned region in loop

L3. Interestingly, several new peaks appeared in the spectra taken at high Mg^{2+} concentrations. A natural interpretation of this observation was to assume that loop L3 of free $CKI1_{RD}$ is present in more conformations in solution, which are in a dynamic equilibrium with an exchange rate on the time scale of the NMR experiment, and that the Mg^{2+} binding locks this loop in a single conformation. Since L3 contains two methionines (M1053 and M1056), we decided to test this hypothesis by running the NMR experiments on a $CKI1_{RD}$ sample selectively labeled with ^{15}N at methionines (Fig. 5). While the spectra of Mg^{2+}-free, selectively labeled $CKI1_{RD}$ showed three intense signals overlapping with peaks assigned to M1008, M1049, and M1099, addition of 20 mM Mg^{2+} increased the number of peaks to six. As the $CKI1_{RD}$ construct contains six methionine residues (not counting the N-terminal methionine), this result proves that the signals of the loop L3 were missing in the Mg^{2+}-free form for dynamic reasons and supports the idea that Mg^{2+} binding favors a single conformation of loop L3. In summary, the backbone NH groups most influenced by the Mg^{2+} binding are located in loop regions surrounding the active site. Met-selective labeling showed that Mg^{2+} binding stabilizes conformation of the flexible loop L3.

Much smaller but still significant effect on the resonance frequency was observed upon beryllofluoridation of the Mg^{2+}-bound protein (Fig. 6B1). The most striking difference was observed in loop L1 and in the N-terminal half of the following helix α1. This region exhibited the largest chemical shift changes upon the Mg^{2+} binding (Fig. 6A1), but, with the exception of D993 and S997, it remained almost unaffected upon beryllofluoridation (Fig. 6B1). On the other hand, significant resonance frequency changes induced by BeF_3^- were found in loops L4 and L5 together with internal helix α4 and strand β5. Resonance frequency changes in the ^1H-^{15}N HSQC NMR spectra were also monitored for the D1050A mutant of $CKI1_{RD}$ ($CKI1_{RD}^{D1050A}$) after Mg^{2+} binding (Fig. 6A2). While loops L4 and L5 of the mutant exhibited resonance frequency changes similar to those observed for the wild type, residues D992 and D993 of the loop L1 were almost unaffected. This result confirms the importance of D1050 in the Mg^{2+} binding and the subsequent structural changes, described in previous section. No resonance frequency changes were observed upon beryllofluoridation of the Mg^{2+}-bound $CKI1_{RD}^{D1050A}$ protein (Fig. 6B2), confirming that D1050 is the active site where beryllofluoridation occurs.

Magnesium- and phosphorylation-induced structural changes have a moderate effect on binding specificity of $CKI1_{RD}$. Our data suggest that the inactive (free) and active (phosphorylated) forms of $CKI1_{RD}$ have an identical overall structure and that the Mg^{2+} binding and phosphorylation induce only local structural changes in specific portions of $CKI1_{RD}$. These changes are located around an Mg^{2+} binding site on the C-terminus of the central β3 strand in a pocket delimited by loops L1, L3, and L5.

To ascertain a potential influence of those structural changes on binding properties of CKI1 during MSP, we inspected the affinity of $CKI1_{RD}$ to AHPs proteins in the presence and absence of Mg^{2+}. The influence of phosphorylation was inspected in the presence of BeF_3^- mimicking specific phosphorylation of $CKI1_{RD}$. The nM orders of dissociation constants identified in the absence of Mg^{2+} did not change dramatically after addition of Mg^{2+} or after modification with beryllium fluoride (Table 2). Nevertheless, the presence of Mg^{2+} ions itself slightly favored the interactions with AHP2 at the expense of interactions with AHP3, thus resulting in a two-fold preference for AHP2 when compared to AHP3. In contrast, the addition of phosphorylation mimicking BeF_3^- in the presence of Mg^{2+} reversed the binding affinities, leading to 1.5-fold higher preference for AHP3 as compared to AHP2. Thus, while either the presence of Mg^{2+} or beryllofluoridation has only a limited influence on the interactions between $CKI1_{RD}$ and AHP proteins, these can further modulate the relative specificity of $CKI1_{RD}$ to individual AHPs.

Discussion

Protein-protein interactions of $CKI1_{RD}$ with its downstream signaling partners determine specificity of the MSP in plants. In contrast to

bacteria, where cross-signaling is believed to be a rare and physiologically rather irrelevant event (2), functional redundancy of proteins in MSP has been suggested to be an important and inherent characteristic of this system in plants (27,28). Using two-hybrid and pull-down assays, AHP proteins were shown to interact with all members of protein families acting both up- and downstream within the MSP pathway in *Arabidopsis*, i.e., with histidine kinases (HKs) and response regulators (27,28). Further, the genetic data suggest additive effects of multiple mutations in *AHP* genes on the sensitivity to cytokinins and thus functional redundancy of individual AHPs (29). Thus, HPt proteins are considered to be rather unspecific integrators that allow an intense cross-talk among individual MSP signaling pathways in *Arabidopsis*.

Here we show that the histidine kinase CKI1 prefers a specific subset of AHP interaction partners, and it interacts *in vivo* with three out of six tested AHP proteins. Our study confirmed the known interactions of CKI1 with AHP2 and AHP3 (13,51), and it newly determined the interaction with AHP5. By two independent *in vivo* methods – bimolecular fluorescence complementation and yeast two-hybrid assays – we proved that interaction of CKI1 with the AHP proteins is mediated by the receiver domain of CKI1.

Importantly, data from our *in vivo* and *in vitro* experiments demonstrate that the binding affinity of $CKI1_{RD}$ to AHP proteins shows a certain level of specificity. $CKI1_{RD}$ exhibits binding specificity for AHP2 and AHP3 with a tight-binding affinity, while the affinity of $CKI1_{RD}$ for AHP5 is an order of magnitude weaker. These findings delimit the previously considered role of HPt proteins in the rather unspecific integration of individual HK signaling. We cannot, however, rule out that the specific recognition of a subset of AHPs by $CKI1_{RD}$ might be affected in the absence of preferred AHPs. The cross-talk of histidine kinase with non-cognate response regulators in the absence of the cognate partner has been demonstrated in bacteria (52), and similar mechanisms might operate in the case of multiple *ahp* mutants in *Arabidopsis*, as suggested by recent genetic studies (19,29). Nevertheless, our data show that the measurement of thermodynamic preferences between signaling partners and recognition of the amino acids required for their binding is an important prerequisite for the determination of MSP specificity in plants.

Structure of $CKI1_{RD}$ and structural dynamics of its Mg^{2+}-dependent BeF_3^- activation. Here we have identified the molecular details as to the structure and structural dynamics of the $CKI1_{RD}$ as a basis for our further understanding of the molecular determinants of catalytic activity and protein-protein interactions in the MSP signaling network in plants. The crystal structure of $CKI1_{RD}$ retains the $(\alpha/\beta)_5$ fold characteristic for bacterial and yeast phosphoreceiver domains (53). This fold is conserved in response regulators of simple two-component signaling systems and in both response regulators and signal receiver domains of hybrid histidine kinases of MSP-based signaling pathways (for review, see 54).

In plants the only known structure of receiver domain is the structure of $ETR1_{RD}$ (55), a receiver domain of sensory histidine kinase involved in ethylene signaling (56). By comparing $ETR1_{RD}$ with $CKI1_{RD}$, we have found that the backbone structures of the two proteins are very similar. Superimposition of secondary structure elements of $CKI1_{RD}$ and $ETR1_{RD}$ (Protein Data Bank entry 1DCF) shows root mean square deviation of 1.57 Å for 113 equivalent C^{α} atom pairs. The length of the secondary structure elements is approximately the same. Major conformational differences between $CKI1_{RD}$ and $ETR1_{RD}$ (25.4% sequence identity for the 134 residues of $ETR1_{RD}$) are located in the loop L3. This γ loop does follow the consensus of the other receiver domain amino acid sequence P-X-M/L-D-G and the loop is positioned in close proximity to the α2-helix. The consensual C-terminal G1058 of loop L3 in the receiver domains of proteins from the CheY-like superfamily, the presence of which is necessary to adopt an α-helical conformation, is substituted with asparagine in $ETR1_{RD}$. This substitution is most probably responsible for the differential conformation of L3 in $ETR1_{RD}$ such that loop L3 is flipped to the opposite side toward the α4-helix (Fig. 3B). This makes $ETR1_{RD}$ unique among all known and structurally determined receiver domains. However, we must consider that $ETR1_{RD}$ without Mg^{2+} forms a homodimer in solution as

well as in the crystal (55). This, together with our findings about conformational heterogeneity of $CKI1_{RD}$ in the absence of Mg^{2+}, makes interpretation of the conformational difference of L3 in comparison to other receiver domains rather difficult. The $CKI1_{RD}$ loop L3, which was not detected by nuclear magnetic resonance in solution, is probably highly flexible and the lock of its internal dynamics upon Mg^{2+} binding is clearly shown by appearance of an additional two methionine residues in comparison to an absence of Mg^{2+} (Fig. 5). If the loop is localized at the active site, then we could assume that the loss of its flexibility is connected with achieving the conformation of $CKI1_{RD}$ that subsequently allows its activation via phosphorylation. Accordingly, Mg^{2+} might cause structural rearrangements in the active site of the $ETR1_{RD}$ that would likely affect also the conformation of its L3. Thus, only the crystal structure of Mg^{2+}-bound $ETR1_{RD}$ could fully explain conformational differences between both *A. thaliana* RDs in their phosphorylation-ready form.

Our data also provide first clues for future identification of the structural changes associated with $CKI1_{RD}$ activation by phosphorylation. In CheY it was proposed that breaking of the salt bridge between D57 and K109 (corresponding to D1050 and K1105 in $CKI1_{RD}$, respectively) by phosphorylation is critical for the conformational change associated with the CheY activation (57,58). Based on absence of the salt bridge between D57 and K109 in the Mg^{2+}-bound CheY, however, Stock et al. (59) suggested that the lysine K109 is rather important for achieving active conformation of the C-terminal portion of phosphorylated CheY – perhaps through an ionic interaction with an oxygen of the acyl-phosphate (or fluorine atoms of BeF_3^-). Here we have shown the presence of a salt bridge between D1050 and K1105 residues both in the Mg^{2+}-free and Mg^{2+}-bound forms of $CKI1_{RD}$. These results suggest that the salt bridge between D1050 and K1105 might be important for a proper orientation of the active site towards Mg^{2+}. That spacing of the active site is thought to act as a template for the transition state during phosphoryl transfer and/or an autodephosphorylation reaction mediated by CheY (59) and possibly also by other receiver domains. Finally, following transphosphorylation, repositioning of the salt bridges from D109 to the phosphoryl group (or BeF_3^-) had been suggested as one of the important structural changes during CheY activation (60). Based on our NMR data, the structural rearrangement following transphosphorylation of D1050 in $CKI1_{RD}$ would be rather minor and, similarly to that of CheY (61), would take place probably in the C-terminal portion of the $CKI1_{RD}$, delimited here by β4 and β5 (Fig. 6B). As the presence of BeF_3^- in the crystal structure of $CKI1_{RD}$ was not determined, however, the detailed structural changes in the activated form of $CKI1_{RD}$ remain to be identified and are a subject of our recent work.

Taken together, our NMR and X-ray experiments show that the main structural changes observed upon magnesium binding stabilize the loop L3 and change the relative positions of D1050 and K1105 in relation to S1082. This suggests that magnesium-mediated remodeling of the active site of $CKI1_{RD}$ is intrinsic to the phosphotransfer catalytic function of CKI1 in MSP in plants.

Effect of Mg^{2+} binding and phosphorylation on the specificity of CKI1-AHP interactions. Phosphorylation of the conserved D1050 residue in $CKI1_{RD}$ converts this domain from an inactive to active form. A correct description of the interactions of CKI1 with its AHP partners thus requires knowledge of AHP binding affinities of both inactive and activated forms of CKI1.

In $CKI1_{RD}$, the most prominent structural changes were Mg^{2+}-induced remodeling of the active site and loss of L3's internal dynamics. By contrast, the effect of beryllofluoridation, mimicking the formation of the labile acyl-phosphate bond, was rather negligible. In the Rcs signaling pathway, one of the few bacterial MSP pathways, the phosphorylation of the C-terminally located phosphoreceiver domain of hybrid sensor kinase RcsC (RcsC-PR) seems to be important for the recognition of its cognate partner, the HPt domain of RcsD HK (8). The addition of BeF_3^- to RcsC-PR preloaded with Mg^{2+} initiated loss of internal dynamics in the region of the interaction interface between RcsC-PR and RcsD. This conformational change led to 5–10 times stronger interaction of RcsC-PR with RcsD. Based on these

findings, it has been suggested that Mg^{2+}-dependent phosphorylation is necessary for the strong interaction of RcsC-PR with the RcsD-HPt domain and that the phosphorylated form of RcsC-PR will be more attractive for its interaction partner (62). In comparison to the aforementioned bacterial system, it seems that $CKI1_{RD}$ is more sensitive to Mg^{2+} and that the structural changes followed by $CKI1_{RD}$ phosphorylation are only minor. Thus, the Mg^{2+}-induced stabilization of the L3 loop might contribute to the molecular recognition of HPt and/or stabilization of the $CKI1_{RD}$ interaction. Accordingly, the *in vitro* affinities of $CKI1_{RD}$ to AHP2 and AHP3 that were comparable in the absence of Mg^{2+} changed to approximately two-fold preference for AHP2 in the presence of Mg^{2+}. This suggests that Mg^{2+}-induced structural changes might contribute to a fine-tuning of the AHPs binding specificity.

This assumption could be supported by continual changes in magnesium homeostasis of the plant with relevant shift under Mg^{2+} deficiency stress. Direct lack of Mg^{2+} but also the presence of competing cations that prevent Mg^{2+} uptake, such as Ca^{2+} in calcareous soils, NH_4^+ and Al_3^+ in acidic soils and Na^+ in saline soils (63), influence intracellular concentration of free form Mg^{2+}. This is also highly affected by light intensity (64) or in rapidly growing plants in the spring (63). Content of Mg^{2+} varies under different physiological conditions and has a direct influence on many processes, including root growth (65), photosynthesis rate (66), or starch reduction in storage tissues (63). Finally, nutrient shortage, including Mg^{2+} starvation, has been shown to affect several signaling pathways in plants (67). Thus, limitation of Mg^{2+} could cause changes in the interaction preference of a respective RD and/or might effectively modify the kinetics of the reaction where the RD acts as a donor of phosphoryl groups for an AHP protein. In this scenario, environmental- and/or developmental-specific changes in Mg^{2+} intracellular concentrations might be important for fine-tuning MSP signaling specificity in plants. Similarly, the BeF_3^--dependent changes in the $CKI1_{RD}$ affinity might reflect differential recognition of the interacting partners in the kinase or phosphatase activity modes of CKI1. Nevertheless, we still cannot exclude the possibility that the affinity changes in the presence or absence of Mg^{2+} and/or BeF_3^- are rather secondary effects of active site remodeling. Thus, the functional importance of the Mg^{2+}- as well as phosphorylation-induced changes in the binding affinity of CKI1-mediated MSP signaling remain to be identified.

As suggested in a previous work, CKI1 and other HKs act through AHP proteins that provide a functional "hub", integrating several signaling pathways mediated by e.g. cytokinin-dependent and cytokinin-independent HK (26). Thus, even slight changes in binding affinity in combination with differences in phosphatase activities reported for individual HKs (26) might substantially affect the final output of the integrated pathways. Therefore, identifying the binding preferences of active and inactive HK_{RD} is a crucial step in establishing the order of phosphoryl group flow in MSP pathways in plants.

References

1. Gao, R., and Stock, A. M. (2009) *Annu. Rev. Microbiol.* **63,** 133–154
2. Koretke, K. K., Lupas, A. N., Warren, P. V., Rosenberg, M., and Brown, J. R. (2000) *Mol. Biol. Evol.* **17,** 1956–1970
3. To, J. P., and Kieber, J. J. (2008) *Trends Plant Sci.* **13,** 85–92
4. Urao, T., Yamaguchi-Shinozaki, K., and Shinozaki, K. (2000) *Trends Plant Sci.* **5,** 67–74
5. Mizuno, T. (2005) *Biosci. Biotechnol. Biochem.* **69,** 2263–2276
6. Laub, M. T., and Goulian, M. (2007) *Annu. Rev. Genet.* **41,** 121–145
7. Xu, Q., Porter, S. W., and West, A. H. (2003) *Structure* **11,** 1569–1581
8. Rogov, V. V., Rogova, N. Y., Bernhard, F., Koglin, A., Lohr, F., and Dotsch, V. (2006) *J. Mol. Biol.* **364,** 68–79
9. Higuchi, M., Pischke, M. S., Mahonen, A. P., Miyawaki, K., Hashimoto, Y., Seki, M., Kobayashi, M., Shinozaki, K., Kato, T., Tabata, S., Helariutta, Y., Sussman, M. R., and Kakimoto, T. (2004) *Proc. Natl. Acad. Sci. U. S. A.* **101,** 8821–8826
10. Nishimura, C., Ohashi, Y., Sato, S., Kato, T., Tabata, S., and Ueguchi, C. (2004) *Plant Cell* **16,** 1365–1377
11. Riefler, M., Novak, O., Strnad, M., and Schmulling, T. (2006) *Plant Cell* **18,** 40–54
12. Urao, T., Yakubov, B., Satoh, R., Yamaguchi-Shinozaki, K., Seki, M., Hirayama, T., and Shinozaki, K. (1999) *Plant Cell* **11,** 1743–1754
13. Urao, T., Miyata, S., Yamaguchi-Shinozaki, K., and Shinozaki, K. (2000) *FEBS Lett.* **478,** 227–232
14. Tran, L. S., Urao, T., Qin, F., Maruyama, K., Kakimoto, T., Shinozaki, K., and Yamaguchi-Shinozaki, K. (2007) *Proc. Natl. Acad. Sci. U. S. A.* **104,** 20623–20628
15. Kakimoto, T. (1996) *Science* **274,** 982–985
16. Pischke, M. S., Jones, L. G., Otsuga, D., Fernandez, D. E., Drews, G. N., and Sussman, M. R. (2002) *Proc. Natl. Acad. Sci. U. S. A.* **99,** 15800–15805
17. Hejatko, J., Pernisova, M., Eneva, T., Palme, K., and Brzobohaty, B. (2003). *Mol. Genet. Genomics* **269,** 443–453
18. Hejatko, J., Ryu, H., Kim, G. T., Dobesova, R., Choi, S., Choi, S. M., Soucek, P., Horak, J., Pekarova, B., Palme, K., Brzobohaty, B., and Hwang, I. (2009). *Plant Cell* **21**, 2008-2021
19. Deng, Y., Dong, H., Mu, J., Ren, B., Zheng, B., Ji, Z., Yang, W. C., Liang, Y., and Zuo, J. (2010) *Plant Cell* **22,** 1232–1248
20. Iwama, A., Yamashino, T., Tanaka, Y., Sakakibara, H., Kakimoto, T., Sato, S., Kato, T., Tabata, S., Nagatani, A., and Mizuno, T. (2007) *Plant Cell Physiol.* **48,** 375–380
21. Desikan, R., Horak, J., Chaban, C., Mira-Rodado, V., Witthoft, J., Elgass, K., Grefen, C., Cheung, M. K., Meixner, A. J., Hooley, R., Neill, S. J., Hancock, J. T., and Harter, K. (2008) *PLoS One* **3,** e2491
22. Hass, C., Lohrmann, J., Albrecht, V., Sweere, U., Hummel, F., Yoo, S. D., Hwang, I., Zhu, T., Schafer, E., Kudla, J., and Harter, K. (2004) *EMBO J.* **23,** 3290–3302
23. Scharein, B., Voet-Van-Vormizeele, J., Harter, K., and Groth, G. (2008) *Anal. Biochem.* **377,** 72–76
24. Hwang, I., and Sheen, J. (2001). *Nature* **413,** 383–389
25. Yamada, H., Suzuki, T., Terada, K., Takei, K., Ishikawa, K., Miwa, K., Yamashino, T., and Mizuno, T. (2001) *Plant and Cell Physiol.* **42,** 1017–1023
26. Mahonen, A. P., Higuchi, M., Tormakangas, K., Miyawaki, K., Pischke, M. S., Sussman, M. R., Helariutta, Y., and Kakimoto, T. (2006) *Curr. Biol.* **16,** 1116–1122
27. Dortay, H., Mehnert, N., Burkle, L., Schmulling, T., and Heyl, A. (2006) *FEBS J.* **273,** 4631–4644
28. Dortay, H., Gruhn, N., Pfeifer, A., Schwerdtner, M., Schmulling, T., and Heyl, A. (2008) *J. Proteome Res.* **7,** 3649–3660
29. Hutchison, C. E., Li, J., Argueso, C., Gonzalez, M., Lee, E., Lewis, M. W., Maxwell, B. B., Perdue, T. D., Schaller, G. E., Alonso, J. M., Ecker, J. R., and Kieber, J. J. (2006) *Plant Cell* **18,** 3073–3087

30. Mason, M. G., Mathews, D. E., Argyros, D. A., Maxwell, B. B., Kieber, J. J., Alonso, J. M., Ecker, J. R., and Schaller, G. E. (2005) *Plant Cell* **17,** 3007–3018
31. Argyros, R. D., Mathews, D. E., Chiang, Y. H., Palmer, C. M., Thibault, D. M., Etheridge, N., Argyros, D. A., Mason, M. G., Kieber, J. J., and Schaller, G. E. (2008). *Plant Cell* **20,** 2102–2116
32. Klumpler, T., Pekarova, B., Marek, J., Borkovcova, P., Janda, L., and Hejatko, J. (2009) *Acta Crystallogr., Sect. F: Struct. Biol. Cryst. Commun.* **65,** 478–481
33. Bradford, M. M. (1976) *Anal. Biochem.* **72,** 248–254
34. Walter, M., Chaban, C., Schutze, K., Batistic, O., Weckermann, K., Nake, C., Blazevic, D., Grefen, C., Schumacher, K., Oecking, C., Harter, K., and Kudla, J. (2004) *Plant J.* **40,** 428–438
35. Horak, J., Grefen, C., Berendzen, K. W., Hahn, A., Stierhof, Y. D., Stadelhofer, B., Stahl, M., Koncz, C., and Harter, K. (2008) *BMC Plant Biol.* **8,** 77
36. Kabsch, W. (2010) *Acta Crystallogr., Sect. D: Biol. Crystallogr.* **66,** 125–132
37. Vagin, A., and Teplyakov, A. *Acta Crystallogr., Sect. D: Biol. Crystallogr.* **66,** 22–25
38. Cohen, S. X., Ben Jelloul, M., Long, F., Vagin, A., Knipscheer, P., Lebbink, J., Sixma, T. K., Lamzin, V. S., Murshudov, G. N., and Perrakis, A. (2008) *Acta Crystallogr., Sect. D: Biol. Crystallogr.* **64,** 49–60
39. Murshudov, G. N., Vagin, A. A., and Dodson, E. J. (1997) *Acta Crystallogr., Sect. D: Biol. Crystallogr.* **53,** 240–255
40. Emsley, P., and Cowtan, K. (2004) *Acta Crystallogr., Sect. D: Biol. Crystallogr.* **60,** 2126–2132
41. Pettersen, E. F., Goddard, T. D., Huang, C. C., Couch, G. S., Greenblatt, D. M., Meng, E. C., and Ferrin, T. E. (2004) *J. Comput. Chem.* **25,** 1605–1612
42. Urbanikova, L., Janda, L., Popov, A., Wiche, G., and Sevcik, J. (2002) *Acta Crystallogr., Sect. D: Biol. Crystallogr.* **58,** 1368–1370
43. Sattler, M., Schleucher, J., and Griesinger, C**.** (1999) *Prog. Nucl. Magn. Reson. Spectrosc.* **34,** 93–158
44. Mulder, F. A. A., van Tilborg, P. J. A., Kaptein, R., and Boelens, R. (1999) *J. Biomol. NMR* **13,** 275–288
45. Delaglio, F., Grzesiek, S., Vuister, G. W., Zhu, G., Pfeifer, J., and Bax, A. (1995). *J. Biomol. NMR* **6,** 277–293
46. Goddard, T. D., and Kneller, D. G. SPARKY 3.115. University of California, San Francisco, USA
47. Borkovcova, P., Pekarova, B., Urbankova, L., Dopitova, R., Brzobohaty, B., Hejatko, J., and Janda, L. (manuscript in preparation)
48. Wilson, D., Pethica, R., Zhou, Y. D., Talbot, C., Vogel, C., Madera, M., Chothia, C., and Gough, J. (2009) *Nucleic Acids Res.* **37,** D380–D386
49. Cho, H. S., Pelton, J. G., Yan, D. L., Kustu, S., and Wemmer, D. E. (2001) *Curr. Opin. Struct. Biol.* **11,** 679–684
50. Pazy, Y., Wollish, A. C., Thomas, S. A., Miller, P. J., Collins, E. J., Bourret, R. B., and Silversmith, R. E. (2009) *J. Mol. Biol.* **392,** 1205–1220
51. Nakamura, A., Kakimoto, T., Imamura, A., Suzuki, T., Ueguchi, C., and Mizuno, T. (1999) *Biosci., Biotechnol., Biochem.* **63,** 1627–1630
52. Silva, J. C., Haldimann, A., Prahalad, M. K., Walsh, C. T., and Wanner, B. L. (1998) *Proc. Natl. Acad. Sci. U. S. A.* **95,** 11951–11956
53. Stock, A. M., Mottonen, J. M., Stock, J. B., and Schutt, C. E. (1989) *Nature* **337,** 745–749
54. West, A. H., and Stock, A. M. (2001). *Trends Biochem. Sci.* **26,** 369–376
55. Muller-Dieckmann, H. J., Grantz, A. A., and Kim, S. H. (1999) *Structure* **7,** 1547–1556
56. Schaller, G. E., and Bleecker, A. B. (1995) *Science* **270,** 1809–1811
57. Bourret, R. B., Drake, S. K., Chervitz, S. A., Simon, M. I., and Falke, J. J. (1993) *J. Biol. Chem.* **268,** 13089–13096
58. Roman, S. J., Meyers, M., Volz, K., and Matsumura, P. (1992) *J. Bacteriol.* **174,** 6247–6255

59. Stock, A. M., Martinez-Hackert, E., Rasmussen, B. F., West, A. H., Stock, J. B., Ringe, D., and Petsko, G. A. (1993) *Biochemistry* **32,** 13375–13380
60. Guhaniyogi, J., Robinson, V. L., and Stock, A. M. (2006) *J. Mol. Biol.* **359,** 624–645
61. Lee, S. Y., Cho, H. S., Pelton, J. G., Yan, D., Berry, E. A., and Wemmer, D. E. (2001) *J. Biol. Chem.* **276,** 16425–16431
62. Rogov, V. V., Schmoe, K., Lohr, F., Rogova, N. Y., Bernhard, F., and Dotsch, V. (2008) *Biochem. Soc. Trans.* **36,** 1427–1432
63. Shaul, O. (2002) *Biometals* **15,** 309–323
64. Marschner, H., and Cakmak, I. (1989) *J. Plant Physiol.* **134,** 308–315
65. Cakmak, I., and Kirkby, E. A. (2008) *Physiol. Plant.* **133,** 692–704
66. Rao, I. M., Sharp, R. E., and Boyer, J. S. (1987) *Plant Physiol.* **84,** 1214–1219
67. Hermans, H., Hammond, J. P., White, P. J., and Verbruggen, N. (2006) *TRENDS Plant Sci.* **11,** 610–617

Footnotes

We wish to thank the EMBL/DESY Hamburg for providing us with synchrotron facilities and D. Tucker for his assistance with data collection. The authors are grateful to Ondrej Šedo for measuring the MALDI-TOF MS spectra. This research was supported by grants from the Czech Science Foundation (Grants nos. 204/08/H054, 525/07/1069, 521/09/1699 and P503/10/217), from the Ministry of Education, Youth and Sports (Grants nos. MSM0021622413, MSM0021622415 and LC06034), and from the 7th Framework Programme of the EC (Contracts 228461, EAST-NMR, and 205872, POSTBIOMIN - FP7-REGPOT-2007-1).

The abbreviations used are: BiFC, bimolecular fluorescence complementation; HK, histidine kinase; HPt, histidine phosphotransfer protein; HSQC, heteronuclear single-quantum coherence; MSP, multistep phosphorelay; PBST, PBS with Tween; RD, receiver domain; TCS, two-component signaling.

Figure legends

Figure 1. CKI1 receiver domain mediates interaction with a specific subset of AHPs *in vivo*. (A-B) Confocal images of abaxial tobacco leaf cells co-expressing the indicated AHP:YFP-N fusion proteins with CKI1:YFP-C (A) and $CKI1_{RD}$:YFP-C (B). YFP fluorescence of the reconstituted fluorophore is documented in the left column; the bars represent 100 μm. The right column shows the corresponding bright field images. Fusion protein expression was confirmed by immunodetection with appropriate antibody in protein extracts from corresponding leaves (1–6). M, protein marker. (C) $CKI1_{RD}$ yeast two-hybrid assay. Growth of the yeast clones expressing BD:$CKI1_{RD}$ and indicated AD:AHP protein was documented after incubation for 4 days by either interaction selective media lacking leucine, tryptophan and adenine (L^-, W^-, Ade^-) or vector selective media (L^-,W^-). The empty pGADT7 was used as a negative control. Expression of all proteins was proven on western blots by immunodetection with appropriate antibodies.

Figure 2. AHP proteins bind to $CKI1_{RD}$ with different affinities. Quantitative analysis of $CKI1_{RD}$-AHP interaction by ELISA. Data are shown as averages from three independent experiments ± SE.

Figure 3. $CKI1_{RD}$ structure and its similarity with $ETR1_{RD}$ structure. (A) A ribbon representation of the $CKI1_{RD}$ structure. The helices (α1–α5) and beta strands (β0–β5) are numbered sequentially. L1–L5 are the loops between helices and beta strands of the same number. Side chains of

catalytic aspartate and of K1105 are shown. (B) Structural comparison of $CKI1_{RD}$ and $ETR1_{RD}$. Superimposition of the C^{α} backbone structures of $CKI1_{RD}$ (green) and $ETR1_{RD}$ (orange) from *A. thaliana* illustrates major difference in loop L3 and minor differences in loops L2 and L4. The remaining parts of the structures overlay well. Side chains of catalytic aspartate D1050 (CKI1) and D659 (ETR1) are shown.

Figure 4. Ribbon diagrams of Mg^{2+}-free (A) and Mg^{2+}-bound (B) form of the active site of $CKI1_{RD}$. Magnesium ion (magenta) is approximately octahedrally coordinated in $CKI1_{RD}$ by short contacts (2.3 Å) with carboxyl oxygens (OD1) of D993 and D1050, carbonyl oxygen of Q1052 and one water molecule (cyan), which forms a hydrogen bond to carboxyl oxygen of D992.

Figure 5. Magnesium binding invokes structural changes within the active site of the $CKI1_{RD}$ in solution. Overlaid two-dimensional $^{1}H,^{15}N$-HSQC spectra of Mg^{2+}-free $CKI1_{RD}$ (green) and Mg^{2+}-bound $CKI1_{RD}$ (red). The left panel shows spectra obtained for uniformly ^{15}N-labelled $CKI1_{RD,}$ while the right panel shows spectra obtained for $CKI1_{RD,}$ with selectively ^{15}N-labelled methionines. Selected residues in two-dimensional $^{1}H,^{15}N$-HSQC spectra are depicted in the corresponding ribbon diagrams of crystal structures of $CKI1_{RD}$ (green), $CKI1_{RD}$ Mg^{2+} (red).

Figure 6. Combined chemical shift changes during titration experiments plotted as a function of residue number. The data were derived from two-dimensional $^{1}H,^{15}N$-HSQC spectra of $CKI1_{RD}$ (A1, B1) and mutant $CKI1_{RD}^{D1050A}$ (A2, B2) measured before and after titration experiments. Differences induced by adding Mg^{2+} to free $CKI1_{RD}$/$CKI1_{RD}^{D1050A}$ and by beryllofluoridation of Mg^{2+}-bound $CKI1_{RD}$/$CKI1_{RD}^{D1050A}$ are displayed in Panels A and B, respectively.

Table 1. X-Ray data collection statistics. Observed reflections are those for which I > 2σ(I).

	$CKI1_{RD}$	$CKI1_{RD}$ Mg^{2+}
Data collection		
Wavelength (Å)	0.8423	0.8123
Space group	*C222₁*	*C222₁*
Cell dimensions		
a, *b*, *c* (Å)	54.5; 99.8; 79.9	54.1; 100.9; 80.1
Resolution range (Å)	19.4–2.00 (2.04–2.00)	20.0 – 2.20 (2.25–2.20)
R_{merge} (all/observed)	9.5/9.2 (34.2/27.5)	4.9/4.0 (28.4/19.1)
$I/\sigma(I)$ (all/observed)	20.7/22.7 (6.8/8.7)	15.5/18.1 (3.10/4.64)
Completeness (all/observed) (%)	99.8/90.6 (99.9/75.8)	92.0/73.2 (88.6/50.4)
Refinement		
Resolution (Å)	2.0	2.2
No. unique reflections (all/observed)	15054/13674 (1439/871)	21328/10328 (3206/629)
R_{work}/ R_{free}	17.6/22.9	17.4/23.7
No. atoms	1265	1243
Protein	1133	1123
Ligand/ion	-	1
Water	132	119
B-factors (Å^2)		
Protein	30.1	37.7
Ligand/ion	-	55.5
Water	40.6	49.9
RMSD		
Bond lengths (Å)	0.033	0.025
Bond angles (º)	2.25	1.91

Table 2. Affinity constants (K_d [nM]) of $CKI1_{RD}$-AHP interactions under conditions of different binding buffers. Affinity constants were determined by ELISA as is described in experimental procedures. Binding buffers used: A, PBST plus 0.05% Tween 20; B, PBST enriched with 5 mM $MgCl_2$; C, PBST enriched with 5 mM $MgCl_2$, 3 mM NaF and 0.6 mM $BeCl_2$.

	Buffer		
Ligand	A	B	C
AHP2	9.17 ± 0.49	6.2 ± 0.98	11.6 ± 2.0
AHP3	10.5 ± 0.73	12.9 ± 0.72	8.0 ± 0.42
AHP5	108 ± 18	152 ± 26	119 ± 32

Figure 1

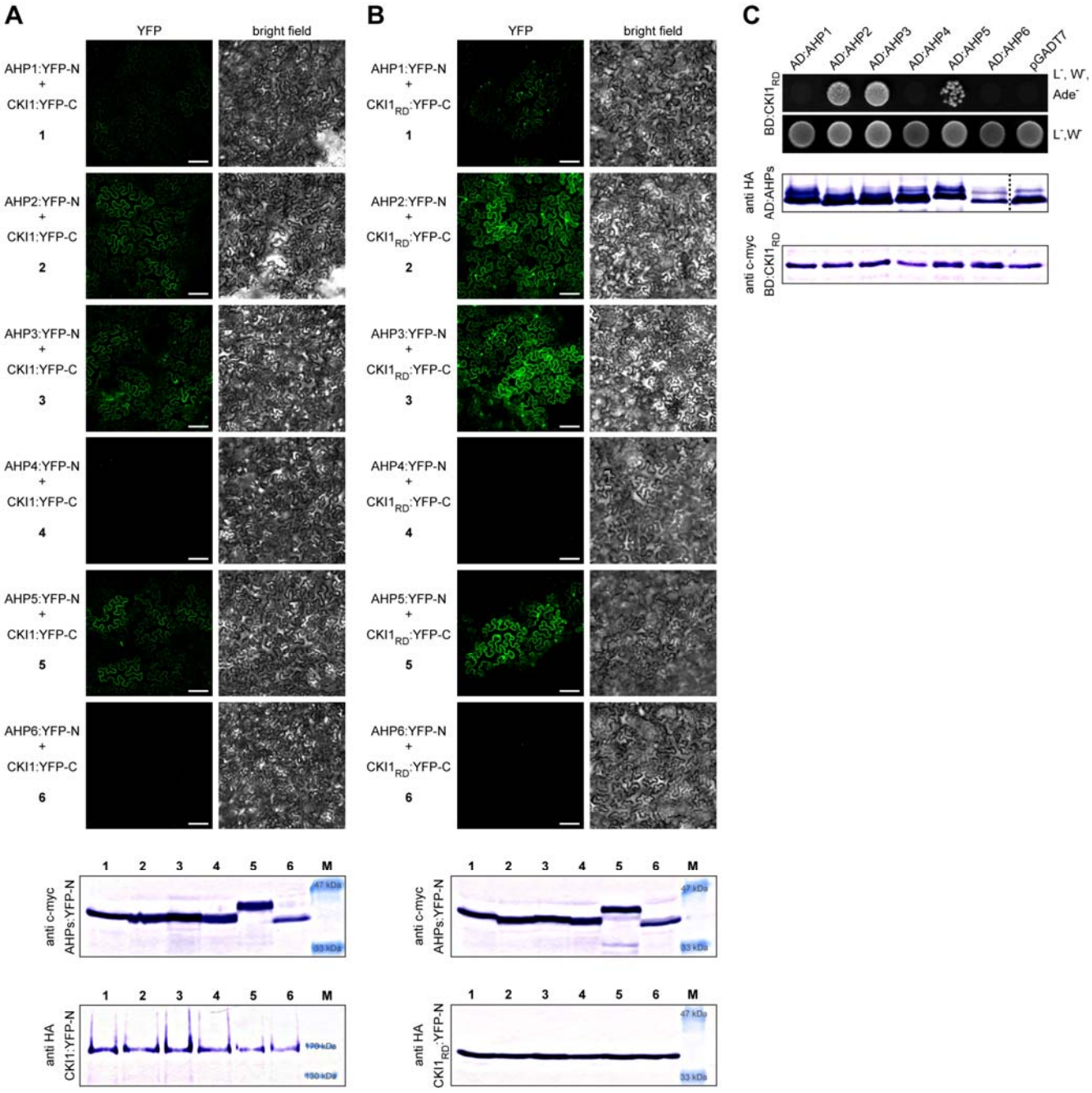
A
YFP
bright field
AHP1:YFP-N + CKI1:YFP-C 1
AHP2:YFP-N + CKI1:YFP-C 2
AHP3:YFP-N + CKI1:YFP-C 3
AHP4:YFP-N + CKI1:YFP-C 4
AHP5:YFP-N + CKI1:YFP-C 5
AHP6:YFP-N + CKI1:YFP-C 6
B
YFP
bright field
AHP1:YFP-N + CKI1RD:YFP-C 1
AHP2:YFP-N + CKI1RD:YFP-C 2
AHP3:YFP-N + CKI1RD:YFP-C 3
AHP4:YFP-N + CKI1RD:YFP-C 4
AHP5:YFP-N + CKI1RD:YFP-C 5
AHP6:YFP-N + CKI1RD:YFP-C 6
C
AD:AHP1
AD:AHP2
AD:AHP3
AD:AHP4
AD:AHP5
AD:AHP6
pGADT7
BD:CKI1RD
L-, W-, Ade-
L-,W-
anti HA AD:AHPs
anti c-myc BD:CKI1RD
1 2 3 4 5 6 M
anti c-myc AHPs:YFP-N
47 kDa
33 kDa
anti HA CKI1:YFP-N
anti HA CKI1RD:YFP-N

Figure 2

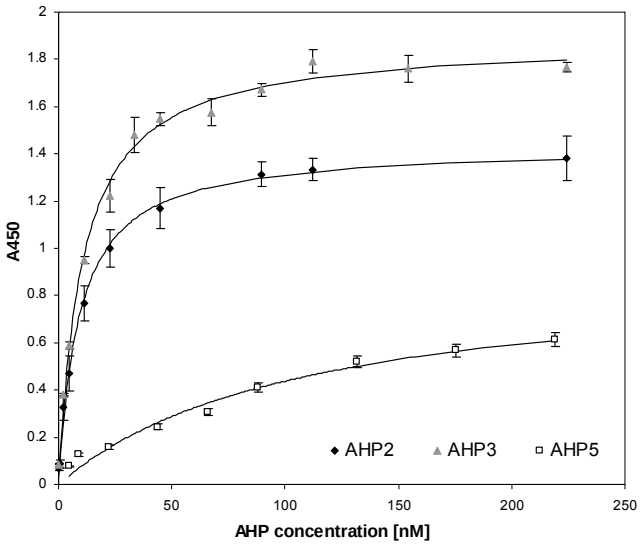
A450
AHP concentration [nM]
AHP2
AHP3
AHP5
0
0.2
0.4
0.6
0.8
1
1.2
1.4
1.6
1.8
2
0
50
100
150
200
250

Figure 3

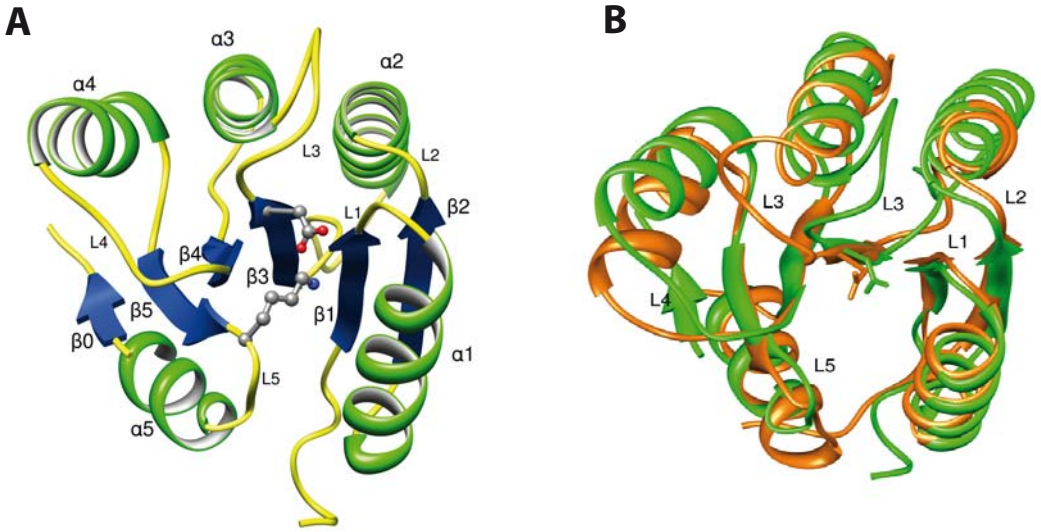

Figure 4

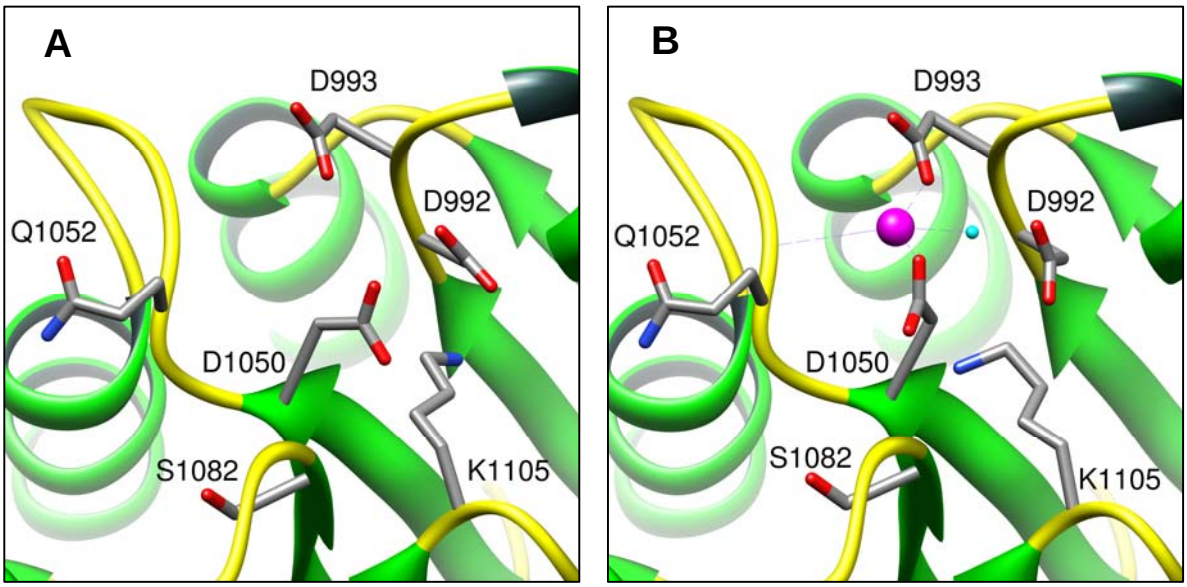
A
D993
D992
Q1052
D1050
S1082
K1105
B
D993
D992
Q1052
D1050
S1082
K1105

Figure 5

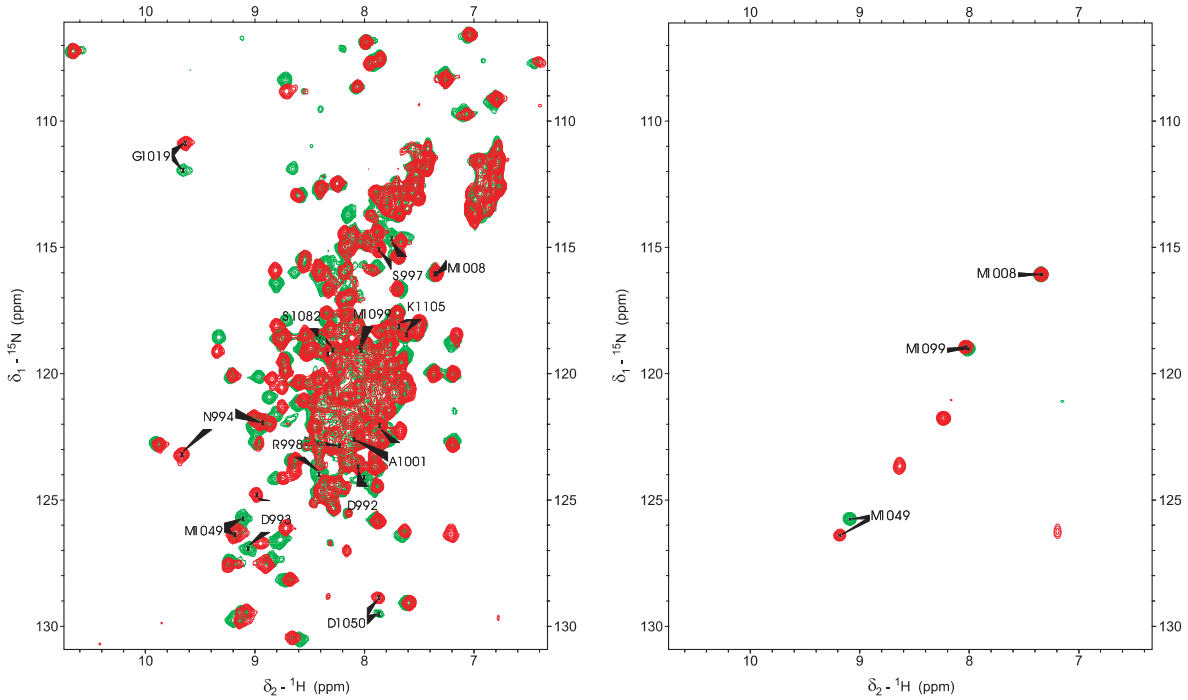
G1019
S997
M1008
S1082
M1099
K1105
N994
R998
A1001
D992
M1049
D993
D1050
δ_1 - ^{15}N (ppm)
δ_2 - ^{1}H (ppm)
M1008
M1099
M1049

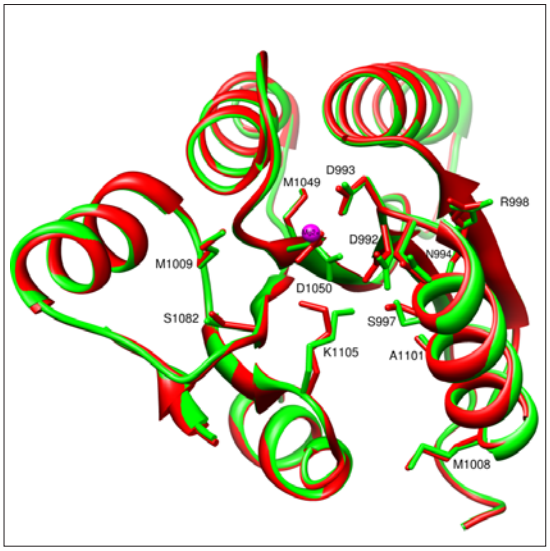
M1049
D993
R998
D992
N994
M1009
D1050
S1082
S997
K1105
A1101
M1008

Figure 6

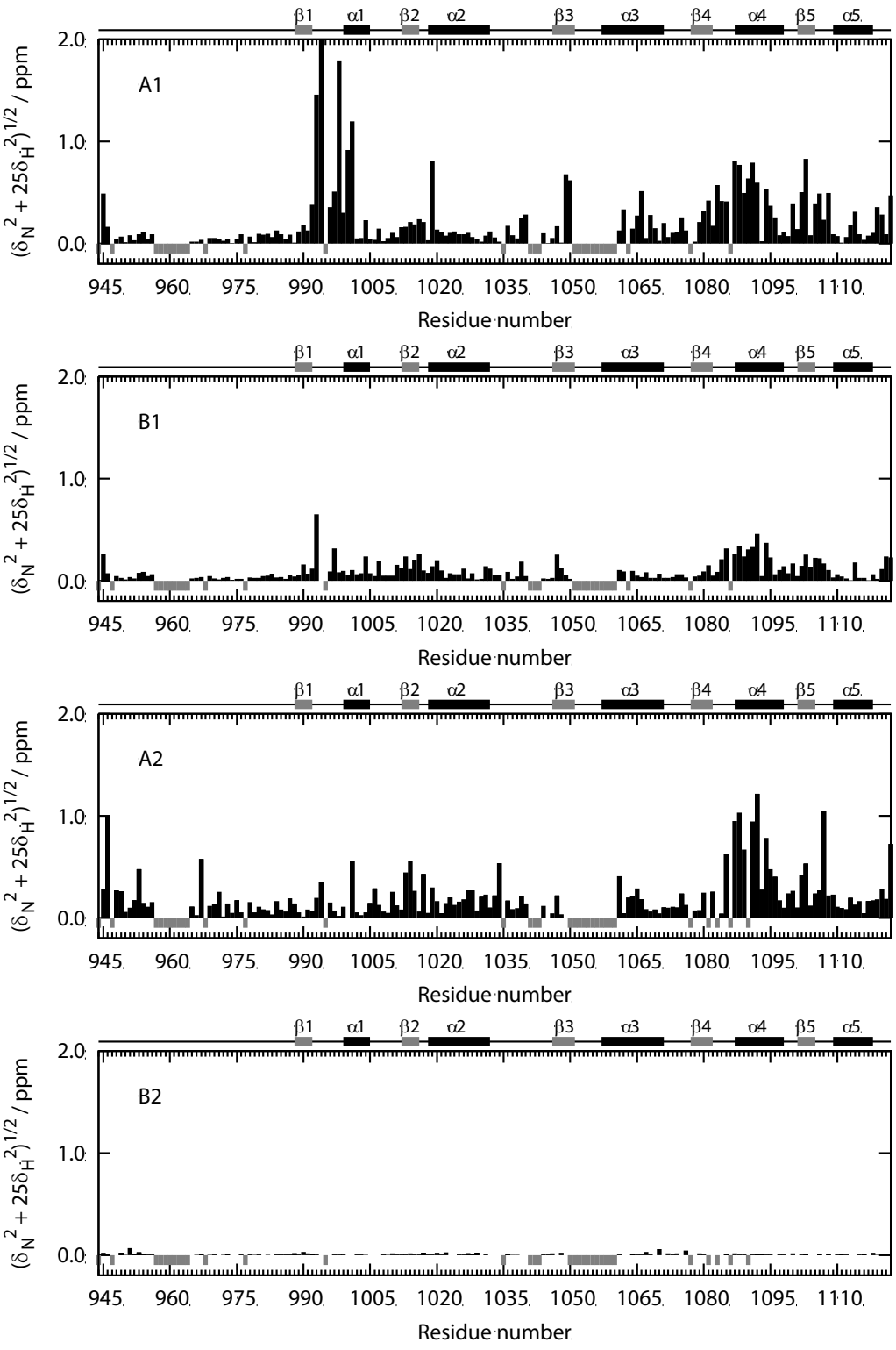
β1 α1 β2 α2 β3 α3 β4 α4 β5 α5
A1
B1
A2
B2
$(\delta_N^2 + 25\delta_H^2)^{1/2}$ / ppm
2.0
1.0
0.0
945 960 975 990 1005 1020 1035 1050 1065 1080 1095 1110
Residue number

Enclosed Publication # 8

Pernisová, M., Klíma, P., Horák, J., Válková, M., Malbeck, J., Souček, P., Reichman, P., Hoyerová, K., Dubová, J., Friml, J., Zažímalová, E. and **Hejátko, J.** (2009) Cytokinins modulate auxin-induced organogenesis in plants via regulation of the auxin efflux. *Proceedings of the National Academy of Sciences of the U.S.A.*, **106**, 3609-3614. IF_{2008}= 9.380

March 3, 2009 | vol. 106 | no. 9 | pp. 2969–3640

PNAS

Proceedings of the National Academy of Sciences of the United States of America www.pnas.org

Plant organogenesis

Legged robots on granular media

Improving nitrogen management

Kelp genes hold sea ice history

Protecting neurons from Alzheimer's

Cytokinins modulate auxin-induced organogenesis in plants via regulation of the auxin efflux

Markéta Pernisová[a], Petr Klíma[b], Jakub Horák[a], Martina Válková[a], Jiří Malbeck[b], Přemysl Souček[c], Pavel Reichman[a], Klára Hoyerová[b], Jaroslava Dubová[a], Jiří Friml[a], Eva Zažímalová[b], and Jan Hejátko[a,1]

[a]Laboratory of Molecular Plant Physiology, Department of Functional Genomics and Proteomics, Institute of Experimental Biology, Faculty of Science, Masaryk University, CZ-625 00 Brno, Czech Republic; [b]Institute of Experimental Botany, The Academy of Sciences of the Czech Republic, CZ-165 02 Prague, Czech Republic; and [c]Institute of Biophysics, The Academy of Sciences of the Czech Republic, CZ-612 65 Brno, Czech Republic

Edited by Marc C. E. Van Montagu, Ghent University, Ghent, Belgium, and approved December 30, 2008 (received for review November 14, 2008)

Postembryonic de novo organogenesis represents an important competence evolved in plants that allows their physiological and developmental adaptation to changing environmental conditions. The phytohormones auxin and cytokinin (CK) are important regulators of the developmental fate of pluripotent plant cells. However, the molecular nature of their interaction(s) in control of plant organogenesis is largely unknown. Here, we show that CK modulates auxin-induced organogenesis (AIO) via regulation of the efflux-dependent intercellular auxin distribution. We used the hypocotyl explants-based in vitro system to study the mechanism underlying de novo organogenesis. We show that auxin, but not CK, is capable of triggering organogenesis in hypocotyl explants. The AIO is accompanied by endogenous CK production and tissue-specific activation of CK signaling. CK affects differential auxin distribution, and the CK-mediated modulation of organogenesis is simulated by inhibition of polar auxin transport. CK reduces auxin efflux from cultured tobacco cells and regulates expression of auxin efflux carriers from the PIN family in hypocotyl explants. Moreover, endogenous CK levels influence *PIN* transcription and are necessary to maintain intercellular auxin distribution *in planta*. Based on these findings, we propose a model in which auxin acts as a trigger of the organogenic processes, whose output is modulated by the endogenously produced CKs. We propose that an important mechanism of this CK action is its effect on auxin distribution via regulation of expression of auxin efflux carriers.

PIN expression | two-component signalling | root meristem | auxin maxima

Postembryonic de novo organogenesis represents an important developmental adaptation evolved in plants. Regeneration of entire bodies in hydras (1) or organs in amphibians (2) has been described. However, in the animal kingdom, these examples are rather exceptional. In contrast, plants evolved postembryonic formation of new organs from differentiated tissues as a strategy that allows physiological and developmental adaptation to changing environmental conditions. However, this strategy requires action by factors that are specifically able to induce developmental programs, leading to the formation of entire organs from virtually differentiated cells.

The interaction of auxin and cytokinin (CK) during plant organogenesis is a phenomenon known for a long time. In their pioneering work, Skoog and Miller (3) identified auxin-to-CK concentration ratios as an important factor regulating the developmental fate of plant tissue explants. Since that time, the role of both growth factors in plant development has been extensively studied. For auxin action, a model involving a spatial and temporal pattern of intercellular auxin distribution and concentration maxima is well established, and the molecular and cellular factors mediating auxin distribution have been identified (4, 5). Differential auxin distribution has been shown to mediate multiple aspects of plant development, such as apical/basal axis formation (6), root patterning (7, 8), tropisms (9–11), and organogenesis (12–15). CK is an important regulator of shoot (16) and root architecture (17–22), and it also regulates seed development (23), abiotic stress (24), and plant senescence (25). CK signaling is mediated by two-component phosphorelay in *Arabidopsis* (for an in-depth recent review, see ref. 26). However, the molecular factors acting downstream of the CK signaling pathway remain mostly unknown.

Here, we use de novo auxin-induced organogenesis (AIO) as a model for characterization of the interactions between CKs and auxin in regulation of plant development. We show that auxin triggers organogenesis and that CK modulates its output through its effect on auxin distribution, which is realized by CK-dependent regulation of expression of auxin transport components.

Results

CK Modulates Auxin-Induced de Novo Organogenesis via Two-Component Signalling. We have used the well-known phenomenon of distinct effects of different CK-to-auxin ratios on the development of plant explants in vitro (3, 27) and adapted this system to study the mechanism underlying de novo organogenesis. Placement of *Arabidopsis* hypocotyls on the media with threshold auxin concentration has resulted in the formation of newly induced root-like organs, even in the absence of exogenous CK. The threshold auxin concentration was identified as the lowest auxin concentration leading to the formation of well-distinguishable organs at different CK concentrations and was identified to be 30 ng/mL (135 nM) for 2,4-dichlorophenoxyacetic acid [2,4-D] and 100 ng/mL (537 nM) for naphthalene-1-acetic acid [NAA] (Fig. 1*A*). In the root-like structures induced by NAA, all important morphological traits of genuine roots could be recognized (i.e., columella, lateral root cap, quiescent center, epidermis, cortex, endodermis, stele). In 2,4-D–induced organs, only the columella-like cells could be distinguished. However, in both 2,4-D– and NAA-induced organs, the columella-like cells revealed DR5 activity, which is consistent with the situation in genuine roots. With an increasing concentration of CK in the media, we observed a decreasing ability of hypocotyl explants to form root-like structures and their gradual disorganization (Fig. 1*A* and Fig. S1, for more details see later in the text). At the CK (kinetin) concentration of 300 ng/mL (1.4 μM, further referred to as the CK threshold), only disorganized callus was produced (Fig. 1*A*), with very rare remnants of distinguishable root-like organs (Fig. S1). After a prolonged period of cultivation at these CK and auxin concentrations, the calli turned green, and new shoots have occasionally been formed from the disorganized tissue (data not shown). However, at auxin concentrations below the organ-inducing threshold, CK alone was unable to induce any organogenic response (Fig. 1 *A* and *B*). This suggests that auxin triggers organogenesis, whereas CK modulates it.

Author contributions: M.P., E.Z., and J. Hejátko designed research; M.P., P.K., J. Horák, M.V., J.M., P.S., P.R., K.H., and J.D. performed research; M.P., P.K., J. Horák, J.F., E.Z., and J. Hejátko analyzed data; and J.F., E.Z., and J. Hejátko wrote the paper.

The authors declare no conflict of interest.

This article is a PNAS Direct Submission.

Freely available online through the PNAS open access option.

[1]To whom correspondence should be addressed. E-mail: hejatko@sci.muni.cz.

This article contains supporting information online at www.pnas.org/cgi/content/full/0811539106/DCSupplemental.

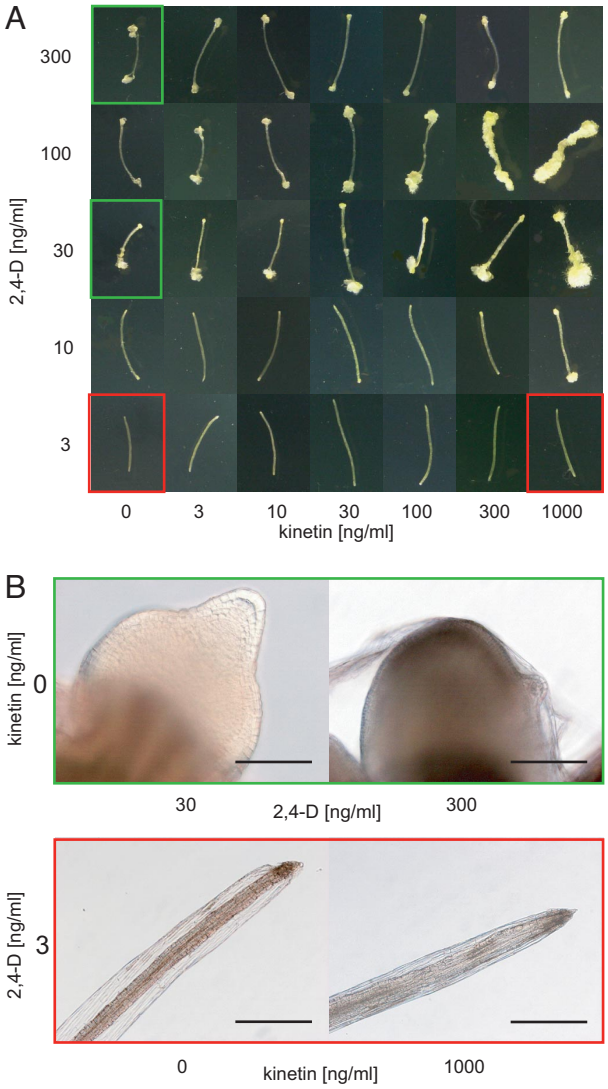

Fig. 1. CK modulates AIO. (*A*) Formation of root-like organs and calli in hypocotyls grown on different combinations of 2,4-D and kinetin. (*B*) Details of the root-like organs (green frames in *A*) formed in the absence of kinetin and at different 2,4-D concentrations. In contrast, no organogenic response was observed at the low auxin concentration and any of the tested kinetin concentrations (red frames in *A*). (Scale bars: 100 μm in green frame and 400 μm in red frame.)

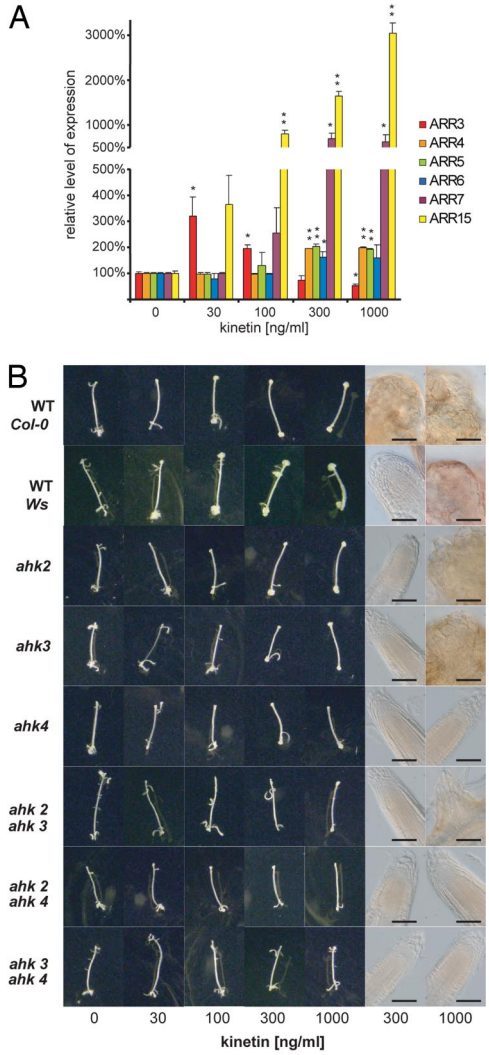

Fig. 2. CK modulates organogenesis via a two-component system. (*A*) Relative expression of CK primary response genes, A-type *ARRs* with the increasing CK concentration in the presence of NAA (537 nM). The statistical significance of identified differences in comparison to the absence of exogenous CKs (*t* test) at alpha 0.05 and 0.01 is designated (* and **, respectively); error bars show SDs. (*B*) Phenotypes of root-like organs induced by NAA (537 nM) at the increasing CK concentrations in WT (*Col-0* and *Ws* ecotypes) and different single and double CK receptor mutants. All mutants are of *Col-0* ecotype except for *ahk4* and *ahk3 ahk4*, which carry *ahk4–1* allele from *Ws* (see *Materials and Methods*). (Scale bar: 50 μm.)

To address the involvement of CK signaling in the observed phenomenon, we analyzed expression of the primary CK response genes (i.e., the A-type *ARR* genes) (28) in hypocotyl explants using quantitative real-time (qRT) PCR in the presence of auxin threshold [NAA (100 ng/mL)] and increasing CK concentration. With the exception of *ARR3*, which peaked at 30 ng/mL (139 nM) kinetin, we have found a gradual increase in the expression levels of all inspected A-type *ARRs* with increasing CK concentration; a particularly steep increase of expression was observed at the CK threshold concentration (Fig. 2*A*). Next, we addressed the involvement of CK perception and its specificity in the observed morphogenic effect. We analyzed the organogenic response in hypocotyl explants isolated from mutants in CK receptors AHK2, AHK3, and AHK4 (29, 30). All single, and particularly double, mutants showed increased resistance to CK in terms of modulation of organogenesis in comparison to corresponding WT (Fig. 2*B*). Differences in the strength of the phenotype in particular single and double *ahk* mutants suggest a certain specificity of individual signaling pathways in the CK-dependent modulation of organogenesis, with a dominant effect of *AHK4*, followed by *AHK3* and *AHK2* (*AHK4* ≥ *AHK3* > *AHK2*; Fig. 2*B*). These findings are in accordance with previous observations (29, 30), thus confirming the suitability of our experimental setup. Collectively, these results show that CKs modulate the auxin-induced organogenic response in *Arabidopsis* via two-component signaling.

AIO Is Accompanied by the Production of Endogenous CKs and Tissue-Specific Activation of CK Signaling. The expression of A-type *ARR*s even in the absence of exogenous CKs (Fig. 2*A* and data not shown) suggests that the AIO might be accompanied by endogenous CK production and subsequent activation of CK signaling. To identify the potential importance of endogenous CKs in AIO, we

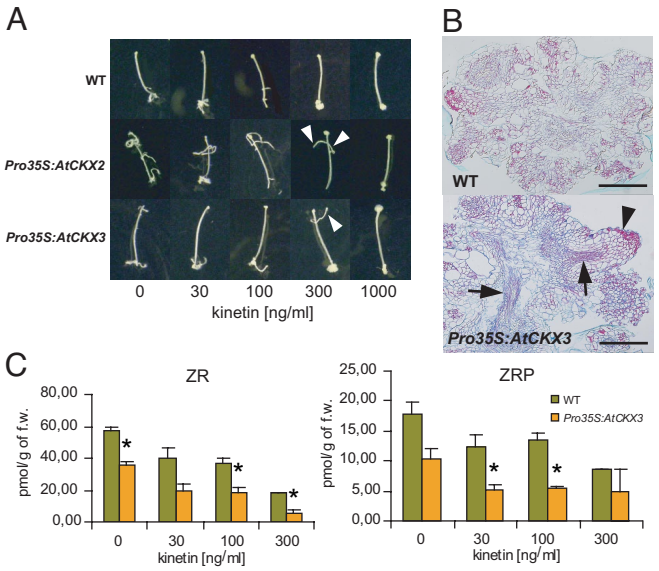

Fig. 3. Auxin induces production of endogenous CKs that contribute to AIO. (*A*) Formation of root-like organs induced by NAA (537 nM). Note that in *Pro35S:AtCKX2* and *Pro35S:AtCKX3* lines, there are still root-like organs distinguishable even at the CK threshold concentration (arrowheads), which is not the case in WT. (*B*) Structure of calli induced by auxin (537 nM NAA) at the CK threshold (1.4 μM kinetin). In the *Pro35S:AtCKX3* line, there are still patterned organs distinguishable (arrowhead) in comparison to WT, where only almost completely disorganized tissue could be detected. Arrows point to the patterned vascular tissue in *Pro35S:AtCKX3* calli. (Scale bar: 200 μm.) (*C*) Levels of endogenous CKs after induction of organogenesis by NAA (537 nM) at different exogenous CK concentrations. The statistical significance of identified differences in comparison to WT (*t* test) at alpha 0.05 is designated (*); error bars show SDs. For the data on all analyzed CK metabolites, see Fig. S2 and Table S1.

inspected organogenesis in hypocotyl explants with endogenous CKs depleted via ectopic overexpression of *CYTOKININ OXIDASE/DEHYDROGENASE* genes (19). In *Pro35S:AtCKX2* and *Pro35S:AtCKX3* explants, we observed partial resistance to CK, as manifested by increased competence of hypocotyl explants to form root-like organs (Fig. S1) and formation of root-like structures even at the CK threshold concentration (Fig. 3 *A* and *B*). Because kinetin has been found to be only a poor substrate of CKX (31), this effect seems to be attributable to a decrease of endogenous CKs rather than to inactivation of exogenously applied CKs. To confirm that, we have measured levels of endogenous CKs in hypocotyl explants cultivated in the absence and presence of exogenous CKs. In the WT hypocotyl explants, endogenous CKs [from active CKs, predominantly *trans*-zeatin-9-riboside (ZR) and ZR phosphate] were found in the hypocotyls grown at the organogenesis-inducing (threshold) auxin concentration in the absence of exogenous CK. The amounts of most of the endogenous CKs were substantially reduced in the *Pro35S:AtCKX3* hypocotyl explants (Fig. 3*C* and Fig. S2). Surprisingly, the addition of exogenous CKs led to the further reduction of endogenously produced CKs in both WT and *AtCKX3* overexpressing hypocotyl explants (Fig. 3*C*). This is presumably attributable to up-regulation of endogenous *AtCKX* expression by exogenous CKs (32). These data show that AIO is accompanied by the production of endogenous CKs that affect its developmental output.

To gain insight into the potential tissue specificity of CK production and action during AIO, we have inspected expression of *ARR5*, one of the earliest expressed CK primary response genes (28). In agreement with our qRT-PCR data, we have observed the activity of *ARR5* promoter in *ProARR5:GUS* hypocotyl explants even in the absence of exogenous CKs (Fig. S3*A*). GUS activity in hypocotyl explants was delimited to the induced root-like organs, suggesting tissue specificity of CK signaling leading to up-regulation of *ARR5* expression. Expression of *ARR5* was reduced in both *Pro35S:AtCKX2* and *Pro35S:AtCKX3* lines (Fig. S3*A* and data not shown, respectively). Altogether, these findings indicate that AIO is accompanied by tissue-specific activation of the CK signaling pathway and endogenous CK production that contributes to the CK-dependent modulation of AIO. Thus, the CK effect on AIO in our system is a sum of both endogenous and exogenous CKs.

CK Affects Auxin Distribution During de Novo Organogenesis. To identify a mechanism of CK action during AIO, we inspected its effect on the morphology of auxin-induced organs in more detail. Interestingly, we found important differences in CK effect on AIO induced by either 2,4-D or NAA. In the absence of exogenous CKs, NAA induces formation of root-like structures with a cellular pattern that resembles *Arabidopsis* roots. The increasing CK concentration led to a decrease in the number of NAA-induced organs (Fig. S1); however, the morphology of formed organs was only slightly affected by CK concentration below the CK threshold (Fig. 4*A*). In contrast, 2,4-D induced formation of only poorly specified root-like organs that only partially resembled *Arabidopsis* roots, and the increasing CK concentration led to a gradual loss of organ structure and patterning (Fig. 4*A*). However, in both cases, the CK threshold led to the loss of organ formation and only unorganized callus was formed (Fig. 4*A*). The 2 types of auxin used, 2,4-D and NAA, differ in the mechanism of their transport in plant cells. While 2,4-D must be taken up into cells actively by AUX/LAX importers (11), NAA enters cells almost entirely via passive diffusion (33). On the other hand, NAA, but not 2,4-D, gets out from cells easily via auxin efflux carriers (33, 34), and can thus be more efficiently transported between cells. Thus, these different effects of CK on NAA- and 2,4-D–induced organogenesis indicated the involvement of auxin transport in this process.

Transport-dependent control of the spatial and temporal pattern of auxin distribution in plant tissues plays an important role in multiple aspects of organogenesis *in planta* (13). Thus, we examined the potential CK effect on the formation of local auxin maxima as visualized by the activity of the auxin response reporter DR5 (35) in organs induced by 2,4-D or NAA. The NAA-induced organs displayed single auxin maxima at the "root tip," which resembles the situation in *Arabidopsis* root primordia (13, 36). With an increasing CK concentration, the auxin maxima in NAA-induced organs were only slightly affected; they became diffuse and weaker, as visible particularly in *DR5rev:GUS* (Fig. 4*B*). On the other hand, 2,4-D–induced organs formed with multiple ectopically located auxin maxima in additional "root tips". The increasing CK concentration resulted in the formation of less focused auxin maxima and their spreading and disorganization. That correlated well with changes in the shape of 2,4-D–induced root-like organs, (i.e., gradual loss of the organ structure and patterning) (Fig. 4*B*). At the CK-threshold concentration, almost complete loss of auxin maxima formation was observed in both NAA- and 2,4-D–induced calli (Fig. 4*B*). Thus, the apparently higher sensitivity of 2,4-D–induced organs to CK-mediated morphogenic effect very probably reflects lower efficiency of efflux carriers to relocate 2,4-D in comparison to NAA. However, at concentrations reaching or higher than the CK threshold, the auxin efflux capacity decreases below the level necessary for formation of defined auxin maxima and, consequently, results in loss of organ patterning in both 2,4-D– and NAA-induced organogenesis.

Moreover, treatment with 1-naphthylphthalamic acid (NPA), a potent inhibitor of polar auxin transport at the level of auxin efflux (37, 38), partially mimics the effect of exogenous CKs (Fig. 4*C*). In the presence of NPA (10 μM) and absence of exogenous CKs, NAA induces the formation of root-like organs similar to those induced by 2,4-D. However, these organs were more sensitive to both endogenous and exogenous CKs. That was manifested by the formation of a large amount of callus and a higher degree of organ

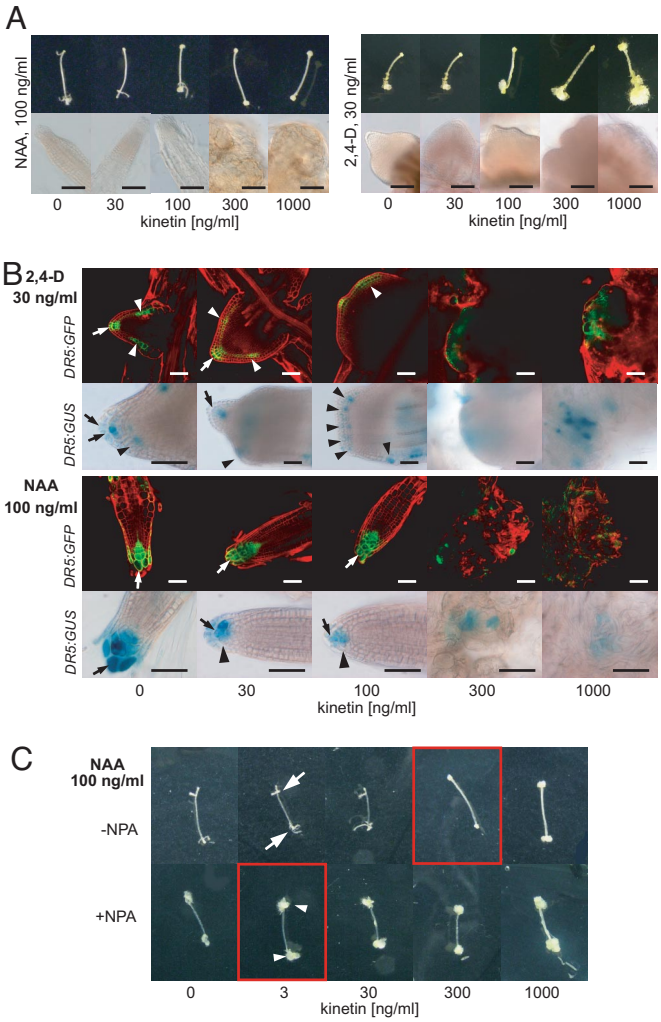

Fig. 4. CK has effects on auxin distribution during de novo organogenesis. (*A*) Phenotype of root-like organs after induction of organogenesis in hypocotyl explants either by NAA (*Left*) or 2,4-D (*Right*). Note the higher organization and patterning resembling *Arabidopsis* roots in the case of root-like organs induced by NAA. (Scale bar: 100 μm.) (*B*) Spatial pattern of auxin maxima as visualized by activity of DR5 on 2,4-D– (*Upper*) and NAA-induced organs (*Lower*). Note the formation of ectopic auxin maxima (arrowheads), their spreading and disorganization, and the more pronounced loss of the organ patterning and structure in the case of organs induced by 2,4-D. The auxin maxima are gradually less pronounced in case of NAA-induced root-like organs (arrowhead). Note the almost complete disappearance of DR5 maxima and loss of organ patterning at the CK threshold concentration [300 ng/mL (1.4 μM) kinetin]. Arrows depict the columella-like cells. (Scale bar: 50 μm.) (*C*) NPA (10 μM) partially mimics the effect of the CK threshold. Note the large amount of calli (arrowheads) formed even at the lowest kinetin concentration [3 ng/mL (14 nM)] in comparison to well-recognizable root-like organs at the same kinetin concentration in the absence of NPA (arrows); this resembles the effect of the CK threshold in the absence of NPA (compare figures in red frames). For details, see Fig. S3.

structure disintegration even at the lowest CK concentration applied, thus resembling the CK threshold (Fig. 4*C* and Fig. S3). Accordingly, in the absence of exogenous CKs, NPA led to the formation of organs whose structure was better preserved and more resembled roots in *Pro35S:AtCKX2* hypocotyl explants in comparison to WT (Fig. S3*B*). This suggests partially synergistic but distinct effects of NPA and CKs on the AIO. Taken together, our results indicate a correlation between auxin distribution and its organogenic effect during de novo AIO and suggest an interference of CKs with the formation of the cellular efflux-dependent local auxin maxima. Nevertheless, it is obvious, and must be considered, that

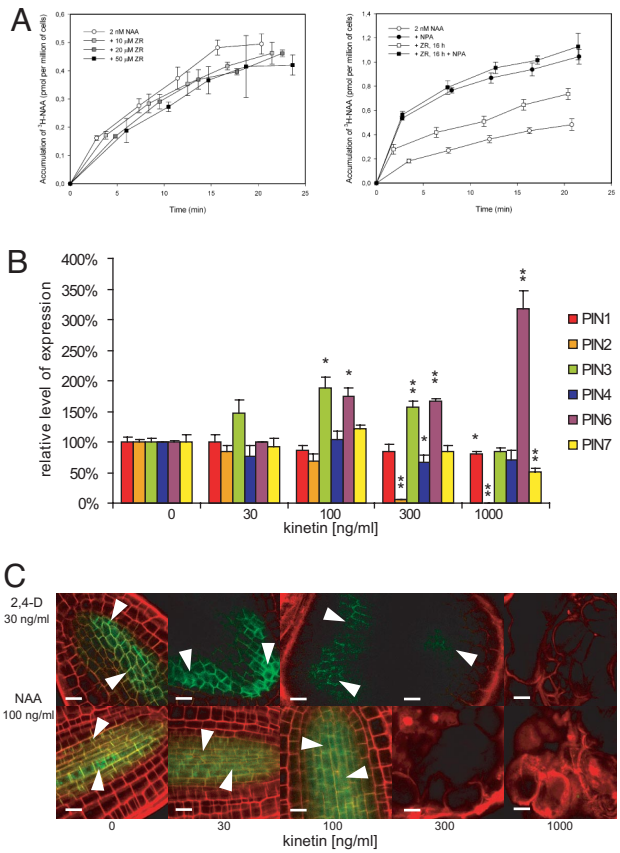

Fig. 5. CKs modulate auxin efflux and *PIN* expression. (*A*) Accumulation of [^{3}H]NAA in BY-2 cells. Although there is no apparent effect on the auxin accumulation in BY-2 cells when CK of different concentrations (10, 20, and 50 μM ZR) was added together with [^{3}H]NAA (*Left*), the 16-hour pretreatment with 5 μM ZR led to an increase in the accumulation of [^{3}H]NAA (*Right*); 2 nM [^{3}H]NAA was used in both cases. This effect could be mimicked by addition of 10 μM NPA (*Right*). Error bars show SDs. (*B*) Relative transcription of *PIN* auxin transporters in hypocotyl explants at different CK concentrations and at the auxin threshold (NAA; 537 nM) as measured by qRT-PCR. The statistical significance of identified differences in comparison to the absence of exogenous CKs (*t* test) at alpha 0.05 and 0.01 is designated (* and **, respectively), and error bars show SDs. (*C*) PIN1-GFP signal (green, arrowheads) in the root-like organs of *ProPIN1:PIN1-GFP* hypocotyl explants at the different CK concentrations. Note that the signal is getting weaker and diffuse and disappears at the CK threshold in the case of both 2,4-D and NAA. (Scale bar: 10 μm.)

apart from the role of CKs in the regulation of auxin distribution, CKs also affect organogenesis via other mechanisms (e.g., regulation of cell proliferation) (3).

CK Affects the Expression of *PIN* Auxin Efflux Carriers and the Cellular Efflux of Auxin. Our results suggest that, as shown for *in planta* organogenesis (12, 13, 15), auxin efflux is also required for control of auxin distribution during de novo-induced organogenesis in our in vitro system. Therefore, we tested the scenario that CK influences AIO through an effect on auxin efflux. Accumulation of radioactively labeled NAA ([^{3}H]NAA) in cultured tobacco BY-2 cells is a reliable system for the measuring and quantification of auxin efflux (34). When CKs were added to the cell suspension just at the beginning of the assay (i.e., together with [^{3}H]NAA), no CK effect on the [^{3}H]NAA accumulation was observed. However, pretreatment of BY-2 cells with CKs (5 μM ZR for 16 h) led to the increase of the [^{3}H]NAA accumulation (i.e., to a decrease of its efflux) (Fig. 5*A*). Similar results were obtained with various other CKs (Fig. S4). Thus, CKs similar to established auxin transport inhibitors, such as NPA, inhibit auxin efflux. However, the long lag

time of CK effect suggests that CKs regulate auxin efflux in BY-2 cells via regulation of expression of genes for efflux carriers or regulatory proteins rather than via direct interference with efflux activity. CK enhances ethylene biosynthesis (39), and the involvement of ethylene in the regulation of auxin transport has been reported (40, 41). Therefore, we analyzed CK effects on the auxin efflux in the presence of aminoethoxy vinyl glycine (AVG), an inhibitor of ethylene production (42). No difference in auxin accumulation in BY-2 cells treated with CK was observed between the absence and presence of AVG (Fig. S4), showing that CKs act on auxin efflux independent of regulation of ethylene biosynthesis.

Next, we addressed the possible mechanisms by which CKs modulate auxin efflux. Auxin carriers from the PIN family were identified to be the rate-limiting regulators of the cellular auxin efflux (34), and their key role in generating differential local auxin distribution has been demonstrated (5). Because cellular output of CK signaling occurs at the level of regulation of gene expression, we tested possible regulation of *PIN* expression by CKs. Using qRT-PCR, we have observed differential transcription of individual *PIN* genes in hypocotyl explants cultivated in the presence of auxin threshold (537 nM NAA) and different CK concentrations. Although the expression of *PIN3* peaked at 100 ng/mL CK (464 nM kinetin) and decreased with further increasing CK concentrations, the expression of *PIN6* was up-regulated at the same CK concentration (100 ng/mL) and further increased at 1,000 ng/mL CK (4.6 μM kinetin) (Fig. 5*B*). The transcription of root-specific *PIN2* (10) dramatically decreased at the CK threshold, presumably reflecting the loss of root identity and formation of only undifferentiated calli (Fig. 5*B*). Interestingly, *PIN1* transcription was only slightly down-regulated even at the highest CK concentration (4.6 μM kinetin) (Fig. 5*B*). However, in both 2,4-D– and NAA-induced root-like organs, the signal of PIN1-GFP was getting weaker and more diffuse with the increasing CK concentrations (Fig. 5*C*). The PIN1-GFP signal was lost in calli at the CK threshold concentration, and only residual PIN1-GFP, apparently not associated with plasma membrane, was occasionally detectable (data not shown); for quantification of the CK effect on *PIN1-GFP* expression, see Fig. S5. Thus, CKs seem to affect the expression of *PIN* genes, possibly at both transcriptional and posttranscriptional levels. Taken together, these results show that CKs regulate expression of PIN auxin efflux carriers during de novo AIO, which provides a plausible mechanism for CK-dependent regulation of auxin efflux.

Endogenous CKs Are Required for Differential Auxin Distribution in *Arabidopsis* Roots. Our results imply that CKs can affect auxin distribution during de novo organogenesis via regulation of auxin efflux from cells. In root development, differential auxin distribution has been shown to regulate activity and patterning of the root meristem (7, 36). Thus, we addressed whether endogenous CKs are required for auxin distribution and root meristem patterning *in planta*. We examined the formation of local auxin maxima (visualized by DR5 activity) in CK-deficient *Pro35S:AtCKX2* and *Pro35S:AtCKX3* plants. In the root tips of these plants, *DR5rev:GFP* expression in columella expanded more laterally in comparison to that of control (Fig. 6*A*). We analyzed 2 lines of each transformant, *Pro35S::AtCKX2* and *Pro35S::AtCKX3*. For *Pro35S::AtCKX2*, 30 and 33 aberrant roots were scored out of 38 and 40 inspected roots, respectively (30 of 38 roots and 33 of 40 roots). For *Pro35S::AtCKX3*, the result was similar (32 of 41 roots and 19 of 23 roots). In WT background, only 5 of 39 inspected roots revealed aberrations in the *DR5rev:GFP* expression pattern. Accordingly, the first 5 columella cells were significantly enlarged in the longitudinal direction in several independent *Pro35S:AtCKX2* and *Pro35S:AtCKX3* lines (Fig. S6). This presumably reflects the dose-dependent role of auxin in the regulation of cell elongation (43) and provides additional evidence for a disturbed auxin gradient in the root tip of *Pro35S:AtCKX2(3)* lines. We also tested whether endogenous CK levels influence *PIN* transcription or polar PIN

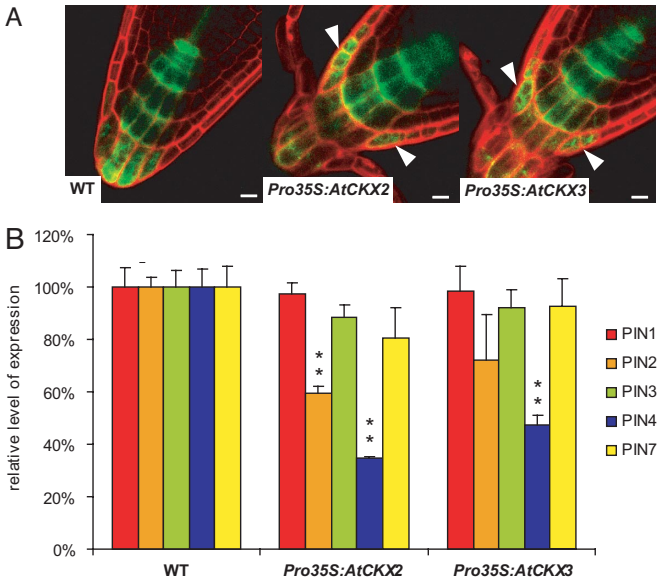

Fig. 6. Endogenous CK levels are required for local auxin maxima formation and mediate *PIN* gene expression in *Arabidopsis* roots. (*A*) Depletion of endogenous CKs in *Pro35S:AtCKX2* and *Pro35S:AtCKX3* lines leads to the defects in auxin response gradients as visualized by *DR5rev:GFP*. Note the lateral expansion of the maxima in transgenic lines (arrowheads) in comparison to WT. (Scale bar: 10 μm.) (*B*) Relative *PIN* transcription measured by qRT-PCR in *Pro35S:AtCKX2* and *Pro35S:AtCKX3* roots in comparison to WT. The statistical significance of differences (*t* test) at alpha 0.01 is marked by **; error bars show SDs.

localization. In the roots of 6-day-old seedlings of both *Pro35S:AtCKX2* and *Pro35S:AtCKX3* lines, polar localization of PIN2 and PIN4 proteins did not differ from that of controls (Fig. S7), but we have found a strong decrease in the *PIN2* and *PIN4* mRNA levels (Fig. 6*B*). Based on these data, we conclude that distinct levels of endogenous CKs are necessary to maintain expression of *PIN* auxin efflux carriers in the root tip, thus regulating formation of local auxin maxima and root meristem development. These data show that the mechanism of CK-dependent regulation of *PIN* transcription and control of differential auxin distribution that we identified during de novo organogenesis also applies for processes *in planta*.

Discussion

Our work addresses the mechanism underlying the role of the phytohormones auxin and CK in plant organogenesis. We show that in contrast to CK, auxin is able to induce a de novo organogenic response in hypocotyl explants. This is in accordance with the recent recognition of auxin and/or its gradients as a general trigger for the change in the developmental program in plants (4, 15). We have found that the auxin-induced organogenic response is accompanied by production of endogenous CKs and the tissue-specific activation of the CK signaling pathway. The activation of *ARR5* expression in the absence of exogenous CKs was also observed in root explants (44). This further confirms our conclusions and implies that auxin might induce similar developmental programs in root and hypocotyl explants, thus strengthening the role of auxin as a universal trigger of organogenesis.

Formation of lateral roots represents one of the examples for postembryonal de novo organogenesis in plants. Recent reports (20, 22) suggest potential involvement of CKs in the regulation of auxin efflux during lateral root formation. Exogenous CKs are supposed to down-regulate expression of all inspected *PIN* genes at early stages of lateral root primordia development (20). However, this does not seem to be the case in the roots of *Pro35S:AtCKX2(3)* lines,

in which at least *PIN2* and *PIN4* are down-regulated after endogenous CK depletion. Our results reflect predominantly the context of primary root meristem, because we have analyzed *PIN* expression in the roots of 6-day-old seedlings, in which only a few lateral roots and lateral root primordia have yet been formed. This implies that CKs affect the expression of individual PIN carriers differentially in particular plant tissues and that complex interactions between CKs and individual members of the auxin-efflux machinery should be further characterized in a spatiotemporal context.

Our results suggest that in addition to recently identified interaction between CK and auxin on the level of signaling (45), CKs modulate auxin distribution via regulation of auxin efflux. This type of regulation represents a thus far unidentified mechanism for well-known CK-auxin interactions during plant development. We propose that changes in endogenous CK levels form an intrinsic part of the auxin-induced organogenic response and that CK-mediated modulation of auxin distribution via regulation of auxin efflux is one of the mechanisms underlying the auxin-CK interaction during organogenesis in plants.

Materials and Methods

Plant Materials. Unless otherwise stated, all plant material used was *Arabidopsis thaliana*, ecotype *Col-0*. For the hypocotyl explant assay, *ahk2–1, ahk3–1*, and *ahk4–1* (30) single-mutant lines and *ahk2–1 ahk3–1*, *ahk3–1 ahk4–1* (30), and *ahk2–2TK cre1–12* (29) double-mutant lines were used. For details of preparation of transgenic lines used, see *SI Text*.

Hypocotyl Explants Assay. Plants were cultivated 1 day in the light and 5 days in the dark in Petri dishes with Murashige and Skoog medium, including Gamborg B5 vitamins in growth chambers (Percival) at 21 °C. Hypocotyls were isolated by removing cotyledons and roots and were placed on Petri dishes with cultivation medium as described (27) and enriched with respective hormone concentrations. Kinetin, 2,4-D, and NAA were purchased from Sigma-Aldrich. Hypocotyl explants were cultivated for 21 days under long-day conditions (16 h light at 21 °C and 8 h dark at 19 °C), a light intensity of 100 $\mu M \cdot m^{-2} \cdot s^{-1}$, and 80% relative humidity.

[^{3}H]NAA Accumulation in BY-2 Cells. The [3H]NAA accumulation assay was performed as described (38).

ACKNOWLEDGMENTS. We thank Yka Helariutta and Chiharu Ueguchi for providing us with seeds of *ahk* mutants, Eva Benkova for *DR5rev:GUS* and *DR5rev:GFP* lines, Kristin Bilyeu for *AtCKX3* cDNA, Joseph Kieber for *ProARR5:GUS* construct, and Guido Jach for pGJ-Bar plasmid. We are grateful to Ivo Lukeš and Tomáš Jendrulek (Olympus C&S, spol. s r. o.) for excellent technical support. This work was supported by the Ministry of Education, Youth, and Sports of the Czech Republic, Project Nos. LC06034 (to M.P., P.K., J. Horák, P.S., K.H., E.Z., and J. Hejátko) and MSM0021622415 (to P.R., J.D., J.F. and J. Hejátko) and by the Grant Agency of the Czech Republic, Project No. 204/08/H054 (to J. Horák and J. Hejátko).

1. Gierer A, *et al.* (1972) Regeneration of hydra from reaggregated cells. *Nat New Biol* 239:98–101.
2. Endo T, Bryant SV, Gardiner DM (2004) A stepwise model system for limb regeneration. *Dev Biol* 270:135–145.
3. Skoog F, Miller CO (1957) Chemical regulation of growth and organ formation in plant tissues cultured in vitro. *Symp Soc Exp Biol* 54:118–130.
4. Vieten A, Sauer M, Brewer PB, Friml J (2007) Molecular and cellular aspects of auxin-transport-mediated development. *Trends Plant Sci* 12:160–168.
5. Tanaka H, Dhonukshe P, Brewer PB, Friml J (2006) Spatiotemporal asymmetric auxin distribution: A means to coordinate plant development. *Cell Mol Life Sci* 63:2738–2754.
6. Friml J, *et al.* (2003) Efflux-dependent auxin gradients establish the apical-basal axis of Arabidopsis. *Nature* 426:147–153.
7. Friml J, *et al.* (2002) AtPIN4 mediates sink-driven auxin gradients and root patterning in Arabidopsis. *Cell* 108:661–673.
8. Blilou I, *et al.* (2005) The PIN auxin efflux facilitator network controls growth and patterning in Arabidopsis roots. *Nature* 433:39–44.
9. Friml J, Wisniewska J, Benkova E, Mendgen K, Palme K (2002) Lateral relocation of auxin efflux regulator PIN3 mediates tropism in Arabidopsis. *Nature* 415:806–809.
10. Luschnig C, Gaxiola RA, Grisafi P, Fink GR (1998) EIR1, a root-specific protein involved in auxin transport, is required for gravitropism in Arabidopsis thaliana. *Genes Dev* 12:2175–2187.
11. Marchant A, *et al.* (1999) AUX1 regulates root gravitropism in Arabidopsis by facilitating auxin uptake within root apical tissues. *EMBO J* 18:2066–2073.
12. Heisler MG, *et al.* (2005) Patterns of auxin transport and gene expression during primordium development revealed by live imaging of the Arabidopsis inflorescence meristem. *Curr Biol* 15:1899–1911.
13. Benkova E, *et al.* (2003) Local, efflux-dependent auxin gradients as a common module for plant organ formation. *Cell* 115:591–602.
14. Reinhardt D, *et al.* (2003) Regulation of phyllotaxis by polar auxin transport. *Nature* 426:255–260.
15. Dubrovsky JG, *et al.* (2008) Auxin acts as a local morphogenetic trigger to specify lateral root founder cells. *Proc Natl Acad Sci USA* 105:8790–8794.
16. Kurakawa T, *et al.* (2007) Direct control of shoot meristem activity by a cytokinin-activating enzyme. *Nature* 445:652–655.
17. Scheres B, *et al.* (1995) Mutations affecting the radial organization of the Arabidopsis root display specific defects throughout the embryonic axis. *Development* 121(1):53–62.
18. Mahonen AP, *et al.* (2006) Cytokinin signaling and its inhibitor AHP6 regulate cell fate during vascular development. *Science* 311:94–98.
19. Werner T, *et al.* (2003) Cytokinin-deficient transgenic Arabidopsis plants show multiple developmental alterations indicating opposite functions of cytokinins in the regulation of shoot and root meristem activity. *Plant Cell* 15:2532–2550.
20. Laplaze L, *et al.* (2007) Cytokinins act directly on lateral root founder cells to inhibit root initiation. *Plant Cell* 19:3889–3900.
21. Dello Ioio R, *et al.* (2007) Cytokinins determine Arabidopsis root-meristem size by controlling cell differentiation. *Curr Biol* 17:678–682.
22. Kuderova A, *et al.* (2008) Effects of conditional IPT-dependent cytokinin overproduction on root architecture of Arabidopsis seedlings. *Plant Cell Physiol* 49:570–582.
23. Riefler M, Novak O, Strnad M, Schmulling T (2006) Arabidopsis cytokinin receptor mutants reveal functions in shoot growth, leaf senescence, seed size, germination, root development, and cytokinin metabolism. *Plant Cell* 18:40–54.
24. Tran LS, *et al.* (2007) Functional analysis of AHK1/ATHK1 and cytokinin receptor histidine kinases in response to abscisic acid, drought, and salt stress in Arabidopsis. *Proc Natl Acad Sci USA* 104:20623–20628.
25. Kim HJ, *et al.* (2006) Cytokinin-mediated control of leaf longevity by AHK3 through phosphorylation of ARR2 in Arabidopsis. *Proc Natl Acad Sci USA* 103:814–819.
26. To JP, Kieber JJ (2008) Cytokinin signaling: Two-components and more. *Trends Plant Sci* 13:85–92.
27. Kubo M, Kakimoto T (2000) The cytokinin-hypersensitive genes of Arabidopsis negatively regulate the cytokinin-signaling pathway for cell division and chloroplast development. *Plant J* 23:385–394.
28. D'Agostino IB, Deruere J, Kieber JJ (2000) Characterization of the response of the Arabidopsis response regulator gene family to cytokinin. *Plant Physiol* 124:1706–1717.
29. Higuchi M, *et al.* (2004) In planta functions of the Arabidopsis cytokinin receptor family. *Proc Natl Acad Sci USA* 101:8821–8826.
30. Nishimura C, *et al.* (2004) Histidine kinase homologs that act as cytokinin receptors possess overlapping functions in the regulation of shoot and root growth in Arabidopsis. *Plant Cell* 16:1365–1377.
31. Popelkova H, *et al.* (2006) Kinetic and chemical analyses of the cytokinin dehydrogenase-catalysed reaction: Correlations with the crystal structure. *Biochem J* 398:113–124.
32. Werner T, Kollmer I, Bartrina I, Holst K, Schmulling T (2006) New insights into the biology of cytokinin degradation. *Plant Biology* 8:371–381.
33. Delbarre A, Muller P, Imhoff V, Guern J (1996) Comparison of mechanisms controlling uptake and accumulation of 2,4-dichlorophenoxy acetic acid, naphthalene-1-acetic acid, and indole-3-acetic acid in suspension-cultured tobacco cells. *Planta* 198:532–541.
34. Petrasek J, *et al.* (2006) PIN proteins perform a rate-limiting function in cellular auxin efflux. *Science* 312:914–918.
35. Ulmasov T, Murfett J, Hagen G, Guilfoyle TJ (1997) Aux/IAA proteins repress expression of reporter genes containing natural and highly active synthetic auxin response elements. *Plant Cell* 9:1963–1971.
36. Sabatini S, *et al.* (1999) An auxin-dependent distal organizer of pattern and polarity in the Arabidopsis root. *Cell* 99:463–472.
37. Katekar GF, Geissler AE (1980) Auxin transport inhibitors: IV. Evidence of a common mode of action for a proposed class of auxin transport inhibitors: The phytotropins. *Plant Physiol* 66:1190–1195.
38. Petrasek J, *et al.* (2003) Do phytotropins inhibit auxin efflux by impairing vesicle traffic? *Plant Physiol* 131:254–263.
39. Chae HS, Faure F, Kieber JJ (2003) The eto1, eto2, and eto3 mutations and cytokinin treatment increase ethylene biosynthesis in Arabidopsis by increasing the stability of ACS protein. *Plant Cell* 15:545–559.
40. Ruzicka K, *et al.* (2007) Ethylene regulates root growth through effects on auxin biosynthesis and transport-dependent auxin distribution. *Plant Cell* 19:2197–2212.
41. Swarup R, *et al.* (2007) Ethylene upregulates auxin biosynthesis in Arabidopsis seedlings to enhance inhibition of root cell elongation. *Plant Cell* 19:2186–2196.
42. Yang SF, Hoffman NE (1984) Ethylene biosynthesis and its regulation in higher-plants. *Annu Rev Plant Physiol Plant Mol Biol* 35:155–189.
43. Hardtke CS (2007) Transcriptional auxin-brassinosteroid crosstalk: Who's talking? *BioEssays* 29:1115–1123.
44. Gordon SP, *et al.* (2007) Pattern formation during de novo assembly of the Arabidopsis shoot meristem. *Development* 134:3539–3548.
45. Muller B, Sheen J (2008) Cytokinin and auxin interaction in root stem-cell specification during early embryogenesis. *Nature* 453:1094–1097.

Supporting Information

Pernisová *et al.* 10.1073/pnas.0811539106

Materials and Methods

Plant Material and Growth Conditions. For the preparation of *Pro35S:AtCKX2* and *Pro35S:AtCKX3* lines, we have cloned *AtCKX3* cDNA and the genomic fragment corresponding to the coding sequence of *AtCKX2* under the control of *CaMV35S* promoter in the pGJ-Bar plasmid, containing *CaMV35S* expression cassette (*CaMV35S* promoter and transcription terminator). Transgenic plants have been obtained by the floral-dip method (1), and several independent single-insertion lines homozygous for the transgene were selected. Selected lines were crossed with *DR5rev:GFP* and *ProARR5:GUS* transgenic lines, and double-homozygous lines were used for the analysis. Plants were cultivated in growth chambers (Percival Scientific, Inc.) under long-day conditions (16 h light/8 h dark) at 21 °C in Petri dishes on Murashige and Skoog medium at a light intensity of 150 $\mu M \cdot m^{-2} \cdot s^{-1}$ and 60% relative humidity or in the soil in the greenhouse under long-day conditions (16 h light at 21 °C and 8 h dark at 19 °C) at a light intensity approximately 100 $\mu M \cdot m^{-2} \cdot s^{-1}$ and 60% relative humidity. BY-2 tobacco cell suspension was cultivated as described by Petrasek *et al.* (2).

qRT-PCR. Total RNA from plant tissue was isolated using the RNAqueous Small Scale Phenol-Free Total RNA Isolation Kit (Ambion) according to the manufacturer's instructions. cDNA was prepared, and qRT-PCR was performed using the DyNAmo Flash SYBR Green qPCR Kit (Finnzymes) according to the manufacturer's instructions on a Rotor-Gene 3000 (CORBETT RESEARCH) instrument. *PIN* transcripts were quantified as previously described (3). All expression levels were normalized to *UBIQUITIN10*.

For quantification of *ARR* transcripts, the following primers were used: fARR3rt (5′-ATC GCC TCT GTC TAT GGT T-3′), rARR3rt (5′-AAG TTC CTT CGT GAG CAA A-3′), fARR4rt (5′-ATT CGT CTC CGC CGT TAT-3′), rARR4rt (5′-CGT CAT CAT CTT CAT CGT CT-3′), fARR5rt (5′-GCT GAT AGA ACC AAG ACT GA-3′), rARR5rt (5′-CTT CCA AAA TAA CAC ACC AC-3′), fARR6rt (5′-ATG GCT GAA GTT ATG CTA CCG AG-3′), rARR6rt (5′-TCA GAT CTT TGC GCG TTT GAG-3′), fARR7rt (5′-GGT GGA GAT TTG ACT GTT AC-3′), rARR7rt (TGG TTT TGC TAA GGT CTT GG-3′), fARR15rt (5′-ATG GCT CTC AGA GAT TTA TCT TC-3′), and rARR15rt (5′-TTA ACC CCT AGA CTC TAA TTT G-3′). All expression levels were normalized to *UBIQUITIN10*: fUBQ10rt (5′-AAC GGG AAA GAC GAT TAC-3′) and rUBQ10rt (5′-ACA AGA TGA AGG GTG GAC-3′).

For individual pairs of primers, the following conditions were used:

UBQ10, ARR3, ARR4: 95 °C/7 min − 35×(95 °C/15 s + 60 °C/20 s + 72 °C/20 s) − 72 °C/1 min − melt

ARR5: 95 °C/7 min − 35×(95 °C/15 s + 56 °C/30 s + 60 °C/30 s) − 60 °C/1 min − melt

ARR6: 95 °C/7 min − 35×(95 °C/20 s + 57 °C/30 s + 72 °C/1 min) − 72 °C/1 min − melt ARR7

ARR15: 95 °C/7 min − 40×(95 °C/20 s + 58 °C/30 s + 72 °C/1 min) − 72 °C/1 min − melt

Microscopy and Histology. Differential interference contrast and fluorescence microscopy were done on an Olympus BX61 microscope (Olympus Optical Co., Ltd.) equipped with a DP50 or DP70 CCD camera (Olympus Optical Co., Ltd.) using appropriate filter sets for detection of GFP (excitation at 460–495 nm and emission 510–550 nm). Confocal microscopy was done on an Olympus IX81 microscope equipped with a Fluoview 500 confocal unit (Olympus Optical Co., Ltd.). Roots and hypocotyl explants of inspected lines were stained with propidium iodide (PI; 10 μg/mL in water for 5 min) and observed using appropriate filter sets (PI excitation at 488–543 nm and emission at 610 nm; GFP excitation at 488 nm and emission at 505–525 nm). *ProARR5:GUS* lines were stained in 0.1 M sodium phosphate buffer (pH 7.0) containing 0.1% X-glc, 1 mM K3[Fe(CN)6], 1 mM K4[Fe(CN)6], and 0.05% Triton X-100 for 1 h at 37 °C and were destained overnight in 80% (vol/vol) ethanol. Tissue clearing was done as previously described (4). For the anatomy studies, hypocotyl segments were fixed in 3% (wt/vol) paraformaldehyde and 1.5% (vol/vol) glutaraldehyde in PBS buffer (pH 7.4), dehydrated in ethanol series, and embedded in Paraplast Plus (Tyco Healthcare Group LP). Longitudinal 3- to 5-μm thick sections were stained with Alcian blue and nuclear fast red as previously described (5). Measurements of the columella cell dimensions were done on micrographs of cleared tissue (4) using analySIS ^ D software (Olympus Soft Imaging Solutions, GmbH). Immunolocalization of PIN2 and PIN4 was performed as described previously (6).

Measurements of Endogenous CKs. The quantification of endogenous CK levels in plant tissue was done as described previously (7).

1. Clough SJ, Bent AF (1998) Floral dip: A simplified method for Agrobacterium-mediated transformation of Arabidopsis thaliana. *Plant J* 16:735–743.
2. Petrasek J, *et al.* (2003) Do phytotropins inhibit auxin efflux by impairing vesicle traffic? *Plant Physiol* 131:254–263.
3. Laplaze L, *et al.* (2007) Cytokinins act directly on lateral root founder cells to inhibit root initiation. *Plant Cell* 19:3889–3900.
4. Malamy JE, Benfey PN (1997) Organization and cell differentiation in lateral roots of Arabidopsis thaliana. *Development* 124:33–44.
5. Benes K, Kaminek M (1973) Use of aluminum lake of nuclear fast red in plant material successively with Alcian blue. *Biologia Plantarum* 15:294–297.
6. Sauer M, Paciorek T, Benkova E, Friml J (2006) Immunocytochemical techniques for whole-mount in situ protein localization in plants. *Nat Protoc* 1:98–103.
7. Kuderova A, *et al.* (2008) Effects of conditional IPT-dependent cytokinin overproduction on root architecture of Arabidopsis seedlings. *Plant and Cell Physiology* 49:570–582.

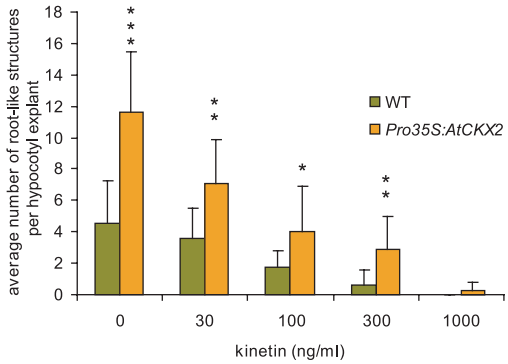

Fig. S1. CK down-regulates the ability of hypocotyl explants to form root-like structures. The effect of increasing CK concentration on the number of root-like structures formed in the presence of 537 nM NAA is shown. The statistical significance of identified differences of WT in comparison to *Pro35S:AtCKX2* (*t* test) at alpha 0.05, 0.01, and 0.001 is designated (*, **, and ***, respectively); error bars show SDs.

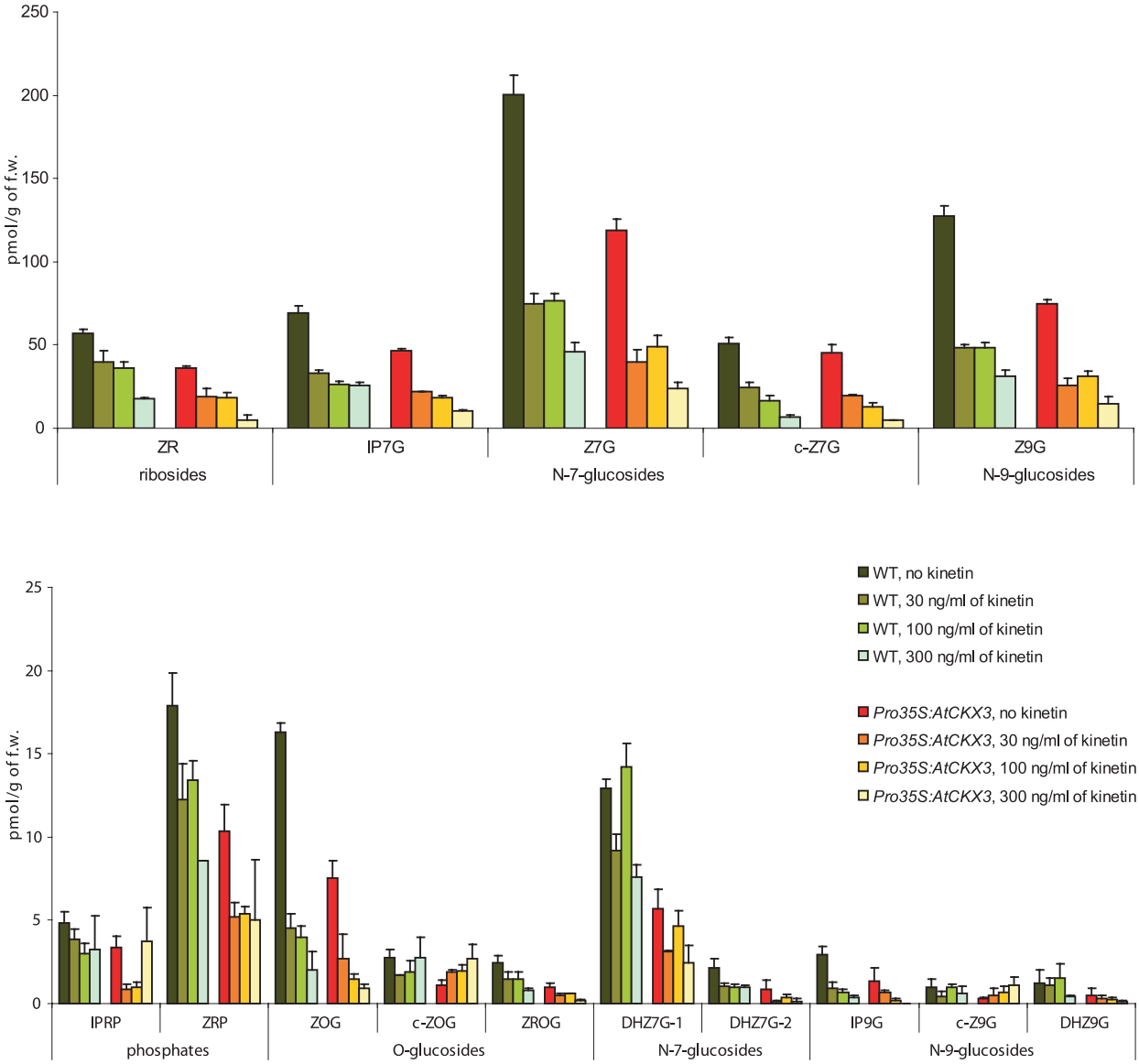

Fig. S2. AIO is accompanied by endogenous CK production. Measurements of endogenous CKs in hypocotyl explants grown at different CK concentrations and at the threshold (organogenesis-inducing) concentration of NAA (537 nM). Results of the representative experiment are presented here. In the graph, zero results were omitted and non-zero results were split into 2 groups (higher and low concentrations) to allow visualization of differences even in the low-concentration CK metabolites. The measurement was repeated 3 times, with very similar results. For the raw data, see Table S1. c-Z7G, *cis*-zeatin-7-glucoside; c-Z9G, *cis*-zeatin-9-glucoside; c-ZOG, *cis*-zeatin-O-glucoside; DHZ7G (1, 2), dihydrozeatin-7-glucoside (1, 2); DHZ9G, dihydrozeatin-9-glucoside; IP7G, isopentenyladenine-7-glucoside; IP9G, isopentenyladenine-9-glucoside; IPRP, isopentenyladenine-9-riboside phosphate; Z7G, *trans*-zeatin-7-glucoside; Z9G, *trans*-zeatin-9-glucoside; ZOG, *trans*-zeatin-O-glucoside; ZR, *trans*-zeatin-9-riboside; ZROG, *trans*-zeatin-9-riboside-O-glucoside; ZRP, *trans*-zeatin-9-riboside phosphate.

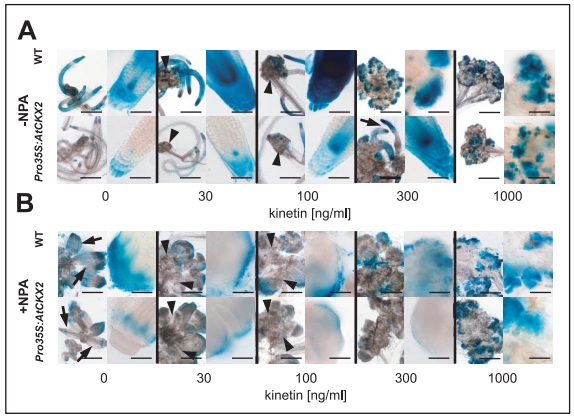

Fig. S3. (*A*) AIO is accompanied by tissue-specific activation of CK signaling. Tissue-specific activity of *ProARR5:GUS* (blue staining) in root-like organs is induced by auxin (537 nM NAA) even in the absence of exogenous CKs in WT (*Upper*) and *Pro35S:AtCKX2* (*Lower*) background. Note the apparent decrease of *ProARR5:GUS* expression in *Pro35S:AtCKX2* (double-homozygous progeny of individual transgenic lines crossing) and the formation of root-like organs even at the CK threshold (arrow). Arrowheads depict the small amounts of undifferentiated callus produced at CK concentrations below the CK threshold. (*B*) CKs and NPA have partially overlapping but distinct effects on AIO. Morphology of NAA-induced root-like organs in *ProARR5:GUS* lines in the presence of NPA (10 μM). Note the apparent better preservation of patterning of root-like organs (arrows) and weaker *ProARR5:GUS* expression in *Pro35S:AtCKX2* background (double-homozygous progeny of crosses between *ProARR5:GUS* and *Pro35S:AtCKX2* lines) in comparison to WT background in the absence of exogenous CKs. Note also the large amount of calli (arrowheads) formed in both WT and *Pro35S:AtCKX2* lines in the presence of the lowest kinetin concentration used (139 nM) in comparison to the absence of NPA (compare with *A*). (Scale bars: 400 μm and 50 μm for overviews and details, respectively.)

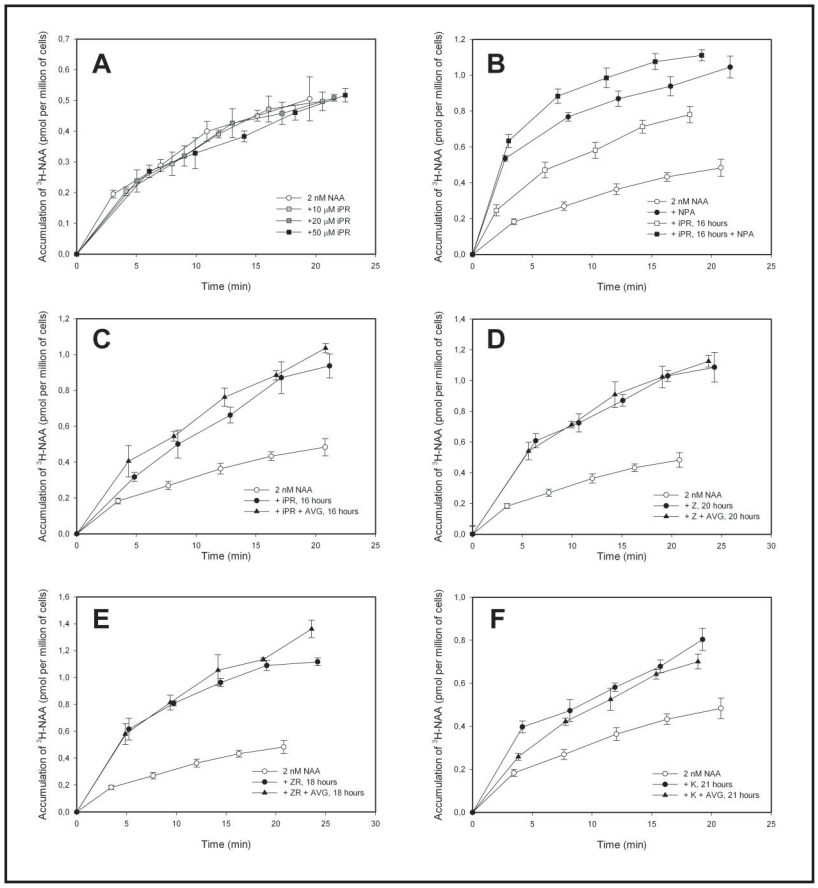

Fig. S4. CKs modulate auxin efflux in BY-2 cells independent of ethylene production. Effect of CK on [^{3}H]NAA accumulation in BY-2 cells. (*A*) Effect of immediate addition of CK at different concentrations. (*B–F*) Effect of pretreatment with different CKs (5 μM) in the presence and absence of the ethylene biosynthesis inhibitor AVG (10 μM). Note that there is no difference in the absence and presence of AVG, suggesting an ethylene-independent effect of CK on auxin efflux in BY-2 cells. iPR, isopentenyl adenosine; Z, *trans*-zeatin; ZR, *trans*-zeatin riboside; K, kinetin. Error bars show SDs.

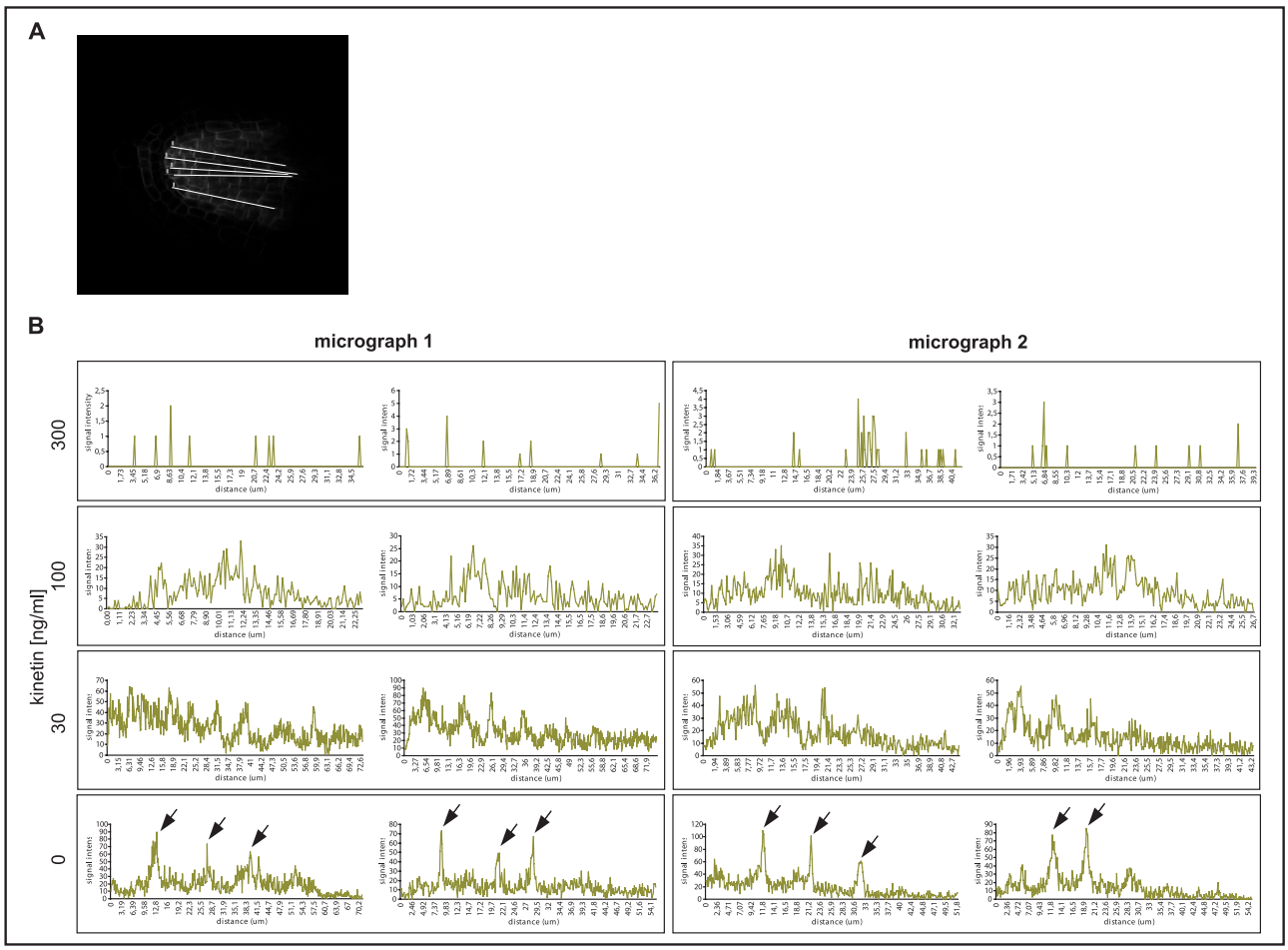

Fig. S5. Quantification of the CK effect on PIN1-GFP signal intensity. (*A*) The PIN1-GFP signal intensity (approximated to the gray value, ranging from 0 to 255 in our 8-bit micrographs) was measured in root-like structures that developed in hypocotyls in the presence of auxin threshold and increasing CK concentration. The signal intensity was measured in the position of an arbitrary line; the lines were oriented longitudinally to include as many of the cell files revealing PIN1-GFP signal as possible. Here, an example of the line positions for one of the micrographs is shown. For each micrograph, 5 measurements in different positions were performed. (*B*) Two micrographs for each CK concentration were evaluated; 2 representative measurements from each micrograph are shown here. Note the gradually decreasing signal intensity with increasing CK concentration. Also note the decreasing intensity in peaks that correspond to plasma membrane-located PIN1-GFP (arrows) and the slightly increased signal intensity between these peaks, suggesting an increased level of intracellular signal. The results of measurements in 2,4-D–induced (135 nM) organs are shown; similar results were obtained for NAA-induced organs (data not shown). All the evaluated micrographs were obtained at the same microscope settings, including the photomultiplier sensitivity level.

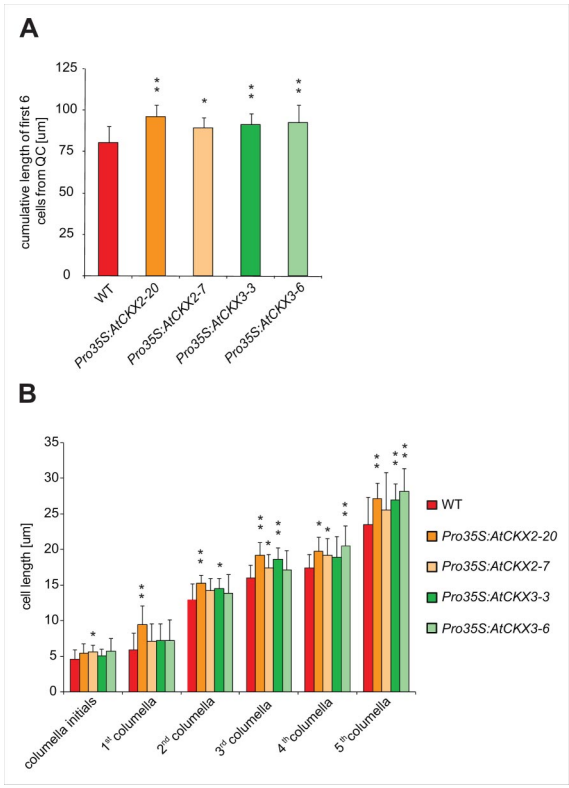

Fig. S6. Columella cells are enlarged in *Pro35S:AtCKX2* and *Pro35S:AtCKX3* lines. Two independent *Pro35S:AtCKX2* and *Pro35S:AtCKX3* lines were inspected. The differences in the sum of the lengths (*A*), together with the differences in the lengths of individual cell layers (columella initials and columella cell files) were compared (*B*). Note that although there was almost no difference identified in the length of the columella initials, the differences were apparent in differentiated columella cell files, suggesting defects in cell differentiation/elongation. The statistical significance of identified differences of *Pro35S::AtCKX2(3)* in comparison to the WT (*t* test) at alpha 0.05 and 0.01 is designated (* and **, respectively). Error bars show SDs.

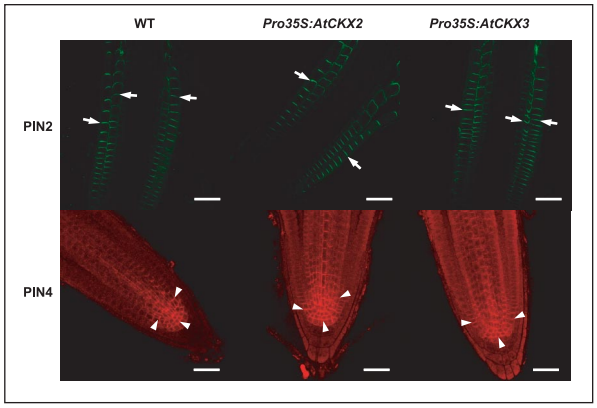

Fig. S7. Endogenous CKs do not affect polar localization of PIN2 and PIN4. Immunolocalization of PIN2 (green signal, arrows) and PIN4 (red signal, arrowheads). Note that both PIN2 and PIN4 keep their polar localization in WT and *Pro35S:AtCKX2* and *Pro35S:AtCKX3* lines. (Scale bar: 50 μM.)

Other Supporting Information Files

Table S1

Enclosed Publication # 9

Kuderová, A., Urbánková, I., Válková, M., Malbeck, J., Brzobohatý, B., Némethová, D. and **Hejátko, J.** (2008) Effects of conditional IPT-dependent cytokinin overproduction on root architecture of *Arabidopsis* seedlings. *Plant and Cell Physiology*, **49**, 570-582. IF_{2008}= 3.542

Plant Cell Physiol. 49(4): 570–582 (2008)
doi:10.1093/pcp/pcn029, available online at www.pcp.oxfordjournals.org
© The Author 2008. Published by Oxford University Press on behalf of Japanese Society of Plant Physiologists.
All rights reserved. For permissions, please email: journals.permissions@oxfordjournals.org

Effects of Conditional IPT-Dependent Cytokinin Overproduction on Root Architecture of *Arabidopsis* Seedlings

Alena Kuderová [1], Ivana Urbánková [1], Martina Válková [1], Jiří Malbeck [2], Břetislav Brzobohatý [1,3], Danka Némethová [4,5] and Jan Hejátko [1,*]

[1] *Laboratory of Plant Molecular Physiology, Department of Functional Genomics and Proteomics, Institute of Experimental Biology, Masaryk University, Kamenice 5, CZ-625 00, Brno, Czech Republic*
[2] *Institute of Experimental Botany, The Academy of Sciences of the Czech Republic V.V.i., Rozvojová 135, CZ-165 02 Prague, Czech Republic*
[3] *Institute of Biophysics, The Academy of Sciences of the Czech Republic V.V.i., Královopolská 135, CZ-612 65, Brno, Czech Republic*
[4] *Institute of Biostatistics and Analyses, Masaryk University, Kamenice 126/3, CZ-625 00 Brno, Czech Republic*
[5] *Research Centre for Environmental Chemistry and Ecotoxicology, Masaryk University, Kamenice 126/3, CZ-625 00, Brno, Czech Republic*

Cytokinin (CK) has been known to inhibit primary root elongation and suggested to act as an auxin antagonist in the regulation of lateral root (LR) formation. While the role of auxin in root development has been thoroughly studied, the detailed and overall description of CK effects on root system morphology, particularly that of developing lateral root primordia (LRPs), and hence its role in organogenesis is still in progress. Here we examine the effects of conditional endogenous CK overproduction on root architecture and consider its temporal aspect during the early development of *Arabidopsis thaliana*. We employed the pOp/LhGR system to induce ectopic *ipt* overexpression with a glucocorticoid dexamethasone at designated developmental points. The transient *CaMV 35S>GR>ipt* transactivation greatly enhanced levels of biologically active CKs of zeatin (Z)-type and identified a distinct developmental interval during which primary root elongation is susceptible to increases in endogenous CK production. Long-term CK overproduction inhibited primary root elongation by reducing quantitative parameters of primary root meristem, disturbed a characteristic graded distribution pattern of auxin response in LRPs and impaired their development. Our findings indicate the impact of perturbed endogenous CK on the regulation of asymmetric auxin distribution during LRP development and imply that there is cross-talk between auxin and CK during organogenesis in *A. thaliana*.

Keywords: *Arabidopsis thaliana* — Auxin–cytokinin cross-talk — *CaMV 35S>GR>ipt* transactivation — DR5 activity — Endogenous cytokinin — Root development.

Abbreviations: AHK, *Arabidopsis thaliana* histidine kinase; CaMV, cauliflower mosaic virus; CK, cytokinin; DAG, days after germination; DEX, dexamethasone; GFP, green fluorescent protein; GR LBD, glucocorticoid ligand-binding domain; GUS, β-glucuronidase; HSP, heat-shock protein; iP, isopentenyl adenine; IPT, isopentenyltransferase; LR, lateral root; LRP, lateral root primordium; Z, zeatin; ZRP, zeatin riboside phosphate.

Introduction

Postembryonic root system development reflects a tremendous plasticity of plants as they adapt to varying environmental conditions. This process of meristem formation and maturation as well as *de novo* organogenesis is regulated by a network of hormonal signals. Plant hormones, cytokines (CKs) and auxins, have been identified as key regulators of the cell proliferation and differentiation during root development. Thus, defining the precise role of CK in primary root meristem maturation and lateral root (LR) formation has recently become a matter of interest.

The *in planta* manipulation of internal plant hormone levels has beeen used to study their biosynthesis (Åstot et al. 2000), interaction (Eklöf et al. 2000, Nordström et al. 2004) or other aspects, and the impact of their enhancement (Faiss et al. 1997, McKenzie et al. 1998, Kunkel et al. 1999). Up to now, studies of phenotypic changes, achieved by exogenous CK application or by overexpression of the bacterial *ipt* gene, have suggested that CKs have a negative role in primary root elongation and LR formation (Medford et al. 1989, Smigocki 1991, Hewelt et al. 1994, Li et al. 2006). In agreement with that, the same conclusion has been drawn from studies on decreasing endogenous CK levels due to the overexpression of the *CK OXIDASE/DEHYDROGENASE* (*CKX*) gene (Werner et al. 2003, Yang et al. 2003). The role of CK in root development has also been addressed in studies on mutants in CK signaling (Higuchi et al. 2004, Nishimura et al. 2004, To et al. 2004, Hutchison et al. 2006, Riefler et al. 2006).

The role of auxin in root meristem development, establishment and maintenance has been thoroughly studied. One way to look at auxin distribution in meristems is by visualizing the expression pattern of reporter genes driven by a synthetic auxin-responsive DR5 promoter (Ulmasov et al. 1997). This has been used to study maximal

*Corresponding author: E-mail, hejatko@sci.muni.cz; Fax, +420-5-4949-2640.

Downloaded from http://pcp.oxfordjournals.org at Masaryk University on August 20, 2010

auxin levels and their developmental significance in the primary root meristem (Sabatini et al. 1999, Friml et al. 2002). The DR5-driven expression pattern has been defined for each stage of developing lateral root primordium (LRP) in a study that attributed a general role to auxin in plant organogenesis (Benkova et al. 2003). Auxin has been regarded as a non-cell-autonomous signal that interacts with other signaling pathways to regulate developmental processes (Swarup et al. 2002). It does so by movement through phloem or by regulated, directional, cell-to-cell movement facilitated by influx (AUX1, LAX family) and efflux (PIN family) protein carriers (reviewed in Friml 2003). This allows auxin to 'meet' CK to regulate the cell cycle synergistically during shoot cell proliferation (Swarup et al. 2002). In the root, however, LR formation is promoted by auxin (Blakely et al. 1988, Casimiro et al. 2003) but this is opposed by the inhibitory influence of CK (Swarup et al. 2002, Werner et al. 2003).

Studies on the homeostatic cross-talk between the two plant hormones at the whole plant level (Nordström et al. 2004) showed that auxin mediates a very rapid negative control of the CK pool (as early as 6 h). In contrast, the effect of CK overproduction on the entire auxin pool in 3-week-old plants was slower (24–48 h), leading the authors to conclude that this was most probably mediated through altered development. The authors also showed strong evidence that LR meristems are the sites of CK biosynthesis. The latter has been confirmed by tissue- and development-specific expression of the *AtIPT* genes (Miyawaki et al. 2004, Takei et al. 2004). In contrast to the results of Nordström et al. (2004), Miyawaki et al. (2004) showed that *AtIPT5* (predominantly expressed in the LRPs) and *AtIPT7* (predominantly expressed in the vascular stele of the root elongation zone) were up-regulated by auxin in roots within 4 h. The above data provide clues about the spatial specificity of the CK-mediated effects. However, little is known about the temporal specificity of the CK action during root development.

Here we present data on the early development of the post-embryonic root. As an alternative to routinely used exogenous CK applications and with the idea of possible differences in exogenous or endogenous CK perception by roots, we specifically aimed at employing the pOp/LhGR transactivation system, or, in other words, *CaMV 35S>GR>ipt* transactivation, to raise endogenous levels of CKs (Craft et al. 2005, Moore et al. 2006, see Materials and Methods). We focused on (i) detailed changes in root morphology due to the *in planta* CK enhancement; and (ii) via the use of DR5-based auxin response reporters, on the role of CK in putative interaction with auxin during LR morphogenesis. In addition, we took advantage of the dexamethasone (DEX)-inducible system and performed transient *ipt* transactivation that allowed us to follow (iii) temporal aspects of CK action during the maturation of primary root meristem. We demonstrate that endogenous CK production affects formation of auxin concentration maxima in developing LRP together with LRP morphology, and we show that CK effects are specific with regard to the state of maturation of the primary root meristem.

Results

Endogenous CK overproduction affects primary root elongation

CK overproduction has been shown to inhibit root elongation (Medford et al. 1989, Smigocki, 1991, Hewelt et al. 1994). To determine the inhibitory effect of the ipt-dependent CK enhancement on root growth in detail, we employed *CaMV 35S>GR>ipt* transactivation using the pOp/LhGR system (Craft et al. 2005) and analyzed root phenotype after continuous, DEX-induced CK overproduction at 6 d after germination (DAG, see Materials and Methods).

Based on the number of transgenes of the used pOp/LhGR transactivation system (double homozygous or heterozygous state of *pOp::ipt* and *CaMV 35S::LhGR* loci, see Materials and Methods), we have identified differences in the strength of the root response. In the case of the strong phenotype response [double homozygous plants (++), Fig. 1C], the average primary root length reached 13% of the untreated control value at 6 DAG (Fig. 1G). From this day on there was no detectable progress in the root development of DEX-treated seedlings. Seedlings of the intermediate phenotype [double heterozygous (+), Fig. 1B] exhibited a lower degree of inhibition. The average primary root length reached 65% of the control value on 6 DAG (Fig. 1G). These results demonstrate two dose-dependent levels of CK-related primary root growth inhibition. Both levels of the root response to the enhanced endogenous CK [(+) and (++)] were subjected to further analysis.

CK overproduction affects quantitative parameters of the primary root meristem

Root growth is a process resulting from cell division in the primary root meristem and from cell elongation occurring predominantly in the elongation zone. However, as the effects of CK on cell elongation may not be specific to CK (Eva Benkova, personal communication, see also Discussion), we have concentrated on the role of endogenous CK in the meristems and inspected primary root meristems in the continuously transactivated plants for possible changes in morphology.

Experiments with lowered endogenous and increased exogenous CK levels (Werner et al. 2003, Ioio et al. 2007, respectively) have demonstrated that CK controls the root

Downloaded from http://pcp.oxfordjournals.org at Masaryk University on August 20, 2010

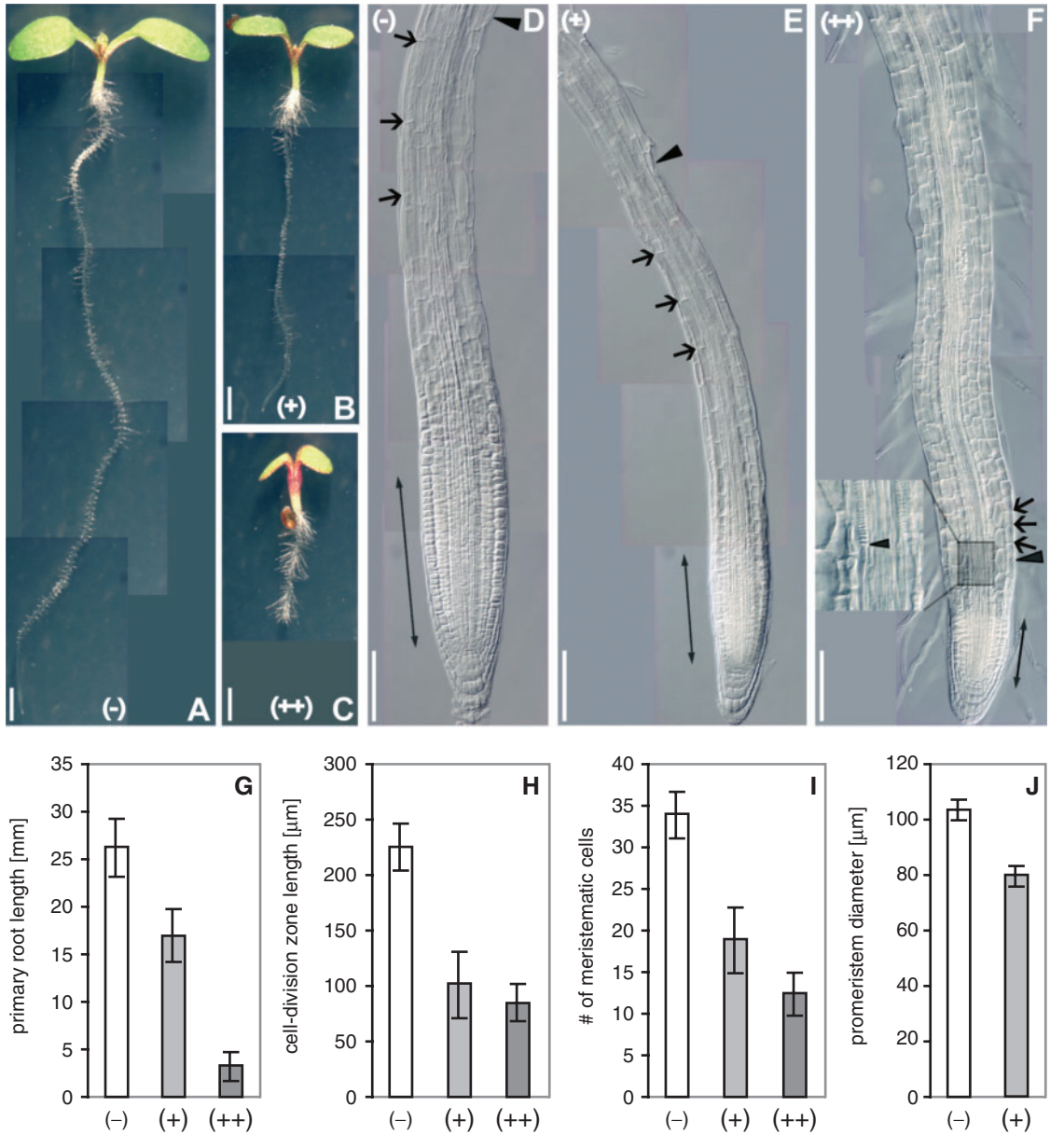

Fig. 1 Overproduction of endogenous CKs affects primary root elongation by reducing quantitative parameters of the primary root meristem. Root growth of *A. thaliana* was evaluated at 6 DAG. Two levels of primary root length reduction are shown as a result of DEX-induced ipt-dependent CK enhancement designated as intermediate (+) and strong (++) compared with uninduced control (−). DEX was present in cultivation media from the moment of germination (continuous *ipt* induction). (A–C) Overall phenotype. (D–F) Detailed view of primary root tips; long arrows indicate the distance between the first and the last dividing cortex cell (estimated morphologically); cell length of differentiated or differentiating cells in close proximity to the first detectable (lignified) protoxylem elements (arrowheads) was apparently reduced in (++) phenotypes (small arrows). (G) Endogenous CK enhancement leads to significantly reduced primary root length (Kruskal–Wallis test: $N = 149$, $Q = 127.581$; $P < 0.001$; multiple comparison: $P < 0.001$). (H) Root length reduction is correlated with reduction of meristematic cell division zone length (ANOVA: $F = 323.742$, $df_1 = 2$, $df_2 = 81$, $P < 0.001$; Tukey post hoc test: $P < 0.001$ in all pairs of groups). (I) Reduction of meristem size is a result of a decreased number of cells within the cell division zone (ANOVA: $F = 328.381$, $df_1 = 2$, $df_2 = 87$, $P < 0.001$; Tukey post hoc test: $P < 0.001$ in all pairs of groups). (J) CK-overproducing seedlings of intermediate phenotype exhibit significantly reduced promeristem diameter (Mann–Whitney U-test: $N = 19$, $P < 0.001$). Genetic background: (−) and (+) mark plants triple heterozygous for the *CaMV 35S::LhGR*, *pOp::ipt* and *DR5::uidA* or *DR5::GFP* loci; (++) marks plants carrying the *CaMV 35S::LhGR* and *pOp::ipt* in the homozygous state. Scale bars: 1 mm (A–C) and 100 µm (D–F). Error bars represent standard deviations.

Downloaded from http://pcp.oxfordjournals.org at Masaryk University on August 20, 2010

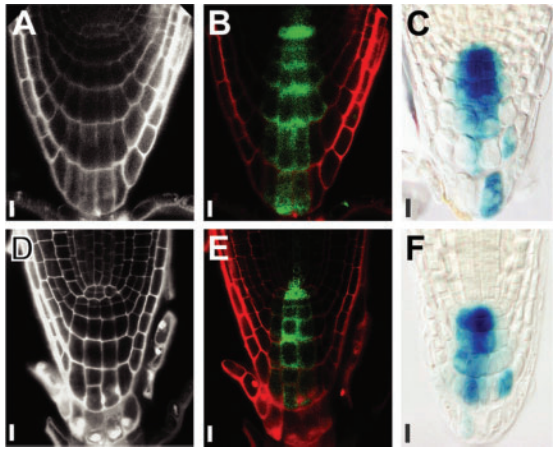

Fig. 2 Enhanced endogenous CK levels do not change stem cell organization and DR5 activity distribution in primary root promeristems of individuals displaying the intermediate phenotype. (A, D, B, E) Propidium iodide (PI)- or (C, F) GUS-stained primary root tips of *A. thaliana* at 6 DAG, triple heterozygous for the *CaMV 35S::LhGR*, *pOp::ipt* and *DR5::GFP*, or *DR5::GUS* loci, respectively. (A–C) Uninduced controls; (D–F) DEX-induced individuals (continuous DEX treatment); (A, D) PI fluorescence; (B, E) the same roots with visualized *DR5::GFP* expression (green signal). (C, F) GUS activity localization (blue staining). Scale bars: 10 µm.

elongation primarily by controlling the size of the meristem rather than by changes in cell division rate. Therefore, we analyzed the impact of increased levels of endogenous CKs on the size of the meristematic cell division zone. At 6 DAG, the longitudinal dimension of the cell division zone was significantly reduced in the roots of individuals displaying the intermediate phenotype [(+), Fig. 1H], predominantly as a result of a reduction in the cell number (Fig. 1I). We also observed a reduced diameter of the primary root tip (measured as a transverse line directed through the quiescent center, Fig. 1J). At 6 DAG, the dimension of the cell division zone in highly activated roots (++) was even more reduced (Fig. 1H), again due to a reduction in the meristematic cell number (Fig. 1I). The average length of the cell division zone of the control, intermediate and strong phenotype was 224.4, 100.5 and 83.5 µm, respectively (Fig. 1H).

Based on these results, we conclude that the increase in endogenous CKs affects root elongation by reducing the number of dividing cells in the meristem. However, in contrast to the observed changes of quantitative parameters, the cellular pattern of the main root promeristem remained unaffected (Fig. 2A, D).

CK overproduction interferes with lateral root development

The negative role of CK in LR formation was previously recognized (Werner et al. 2003, Li et al. 2006, Riefler et al. 2006). Recently, new molecular evidence has emerged, suggesting action of endogenous CKs during LR development (Miyawaki et al. 2004, Takei et al. 2004). To identify the developmental aspects of CK action during LR formation, we have screened the roots of transactivated, 6-day-old seedlings displaying the intermediate and the strong phenotype responses to determine the frequencies at which LRPs had (i) initiated (Beeckman et al. 2001, Casimiro et al. 2001); and (ii) further developed (Malamy and Benfey 1997).

To describe the effects of endogenous CK production on the initiation of LRP, we have inspected the total number of newly established LR meristems in continuously transactivated plants. The total number of LR meristems per root was significantly reduced by both levels of ipt-dependent CK overproduction. It decreased on average from 8.8 in the control (−) to 7.2 in roots of intermediate phenotype (+), i.e. to 82% of the control value, and from 9.8 to 2.9 in roots with a strong response (++), i.e. to 30% of the control value, respectively (Fig. 3A). However, considering the reduction of the primary root length (Fig. 1G), the LRP density of the induced individuals increased somewhat (Fig. 3B). LRPs frequently occurred in proximity to each other in the strong (++) phenotype (Fig. 3C).

As the next step, we analyzed the potential impact of endogenous CKs on development of LRPs. To do that, we have evaluated frequencies of individual stages of LRP development as defined by Malamy and Benfey (1997) in continuously transactivated plants. In the 6-day-old untreated (−) seedlings there were few LRs or LRPs of higher developmental stages. LRPs of stages II to IV prevailed (Fig. 3D, E). The distribution of LRPs in transactivated seedlings of the intermediate (+) phenotype at 6 DAG shifted in favor of stages II–IV at the expense of the latest stages just before and after emergence (Fig. 3D, F); there were no LRs, only one LRP which was just about to emerge, and one LRP having reached the epidermis. In strongly (++) responding roots of continuously transactivated plants (Fig. 3E), the LRPs became arrested even earlier in development. There were only two LRPs at stage V, while later stages were completely missing, indicating that the ipt-dependent, CK-related effects were dose dependent (Fig. 3G).

Thus, while reduction of the root length due to *ipt* overexpression does not allow us to draw a clear conclusion about the effect of increased endogenous CKs on the initiation of LRPs, our results demonstrate that in response to the endogenous CK overproduction, growth of LRPs is inhibited during developmental stages II–IV and their transition to stage V.

CK overproduction impairs auxin maxima in LRP

The dependence of LRP development on the correct establishment of local auxin maxima was previously

Downloaded from http://pcp.oxfordjournals.org at Masaryk University on August 20, 2010

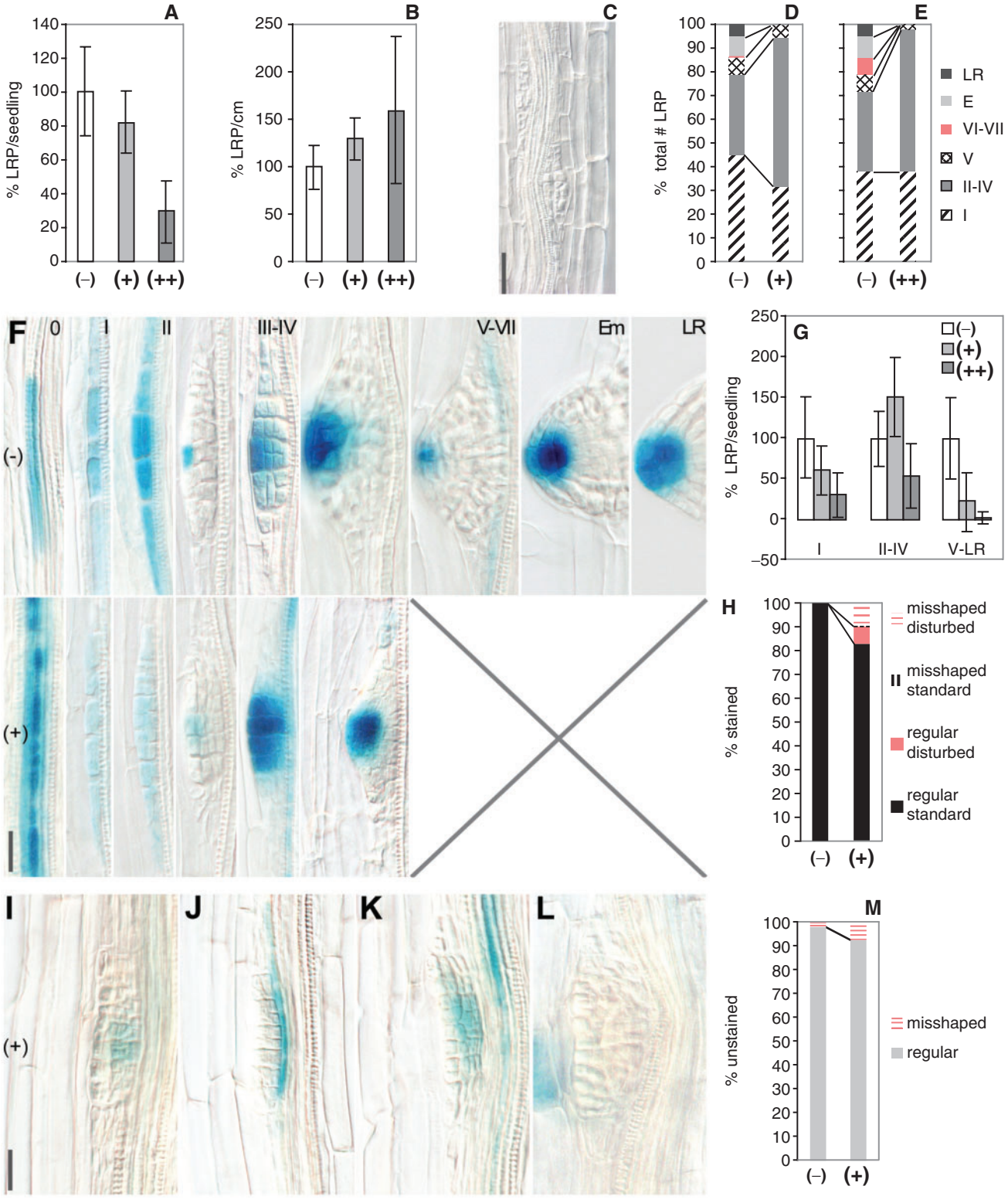

Fig. 3 Effects of endogenous CK overproduction on initiation, development and the DR5 activity distribution pattern of LRPs. Each graph or image displays the effect of DEX-induced intermediate (+) or strong (++) endogenous CK overproduction on LR formation compared with uninduced control (–) at 6 DAG. DEX was present in cultivation media from the moment of germination (continuous *ipt* induction). (A) Both levels of CK overproduction result in a significant decrease of the total number of the observed LRPs per root

Downloaded from http://pcp.oxfordjournals.org at Masaryk University on August 20, 2010

demonstrated by Benkova et al. (2003). To assess whether the observed retardation in LRP development in the CK-overproducing lines is accompanied by disturbed auxin concentration gradients, we closely examined LRPs for auxin reporter maxima in crosses between *ipt*-inducible and *DR5::GUS* (β-glucuronidase) lines (triple heterozygous for *pOp::ipt*, *CaMV 35S::LhGR* and *DR5::GUS*). At 6 DAG, 23% of LRPs were stained in control seedlings whereas 77% were not stained. The roots of continuously DEX-treated seedlings (+) contained a slightly higher number of unstained LRPs (79%). In the DEX-induced seedlings, 16% of the stained LRPs (11/71) displayed a disturbed *DR5::GUS* expression pattern (Fig. 3H), manifested by a loss of a sharp maximum at the distal part of the primordium (Fig. 3I), whereas only one such primordium (a future adventitious root at the root–shoot junction—not included in our results) was observed in the uninduced control. These results provide evidence of the impact of CK overproduction on auxin maxima distribution during LRP development.

The 55% of LRPs with impaired auxin distribution (6/11) were irregularly shaped in the induced plants (Fig. 3H, J, K). Misshaped LRPs also occurred to a greater degree among the unstained LRPs of CK-overproducing roots [7% (19/260), compared with 2% (4/209) of unstained LRPs in control, Fig. 3L, M]. These differences between the uninduced and induced populations demonstrate that long-term, continuous CK overproduction results in local disturbances in auxin graded distribution and morphological defects during LRP development. However, in contrast to identified changes of auxin maxima during LRP development, there was no apparent dislocation and very weak to no change in the intensities of the spatial pattern of DR5 activity in the main root meristem in response to continuous *ipt* transactivation (Fig. 2B, E and C, F). This is in agreement with the above-mentioned absence of detectable changes in the cellular pattern of the main root promeristem (Fig. 2A, D).

Temporal pulses of ipt expression reveal a developmental window for sensitivity of primary root elongation to endogenous CK

To determine the potential time specificity of CK action in *Arabidopsis*, we induced transient *ipt* overexpression at distinct intervals (lasting 24 h each), covering primary root development from the moment of germination to the first LRP emergence, i.e. the first 6 DAG (see Materials and Methods). Based on the extent of root growth retardation, the six tested samples can be divided into two groups (Fig. 4A). Samples that were induced during 2, 3 and 4 DAG displayed a greater level of reduction in primary root length compared with samples treated by DEX during 1, 5 and 6 DAG. From the long-term perspective, the former (2, 3, 4) but not the latter group (1, 5, 6) never reached the final primary root length of the control (−) after further cultivation under non-inductive conditions (Fig. 4A, C). No effects on the root growth were detected in the similarly treated wild-type plants (data not shown). The intervals 3 and 6 were chosen for further analyses and designated as 'early' and 'late' pulses of the *ipt* transactivation, respectively. Detailed measurements of the primary root length during the first 12 DAG showed that after the early pulse, root elongation nearly stopped for the next 4–5 d. In contrast, this inhibition only lasted for another 24 h after application of the late pulse of *ipt* transactivation (Fig. 4D). The elongation rate of

(Kruskal–Wallis test: $N = 151$, $Q = 92.359$; $P < 0.001$; multiple comparison: $P < 0.003$). (B) Overall LRP density slightly increased (Kruskal–Wallis test: $N = 151$, $Q = 30.208$, $P < 0.001$; comparing sample (−) and samples (+) and (++) in multiple comparisons: $P < 0.005$). However, no significant difference was found between the intermediate and strongly responding roots (multiple comparison: $P = 0.098$). (C) LRPs in a root of the strong phenotype in close proximity to each other. (D, E) Frequencies of individual stages of LRPs scored in plants exhibiting the intermediate (D) and strong (E) phenotype. LRPs become arrested at developmental stages II–IV and their transition to stage V, by both the intermediate ($\chi^2 = 82.296$, $df = 5$; $P < 0.001$) and the strong level ($\chi^2 = 65.104$, $df = 5$; $P < 0.001$) of enhanced CKs. (F) DR5 activity during LRP development in uninduced controls (−) vs. plants with intermediate CK overproduction (+); the later stages of LRPs and LRs were not identified after *ipt* transactivation. (G) Endogenous CK production changes the distribution of developing LRPs grouped as initiating (I), gradually acquiring auxin-autonomous status at stage IV (II–IV), and close to or at the stage of emergence (V–LR); the relative prevalence of LRPs at stages II–IV suggests interference of enhanced CK production with polar cell-to-cell auxin transport (Kruskal–Wallis test, $N = 151$, $Q = 61.162$ for stage I, $Q = 58.503$ for stages II–IV and $Q = 96.123$ for stages V–LR, multiple comparisons: $P < 0.001$; the difference between samples (+) and (++) for stages V–LR was not significant: $P = 0.325$). (H) Endogenous CK enhancement results in changed *DR5::uidA* expression pattern (χ^2 goodness-of-fit: $\chi^2 = 16.100$, $df = 3$; $P = 0.001$) and morphology ($\chi^2 = 7.983$, $df = 1$; $P = 0.005$) in LRPs. Standard denotes LRPs displaying the *DR5::uidA* expression pattern reflecting correctly located auxin-graded distribution. Disturbed denotes LRPs missing a well-defined auxin-graded distribution pattern, frequently misplaced and shifted towards the base of a primordium. Regular vs. misshaped denotes LRPs exhibiting normal compared with abnormal morphology. (I) An example of an LRP with a disturbed auxin-graded distribution pattern. (J, K) LRPs with a misplaced *DR5::uidA* expression pattern and abnormal morphology. (L) An example of a misshaped LRP with missing detectable DR5 activity maximum. (M) Endogenous CK enhancement results in increased frequencies of misshaped LRPs among those with an undetectable *DR5::uidA* expression pattern (χ^2 goodness-of-fit: $\chi^2 = 7.983$, $df = 1$; $P = 0.005$). Genetic background: (−) and (+) mark plants triple heterozygous for the *CaMV 35S::LhGR*, *pOp::ipt* and *DR5::uidA* loci; (++) marks plants carrying the *CaMV 35S::LhGR* and *pOp::ipt* in the homozygous state. (I–VII) Individual stages of LRP development defined by Malamy and Benfey (1997); Em, emerging LRP; LR, lateral roots soon after emergence. Scale bars = 20 μm.

Downloaded from http://pcp.oxfordjournals.org at Masaryk University on August 20, 2010

the primary root, measured as the increase in root length per day, was significantly lower after application of the early compared with the late pulse when measured during the first 6 d following DEX treatment (Fig. 4E). Fig. 4B demonstrates that the increase in the *ipt* transcripts was similar and transient after 24 h of DEX uptake in both cases. These results indicate a development-specific response to the transcriptional activation of the *ipt* gene.

Both early and late pulses of ipt overexpression greatly enhance the endogenous levels of biologically active zeatin-type CKs

To define the enhanced ipt-dependent CK profile at each of the two chosen intervals of development (early and late), we performed quantitative CK analysis. Of all the measured CKs (Fig. 5 and Supplementary Table S1), the zeatin-type (Z-type) metabolites prevailed at both stages of development, comprising mostly active forms, which in turn were mostly represented by riboside phosphates, with zeatin riboside phosphate (ZRP) as a major compound. Z-type metabolite levels increased from 285 to 2,250 (i.e. by an order of magnitude) and from 62 to 8,570 (i.e. by two orders of magnitude) pmol g^{-1} FW at the end of the early and the late ipt pulse, respectively. That means that while levels of most active CKs of the uninduced control were significantly higher at the early than at the late stage (−, Fig. 5), this ratio was reversed in favor of the late stage after *ipt* overexpression (+, Fig. 5).

We have further identified several differences in relative distribution of CK metabolites between uninduced controls at early and late intervals. Uninduced levels of CK conjugates were lower at the early compared with the late stage, which became even more apparent after *ipt* overexpression (Fig. 5). Also a significantly lower proportion of the CKX-degradable to CKX-non-degradable CKs was found in control plants at early than at late intervals (Supplementary Fig. S2E). Not only were the differences in relative distribution of CK metabolites detectable in uninduced controls, but minor differences also occurred between the early and late samples after *ipt* transactivation. For example, the proportion of the iP-type- to Z-type CKs and that of *N*-7-glucosides to other conjugates was significantly higher in early than in late stage (see Supplementary Fig. S2A–E).

Thus the fact that enhanced CK levels, measured at the end of both developmental intervals, resulted in the stronger response of 3-day-old compared with 6-day-old roots indicates the temporal aspect of the CK-mediated inhibition of primary root elongation. Furthermore, significant differences in the spectrum of uninduced CK levels between the early and the late intervals indicate differences in the basal status of CK metabolism. These differences might play a role in the observed differential root response that we suggest is development specific.

Discussion

Effects of enhanced CK levels on the development of the primary root

Reduced root growth in response to enhanced endogenous CK content has previously been observed (Medford et al. 1989). The phenotype of plants exposed to exogenous CK and transgenic lines with reduced endogenous CK suggests a negative role for CK in the regulation of the size of root meristems (Beemster and Baskin 2000, Werner et al. 2003, respectively). However, disruption of CK signaling results in reduction of the root meristem size, too (Higuchi et al. 2004, Nishimura et al. 2004, Hutchison et al. 2006), suggesting a positive role for the CK particularly in root meristem maturation. These findings led to the hypothesis explaining this phenomenon by what is called supraoptimal endogenous CK levels in the root (Ferreira and Kieber 2005). Thus, reducing the CK contents within physiological limits to optimal levels (e.g. by CKX activity) would lead to an acceleration of root growth, while a complete inhibition of CK signaling would result in reduction of primary root growth, which is correlated with a reduction in meristem size. Similarly, overdose of the root with CK would lead to meristem reduction, too. Our observation of meristem reduction as a result of the ipt-dependent CK enhancement is in agreement with this hypothesis.

Miyawaki et al. (2004) have reported that expression of the *Arabidopsis* CK biosynthesis gene *AtIPT5* was localized in the root cap soon after germination, but this signal decreased with time and was undetectable 7 DAG. Recently, Ioio et al. (2007) demonstrated that CK delimits the size of the root meristem by induction of cell differentiation at the transition zone. Thus, temporal and spatial specificity of CK action must be considered when discussing the role of CK in the complex regulation of formation and maintenance of the root meristems.

In the transactivation system used here, *ipt* overexpression preferentially occurred in more differentiated parts of the root (see Supplementary material and Fig. S1). Thus, low (in our system undetectable) expression might occur in the root meristem, leading to an increase of endogenous CK sufficient for the observed phenotype changes. Alternatively (and more probably), CK is distributed from the place of its biosynthesis towards the root meristem through vascular tissues (see also the next section of the Discussion). The latter conclusion is fully in agreement with the above-mentioned data of Ioio et al. (2007) who identified vascular tissue at the transition

Downloaded from http://pcp.oxfordjournals.org at Masaryk University on August 20, 2010

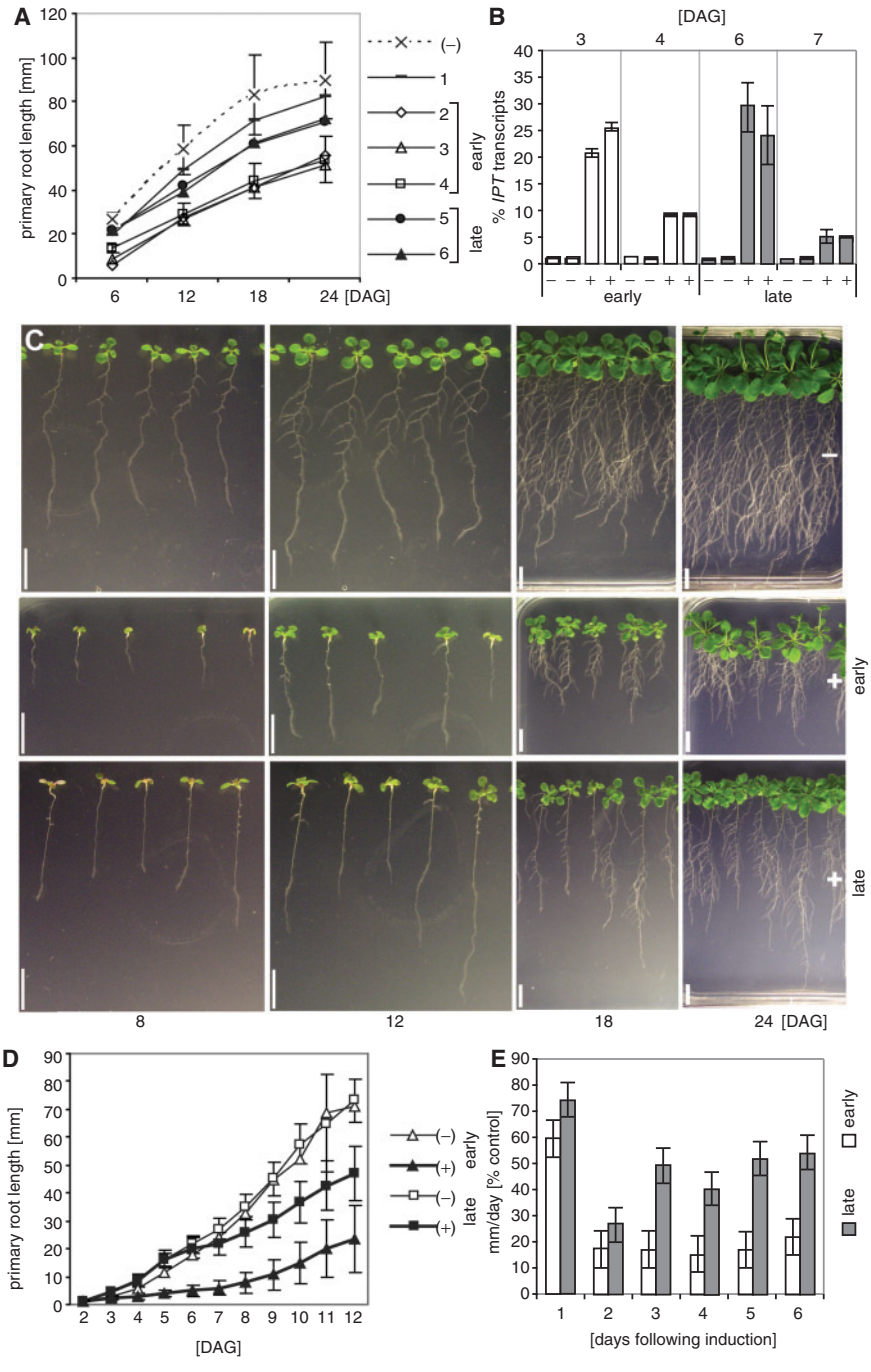

Fig. 4 Stage-specific inhibition of primary root elongation as a result of transiently induced endogenous CK overproduction. Six groups of individuals were temporarily exposed to DEX-mediated induction of *ipt* overexpression for 24 h at 0–24 (1), 24–48 (2), 48–72 (3), 72–96 (4), 96–120 (5) or 120–144 h (6) intervals between day 0 and 6 after germination. (A) Average primary root length of each group measured at 6, 12, 18 and 24 DAG demonstrates distinct long-term inhibition of root elongation after early (intervals 2, 3, 4) but not late (intervals 5, 6) exposure to DEX. (B) Temporal early (2–3 DAG) and late (5–6 DAG) treatment by DEX (white or gray columns, respectively) results in an adequate and transient increase in amounts of *ipt* transcripts relative to *ACTIN2* and *ACTIN8* transcripts; presented are mean values of two replications of quantitative real-time PCR of two independent biological samples obtained by RNA isolation from hundreds of individuals. After the early or late treatment, RNA was isolated from the seedlings immediately (3, 6) or after an additional 24 h of cultivation in the absence of DEX (4, 7). (C) Phenotypes of seedlings at 8, 12, 18 and 24 DAG after transient *ipt* transactivation in early (2–3 DAG) and late (5–6 DAG) intervals (+) as compared with uninduced control (–). (D) Significant reduction of primary root length was detected soon after early and late DEX treatment (+) compared with controls transferred to DEX-free media for 24 h (–) [Mann–Whitney U-test, early: $N = 80$, $P < 0.001$, late: N from 50 to 67, $P < 0.001$; comparison of (+) and (–) on days 1, 2, 3, 4, 5 and 6 following induction]. (E) The elongation rate of the primary root was significantly lower after application of the early compared with the late pulse during the first days following DEX treatment [Mann–Whitney U-test: N from 69 to 74, $P < 0.008$ on days 1, 2, 3, 4, 5 and 6 following induction]. (+) DEX-treated samples, (–) uninduced control.

between the meristematic cell division and elongation zones as the essential site of CK action.

Beemster and Baskin (2000) have described the effects of exogenously applied CK not only on the meristem, but also outside the meristem, in the elongation zone. Our results seem to confirm both of these effects (Fig. 1). However, besides its direct action, CK was shown to enhance endogenous levels of ethylene (Rashotte et al. 2005). Recently it has been reported that ethylene inhibits root growth via induction of auxin biosynthesis and auxin basipetal transport, accompanied by accumulation of the auxin-responsive DR5::GUS reporter signal in the elongation zone and auxin-dependent inhibition of cell elongation (Růžička et al. 2007, Swarup et al. 2007). In contrast, ethylene does not affect the number of dividing cells in the root meristem (Růžička et al. 2007). Thus, while the

Downloaded from http://pcp.oxfordjournals.org at Masaryk University on August 20, 2010

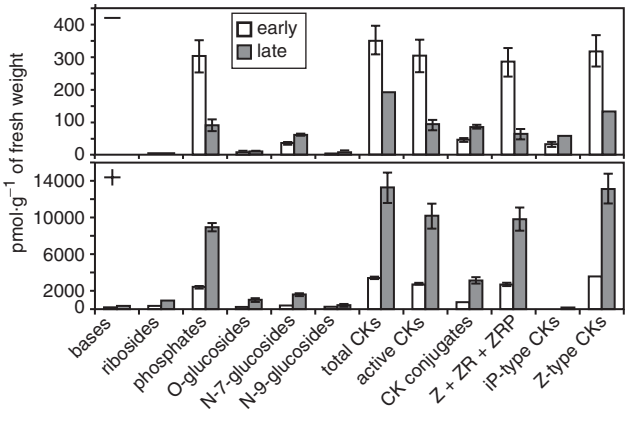

Fig. 5 (−) Uninduced and (+) greatly enhanced DEX-induced endogenous CK levels measured at the end of the transient 24 h pulse of *ipt* expression. Early (2–3 DAG) and late (5–6 DAG) pulses of endogenous CK overproduction are compared. The amounts of every group of CKs differed significantly between the early and the late pulses of uninduced samples (Mann–Whitney U-test, in each comparison $P<0.05$) except for iP-type CKs ($P=0.201$). The amounts of every group of CKs differed significantly between the early and the late pulses of induced samples (Mann–Whitney U-test, in each comparison $P<0.05$) except for iP-type CKs ($P=0.522$). CKs are arranged in various categories in terms of their biological relevance. For terminology see Supplementary Table S1 and footnotes.

negative effect of increased endogenous CK on cell elongation might be an additive effect of both CK end ethylene or even specific to ethylene, the negative CK effect on the number of cells within the cell division zone in primary root meristems is ethylene independent.

Effects of enhanced CK levels on auxin distribution and the development of LRPs

Our results show that the root responds to an ipt-dependent increase in endogenous CK levels by arresting LRPs mostly at the developmental stages II–IV, suggesting sensitivity and a negative response of developing LRPs to enhanced CKs at these developmental stages. In agreement with that, Lohar et al. (2004) observed a repression of the CK response during LRP development in *Lotus* at a stage of pericycle cell division corresponding to stages III–IV in *Arabidopsis thaliana*. In contrast, exogenous application of CK inhibited LRP initiation in *A. thaliana* (Li et al. 2006, Laplaze et al. 2007). These observations suggest differences in the developmental impact of exogenous application versus endogenous manipulation of CK levels. In agreement with this idea, endogenous and exogenous CK levels seem to be monitored by distinct *A. thaliana* histidine kinases (AHKs). While AHK4/CRE1/WOL was shown to mediate the negative effect of the exogenously applied CKs on LRP initiation and root elongation (Li et al. 2006, Higuchi et al. 2004, respectively), AHK2 and AHK3 seem to be responsible for the negative effect of endogenous CKs on LR formation in *A. thaliana* (Riefler et al. 2006). Taken together, CKs may participate in regulating LR development at different stages through the regulation of distinct CK-dependent signaling pathways that might reflect both intrinsic developmental programs and other environmental stimuli and adaptive responses.

CaMV 35S>GR>ipt transactivation, used in this work, allows *ipt* overexpression in all root tissues, including pericycle cell files and early stages of LRPs (Supplementary Fig. S1). While our manuscript was under review, new results were published describing use of GAL4-GFP (green fluorescent protein) enhancer trap lines in order to induce *ipt* expression specifically in initiating pericycle cells or developing LRPs (Laplaze et al. 2007). The authors demonstrated that *ipt* induction in xylem pole pericycle cells (LR founder cells) leads to changes in the cellular pattern of developing LRPs and arrest of LRP development at stage V, while *ipt* induction in developing LRPs does not affect LR formation. From this new point of view, the growth arrest at stages II–IV and the irregular morphology of LRPs that we observed should be a consequence of CK action occurring as early as LRPs initiate. These results also suggest that although the *CaMV 35S>GR>uidA* transactivated roots exhibit differences in intensities of the GUS reporter expression between mature (differentiated) and apical (formed by elongating and rapidly dividing cells) parts of the primary root (Supplemental material, Fig. S1), this system seems to distribute CK sufficiently throughout the root, very probably via the root vascular tissues.

LRP initiation, their further development and the moment of emergence seem to be specific stages of an otherwise continuous process also in terms of the origin of auxin supply. The initiation of the very first LRP, which occurs as soon as 40 h after germination (Beeckman et al. 2001) in acropetal sequence (Dubrovsky et al. 2006), seems to depend solely on the primary root basipetal auxin transport (Casimiro et al. 2001, De Smet et al. 2007), while their emergence is positively correlated with functional primary root acropetal auxin transport via the phloem (Reed et al. 1998, Casimiro et al. 2001). Between these two stages, 3–5 cell-layer LRPs have been proposed to acquire an independent auxin-autonomous status temporarily (Laskowski et al. 1995). Our data on the frequencies of initiating LRPs in response to endogenous CK production demonstrate that LRP initiation is not fully inhibited but proceeds further in the used transactivation system, indicating a low impact of CK on the basipetal auxin transport. In contrast, the reduced frequencies of late developmental stages before emergence (VI–VII), and the arrest of LRPs at the auxin-autonomous stage IV as a

Downloaded from http://pcp.oxfordjournals.org at Masaryk University on August 20, 2010

consequence of CK overproduction, imply possible interference of CK with polar cell-to-cell auxin transport within developing LRPs.

Benkova et al. (2003) demonstrated the importance of establishing local active auxin transport during LRP initiation and development. Auxin accumulates at the position of a future primordium, and, as the LRP develops, its graded distribution becomes established, with the maximum located at the tip of the primordium. Disruption in the polar auxin distribution that is dependent on proteins from the PIN family (Petrášek et al. 2006) correlates with defects in patterning during LRP development. Individual *pin* mutants exhibited changed frequencies of initiated LRPs and LRPs with abnormal development accompanied by defects in DR5 activity distribution. The impairment of the DR5 activity distribution in developing LRPs and the increased frequency of defects in LRP patterning that we observed due to CK overproduction indicate that enhanced CK levels interact with auxin during LRP morphogenesis via regulation of the auxin distribution. Our conclusions are in agreement with those of Laplaze et al. (2007) who, in addition to changed DR5-driven *uidA* expression, also observed affected *PIN1* and *PIN6* expression patterns in roots treated with exogenous CK.

However, in contrast to changes scored in the developing LRPs, we observed neither significant changes in the spatial pattern of the DR5 activity maximum, nor any obvious changes in the cell division pattern in the main root promeristem of the seedlings exhibiting the intermediate phenotype (Fig. 2). Thus, the intermediate level of endogenous CK enhancement described here does not affect components directly involved in the maintenance of auxin distribution responsible for stem cell organization in the main root meristem.

Developmental specificity of the root response to CK overproduction

A temporary induction of *ipt* transactivation in the pOp/LhGR system made it possible for us to identify a development-specific primary root response to enhanced endogenous CK levels. Transient pulses of *ipt* overexpression specified a time interval, between the second and the fourth day of *Arabidopsis* seedling development, during which primary root elongation was inhibited to a greater extent than 1 or 2 d later. There are several interesting aspects to consider. First, after germination, the final number of dividing cells of the primary root meristem gradually increases until it reaches a finite number, which is not earlier than 5 DAG (Ioio et al., 2007). In the experiments presented here, transient *ipt* overexpression revealed that there is a mechanism that attenuates the response to endogenous CK overproduction when the meristem cell number is finite compared with younger primary roots. Secondly, Bhalerao et al. (2002) have shown that a sharp basipetal IAA concentration gradient is established in the root tip as late as 6 DAG, and that shoot-derived auxin appears in the primary root as a sudden IAA pulse between the fifth and the seventh day of root development, not reaching the root apex earlier than 7 or 8 DAG. The results describing opposite roles for CK and auxin in the root meristem size have been published (Beemster and Baskin 2000, Ioio et al. 2007). Thus CK may be 'allowed' to act and produce a stronger response before the sharp auxin concentration gradient in the primary root tip becomes established and/or a further pulse of auxin 'arrives' from the shoot. Thirdly, differential expression of *AtIPT* genes (Miyawaki et al. 2004, Takei et al. 2004) has recently brought a more advanced view of CK action during root development. *AtIPT1::GUS* was expressed in xylem precursor cells of primary root meristems but the signal was no longer detectable starting from 5 DAG onwards. *AtIPT1::GFP* also exhibited a temporary expression pattern in young roots with an immature vascular system. *AtIPT5::GUS* expression in the columella of the primary root apex disappears at the seventh day of root development. *AtIPT5::GUS* expression in the LRP diminishes and is lost after LR emergence. Based on these observations, it seems that in developing root meristems there is a specific time point at which the termination of expression of CK biosynthesis genes is correlated with (i) root meristem maturation; (ii) the establishment of the sharp basipetal auxin concentration gradient; and, possibly, (iii) the increase in the shoot-derived auxin concentration in the primary root. The fact that the responsiveness of a 3-day-old plant is greater to the transient increase of endogenous CK compared with a 6-day-old plant is in agreement with the above findings. It implies a possible role for CK during primary meristem maturation together with the existence of mechanisms to fine-tune the concentration of CK and auxin temporally at specific stages of root development. Whether this can be generalized and whether all the above-mentioned aspects can be applied to LR development before and early after LRs emerge from the primary root is not quite clear. However, it is very probable that LR development should still be influenced by CK and auxin metabolism originating in the primary root.

Based on a detailed quantitative analysis of CK levels, our data indicate that the level and spectrum of various forms of CKs most probably change temporally during plant development. The different strength of the induced root response at the two different developmental intervals resulted from quantitatively saturated and a qualitatively similar proportion of CK metabolites. This suggests the presence of development-specific mechanisms involved in

Downloaded from http://pcp.oxfordjournals.org at Masaryk University on August 20, 2010

the regulation of CK metabolism and/or signaling during the first 6 d of *A. thaliana* development. One indication for the higher sensitivity of the 3-day-old meristem to the increased levels of endogenous CKs may be the observed qualitative differences in the proportion of CK metabolites in controls (uninduced plants) between day 3 and 6 (see Supplementary Fig. S2E). The observed difference in the proportion of *N*-7- glucosides in early and late stages after *ipt* transactivation (Supplementary Fig. S2D) suggests that the mechanisms involved in the maintenance of CK homeostasis by CK glycosylation might differ in early and late intervals. Thus, differences in the specificity of inactivation of CKs by glucosylation might be one of the factors responsible for the developmental-specific sensitivity of the immature root meristems in *A. thaliana*. However, further studies would have to be done to define the particular molecular mechanisms regulating the complex net of CK metabolism and signaling during early root development.

Materials and Methods

Plant material and the pOp/LhGR system

Arabidopsis thaliana lines of the Columbia (Col-0) ecotype were used in this study. Glucocorticoid-inducible overexpression of the *ipt* gene from *Agrobacterium tumefaciens* or the *uidA* gene was achieved by use of the pOp/LhGR system for transcriptional activation or, in other words, by *CaMV 35S>GR>ipt* or *CaMV 35S>GR>uidA* transactivation (Craft et al. 2005, Moore et al. 2006). Briefly, the system is based on interaction of two components. The first component comprises a gene of interest (e.g. *ipt* or *uidA*) placed under control of a synthetic pOp promoter; *lac* operators are part of the pOp promoter. The second component is a chimeric transcription factor LhGR, consisting of (i) a mutant *lac* repressor that binds its operator with increased affinity; (ii) a transcription activation domain-II from *GAL4* of *Saccharomyces cerevisiae*; and (iii) a glucocorticoid ligand-binding domain (GR LBD). The LhGR is expressed constitutively from the CaMV 35S promoter, but the transcriptional activation of expression of a target gene will not take place under normal conditions because the GR LBD is occupied by the plant heat-shock proteins (HSP 90 complex). HSP 90 is released and the target gene expression is activated in the presence of a glucocorticoid ligand, e.g. DEX.

We performed both continuous and transient *CaMV 35S>GR>ipt* or *uidA* transactivations. Induction of the continuous target gene expression was swiched on at germination and lasted 6 d, followed by phenotype evaluation at 6 DAG. Induction of the 24 h transient *ipt* expression was carried out at six developmental points. Each of the six samples was exposed to DEX for 24 h intervals at 0–24, 24–48, 48–72, 72–96, 96–120 or 120–144 h after germination.

The *CaMV 35S>GR>ipt* transactivation in *A. thaliana* can yield a wide range of CK-related phenotypes. Their severity depends on the rate and level of *ipt* expression and the concentration of DEX, but is also influenced by the number of engineered *lac* operators and the character of the flanking genomic sequences (Craft et al. 2005, Moore et al. 2006). Continuous DEX treatment of a transgenic line homozygous for *pOp::ipt* (in Craft et al. 2005 referred to as pOp^{BK}-*ipt*; the number of operators equals two in this construct) and *CaMV 35S::LhGR-N* fusions yielded a strong (++) phenotype response (Fig. 1C). The same line was used to perform transient 24 h DEX induction of CK overproduction. Continuous DEX treatment of the F_1 generations of the crosses between the *CaMV 35S>GR>ipt* and *DR5::GUS* (Ulmasov et al. 1997) or *DR5rev::GFP* (Benkova et al., 2003) lines resulted in an intermediate (+) phenotype response (Fig. 1B). To study the morphology of root meristems, both transgenic lines were used. Heterozygous line was used to assess potential changes in morphogenesis and the spatial pattern of auxin response of developing LRPs. The *CaMV 35S>GR>uidA* transactivation was carried out to define the spatial pattern of expression of a target gene driven from the pOp promoter, i.e. the expression pattern of *pOp::uidA* (referred to as pOp^{BK}-*GUS*, two *lac* operators, Craft et al., 2005; see the Supplementary material, Fig. S1).

Growth conditions and dexamethasone induction of a target gene from the pOp promoter

Seeds were sterilized in 70% ethanol for 2 min, allowed to dry, and plated on solidified medium containing a basal Murashige and Skoog mixture including MES buffer, 1% sucrose and 1.25% agar, pH 5.6. The plates were sealed with gas-permeable tape (Spofapor, Chemofarma, a.s., Ústí nad Labem, Czech Republic) and kept in darkness at 4°C for 3 d. The seeds germinated and the plants grew on vertically positioned plates under long-day conditions (16 h light, 21°C, and 8 h dark, 19°C) in three-shelf growth chambers with an average photosynthetic photon flux density of 140 μmol m^{-2} s^{-1} (Percival Scientific, Ltd., Perry, IA, USA). *ipt* or *uidA* (GUS) expression was induced by 10 μM DEX (Sigma, St. Louis, MO, USA) (Craft et al. 2005, Moore et al. 2006) via its uptake by roots from solid medium. Seeds either germinated on DEX-containing medium and seedlings were screened at 6 d of continuous *ipt* or *uidA* induction, i.e. at 6 DAG, or the seeds or seedlings were temporarily transferred to DEX-containing medium for 24 h (transient pulses of *ipt* expression, see the above paragraph).

Histochemistry, GFP localization and microscopy

Before roots were analyzed in detail, the overall phenotype of seedlings was viewed, documented and analyzed by using a digital camera, SZX 9 stereo microscope and image analysis software [(analySIS), (Olympus C&S, s.r.o., Praha, Czech Republic)].

Histochemical staining for GUS activity was performed in 0.1 M sodium phosphate buffer, pH 7.0, containing 0.1 M Triton X-100, 0.1% X-glc, 5 mM EDTA, 2.5 mM $K_3[Fe(CN)_6]$ and 2.5 mM $K_4[Fe(CN)_6]$ for 8 h at 37°C unless otherwise stated. The reaction was stopped by placing the seedlings in 70% ethanol. The seedlings were cleared (Malamy and Benfey 1997) and mounted in 50% glycerol. The roots were screened for the frequency of LRP, *DR5::GUS* expression pattern, or a morphological boundary between the last dividing and the first elongating cortex cell of the primary root meristem viewed by Nomarski optics using a BX61 microscope equipped with a DP50 camera (Olympus C&S, s.r.o., Praha, Czech Republic). In the case of the intermediate phenotypes, we have viewed 271 LRPs among 31 untreated individuals and 331 LRPs among 46 DEX-treated individuals. In another experiment, 304 LRPs of 31 untreated seedlings were compared with 126 LRPs of 43 highly activated individuals displaying the strong phenotype.

Epifluorescence or confocal microscopy was used to localize the *DR5rev::GFP* expression pattern. The seedlings were transferred directly from plates to 5% glycerol on the microscopic

Downloaded from http://pcp.oxfordjournals.org at Masaryk University on August 20, 2010

slides. Prior to confocal microscopy (Sarastro 2000; Molecular Dynamics, Sunnyvale, CA, USA), the roots were stained with 10 μM propidium iodide, and GFP and propidium iodide fluorescence was further detected as described in Ottenschläger et al. (2003).

Quantitative real-time PCR

ipt expression was induced by 10 μM DEX at two different time intervals. Total RNA was isolated from the whole DEX-induced as well as control seedlings through the use of TRIzol® Reagent (Invitrogen, Carlsbad, CA, USA). The samples were treated with DNase (Ambion, Austin, TX, USA) prior to cDNA synthesis, which was carried out in the presence of oligo(dT) primer and Superscript II reverse transcriptase (Invitrogen, Carlsbad, CA, USA). To quantify *ipt* and actin gene expression, real-time PCR was performed using Rotor-Gene-3000 equipment and software (Corbett Research, Biocompare, Inc., San Francisco, CA, USA). Taq DNA polymerase (Top Bio, Praha, Czech Republic) was used for DNA amplification. The detection of increasing numbers of amplicons was based on the fluorescence of the DNA intercalator SYBR® Green I (Molecular Probes™, Invitrogen, Carlsbad, CA, USA). *Ipt* expression levels were normalized to *ACTIN2* and *ACTIN8* levels. The sequences of the PCR primers were as follows: forward primer recognizing *ACTIN2* and *8*, 5′-GGT GAT GGT GTG TCT-3′; reverse primer recognizing *ACTIN2* and *8*, 5′-ACT GAG CAC AAT GTT AC-3′; *ipt* forward primer, 5′-ATC CTC CCT CAA GAA TAA GC-3′; *ipt* reverse primer, 5′-CTG AAA GGA ACG ACG C-3′.

Extraction, purification and quantitative analysis of CKs

CK extraction, purification and quantitation were performed as described in Lexa et al. (2003) with some minor modifications (see Supplementary material). A total of 27 substances were measured in CK extracts of DEX-treated as well as control *CaMV 35S>GR>ipt* individuals (see Supplementary Table S1). The mean values of biologically active CKs (grouped as free bases, ribosides and riboside phosphates), biologically inactive CK conjugates (*O*-glucosides, *N*-7-glucosides and *N*-9-glucosides), and those classified as iP-type and Z-type CK metabolites are presented in Fig. 5.

Supplementary material

Supplementary material mentioned in the article is available to online subscribers at the journal website www.pcp.oxfordjournals.org.

Funding

Ministry of Education, Youth and Sport of the Czech Republic (LC06034, MSM0021622415); the Academy of Sciences of the Czech Republic (AVOZ50040507); the Grant Agency of the Academy of Sciences of the Czech Republic (IAA600380507).

Acknowledgments

We are indebted to Ian Moore and Markéta Šámalová for their kind gift of the *A. thaliana* lines allowing *CaMV 35S>GR>ipt* and *CaMV 35S>GR>uidA* transactivation. We thank Eva Benková and Jiří Friml for kindly providing us with the *DR5::GUS* and *DR5rev::GFP* lines. We are grateful to Jiří Široký and Boris Vyskot for great technical help and for allowing us to use laser confocal microscopy equipment and Přemysl Souček for his help with quantitative real-time PCR. We are grateful to Ian Moore and Jiří Friml for helpful comments and expert advice.

References

Åstot, C., Doležal, K., Nordström, A., Wang, Q., Kunkel, T., Moritz, T., Chua, N.H. and Sandberg, G. (2000) An alternative cytokinin biosynthesis pathway. *Proc. Natl Acad. Sci. USA* 97: 14778–14783.

Beeckman, T., Burssens, S. and Inzé, D. (2001) The peri-*cell*-cycle in *Arabidopsis*. *J. Exp. Bot* 52: 403–411.

Beemster, G.T.S. and Baskin, T.I. (2000) *STUNTED PLANT1* mediates effects of cytokinin, but not of auxin, on cell division and expansion in the root of Arabidopsis. *Plant Physiol* 124: 1718–1727.

Benková, E., Michniewicz, M., Sauer, M., Teichmann, T., Seifertová, D., Jürgens, G. and Friml, J. (2003) Local, efflux-dependent auxin gradients as a common module for plant organ formation. *Cell* 115: 591–602.

Bhalerao, R.P., Eklöf, J., Ljung, K., Marchant, A., Bennett, M. and Sandberg, G. (2002) Shoot-derived auxin is essential for early lateral root emergence in *Arabidopsis* seedlings. *Plant J* 29: 325–332.

Blakely, L.M., Blakely, R.M., Colowit, P.M. and Elliott, D.S. (1988) Experimental studies on lateral root formation in radish seedling roots. *Plant Physiol* 87: 414–419.

Casimiro, I., Marchant, A., Bhalerao, R.P., Beeckman, T., Dhooge, S., Swarup, R., Graham, N., Inzé, D., Sandberg, G., Casero, P.J. and Bennett, M. (2001) Auxin transport promotes *Arabidopsis* lateral root initiation. *Plant Cell* 13: 843–852.

Casimiro, I., Beeckman, T., Graham, N., Bhalerao, R., Zhang, H., Casero, P., Sandberg, G. and Bennett, M.J. (2003) Dissecting *Arabidopsis* lateral root development. *Trends Plant Sci* 8: 165–171.

Craft, J., Šámalová, M., Baroux, C., Townley, H., Martinez, A., Jepson, I., Tsiantis, M. and Moore, I. (2005) New pOp/LhG4 vectors for stringent glucocorticoid-dependent transgene expression in *Arabidopsis*. *Plant J* 41: 899–918.

De Smet, Dubrovsky, J.G., Gambetta, G.A., Hernández-Barrera, A., Shishkova, S. and González, I. (2006) Lateral root initiation in *Arabidopsis*: developmental window, spatial patterning, density and predictability. *Ann. Bot* 97: 903–915.

De Smet, Tetsumura, T., Rybel, B.D., Frei dit Frey, N., Laplaze, L., et al. (2007) Auxin-dependent regulation of lateral root positioning in the basal meristem of *Arabidopsis*. *Development* 134: 681–690.

Eklöf, S., Åstot, C., Sitbon, F., Moritz, T., Olsson, O. and Sandberg, G. (2000) Transgenic tobacco plants co-expressing *Agrobacterium iaa* and *ipt* genes have wild-type hormone levels but display both auxin- and cytokinin-overproducing phenotypes. *Plant J* 23: 279–284.

Faiss, M., Zalubilová, J., Strnad, M. and Schmülling, T. (1997) Conditional transgenic expression of the *ipt* gene indicates a function for cytokinins in paracrine signaling in whole tobacco plants. *Plant J* 12: 401–415.

Ferreira, F.J. and Kieber, J.J. (2005) Cytokinin signaling. *Curr. Opin. Plant Biol* 8: 518–525.

Friml, J., Benková, E., Blilou, I., Wisniewska, J., Hamann, T., Ljung, K., Woody, S., Sandberg, G., Scheres, B., Jürgens, G. and Palme, K. (2002) AtPIN4 mediates sink-driven auxin gradients and root patterning in *Arabidopsis*. *Cell* 108: 661–673.

Friml, J. (2003) Auxin transport—shaping the plant. *Curr. Opin. Plant Biol* 6: 7–12.

Hewelt, A., Prinsen, E., Schell, J., Van Onckelen, H. and Schmülling, T. (1994) Promoter tagging with a promoterless *ipt* gene leads to cytokinin-induced phenotypic variability in transgenic tobacco plants: implications of gene dosage effects. *Plant J* 6: 879–891.

Higuchi, M., Pischke, M.S., Mahonen, A.P., Miyawaki, K., Hashimoto, Y., et al. (2004) In planta functions of the *Arabidopsis* cytokinin receptor family. *Proc. Natl Acad. Sci. USA* 101: 8821–8826.

Hutchison, C.E., Li, J., Argueso, C., Gonzalez, M., Lee, E., et al. (2006) The *Arabidopsis* histidine phosphotransfer proteins are redundant positive regulators of cytokinin signaling. *Plant Cell* 18: 3073–3087.

Downloaded from http://pcp.oxfordjournals.org at Masaryk University on August 20, 2010

Ioio, R.D., Linhares, F.S., Scacchi, E., Casamitjana-Martinez, E., Heidstra, R., Costantino, P. and Sabatini, S. (2007) Cytokinins determine *Arabidopsis* root-meristem size by controlling cell differentiation. *Curr. Biol* 17: 678–682.

Kunkel, T., Niu, Q.W., Chan, Y.S. and Chua, N.H. (1999) Inducible isopentenyl transferase as a high-efficiency marker for plant transformation. *Nat. Biotechnol* 17: 916–919.

Laplaze, L., Benkova, E., Casimiro, I., Maes, L., Vanneste, S., et al. (2007) Cytokinins act directly on lateral root founder cells to inhibit root initiation. *Plant Cell* 19: 3889–3900.

Laskowski, M.J., Williams, M.E., Nusbaum, H.C. and Sussex, I.M. (1995) Formation of lateral root meristems is a two-stage process. *Development* 121: 3303–3310.

Lexa, M., Genkov, T., Malbeck, J., Macháčková, I. and Brzobohatý, B. (2003) Dynamics of endogenous cytokinin pools in tobacco seedlings: a modelling approach. *Ann. Bot* 91: 585–597.

Li, X., Mo, X., Shou, H. and Wu, P. (2006) Cytokinin-mediated cell cycling arrest of pericycle founder cells in lateral root initiation of *Arabidopsis*. *Plant Cell Physiol* 47: 1112–1123.

Lohar, D.P., Schaff, J.E., Laskey, J.G., Kieber, J.J., Bilyeu, K.D. and Bird, D.M. (2004) Cytokinins play opposite roles in lateral root formation, and nematode and rhizobial symbioses. *Plant J* 38: 203–214.

Malamy, J.E. and Benfey, P.N. (1997) Organization and cell differentiation in lateral roots of *Arabidopsis thaliana*. *Development* 124: 33–44.

McKenzie, M.J., Mett, V.V., Stewart Reynolds, P.H. and Jameson, P.E. (1998) Controlled cytokinin production in transgenic tobacco using a copper-inducible promoter. *Plant Physiol* 116: 969–977.

Medford, J.I., Horgan, R.H., El-Sawi, Z. and Klee, H.J. (1989) Alterations of endogenous cytokinins in transgenic plants using a chimeric isopentenyl transferase gene. *Plant Cell* 1: 403–413.

Miyawaki, K., Matsumoto-Kitano, M. and Kakimoto, T. (2004) Expression of cytokinin biosynthetic isopentenyltransferase genes in *Arabidopsis*: tissue specificity and regulation by auxin, cytokinin and nitrate. *Plant J* 37: 128–138.

Moore, I., Šámalová, M. and Kurup, S. (2006) Transactivated and chemically inducible gene expression in plants. *Plant J* 45: 651–683.

Nishimura, C., Ohashi, Y., Sato, S., Kato, T., Tabata, S. and Ueguchi, C. (2004) Histidine kinase homologs that act as cytokinin receptors possess overlapping functions in the regulation of shoot and root growth in *Arabidopsis*. *Plant Cell* 16: 1365–1377.

Nordström, A., Tarkowski, P., Tarkowska, D., Norbaek, R., Åstot, C., Doležal, K. and Sandberg, G. (2004) Auxin regulation of cytokinin biosynthesis in *Arabidopsis thaliana*: a factor of potential importance for auxin–cytokinin-regulated development. *Proc. Natl Acad. Sci. USA* 101: 8039–8044.

Ottenschläger, I., Wolff, P., Wolverton, C., Bhalerao, R.P., Sandberg, G., Ishikawa, H., Evans, M. and Palme, K. (2003) Gravity-regulated differential auxin transport from columella to lateral root cap cells. *Proc. Natl Acad. Sci. USA* 100: 2987–2991.

Petrášek, J., Mravec, J., Bouchard, R., Blakeslee, J.J., Abas, M., et al. (2006) PIN proteins perform a rate-limiting function in cellular auxin efflux. *Science* 312: 914–918.

Rashotte, A.M., Chae, H.S., Maxwell, B.B. and Kieber, J.J. (2005) The interaction of cytokinin with other signals. *Physiol. Plant* 123: 184–194.

Reed, R.C., Brady, S.R. and Muday, G.K. (1998) Inhibition of auxin movement from the shoot into the root inhibits lateral root development in *Arabidopsis*. *Plant Physiol* 118: 1369–1378.

Riefler, M., Novák, O., Strnad, M. and Schmülling, T. (2006) *Arabidopsis* cytokinin receptor mutants reveal functions in shoot growth, leaf senescence, seed size, germination, root development, and cytokinin metabolism. *Plant Cell* 18: 40–54.

Růžička, K., Ljung, K., Vanneste, S., Podhorská, R., Beeckman, T., Friml, J. and Benková, E. (2007) Ethylene regulates root growth through effects on auxin biosynthesis and transport-dependent auxin distribution. *Plant Cell* 19: 2197–2212.

Sabatini, S., Beis, D., Wolkenfelt, H., Murfett, J., Guilfoyle, T., Malamy, J., Benfey, P., Leyser, O., Bechtold, N., Weisbeek, P. and Scheres, B. (1999) An auxin-dependent distal organizer of pattern and polarity in the *Arabidopsis* root. *Cell* 99: 463–472.

Smigocki, A.C. (1991) Cytokinin content and tissue distribution in plants transformed by a reconstructed isopentenyl transferase gene. *Plant Mol. Biol* 16: 105–115.

Swarup, R., Parry, G., Graham, N., Allen, T. and Bennett, M. (2002) Auxin cross-talk: integration of signalling pathways to control plant development. *In* Plant Molecular Biology. Edited by Perrot-Rechenmann, C. and Hagen, G. vol. 49. pp. 411–426. Kluwer Academic Publishers, Dordrecht, The Netherlands.

Swarup, R., Perry, P., Hagenbeek, D., Van Der Straeten, D., Beemster, G.T., Sandberg, G., Bhalerao, R., Ljung, K. and Bennett, M.J. (2007) Ethylene upregulates auxin biosynthesis in *Arabidopsis* seedlings to enhance inhibition of root cell elongation. *Plant Cell* 19: 2186–2196.

Takei, K., Ueda, N., Aoki, K., Kuromori, T., Hirayama, T., Shinozaki, K., Yamaya, T. and Sakakibara, H. (2004) AtIPT3 is a key determinant of nitrate-dependent cytokinin biosynthesis in *Arabidopsis*. *Plant Cell Physiol* 45: 1053–1062.

To, J.P., Haberer, G., Ferreira, F.J., Deruere, J., Mason, M.G., Schaller, G.E., Alonso, J.M., Ecker, J.R. and Kieber, J.J. (2004) Type-A *Arabidopsis* response regulators are partially redundant negative regulators of cytokinin signaling. *Plant Cell* 16: 658–671.

Ulmasov, T., Murfett, J., Hagen, G. and Guilfoyle, T.J. (1997) Aux/IAA proteins repress expression of reporter genes containing natural and highly active synthetic auxin response elements. *Plant Cell* 9: 1963–1971.

Werner, T., Motyka, V., Laucou, V., Smets, R., Van Onckelen, H. and Schmülling, T. (2003) Cytokinin-deficient transgenic *Arabidopsis* plants show multiple developmental alterations indicating opposite functions of cytokinins in the regulation of shoot and root meristem activity. *Plant Cell* 15: 2532–2550.

Yang, S., Yu, H., Xu, Y. and Goh, C.J. (2003) Investigation of cytokinin-deficient phenotypes in *Arabidopsis* by ectopic expression of orchid DSCKX1. *FEBS Lett* 555: 291–296.

(Received December 1, 2007; Accepted February 18, 2008)

Downloaded from http://pcp.oxfordjournals.org at Masaryk University on August 20, 2010

Supplemental Data, Kuderova et al.

Supporting data

Expression of DEX-induced *CaMV 35S>GR>uidA* transactivation preferentially occurs in the more differentiated part of the primary root

To identify spatial specificity of the *CaMV 35S>GR>ipt* transactivation, we have inspected GUS activity in plants carrying *uidA* under control of pOp promoter in the identical genetic background (plants homozygous for *CaMV 35S::LhGR*) used for the *CaMV 35S>GR>ipt* transactivation. In six-day-old seedlings after continuous DEX-treatment, maximal β-GLUCURONIDASE (GUS) activity was found in the older part of the root, extending but weakening towards the root apex (Fig. S1). While all cell files of the older part of the root exhibited strong GUS activity (Fig. S1B, F, G), the staining was more pronounced in the vascular tissues of the younger part of the root (Fig. S1C, D, H), where it gradually weakened and disappeared (Fig. S1A). Unlike the less stringent conditions of GUS product localization (Fig. S1B-E), the presence of 2.5 mM $K_3[Fe(CN)_6]$ and 2.5 mM $K_4[Fe(CN)_6]$ (preventing secondary diffusion of GUS product) in the substrate solution (Fig. S1A, F-I) resulted in a relatively weak signal in a number of developing LRP compared with other cell files of the primary root. After emergence, the developing meristems of the LRs and the primary root meristem were void of the signal (Fig. S1E, G, I). A sharp boundary was visible at the root/shoot junction (Fig. S1J), most likely reflecting the uptake of DEX by root hairs and root epidermal cells, its subsequent penetration to lower cell files, and its further distribution through vascular tissues to the rest of the root as well as to the hypocotyl (Fig. S1K) and the rest of the aerial part of the seedling (Fig. S1L-N). The initiation at root/shoot junction and spatial localization of this *pOp::uidA*

expression pattern was unchanged when screened soon after germination or induced temporarily between day 2 and 3 or between day 5 and 6 after germination (not shown).

Supplementary materials and methods

Extraction, purification, and quantitative analysis of CKs

Detection and quantitation were carried out using an HPLC/MS system consisting of an HTS-Pal auto-sampler with a cooled sample stack (CTC Analytics, Zwingen, Switzerland), quaternary HPLC pump (Rheos 2200, Flux Instruments, Basel, Switzerland), Delta Chrom CTC 100 Column oven (Watrex, Praha, CR), and TSQ Quantum Ultra AM triple-quad high resolution mass spectrometer (Thermo Electron, San Jose, USA) equipped with an electrospray interface. The dried extract was re-dissolved in diluted acetonitrile and filtered. A 5 µl aliquot was injected onto a C_{18} HPLC Synergy Hydro-RP column, 250×2 mm, 4 µm (Phenomenex, Torrance, USA) and analyzed using ternary gradient elution (water/acetonitrile/0.01% acetic acid) starting at 8% acetonitrile for 5 min, followed by increase in acetonitrile to 15% for 10 min, and subsequently to 50% for 11 min. The proportion of 0.01% acetic acid was maintained at 25% throughout the analysis. The rest of the sample was removed from the column by increasing the content of acetonitrile to 90% for 9 min. Before the next injection, the column was equilibrated using 8% acetonitrile for 20 min. The mass spectrometer was operated in the positive SRM (single reaction monitoring) mode with monitoring of 2 to 4 transitions for each compound. The most intensive ion was used for quantification and the rest was used for identity confirmation. CKs were quantified using a multilevel calibration graph with [^{2}H] labeled cytokinins

as internal standards. The detection limits of different cytokinins varied from 0.05 to 0.1 pmol/sample.

Statistical analyses

We used the Kruskal-Wallis test to compare the values of continuous parameters among samples (groups) followed by multiple comparisons when significant differences were found among samples. To compare the values of parameters between only two samples (groups), the Mann-Whitney U test was used. When appropriate (normal distribution of data, homogeneity of variances), the parametric t-test and ANOVA followed by the Tuckey post-hoc test were used to compare values among two or more groups, respectively. The Bonferonni correction was used to cope with multiple usage of the Mann-Whitney U test when comparing proportional values of groups of CKs. The χ^2 goodness-of-fit was used to analyze the dependence of two categorical parameters (i.e. number of LRP in different growth stages in two groups of seedlings, number of different types of stained LRP in two groups, etc.). Data analyses were performed using Microsoft EXCEL 2002 and Statistical software for Windows 7.1.

Supplementary figure legends

Figure S1. *pOp::GUS* expression pattern at 6 DAG of seedlings subjected to the *CaMV 35S>GR>uidA* transactivation. (A) The whole seedling. (B-I) Details of root sections viewed sequentially in the direction from the root/shoot junction to the root tip; (B-E) less or (F-I) more stringent conditions of GUS product localization. By lower stringency is meant treatment of seedlings with substrate solution lacking $K_3[Fe(CN)_6]/K_4[Fe(CN)_6]$. By higher stringency is meant

preventing potential secondary GUS product diffusion by adding $K_3[Fe(CN)_6]/K_4[Fe(CN)_6]$ to the substrate solution (see Materials and methods). (J) Root/shoot junction, (K) hypocotyl, (L) shoot apical meristems, (M) cotyledon vasculature, and (N) the tip of cotyledon. In (A) and (J-N) more stringent conditions were applied. Scale bars: 1 mm (A) and 25 μm (B-N).

Figure S2. Comparison of the relative distribution of (-) uninduced and (+) induced endogenous CKs extracted from seedlings of the *CaMV 35S>GR>ipt* line of *A. thaliana* that were subjected to a transient pulse of *ipt* overexpression between the 2nd and 3rd DAG (early) and between the 5th and 6th DAG (late). CKs are arranged in various categories in terms of their biological relevance. (A) Proportion of biologicaly active CKs to their conjugated forms was significantly higher in uninduced controls (-) compared with CK overproducing individuals (+) after early ipt pulse (Mann-Whitney U test, N = 10, P = 0.011). Other differences were not significant. (B) Proportion of the iP-type- to Z-type CKs was significantly higher at early than at late stage in *IPT*-overexpressing seedlings (Mann-Whitney U test, N = 11, P = 0.006). Other differences were not significant. (C) Proportion of ribosides and free bases to nucleotide phosphates were not significantly different between early and late ipt pulse. (D) Proportion of N-7-glucosides to other conjugates was significantly higher at early than at late stage in *IPT*-overexpressing seedlings (Mann-Whitney U test, N = 12, respectively, P = 0.006). (E) Significantly lower proportion of the CKX-degradable- to CKX-nondegradable CKs was found in uninduced control at early than at late stage (Mann-Whitney U test, N = 10, P = 0.011). (CK conjugates) inactive reversibly conjugated *O*-glucosides and irreversibly inactivated *N*-7- or *N*-9- glucosides;

(active CKs) biologically active free bases, ribosides and ribotides (riboside phosphates); (Z-type CKs) *cis*- or *trans*-zeatin in the form of free bases, ribosides, ribotides and CK conjugates; (iP-type CKs) isopentenyl adenine in the form of free bases, ribosides, ribotides and CK conjugates; (phosphates) riboside phosphates;(bases) free bases; (CKs degradable by CKXs) isopentenyl adenine and *trans*-zeatin in the form of free bases and ribosides; (CKs nondegradable by CKXs) *cis*-zeatin and dihydrozeatin in the form of free bases and ribosides; for detailed terminology see Tab. S1 and the legend to Tab. S1.

Table S1. Endogenous CK levels in seedlings of the *CaMV 35S>GR>ipt* line of *A. thaliana* subjected to the "early" (3) or "late" (6) transient 24 h pulse of *ipt* overexpression; DEX-induced (+) or uninduced (-) CK levels; values represent the mean of LC/MS/MS measurements of CK metabolites arranged and grouped as biologically active free bases, ribosides (R), and ribotides (riboside phosphates, RP), inactive reversibly conjugated *O*-glucosides (OG), irreversibly inactivated *N*-7- (7G) or *N*-9- (9G) glucosides, and *trans*-zeatin (tZ)- and isopentenyl adenine (iP)-type CKs; *cis*-zeatin (cZ), dihydrozeatin (DHZ); DHZ7G-1 and DHZ7G-2 are enantiomers of dihydrozeatin *N*-7-glucoside.

Supplementary figures and tables

Figure S1, Kuderová et al.

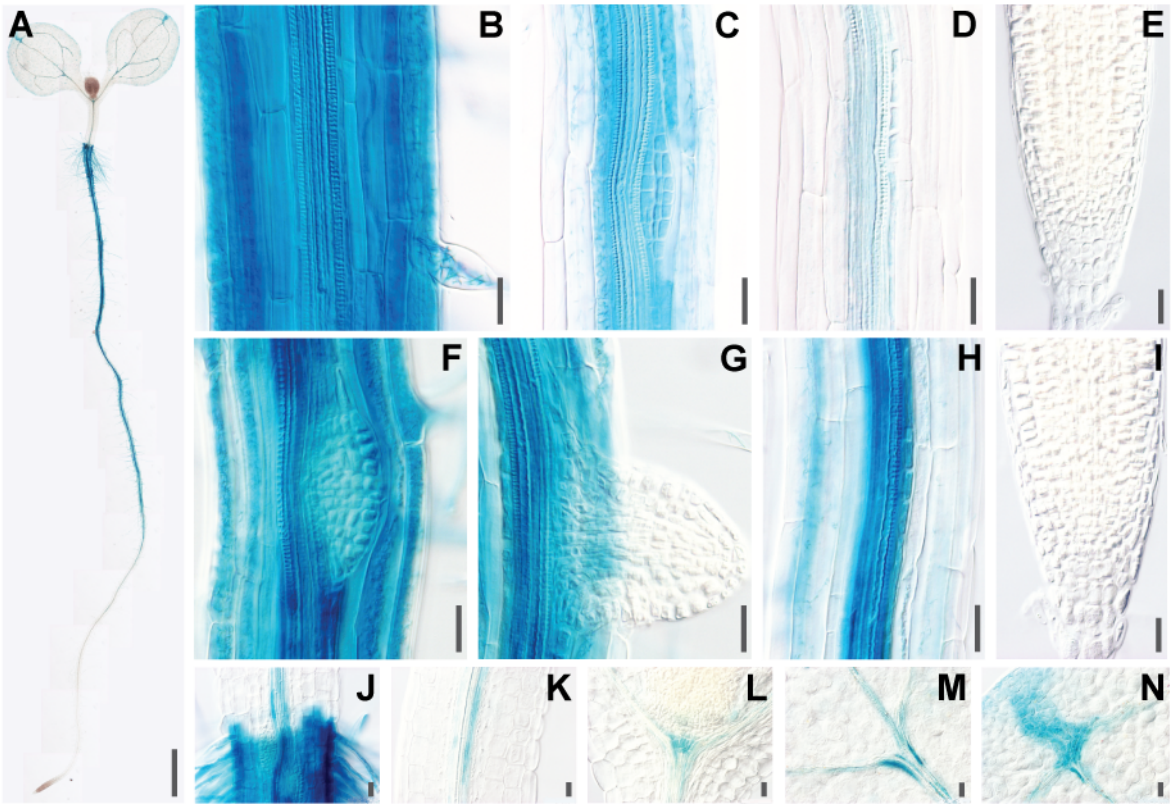

Figure S2, Kuderova et al.

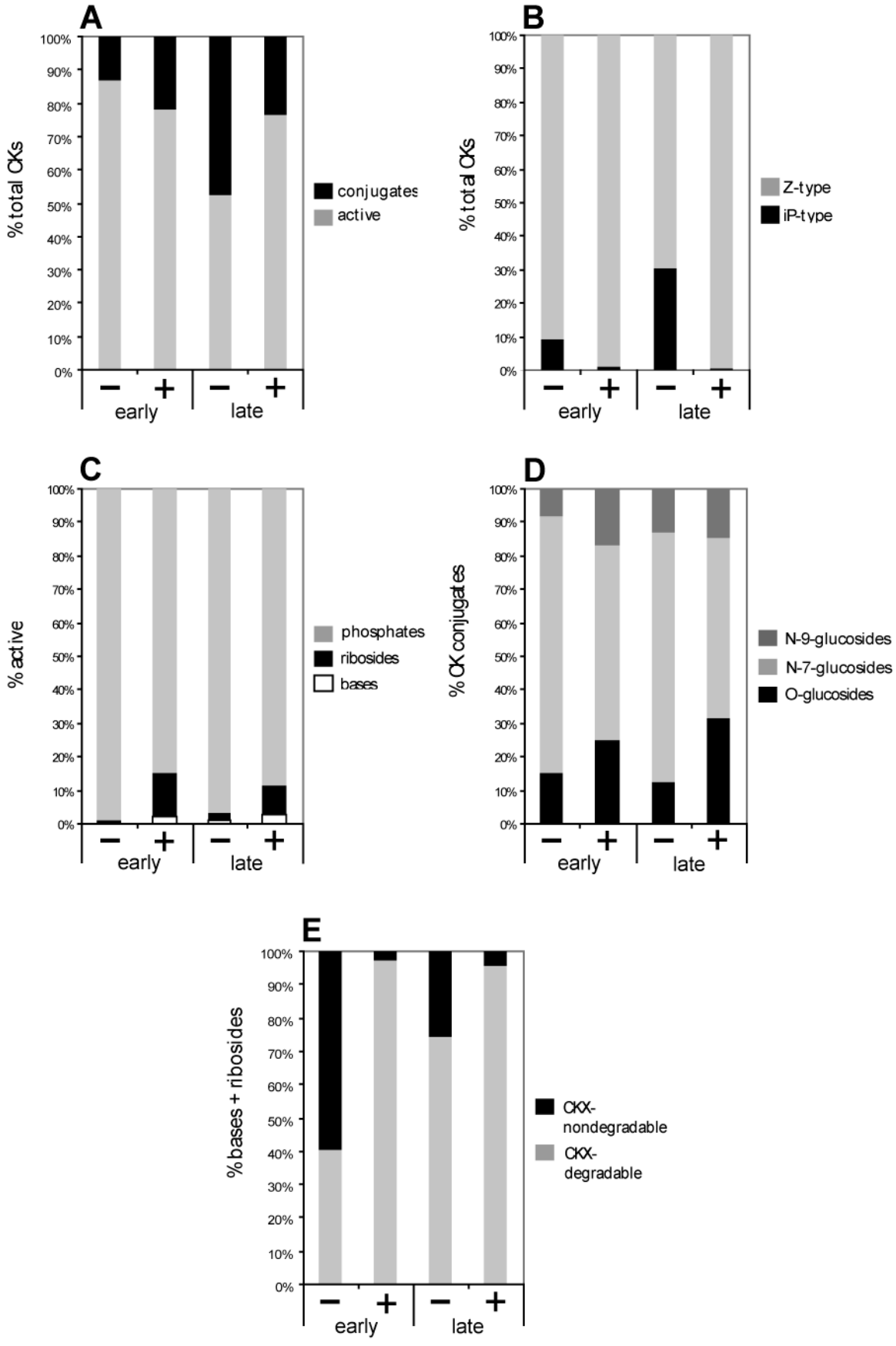

Table S1, Kuderova et al.

		bases				ribosides				phosphates		
(-)3		iP	tZ	cZ	DHZ	iPR	ZR	cZR	DHZR	iPRP	ZRP	cZRP
	Valid N	4	4	4	4	4	4	4	4	4	4	2
	Mean	0,118	0,6	0	0,09	0,35	0,39	1,87	0,112	7,8	285	16
	Confidence	-0,144	-0,5		-0,19	-0,34	-0,35	0,65	-0,215	-2,8	195	
	Confidence	0,380	1,6		0,36	1,04	1,13	3,08	0,439	18,4	375	
	Std.Dev.	0,164	0,6	0	0,17	0,43	0,47	0,76	0,206	6,7	57	0
(+)3												
	Valid N	6	6	6	6	6	6	6	6	8	8	7
	Mean	0,3	65	0,06	0,57	2,4	342	2,43	9,6	14,4	2250	22
	Confidence	-0,4	52	-0,09	0,30	1,5	306	1,06	7,1	11,2	2005	13
	Confidence	0,9	77	0,21	0,83	3,2	377	3,80	12,1	17,7	2495	31
	Std.Dev.	0,6	12	0,15	0,25	0,8	34	1,30	2,4	3,9	293	10
(-)6												
	Valid N	6	6	6	6	6	6	6	6	4	4	4
	Mean	0,24	0,726	0,0444	0	0,530	0,83	0,76	0	23	62	3,7
	Confidence	-0,15	0,101	-0,0665		-0,162	-0,03	0,20		21	33	2,0
	Confidence	0,64	1,351	0,1553		1,221	1,69	1,31		26	92	5,4
	Std.Dev.	0,38	0,595	0,1056	0	0,659	0,82	0,53	0	2	18	1,1
(+)6												
	Valid N	6	6	6	6	6	6	6	6	12	10	10
	Mean	0,11	233	0,4482	11,3	0,430	853	2,3	38	31	8570	27
	Confidence	-0,17	190	-0,3385	7,3	-0,004	800	0,6	33	26	7316	20
	Confidence	0,38	276	1,2348	15,3	0,863	907	3,9	43	36	9824	35
	Std.Dev.	0,26	41	0,7496	3,8	0,413	51	1,6	5	8	1752	10

	O-glucosides						N-7-glucosides					
(-)3	DHZRP	ZOG	cZOG	DHZOG	ZROG	cZROG	DHZROG	iP7G	Z7G	cZ7G	DHZ7G-1	DHZ7G-2
	2	4	4	4	4	4	4	4	4	4	4	4
	4,0	5,2	1,17	0,42	0,3	0	0,04	23	12	0	0,55	0,07
	-13,2	3,9	-1,79	-0,38	-0,7		-0,09	20	6		-0,04	-0,15
	21,1	6,4	4,12	1,22	1,4		0,17	27	19		1,14	0,29
	1,9	0,8	1,86	0,50	0,7	0	0,08	2	4	0	0,37	0,14
(+)3												
	8	6	6	6	6	6	6	6	6	6	6	6
	46	175	0,83	2,2	12	0,14	0,27	20	413	0	9,2	2,14
	40	150	-0,37	1,4	10	-0,22	-0,07	16	380		7,4	1,04
	52	200	2,02	2,9	14	0,50	0,62	24	446		10,9	3,23
	7	23	1,14	0,7	2	0,34	0,33	4	31	0	1,7	1,04
(-)6												
	4	4	6	6	6	6	6	6	4	6	3	6
	1,186	9,2	1,6	0,62	0,43	0	0,02	32	28	0,4	1,6	0,04
	-0,639	5,9	-2,5	0,18	-0,41		-0,04	28	25	-0,6	1,2	-0,05
	3,011	12,5	5,6	1,07	1,27		0,08	36	30	1,4	1,9	0,12
	1,147	2,1	3,8	0,42	0,80	0	0,06	4	1	0,9	0,2	0,09
(+)6												
	10	6	6	6	6	6	6	6	6	6	6	6
	252	768	1,1	46	109	0	3,3	24	1433	0	92	54
	218	595	-1,8	31	92		2,4	22	1348		69	38
	286	942	4,0	61	126		4,3	26	1519		115	70
	48	165	2,8	14	16	0	0,9	2	82	0	22	15

	N-9-glucosides												
(-)3	iP9G	Z9G	cZ9G	DHZ9G	bases	ribosides	phosphates	glucosides	glucosides	glucosides	total CKs	active CKs	conjugates
	4	4	4	4	4	4	4	4	4	4	4	4	4
	1,07	2,1	0	0,56	0,753	2,717	302,8	7,10	36,20	3,73	353,295	306,270	47,03
	0,34	-1,8		0,04	-0,082	0,802	206,0	2,17	28,28	-0,02	267,611	209,428	35,57
	1,81	6,0		1,08	1,588	4,632	399,6	12,03	44,11	7,48	438,979	403,113	58,48
	0,46	2,4	0	0,33	0,524	1,203	60,8	3,10	4,98	2,36	53,848	60,860	7,20

	N-9-glucosides				grouped CKs								
(+)3	iP9G	Z9G	cZ9G	DHZ9G	bases	ribosides	phosphates	glucosides	glucosides	glucosides	total CKs	active CKs	conjugates
	6	6	6	6	6	6	8	6	6	6	6	6	6
	0,69	127	0,1	1,06	65,38	356,05	2329,8	190,39	444,45	128,51	3491,69	2728,34	763,35
	0,00	116	-0,1	0,28	52,20	318,28	2082,0	166,79	410,23	117,35	3138,50	2377,46	708,06
	1,38	138	0,3	1,85	78,55	393,81	2577,6	213,99	478,67	139,66	3844,88	3079,22	818,64
	0,66	10	0,2	0,75	12,56	35,98	296,4	22,49	32,61	10,63	336,55	334,35	52,69

	N-9-glucosides												
(-)6	iP9G	Z9G	cZ9G	DHZ9G	bases	ribosides	phosphates	glucosides	glucosides	glucosides	total CKs	active CKs	conjugates
	6	4	6	6	6	6	4	4	4	4	2	4	3
	1,22	8,8	0,4	0,353	1,0119	2,115	90,386	10,14	60,88	10,836	191,3383	93,3786	84,702
	0,32	4,6	-0,3	-0,108	0,7341	1,111	60,321	6,30	52,42	4,567	145,3640	64,6956	75,819
	2,13	12,9	1,1	0,813	1,2897	3,119	120,451	13,99	69,34	17,105	237,3125	122,0616	93,584
	0,86	2,6	0,7	0,438	0,2647	0,957	18,894	2,42	5,32	3,940	5,1170	18,0258	3,576

	N-9-glucosides												
(+)6	iP9G	Z9G	cZ9G	DHZ9G	bases	ribosides	phosphates	glucosides	glucosides	glucosides	total CKs	active CKs	conjugates
	6	6	6	6	6	6	10	6	6	6	6	6	6
	1,57	418	0	15	245,2048	893,847	8879	927,6	1603	434,41	12753,7563	9788,3847	2965,37
	0,97	317		10	199,0556	838,116	7620	726,3	1497	328,57	10355,8980	7595,9401	2585,30
	2,17	520		19	291,3540	949,577	10139	1129,0	1710	540,24	15151,6146	11980,8292	3345,44
	0,57	97	0	4	43,9753	53,105	1760	191,9	102	100,85	2284,9027	2089,1653	362,17

ZR + ZRP	P-type CKs	Z-type CKs
4	4	4
285,94	32,613	320,682
196,21	20,703	223,205
375,67	44,523	418,159
56,39	7,485	61,259

ZR + ZRP	P-type CKs	Z-type CKs
6	6	5
2640	38,39	3576,11
2294	31,58	3368,43
2985	45,19	3783,78
329	6,48	167,26

ZR + ZRP	P-type CKs	Z-type CKs
4	4	2
63,834	58,015	134,1383
34,123	54,921	65,2929
93,545	61,109	202,9836
18,672	1,944	7,6626

ZR + ZRP	P-type CKs	Z-type CKs
6	6	6
9437	55,275	12698,4815
7255	45,554	10305,3009
11619	64,996	15091,6621
2079	9,263	2280,4453

Enclosed Publication # 10

Benková, E. and **Hejátko, J.** (2009) Hormone interactions at the root apical meristem. *Plant Molecular Biology*, **69**, 383-396. IF_{2008}= 3.541

Plant Mol Biol (2009) 69:383–396
DOI 10.1007/s11103-008-9393-6

Hormone interactions at the root apical meristem

Eva Benková · Jan Hejátko

Received: 23 May 2008 / Accepted: 27 August 2008 / Published online: 19 September 2008
© Springer Science+Business Media B.V. 2008

Abstract Plants exhibit an amazing developmental flexibility. Plant embryogenesis results in the establishment of a simple apical–basal axis represented by apical shoot and basal root meristems. Later, during postembryonic growth, shaping of the plant body continues by the formation and activation of numerous adjacent meristems that give rise to lateral shoot branches, leaves, flowers, or lateral roots. This developmental plasticity reflects an important feature of the plant's life strategy based on the rapid reaction to different environmental stimuli, such as temperature fluctuations, availability of nutrients, light or water and response resulting in modulation of developmental programs. Plant hormones are important endogenous factors for the integration of these environmental inputs and regulation of plant development. After a period of studies focused primarily on single hormonal pathways that enabled us to understand the hormone perception and signal transduction mechanisms, it became obvious that the developmental output mediated by a single hormonal pathway is largely modified through a whole network of interactions with other hormonal pathways. In this review, we will summarize recent knowledge on hormonal networks that regulate the development and growth of root with focus on the hormonal interactions that shape the root apical meristem.

E. Benková (✉)
Department of Plant Systems Biology, Flanders Institute for Biotechnology (VIB), Gent University, Technologiepark 927, 9052 Gent, Belgium
e-mail: eva.benkova@psb.ugent.be

J. Hejátko
Laboratory of Molecular Plant Physiology, Department of Functional Genomics and Proteomics, Institute of Experimental Biology, Masaryk University, Kamenice 5 62500, Brno, Czech Republic

Keywords Root meristem · Hormonal cross-talk · Abscisic acid · Auxin · Brassinosteroid · Cytokinin · Ethylene · Gibberellin · *Arabidopsis*

Introduction: *when root grows*

The root meristem is an organ of well-defined structure with stereotypical patterns of cell types along radial and longitudinal axes. The radial pattern is organized in concentric rings of lateral root cap, epidermis, ground tissue (cortex and endodermis) and a pericycle surrounding a central stele (Dolan et al. 1993; van den Berg et al. 1998). The radial patterning is laid down during embryogenesis and maintained by stem cell niche activity consisting of four sets of initials: the lateral root cap/epidermal, the cortical/endodermal, the columella and the pericycle/vascular initials surrounding quiescent centre (QC) (Dolan et al. 1993; van den Berg et al. 1998). Stem cells have the capacity for prolonged self-renewal (Watt and Hogan 2000). Each stem cell undergoes an asymmetric division to produce one daughter cell that remains under the influence of a short-range signal from the QC, preventing differentiation and maintaining the stem cell status and the other daughter cell becomes part of differentiated tissues (van den Berg et al. 1998).

Along the longitudinal axis, the root meristem forms a distal root tip, including stem cell niche, columella and lateral root cap, proximal meristem with a population of rapidly dividing cells and elongation zone where cells leaving the root meristem undergo rapid elongation and mature (Dolan et al. 1993). The longitudinal root meristem organization is completed during the postembryonic development when the balance in the rate of generation of new cells in the proximal root meristem and the

differentiation of daughter cells leaving root meristem is established, resulting in the formation of the root meristem of stable size (Dello Ioio et al. 2007; Dolan et al. 1993).

The identification of mutants with defects in the root meristem organization has provided a basis for understanding the mechanisms of radial and longitudinal patterning in the root. Organization of root meristem along the longitudinal axis is primarily under the control of the plant hormone auxin and of the downstream auxin-acting family of *PLETHORA* (*PLT*) (AP2-like transcription factors) genes. The *PLT* expression follows the auxin gradient along the root meristem with its maxima in the stem cell niche region. *PLT* genes have been shown to act in a dosage dependent manner, high activity promotes stem cell identity and maintenance, whereas low levels promote mitotic activity of stem cell daughters; and even lower levels are required for cell differentiation (Aida et al. 2004; Galinha et al. 2007).

In parallel with the auxin and PLT pathway, the SHORTROOT/SCARECROW (SHR/SCR) pathway regulates the radial patterning, and they converge to specify and regulate function of the stem cell niche. Plants homozygous for the *scr* and *shr* mutations are defective in the division of the cortex/endodermis initial daughter cell, resulting in the formation of a single layer of ground tissue instead of two (Benfey et al. 1993; Scheres et al. 1995). Functional studies revealed that SHR, a transcription factor of the GRAS family, acts upstream of the SCR transcription factor (Helariutta et al. 2000). SHR moves from the central vasculature, place of its transcription, into the surrounding tissue layer, where after heterodimerization with SCR, it stimulates by a positive feedback loop the expression of *SCR* gene (Cui et al. 2007; Di Laurenzio et al. 1996; Nakajima et al. 2001). Ectopic expression experiments suggested that the SHR movement is limited to a single cell layer and that heterodimerization with SCR might be the mechanism to sequester the SHR protein in the nucleus and restrain its movement to a single cell layer adjacent to the stele (Cui et al. 2007). Recently, two zinc-finger proteins, MAGPIE (MGP) and JACKDAW (JKD), have been identified as factors required for radial patterning and contribute to refining the SHR and SCR action range (Welch et al. 2007).

Both auxin/PLT and SHR/SCR pathways are closely interconnected with the activities of several hormonal pathways. The PLT pathway acts downstream of the auxin signalling (Aida et al. 2004; Galinha et al. 2007), whereas among the eight direct targets of SHR, as elegantly identified by a set of microarray analyses (Levesque et al. 2006), one is involved in the brassinosteroid pathway (cytochrome P450/BRox62 regulating brassinosteroid biosynthesis; (Shimada et al. 2003)) and the other in the gibberellin signalling (SNEEZY/SLEEPY2 (SNE) F-box protein (Levesque et al. 2006)). Several other indirect targets are the molecular components of auxin biosynthesis *SUR2*(*SUPERROOT*) (Barlier et al. 2000), signalling *IAA12/BDL*(*BODENLOS*) and *ARF5/MP*(*MONOPTEROS*) (Hamann et al. 2002; Hardtke and Berleth 1998) and transport *PIN3* and *PIN7* (Friml et al. 2003a; Friml et al. 2002b); brassinosteroid perception *BRL3* (Cano-Delgado et al. 2004) and biosynthesis *Cyp90D1* (Kim et al. 2005) and gibberellin signalling R*GL1* and *RGL2* (Lee et al. 2002; Wen and Chang 2002); and *GA3* biosynthesis (Helliwell et al. 1998; Levesque et al. 2006). This clearly reflects that root development requires not only transcriptional network but also network of hormonal signalling.

Indeed, besides the plant hormone auxin, the key hormonal regulator of the root organogenesis, other plant hormones, e.g. cytokinin (Dello Ioio et al. 2007; Mahonen et al. 2006; Werner et al. 2003), ethylene (Ortega-Martinez et al. 2007; Swarup et al. 2007), brassinosteroids (Mouchel et al. 2006), gibberellin (Fu and Harberd 2003; Ubeda-Tomas et al. 2008) and abscisic acid (Achard et al. 2003) also participate in the regulation of different aspects of root organogenesis and activity. Lately, it became obvious that single hormone input is strongly modulated by other hormonal pathways acting in parallel. Characterization of these interactions and their impact on the root meristem development will be discussed in detail in the following sections.

Auxin: *the hormonal regulator of root development*

Auxin has been shown to regulate an extremely broad range of developmental processes, such as embryogenesis, organogenesis of leaves, flowers, ovules or lateral roots, gravitropic responses and apical hook formation. The whole process of root organogenesis, begining with the establishment of the root pole in embryos (Friml et al. 2003a; Weijers et al. 2006), positioning and formation of stem cell niche (Blilou et al. 2005; Sabatini et al. 1999), maintenance of mitotic activity in proximal meristem (Beemster and Baskin 2000; Dello Ioio et al. 2007; Galinha et al. 2007; Stepanova et al. 2008) and rapid elongation and differentiation of cells leaving the root meristem (Rahman et al. 2007) has been shown to be under the control of auxin. A real breakthrough in our understanding of how auxin molecule can lead to such a variety of developmental responses is the discovery of the instructive function of the auxin gradient formed along the longitudinal axis of the root meristem (Benkova et al. 2003; Friml et al. 2002a; Sabatini et al. 1999). The auxin gradient is generated by the concerted action of AUX/LAX auxin influx carriers (Bennett et al. 1996; Yang et al., 2006), PIN auxin efflux carriers (Galweiler et al. 1998; Luschnig et al. 1998; Friml et al. 2002a, b; Friml et al. 2003b; Petrášek

et al. 2006) and members of the multi-drug-resistant/P-glycoprotein (MDR/PGP) subfamily of ATP-binding cassette (ABC) proteins (Blakeslee et al., 2007). Interference with its establishment results in dramatic patterning and developmental defects in the root meristem (Blilou et al. 2005; Friml et al. 2002a; Sabatini et al. 1999).

It is still not precisely known how the auxin gradient achieves the specificity of the response required for the different aspects of the root meristem development by using the signal transduction pathway consisting of four TIR/AFB auxin receptors of the F-box protein family (Dharmasiri et al. 2005), 29 AUX/IAA negative regulators (Overvoorde et al. 2005) and 23 ARF (AUXIN RESPONSE FACTORS) transcription factors (Okushima et al. 2005), activating the expression of downstream auxin response genes. It has been proposed that certain combinations of AUX/IAAs and ARFs determine the response specificity (Hamann et al. 2002; Knox et al. 2003; Weijers et al. 2005). In the case of root development, the specific pair of IAA12/BDL and ARF5/MP was identified to determine the establishment of root pole in early embryogenesis (Hamann et al. 2002). Beside the *BDL-MP* pair, some other genes of the auxin signalling pathway (*SHY2/IAA3, AXR3/IAA17* and *AXR2/IAA7*) were shown to be involved in different aspects of root growth (Leyser et al. 1996; Nagpal et al. 2000; Tian and Reed 1999), although their direct ARF counterparts are still unknown. The *PLT* gene family seems to play an important role in the developmental interpretation of the auxin gradient. *PLT* genes respond in an auxin concentration-dependent manner to regulate stem cell identity and maintenance, mitotic activity of stem cells' daughters and cell differentiation (Galinha et al. 2007).

Auxin: universal partner in hormonal interactions?

Interestingly, many mutants in the auxin pathway exhibit not only auxin-related root phenotypes but also an altered sensitivity to other hormones. For example, root growth of the auxin transport mutants *aux1* and *pin2* is also ethylene resistant (Roman et al. 1995). Similarly, mutants in the auxin signalling *shy2-2/iaa3*, *axr2/iaa7* and *tir1* do not exclusively exhibit an auxin-resistant root phenotype, but also exhibit a changed sensitivity to other hormones such as cytokinins, abscisic acid or ethylene (Alonso et al. 2003; Tian and Reed 1999; Wilson et al. 1990). This promiscuous behaviour of mutants points out that auxin regulated events in root growth are tightly interconnected with other hormonal pathways and in many interactions auxin seems to act downstream of other hormonal pathways. From longstanding investigations on regulatory pathways in root development, auxin has emerged as one of the key factors involved in many very specific aspects of root organogenesis. Therefore, from practical reasons, auxin and its interactions will be discussed in the context of respective hormonal pathways (see Fig. 1).

Ethylene *is all around … and interacts*

Typically, seedlings germinated at high ethylene concentrations have short hairy roots, a phenotype in some aspects resembling auxin-treated roots. Detailed developmental studies revealed that ethylene affects root growth primarily by inhibiting the rapid expansion of cells leaving the root meristem (Le et al. 2001; Ruzicka et al. 2007; Swarup et al. 2007). More recently, ethylene has also been demonstrated to participate in the regulation of the cell division activity of the QC. Manipulation of the ethylene pathway by genetic or chemical tools affected the division activity of the QC suggesting its functions in maintenance of stem cell niche by regulating the balance between proliferation and quiescence of stem cells (Ortega-Martinez et al. 2007).

As mentioned above mutations in many auxin transport or signalling components cause aberrant responses to ethylene, thus pointing to an ethylene–auxin interaction. Mutations in the auxin influx and efflux carrier genes *AUX1* and *EIR1/AGR/PIN2* (Luschnig et al. 1998; Pickett et al. 1990; Roman et al. 1995), several components of the auxin signalling cascade, including the auxin receptor *TIR1* (Alonso et al. 2003) and the AUX/IAA regulators *axr2/iaa7* (Wilson et al. 1990) and *axr3/iaa17* (Leyser et al. 1996; Swarup et al. 2007) confer ethylene insensitive root growth phenotypes. Stepanova et al. (2005) demonstrated that mutations in two *Arabidopsis* genes *ASA1* and *ASB1* encoding subunits of the anthranilate synthase enzyme that synthesizes an auxin precursor also confer ethylene insensitive root growth phenotypes. Gene interaction studies have positioned these auxin pathway components downstream of the ethylene signal transduction pathway (Roman et al. 1995; Stepanova et al. 2005), suggesting that ethylene inhibition of root growth requires auxin biosynthesis, transport and responses. The hypothesis is further corroborated by other findings. As indicated by Rahman et al. (2001), *aux1* root growth can be sensitized to ethylene when cultured in the presence of auxin. Accordingly, ethylene sensitivity of the ethylene response reporter EBS in roots depends on auxin (Stepanova et al. 2007). Measurements of the auxin biosynthesis rate upon ethylene treatment revealed a stimulatory effect of ethylene on the auxin biosynthetic pathway (Swarup et al. 2007). Indeed, several genes of the auxin biosynthesis pathways were isolated and found to be under transcriptional control of ethylene. Beside *ASA1* and *ASB1,* (Stepanova et al. 2005), recently, a small family of genes encoding a long-anticipated tryptophan aminotransferase, TAA1, regulating the indole-3-pyruvic acid branch of the auxin biosynthetic pathway (Stepanova et al. 2008; Tao et al. 2008) has been

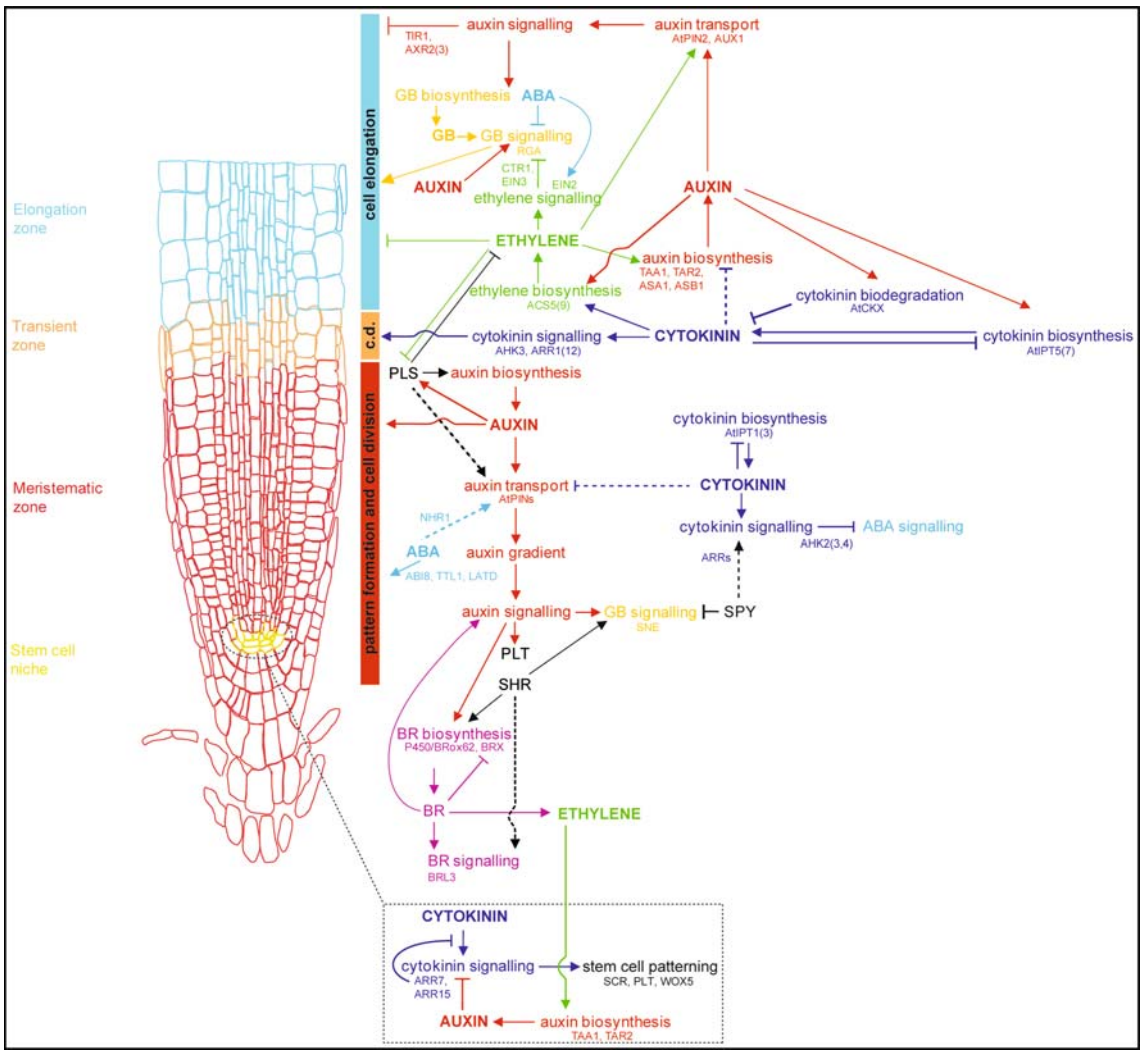

Fig. 1 Scheme of the hormonal cross-talk involved in the regulation of the root apical meristem growth and development. Selected regulators of the cross-talk are highlighted. Dashed lines correspond to not completely clear or mostly indirect regulations. c.d. is transition zone where differentiation starts

identified. Interestingly, *TAA1* and its close homologue *TAR2* are expressed in different organs including root meristem. Lack of their functions caused a drastic reduction in the meristem size and collapse of the root meristem, similar to mutants with reduced auxin levels due to a defective auxin transport (Benjamins et al. 2001; Blilou et al. 2005). Thus, analysis of *TAA1* and its homologues represents an important and for a long time missing link between local auxin production, tissue-specific ethylene effects and organ development, including root meristem (Stepanova et al. 2008).

A mechanistic model integrating our recent knowledge on the auxin - ethylene cross talk in roots has been proposed (Ruzicka et al. 2007; Stepanova et al. 2007; Swarup et al. 2007). According to this model, ethylene stimulates auxin biosynthesis in different plant organs via its known signalling pathway. In addition, ethylene increases the auxin transport capacity by regulating the transcription of several auxin transport components, including *PIN1*, *PIN2* and *AUX1* (Ruzicka et al. 2007). The additionally produced auxin is redistributed by polar auxin transport towards the root tip. The major components of the auxin transport in these tissues, AUX1 and PIN2, mediate the auxin delivery into cells of the elongation zone, where auxin accumulates and induces local auxin responses that inhibit cell elongation and overall root growth (Ruzicka et al. 2007; Stepanova et al. 2007; Swarup et al. 2007). Thus, inhibition of auxin responses in several mutants of the auxin signalling results in ethylene insensitive root growth. As revealed by tissue targeted inhibition of auxin responses, ethylene inhibition of root growth requires auxin responses in multiple cell layers of the elongation zone tissues (Swarup et al. 2007). However, this mechanism can account for most, but not all, ethylene effects on the root

growth. Some of the auxin insensitive mutants, e.g. *slr/iaa14* (Fukaki et al. 2002), *shy2-2/iaa3* (Tian and Reed 1999) or *nph4-1/arf7, arf19* (Okushima et al. 2005) are strongly resistant to auxin, but not or weakly to ethylene (Li et al. 2006a; Ruzicka et al. 2007). In addition, auxin transport mutants *aux1* and *pin2* do not exhibit complete ethylene resistance. Based on the extensive gene expression analysis, Stepanova et al. (2007) predicted that besides an auxin-mediated ethylene response there are at least three other types of interactions between auxin and ethylene. Thus, although an important part of the ethylene effect on root growth is performed through the auxin pathway, there appears to be a direct ethylene-specific, auxin response-independent component for this regulation.

Maintenance of a proper ethylene–auxin concentration balance along the root meristem seems to be one of the important mechanisms involved in ethylene–auxin regulated root growth. Besides the previously described control of the auxin biosynthesis by ethylene, auxin control over ethylene biosynthesis is also well established (Bleecker and Kende 2000; Liang et al. 1992; Yang and Hoffman 1984). One of the rate-limiting enzymes in the ethylene synthesis pathway is 1-aminocyclopropane-1-carboxylate synthases (ACS). Numerous ACS genes are expressed in the root meristem in a tissue-specific manner (Tsuchisaka and Theologis 2004) and their expression is enhanced upon auxin treatment (Tsuchisaka and Theologis 2004). This complicated regulatory loop between auxin and ethylene biosynthetic pathways suggests the presence of a complex feedback mechanism involving components that tightly control the actual auxin–ethylene level in root cells. One of the candidates for such a component might be the *POLARIS* (*PLS*) gene encoding a short 36-amino acid peptide. Mutation in *PLS* results in an enhanced ethylene phenotype, repressed auxin transport and auxin accumulation (Casson et al. 2002; Chilley et al. 2006). *PLS* transcription itself is under the negative control of ethylene and is stimulated by auxin. The *pls* mutant phenotype can be restored by genetic and pharmacological inhibition of the ethylene action, implicating PLS as a negative regulator of ethylene responses. Chilley et al. (2006) proposed a model in which the *PLS* transcription is activated at the root tip by the relatively high auxin concentration that accumulates and is required for correct cell division at that position (Blilou et al. 2005; Friml et al. 2002a; Sabatini et al. 1999). Here, PLS acts as a negative regulator of ethylene signalling, which is inhibitory to cell division and expansion, and therefore root growth. Although some aspects of *pls* phenotype are seemingly in contradiction with previously shown stimulatory effect of ethylene on auxin biosynthesis, PLS might be an important component of the ethylene sensing mechanism for the tuning auxin pathway action during root development.

Cytokinin: *antagonist in root*

The negative role of cytokinin (CK) on root growth is a long-known phenomenon that has been proven by both exogenous CK application and overexpression of the bacterial *ISOPENTENYLTRANSFERASE* (*IPT)* gene (Hewelt et al. 1994; Kuderova et al. 2008; Li et al. 2006b; Medford et al. 1989; Smigocki 1991). Accordingly, decreased endogenous CK levels via overexpression of the *CYTOKININ OXIDASE/DEHYDROGENASE* (*CKX*) gene results in an opposite effect i.e. enhanced root meristem and the root growth (Werner et al. 2003; Yang et al. 2003).

Interestingly, studies on mutants of CK signalling revealed a positive role of CK in the root meristem. The root meristem was reduced in the triple cytokinin receptor mutant *ahk2,ahk3,ahk4* and multiple mutant in *ahp* members of the signal transduction cascade (Higuchi et al. 2004; Hutchison et al. 2006; Nishimura et al. 2004; Riefler et al. 2006; To et al. 2004). Based on the phenotypes of CK signalling mutants, the modulation of CK levels led to the hypothesis of "supraoptimal" CK concentration in the root meristem (Ferreira and Kieber 2005), according to which, downregulation of the endogenous CK levels to optimal levels via *CKX* overexpression enhances root growth. However, both complete absence of the CK signal in CK signalling mutants and its abundance after *IPT* overexpression and/or exogenous application, respectively, exert optimal levels and lead to inhibitory effects (Ferreira and Kieber 2005).

A role for CK during embryonal root formation has been suggested by the *wooden leg* (*wol*) mutant identified for its defect in the radial root patterning (Scheres et al. 1995). In the *wol* embryos, the last series of divisions in the stele is missing, leading to the formation of the pericycle with a reduced cell number (Scheres et al. 1995). In the postembryonal development, *wol* mutation affects the asymmetric division of the procambium, resulting in a defective vasculature without phloem and formed exclusively by the protoxylem (Mahonen et al. 2000; Scheres et al. 1995). *WOL* was found to be allelic to the CK receptor *AHK4/CRE1*, thus pointing to a role for CK as a negative regulator of the protoxylem differentiation from the procambium. CK inhibition of the protoxylem differentiation allows procambial cells to undergo another developmental pathway, leading to phloem formation. *AHP6*, the downstream component of the CK transduction pathway, has been revealed to act in a negative regulatory feedback loop, antagonizing the CK effects (Mahonen et al. 2006).

Interestingly, the *wol* defect in the vasculature formation is rescued by the *fass* (*fs*) mutation (Scheres et al. 1995), allelic to *TONNEAU2* that codes for the putative novel protein phosphatase 2A regulatory subunit (Camilleri et al.

2002). It seems that additional cell layers in the radial pattern of the *fs* mutant (Torres-Ruiz and Jurgens 1994) allow phloem differentiation while the reduced number of cells in the stele of *wol* is "used up" by xylem pole-directed protoxylem differentiation (Scheres et al. 1995). However, missexpression of *AHP6* in *wol* embryos (Mahonen et al. 2006) suggests that positional, CK-mediated information rather than the cell number is critical for the proper vascular specification. As demonstrated also by the conditional expression of *CKX*, phenocopying *wol*, CK is a sufficient and necessary signal to provide this information during both embryonal and postembryonal root meristem development (Mahonen et al. 2006). That *fs* mutation is accompanied with increased levels of auxin and ethylene (Fisher et al. 1996) might imply a hormonal origin of *wol* complementation and suggest a role for CK/auxin/ethylene interplay during embryonal radial root pattern specification.

The role of CK in the embryonal specification of the root meristem stem cells was recently described (Muller and Sheen 2008). In the set of elegant experiments using CK-responsive synthetic reporter, authors have shown that output of CK signalling is antagonized by auxin. This effect is mediated by auxin-inducible expressions of *ARR7* and *ARR15* type-A response regulators acting as negative regulators of CK signalling. In the absence of auxin, expression of *ARR7* and *ARR15* are balanced with CK signalling levels (CK induce expression of type-A ARRs, which in turn inhibit CK signalling phosphorelay). However, auxin-mediated local expression of *ARR7* and *ARR15* bypasses the CK feedback loop and counteracts CK signalling. In conditional *arr7* and *arr15* double mutants, ectopic CK phosphorelay output was detected, accompanied with defects in root stem cell region and misexpression of *SCR, PLT1* and *WUSCHEL_RELATED-HOMEOBOX 5* (*WOX5*) genes (Muller and Sheen 2008). These results provide insight into the molecular mechanism of long-known antagonistic effects of CK and auxin interaction and introduce the role of these interactions in root meristem establishment during the early embryogenesis.

Biometric analysis on root growth (Beemster and Baskin 2000) demonstrated that CK reduces the relative elongation rate and blocks the increase of the meristem size. In some aspects, CK regulated root growth resembles typical ethylene-induced inhibition. CK was found to stimulate ethylene production and root growth of ethylene insensitive mutants to be CK resistant (Cary et al. 1995). Moreover, inhibitors of ethylene signalling and biosynthesis partially relieve roots from CK inhibition. These results suggest that part of the CK effects on root growth is mediated through ethylene. Molecular characterization of the *ACS5* and *ACS9* genes in *ethylene overproduction* (*eto2 and eto3*) mutants revealed that dominant *eto2* mutation does not increase the specific activity of the ethylene biosynthesis ACS5 enzyme, rather it increases the half-life of the protein. Similarly, CK treatment was shown to enhance the stability of ACS5 by a mechanism that is at least partially independent of the *eto2* mutation (Chae et al. 2003).

Altogether, rapid expansion of cells in the root transition zone seems to be under the control of at least three hormonal pathways—cytokinin, ethylene and auxin downstream of this regulatory chain. Importantly, feedback loop mechanisms comprising control of the CK biosynthesis by auxin (Eklof et al. 1997; Nordstrom et al. 2004), or the ethylene biosynthesis by auxin (Tsuchisaka and Theologis 2004; Yang and Hoffman 1984) represent an important part of the homeostatic mechanism.

Recently, Dello Ioio et al. (2007) have analysed the role of CK in the root meristem formation and have demonstrated that CK does not interfere with specification of the QC and stem cell function, nor with the overall division rate in the proximal meristem. CK affects primarily the rate of meristematic cell differentiation, resulting in shortening of the meristematic zone. Accordingly, depletion of CK by overexpression of *CKX* or by mutation of three *Arabidopsis* cytokinin biosynthesis genes *ipt2,ipt3,ipt7* increases the root meristem size (Dello Ioio et al. 2007; Werner et al. 2003). The role of CK signalling in longitudinal root patterning has been further confirmed by the expansion of the root meristem in the *ahk3* and response regulator mutants *arr1* and *arr12*.

Important knowledge on the CK control mechanism on the root meristem development has arisen from the targeted depletion of CK in different root meristem tissue layers. Depletion of CK restricted to the vasculature of the transition zone was sufficient to reduce the rate of cell differentiation of all other tissues and, thus, to diminish the root meristem size. Such a type of non-cell autonomous effect suggests that CK acts by antagonizing other signals. As proposed by Dello Ioio et al. (2007), a candidate for such a signalling molecule would be auxin, which as described above, is critical for the control of cell division and root meristem size. Application of auxin at low concentrations causes an increase in the meristem size (Beemster and Baskin 2000; Dello Ioio et al. 2007). On the other hand, depletion of CK by CKX has no additional effects on the meristem size in the auxin efflux carrier triple mutant *pin2,pin3,pin7*. Thus, the balance between the auxin and cytokinin pathways regulates important aspects of root development and establishment and maintenance of the meristem size. The molecular mechanisms are so far illusive, although several modes of interaction are conceivable.

First, CK and auxin biosynthesis are dependent on each other and perturbation in the abundance of one affects the other. An increase in auxin concentration leads to a decrease in the CK level (Eklof et al. 1997; Nordstrom

et al. 2004), and slow inhibitory effect of CK on auxin biosynthesis was described (Nordstrom et al. 2004). Auxin has also been shown to contribute to the CK degradation via stimulation of the CKX activity (Palni et al. 1988). In contrast, expression of two genes for CK biosynthetic enzymes AtIPT5 and AtIPT7 in *Arabidopsis* is induced by exogenous auxin (Miyawaki et al. 2004).

Second, the activity of the polar auxin transport machinery, the principal director of the auxin distribution in the root meristem, might be modulated by CK. Recently, CK has been shown to affect the local auxin gradient formation and expression of *PIN* auxin efflux carriers during lateral root development (Kuderova et al. 2008; Laplaze et al. 2007).

Third, auxin and cytokinin can regulate a common set of genes. A promising candidate for the downstream molecular component is *PROPORZ1* (*PRZ1*). This putative transcriptional adaptor protein has been shown to be essential for the developmental switch from cell proliferation to differentiation in response to variations in auxin and CK concentrations (Sieberer et al. 2003). Expression of several other genes was found to be under control of auxin and cytokinin. For example, transcription of the root-specific putative homeobox gene *ATHB53* is differentially regulated by auxin and CK (Son et al. 2005), and interestingly, CK regulates also expression of genes of the auxin signalling pathway (*SHY2-2/IAA3*, *AXR3/IAA17* or *SAUR-AC1*) (Rashotte et al. 2005).

Brassinosteroid: *forget-me-not*

Typically, effects of brassinosteroids (BRs) on root growth strongly depend on the BR concentration used. Exogenous BRs stimulate root growth at low concentrations, but have an inhibitory effect at higher BR levels (Mussig et al. 2003). BR-deficient mutants, such as *dwarf1-6*/(*dwf1-6*) and *cabbage3*/(*cbb3*) (allelic to *cpd*), defective in brassinosteroid biosynthesis (Kauschmann et al., 1996; Szekeres et al., 1996), show shorter roots than wild-type plants (Mussig et al. 2003). Root-specific BR-deficiency in *brevis radix*/(*brx*) mutant causes reduced root growth due to reduction in the meristem size, and mature cell size as well (Mouchel et al. 2004). *BRX,* isolated as quantitative trait locus affecting root growth in the *Arabidopsis* accession Umkirch-1 (Uk-1), is a member of a small gene family representing most probably a novel class of transcriptional factors involved in the regulation of expression of a rate-limiting enzyme in brassinosteroid biosynthesis (Mouchel et al. 2006).

Transcriptome profile analyses in roots of two BR mutants, *dwf1-6* and (Mussig et al. 2003) and *brx* (Mouchel et al. 2006), revealed a link between BR and the auxin pathway in root development. Test of auxin response in *brx* via microarray analysis showed that almost none of tested auxin response genes responded normally to auxin in the BR-deficient *brx* mutant, but this auxin responsiveness was largely restored by brassinollide treatment. Accordingly, expression of the auxin reporter *DR5* (Sabatini et al. 1999; Ulmasov et al. 1997) in *brx* was fully sensitized to auxin by BR supply (Mouchel et al. 2006). Altogether, these results suggested that optimal BR levels are rate limiting for auxin-induced transcriptional responses. BR does not seem to act through regulation of endogenous auxin content, because as shown by Nakamura et al. (2003), BR did not increase the endogenous auxin levels of either the control plant or the BR-deficient mutant *deetiolated2*/*det2*. Furthermore, the levels of *AUX/IAA* transcripts were lower in the *det2* mutant than in the control, even though endogenous auxin levels were elevated in the *det2* background (Nakamura et al. 2003).

Accordingly, negative regulators of auxin signalling *IAA14* and *IAA2* showed weaker expression in roots of *dwf1-6* (Fukaki et al. 2002; Mussig et al. 2003) and the *NIT3* gene, encoding enzyme involved in IAA biosynthesis (Kutz et al. 2002) exhibited higher transcript level in the *dwf1-6* mutant background (Mussig et al. 2003).

Brassinosteroids are known to stimulate the production of ethylene in shoots and roots (Arteca and Arteca 2001; Schlagnhaufer and Arteca 1985; Yi et al. 1999). In line with these observations, expression data point to a positive BR effect on genes involved in ethylene biosynthesis and ethylene response in roots (Mussig et al. 2003). Thus, part of the BR inhibitory effect on root growth might be mediated through ethylene. More detailed studies are needed to dissect the ethylene effects in the context of BR action. However, analysis of the auxin and ethylene resistant mutants *axr1* points to the existence of ethylene-independent BR-regulated root growth (Clouse et al. 1993). A direct BR-ethylene feedback loop might exist that specifically interferes with BR transport, BR biosynthesis, or BR responses.

Also another mutant in BR biosynthesis, *sax1* (*hypersensitive to abscisic acid and auxin*), with roots oversensitive to auxin and ABA suggests that BR interacts with multiple hormonal pathways (Ephritikhine et al. 1999).

Gibberellins: *you have to beat me*

Although gibberellin (GA) has been recognized for a long time mainly as a regulator of shoot growth, its important role in the regulation of root growth has been demonstrated as well. The GA-deficient mutant *ga1-3* exhibits shorter roots. Loss of DELLA proteins GAI and RGA, negative inhibitors of GA signalling, suppress the *ga1-3* root phenotype, showing that GA pathway acts in the regulation of root growth (Fu and Harberd 2003). An elegant set of

experiments has recently been performed to map the site of GA action for regulating root growth (Ubeda-Tomas et al. 2008). When gai, a mutant non-degradable DELLA protein, was expressed in selected root tissues, the root growth was retarded specifically when *gai* was expressed in endodermal cells. These results demonstrated that the endodermis represents the primary GA-responsive tissue and that endodermal cell expansion is rate limiting for elongation of other tissues and, therefore, of the root as a whole (Ubeda-Tomas et al. 2008). In work of Paquette and Benfey (2005) also a role of GA in radial patterning of root meristem has been revealed and GA shown to act as negative regulator of the middle cortex formation—the third layer of the root ground tissue rapidly differentiating to cortex.

GA stimulates growth by promoting the destruction of DELLA proteins, a subfamily of the GRAS family of putative transcriptional regulators (Dill et al. 2001; Fu and Harberd 2003). Thus, DELLA proteins restrain the plant growth, whereas GA relieves the DELLA-mediated growth inhibition by targeting the DELLA proteins for destruction. GA-mediated destabilization of DELLA proteins involves GA-stimulated phosphorylation, polyubiquitination via a specific SCF E3 ubiquitin ligase complex and subsequent destruction in the 26S proteasome (Fu et al. 2002; McGinnis et al. 2003; Sasaki et al. 2003).

As demonstrated by several laboratories, GA-regulated root growth involves interaction with other hormonal pathways, e.g. auxin (Fu and Harberd 2003), cytokinin (Greenboim-Wainberg et al. 2005), ethylene (Achard et al. 2006) or ABA (Achard et al. 2006) and the regulation of DELLA proteins stability might represent an important cross-point.

GA and auxin pathways converge in roots to regulate cell expansion and tissue differentiation. GA-induced root elongation was inhibited by the removal of the shoot apex, which is a major auxin source, and this effect was reversed by auxin application suggesting that GA stimulation of root elongation requires auxin. Moreover, application of the auxin-transport inhibitor 1-*N*-naphthylphthalamic acid (NPA), or a mutation in the auxin efflux carrier *PIN1* attenuated the effect of GA on root elongation and on RGA degradation in root cells. GA-induced RGA degradation was also inhibited in the auxin resistant mutant *axr1*. These observations indicate that auxin promotes the growth of roots by enhancing the GA-induced destabilization of some of the DELLA proteins (Fu and Harberd 2003). Thus, the DELLA protein RGA seems to act as integrator of GA and auxin signals in the root.

Positive regulation of GA biosynthesis by auxin might be involved in these interactions. A stimulatory effect of the auxin on GA biosynthesis was demonstrated and several components of auxin signalling pathway seem to be included in this regulation (Frigerio et al. 2006).

GA has been shown to antagonize ethylene inhibitory effects on root growth (Achard et al. 2003). Ethylene insensitive root growth of the *gai rga* GA-insensitive mutant indicates that ethylene regulates root growth in a DELLA-dependent manner. In agreement with this observation, ethylene counteracted GA-induced destabilization of the RGA protein in root cell nuclei. The effect of ethylene on RGA stability was mimicked by the loss of its signalling suppressor CONSTITUTIVE TRIPLE RESPONSE1 (CTR1) (Guo and Ecker 2004), suggesting that the ethylene's RGA stabilizing signal is transduced via a CTR1-dependent pathway (Achard et al. 2003).

Analysis of *SPINDLY* (*SPY*) gene revealed antagonistic interaction of GA and CK in root growth (Greenboim-Wainberg et al. 2005). Mutation of *SPY* results in phenotypes resembling that of wild-type plants treated with exogenous GA and overexpression of *SPY* produced phenotypes consistent with a reduced GA action (Izhaki et al. 2001; Swain et al. 2001). This suggests that SPY functions as a negative regulator of the GA-signal transduction. Inhibition of root elongation by CK was greatly suppressed in the *spy* mutant background, and accordingly, exogenous application of GA antagonized the inhibitory effect of CK on root growth. Both GA and *spy* interfered with the induction of CK primary response gene *ARR5*. Thus, SPY is a potential molecular component that integrates GA and CK pathways in root growth and acts as a repressor of GA responses and a positive regulator of CK signalling. Based on the comparison of GA and CK sensitivities of *spy* mutants, it seems that GA suppresses CK responses at least partially via SPY (Greenboim-Wainberg et al. 2005).

In the shoot apical meristem *KNOTTED*-like homeobox genes were shown to play an important role in the establishment of the hormonal balance between CK and GA. They activate CK biosynthesis and repress *GA 20-oxidase* gene expression and, hence, GA biosynthesis, thus promoting meristem activity (Jasinski et al. 2005; Yanai et al. 2005). Several members of this gene family were shown to be expressed in distinct domains and cell types of the main root (Truernit et al. 2006), but their role in the hormonal interactions and its relevance for root growth regulation remains to be examined in detail.

Abscisic acid: *not only stress*

The role of abscisic acid (ABA) in the regulation of root growth is still not completely clear. However, recent genetic and molecular studies started to unravel the importance of ABA regulation in root meristem formation and root growth. An example of genes involved in ABA-mediated control of the root meristem is the *TETRATRICOPEPTIDE-REPEAT THIOREDOXIN-LIKE 1* (*TTL1*) gene. Mutation in *TTL1* causes reduced root

elongation and disorganization of the root meristem. TTL1 mediates the sensitivity to ABA and to osmotic stress and is supposed to participate in ABA signalling in *Arabidopsis* (Rosado et al. 2006). ABA has been shown to rescue the root meristem phenotype of *Medicago* mutant *latd*. *latd* roots have disorganized root tip that is defective in meristem organization, columella root cap formation and root growth (Liang et al. 2007). *latd* mutants exhibit normal ABA levels, but reduced sensitivity to ABA, suggesting that LATD functions in the ABA signalling.

Multiple ABA effects are associated with ethylene action. There are several hints that functional ethylene signalling is necessary for root responses to ABA. The ABA effect on the root growth was restrained by inhibitors of the ethylene perception, but not by reduced ethylene biosynthesis, suggesting that, in contrast to CK, ABA does not operate through ethylene biosynthesis, as confirmed by the measurements of ethylene production upon ABA treatment. Vice versa, ethylene seems to inhibit root responsiveness to ABA (Ghassemian et al. 2000). Close interplay of ABA and ethylene in root development indicates *era3* mutant identified in a screen for ABA hypersensitive germination mutant. The *era3* mutation was found to be allelic to the ethylene insensitive *ein2* mutant (Beaudoin et al. 2000; Ghassemian et al. 2000). Interestingly, the *era3* roots are not only resistant to CK and ethylene as previously shown for the *ein2* mutant in ethylene signalling (Cary et al. 1995) but also to ABA. Moreover, they are sensitive to auxin and accumulate more ABA (Ghassemian et al. 2000). Thus, *era3* represents an important candidate to investigate ABA and ethylene signalling interaction in the root development. The *abi8/eld1/kob1* mutant with altered ABA-responsive gene expression was shown to be necessary for the meristematic activity in the root (Brocard-Gifford et al. 2004). *ABI8/ELD1/KOB1* encodes a protein of unknown function and, in contrast to most of the other ABA insensitive mutations, the *abi8* phenotype cannot be suppressed by inhibition of the ethylene pathway. Thus, ABI8 might function in parallel or downstream of the EIN2 and EIN3 components of the ethylene signalling pathway (Brocard-Gifford et al. 2004).

The *nhr1* mutation uncovers interaction between ABA and auxin (Eapen et al. 2003). Semi-dominant *nhr1* mutation was identified in a screen for lack of hydrotropic root responses. *NHR1* affects root meristem formation via regulation of the QC, columella initials and root cap specification and affects cell proliferation in the root meristem. *nhr1* shows reduced sensitivity to ABA, NAA and to the auxin efflux inhibitor NPA. Authors hypothesize that NHR1 is involved in the ABA-dependent mechanism of efflux mediated auxin redistribution, allowing positive hydrotropic response of the root (Eapen et al. 2003).

Similarly to ethylene, salt stress-induced ABA increases the stability of DELLA negative regulators of the GA pathway (Achard et al. 2006; Fu and Harberd 2003; Vriezen et al. 2004). The quadruple DELLA mutant *gai,rga,rgl1,rgl2* is resistant to the growth-inhibitory effects of ABA. Furthermore, EIN3, a negative regulator of the ethylene signalling, was found to promote salt tolerance via enhancement of the DELLA function (Achard et al. 2006). Thus, DELLA proteins integrate ABA and ethylene signalling in the regulation of the root growth. As ABA and ethylene signalling are involved in different abiotic and biotic responses, this mechanism might mediate environmental regulation of the root growth response (Achard et al. 2006).

Recently, important connection between CK and ABA signalling was described in *Arabidopsis*. Homologue of CK receptors, sensory histidine kinase AHK1, was found to be a positive regulator of drought and salt stress responses and ABA signalling. In contrast, CK receptors AHK2, AHK3 and AHK4 were identified to be negative regulators of the ABA signalling, acting in case of AHK2 and AHK3 via negative regulation of many stress- and/or ABA-inducible genes (Tran et al. 2007).

Conclusion

The current status of knowledge on root development indisputably points out that a complex hormonal network participates in the regulation of root formation and growth from the moment of its initiation in the embryo. Essentially, all hormonal pathways are involved and control different developmental aspects of the root meristem formation. Auxin seems to be the most universal factor acting in all root developmental events (Dinneny and Benfey 2008; Galinha et al. 2007). CK has been shown to be a critical factor in radial root patterning (Mahonen et al. 2006; Scheres et al. 1995), establishment of root stem cells during early embryogenesis (Muller and Sheen 2008) and establishment of the root meristem size by controlling the balance between cell division and differentiation of cells leaving the root meristem (Dello Ioio et al. 2007). Ethylene and GA act primarily on the rapid elongation of cells leaving the root meristem (Fu and Harberd 2003; Ruzicka et al. 2007; Swarup et al. 2007; Ubeda-Tomas et al. 2008). BR deficiency affects both the division activity of the root meristem and rapid cell elongation (Mouchel et al. 2004), and ABA mediates the environmental regulation of root growth responses (Achard et al. 2006). Importantly, each hormonal pathway functions in the context of the whole hormonal network and they mutually modulate their actions. Thus, for example, auxin regulated processes require a minimal level of BR (Mouchel et al. 2006). Maintenance of the root meristem size is balanced by antagonistic activities of CK and auxin (Dello Ioio et al.

2007), and the gibberellin pathway is differently modulated by auxin and ethylene (Achard et al. 2003; Fu and Harberd 2003). Although our knowledge on the molecular components and pathways that mediate developmental responses to hormones has improved enormously in recent years, molecular mechanisms standing behind their interactions are poorly understood. However, from most of the recent studies, it became obvious that diverse mechanisms of hormonal interactions have evolved to coordinate activity of hormonal pathways in certain developmental processes. There are several examples of mutual regulations on the level of hormone metabolism and distribution (Laplaze et al. 2007; Stepanova et al. 2005; Stepanova et al. 2008; Tsuchisaka and Theologis 2004). Transcriptional or post-translational control over the key molecular components of signal transduction pathways by other hormonal signals is another example of a cross-talk strategy (Fu and Harberd 2003; Chae et al. 2003; Muller and Sheen 2008). There are rare cases in which activation of one hormonal pathway might branch and stimulate transduction component of another pathway (Hass et al. 2004). Hormonal signalling pathways might also differentially regulate expression or activity of common target gene (Chilley et al. 2006; Son et al. 2005). Several other modes of hormonal interactions could be predicted. Although we have no real evidence for their existence today, they might be revealed in the future years. In this context, we would like to note that although sometimes experimental findings might lead to contradictory conclusions on the mode of hormonal interactions (Ferreira and Kieber 2005), these "inconsistencies" might point to a very important feature of the hormone behaviour—its action is extremely dependent on concentration and developmental stage (Kuderova et al. 2008; Mussig et al. 2003). It has been nicely demonstrated by Kuderova et al. (2008) that the strength of the effects of temporal pulses of endogenous CK via regulated expression of the bacterial *IPT* depends on the developmental status of the root. Consequently, the same hormone can, during one developmental process, set up different interactions in relation to the actual concentration and developmental stage.

Recent investigations have created a good outline of different possible modes of interactions between hormones, which in combination with the fast progress in understanding single hormonal pathways represents a promising start to reveal concrete cross-talk molecular components, which is the challenge of future research.

Acknowledgement We would like to thank Dr. Kamil Ruzicka and Dr. Jiri Friml for critical reading of the manuscript and Martine De Cock for help in preparing it. This work was supported by the Ministry of Education, Youth and Sports of the Czech Republic (LC06034 and MSM0021622415) (JH).

References

Achard P, Vriezen WH, Van Der Straeten D, Harberd NP (2003) Ethylene regulates arabidopsis development via the modulation of DELLA protein growth repressor function. Plant Cell 15:2816–2825. doi:10.1105/tpc.015685

Achard P, Cheng H, De Grauwe L, Decat J, Schoutteten H, Moritz T, Van Der Straeten D, Peng J, Harberd NP (2006) Integration of plant responses to environmentally activated phytohormonal signals. Science 311:91–94. doi:10.1126/science.1118642

Aida M, Beis D, Heidstra R, Willemsen V, Blilou I, Galinha C, Nussaume L, Noh YS, Amasino R, Scheres B (2004) The PLETHORA genes mediate patterning of the Arabidopsis root stem cell niche. Cell 119:109–120. doi:10.1016/j.cell.2004.09.018

Alonso JM, Stepanova AN, Solano R, Wisman E, Ferrari S, Ausubel FM, Ecker JR (2003) Five components of the ethylene-response pathway identified in a screen for weak ethylene-insensitive mutants in Arabidopsis. Proc Natl Acad Sci USA 100:2992–2997. doi:10.1073/pnas.0438070100

Arteca JM, Arteca RN (2001) Brassinosteroid-induced exaggerated growth in hydroponically grown Arabidopsis plants. Physiol Plant 112:104–112. doi:10.1034/j.1399-3054.2001.1120114.x

Barlier I, Kowalczyk M, Marchant A, Ljung K, Bhalerao R, Bennett M, Sandberg G, Bellini C (2000) The SUR2 gene of Arabidopsis thaliana encodes the cytochrome P450 CYP83B1, a modulator of auxin homeostasis. Proc Natl Acad Sci USA 97:14819–14824. doi:10.1073/pnas.260502697

Beaudoin N, Serizet C, Gosti F, Giraudat J (2000) Interactions between abscisic acid and ethylene signaling cascades. Plant Cell 12:1103–1115

Beemster GT, Baskin TI (2000) Stunted plant 1 mediates effects of cytokinin, but not of auxin, on cell division and expansion in the root of Arabidopsis. Plant Physiol 124:1718–1727. doi:10.1104/pp.124.4.1718

Benfey PN, Linstead PJ, Roberts K, Schiefelbein JW, Hauser MT, Aeschbacher RA (1993) Root development in Arabidopsis: four mutants with dramatically altered root morphogenesis. Development 119:57–70

Benjamins R, Quint A, Weijers D, Hooykaas P, Offringa R (2001) The PINOID protein kinase regulates organ development in Arabidopsis by enhancing polar auxin transport. Development 128:4057–4067

Benkova E, Michniewicz M, Sauer M, Teichmann T, Seifertova D, Jurgens G, Friml J (2003) Local, efflux-dependent auxin gradients as a common module for plant organ formation. Cell 115:591–602. doi:10.1016/S0092-8674(03)00924-3

Bennett MJ, Marchant A, Green HG, May ST, Ward SP, Millner PA, Walker AR, Schulz B, Feldmann KA (1996) Arabidopsis AUX1 gene: a permease-like regulator of root gravitropism. Science 273:948–950. doi:10.1126/science.273.5277.948

Blakeslee JJ, Bandyopadhyay A, Lee OR, Mravec J, Titapiwatanakun B, Sauer M, Makam SN, Cheng Y, Bouchard R, Adamec J, Geisler M, Nagashima A, Sakai T, Martinoia E, Friml J, Peer WA, Murphy AS (2007) Interactions among PIN-FORMED and P-glycoprotein auxin transporters in Arabidopsis. Plant Cell 19:131–147. doi:10.1105/tpc.106.040782

Bleecker AB, Kende H (2000) Ethylene: a gaseous signal molecule in plants. Annu Rev Cell Dev Biol 16:1–18. doi:10.1146/annurev.cellbio.16.1.1

Blilou I, Xu J, Wildwater M, Willemsen V, Paponov I, Friml J, Heidstra R, Aida M, Palme K, Scheres B (2005) The PIN auxin efflux facilitator network controls growth and patterning in Arabidopsis roots. Nature 433:39–44. doi:10.1038/nature03184

Brocard-Gifford I, Lynch TJ, Garcia ME, Malhotra B, Finkelstein RR (2004) The Arabidopsis thaliana ABSCISIC ACID-INSENSITIVE8 encodes a novel protein mediating abscisic acid and sugar responses essential for growth. Plant Cell 16:406–421. doi:10.1105/tpc.018077

Camilleri C, Azimzadeh J, Pastuglia M, Bellini C, Grandjean O, Bouchez D (2002) The Arabidopsis TONNEAU2 gene encodes a putative novel protein phosphatase 2A regulatory subunit essential for the control of the cortical cytoskeleton. Plant Cell 14:833–845. doi:10.1105/tpc.010402

Cano-Delgado A, Yin Y, Yu C, Vafeados D, Mora-Garcia S, Cheng JC, Nam KH, Li J, Chory J (2004) BRL1 and BRL3 are novel brassinosteroid receptors that function in vascular differentiation in Arabidopsis. Development 131:5341–5351. doi:10.1242/dev.01403

Cary AJ, Liu W, Howell SH (1995) Cytokinin action is coupled to ethylene in its effects on the inhibition of root and hypocotyl elongation in Arabidopsis thaliana seedlings. Plant Physiol 107:1075–1082. doi:10.1104/pp.107.4.1075

Casson SA, Chilley PM, Topping JF, Evans IM, Souter MA, Lindsey K (2002) The POLARIS gene of Arabidopsis encodes a predicted peptide required for correct root growth and leaf vascular patterning. Plant Cell 14:1705–1721. doi:10.1105/tpc.002618

Clouse SD, Hall AF, Langford M, Mcmorris TC, Baker ME (1993) Physiological and molecular effects of brassinosteroids on Arabidopsis-Thaliana. J Plant Growth Regul 12:61–66. doi:10.1007/BF00193234

Cui H, Levesque MP, Vernoux T, Jung JW, Paquette AJ, Gallagher KL, Wang JY, Blilou I, Scheres B, Benfey PN (2007) An evolutionarily conserved mechanism delimiting SHR movement defines a single layer of endodermis in plants. Science 316:421–425. doi:10.1126/science.1139531

Dello Ioio R, Linhares FS, Scacchi E, Casamitjana-Martinez E, Heidstra R, Costantino P, Sabatini S (2007) Cytokinins determine Arabidopsis root-meristem size by controlling cell differentiation. Curr Biol 17:678–682. doi:10.1016/j.cub.2007.02.047

Dharmasiri N, Dharmasiri S, Estelle M (2005) The F-box protein TIR1 is an auxin receptor. Nature 435:441–445. doi:10.1038/nature03543

Di Laurenzio L, Wysocka-Diller J, Malamy JE, Pysh L, Helariutta Y, Freshour G, Hahn MG, Feldmann KA, Benfey PN (1996) The SCARECROW gene regulates an asymmetric cell division that is essential for generating the radial organization of the Arabidopsis root. Cell 86:423–433. doi:10.1016/S0092-8674(00)80115-4

Dill A, Jung HS, Sun TP (2001) The DELLA motif is essential for gibberellin-induced degradation of RGA. Proc Natl Acad Sci USA 98:14162–14167. doi:10.1073/pnas.251534098

Dinneny JR, Benfey PN (2008) Plant stem cell niches: standing the test of time. Cell 132:553–557. doi:10.1016/j.cell.2008.02.001

Dolan L, Janmaat K, Willemsen V, Linstead P, Poethig S, Roberts K, Scheres B (1993) Cellular organisation of the Arabidopsis thaliana root. Development 119:71–84

Eapen D, Barroso ML, Campos ME, Ponce G, Corkidi G, Dubrovsky JG, Cassab GI (2003) A no hydrotropic response root mutant that responds positively to gravitropism in Arabidopsis. Plant Physiol 131:536–546. doi:10.1104/pp.011841

Eklof S, Astot C, Blackwell J, Moritz T, Olsson O, Sandberg G (1997) Auxin-cytokinin interactions in wild-type and transgenic tobacco. Plant Cell Physiol 38:225–235

Ephritikhine G, Pagant S, Fujioka S, Takatsuto S, Lapous D, Caboche M, Kendrick RE, Barbier-Brygoo H (1999) The sax1 mutation defines a new locus involved in the brassinosteroid biosynthesis pathway in Arabidopsis thaliana. Plant J 18:315–320. doi:10.1046/j.1365-313X.1999.00455.x

Ferreira FJ, Kieber JJ (2005) Cytokinin signaling. Curr Opin Plant Biol 8:518–525. doi:10.1016/j.pbi.2005.07.013

Fisher RH, Barton MK, Cohen JD, Cooke TJ (1996) Hormonal studies of fass, an Arabidopsis mutant that is altered in organ elongation. Plant Physiol 110:1109–1121

Frigerio M, Alabadi D, Perez-Gomez J, Garcia-Carcel L, Phillips AL, Hedden P, Blazquez MA (2006) Transcriptional regulation of gibberellin metabolism genes by auxin signaling in Arabidopsis. Plant Physiol 142:553–563. doi:10.1104/pp.106.084871

Friml J, Benkova E, Blilou I, Wisniewska J, Hamann T, Ljung K, Woody S, Sandberg G, Scheres B, Jurgens G, Palme K (2002a) AtPIN4 mediates sink-driven auxin gradients and root patterning in Arabidopsis. Cell 108:661–673. doi:10.1016/S0092-8674(02)00656-6

Friml J, Wisniewska J, Benkova E, Mendgen K, Palme K (2002b) Lateral relocation of auxin efflux regulator PIN3 mediates tropism in Arabidopsis. Nature 415:806–809

Friml J, Vieten A, Sauer M, Weijers D, Schwarz H, Hamann T, Offringa R, Jurgens G (2003) Efflux-dependent auxin gradients establish the apical–basal axis of Arabidopsis. Nature 426:147–153. doi:10.1038/nature02085

Fu X, Harberd NP (2003) Auxin promotes Arabidopsis root growth by modulating gibberellin response. Nature 421:740–743. doi:10.1038/nature01387

Fu X, Richards DE, Ait-Ali T, Hynes LW, Ougham H, Peng J, Harberd NP (2002) Gibberellin-mediated proteasome-dependent degradation of the barley DELLA protein SLN1 repressor. Plant Cell 14:3191–3200. doi:10.1105/tpc.006197

Fukaki H, Tameda S, Masuda H, Tasaka M (2002) Lateral root formation is blocked by a gain-of-function mutation in the SOLITARY-ROOT/IAA14 gene of Arabidopsis. Plant J 29:153–168. doi:10.1046/j.0960-7412.2001.01201.x

Galinha C, Hofhuis H, Luijten M, Willemsen V, Blilou I, Heidstra R, Scheres B (2007) PLETHORA proteins as dose-dependent master regulators of Arabidopsis root development. Nature 449:1053–1057. doi:10.1038/nature06206

Galweiler L, Guan C, Muller A, Wisman E, Mendgen K, Yephremov A, Palme K (1998) Regulation of polar auxin transport by AtPIN1 in Arabidopsis vascular tissue. Science 282:2226–2230. doi:10.1126/science.282.5397.2226

Ghassemian M, Nambara E, Cutler S, Kawaide H, Kamiya Y, McCourt P (2000) Regulation of abscisic acid signaling by the ethylene response pathway in Arabidopsis. Plant Cell 12:1117–1126

Greenboim-Wainberg Y, Maymon I, Borochov R, Alvarez J, Olszewski N, Ori N, Eshed Y, Weiss D (2005) Cross talk between gibberellin and cytokinin: the Arabidopsis GA response inhibitor SPINDLY plays a positive role in cytokinin signaling. Plant Cell 17:92–102. doi:10.1105/tpc.104.028472

Guo H, Ecker JR (2004) The ethylene signaling pathway: new insights. Curr Opin Plant Biol 7:40–49. doi:10.1016/j.pbi.2003.11.011

Hamann T, Benkova E, Baurle I, Kientz M, Jurgens G (2002) The Arabidopsis BODENLOS gene encodes an auxin response protein inhibiting MONOPTEROS-mediated embryo patterning. Genes Dev 16:1610–1615. doi:10.1101/gad.229402

Hardtke CS, Berleth T (1998) The Arabidopsis gene MONOPTEROS encodes a transcription factor mediating embryo axis formation and vascular development. EMBO J 17:1405–1411. doi:10.1093/emboj/17.5.1405

Hass C, Lohrmann J, Albrecht V, Sweere U, Hummel F, Yoo SD, Hwang I, Zhu T, Schafer E, Kudla J, Harter K (2004) The response regulator 2 mediates ethylene signalling and hormone

signal integration in Arabidopsis. EMBO J 23:3290–3302. doi:10.1038/sj.emboj.7600337

Helariutta Y, Fukaki H, Wysocka-Diller J, Nakajima K, Jung J, Sena G, Hauser MT, Benfey PN (2000) The SHORT-ROOT gene controls radial patterning of the Arabidopsis root through radial signaling. Cell 101:555–567. doi:10.1016/S0092-8674(00)80865-X

Helliwell CA, Sheldon CC, Olive MR, Walker AR, Zeevaart JA, Peacock WJ, Dennis ES (1998) Cloning of the Arabidopsis ent-kaurene oxidase gene GA3. Proc Natl Acad Sci USA 95:9019–9024. doi:10.1073/pnas.95.15.9019

Hewelt A, Prinsen E, Schell J, Van Onckelen H, Schmulling T (1994) Promoter tagging with a promoterless ipt gene leads to cytokinin-induced phenotypic variability in transgenic tobacco plants:implications of gene dosage effects. Plant J 6:879–891. doi:10.1046/j.1365-313X.1994.6060879.x

Higuchi M, Pischke MS, Mahonen AP, Miyawaki K, Hashimoto Y, Seki M, Kobayashi M, Shinozaki K, Kato T, Tabata S, Helariutta Y, Sussman MR, Kakimoto T (2004) In planta functions of the Arabidopsis cytokinin receptor family. Proc Natl Acad Sci USA 101:8821–8826. doi:10.1073/pnas.0402887101

Hutchison CE, Li J, Argueso C, Gonzalez M, Lee E, Lewis MW, Maxwell BB, Perdue TD, Schaller GE, Alonso JM, Ecker JR, Kieber JJ (2006) The Arabidopsis histidine phosphotransfer proteins are redundant positive regulators of cytokinin signaling. Plant Cell 18:3073–3087. doi:10.1105/tpc.106.045674

Chae HS, Faure F, Kieber JJ (2003) The eto1, eto2, and eto3 mutations and cytokinin treatment increase ethylene biosynthesis in Arabidopsis by increasing the stability of ACS protein. Plant Cell 15:545–559. doi:10.1105/tpc.006882

Chilley PM, Casson SA, Tarkowski P, Hawkins N, Wang KL, Hussey PJ, Beale M, Ecker JR, Sandberg GK, Lindsey K (2006) The POLARIS peptide of Arabidopsis regulates auxin transport and root growth via effects on ethylene signaling. Plant Cell 18:3058–3072. doi:10.1105/tpc.106.040790

Izhaki A, Swain SM, Tseng TS, Borochov A, Olszewski NE, Weiss D (2001) The role of SPY and its TPR domain in the regulation of gibberellin action throughout the life cycle of Petunia hybrida plants. Plant J 28:181–190. doi:10.1046/j.1365-313X.2001.01144.x

Jasinski S, Piazza P, Craft J, Hay A, Woolley L, Rieu I, Phillips A, Hedden P, Tsiantis M (2005) KNOX action in Arabidopsis is mediated by coordinate regulation of cytokinin and gibberellin activities. Curr Biol 15:1560–1565. doi:10.1016/j.cub.2005.07.023

Kim GT, Fujioka S, Kozuka T, Tax FE, Takatsuto S, Yoshida S, Tsukaya H (2005) CYP90C1 and CYP90D1 are involved in different steps in the brassinosteroid biosynthesis pathway in Arabidopsis thaliana. Plant J 41:710–721. doi:10.1111/j.1365-313X.2004.02330.x

Knox K, Grierson CS, Leyser O (2003) AXR3 and SHY2 interact to regulate root hair development. Development 130:5769–5777. doi:10.1242/dev.00659

Kuderova A, Urbankova I, Valkova M, Malbeck J, Nemethova D and Hejatko J (2008) Effects of conditional IPT-dependent cytokinin overproduction on root architecture of Arabidopsis seedlings. Plant Cell Physiol 49:570–582

Kutz A, Muller A, Hennig P, Kaiser WM, Piotrowski M, Weiler EW (2002) A role for nitrilase 3 in the regulation of root morphology in sulphur-starving Arabidopsis thaliana. Plant J 30:95–106. doi:10.1046/j.1365-313X.2002.01271.x

Laplaze L, Benkova E, Casimiro I, Maes L, Vanneste S, Swarup R, Weijers D, Calvo V, Parizot B, Herrera-Rodriguez MB, Offringa R, Graham N, Doumas P, Friml J, Bogusz D, Beeckman T, Bennett M (2007) Cytokinins act directly on lateral root founder cells to inhibit root initiation. Plant Cell 19:3889–3900. doi:10.1105/tpc.107.055863

Le J, Vandenbussche F, Van Der Straeten D, Verbelen JP (2001) In the early response of Arabidopsis roots to ethylene, cell elongation is up- and down-regulated and uncoupled from differentiation. Plant Physiol 125:519–522. doi:10.1104/pp.125.2.519

Lee S, Cheng H, King KE, Wang W, He Y, Hussain A, Lo J, Harberd NP, Peng J (2002) Gibberellin regulates Arabidopsis seed germination via RGL2, a GAI/RGA-like gene whose expression is up-regulated following imbibition. Genes Dev 16:646–658. doi:10.1101/gad.969002

Levesque MP, Vernoux T, Busch W, Cui H, Wang JY, Blilou I, Hassan H, Nakajima K, Matsumoto N, Lohmann JU, Scheres B, Benfey PN (2006) Whole-genome analysis of the SHORT-ROOT developmental pathway in Arabidopsis. PLoS Biol 4:e143. doi:10.1371/journal.pbio.0040143

Leyser HM, Pickett FB, Dharmasiri S, Estelle M (1996) Mutations in the AXR3 gene of Arabidopsis result in altered auxin response including ectopic expression from the SAUR-AC1 promoter. Plant J 10:403–413. doi:10.1046/j.1365-313x.1996.10030403.x

Li J, Dai X, Zhao Y (2006a) A role for auxin response factor 19 in auxin and ethylene signaling in Arabidopsis. Plant Physiol 140:899–908. doi:10.1104/pp.105.070987

Li X, Mo X, Shou H, Wu P (2006b) Cytokinin-mediated cell cycling arrest of pericycle founder cells in lateral root initiation of Arabidopsis. Plant Cell Physiol 47:1112–1123. doi:10.1093/pcp/pcj082

Liang X, Abel S, Keller JA, Shen NF, Theologis A (1992) The 1-aminocyclopropane–1-carboxylate synthase gene family of Arabidopsis thaliana. Proc Natl Acad Sci USA 89:11046–11050. doi:10.1073/pnas.89.22.11046

Liang Y, Mitchell DM, Harris JM (2007) Abscisic acid rescues the root meristem defects of the Medicago truncatula latd mutant. Dev Biol 304:297–307. doi:10.1016/j.ydbio.2006.12.037

Luschnig C, Gaxiola RA, Grisafi P, Fink GR (1998) EIR1, a root-specific protein involved in auxin transport, is required for gravitropism in Arabidopsis thaliana. Genes Dev 12:2175–2187. doi:10.1101/gad.12.14.2175

Mahonen AP, Bonke M, Kauppinen L, Riikonen M, Benfey PN, Helariutta Y (2000) A novel two-component hybrid molecule regulates vascular morphogenesis of the Arabidopsis root. Genes Dev 14:2938–2943. doi:10.1101/gad.189200

Mahonen AP, Bishopp A, Higuchi M, Nieminen KM, Kinoshita K, Tormakangas K, Ikeda Y, Oka A, Kakimoto T, Helariutta Y (2006) Cytokinin signaling and its inhibitor AHP6 regulate cell fate during vascular development. Science 311:94–98. doi:10.1126/science.1118875

McGinnis KM, Thomas SG, Soule JD, Strader LC, Zale JM, Sun TP, Steber CM (2003) The Arabidopsis SLEEPY1 gene encodes a putative F-box subunit of an SCF E3 ubiquitin ligase. Plant Cell 15:1120–1130. doi:10.1105/tpc.010827

Medford JI, Horgan R, El-Sawi Z, Klee HJ (1989) Alterations of Endogenous Cytokinins in Transgenic Plants Using a Chimeric Isopentenyl Transferase Gene. Plant Cell 1:403–413

Miyawaki K, Matsumoto-Kitano M, Kakimoto T (2004) Expression of cytokinin biosynthetic isopentenyltransferase genes in Arabidopsis: tissue specificity and regulation by auxin, cytokinin, and nitrate. Plant J 37:128–138. doi:10.1046/j.1365-313X.2003.01945.x

Mouchel CF, Briggs GC, Hardtke CS (2004) Natural genetic variation in Arabidopsis identifies BREVIS RADIX, a novel regulator of cell proliferation and elongation in the root. Genes Dev 18:700–714. doi:10.1101/gad.1187704

Mouchel CF, Osmont KS, Hardtke CS (2006) BRX mediates feedback between brassinosteroid levels and auxin signalling in root growth. Nature 443:458–461. doi:10.1038/nature05130

Muller B and Sheen J (2008) Cytokinin and auxin interaction in root stem-cell specification during early embryogenesis. Nature 453:1094–1097

Mussig C, Shin GH, Altmann T (2003) Brassinosteroids promote root growth in Arabidopsis. Plant Physiol 133:1261–1271. doi:10.1104/pp.103.028662

Nagpal P, Walker LM, Young JC, Sonawala A, Timpte C, Estelle M, Reed JW (2000) AXR2 encodes a member of the Aux/IAA protein family. Plant Physiol 123:563–574. doi:10.1104/pp.123.2.563

Nakajima K, Sena G, Nawy T, Benfey PN (2001) Intercellular movement of the putative transcription factor SHR in root patterning. Nature 413:307–311. doi:10.1038/35095061

Nakamura A, Higuchi K, Goda H, Fujiwara MT, Sawa S, Koshiba T, Shimada Y, Yoshida S (2003) Brassinolide induces IAA5, IAA19, and DR5, a synthetic auxin response element in Arabidopsis, implying a cross talk point of brassinosteroid and auxin signaling. Plant Physiol 133:1843–1853. doi:10.1104/pp.103.030031

Nishimura C, Ohashi Y, Sato S, Kato T, Tabata S, Ueguchi C (2004) Histidine kinase homologs that act as cytokinin receptors possess overlapping functions in the regulation of shoot and root growth in Arabidopsis. Plant Cell 16:1365–1377. doi:10.1105/tpc.021477

Nordstrom A, Tarkowski P, Tarkowska D, Norbaek R, Astot C, Dolezal K, Sandberg G (2004) Auxin regulation of cytokinin biosynthesis in Arabidopsis thaliana: a factor of potential importance for auxin-cytokinin-regulated development. Proc Natl Acad Sci USA 101:8039–8044. doi:10.1073/pnas.0402504101

Okushima Y, Overvoorde PJ, Arima K, Alonso JM, Chan A, Chang C, Ecker JR, Hughes B, Lui A, Nguyen D, Onodera C, Quach H, Smith A, Yu G, Theologis A (2005) Functional genomic analysis of the AUXIN RESPONSE FACTOR gene family members in Arabidopsis thaliana: unique and overlapping functions of ARF7 and ARF19. Plant Cell 17:444–463. doi:10.1105/tpc.104.028316

Ortega-Martinez O, Pernas M, Carol RJ, Dolan L (2007) Ethylene modulates stem cell division in the Arabidopsis thaliana root. Science 317:507–510. doi:10.1126/science.1143409

Overvoorde PJ, Okushima Y, Alonso JM, Chan A, Chang C, Ecker JR, Hughes B, Liu A, Onodera C, Quach H, Smith A, Yu G, Theologis A (2005) Functional genomic analysis of the AUXIN/INDOLE–3-ACETIC ACID gene family members in Arabidopsis thaliana. Plant Cell 17:3282–3300. doi:10.1105/tpc.105.036723

Palni LMS, Burch L, Horgan R (1988) The Effect of Auxin Concentration on Cytokinin Stability and Metabolism. Planta 174:231–234. doi:10.1007/BF00394775

Paquette AJ, Benfey PN (2005) Maturation of the ground tissue of the root is regulated by gibberellin and SCARECROW and requires SHORT-ROOT. Plant Physiol 138:636–640. doi:10.1104/pp.104.058362

Petrášek J, Mravec J, Bouchard R, Blakeslee JJ, Abas M, Seifertová D, Wisniewska J, Tadele Z, Kubes M, Covanová M, Dhonukshe P, Skupa P, Benková E, Perry L, Krecek P, Lee OR, Fink GR, Geisler M, Murphy AS, Luschnig C, Zazímalová E, Friml J (2006) PIN proteins perform a rate-limiting function in cellular auxin efflux Science 312:914–918. doi:10.1126/science.1123542

Pickett FB, Wilson AK, Estelle M (1990) The aux1 Mutation of Arabidopsis Confers Both Auxin and Ethylene Resistance. Plant Physiol 94:1462–1466

Rahman A, Amakawa T, Goto N, Tsurumi S (2001) Auxin is a positive regulator for ethylene-mediated response in the growth of arabidopsis roots. Plant and Cell Physiology 42:301–307. doi:10.1093/pcp/pce035

Rahman A, Bannigan A, Sulaman W, Pechter P, Blancaflor EB, Baskin TI (2007) Auxin, actin and growth of the Arabidopsis thaliana primary root. Plant J 50:514–528. doi:10.1111/j.1365-313X.2007.03068.x

Rashotte AM, Chae HS, Maxwell BB, Kieber JJ (2005) The interaction of cytokinin with other signals. Physiologia Plantarum 123:184–194. doi:10.1111/j.1399-3054.2005.00445.x

Riefler M, Novak O, Strnad M, Schmulling T (2006) Arabidopsis cytokinin receptor mutants reveal functions in shoot growth, leaf senescence, seed size, germination, root development, and cytokinin metabolism. Plant Cell 18:40–54. doi:10.1105/tpc.105.037796

Roman G, Lubarsky B, Kieber JJ, Rothenberg M, Ecker JR (1995) Genetic analysis of ethylene signal transduction in Arabidopsis thaliana: five novel mutant loci integrated into a stress response pathway. Genetics 139:1393–1409

Rosado A, Schapire AL, Bressan RA, Harfouche AL, Hasegawa PM, Valpuesta V, Botella MA (2006) The Arabidopsis tetratricopeptide repeat-containing protein TTL1 is required for osmotic stress responses and abscisic acid sensitivity. Plant Physiol 142:1113–1126. doi:10.1104/pp.106.085191

Ruzicka K, Ljung K, Vanneste S, Podhorska R, Beeckman T, Friml J, Benkova E (2007) Ethylene regulates root growth through effects on auxin biosynthesis and transport-dependent auxin distribution. Plant Cell 19:2197–2212. doi:10.1105/tpc.107.052126

Sabatini S, Beis D, Wolkenfelt H, Murfett J, Guilfoyle T, Malamy J, Benfey P, Leyser O, Bechtold N, Weisbeek P, Scheres B (1999) An auxin-dependent distal organizer of pattern and polarity in the Arabidopsis root. Cell 99:463–472. doi:10.1016/S0092-8674(00)81535-4

Sasaki A, Itoh H, Gomi K, Ueguchi-Tanaka M, Ishiyama K, Kobayashi M, Jeong DH, An G, Kitano H, Ashikari M, Matsuoka M (2003) Accumulation of phosphorylated repressor for gibberellin signaling in an F-box mutant. Science 299:1896–1898. doi:10.1126/science.1081077

Shimada Y, Goda H, Nakamura A, Takatsuto S, Fujioka S, Yoshida S (2003) Organ-specific expression of brassinosteroid-biosynthetic genes and distribution of endogenous brassinosteroids in Arabidopsis. Plant Physiol 131:287–297. doi:10.1104/pp.013029

Scheres B, Dilaurenzio L, Willemsen V, Hauser MT, Janmaat K, Weisbeek P, Benfey PN (1995) Mutations Affecting the Radial Organization of the Arabidopsis Root Display Specific Defects Throughout the Embryonic Axis. Development 121:53–62

Schlagnhaufer CD, Arteca RN (1985) Brassinosteroid-Induced Epinasty in Tomato Plants. Plant Physiol 78:300–303

Sieberer T, Hauser MT, Seifert GJ, Luschnig C (2003) PROPORZ1, a putative Arabidopsis transcriptional adaptor protein, mediates auxin and cytokinin signals in the control of cell proliferation. Curr Biol 13:837–842. doi:10.1016/S0960-9822(03)00327-0

Smigocki AC (1991) Cytokinin content and tissue distribution in plants transformed by a reconstructed isopentenyl transferase gene. Plant Mol Biol 16:105–115. doi:10.1007/BF00017921

Son O, Cho HY, Kim MR, Lee H, Lee MS, Song E, Park JH, Nam KH, Chun JY, Kim HJ, Hong SK, Chung YY, Hur CG, Cho HT, Cheon CI (2005) Induction of a homeodomain-leucine zipper gene by auxin is inhibited by cytokinin in Arabidopsis roots. Biochem Biophys Res Commun 326:203–209. doi:10.1016/j.bbrc.2004.11.014

Stepanova AN, Hoyt JM, Hamilton AA, Alonso JM (2005) A Link between ethylene and auxin uncovered by the characterization of two root-specific ethylene-insensitive mutants in Arabidopsis. Plant Cell 17:2230–2242. doi:10.1105/tpc.105.033365

Stepanova AN, Yun J, Likhacheva AV, Alonso JM (2007) Multilevel interactions between ethylene and auxin in Arabidopsis roots. Plant Cell 19:2169–2185. doi:10.1105/tpc.107.052068

Stepanova AN, Robertson-Hoyt J, Yun J, Benavente LM, Xie DY, Dolezal K, Schlereth A, Jurgens G, Alonso JM (2008) TAA1-

mediated auxin biosynthesis is essential for hormone crosstalk and plant development. Cell 133:177–191. doi:10.1016/j.cell.2008.01.047

Swain SM, Tseng TS, Olszewski NE (2001) Altered expression of SPINDLY affects gibberellin response and plant development. Plant Physiol 126:1174–1185. doi:10.1104/pp.126.3.1174

Swarup R, Perry P, Hagenbeek D, Van Der Straeten D, Beemster GT, Sandberg G, Bhalerao R, Ljung K, Bennett MJ (2007) Ethylene upregulates auxin biosynthesis in Arabidopsis seedlings to enhance inhibition of root cell elongation. Plant Cell 19:2186–2196. doi:10.1105/tpc.107.052100

Tao Y, Ferrer JL, Ljung K, Pojer F, Hong F, Long JA, Li L, Moreno JE, Bowman ME, Ivans LJ, Cheng Y, Lim J, Zhao Y, Ballare CL, Sandberg G, Noel JP, Chory J (2008) Rapid synthesis of auxin via a new tryptophan-dependent pathway is required for shade avoidance in plants. Cell 133:164–176. doi:10.1016/j.cell.2008.01.049

Tian Q, Reed JW (1999) Control of auxin-regulated root development by the Arabidopsis thaliana SHY2/IAA3 gene. Development 126:711–721

To JP, Haberer G, Ferreira FJ, Deruere J, Mason MG, Schaller GE, Alonso JM, Ecker JR, Kieber JJ (2004) Type-A Arabidopsis response regulators are partially redundant negative regulators of cytokinin signaling. Plant Cell 16:658–671. doi:10.1105/tpc.018978

Torres-Ruiz RA, Jurgens G (1994) Mutations in the FASS gene uncouple pattern formation and morphogenesis in Arabidopsis development. Development 120:2967–2978

Tran LS, Urao T, Qin F, Maruyama K, Kakimoto T, Shinozaki K, Yamaguchi-Shinozaki K (2007) Functional analysis of AHK1/ATHK1 and cytokinin receptor histidine kinases in response to abscisic acid, drought, and salt stress in Arabidopsis. Proc Natl Acad Sci USA 104:20623–20628. doi:10.1073/pnas.0706547105

Truernit E, Siemering KR, Hodge S, Grbic V, Haseloff J (2006) A map of KNAT gene expression in the Arabidopsis root. Plant Mol Biol 60:1–20. doi:10.1007/s11103-005-1673-9

Tsuchisaka A, Theologis A (2004) Unique and overlapping expression patterns among the Arabidopsis 1-amino-cyclopropane–1-carboxylate synthase gene family members. Plant Physiol 136:2982–3000. doi:10.1104/pp.104.049999

Ubeda-Tomas S, Swarup R, Coates J, Swarup K, Laplaze L, Beemster GT, Hedden P, Bhalerao R, Bennett MJ (2008) Root growth in Arabidopsis requires gibberellin/DELLA signalling in the endodermis. Nat Cell Biol 10:625–628. doi:10.1038/ncb1726

Ulmasov T, Murfett J, Hagen G, Guilfoyle TJ (1997) Aux/IAA proteins repress expression of reporter genes containing natural and highly active synthetic auxin response elements. Plant Cell 9:1963–1971

van den Berg C, Weisbeek P, Scheres B (1998) Cell fate and cell differentiation status in the Arabidopsis root. Planta 205:483–491. doi:10.1007/s004250050347

Vriezen WH, Achard P, Harberd NP, Van Der Straeten D (2004) Ethylene-mediated enhancement of apical hook formation in etiolated Arabidopsis thaliana seedlings is gibberellin dependent. Plant J 37:505–516. doi:10.1046/j.1365-313X.2003.01975.x

Watt FM, Hogan BL (2000) Out of Eden: stem cells and their niches. Science 287:1427–1430. doi:10.1126/science.287.5457.1427

Weijers D, Benkova E, Jager KE, Schlereth A, Hamann T, Kientz M, Wilmoth JC, Reed JW, Jurgens G (2005) Developmental specificity of auxin response by pairs of ARF and Aux/IAA transcriptional regulators. EMBO J 24:1874–1885. doi:10.1038/sj.emboj.7600659

Weijers D, Schlereth A, Ehrismann JS, Schwank G, Kientz M, Jurgens G (2006) Auxin triggers transient local signaling for cell specification in Arabidopsis embryogenesis. Dev Cell 10:265–270. doi:10.1016/j.devcel.2005.12.001

Welch D, Hassan H, Blilou I, Immink R, Heidstra R, Scheres B (2007) Arabidopsis JACKDAW and MAGPIE zinc finger proteins delimit asymmetric cell division and stabilize tissue boundaries by restricting SHORT-ROOT action. Genes Dev 21:2196–2204. doi:10.1101/gad.440307

Wen CK, Chang C (2002) Arabidopsis RGL1 encodes a negative regulator of gibberellin responses. Plant Cell 14:87–100. doi:10.1105/tpc.010325

Werner T, Motyka V, Laucou V, Smets R, Van Onckelen H, Schmulling T (2003) Cytokinin-deficient transgenic Arabidopsis plants show multiple developmental alterations indicating opposite functions of cytokinins in the regulation of shoot and root meristem activity. Plant Cell 15:2532–2550. doi:10.1105/tpc.014928

Wilson AK, Pickett FB, Turner JC, Estelle M (1990) A dominant mutation in Arabidopsis confers resistance to auxin, ethylene and abscisic acid. Mol Gen Genet 222:377–383. doi:10.1007/BF00633843

Yanai O, Shani E, Dolezal K, Tarkowski P, Sablowski R, Sandberg G, Samach A, Ori N (2005) Arabidopsis KNOXI proteins activate cytokinin biosynthesis. Curr Biol 15:1566–1571. doi:10.1016/j.cub.2005.07.060

Yang SF, Hoffman NE (1984) Ethylene Biosynthesis and Its Regulation in Higher-Plants. Annual Review of Plant Physiology and Plant Molecular Biology 35:155–189. doi:10.1146/annurev.arplant.35.1.155

Yang S, Yu H, Xu Y, Goh CJ (2003) Investigation of cytokinin-deficient phenotypes in Arabidopsis by ectopic expression of orchid DSCKX1. FEBS Lett 555:291–296. doi:10.1016/S0014-5793(03)01259-6

Yang Y, Hammes UZ, Taylor CG, Schachtman DP, Nielsen E (2006) High-affinity auxin transport by the AUX1 influx carrier protein. Curr Biol 16:1123–1127

Yi HC, Joo S, Nam KH, Lee JS, Kang BG, Kim WT (1999) Auxin and brassinosteroid differentially regulate the expression of three members of the 1-aminocyclopropane-1-carboxylate synthase gene family in mung bean (Vigna radiata L.). Plant Mol Biol 41:443–454. doi:10.1023/A:1006372612574